

Dipl.-Ing.(FH), M.Sc. Sandra Hellmers

*Hydrological Impacts of Climate Change  
on Flood Probability in Small Urban Catchments  
and Possibilities of Flood Risk Mitigation*



Sandra Hellmers

**Hydrological Impacts of Climate Change on Flood Probability  
in Small Urban Catchments and Possibilities of Flood Risk Mitigation**

**Hydrologische Auswirkungen des Klimawandels auf die  
Hochwasserwahrscheinlichkeit und Maßnahmen zu deren  
Kompensation in kleinen städtischen Einzugsgebieten**

**Hamburger Wasserbau-Schriften**

Band 13

Publicated by

Prof. Dr.-Ing. Erik Pasche

**Hydrological Impacts of Climate Change on Flood Probability  
in Small Urban Catchments and Possibilities of Flood Risk Mitigation**

Master's Thesis at the Institute of River and Coastal Engineering

by Sandra Hellmers

**Institute of River and Coastal Engineering,  
University of Technology Hamburg – Harburg**

**2010**

**All rights reserved. Reproduction in whole or in part without permission of the Institute is prohibited.**

Cover Design: Kerstin Schürmann, [www.formlabor.de](http://www.formlabor.de)  
Cover Foto: Sandra Hellmers  
Editor: Sandra Hellmers

ISBN 978-3-937693-13-2  
ISSN 1612-8699

1. Edition, Institute of River and Coastal Engineering TUHH, Hamburg

## **Preface**

*Dear Reader,*

*like many other disciplines the hydrological science community is strongly affected by the societal discussion about the consequences of a changing climate. Based on future economic and demographic development scenarios the progress of the climate system can be simulated with computer models. Further on the calculated climate variables are used in specific impact models such as detailed hydrological simulations, which use rainfall-runoff as well as water balance models to understand the consequences of these changing climate conditions on the hydrological cycle.*

*So far the temporal and spatial resolution of the available climate data has not been sufficient enough in order to use it directly in hydrological models for flood analysis. However, within the German BMBF-project KLIMZUG-Nord ([www.klimzug-nord.de](http://www.klimzug-nord.de)) climate data has been provided with a spatial resolution of 1km<sup>2</sup> and a temporal resolution of 1 h which allows the analysis of discharge simulations in smaller river catchments for the first time.*

*In her Master's thesis Sandra Hellmers developed a new method to derive extreme floods from this climate data and to classify them statistically. For these hydrological studies she used the non-linear semi-distributive rainfall-runoff model KALYPSO-Hydrology and demonstrated the improvements for flood analysis in rural and urban areas in the case study area of the river basin Krückau in Northern Germany. Furthermore she proved that extreme precipitations cannot be linearly transferred into extreme runoff. In order to resolve the various complex, interacting processes between the terrain, ground, river network and the urban drainage system very precise modelling instruments are needed. These model requirements are also necessary to quantify the effectiveness of non-structural measures such as SUDS (Sustainable Drainage System) and surface conveyance measures.*

*Sandra Hellmers' research work is outstanding as her new method of climate impact assessment on the hydrological cycle is innovative, physically sound and so generic that it can be used as good guidance for hydrological impact studies of climate change. The new method to simulate the attenuation and retention effects of SUDS fully parametrises the components of SUDS thereby opening this method to scenario studies of urban drainage systems with various combinations and intensities of SUDS components.*

*On this background I decided to publish her Master's thesis in the „Hamburger Wasserbau-Schriften“. I hope many practitioners and other researchers will benefit from this pioneering work and make use of this method for their own climate impact studies. They are invited to make use of the software KALYPSO-Hydrology which can be downloaded from <http://kalypso.sourceforge.net>.*

*Hamburg, 08.11.2010*

*Prof. Dr.-Ing. Erik Pasche*

*(Head of the Institute of River and Coastal Engineering at the TUHH)*

## Abstract

Impacts of climate change on the ecology, the human and the economy are already apparent and probably increase significantly in future. The magnitude and frequency of extreme rainfall is thereby assumed to change, which could affect the flood regime in river catchments substantially. Especially flooding in small urban catchments (SUCAs) is strongly dependent on intensive rainfall events which cause exceeding flow from small rivers, streams and storm water sewer systems. Developing a detailed and comprehensive methodology to quantify the hydrological impacts of climate change on flood probability in SUCAs is a required and forward-looking task, which has been worked out and described in this thesis.

To cope with the impacts on flood risk in SUCAs, it is emergent to introduce and implement effective, flexible as well as adaptable possibilities of flood probability reduction, whereas sustainable drainage systems (SUDSs) have been identified as appropriate measures. To assess the effectiveness of these techniques, a software tool for simulating SUDS elements (namely: green roofs) on a catchment level has been programmed.

The developed methodology in this thesis comprises the pre-processing of climate model as well as climate scenario data series, the processing of climate scenario results, the post-processing of calculated climate change impacts including the computation of climate change factors and the assessment of the effectiveness of SUDSs in post-impact studies.

This methodology has been applied for climate change impact studies in one of the catchments in the region of the KLIMZUG-Nord project. An increase of the frequency and magnitude of extreme events has been calculated especially for summer periods, whereas for winter periods the average precipitation is computed to increase significantly. With the IPCC scenario A1B, in the climate period from 2040 to 2070, an increase of 13.3% for 100year summer rainfall intensities with durations of 1hour, as well as an increase of 22.5% for 100year peak discharges in summer periods has been calculated. Additionally, simulations for the IPCC scenarios B1 and A2 have been performed, but the results display lower changes in extreme events for the time period around 2050.

The new developed software tool for simulating green roofs has been tested in adaptation scenario studies, along with the simulation of swales and swale-filter-drain systems. The appropriateness of the simulation results of hydrological processes in each SUDS element and the effectiveness of SUDSs on a catchment level has been verified. The compensation of climate change impacts on the flood probability in SUCAs has been achieved with the combination of different SUDS measures, which display larger effectiveness for events with higher probabilities of occurrence.

## Zusammenfassung

Die Auswirkungen des Klimawandels auf die Ökologie, den Menschen und die Ökonomie sind bereits spürbar und werden voraussichtlich in Zukunft erheblich zunehmen. Veränderungen der Häufigkeit und Intensität von Starkniederschlägen sind dabei zu erwarten, die wiederum erhebliche Auswirkungen auf die Hochwasserverhältnisse in Flusseinzugsgebieten zur Folge haben können. Insbesondere Überschwemmungen von kleinen Einzugsgebieten in urbanen Räumen durch Gewässer und Entwässerungsnetze werden durch Starkniederschläge verursacht. Die Entwicklung einer umfassenden und detaillierten Methodik zur Quantifizierung der hydrologischen Auswirkungen des Klimawandels auf die Hochwasserwahrscheinlichkeit in kleinen städtischen Einzugsgebieten ist eine erforderliche und zukunftsweisende Aufgabe, die in dieser Arbeit erläutert und ausgearbeitet wurde.

Um den Einflüssen des Klimawandels auf Hochwasser in städtischen Einzugsgebieten zu begegnen, ist es notwendig effektive und flexibel anpassbare Maßnahmen zur Reduktion der Hochwasserwahrscheinlichkeit zu ergreifen und umzusetzen. Nachhaltige Regenwasserbewirtschaftung (RWB) wurde hierfür als geeignete Vorgehensweise erkannt und für den Nachweis der Effektivität von diesen Maßnahmen wurde ein Software-Tool für die Simulation von RWB-Elementen (hier: Gründächer) auf Einzugsgebietsebene programmiert.

Die entwickelte Methodik umfasst die Aufbereitung der Daten von Klimamodellen (Pre-Processing), die Berechnung sowie Analyse der Klimaszenarienergebnisse (Processing), die Nachbereitung der berechneten Auswirkungen (Post-Processing) einschließlich der Berechnung von Klimawandelfaktoren und den Nachweis der Effektivität von RWB-Maßnahmen.

Für Studien über die Folgen des Klimawandels in einem der Einzugsgebiete des KLIMZUG-Nord Projektes wurde diese Methodik angewendet. Für das IPCC Szenario A1B der Klimaperiode von 2040 bis 2070 wurde eine Zunahme von 13,3% für 100jährige Starkniederschläge im Sommer, sowie eine Erhöhung von 22,5% für 100jährige Sommerhochwasserereignisse berechnet. Zusätzlich wurden Berechnungen der IPCC Szenarien B1 und A2 ausgeführt, die jedoch geringere Auswirkungen des Klimawandels für den Zeitraum um 2050 aufzeigen. Das entwickelte Software-Tool für die Simulation von Gründächern wurde zusammen mit der Modellierung von Mulden und Mulden-Filter-Rigolen Systemen getestet. Die Genauigkeit der Simulation der hydrologischen Prozesse in den jeweiligen RWB-Elementen und die Berechnung deren Effektivität auf Einzugsgebietsebene wurden nachgewiesen. Durch die Kombination von mehreren RWB-Maßnahmen wurde sogar eine Kompensation der Auswirkungen des Klimawandels auf die Hochwasserwahrscheinlichkeit erreicht.

## **Acknowledgement**

I would like to take the opportunity to express my gratitude to all those people who supported me during this Master Thesis.

My sincere thanks are due to Prof. Dr.-Ing. Erik Pasche, for the scientific guidance, continuous challenge and encouragement to work on this Thesis in the scope of the KLIMZUG-Nord project, with the possibility to continue my research at the Institute of River and Coastal Engineering in this forward-looking topic.

I am especially grateful to Claudia Brüning for discussions and supporting me in implementing the developed software tool, and for giving me an introduction to the FORTRAN programming language used in the core of Kalypso Hydrology.

Further on, I owe thanks to Dejan Antanaskovic for assisting me in the pre-processing of climate model data by programming an auxiliary Java tool. And my thanks are due to Niloufar Behzadnia for the countless and helpful discussions about the application of the GUI of Kalypso Hydrology. Additionally, I owe thanks to her together with Gehad Ujeyl for giving me the opportunity to run the vast number of simulations on several computers.

I express my sincere gratitude to Nataša Manojlovic for her support in receiving the required data and the helpful suggestions during the final writing of my thesis.

And thanks are due to Diana Rechid from the Max-Planck-Institute of Meteorology in Hamburg, for discussions about climate model data and support of valuable literature.

---

## Table of Contents

|  |           |
|--|-----------|
| <b>1. Introduction</b> .....   | <b>1</b>  |
| <b>2. How do Flood Impact Studies deal with Climate Change Scenarios?</b> .....              | <b>4</b>  |
| <b>2.1 Climate Change Impact Studies about Extreme Events and Flooding</b> .....             | <b>5</b>  |
| <b>2.2 Strategies for Mitigating Climate Change Impacts on Urban Flooding</b> .....          | <b>12</b> |
| 2.2.1 Research Projects of Adaptation Strategies .....                                       | 12        |
| 2.2.2 Sustainable Climate Change Adaptation Strategies for Flood Probability Reduction.....  | 14        |
| <b>2.3 Open Research Questions and Objectives</b> .....                                      | <b>17</b> |
| <b>3. Methodological Approach</b> .....  | <b>19</b> |
| <b>3.1 Methodology Scheme</b> .....  | <b>19</b> |
| <b>3.2 Hydrological Modelling</b> .....  | <b>20</b> |
| <b>3.3 Pre-Processing of Climate Model Data</b> .....  | <b>22</b> |
| 3.3.1 Criteria for Selecting Climate Model Data .....  | 22        |
| 3.3.2 Climate Model Types .....  | 24        |
| 3.3.2.1 <i>Global Circulation Models (GCMs)</i> .....  | 24        |
| 3.3.2.2 <i>Regional Climate Models (RCMs)</i> .....  | 25        |
| 3.3.3 Climate Change Scenarios .....   | 26        |
| 3.3.4 Climate Model Data Sources and Formats.....  | 27        |
| 3.3.5 Calculation of Additional Data Series .....  | 29        |
| 3.3.6 Differentiation of Seasons .....   | 30        |
| <b>3.4 Processing of Climate Change Scenario Results</b> .....                               | <b>30</b> |
| 3.4.1 Climate Variables .....  | 31        |
| 3.4.2 Data Series of Flood Events .....  | 31        |
| 3.4.3 Control Scenario Data Series .....   | 31        |
| 3.4.4 Future Climate Scenario Data Series .....  | 32        |
| 3.4.5 Statistical Evaluations of Extreme Rainfall and Flood Probabilities .                  | 32        |
| 3.4.5.1 <i>Trend Adjustment</i> .....  | 33        |
| 3.4.5.2 <i>Extreme Rainfall Probability Distribution Functions</i> .....                     | 34        |
| 3.4.5.3 <i>Flood Peak Probability Distribution Functions</i> .....                           | 35        |
| 3.4.5.4 <i>Outlier Tests</i> .....   | 37        |
| 3.4.5.5 <i>Goodness-of-Fit Tests</i> .....   | 39        |
| <b>3.5 Post-Processing of Scenario Results</b> .....   | <b>39</b> |
| 3.5.1 The Magnitude of Climate Change Impacts .....  | 39        |
| 3.5.2 Computation of Climate Change Factors (CCFs) .....                                     | 40        |
| 3.5.3 Design Events for Post-Impact Studies.....   | 41        |
| <b>3.6 Post-Impact Studies to Mitigate Climate Change Impacts on Flood Probability</b> ..... | <b>42</b> |

---

---

|   |            |
|---|------------|
| 3.6.1 Theoretical Approach to Model SUDS .....                              | 43         |
| 3.6.1.1 <i>Green Roofs</i> .....  | 43         |
| 3.6.1.2 <i>Swales and Swale-Filter-Drain Systems</i> .....                  | 45         |
| 3.6.2 Criteria for Testing the Approach .....                               | 46         |
| 3.6.3 Combination of Adaptation Measure Scenarios.....                      | 47         |
| 3.6.4 Planning Criteria for Sustainable Drainage Systems .....              | 48         |
| 3.6.4.1 <i>Restrictions of Spatial Distribution</i> .....                   | 48         |
| 3.6.4.2 <i>Design Criteria of SUDS Measures</i> .....                       | 49         |
| 3.6.4.3 <i>Design Storm Conditions</i> .....                                | 51         |
| <b>3.7 Comparative and Uncertainty Studies .....</b>                        | <b>52</b>  |
| <b>4. Implementation of a SUDS Software Tool .....</b>                      | <b>55</b>  |
| <b>4.1 Catchment Level Approach .....</b>                                   | <b>55</b>  |
| <b>4.2 Implementation Procedure.....</b>                                    | <b>56</b>  |
| <b>4.3 Development of an Add-On Tool .....</b>                              | <b>65</b>  |
| <b>5. Application Scenario Studies .....</b>                                | <b>70</b>  |
| <b>5.1 Applied Hydrological Model of the Krückau Catchment .....</b>        | <b>70</b>  |
| 5.1.1 Scenario Study Area.....  | 70         |
| 5.1.2 Hydrological Model Set-Up .....                                       | 71         |
| <b>5.2 Pre-Processing of Climate Model Data .....</b>                       | <b>73</b>  |
| 5.2.1 Selection of Climate Model Data Series .....                          | 73         |
| 5.2.2 Pre-Processing of Climate Model Data Series .....                     | 75         |
| <b>5.3 Processing of Results of Climate Variables .....</b>                 | <b>76</b>  |
| 5.3.1 Climate Control Scenarios [1971 – 2000].....                          | 77         |
| 3.6.1.1 <i>Average Climate Data Results</i> .....                           | 77         |
| 3.6.1.2 <i>Statistical Evaluations of Rainfall Events</i> .....             | 78         |
| 5.3.2 Future Climate Scenarios [2040 – 2070].....                           | 81         |
| 3.6.2.1 <i>Trend Line Analysis of Climate Variables</i> .....               | 81         |
| 3.6.2.2 <i>Number of Occurrences of Daily Rainfall Thresholds</i> .....     | 83         |
| 3.6.2.3 <i>Statistical Evaluations of Rainfall Events</i> .....             | 85         |
| <b>5.4 Processing of Flood Probability Scenario Results.....</b>            | <b>87</b>  |
| 5.4.1 Locations of Interest.....  | 88         |
| 5.4.2 Differentiation of Simulation Timesteps.....                          | 89         |
| 5.4.3 Statistical Evaluations of Flood Peaks .....                          | 90         |
| 3.6.3.1 <i>Climate Control Scenario Results [1971 – 2000]</i> .....         | 94         |
| 3.6.3.2 <i>Future Climate Scenario Results [2040 – 2070]</i> .....          | 95         |
| <b>5.5 Post-Processing of Climate Change Scenario Results.....</b>          | <b>96</b>  |
| 5.5.1 Post-Processing of Rainfall Probability Results [Scenario 0-A1B]..... | 97         |
| 5.5.2 Post-Processing of Flood Peak Probability Results [Scenario0-A1B] ... | 98         |
| 5.5.3 Design Event for Post-Impact Studies .....                            | 100        |
| <b>5.6 Simulation of Adaptation Measures .....</b>                          | <b>102</b> |
| 5.6.1 Design of SUDS Techniques .....                                       | 103        |

---

---

|            |   |            |
|------------|---|------------|
| 5.6.1.1    | <i>Potential Spatial Distribution of SUDSs</i>                | 103        |
| 5.6.1.2    | <i>Design of SUDS Elements</i>                                | 107        |
| 5.6.2      | Testing Results of the SUDS Software Tool                     | 109        |
| 5.6.2.1    | <i>Simulations of Green Roofs</i>                             | 109        |
| 5.6.2.2    | <i>Simulations of Swales</i>                                  | 112        |
| 5.6.2.3    | <i>Simulations of Swale-Filter-Drain System</i>               | 114        |
| 5.6.3      | Assessment of the Effectiveness of SUDS in Adaptation         |            |
| Scenarios  |   | 117        |
| 5.6.3.1    | <i>Catchment of the Eckhorner Au</i>                          | 118        |
| 5.6.3.2    | <i>Upper Krückkau Catchment (Kaltenkirchen and Barmstedt)</i> | 119        |
| 5.6.3.3    | <i>Elmshorn - Node Langeloh</i>                               | 119        |
| 5.6.3.4    | <i>Elmshorn - End Node of the Krückkau Catchment</i>          | 121        |
| 5.6.3.5    | <i>Sub-Catchments in Elmshorn</i>                             | 123        |
| <b>6.</b>  | <b>Discussion</b>   | <b>127</b> |
| <b>6.1</b> | <b>Comparative Studies</b>                                    | <b>127</b> |
| 6.1.1      | Discussion of Changes in Climate Variables                    | 127        |
| 6.1.1.1    | <i>Climate Control Scenario Results [1971 – 2000]</i>         | 127        |
| 6.1.1.2    | <i>Future Climate Scenario Results [2040 – 2070]</i>          | 129        |
| 6.1.2      | Discussion of Changes in Flood Probability                    | 133        |
| 6.1.2.1    | <i>Reference Scenario 0 Results [1971 – 2000]</i>             | 134        |
| 6.1.2.2    | <i>Climate Control Scenario Results [1971 – 2000]</i>         | 135        |
| 6.1.2.3    | <i>Future Climate Scenario Results [2040 – 2070]</i>          | 135        |
| 6.1.3      | Discussion of Post-Processing Results                         | 136        |
| 6.1.4      | Discussion of SUDS Adaptation Scenario Results                | 138        |
| <b>6.2</b> | <b>Uncertainty Analysis in Climate Change Impact Studies</b>  | <b>139</b> |
| <b>7.</b>  | <b>Conclusion and Outlook</b>                                 | <b>142</b> |
| <b>7.1</b> | <b>Conclusion</b>   | <b>142</b> |
| <b>7.2</b> | <b>Outlook</b>  | <b>147</b> |
| <b>8.</b>  | <b>Bibliography</b>   | <b>150</b> |
| <b>9.</b>  | <b>Appendices</b>   | <b>162</b> |

---

---

## **List of Appendices**

| <b>Nr.</b>  | <b>Title</b>  | <b>Page</b> |
|---|---|-------------|
| <b><i>Attachments: Methodology</i></b>                  |   |             |
| 1   | Climate Models  | 162         |
| 2   | Calculation of Additional Climate Change Data Series                  | 164         |
| 3   | Statistical Evaluations   | 167         |
| 3.1   | Adjustment of Trends in Data Time Series                              | 167         |
| 3.2   | Statistical Evaluation of Extreme Rainfall Events with Partial Series | 167         |
| 4   | Grubbs Test Values (DIN 53 804)                                       | 171         |
| <b><i>Attachments: Implementation</i></b>               |   |             |
| 5   | Nassi-Shneiderman Diagrams  | 172         |
| 5.1   | Definitions and Auxiliary Explanations                                | 172         |
| 5.2   | Green Roof Main Routine   | 174         |
| 5.3   | Drained Area per Outlet Pipe  | 175         |
| 5.4   | First Internal Layer Loop   | 177         |
| 5.5   | Second Internal Layer Loop  | 178         |
| 5.6   | Third Internal Layer Loop   | 179         |
| 5.7   | Water Balance in Drainage and Substrate Layer                         | 180         |
| 5.8   | Flow Through Down Pipe  | 181         |
| 5.9   | Water Balance in Storage layer  | 182         |
| 5.10  | Flow Through Overflow Pipe  | 183         |
| 5.11  | Derivation of Equations   | 184         |
| 6   | Application of Spreadsheet and ASCII Files                            | 185         |
| <b><i>Attachments: Application Scenario Studies</i></b> |   |             |
| 7   | Climate Model Data Variables  | 189         |
| 8   | Probability of Extreme Rainfall Events in the Past [1971 - 2000]      | 190         |
| 9   | Average Changes in Climate Variables [2040 - 2070]                    | 202         |
| 10  | Number of Occurrence of Daily Precipitation Intensities [2040 - 2070] | 207         |
| 11  | Probability of Extreme Rainfall Events in the Future [2040 - 2070]    | 209         |
| 12  | Differentiation of Simulation Time Steps                              | 215         |
| 13  | Trend Adjustment of Flood Peak Data Series                            | 217         |
| 14  | Probability of Flood Peak Events                                      | 221         |
| 14.1  | Log-Pearson Type III and Log-Normal Type III Distributions            | 221         |
| 14.2  | Flood Probability Distribution Curves                                 | 222         |
| 14.3  | Tables: Control Scenario Results [1971 - 2000]                        | 233         |
| 14.4  | Tables: Future Scenario Results [2040 - 2070]                         | 234         |
| 15  | Post-Processing Results   | 237         |
| 15.1  | Post-Processing of Design Rainfall Events                             | 237         |
| 15.2  | Post-Processing of Design Flood Events                                | 238         |
| 16  | Photos of Site Visit in Elmshorn                                      | 241         |
| 17  | Testing Results of Software Tool                                      | 247         |
| 18  | Results of SUDS Adaptation Scenarios                                  | 250         |

---

---

**Attachment: Discussion**

|    |  |     |
|----|--|-----|
| 19 | Discussion About Climate Change Factors (CCF) Calculations | 259 |
|----|--|-----|

**List of Figures**

| Figure | Title   | Page |
|--------|---|------|
| 2.1    | Number of wet days calculated in the UFOPLAN. [adopted from <a href="#">Jacob et al., 2008</a> ]  | 7    |
| 2.2    | Statistical results of rainfall intensities of the REMO control scenario data (Mean) and observed rain gauge data (HSE) for the time period (1979 – 2000) at the station R005 with the largest deviations. (adopted from <a href="#">Bischoff, 2007</a> ).  | 7    |
| 2.3    | Effects of bias correction methods on the projected changes of daily precipitation in Romania. (adopted from <a href="#">CLAVIER [2], 2009</a> )  | 8    |
| 2.4    | Projected average change of river discharge with a return period of once in 100years of the IPCC scenarios B2 and A2 (2071 – 2100) compared to the control period (1961 – 1990). The results are the mean changes of four different model combinations (ensembles). (adopted from <a href="#">Feyen &amp; Dankers, 2009</a> ) | 11   |
| 2.5    | Number of model and scenario results (of a total of eight combinations) showing a decrease (a) or increase (b) of 5% in the 100year river discharge for the period 2071 to 2100 compared to the control period (1961 – 1990). (adopted from <a href="#">Feyen &amp; Dankers, 2009</a> )                                       | 11   |
| 3.1    | Methodological Scheme.  | 19   |
| 3.2    | Conceptual Structure of a Global Circulation Model and Downscaling Approach. (adopted from <a href="#">Viner, 2000</a> ; <a href="#">STARDEX, Final Report, n. d.</a> )   | 24   |
| 3.3    | Schematic illustration of the four qualitative storylines (A1, A2, B1 and B2) derived in the SRES of the IPCC. (adopted from <a href="#">IPCC, 2000</a> )   | 27   |
| 3.4    | Example of a climate model data series (precipitation) on a raster with 18 cells in NetCDF format, which are averaged over 4 grid cells and transferred to separate time series.  | 29   |
| 3.5    | Developed method for statistical evaluations.   | 33   |
| 3.6    | Concept of the layer theory for green roofs. (published earlier in <a href="#">Brüning &amp; Hellmers, 2009</a> )   | 43   |
| 3.7    | Concept of the layer theory for swales (adopted from <a href="#">Brüning &amp; Hellmers, 2009</a> )   | 45   |
| 3.8    | Concept of the layer theory for swale-filter-drain systems (adopted from <a href="#">Brüning &amp; Hellmers, 2009</a> )   | 45   |
| 3.9    | Complexity of Climate Scenarios (0-CCX), SUDS Adaptation Scenarios and Future Urban Development Scenarios   | 47   |
| 3.10   | Simplified illustration of the increasing range of uncertainties in the model chain. (adopted from <a href="#">Viner, 2002</a> )  | 53   |
| 3.11   | Simplified illustration of the uncertainties assumed for two elements of the uncertainty chain.   | 53   |

---

---

|             |  |            |
|-------------|--|------------|
| <b>4.1</b>  | Representation of SUDS in the data model (published earlier in <a href="#">Pasche et al., 2009</a> ; <a href="#">Brüning et al., 2009</a> ; <a href="#">Brüning &amp; Hellmers, 2009</a> )                             | <b>55</b>  |
| <b>4.2</b>  | Creation of hydrotopes with the attributes of SUDS in the data model (published earlier in <a href="#">Pasche et al., 2009</a> ; <a href="#">Brüning et al., 2009</a> ; <a href="#">Brüning &amp; Hellmers, 2009</a> ) | <b>56</b>  |
| <b>4.3</b>  | Outline of the main sub-routines in the Model Kalypso Hydrology and the embedded new sub-routines for simulating SUDS elements.  | <b>57</b>  |
| <b>4.4</b>  | Outline of the SUDS Sub-Routines.  | <b>58</b>  |
| <b>4.5</b>  | Relation between water level (hw) and soil water content (sw_sat) in the software tool.  | <b>61</b>  |
| <b>5.1</b>  | Map of the Krückau catchment area with the main urban areas, indicated sealing rates and rainfall gauging stations.  | <b>72</b>  |
| <b>5.2</b>  | Rainfall gauging stations (blue) and REMO data raster on a regular grid (red) of the datastream D3 covering the catchment area of the river Krückau. [downloaded REMO data raster: green].                             | <b>76</b>  |
| <b>5.3</b>  | Probability distribution curves of hourly extreme rainfall events [mm/h] in the summer periods.  | <b>80</b>  |
| <b>5.4</b>  | Differences between the probability distribution curves of REMO climate model and observed hourly data series.   | <b>81</b>  |
| <b>5.5</b>  | Number of days which are defined as wet days (>25mm/day) in the IPCC scenarios (B1, A1B, A2) compared to the computed control scenario (C20).  | <b>84</b>  |
| <b>5.6</b>  | Probability distribution curves of summer rainfall intensities in [mm/h] of future climate scenarios A1B, B1 and A2 compared to the control scenario C20.  | <b>86</b>  |
| <b>5.7</b>  | Nodes and sub-catchments of interest for the flood probability analysis.   | <b>89</b>  |
| <b>5.8</b>  | Results of the flood hydrographs at the node Langelohe with 15minute and hourly simulation timesteps.  | <b>90</b>  |
| <b>5.9</b>  | Comparison of the Log-Normal Type III and the Log-Pearson Type III Distribution Curves of summer flood peaks.  | <b>94</b>  |
| <b>5.10</b> | Illustration of post-processed future summer rainfall intensities and the shift in return periods T [a].   | <b>97</b>  |
| <b>5.11</b> | Illustration of a shift in return periods of post-processed flood peak probabilities by climate change impacts.  | <b>98</b>  |
| <b>5.12</b> | Testing results of the climate change factor (CCF) calculations for the node Kölln (Eckhorner Au).   | <b>99</b>  |
| <b>5.13</b> | Design Flood Event selected for Post-Impact Studies.   | <b>100</b> |
| <b>5.14</b> | Combination of SUDSs on a residential estate. (adopted from <a href="#">UMBW, n.d.</a> )   | <b>106</b> |
| <b>5.15</b> | Water storage and flow processes in the green roof elements with the design rainfall event (HP <sub>5,C</sub> ) [sub-catchment: ELMSH_E13_04].   | <b>111</b> |
| <b>5.16</b> | Water storage and infiltration processes in the swale element of the sub-catchment ELMSH_E13_04 with the design rainfall event (HP <sub>5,C</sub> ).   | <b>114</b> |
| <b>5.17</b> | Water storage and infiltration processes in the swale-filter-drain system of the sub-catchment KAKI_3 with the design rainfall event (HP <sub>5,C</sub> ).   | <b>116</b> |

---

---

|             |   |            |
|-------------|---|------------|
| <b>5.18</b> | Flood peak probability curves of the climate change and SUDS Adaptation Scenarios at the node: Langelohé in Elmshorn.   | <b>120</b> |
| <b>5.19</b> | Flood peaks (HQ <sub>100</sub> ) in hydrographs of SUDS adaptation and climate scenarios [node Langelohé in Elmshorn].  | <b>121</b> |
| <b>5.20</b> | Flood peak probability curves of the climate change and SUDS adaptation scenarios at the End Node of the Krückau Catchment.   | <b>121</b> |
| <b>5.21</b> | Reduction of the flood peaks by projected (climate change) SUDS adaptation scenarios related to the reference Scenario 0 at the End Node of the Krückau catchment.  | <b>122</b> |
| <b>5.22</b> | Reduction of the flood peaks referred to the projected (climate change) Natural State Scenario at the End Node of the Krückau catchment.  | <b>123</b> |
| <b>5.23</b> | Flood peak probability curves of the climate change and SUDS adaptation scenarios of the Sub-catchment ELMS_E06_02.   | <b>124</b> |
| <b>5.24</b> | Reduction of the flood peaks by projected (climate change) SUDS adaptation scenarios related to the reference Scenario 0 of the Sub-catchment ELMS_E06_02.  | <b>125</b> |
| <b>5.25</b> | Reduction of the flood peaks referred to the projected (climate change) Natural State Scenario of the Sub-catchment ELMS_E06_02.  | <b>125</b> |
| <b>6.1</b>  | Comparison of the statistical evaluations of the PÜK and the computed Scenario 0 in this thesis   | <b>134</b> |
| <b>6.2</b>  | Comparison of the approaches to calculate climate change factors (CCFs)   | <b>137</b> |
| <b>6.3</b>  | Comparison of flood peak probabilities simulated with three hydrological models using the climate data series of the CGCM2. (past [1971-2000] = solid bars; future [2071-2100] = striped bars) [adopted from <a href="#">Ludwig et al., 2009</a> ]. | <b>141</b> |
| <b>7.1</b>  | Illustration of the work flow to quantify climate change impacts on the flood probability in SUCAs and simulating adaptation measure scenarios (SUDS-Scenarios); with notes for optimisation and outlook.   | <b>143</b> |

### **List of Tables**

| <b>Table</b> | <b>Title</b>  | <b>Page</b> |
|--------------|---|-------------|
| <b>2.1</b>   | Rainfall related core extreme indices in the UFOPLAN. (adopted from <a href="#">Jacob et al., 2008</a> )  | <b>6</b>    |
| <b>2.2</b>   | SUDS elements defined in the project CRUE ERA-Net. (adopted from <a href="#">Pasche et al., 2008</a> )  | <b>15</b>   |
| <b>2.3</b>   | Research about SUDS modelling tools implemented in current software applications. ( <a href="#">Hellmers, 2009</a> )                                | <b>16</b>   |
| <b>3.1</b>   | Correction factors of precipitation data series. ( <a href="#">ATV-A 121, 1985</a> )  | <b>34</b>   |
| <b>3.2</b>   | Standard drained roof area per outlet pipe in Germany.  | <b>50</b>   |
| <b>4.1</b>   | Scheme of the Hydrotope-ASCII file.   | <b>66</b>   |
| <b>5.1</b>   | REMO grid cell coordinates (Datastream D3) transferred to Gauß-Krüger-Coordinates. (E: Easting [km]; N:Northing [km], left bottom corner of cells). | <b>75</b>   |

---

---

|             |   |            |
|-------------|---|------------|
| <b>5.2</b>  | Results of the comparison between observed and REMO control scenario data series.   | <b>77</b>  |
| <b>5.3</b>  | Results of the Grubbs Test with the observed and REMO control scenario data series of extreme rainfall events.  | <b>79</b>  |
| <b>5.4</b>  | Changes per hydrological season of temperature [°C], precipitation [%] as well as evaporation [%].  | <b>82</b>  |
| <b>5.5</b>  | Summary of the number of days meeting the defined threshold categories.   | <b>83</b>  |
| <b>5.6</b>  | Results of the Grubbs Tests of the future scenario studies of extreme rainfall events.  | <b>85</b>  |
| <b>5.7</b>  | Average change in extreme rainfall [mm/h] derived by future climate scenarios referred to the REMO C20 control scenario.  | <b>86</b>  |
| <b>5.8</b>  | Nodes and sub-catchments of interest for the flood probability scenario studies.  | <b>88</b>  |
| <b>5.9</b>  | Identification of outliers in the flood peak data series with the Grubbs Test.  | <b>91</b>  |
| <b>5.10</b> | Average Difference between the REMO C20 and the Scenario 0 flood peak data series for the hydrological year periods.  | <b>94</b>  |
| <b>5.11</b> | Average changes in future climate scenarios referred to the REMO C20 control scenario.  | <b>95</b>  |
| <b>5.12</b> | CCFs for calculating rainfall events with a duration of one hour and specific return periods T (a) with respect to the Scenario 0-A1B results in the Krückau catchment.                         | <b>98</b>  |
| <b>5.13</b> | CCFs of design flood events for the Krückau catchment for specific return periods T [a] to compute the flood peaks with the Scenario 0-A1B results.   | <b>99</b>  |
| <b>5.14</b> | Applied matching coefficients for adjusting the observed rainfall intensity to the projected climate change rainfall intensity with a return period of once in five years.                      | <b>101</b> |
| <b>5.15</b> | Average matching coefficients for the simulation of design flood events.  | <b>101</b> |
| <b>5.16</b> | Summary of the suggested potential spatial distribution of SUDSs in the urban sub-catchments of Elmshorn, Barmstedt and Kaltenkirchen.  | <b>106</b> |
| <b>5.17</b> | Summary of the results of the SUDS design and simulation with the design rainfall event [HP <sub>5,C</sub> ].   | <b>109</b> |
| <b>5.18</b> | Water balance calculation results of green roofs [HP <sub>5,C</sub> ].  | <b>110</b> |
| <b>5.19</b> | Water balance calculation results of green roofs [HQ <sub>100,C</sub> ].  | <b>110</b> |
| <b>5.20</b> | Water balance calculation results of swales [HP <sub>5,C</sub> ].   | <b>112</b> |
| <b>5.21</b> | Water balance calculation results of swales [HQ <sub>100,C</sub> ].   | <b>113</b> |
| <b>5.22</b> | Water balance calculation results of swale-filter-drain systems [HP <sub>5,C</sub> ].   | <b>115</b> |
| <b>5.23</b> | Water balance calculation results of swale-filter-drain systems [HQ <sub>100,C</sub> ].   | <b>115</b> |
| <b>5.24</b> | Eight SUDS adaptation scenarios.  | <b>118</b> |
| <b>6.1</b>  | Relative change of temperature published in the UFOPLAN for the period: 2021-2050 and the scenarios A1B, A2 and B1 related to (1961 – 1990). (adopted from <a href="#">Jacob et al., 2008</a> ) | <b>129</b> |

---

---

|            |  |            |
|------------|--|------------|
| <b>6.2</b> | Relative change of temperature published in the UFOPLAN for the period: 2071-2100 and the scenarios A1B, A2 and B1 related to (1961 – 1990). (adopted from <a href="#">Jacob et al., 2008</a> ). | <b>129</b> |
| <b>6.3</b> | Changes per hydrological season in Temperature [°C] (2040 – 2070) calculated for the Krückau catchment related to the period 1971 – 2000.  | <b>130</b> |
| <b>6.4</b> | Change of precipitation published in the UFOPLAN for the period: 2021-2050 and the scenarios A1B, A2 and B1 related to (1961 – 1990). (adopted from <a href="#">Jacob et al., 2008</a> ).        | <b>131</b> |
| <b>6.5</b> | Change of precipitation published in the UFOPLAN for the period: 2071-2100 and the scenarios A1B, A2 and B1 related to (1961 – 1990). (adopted from <a href="#">Jacob et al., 2008</a> ).        | <b>131</b> |
| <b>6.6</b> | Relative changes per hydrological season in precipitation [%] (2040 – 2070) calculated for the Krückau catchment related to the period from 1971 to 2000.  | <b>131</b> |
| <b>6.7</b> | Relative changes per hydrological season in evaporation [%] (2040 – 2070) calculated for the Krückau catchment related to the period from 1971 to 2000.  | <b>132</b> |
| <b>6.8</b> | Total variance of precipitation in [%] derived by four sources of uncertainty (adopted from <a href="#">Déqué et al., 2007</a> ).  | <b>140</b> |

### **List of Abbreviations**

|                |  |
|----------------|--|
| AR4            | Fourth Assessment Report   |
| ASCII          | American Standard Code for Information Interchange   |
| BALTEX         | BALTic Sea EXperiment ( <a href="http://www.baltex-research.eu/">www.baltex-research.eu/</a> )   |
| BfG            | German Federal Institute of Hydrology  |
| BMBF           | German Federal Ministry of Education and Research  |
| BMVBS          | Federal Ministry of Transport, Building and Urban Affairs  |
| BWK            | Bund der Ingenieure für Wasserwirtschaft, Abfallwirtschaft und Kulturbau   |
| CCF            | Climate Change Factor  |
| CDO            | Climate Data Operators   |
| CERA           | Climate and Environmental Retrieval and Archive server   |
| CLAVIER        | Climate change and variability: impact on central and eastern Europe<br><a href="http://www.clavier-eu.org/">http://www.clavier-eu.org/</a>  |
| DWD            | German Weather Service   |
| EEA            | European Environmental Agency  |
| ELBE-DSS       | Elbe Decision Support System project   |
| ERA40          | Reanalyse Data series over 40 years  |
| ERA-Net CIRCLE | Climate Impact Research Coordination for a larger Europe;<br><a href="http://www.circle-era.net">www.circle-era.net</a>  |
| ERA-Net CRUE   | 1st ERA-Net CRUE Funding Initiative: 'Risk assessment and risk management: Effectiveness and efficiency of non-structural flood risk management measures' : <a href="http://www.crue-eranet.net">www.crue-eranet.net</a> |

---

---

|              |  |
|--------------|--|
| GCM          | Global Circulation Model   |
| GHG          | Green House Gas  |
| GKSS         | Gesellschaft für Kernenergieverwertung in Schiffbau und Schifffahrt mbH  |
| GLOWA ELBE   | Global Change in the Elbe region   |
| GLOWA-Danube | Global Change at River Danube  |
| GUI          | Graphical User Interface   |
| GVOBI        | Law and Ordinance Gazette of Schleswig-Holstein  |
| HERPEX       | Hydrologic Ensemble Prediction Experiment (source: <a href="http://hydis8.eng.uci.edu/hepex/">http://hydis8.eng.uci.edu/hepex/</a> )   |
| HLUG         | Hessian Agency for the Environment and Geology   |
| HSE          | Hamburg Public Sewage Company (Hamburger Stadtentwässerung)  |
| INKLIM       | Integrated Climate Protection Programme; <a href="http://klimawandel.hlug.de/forschungsprojekte/inklim-2012-baustein-ii-plus.html">http://klimawandel.hlug.de/forschungsprojekte/inklim-2012-baustein-ii-plus.html</a> |
| IPCC         | Intergovernmental Panel on Climate Change  |
| DKRZ         | German Climate Computing Centre (Deutsches Klimakonsortium)  |
| KLIMZUG      | KLImawandel ZUKunfts-fähig Gestalten   |
| KLIWA        | Climate Change and Consequences for Water Management <a href="http://www.kliwa.de/">www.kliwa.de/</a>  |
| KLIWAS       | Consequences of climate change for navigable waterways and options for the economy and inland navigation <a href="http://www.kliwas.de">www.kliwas.de</a>  |
| LANU         | Ministry of agriculture, environment and rural areas of the Federal State Schleswig-Holstein   |
| LSBG         | Agency for Roads, Bridges and Waters   |
| LLUR         | The State Agency for Nature and Environment of the Federal State Schleswig-Holstein  |
| MICE         | Modelling the Impact of Climate Extremes ( <a href="http://www.cru.uea.ac.uk/projects/mice">www.cru.uea.ac.uk/projects/mice</a> )  |
| MLUR         | Ministry of Environment, Nature and Forests of the Federal State Schleswig-Holstein  |
| MPI-M        | Max-Planck Institute of Meteorology  |
| NetCDF       | Network Common Data Form   |
| PÜK          | Planungsgemeinschaft Überschwemmungsgebiete an der Krückau   |
| PRUDENCE     | Prediction of regional scenarios and uncertainties for defining European climate change risks and effects: <a href="http://prudence.dmi.dk/">http://prudence.dmi.dk/</a>   |
| RCM          | Regional Climate Model   |
| SGA          | Service Group Adaptation   |
| SRES         | Special Report on Emissions Scenarios  |
| STARDEX      | Statistical and regional dynamical downscaling of extremes for European regions <a href="http://www.cru.uea.ac.uk/projects/stardex">www.cru.uea.ac.uk/projects/stardex</a> )   |
| SUDS         | Sustainable Drainage Systems (In Germany known as  |

---

---

|             |  |
|-------------|--|
|             | “Regenwasserbewirtschaftungsmaßnahmen”)  |
| TAR         | Third Assessment Report  |
| TUHH        | Technical University of Hamburg Harburg  |
| UFOPLAN     | Umweltforschungsplan (Environmental Research Plan)   |
| UBA         | Federal Environmental Agency   |
| UCAR        | University Corporation for Atmospheric Research  |
| UMBW        | Agency for Environment and Transport Baden-Württemberg                                     |
| WCED        | World Commission on Environment and Development  |
| WDCC        | World Data Centres for Climate   |
| WHG         | Act on Managing Water Resources  |
| ZMAW        | Centre for marine and atmospheric sciences <a href="http://www.zmaw.de">www.zmaw.de</a>    |
| *_1 and *_2 | Abbreviation of the first realisation (*_1) and second realisation (*_2) of climate models |

### **List of Variables**

|                          |   |
|--------------------------|---|
| $A_u$                    | Drained Sealed Areas [km <sup>2</sup> ]   |
| $A_{Hydrotope}$          | Area of Hydrotope [km <sup>2</sup> ]  |
| $A_{land\ use\ area}$    | Area of a land use unit [km <sup>2</sup> ]  |
| $A_s$                    | Area of the SUDS device [km <sup>2</sup> ]  |
| $A_{SUDS,total}$         | Total area of the SUDSs in a sub-catchment [km <sup>2</sup> ]   |
| $\alpha$                 | Significance level in statistical evaluations (e.g. 0.001 or 0.005) [-]   |
| $\alpha_t$               | Critical value in Grubbs Test [-]   |
| $D$                      | Duration [h]  |
| $d_{pipe}$               | Diameter of a pipe [mm]   |
| $Et_a$                   | Actual evapotranspiration [mm]  |
| $Et_p$                   | Potential evaporation [mm]  |
| $f_{T,C}$                | Climate change factor for a specific return period (T) of the extreme event [-]   |
| $g$                      | Acceleration due to gravity [9.81m/s <sup>2</sup> ]   |
| $H_T$                    | Extreme event with a specific return period (T)   |
| $H_{T,C}$                | Extreme event per return period (T) under climate change conditions (C)   |
| $\Delta H_{T,C,[\%]}$    | Percentage change of the extreme event under climate change conditions (C) with a specific return period (T)            |
| $\Delta H_{T,C,abs}$     | Absolute change of the extreme event under climate change conditions (C) with a specific return period (T)              |
| $H_{T,IPCC-sceanrio}$    | Extreme event with a return period (T) computed in an IPCC climate change scenario (C)                                  |
| $H_{T,control-sceanrio}$ | Extreme event with a return period (T) computed in the control scenario of the past                                     |
| $h_{ex}$                 | Water level above the overflow pipe on a green roof [mm]  |
| $h_{ov}$                 | Height of the overflow pipe on a green roof [mm]  |
| $HP_{D,T}$               | Design rainfall intensity with a specific duration (D) and return period (T) of observed data series [mm/D]             |
| $HP_{D,T,C}$             | Design rainfall intensity with a specific duration (D) and return period (T) under climate change conditions (C) [mm/D] |

---

---

|               |  |
|---------------|--|
| $HQ_T$        | Design flood peak with a defined return period (T) calculated with observed rainfall data series [m <sup>3</sup> /s] |
| $HQ_{T,C}$    | Design flood peak with a defined return period (T) under climate change conditions (C) [m <sup>3</sup> /s]           |
| $Inf$         | Potential inflow into the soil layer of SUDS element [l/m <sup>2</sup> ]   |
| $\Sigma P$    | Sum of precipitation per day [mm/day]  |
| $G$           | Grubbs Test Value [-]  |
| $\Delta G$    | Difference between Grubbs Test value (G) and critical value $\alpha_c$   |
| $h_w$         | Water level in a layer of a SUDS element [mm]  |
| $k_f$         | Permeability coefficient [m/s]   |
| $\mu$         | Coefficient in the Poleni equation [-]   |
| $\lambda$     | Flow resistance according to the Colebrook-White approach [-]  |
| $k_s$         | Equivalent sand roughness [mm]   |
| $M$           | Number of years in a time period [a]   |
| $MIN$         | Minimum of results [-]   |
| $N$           | Number of values in a data series [-]  |
| $n$           | Number of statistical evaluations [-]  |
| $perk$        | Percolation of water in the soil layers of a SUDS element [l/m <sup>2</sup> ]  |
| $Q_{outflow}$ | Flow from a SUDS element (drainage or overflow) [m <sup>3</sup> /s]  |
| $S$           | Standard deviation [-]   |
| $\Delta sw$   | Change of the soil water content in layers of SUDS elements [l/m <sup>2</sup> ]                                      |
| $T$           | Return Period in years [a]   |
| $\Delta t$    | Simulation time step [h]   |
| $Y_i$         | Value i of the data series [-]   |
| $Y_{i,max}$   | Exceptional or extreme value [-]   |
| $\bar{Y}$     | Sample mean [-]  |

*Explanations of the used variables for the implementation of the software tool and FORTRAN language definitions are summarized in attachment 5.1.*

# 1 Introduction

Climate change is an emergent, important and highly political issue nowadays, due to the increased changing rate of the current ice age to a warmer climate state (IPCC AR4, 2007b). It is stated in the Fourth Assessment Report (AR4) of the Intergovernmental Panel on Climate Change (IPCC), that in the last decades, earth temperature increased about 0.6°C (in Germany about 1°C), whereas in the last 1000 years (before 1990) it increased only by a maximum of 1°C (BMVBS, 2007). This fast change in the temperature rate is projected to further increase in climate change scenarios till 2100, reaching temperatures between 2°C and 6°C above values measured in 1990 (BMVBS, 2007). Climate change is an ongoing process of the development of the earth, so it is not a “new” phenomenon, but it is stated that the current accelerated change of the temperature can not be explained solely by natural variability. Human activities have an impact on the earth atmosphere, especially by increasing green house gas (GHG) emissions (IPCC AR4, 2007b). Therefore, mitigation strategies have to be developed to reduce exceedingly the emissions of GHG as stated in the Kyoto Protocol (1997).

With global warming, impacts are derived which could have more or less significant influences on nature and on human life, for example by the rise of the sea level and increasing frequency as well as intensity of extreme weather conditions, which could lead to heat records, droughts or extreme rainfalls (IPCC AR4, 2007c). Such impacts of more frequent and intensive weather events in the past decades can be assumed to have already caused more losses and damages in some regions in combination with simultaneous increased wealth and exposure (IPCC AR4, 2007d; Pfister et al., 2005).

Future scenarios have been developed with consideration of changes in GHG emissions and changes in the worldwide development of population as well as energy consumption. Nowadays, the so called Special Report on Emissions Scenarios (SRES), published by the IPCC in 2000 (IPCC, 2000), are primarily used as a basis for climate change studies. The difference between the scenarios is mainly based on the economic and demographic development (BMVBS, 2007). Whereas, to quantify the climate response on the scenarios, numerical climate models are used, which are based on physical, chemical and biological principles combined with empirical and statistical methods.

SRES enable the analysis of a range of climate changes and the impacts on the environment (e.g. habitats, diversity of species, forests), the human live (e.g. fresh water resources) and economy (e.g. industry, settlements and society). Such climate impact studies are done for example in the AR4 by the IPCC in the Working Group II about “Impacts, Adaptation and Vulnerability” with climate components like the

long-term average temperature or precipitation change in Africa, Asia, Europe, Australia, America and the Polar Regions (IPCC AR4, 2007e).

Since the demand for climate change scenario studies has been increased and more powerful computers are available for climate change researches, international and national climate research projects were subsequently drawn up around the globe. Among others, in Germany a network project started in the beginning of 2009 which has a focus on regional climate change studies. The network project is known as KLIMZUG: ‘KLIMawandel ZUkunftsfähig Gestalten’<sup>1</sup>. It consists of seven regional project areas, one of these being the Metropolitan Region of Hamburg (KLIMZUG-Nord)<sup>2</sup>. The aim is, to develop a master plan till 2014 with techniques and methods to mitigate the impacts by climate change and to ensure the adaptation of the society and ecology to increased risks derived by climate change.

The prevalent open task at the beginning of this project is the development of strategies, to quantify the climate change impacts on a local scale for the Metropolitan Region of Hamburg. In contrast to projects covering wide spread areas, local scale studies require detailed data analyses with an appropriate small spatial and temporal resolution.

Especially demanding are studies of climate change impacts on extreme events, which have a low probability of occurrence, but could derive a vast number of serious consequences. In this context, extreme rainfall events in urban areas, which are the main drivers of pluvial flooding, require special consideration and strategies. Significant impacts in urban areas are derived, where surfaces are strongly modified by sealing with low retention capacities for surface runoff and the exposure to flooding is high (WMO/GWP, 2008). In small urban catchments (SUCAs) pluvial flooding could be derived in combination with fluvial flooding from small rivers, streams and the drainage systems, which appear to be overloaded by surface runoff after extreme rainfall events. SUCAs are characterised by catchments in complete urban areas or with urbanised areas downstream of the river catchments, but natural or rural areas in the upstream part. For example in Hamburg, a thunderstorm in July 2002 caused serious flood problems with a total damage of more than 15million Euro (Pasche et al., 2008). This type of flooding is of particular importance in urban flood risk management which is the product of the probability of flooding and the derived consequences. Both issues vary greatly according to future urban developments as well as climate change impacts (Pasche et al., 2008). Additionally it is stated that a large range of uncertainty has to be taken into account in the calculations of extreme rainfall events with climate models and it varies significantly between study

---

<sup>1</sup> KLIMZUG: [www.klimzug.de](http://www.klimzug.de)

<sup>2</sup> KLIMZUG-Nord: [www.klimzug-nord.de](http://www.klimzug-nord.de)

locations (Fowler & Ekström, 2009). This calls for a comprehensive and detailed study about the *hydrological impacts of climate change on flood probability in small urban catchments*, which takes into account a variety of future climate scenarios.

Additionally, the development and assessment of the effectiveness of adaptable *possibilities of flood risk mitigation* to reduce or compensate the increase of flood probability derived by climate change impacts in SUCAs is required. Whereas, traditional measures, like enlarging storm water sewage pipes, are not appropriate to cope with the uncertainties in climate change and flood probability studies (Pasche et al., 2008).

The main open questions and objectives are defined after a research about current studies and projects, which discuss the question: ‘*How do Flood Impact Studies Deal with Climate Change Scenarios?*’. In this context, the demand for adaptation strategies in current research studies as possibilities for future flood risk mitigation are outlined (*chapter 2*). With the defined open questions and objectives, a detailed methodology has been developed to quantify climate change impacts on flood probabilities and assessing the effectiveness of adaptation measures for increased flood probabilities in SUCAs (*chapter 3*). For the simulation of the defined flood probability reduction measures, a software tool has been worked out in the scope of this thesis. The implementation procedure of this software tool is pointed out in *chapter 4*. The actual need for research of this topic made it possible that the derived methodology in this thesis could be applied right away for an area in the KLIMZUG-Nord project (*chapter 5*) and it aims for being applied in further studies in the network-project. The results of the scenario studies are discussed in comparative studies in *chapter 6*, where as well uncertainties have to be taken into account with the application of numerical models, the assumptions for scenarios and the computation of impacts.

## 2 How do Flood Impact Studies deal with Climate Change Scenarios?

Flooding occurs, when land is exceptionally covered by water, whereas larger consequences are derived by flood events with lower probabilities of occurrence: e.g. which occur only once in 100 years. In this context the product of the probability of occurrence of flooding and the derived consequences is defined as flood risk, which has to be managed as well with regard on climate change impacts as stated in the EU Floods Directive ([European Parliament, 2007](#)). The EU Member States are required by this directive to assess all waters (water courses and coast lines) which are in risk of flooding and to map the flood extents. The risk on human and assets have to be assessed and adequate measures shall be implemented to reduce the probability of flooding as well as the consequences.

Flooding is caused by a variety of drivers, e.g. extreme rainfall events, increased sea level rise as well as storm surges and modification of the land surface. These examples outline already the complexity to analyse flood impacts, which comprises as well socioeconomic factors like future urban developments in flood prone areas with a higher exposure ([Feyen & Dankers, 2009](#)). Considering additionally the impacts derived in future climate scenarios, increases the complexity further on, whereas especially extreme rainfall events are heavily affected by climate change impacts.

In this context, a focus has been set on flooding which is mainly driven by extreme rainfall events. This is most significant in small urban catchments (SUCAs), where short term extreme rainfall events appear to cause flooding by small rivers, streams and the surface water drainage systems ([Pasche et al., 2008](#)). This type of flooding is highly complex and requires small scale analysis of extreme rainfall events, which is a challenging task in current climate change research studies outlined in the following paragraphs, where studies about climate change impacts on extreme rainfall and flood probability are analysed.

The demand for studies about climate change adaptation strategies, and in this context about *possibilities of flood risk mitigation*, is increasing. It has to be pointed out, that the assumption of impacts on the probability of flooding in climate scenarios is very complex and a range of uncertainties have to be taken into account. Therefore, flexible and no-regret strategies have to be preferred ([The Federal Government, 2008](#)), which are outlined with a focus on flood probability reduction measures in SUCAs.

## **2.1 Climate Change Impact Studies about Extreme Events and Flooding**

In research projects it has been pointed out that calculated climate change impacts from one region can not be transferred one to one to other regions and that several scenarios as well as seasonal differentiations should be simulated to gain a range of climate change impact results (e.g. UFOPLAN<sup>1</sup>, BALTEX<sup>2</sup>, CLAVIER<sup>3</sup>, ENSEMBLES<sup>4</sup>, PRUDENCE<sup>5</sup>). In the UFOPLAN for example regional studies of changes in seasonal precipitation and extreme events have been done (Jacob et al., 2008). For the scenario studies, the regional climate model REMO developed at the Max-Planck-Institute of Meteorology (MPI-M) in Hamburg has been applied which provide data series with a spatial resolution of 10km x 10km. Currently these data series display the highest spatial resolution for German research studies provided by a dynamical regional climate model (RCM). According to the findings in the project CLAVIER and by Iorio et al. (2004) regional impacts by extreme events become more representative with higher spatial resolution.

In the UFOPLAN average precipitation changes are published for the federal states of Germany, which have been simulated with the model REMO (Jacob et al., 2008). The range between the scenarios is significant. For Hamburg a decrease of about 7% of the yearly average precipitation from one scenario and from another scenario an increase of 8 % is projected for the climate period from 2021 to 2050 related to 1961 to 1990. Further on, it is displayed how climate change impacts differ between regions, which are close to each other like Hamburg and Schleswig-Holstein, which emphasizes the need for regional small scale studies.

The yearly average precipitation changes are less significant than analyzing the average changes of the seasonal periods. For example, for Schleswig-Holstein an increase of precipitation of 15% in winter periods, whereas for summer periods a decrease of precipitation of about –11% is calculated for the climate period from 2021 to 2050 related to 1961 to 1990. These significant differences are flattened by computing only the yearly average precipitation. This emphasizes, that a differentiation in seasons has to be studied.

Unlike mean seasonal changes of precipitation, extreme events have a low probability of occurrence. Like in other scientific analysis, it is difficult to interpret and get well-founded conclusions from a small size of data sets. One method is to

---

<sup>1</sup> UFOPLAN = Umweltforschungsplan; funded by the Federal Environmental Agency (UBA)

<sup>2</sup> BALTEX = BALTic Sea EXperiment : [www.baltex-research.eu/](http://www.baltex-research.eu/) and BACC (2008)

<sup>3</sup> CLAVIER = CLimate ChAnge and Variability: Impact on Central and Eastern Europe  
<http://www.clavier-eu.org/>

<sup>4</sup> ENSEMBLES = Project funded by the European Commission and co-ordinated by the Hadley Centre for Climate Prediction and Research at the UK Met Office; <http://ensembles-eu.metoffice.com/>

<sup>5</sup> PRUDENCE = Prediction of Regional scenarios and Uncertainties for Defining European Climate change risks and Effects: <http://prudence.dmi.dk/>

---

define ‘core extreme indices’ of extremes. An advance for this was made in the European Commission funded projects: STARDEX<sup>1</sup> and MICE<sup>2</sup>, which focussed on changes in temperature, precipitation and wind extremes from climate models to assess the impacts on three economic sectors: forestry, tourism and insurance & civil protection (Hanson et al., 2007). In this context, an increase in the magnitude of short and long-duration extreme precipitation has been projected for northern Europe, whereas the change of extreme precipitation in the summer period is less clear due to larger differences between the projections with different models (Feyen & Dankers, 2009). In the UFOPLAN ‘core extreme indices’ have been used to analyze the impacts of climate change on extreme events in Germany with results of the climate model (RCM) REMO (Table 2. 1).

**Table 2. 1 Rainfall core extreme indices in the UFOPLAN. (adopted from Jacob et al., 2008)**

| <b>Rainfall related core extreme indices in the UFOPLAN</b>                              | <b>User-friendly name</b>        |
|--|----------------------------------|
| Number of days with more than 25mm rainfall per day                                      | Number of wet days               |
| Yearly maximum of daily precipitation sums in mm per year                                | Greatest 1-day rainfall (amount) |
| Yearly maximum of 5-day precipitation sums in mm per year                                | Greatest 5-day rainfall (amount) |
| Maximum number of consecutive dry days per year with precipitation less than < 0.1mm/day | Length of dry period             |

Such extreme core indices are chosen from a climatic meteorological perspective rather than in terms of impacts like flooding, to point out the magnitude (e.g. greatest 1-day rainfall), the frequency (e.g. number of wet days) and the persistence (e.g. length of dry period) (STARDEX, Final Report, n. d.).

For Germany the changes of the number of wet days are depicted in Fig. 2. 1 for the IPCC scenarios A1B, A2 and B1. However, urban flooding is strongly dependent on changes of short-term intense rainfall events with durations of minutes up to some hours. A study about these changes has been done by Bischoff (2007), by using control scenario data (1970 – 2000) of the REMO model for the region of Hamburg to work out statistics according to the ATV-A 121 (1985).

The return periods of extreme events generated by the control scenario data of the REMO model from 1970 to 2000 have been compared with the statistical results of observed rainfall data from gauging stations provided by the Hamburg Public Sewage Company (HSE). Projected future scenarios have not been analyzed by Bischoff (2007). The return periods (T) of rainfall events with intensities in [mm/D] and durations of D=60minutes, D=360minutes and D=1440minutes have been analysed for seven rain gauge stations in Hamburg and corresponding geographical raster data computed with the model REMO.

---

<sup>1</sup> STARDEX = STAtistical and Regional dynamical Downscaling of EXtremes for European regions ([www.cru.uea.ac.uk/projects/stardex](http://www.cru.uea.ac.uk/projects/stardex))

<sup>2</sup> MICE = Modelling the Impact of Climate Extremes ([www.cru.uea.ac.uk/projects/mice](http://www.cru.uea.ac.uk/projects/mice))

One of the statistical evaluation results is illustrated in Fig. 2. 2 (Bischoff, 2007). For all durations, the linear of the statistical results of the control scenario (REMO) show larger gradients than the observed rain gauge data. The highest average deviation between 43% and 63% is displayed for the statistical results of rainfall events with the duration of 60minutes (Bischoff, 2007). This deviation is mainly derived by the use of observed rain gauge data which are influenced by measuring errors, and REMO data series which are not bias corrected according to a detailed validation with e.g. the Reanalyse Data (known as ERA40) (Bischoff, 2007). The Reanalyse Data Series of 40 years

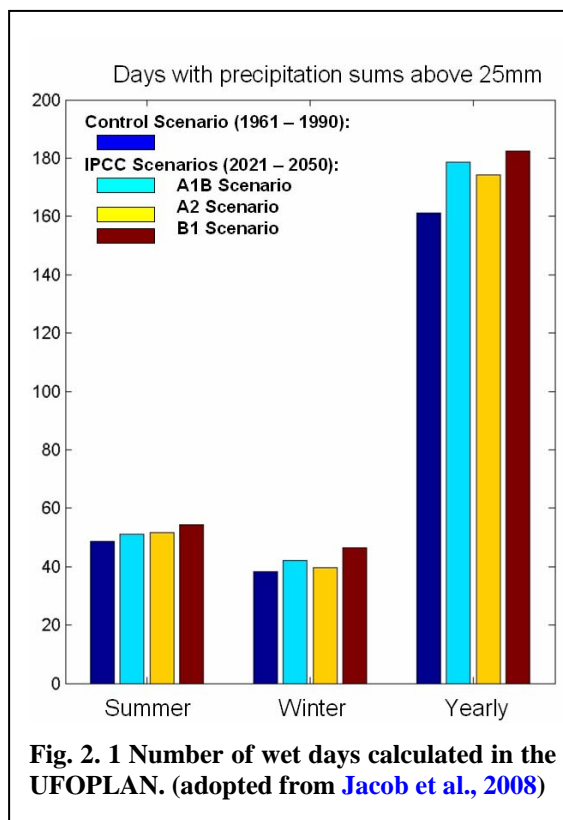


Fig. 2. 1 Number of wet days calculated in the UFOPLAN. (adopted from Jacob et al., 2008)

(ERA40) of the European Centre for Medium-Range Weather Forecasting are derived with overall conventional observations and satellite data streams from 1957 till 2001 (Hagemann et al., 2005). These ERA 40 data series can be applied for bias correction methods of climate model data results e.g. done in the projects UFOPLAN and CLAVIER.

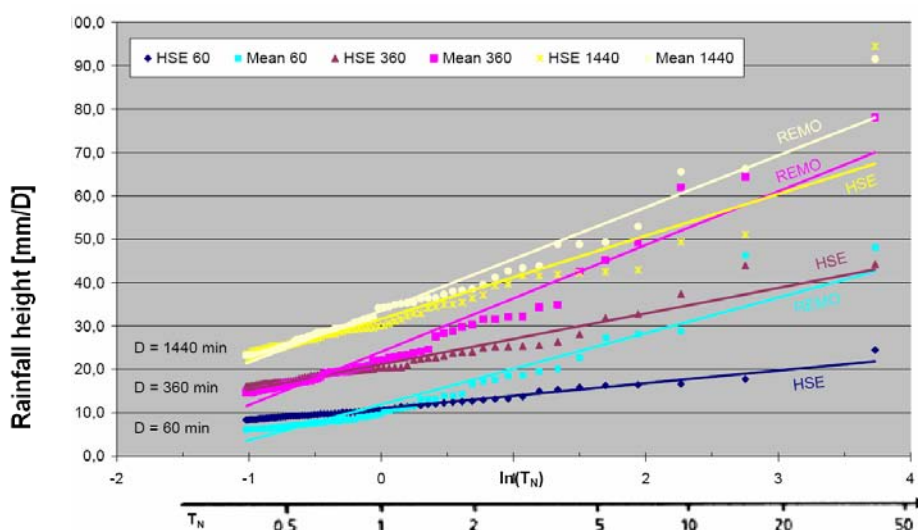
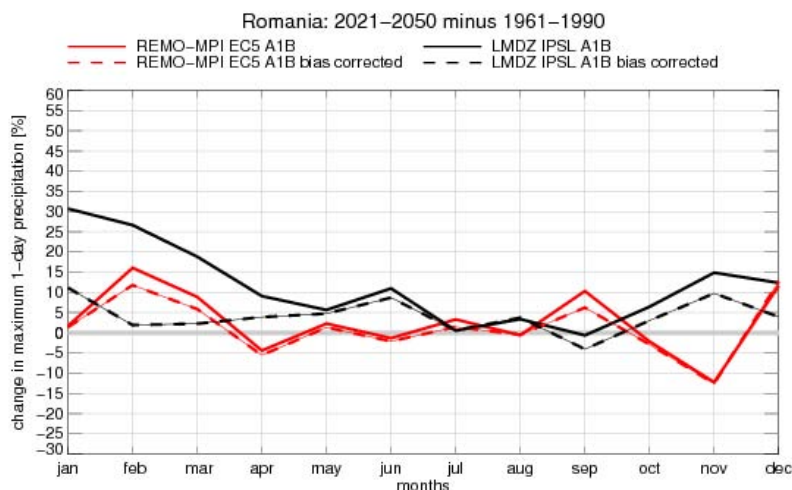


Fig. 2. 2 Statistical results of rainfall intensities of the REMO control scenario data (Mean) and observed rain gauge data (HSE) for the time period (1979 – 2000) at the station R005 with the largest deviations. (adopted from Bischoff, 2007)

In the EU funded project CLAVIER which ran from 2006 till August 2009, the influence of correction methods based on ERA 40 data series have been analysed. The focus of this project has been the assessment of detailed local and regional climate change impacts, which includes along other the changes of extreme events and the impacts on flooding. The regional climate models REMO and LMDZ<sup>1</sup> have been used and the climate model results have been corrected with an empirical statistical bias correction method: known as Quantile Mapping (CLAVIER [1], 2009). In this method the modelled cumulative frequency distributions of the data series are compared with the observed cumulative frequency distributions (ERA40 series). In this regard, the mean and variability of the simulated temperature and precipitation amounts were corrected (CLAVIER [1], 2009).

In the project CLAVIER and by Van Pelt et al. (2009), it has been analysed how bias-correction methods affects the projected changes of extreme events. In the CLAVIER project, data series of extreme core indices, like the maximum 1-day precipitation amounts, have been produced with the regional climate models REMO and LMDZ (CLAVIER [2], 2009). In Fig. 2. 3 are the effects of the bias correction shown of the climate model data series. The bias correction has the most influence on the precipitation extremes in the winter month of the LMDZ climate model results. The projected data series results with the REMO model remain more or less unchanged by the Quantile Mapping bias correction.



**Fig. 2. 3** Effects of bias correction methods on the projected changes of daily precipitation in Romania. (adopted from CLAVIER [2], 2009)

In Van Pelt et al. (2009) two correction methods have been compared for simulating river discharges with the hydrological model HBV<sup>2</sup>. The results of this study show that the use of a bias correction method can have a large influence on the simulated

<sup>1</sup> LMDZ = regional climate model developed at the Laboratoire de Météorologie Dynamique

<http://www.lmd.jussieu.fr/>

<sup>2</sup> HBV = Hydrologiska Byråns Vattenbalansavdelning model;

<http://www.smhi.se/sgn0106/ef/hydrologi/hbv.htm>

discharge. But it is stated as well, that bias correction methods generates an additional uncertainty, next to other uncertainties that arise from e.g. model parameterization and downscaling techniques (Van Pelt et al., 2009). The application of bias correction methods is debatable in research studies (e.g. CLAVIER; Van Pelt et al., 2009; BALTEX). A detailed, critical and comprehensive analyse of different correction methods has been done by Fowler et al. (2007), but can not be outlined in the context and focus of this paper.

Climate Change research studies about the European river catchments have been worked out, which published different changes in frequency and magnitude of floods (e.g. Feyen & Dankers (2009); CLAVIER; BALTEX; KLIWA<sup>1</sup>; KLIWAS<sup>2</sup>; INKLIM 2012 II plus<sup>3</sup>). In the project KLIWA the changes in flood discharge, mean discharge and extreme precipitation were analysed for the period 1971 to 2000 and the future climate scenario period (2021 – 2050) in the Federal State Baden-Württemberg of Germany (KLIWA, 2006). The KLIWAS project started in June 2007 with the German Federal Institute of Hydrology (BfG) having the overall responsibility (BMVBS, 2007). In this project the flow regime in waterways has been investigated for climate change scenarios. A focus has been set here as well on the change in the frequency and intensity of extreme events, but more on low, instead of high discharge extremes (BMVBS, 2007). The data series of the global circulation model (GCM) ECHAM4<sup>4</sup>, the regional model REMO and the hydrological water balance model LARSIM<sup>5</sup> have been used (BMVBS, 2007). The project INKLIM 2012 II plus, focused on the analysis of the impacts by climate change on the flood peaks and discharge of rivers in the Hessian part of the river Rhine catchment (HLUG, 2005). In the project the highest increase in flood peak have been defined for the A1B scenario with 20% for the climate period 2051 - 2080 and it has been stated that the results of extreme floods simulations differ significantly among the IPCC-scenarios (Brahmer, 2008). Further studies comprise the projects funded by the German Federal Ministry of Education and Research (BMBF), e.g. GLOWA ELBE, ELBE-DSS, GLOWA-Danube<sup>6</sup> (BMVBS, 2007).

In impact studies of extreme rainfall and flood events, climate change factors (CCFs) have been computed or applied. These are used for the adjustment of current design

---

<sup>1</sup> KLIWA= Climate Change and Consequences for Water Management [www.kliwa.de](http://www.kliwa.de)

<sup>2</sup> KLIWAS = Consequences of climate change for navigable waterways and options for the economy and inland navigation [www.kliwas.de](http://www.kliwas.de)

<sup>3</sup> INKLIM = Integrated Climate Protection Programme;  
<http://klimawandel.hlug.de/forschungsprojekte/inklim-2012-baustein-ii-plus.html>

<sup>4</sup> ECHAM4 = global circulation model developed at the MPI-M (ECHAM5 see Attach 1.1)

<sup>5</sup> LARSIM = hydrological water balance model <http://larsim.sourceforge.net>

<sup>6</sup> GLOWA ELBE= Global Change in the Elbe region; ELBE-DSS = Elbe Decision Support System.; GLOWA-Danube = Global Change at River Danube

flood and rainfall events to projected future climate state design conditions. The approach of using CCFs has been done for example in the project INKLIM 2012 II plus (Brahmer, 2008), KLIWA (Katzenberger, 2004) and in a local project study in Hamburg by the Golder Associates (2009). In the KLIWA Project, CCFs have been worked out for the results of the pilot project area Neckar (ca. 14.000km<sup>2</sup>) with a focus on the year 2050 (Katzenberger, 2004). The Wandse project has been assigned by the Agency for Roads, Bridges and Waters of Hamburg (LSBG) in 2009 to analyse the change in flood probabilities projected with the IPCC scenario A1B computed by the regional climate model REMO. The approaches to compute the CCFs are based on different methods by taking into account the changed runoff rates in the catchment with a spatial distribution of the flood peak changes (Golder Associates, 2009) or without taking into account the specific spatial distribution of the catchment (Katzenberger, 2004).

The results of the different climate change research studies, especially with regard on flooding, vary significantly which can be assigned to the use of different climate scenarios, climate as well as hydrological models and to the specific characteristics of catchments (Feyen & Dankers, 2009). The statement of defining reliable scenarios for flooding is described by the IPCC with low confidence (Handmer et al., 1999). The amount of increase in flooding is very uncertain and is likely to vary significantly between catchments and climate change research projects (Handmer et al., 1999).

Dankers & Feyen (2009) evaluated changes in flood events and flood hazard in Europe using the results of climate model ensembles<sup>1</sup> and the hydrological model LISFLOOD<sup>2</sup>, which has been developed for flood forecasting on a European scale. The ensembles have been derived with the RCMs HIRHAM<sup>3</sup> and RCAO<sup>4</sup> within the scope of the project PRUDENCE<sup>5</sup>. Both RCMs have been forced with boundary conditions of two different global circulation models (GCM): HadAM3H<sup>6</sup> and ECHAM4. The ensemble results of the IPCC scenario A2 and B2 of the climate models have been used to drive the hydrological model LISFLOOD with a focus on the analyse of maximal discharges. The results for the German and Dutch river catchments (Rhine, Ijssel, Ems, Weser, Elbe and Warnow/Peene) are illustrated in Fig. 2. 4 for the IPCC scenarios B2 and A2.

---

<sup>1</sup> Ensembles are a set of different climate model set ups used to deal with uncertainties.

<sup>2</sup> LISFLOOD = Distributed Water Balance and Flood Simulation Model [http://natural-hazards.jrc.ec.europa.eu/activities\\_lisflood.html](http://natural-hazards.jrc.ec.europa.eu/activities_lisflood.html)

<sup>3</sup> HIRHAM = RCM developed by the Climate Research Division at the Danish Climate Centre (DMI) ([www.dmi.dk](http://www.dmi.dk)) and the MPI-M in Hamburg

<sup>4</sup> RCAO = RCM developed by the Rossby Centre of the Swedish Meteorological and Hydrological Institute (SMHI)

<sup>5</sup> PRUDENCE: Prediction of Regional scenarios and Uncertainties for Defining European Climate change risks and Effects ([www.prudence.dmi.dk](http://www.prudence.dmi.dk))

<sup>6</sup> HadAM3H = GCM from the Hadley Centre (U.K.)

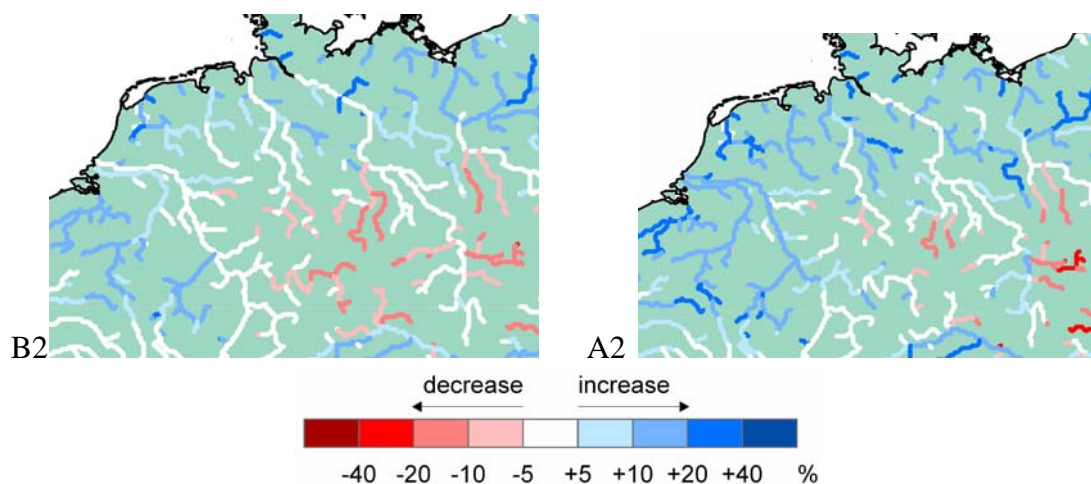


**Fig. 2. 4** Projected average change of river discharge with a return period of once in 100years of the IPCC scenarios B2 and A2 (2071 – 2100) compared to the control period (1961 – 1990). The results are the mean changes of four different model combinations (ensembles). (adopted from Feyen & Dankers, 2009)

For all catchments the increase of the 100-year discharge is larger with the A2-scenario than with the B2-scenario. For the catchment of the Rhine and the Ijssel an increase between 10% and 20% is projected with the A2 scenario, especially in the downstream parts, but with the B2 scenario the 100-year river discharge for the Rhine catchment even decreases for the upstream catchment area. The projected change of the 100-year discharge of the Weser and Elbe catchments are lower than for the other catchment areas. As illustrated in Fig. 2. 4 varying and even opposite changes of the river discharge could be projected for the time period 2071 – 2100 with different IPCC emissions scenarios.

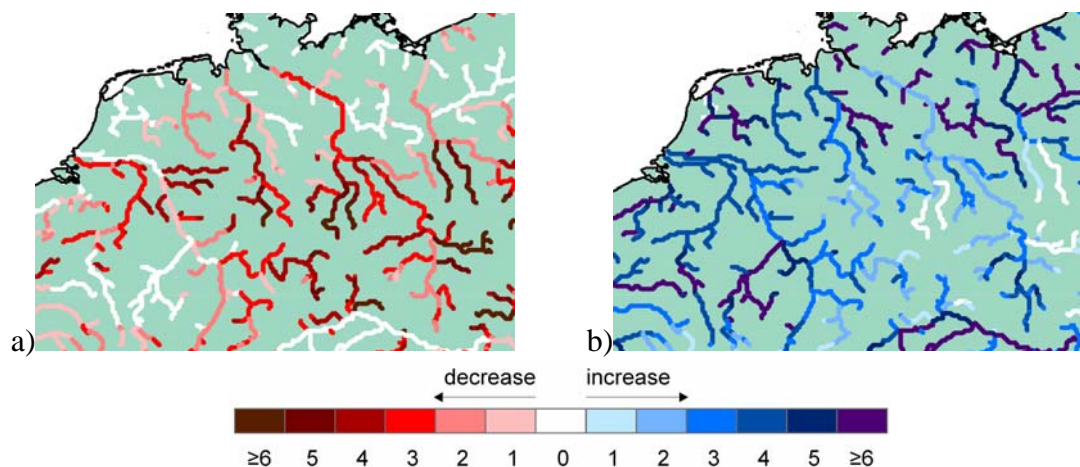


**Fig. 2. 5** Number of model and scenario results (of a total of eight combinations) showing a decrease (a) or increase (b) of 5% in the 100year river discharge for the period 2071 to 2100 compared to the control period (1961 – 1990). (adopted from Feyen & Dankers, 2009)

Additionally, the utilized combination of GCMs and RCMs has a significant impact on the change of the flood events. Feyen & Dankers (2009) illustrated this deviations in a map (Fig. 2. 5) with the number of model and scenario combinations which illustrate a change (increase or decrease) of more than 5% (Feyen & Dankers, 2009).

Overall eight model and scenario combinations have been used, but only in a few river sections more than six model and scenario combination show a corresponding increase or decrease of 5% of the 100year river discharge.

The deviations in the model results point out the large range of scenario results of climate change impacts and calls for the need to analyze involved uncertainties. All variations in the modelling chain composed of the elements: Assumptions of Emission Scenarios [1]→ Global Circulation Modelling (GCM)[2] → downscaling with Regional Climate Models (RCMs)[3] → Climate and Model Variability [4]→ and Impact Models (Hydrological Models) [5] contribute to uncertainties of the simulation results (Feyen & Dankers, 2009; Fowler et al., 2007).

## 2.2 Strategies for Mitigating Climate Change Impacts on Urban Flooding

Even if the ambitious target is reached, to restrict the increase of the global mean temperature till 2050 to less than 2°C compared to the pre-industrial times, consequences are derived in the future, which the environment and man has to cope with (The Federal Government, 2008). It has been stated by Zebisch et al. (2005) that the need to avoid or at least mitigate subsequently Green House Gas (GHG) emissions is regarded as most important reaction on the increased rate of climate change, but that the need for adaptation on climate change impacts has been just becoming a growing concern world wide. In the published framework about the *German Strategy for Adaptation to Climate Change* by the Federal Government, the climate policy has been based on both pillars, which are inseparable linked, because the rise in GHG emissions and therewith the rise in temperature will lead to the need of larger adaptation efforts (The Federal Government, 2008).

The objective of adaptation to climate change impacts can not be defined with a long-term single focus, because it aims for managing the complex impacts of climate change on man and environment, property and quality of life as well as economical and social development. Adaptation has to be regarded here as the reduction of the vulnerability of man as well as the environment to unavoidable changes of impacts and to maintain or increase the capacity of the natural, societal and economic systems. (The Federal Government, 2008).

### 2.2.1 Research Projects of Adaptation Strategies

In the 1990s the global community committed to initiate measures for adaptation to climate change under the UN Framework Convention on Climate Change<sup>1</sup>. The next step was taken by an international community which launched the ‘Nairobi Work Programme’<sup>2</sup> which aims to help all countries to decide about adapting to climate

---

<sup>1</sup>UN Framework Convention on Climate Change = [www.unfccc.int](http://www.unfccc.int)

<sup>2</sup>Nairobi Work Programme = <http://www.unep.org/NairobiConvention>

change. Financial funding for adaptation measures has been made available in 2008 under the Kyoto Protocol<sup>1</sup>. On the European level the Green Paper (Adapting to Climate Change in Europe – options for EU action, July 2007) and the White Paper (Adapting to climate change: Towards a European Framework for Action, April 2009) have been published (European Commission, 2009). The current European research project ERA-Net CIRCLE<sup>2</sup> contributes to the networking of institutions, with research on climate change effects and adaptation under the 6<sup>th</sup> and 7<sup>th</sup> Research Framework Programme.

In Germany currently three major research projects of Adaptation Strategies concerned with hydrological impacts and urban flooding are funded by the Federal Ministry of Education and Research (BMBF) (The Federal Government, 2008):

- KLIMAZWEI (with KLIMANET)
  - *Research for climate protection and protection from climate impacts*
  - It is part of the framework programme “Research for Sustainability”
  - 40 sub-projects are funded from 2006 to 2009 ([www.klimazwei.de](http://www.klimazwei.de))
  - KLIMANET is one of the sub-projects which develops water sensible urban developments and focused on the adaptation of urban drainage systems on extreme rainfall events (Staufner et al., 2008).
- KLIMZUG
  - *Managing Climate Change in Regions for the Future*
  - A regional approach is pursued with seven joint sub-projects: DynAKlim (region: Northern Ruhr Basin), INKA BB (region: Brandenburg-Berlin), KLIMZUG-Nord (Hamburg Metropolitan Region), KLIMZUG Nordhessen (region: Northern Hesse), NordWest2050 (Bremen-Oldenburg), RADOST (German Baltic Sea region), REGKLAM (Model Region of Dresden). Funded from 2009 to 2014 ([www.klimzug.de](http://www.klimzug.de))
  - The aim of these projects is to integrate the projected climate change impacts and the associated extreme weather forms in regional planning and development processes.
- GLOWA
  - *Global change in the hydrological cycle*
  - The aim is to develop a basis for decision making that permit sustainable management of the vital resource water. ([www.glowa.org](http://www.glowa.org)) [2000 till 2009]

---

<sup>1</sup> Kyoto Protocol = [www.kyoto-protokoll.de](http://www.kyoto-protokoll.de)

<sup>2</sup> Climate Impact Research Coordination for a Larger Europe [www.circle-era.net](http://www.circle-era.net)

---

A common basis for methods and data, related to climate change research, is provided by the Service Group Adaptation (SGA)<sup>1</sup> at the MPI-M in Hamburg since 2005, which supports the dialogue between climate system and adaptation research as well as stakeholders on a practical level.

The main question is now, how to handle a situation, which could occur in its full extent in a couple of decades and is accompanied with a significant range of uncertainty (Katzenberger, 2004). A strategy has to be developed which makes it possible to define reasonable steps for adaptation. Sequences of small steps in shorter time horizons are more appropriate here, to have the possibility later on for adjusting the strategy when new knowledge about the impacts of climate change is gained. This approach can be defined as “flexible and no regret”-strategy (Katzenberger, 2004). Additionally sustainable developments have to be pursued, whereas the mostly referred definition comes from the Bruntland Report *Our Common Future*: "... Sustainable development is development that meets the needs of the present without compromising the ability of future generations to meet their own needs." (Bruntland, 1987; p. 43).

### **2.2.2 Sustainable Climate Change Adaptation Strategies for Flood Probability Reduction**

With the principle of sustainability, it has to be assured that any planned adaptation measures for flood probability reduction don't cause negative effects at other locations according to the EU Flood Directive (European Parliament, 2007).

A focus has to be set here on understanding the drivers of urban flooding to find sustainable climate change adaptation strategies. In this context, the interconnection between rainfall causing surface runoff in SUCAs, which in turn cause flooding and as a response damage and risk to residents have to be analysed (WMO/GWP, 2008). It is expected that the initial driver, extreme rainfall events, will be mostly affected by climate change impacts. Secondly the surface runoff volume is significantly larger on sealed areas, where the infiltration and retention of rainfall water is minimized. This is mostly affected by future urbanisation. Both factors together derive the main causes for future changes in flood probability in SUCAs. In the third stage, consequences of flooding are affected by changes in the exposure and vulnerability of SUCAs, but in this thesis a focus has been set on the quantification of the flood probability rather than the derived consequences.

Flexible and sustainable adaptation measures for mitigating urban flooding have been defined e.g. within the KlimaNet, the KLIMZUG and the 1st ERA-Net CRUE

---

<sup>1</sup> [www.mad.zmaw.de/projects-at-md/sg-adaptation](http://www.mad.zmaw.de/projects-at-md/sg-adaptation)

Funding Initiative<sup>1</sup>. Among others, sustainable drainage systems (SUDSs) have been identified as possible strategies for flood probability reduction in SUCAs.

In contrast to conventional drainage systems with the main purpose of draining rainfall as fast as possible to the nearest receiving watercourse; the main purpose of SUDSs is to retain and reduce the rainfall water which causes surface runoff as close as possible to the source by infiltration or storage facilities. The main principles of SUDSs are based on collecting, temporary storing, purification at the source, subsequently discharging at a controlled rate, purification and improving the urban environment (Kellagher & Laughlan, 2005). The main components of SUDSs have been summarized in the project CRUE ERA-Net as listed in Table 2. 2.

**Table 2. 2 SUDS elements defined in the project CRUE ERA-Net. (adopted from Pasche et al., 2008)**

|                                | <b>SUDS Technique</b>                  | <b>Description</b>   |
|--------------------------------|--|--|
| <b>Source Control Measures</b> | <b>Green roofs</b>                     | Vegetated roofs that reduce the volume and rate of runoff and remove pollution.  |
|                                | <b>Rainwater re-use (harvesting)</b>   | Involves the collection and storage of rainwater on site and its use as a substitute for mains water, for example in watering gardens or for flushing toilets.   |
|                                | <b>Permeable pavements (Unsealing)</b> | Through porous pavement rain water directly infiltrates into the subsoil. Here it can be stored in an underground reservoir before slowly percolating into deeper parts of the underground.  |
| <b>Infiltration Techniques</b> | <b>Filter trenches</b>                 | A filter trench is a shallow, excavated trench that has been filled with permeable material to create an underground reservoir.  |
|                                | <b>Filter drains</b>                   | Filter drains are similar to filter trenches through which a perforated pipe runs. This facilitates the storage, filtering and some infiltration of water passing from the source to the discharge point.  |
|                                | <b>Filter strips</b>                   | Filter stripes are vegetated areas of gently sloping ground designed to drain water evenly off and to filter out silt & other particulates.  |
|                                | <b>Soakaways</b>                       | These are sub-surface structures that infiltrate runoff water.   |
| <b>Detention Structures</b>    | <b>Swales</b>                          | Swales are grassed depressions which lead surface water overland from the drained surface to a storage or discharge system and permits infiltration.   |
|                                | <b>Bioretention area</b>               | Such areas are depressed in the landscape, which are allowed to collect runoff so that it percolates through the soil below the area into an underdrain, thereby promoting pollutant removal.  |
|                                | <b>Detention basin</b>                 | Such basins are designed to hold back storm runoff for a few hours and to allow the settlement of solids. They permit infiltration and are dry outside of storm periods.   |
|                                | <b>Ponds &amp; wetlands</b>            | These are areas of permanent water, designed to accommodate considerable variations in water levels during storms, thereby enhancing flood-storage capacity. They can be fed by swales, filter drains or piped systems, and the use of inlet and outlet sumps will enhance performance by trapping silt and preventing clogging of the outlet. |

---

<sup>1</sup>CRUE ERA-Net = 1st ERA-Net CRUE Funding Initiative: 'Risk assessment and risk management: Effectiveness and efficiency of non-structural flood risk management measures' : [www.crue-eranet.net](http://www.crue-eranet.net)

SUDSs include source control measures (e.g. green roofs), detention structures (e.g. ponds, swales) and infiltration techniques (e.g. filter drains, soakaways) (Pasche et al., 2008). Additionally they can be combined in many ways like green roofs draining into swales with filter drains placed underneath (Pasche et al., 2009; Brüning et al. 2009; Brüning & Hellmers, 2009).

It has been stated that a large potential for the reduction of the surface runoff volume from SUCAs is represented by disconnecting roof areas. In residential areas the spatial distribution is assumed to be about 20% to 30% and represent a ratio of 60% of the drainage relevant sealed urban area. In commercial areas this ratio can be even higher (UMBW, n.d.).

For the assessment of the hydrological effectiveness of SUDSs to mitigate flood probability in SUCAs, practical experiences are rare up to now especially for extreme storm events in urban catchments and with respect to future climate scenarios (Kellagher & Laughlan, 2005). The effectiveness of SUDSs elements on single allotments can be determined with hydraulic calculations, but the assessment of their effectiveness on the catchment level in SUCAs is very complex and requires computer models (Pasche et al., 2009). Only a few of the SUDSs techniques are implemented in commercially or public available hydrological and/or hydraulic software tools (Hellmers, 2009) (Table 2. 3).

**Table 2. 3 Research about SUDS modelling tools implemented in current software applications. (Hellmers, 2009)**

|                           | Swales | Swales with filter drains | Filter (strips) | Gravel filled trenches | Wetlands | Cisterns | Porous pavement | Green roofs | Detention ponds | Infiltration ponds |
|---------------------------|--------|---------------------------|-----------------|------------------------|----------|----------|-----------------|-------------|-----------------|--------------------|
| <b>InfoSWMM</b>           | X      | -                         | X               | X                      | X        | X        | X               | X           | X               | -                  |
| <b>HydroCAD</b>           | X      | X                         | X               | X                      | X        | X        | X               | X           | X               | -                  |
| <b>MIKE Urban (MOUSE)</b> | X      | -                         | -               | -                      | X        | X        | -               | -           | X               | -                  |
| <b>InfoWorks CS</b>       | X      | -                         | -               | X                      | -        | X        | -               | -           | X               | X                  |
| <b>WinDes</b>             | X      | -                         | -               | -                      | -        | X        | X               | -           | X               | -                  |
| <b>STORM.RWB</b>          | X      | X                         | X               | -                      | -        | X        | -               | -           | X               | X                  |

X = SUDS module available; "-" = SUDS module not available

It can be stated that modelling SUDSs techniques like swales, cisterns or detention ponds is supported by the most investigated software tools in the study, but modelling combined swale-filter-drain systems and green roofs is rarely facilitated.

### 2.3 Open Research Questions and Objectives

In current research studies it is an open task to develop a comprehensive and detailed methodology to quantify the hydrological impacts by climate change on the flood probability in small urban catchments (SUCAs). In addition, it is emergent to comprise a systematic procedure for subsequent post-impact studies of adaptation measures. This is especially challenging due to the analysis of extremes in complex small study regions with a variety of land use characteristics. In this context it is undetermined, what engineers and hydrologists have to be aware of, when setting up scenario studies with climate model data.

Climate change research studies focus mainly on larger river catchments like the Rhine (Feyen & Dankers, 2009), the Danube catchments (CLAVIER) and the Baltic Sea river catchments (BALTEX). But this thesis contributes to the research of small scale areas of SUCAs, which are significantly affected by flooding after extreme rainfall events, due to the generation of fast surface runoff in densely urbanised areas. For this purpose, a fine and detailed spatial resolution of the climate model data is required for climate change scenario studies. It is questionable, if the current smallest spatial resolution of about 10km x 10km provided by the regional climate model REMO (MPI-M) could fulfil the requirements for scenario studies of flood probabilities in SUCAs.

The studied extreme core indices in the projects STARDEX, MICE and the UFOPLAN are indicated as moderate with the number of wet days and daily precipitation sums used e.g. in the INKLIM 2012 II Plus project to study the impacts of climate change on the flood regime in the overall Lahn catchment (Brahmer, 2008). However, for the analysis of flood probabilities in SUCAs, data series with a higher temporal resolution of minutes are required, to simulate the fast surface runoff processes in urban areas. The smallest timestep of currently available climate model data series is in hours (REMO, CLM<sup>1</sup>). In this context, it is an open question if the computation of flood probabilities are notwithstanding reasonable with these provided time steps of climate model data series.

It has been stated as questionable, if the IPCC scenario with the largest projected increase in future CO<sub>2</sub> emissions and highest temperature change, results as well to a larger increase of the probability of extreme rainfall events and flooding in SUCAs.

Furthermore, it is not possible to imply per se that extreme rainfall events changes in the same way as mean precipitation. But it is discussable, to find out a correlation between the interaction of the change in temperature, evaporation, mean precipitation and the change of extreme rainfall as well as flood probabilities.

---

<sup>1</sup> CLM = Climate Local Model; Features in Attachment 1.2

As stated in the results of the CLAVIER project, by [Van Pelt et al. \(2009\)](#) and by [Fowler et al. \(2007\)](#) the application of bias correction methods is debatable in research studies. An additional uncertainty source could be even derived by the application ([Van Pelt et al., 2009](#)). Therefore it is intended to derive another solution for computing climate change impacts on flood probabilities.

For the applicability of climate change scenario study results in post-impact studies (like for the simulation of adaptation measures e.g. SUDS), the computation of climate change factors (CCF) is useful to project extreme design rainfall and design flood events under climate change conditions. For this purpose, no standard or 'best practice' solution is provided and a comparison of the applicability of different approaches is required.

Assessing the effectiveness of possibilities for mitigating flood probabilities, which are flexible and sustainable, is an emergent task in climate change research studies (paragraph 2.2). In this context, SUDSs have been identified as appropriate measures for this purpose. Therefore, it has been defined as an objective in this thesis to develop a theoretical approach for modelling SUDS elements (namely: green roofs) and to implement it in a hydrological model, which is tested and used for climate change scenario studies. The challenge of this task is derived by developing a software tool which enables the simulation of detailed hydrological processes in the SUDS element, but can be applied as well for assessing the effectiveness of SUDSs on a catchment level.

### 3 Methodological Approach

In current research studies a detailed and comprehensive methodology to quantify the impacts on flood probability derived by climate change is required, especially for local scale and complex study areas like small urban catchments (SUCAs).

Secondly, it is required to assess the effectiveness of possibilities of flood risk mitigation. In this context, it has been induced as challenge to develop a software tool which enables the simulation of the defined appropriate measures in chapter 2, namely sustainable drainage systems (SUDSs).

The main steps of the developed methodology in this thesis are summarized first, to provide an overview of the complexity of the two defined main objectives, before going into the details.

#### 3.1 Methodology Scheme

The developed methodology consists of two main columns. In the first [methodology part \(A\)](#), the developed theoretical approach for calculating the *Hydrological Impacts by Climate Change on Flood Probability* is depicted. And in the [methodology part \(B\)](#), an approach for assessing the effectiveness of SUDS as *Possibilities of Flood Risk Mitigation* is defined (Fig. 3. 1).

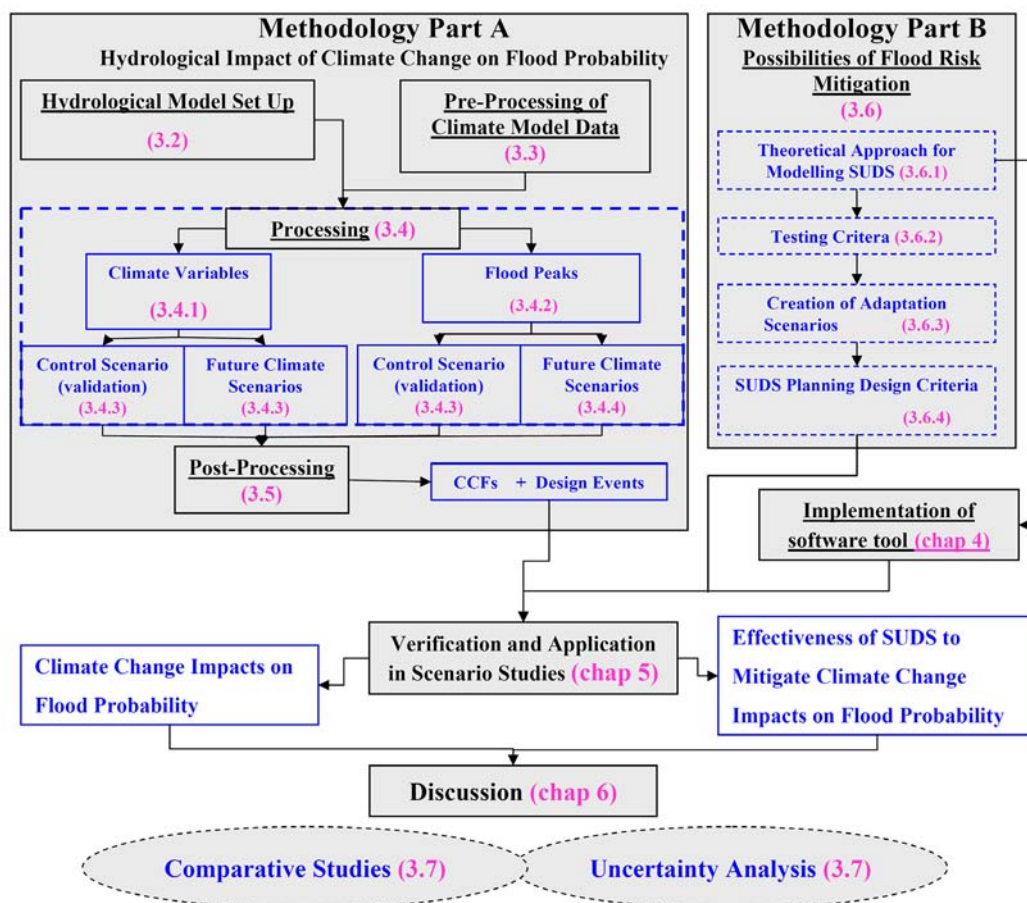


Fig. 3. 1 Methodological Scheme.

In the [methodology part \(A\)](#) the hydrological model has to be set up, which is applicable for flood peak simulations in urban catchments [\(3.2\)](#). In the second step the climate model data series for the climate change scenarios have to be selected and pre-processed to be used for hydrological simulations [\(3.3\)](#). Thereafter, the data and results of climate change scenarios are processed in analyses [\(3.4\)](#), whereas a differentiation had to be done between climate variables [\(3.4.1\)](#) and flood peak simulation results [\(3.4.2\)](#). For both, it is required to analyse the control scenario data series referred to the observed data series of the past (validation) [\(3.4.3\)](#) and to analyse the future climate scenario results [\(3.4.4\)](#). The results of these scenario studies have to be post-processed to compute the magnitude of change derived in climate scenarios and to calculate applicable climate change factors (CCFs) [\(3.5\)](#). Therewith the change in design events of extreme rainfall and flood peak events with a specific probability of occurrence can be computed, which are used in subsequent post-impact studies.

In the second [part \(B\)](#) a methodology for assessing the effectiveness of possibilities of flood risk mitigation has been developed. First, the theoretical approach for modelling SUDSs and criteria for testing it, are defined. To assess the effectiveness of SUDS for the mitigation of climate change impacts on the flood probability, adaptation scenarios have to be created. Further on, criteria for the planning of SUDSs are summarized. The theoretical approach for modelling SUDSs has been implemented in a software tool, which is outlined in [chapter 4](#). The effective and appropriate applicability of the methodology and the developed software tool is demonstrated as well as verified in scenario studies ([chapter 5](#)).

Additionally the theory of comparative studies and uncertainty analysis is depicted in the methodology of this thesis [\(3.7\)](#) which is applied for the discussion of the scenario study results in [chapter 6](#).

### **3.2 Hydrological Modelling**

In this thesis, hydrological impacts by climate change on the flood probability in SUCAs are analysed by simulating river peak flow and calculating the statistical evaluation.

Hydrological processes are simulated in GCMs (e.g. ECHAM5) and in dynamical RCMs (e.g. REMO and CLM) as well, but the results of surface runoff and discharge in water courses are only roughly simulated and not appropriate for flood probability analyses. In fact, accurate modelling results of the flow regime in catchments<sup>1</sup> are required ([Blyth, 2009](#)), because the generation of flooding is a highly non-linear process which is influenced by the magnitude, intensity and timing of precipitation as well as antecedent conditions like the soil moisture and interception of water ([Feyen & Dankers, 2009](#)). Additionally the river morphology,

---

<sup>1</sup> Catchments are drainage basins, where rainfall water is drained to a body of water.

the land type and flood control measures like reservoirs and polders have a significant impact on the progress of the flood wave. For example surface runoff occurs when water can not infiltrate into the soil and is forced to run over the land. This surface runoff reaches the conduit or river much faster than the water which travels through sub-surface routes to the conduit system. The difference in travel time has a large influence on the runoff hydrograph and much research as well as effort has been done to simulate the timing of flood waves in water courses with hydrological models (Blyth, 2009; Pasche 2003).

For the simulation of the hydrological and hydraulic processes (e.g. infiltration, runoff, groundwater flow) the catchment has to be divided into sub-catchments according to the topology, hydrological relevant characteristics of the area, retention structures like ponds, drainage networks and with regard to potential flood risk areas. In well-applied software models (e.g. InfoWorksCS<sup>1</sup>, SWMM<sup>2</sup> as well as Kalypso Hydrology<sup>3</sup>) the flow regime is simulated on the basis of the reservoir theory (VICAIRE, 2006) by connecting sub-catchments with nodes<sup>4</sup> and strands.

Therewith the resulting flow components calculated on the sub-catchment level are transferred to the respective node and are further processed in strands, which display the connection elements (streams, pipes, open river sections) of the conduit network.

For the retention and translation processes in the strands and sub-catchments, different approaches are used in software tools, which can be based on modelling the discharge in pipe networks (e.g. Hystem/Extran<sup>5</sup>) or modelling open channel flow (e.g. Kalypso Hydrology). In a few software models it is possible to simulate pipe and open channel flow (e.g. InfoWorksCS). Concerning this matter, a criteria analysis for comparing software tools has been worked out in a previous work (Hellmers, 2009) which has been applied for comparing the software models InfoWorksCS and Kalypso Hydrology. The selection of the appropriate software model depends on manifold criteria including the availability of the software, the needed effort of the user to use it, the required purpose of use (e.g. river or pipe network simulation), restrictions of the model to be used in specific locations (e.g. mountains or low lands; urban areas or rural areas) and the costs of the software can be an important criteria. When an integrated approach of different disciplines is required, where several models have to be applied, it is as well an important criterion that the output of one model can be directly used for another model (Hellmers, 2009). Additionally, for climate change scenario studies, it has to be possible to

---

<sup>1</sup> [http://www.wallingfordsoftware.com/products/infoworks\\_cs/](http://www.wallingfordsoftware.com/products/infoworks_cs/)

<sup>2</sup> <http://www.epa.gov/ednrmrl/models/swmm/>

<sup>3</sup> <http://sourceforge.net/projects/kalypso/>

<sup>4</sup> Nodes are like river stations.

<sup>5</sup> [http://www.itwh.de/S\\_extinfo.htm](http://www.itwh.de/S_extinfo.htm)

import data series of climate models into the software tool, which include time series of precipitation, temperature and evaporation (if appropriate).

### ***Hydrological Model Set-Up***

For setting up the model a comprehensive data acquisition and pre-processing is necessary to assure qualitative results. The procedure to set up a hydrological model including the calibration and validation has been worked out previously (Hellmers, 2009). The most important data sources for setting up the models for climate change scenario simulations comprise:

- Data and Information about the drainage and conduit system,
- Land use data and topographical data,
- Pedological and geological information,
- Observed meteorological and hydrological data (for validation / calibration),
- Data series of future climate scenarios derived with climate models.

The allocation of observed meteorological data series depends on the type of the data. E.g. satellite data series are provided in a grid distribution and therewith the allocation of the data series in the catchment is done on the basis of the supplied raster. Observed data series from weather stations is provided as a point measure, which has to be distributed to the sub-catchments with methods like the Thiessen-Polygon or Kriging-Method (ASCE, 1996).

With observed meteorological and discharge data series of gauging stations in the conduits, the hydrological model has to be calibrated and validated. A detailed explanation of the calibration theory is given in Hellmers (2009) and has been applied for a study area in Garforth: Yorkshire, UK.

## **3.3 Pre-Processing of Climate Model Data**

For the analysis of flood probability changes derived in future climate scenarios, time series of climate models are required. For this purpose, the data series of a variety of climate models as well as climate scenario combinations can be selected.

### **3.3.1 Criteria for Selecting Climate Model Data**

Worldwide different global and regional climate models are used which are based on different approaches (IPCC AR4, 2007a). The selection of the adequate climate model as well as scenario combination for specific impact studies is an integrative process. For this purpose six criteria have been defined in this methodology.

#### ***1. Comparability with related climate change research studies or projects.***

- a. In climate change impact studies the comparability of related project outcomes is the basis to assume the reasonability of scenario study results and the range of uncertainties. Therefore a research about

related studies in the project area and about the applied climate models as well as scenario combinations is required in the beginning.

### ***2. Type of global circulation and regional (downscaling) climate models.***

- a. Global Circulation Models (GCMs) (IPCC AR4, 2007a):
  - i. Ocean Global Circulation Models (OGCM),
  - ii. Atmospheric Global Circulation Models (AGCM),
  - iii. Atmospheric Ocean Global Circulation Models (AOGCM).

It is recommended that the output data of the more advanced AOCGMs is taken to provide the boundary conditions for the downscaling in a regional climate models (RCMs) (IPCC AR4, 2007a).

- b. RCMs are used for downscaling GCM data series. Two types are currently available:
  - i. RCMs based on dynamical process simulations,
  - ii. RCMs based on statistical calculations.

A comparison of the main features of RCMs is outlined in (3.3.2.2) to select the appropriate type for flood probability analysis.

### ***3. Availability of required data variables.***

Climate models provide a limited package of climate and hydrological variables for different temporal aggregations. The completeness of the required data series for specific hydrological modelling purposes has to be detected before selecting the final climate model and scenario combinations.

### ***4. Spatial resolution of climate model data series.***

Especially for the analysis of extreme events and local study areas, the smallest available spatial resolution is preferred for impact studies.

### ***5. Scenario combinations.***

Three main scenario combinations can be considered with climate model data, which could be further extended to more complex combinations:

- a. Using climate model data of different future IPCC scenarios (e.g. A1B, B1 and A2).
- b. Comparing the results of different climate models for the same IPCC-scenario.
- c. In case of several model runs, scenarios can be based on different climate model realisations<sup>1</sup>. For example, scenarios could be set up

---

<sup>1</sup> Realisations of climate models depend on the initial beginning of the model run. When these initial conditions are changed, the results of the climate model are different.

---

with the data series of the REMO-UBA experiment<sup>1</sup> (Jacob & Mahrenholz, 2006), which displays the first run<sup>2</sup> and the recently published data of the REMO-BFG experiment (Jacob & Lorenzo, 2009) could be the second realisation of the REMO model to be used.

**6. Definition of climate time periods.**

- a. Climate model simulations cover a time period of about 40 years for control scenarios in the past (e.g. 1961 – 2000) and a period of 100 years from 2001 to 2100 for future climate scenarios. Time periods with a length of 30 years are widely-used for climate scenario studies in the past and the future (IPCC TAR, 2001).

**3.3.2 Climate Model Types**

**3.3.2.1 Global Circulation Models (GCMs)**

In research studies, the more advanced coupled AOGCMs are utilized, which are continuously improved regarding spatial resolution and the included dynamical process simulations (e.g. on land surfaces or sea-ice). A detailed analysis of 23 AOGCMs has been done in the fourth assessment report (AR4) of the IPCC (IPCC AR4, 2007a). In Germany, the currently mostly applied AOGCM has been developed by the MPI-M<sup>3</sup>, known as ECHAM5 with a horizontal raster resolution of about 220km x 220km and 31 vertical layers (BMVBS, 2007). An example of a horizontal and vertical GCM raster is illustrated in Fig. 3. 2.

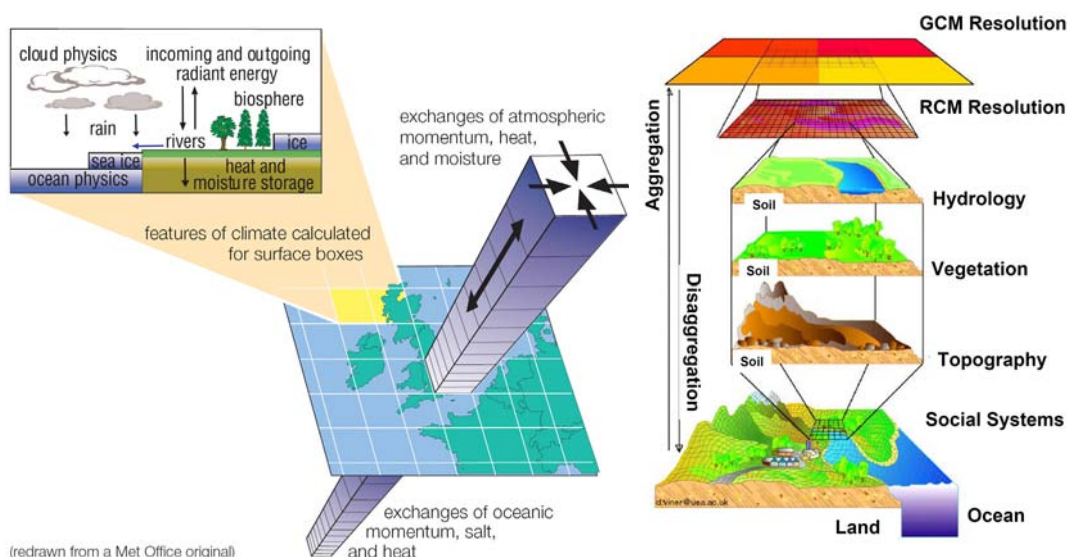


**Fig. 3. 2 Conceptual Structure of a Global Circulation Model and Downscaling Approach. (adopted from Viner, 2000; STARDEX, Final Report, n. d.)**

<sup>1</sup> A climate model “experiment” is a scientific project, for which the data has been computed primarily.

<sup>2</sup> In the thesis the differentiation between the first and the second run is abbreviated with \*\_1 and the second run with \*\_2.

<sup>3</sup> MPI-M = Max-Planck-Institute for Meteorology in Hamburg.

Specific features of the simulation of the land surface comprised by ECHAM5 is the representation of the soil moisture as a single layer ‘bucket’, the incorporation of the vegetation canopy and a river routing scheme (IPCC AR4, 2007a). Further details are listed in Attachment 1.1 of the thesis. For climate change scenario impact analysis it is required to post-process the coarse global climate model data to a finer resolution. This procedure of bridging the spatial resolution gap is known as “downscaling” (Fowler et al., 2007).

### 3.3.2.2 Regional Climate Models (RCMs)

With the application of regionalisation procedures, the GCM data can be downscaled to a spatial grid of 10km x 10km (BMVBS, 2007). Downscaling techniques are based on statistical or dynamical approaches, which have been compared, especially for hydrological impact studies by Fowler et al. (2007). As stated in their research study, little attention has been given up to now to the choice of downscaling method when quantifying the impacts of climate change, although it can have influences on the results of impact studies (Fowler et al., 2007).

#### *Dynamical RCMs*

Dynamical climate models are based on numerical simulations of vertical and horizontal meteorological as well as hydrological processes in each box of a model-grid. The boundary input data for the RCM computations are provided by GCMs. This is also known as nesting strategy (Spekat et al., 2007). A finer resolution of regional climate models can be gained by a “double nesting”, like with the regional climate model REMO in the REMO-UBA and REMO-BFG experiment which provide the smallest spatial distribution of 10km x 10km for Germany (Jacob & Mahrenholz, 2006; Jacob & Lorenzo, 2009). With regional dynamical climate models it is possible to simulate orographic precipitation, extreme climate events and regional scale climate anomalies (Fowler et al., 2007). The physical vertical processes are calculated in columns over the grid cells per timestep in a raster. Here the energy flux, clouds formation and the water cycle processes are simulated like by GCMs but on a smaller scale (see Fig. 3. 2). The soil water simulation can be based on different layers like in the REMO model, where the soil structure is divided into 5 layers (Jacob et al., 2008).

The two developed and mostly applied dynamical climate models in Germany are REMO and CLM, which are based on the leap-frog-scheme (Jacob et al., 2008; Schättler, 2009). In this scheme, a tendency of the horizontal processes is calculated first and then the dynamical result is gained, which is used to start the calculation again. This scheme leads to uncertainties regarding the results of single cells and could lead to “noises” (CLAVIER[1], 2009). Therefore it is advised to compute the average of at least 4 to 9 grid cells (CLAVIER[1], 2009).

For impact studies, physical consistent pictures are required of future climate variables, including changes in climate variability and the occurrence of such various weather phenomena as extreme events (Bader et al., 2008). This criterion is fulfilled by dynamical climate models, which compute the variables per timestep with numerical equations.

A drawback of the dynamical RCMs is the required higher computationally expenses in comparison to the RCMs using statistical downscaling techniques. A summary of dynamical RCM features is given in Attachment 1.2 for the REMO and CLM model.

### ***Downscaling models based on statistical calculations***

Statistical downscaling techniques are based on the assumption that the GCMs simulate adequately enough the atmospherically processes (Spekat et al., 2007). In this way, statistical relationships are defined between the wide-spread weather patterns and the local effects. For the definition of the relationship, long and reliable observed historical data series for the calibration of the RCM are required (Fowler et al., 2007). In contrast to the grid-based model output from dynamical RCMs, statistical based RCMs provide data series for respective weather stations (Fowler et al., 2007). Statistical downscaling models require less computational expenses than dynamical RCMs (Spekat et al., 2007). In Germany, the mostly applied climate model based on statistical downscaling is the WETTREG model, for which the main features are listed in attachment 1.2.

### **3.3.3 Climate Change Scenarios**

The Special Report on Emissions Scenarios (SRES) presented by the IPCC in 2000 (IPCC, 2000) are generally used as a basis for climate change scenario studies (BMVBS, 2007). The differentiation between the scenarios is based on economic and demographic developments. Comprised are a number of four emissions scenario families (A1, B1, A2, B2; Fig. 3. 3), which represent assessments of future greenhouse gas concentrations (IPCC, 2000). None of the SRES can be assigned to a range of probability to occur in the future (IPCC, 2000).

#### ***A1 scenario family***

The A1 scenario group displays a possible future with rapid economic, global population growth which reaches a peak in the middle of the 21<sup>st</sup> century. After 2050 a fast introduction of more efficient new technologies and a decline of the economic as well as population growth are projected. In this scenario family the cultural and social as well as the regional differences in per capita income are reduced in the future. The three sub-groups (A1FI, A1T and A1B) describe the use of different technologies: A1FI = fossil intensive, A1T = non-fossil energy sources and A1B =

balanced energy source of different types (IPCC, 2000). [Indicated as medium CO<sub>2</sub> emissions scenario]

**A2 scenario family**

In the A2 scenario family the change of technologies is slower than in the other storylines. The world is described very heterogeneous with primarily regional oriented economic development and larger differences in economic growth. The global population is growing continuously in this scenario family (IPCC, 2000). [Indicated as high CO<sub>2</sub> emissions scenario]

**B1 scenario family**

Like in the A1 scenario family, the global population increases till the mid-century and declines thereafter. Contrary to the other storylines, a strongly service and information oriented economy is projected which leads to a reduction of used material and the introduction of clean as well as resource-efficient technologies. In this scenario family a focus is set on economic, social and environmental sustainability (IPCC, 2000). [Indicated as low CO<sub>2</sub> emissions scenario]

**B2 scenario family**

The increase of the global population growth displayed in the B2 scenario family is lower as in the other scenarios, but continuous. The technological change is less rapid than in the B1 and A1 storyline. Meanwhile an orientation toward environmental protection and social equity is displayed. The emphasis is set on local solutions and on regional levels (IPCC, 2000). [Indicated as medium CO<sub>2</sub> emissions Scenario]



Fig. 3. 3 Schematic illustration of the four qualitative storylines (A1, A2, B1 and B2) derived from the SRES of the IPCC. (adopted from IPCC, 2000)

**3.3.4 Climate Model Data Sources and Formats**

Climate model data series for scenario studies in Germany and partly for Europe are available from the Climate and Environmental Retrieval and Archive server (CERA)<sup>1</sup>. It is one of 52 World Data Centres for Climate (WDCC) in 12 countries.

<sup>1</sup>CERA: <http://cera-www.dkrz.de>

The mission of these centres is the collection, storage and distribution of data for climate research<sup>1</sup>.

The results of climate model data can be selected by the experiment, by the data series of different variables (e.g. precipitation), by the name (acronym) or the topic. The selected entries can be stored in user process lists, where it is available to be downloaded. The total size of the data series can be very large; e.g. the complete hourly data series of precipitation from the REMO-UBA experiment comprise a size of 70GB. Therefore it is necessary to predefine the area of interest and to reduce the required time period before downloading the data series. The geographical raster and the format of the data series vary between climate models, whereas the NetCDF format<sup>2</sup> is often provided and described below. Post-processed data series are available for the REMO and CLM model, which are indicated as datastream D3 on the CERA server. These data series provide additional data values and are interpolated on a regular geographical grid. The grid cells are always defined by the left bottom corner in the climate model raster.

### *NetCDF formats:*

The structure of a NetCDF file is described in the header of each data block. It can comprise one- or more dimensional arrays (UCAR, 2007). The University Corporation for Atmospheric Research (UCAR) developed this format with the purpose of creating a file format, which provides all the information needed to read the data and the data itself (UCAR, 2007).

For reading and processing NetCDF files, the MPI-M developed a package of Climate Data Operators (CDO)<sup>3</sup> which can be used on UNIX or Linux computer operating systems. An example of a climate model data raster consisting of 18 cells on a regular grid is given in Fig. 3. 4.

For the import of the climate model data series in hydrological models, two pre-processing steps are required:

1. In case of using data series of dynamical RCMs, which are based on the leap-frog-scheme (e.g. REMO, CLM), the averages of at least four to nine grid cells are recommended to be applied for impact studies [CLAVIER [1], 2009; REMO User Leaflet, n. d.].
2. The NetCDF format has to be transferred to time series, comprising the data of each averaged grid cell.

---

<sup>1</sup> For the download and processing of climate model data for Germany, a user account has to be set up, which can be requested currently to [data@dkrz.de](mailto:data@dkrz.de).

<sup>2</sup> NetCDF = Network Common Data Form

<sup>3</sup> [www.mpimet.mpg.de/cdo](http://www.mpimet.mpg.de/cdo)

For the computation of the averaged grid data and the following transformation of the grid data to time series, a Java Application has been developed by Dejan Antanaskovic from the Institute of River and Coastal Engineering at the Technical University of Hamburg Harburg (TUHH). The principle of overlapping averaged grids is shown in Fig. 3. 4, whereas an example of averaging the data of four grid cells on the 01.01.2030 at 1:59 is illustrated. The averaging of the grids starts with the bottom left grid cell. In this way, the data is gained for 10 averaged grid cells which are copied per timestep into a time series file (e.g. \*.csv-file). The data for each grid cell is indicated by a semicolon and has to be transferred to separate time series before it can be imported into hydrological models. This is illustrated for the first grid cell on the 01.01.2030 at 0:59 till 4:49 in Fig. 3. 4.

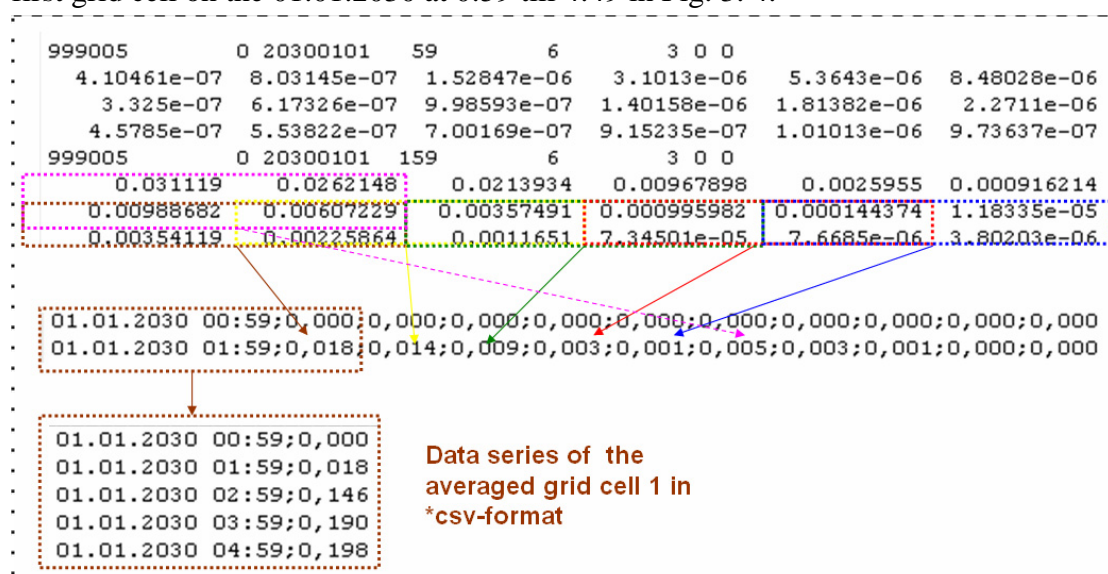


Fig. 3. 4 Example of a climate model data series (precipitation) on a raster with 18 cells in NetCDF format, which are averaged over 4 grid cells and transferred to separate time series.

The command for the transfer of NetCDF formats to an other format is:

- **cdo output** “file-name.nc” > “output-file-name.txt”

The command for averaging grid cells and transferring the results to a time series with the developed add-on Java tool is:

- **-jar transform.jar** “name of netcdf-format-file.txt” “name of the transferred file\*.csv”

### 3.3.5 Calculation of Additional Data Series

A number of hydrological models (e.g. MIKE, InfoWorksCS, Kalypso Hydrology) use time series of evaporation for the calculation of the water balance in catchments. A differentiation has to be defined between the evaporation from free water surfaces and the more complex evapotranspiration from land surfaces, which comprise the

sum of the evaporation from free soil surfaces and the transpiration from plants/flora ([DVWK-238, 1996](#)).

Regarding the available data sets from climate models, there is a limitation of evaporation data series for scenario studies. E.g. the dynamical climate models REMO and CLM provide data sets of the actual evapotranspiration, but not the potential evaporation. For this purpose, an approach for the calculation of the potential evaporation (here: grass-reference evaporation) with climate model data of REMO or CLM is outlined in the Attachment 2.

### 3.3.6 Differentiation of Seasons

The magnitude of impacts derived in climate scenarios can differ significantly between seasons as stated in the UFOPLAN ([Jacob et al., 2008](#)) and in the project CLAVIER. In impact studies a differentiation can be done with four seasons or with hydrological year periods:

1. According to four seasons (e.g. [Jacob et al., 2008](#); [Déqué et al., 2007](#)):
  - Winter (December, January, February)
  - Spring (March, April, May)
  - Summer (June, July, August)
  - Autumn (September, October, November)
  
2. According to periods of hydrological years, which are widely-used in hydrological impact studies with a differentiation described in DIN 4049 (e.g. used in the project: KLIWA, [www.kliwa.de](http://www.kliwa.de)):
  - Winter (November till April; 01.11 – 30.04)
  - Summer (May till September; 01.05 – 31.10)

## 3.4 Processing of Climate Change Scenario Results

Computed climate data series describe the statistical sums and averages of weather phenomena ([IPCC AR4, 2007b](#)), whereas it is not possible to compare climate data series neither of the past nor of the future according to a specific point in the time series. In fact, strategies have to be defined to quantify the overall change of variables in a selected climate period. For flood probability studies, a differentiation between (input) climate variables (3.4.1) and simulated flood peak data series (3.4.2) has to be made. For both data sets, it is required to analyse data series of the past (3.4.3), before future climate impacts derived in IPCC-scenarios are computed (3.4.4).

The following strategies are suggested to quantify climate change impacts:

- Comparison of summations (e.g. yearly, seasonal or monthly precipitation).
- Analysis of averages (e.g. yearly, seasonal or monthly temperature).
- Trend analysis of yearly, seasonal or monthly changes.

- Number of occurrence of values above a threshold (e.g. number of wet days).
- Statistical evaluations for the analysis of extremes (e.g. flood peaks).

For the analysis of extreme rainfall events and the change in flood probability, approaches for statistical evaluations are outlined in more detail in 3.4.5.

### 3.4.1 Climate Variables

For the interpretation of impacts on flood peak probabilities, it is important to analyse as well the changes in climate variables (precipitation, temperature and evaporation) which are the external drivers for the water balance calculations in catchments with hydrological models. Most significant are here the impacts on precipitation and especially extreme rainfall events.

The analysis can be done with seasonal averages (e.g. of temperatures) or summations (e.g. for precipitation). Further on it is recommended to compare the intensity and frequency of extreme events in statistical evaluations.

### 3.4.2 Data Series of Flood Events

With hydrological models flood hydrographs are computed. Therewith the changes in the flood volume and flood peaks can be derived for the control scenario data series and future climate scenarios. The computation of statistical evaluations of flood peak data series is recommended to be done as outlined in (3.4.5).

### 3.4.3 Control Scenario Data Series

The computed control scenario data series of climate models are based on initial climate conditions of the past. The results of these control scenarios are provided by the climate model operators for time periods between 1950 and 2000 (<http://cera-www.dkrz.de>). Although the climate model calculations are based on initial values of the past, the computed data series can not be compared directly with data series of weather phenomena observed in the past. The same is true with any short term trends due to the variability of the climate (IPCC TAR, 2001). The comparability is restricted on the overall statistical computed and observed climate.

It is expected that the results of the computed and observed data series analysis differ to a more or less significant degree. These differences are derived by uncertainties in the computation of climate model data series, climate variability and can be as well introduced in observed data series by systematic errors or by inaccuracies of measuring techniques (Rudolf & Rubel, 2005).

To handle these differences, a validation of the climate model data series and correction methods can be applied like in the CLAVIER project or by Van Pelt et al. (2009) outlined in (2.1). Due to the derived additional source of uncertainties with correction methods (Van Pelt et al., 2009) and the limited scope of the thesis to validate a variety of methods, a different approach has been defined to assess the

changes in flood probability. However, for this purpose a detailed analysis of the observed and computed control scenario data series have to be provided.

#### **3.4.4 Future Climate Scenario Data Series**

For the computation of the impacts derived in future climate scenarios, the average changes of the climate can be analysed with trend lines, averages and summations of e.g. precipitation, temperature and evaporation. With regard to trend analyses, it is recommended to compare the change of the future scenarios to the average of the control scenario climate period of the past. In this way, it is assured that the average trends in the projected scenarios are calculated.

The changes derived in daily precipitation intensities in the climate scenarios can be analysed with the number of days with rainfall heights above or in a range of defined thresholds. This approach is widely used in climate impact studies (e.g. [Jacob et al., 2008](#); [Bischoff, 2007](#); [North-German Climate Atlas \(online\)](#)). The aim is here to set up a basis for the comparison of the results with related climate change studies of extreme events. According to the UFOPLAN ([Jacob et al., 2008](#)) days with rainfall above 25mm/day are defined as “wet days”. For the comparability this threshold value could be used as maximum and it is recommended to use at least two more threshold values:

- Number of days with  $15\text{mm/day} \leq \Sigma P^1 \leq 20 \text{ mm/day}$
- Number of days with  $20\text{mm/day} \leq \Sigma P \leq 25 \text{ mm/day}$
- Number of days with  $25\text{mm/day} \leq \Sigma P$

The second approach of using statistical evaluations for the study of extreme rainfall and flood events is less often applied and only some related studies can be referred here (e.g. INKLIM 2012 II plus). The main reasons are the larger uncertainties, which are derived within extreme event simulations with current state of the art climate models ([STARDEX, Final Report, n. d.](#)).

#### **3.4.5 Statistical Evaluations of Extreme Rainfall and Flood Probabilities**

The purpose of the statistical evaluation is, to gain a correlation between the magnitude and frequency of extreme rainfall as well as flood peaks. Approaches for statistical evaluations are recommended in the technical bulletin [ATV-A 121 \(1985\)](#) and [DVWK-101 \(1979\)](#). These guidelines are widely used in practise in Germany. Additionally, approaches for the adjustment of trends, outlier identifications and goodness-of-fit tests are introduced in this methodology. In Fig. 3. 5 the developed procedure of the statistical evaluation of flood peaks as well as extreme rainfall events is illustrated.

---

<sup>1</sup>  $\Sigma P$  = Sum of Precipitation per day [mm/day]

---

The trends in the data series are adjusted to a reference year (3.4.5.1) before a probability distribution curve is computed (3.4.5.2 and 3.4.5.3). Then an outlier test is recommended (3.4.5.4). When the outlier test is positive, due to an outlier which distort the statistical results, the trend adjustments as well as the statistical evaluations have to be calculated again. It is recommended to repeat this procedure till the outlier test is negative, which means there are no outliers identified or the outliers are adequately re-presented in the statistical evaluation.

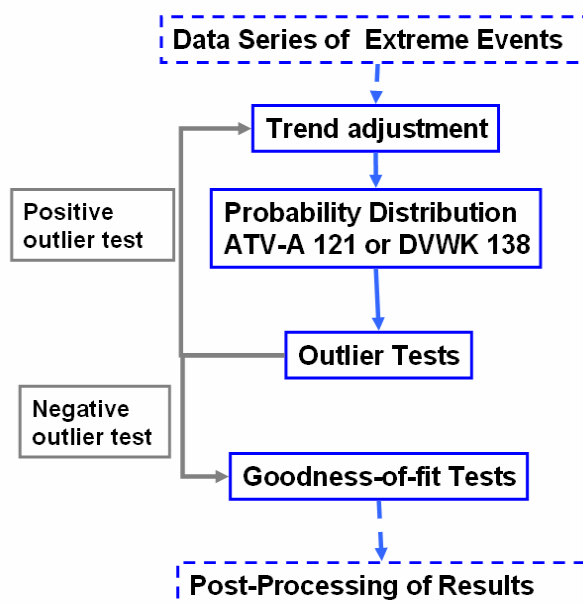


Fig. 3. 5 Developed method for statistical evaluations.

#### 3.4.5.1 Trend Adjustment

Climate variables as well as flood peak data series could display significant increasing or declining trends. In statistical evaluations it is recommended to adjust the trends of the series before computing the probability distribution functions for a reference time (Hänggi & Weingartner, 2009). In the considered time periods of the climate scenarios, different signals of trends could be displayed, which are significant for being taken into account for statistical evaluations.

For example a data series displays an increasing trend from the beginning of the time series to the end. The last date of the time series is taken as reference. Without a trend adjustment the lower data values at the beginning of the data series contribute to a lower statistical result. After a trend adjustment, the values at the beginning of the time series are adjusted according to the displayed increasing trend towards the reference year. In this way a trend adjusted statistical evaluation for the reference date is computed. One approach of a linear trend adjustment calculation is outlined in Attachment 3.1. For observed data series and computed control scenario data series of the past, a trend adjustment to the last year in the series is recommended to define the reference year as close as possible to the today's situation. For the climate change scenarios of the future (e.g. 2040 – 2070) a trend adjustment to the middle of the time period is suggested, to point out the statistical results of the climate period around the reference year.

*3.4.5.2 Extreme Rainfall Probability Distribution Functions*

For statistical evaluations it has to be assured that the extreme rainfall events are independent. With respect to the comparability, observed and computed climate model data series have to be aggregated to equal time steps (e.g. 5min, 1h, 24h) (ATV-A 121, 1985). By the computation of such equidistant data series, extreme rainfall heights are in general underestimated by e.g. division of short term extremes (KOSTRA-Atlas, 1997; ATV-A 121, 1985). Therefore it is recommended to apply the following factors with respect to the required summation intervals:

**Table 3. 1 Correction factors of precipitation data series. (ATV-A 121, 1985)**

| Number of aggregation intervals | 1    | 2    | 3    | 4    | 5    | 6    |
|---------------------------------|------|------|------|------|------|------|
| Correction factor               | 1.14 | 1.07 | 1.04 | 1.03 | 1.03 | 1.02 |

In the ATV-A 121 (1985) as well as in the KOSTRA-Atlas (1997) it is advised to use consistent methods and approaches for extreme rainfall statistical evaluations, which are recommended to be done with ‘partial series’ or ‘yearly series’.

‘**Partial series**’ consists of values above a threshold, independent from the year in which it occurs. The number of values in the partial series (N) should not exceed 3 to 4 times the length of the time period in years (M) (ATV-A 121, 1985).

The other method is based on the use of the maximum value per year and is known as the ‘**yearly series**’. Therewith, a relative low maximal event in one year, which is exceeded several times in other years, is considered as well in the statistical evaluation of extremes (KOSTRA-Atlas, 1997; ATV-A 121, 1985).

For statistical evaluations with partial series a calculation of Exponential-Distributions and with yearly series Extremal-I-Distributions (known as Gumbel Distributions) are recommended. According to the guidelines, both approaches are equally adequate for statistical evaluations of extreme rainfall events (KOSTRA-Atlas, 1997; ATV-A 121, 1985). But the partial series is recommended if the length of the time period in years (M) is smaller or equal to 30 years and when errors occurred in the data series of single years (KOSTRA-Atlas, 1997). The computation of the probability distribution function for extreme rainfall events with partial series is outlined in Attachment 3.2.

Especially for climate change studies, it is important to differentiate between summer and winter extreme rainfall events. It is suggested to compute statistical evaluations of seasonal extreme events as well with partial series covering 3 to 4 times the length of the time period in years (M).

### 3.4.5.3 Flood Peak Probability Distribution Functions

The required data for the statistical evaluations of flood peak probabilities is computed with discharge hydrographs simulated by hydrological models at specific nodes in the network system. It has to be assured that the hydrographs display independent discharge events (DVWK-101, 1979).

A widely used recommendation for the calculation of flood probabilities in Germany has been published in the technical bulletin DVWK-101 (1979) and has been updated in the DVWK-251 (1999). Statistical analysis can be computed with annual maximal flood peaks (yearly series), when data series of at least 30 years are available. But it has to be taken into account that in dry years the maximal flood peak could be smaller than a 2<sup>nd</sup> or even 3<sup>rd</sup> range flood event in a wet year. This variability could distort the statistical results and could be avoided by using the flood peak results above a specific threshold value in the corresponding time period. In this way a partial series is gained which is recommended to be used for data series shorter or equal to 30 year periods (DVWK-101, 1979). It is suggested to define the threshold value according to the smallest maximal yearly peak discharge within the time period of interest and that the number of flood peaks (N) is about five times as large as the number of years (M) in the time period (DVWK-101, 1979).

$$N = 5 * M$$

**eq.3. 1**

But in practice it is prevalent to define the threshold value in that way, that the partial series comprises a number of flood peaks (N), which is two to three times as large as the number of years (M) in the time period (DVWK-101, 1979).

$$N = (2 \text{ to } 3) * M$$

**eq.3. 2**

In this context, for climate periods covering 30 years a number of minimal 60 to 90 discharge peaks shall be taken into account for the statistical evaluation with partial series.

Like for the extreme rainfall event statistical evaluations, it is important to take into account a differentiation between the summer and winter flood peak impacts. For this purpose it is recommended to use a number of at least two to three flood events (N) per winter and summer period for each year in the time period (M).

In contrast to the consistent extreme rainfall probability distribution function recommended by the KOSTRA-Atlas (1997) and the ATV-A 121 (1985), a variety of distribution functions are used in practice for flood peak probability analysis. The

mostly approved approaches are based on the scheme of PEARSON or extremal distributions (DVWK-101, 1979):

- ***Distribution functions based on the scheme of PEARSON:***
  - Pearson, Log-Pearson and Log-Pearson-Type-III-Distribution
  - Normal, Log-Normal and Log-Normal-Type-III-Distribution
  - Weibull and Log Weibull
  
- ***Extremal Distributions:***
  - Gumbel and Log-Gumbel distribution

A comprehensive test of nine distribution functions have been done by Rao & Srinivas (2008) for an analysis of the applicability for flood frequency analysis in a specific region. From the nine distributions the Pearson type III, Log-Normal type III and the Log-Pearson type III distributions came out with the best statistical distribution results.

The flood frequency analysis with the Log-Pearson Type III Distribution is recommended as well by the U.S. Water Resources Council (Fang et al., 1994) and the DVWK-101 (1979). At the Institute of River and Coastal Engineering at the TUHH in Hamburg a software application has been developed in the JAVA programming language for flood frequency analyses (Yao Hu, 2008). Implemented are the statistical calculations with the Log-Pearson-Type-III-Distribution and the Log-Normal-Type-III-Distribution including a Goodness-of-Fit test with the Kolmogorov-Smirnov method (see 3.4.5.5).

This tool is applicable for statistical analysis of flood probability changes derived in climate scenarios. But further processing work is required to gain a direct comparison of the probability distribution curves for climate change scenarios. The statistical results of flood frequencies of interest can only be computed for each scenario and data series separately. The data could be collected in pivot tables of a spreadsheet application like the software “Excel” provided by Microsoft Office or “Calc” by Open Office. Here the results of the separate flood frequency distributions can be further processed and compared. The empirical distribution can not be transferred from the statistical tool to a spreadsheet application, but could be calculated with the following equation (Yao Hu, 2007):

$$T = \frac{M}{N} * \frac{1}{1 - \frac{k}{(N+1)}}$$

with :

- k = Index of the flood event
- N = Number of flood events
- M = Length of the time period [a]
- T = Return period of the flood peak [a]

eq.3. 3

### *Extrapolation of results*

An extrapolation of the statistical results should not exceed 2 to 3 times the length of the considered time period in years (DVWK-101, 1979). In climate change studies a time period of about 30 years is mostly defined (see chapter 2). Therewith an extrapolation of the results up to a probability of occurrence of once in 60 to 90 years is supported. Further extrapolations involve a higher rate of uncertainties and the plausibility of the results has to be discussed (DVWK-101, 1979).

#### *3.4.5.4 Outlier Tests*

According to the technical bulletin [ATV-A 121 \(1985\)](#) exceptional high or low values in data series could 'distort' the statistical evaluation of the main data series. Such extreme values are defined as outliers and have to be analysed separately. In the [ATV-A 121 \(1985\)](#) three types of outliers are itemised:

- Outliers derived by systematic errors: The exceptional value is derived from an incorrect or inaccurate measurement or computation, which has to be corrected or if not possible, it has to be taken out from the data series.
- The outlier displays an event with a very low probability of occurrence, which exceeds the extent of the data series and is not appropriately displayed in the distribution curves. These outliers distort the statistical results and have to be handled separately.
- The outlier is displayed with an adequate probability of occurrence in the data series and the overall statistical evaluation of the probability distribution curve is represented. In this case the outlier (exceptional value) has to be taken into account for the statistical evaluation.

### *Identification of outliers:*

It has to be assured that the exceptional value is not caused by incorrect measurements, which is the first type of outlier described by the bulletin [ATV-A 121 \(1985\)](#). When this is not the case, the identification of outliers can be done according to experiences, results of other data series which are comparable or with mathematical identification tests.

For continual data series with a number of values of  $(N) \leq 29$ , the mathematical Dixon Test and for  $(N) \geq 30$ , the Grubbs Test is recommended (Durner, 1999). Due to the length of data series for climate change scenario studies of at least 30 years, the Grubbs-Test is considered as relevant outlier test in this methodology.

### *Grubbs Test*

The Grubbs Test is based on the assumption that the data series can be reasonable approximated by a normal distribution (NIST, 2006). It displays the highest deviation

---

between the exceptional value ( $Y_{i,max}$ ) and the sample mean ( $\bar{Y}$ ) divided by the standard deviation ( $S$ ) of the data series. The test value ( $G$ ) is calculated with the following equation (NIST, 2006):

$$G = \frac{Y_{i,max} - \bar{Y}}{S}$$

eq.3. 4

The calculation of the sample mean value ( $\bar{Y}$ ) is done with the number of values in the data series ( $N$ ) and the respective value of the data series ( $Y_i$ ) (adopted from DVWK-101, 1979):

$$\bar{Y} = \frac{1}{N} * \sum_{i=1}^N Y_i$$

eq.3. 5

The calculation of the standard deviation ( $S$ ) is done with the equation adopted from DVWK-101 (1979):

$$S = \sqrt{\frac{1}{N-1} * \sum_{i=1}^N (Y_i - \bar{Y})^2}$$

eq.3. 6

The significance level ( $\alpha$ ) has to be selected (e.g. 0.001 or 0.005) which defines the respective critical value ( $\alpha_t$ ) in the table of the DIN 53 804 attached to the thesis (Attachment 4). If the difference ( $\Delta G$ ) between the test value ( $G$ ) and the critical value ( $\alpha_t$ ) is larger than zero ( $\Delta G > 0$ ) the exceptional value is defined as outlier.

$$\Delta G = G - \alpha_t$$

eq.3. 7

### ***Dealing with outliers:***

After the identification of outliers with the recommended Grubbs Test, it has to be discussed, if the outlier distorts the results of the statistical evaluation (outlier type 2; ATV-A 12, 1985) or should be taken into account for the probability distribution function (outlier type 3; ATV-A 121, 1985). At this, careful consideration is required by neglecting outliers in statistical evaluations (NIST, 2006).

An example of a too fast reliability on the outlier test result and deleting outliers which had been very important for the statistical result is the detection of the hole in the ozone layer. Researchers relied on the results of computer programs which eliminated outliers with mathematical methods. It is assumed that the hole in the ozone layer would have been detected earlier, if outliers would not have been deleted (Durner, 1999; Schendera, 2007).

Outliers are important for the probability distribution when they are displayed with a corresponding larger probability of occurrence. If this is the case, the outliers shall be included in the statistical data series. Experience and results of comparable projects are helpful to decide about the adequate handling of outliers.

When an **outlier test is positive**, which means the outlier shall be neglected from the statistical evaluation, the trend adjustment as well as the statistical distribution function has to be calculated again. It is recommended to repeat this procedure till the **outlier test is negative**, which means that there are no outliers identified or the outliers are adequately represented in the statistical evaluation.

### 3.4.5.5 Goodness-of-Fit tests

To test the accuracy of the distribution functions, several statistical tests could be applied (Rao & Srinivas, 2008). Recommended are the Chi-Square Test, the Anderson-Darling Test or the Kolmogorov-Smirnov Test in order to verify the fitting of the distribution curves (NIST, 2006; Rao & Srinivas, 2008).

The tests are based on analysing the distribution of the average behaviour of the probability curve (NIST, 2006). But for the statistical analysis of extreme events it is more important to analyse the adequacy of the curve for extreme events. For this purpose it is important that the empirical distribution of the extreme events is computed and illustrated in graphs together with the calculated theoretical distribution functions. In this way it is possible to find out the distribution function, which fits best. The calculation of the empirical distribution of rainfall extremes is provided in Attachment 3.2 and for flood probabilities in (eq. 3.3).

## 3.5 Post-Processing of Scenario Results

The magnitude of climate change impacts can not be derived by comparing directly the computed future climate scenario results with observed data series, but has to be calculated in correlation to the control scenario data results (3.5.1). With the computed magnitude of change, climate change factors (CCFs) can be calculated (3.5.2) and design events for post-impact studies can be defined (3.5.3).

### 3.5.1 The Magnitude of Climate Change Impacts

The change in extreme rainfall and flood peak events can be calculated with the difference between the climate change scenarios and the computed control scenario. On the one hand the *percentage change* of the extreme rainfall [mm/D] or flood peak [m<sup>3</sup>/s] ( $\Delta H_{T,C,[\%]}$ ) per return period (T) and under climate change conditions (C) can be calculated, or the *absolute value* of change ( $\Delta H_{T,C,abs}$ ) can be computed. In both approaches the magnitude of change has to be referred to the observed data series of the past ( $H_T$ ) to obtain the projected extreme event ( $H_{T,C}$ ) under climate change conditions.

The calculation of the percentage change of the extreme rainfall or flood peak per probability of occurrence ( $\Delta H_{T,C,[\%]}$ ) is depicted in eq.3. 8. The difference between the extreme precipitation height ('HP' in mm/D) or flood peak ('HQ' in m<sup>3</sup>/s) with a return period (T) computed in an IPCC climate change scenario ( $H_{T,IPCC-scenario}$ ) and the respective extreme event computed with the control scenario data of the past ( $H_{T,control-scenario}$ ) is calculated.

$$\Delta H_{T,C,[\%]} = \frac{(H_{T,IPCC-scenario} - H_{T,control-scenario})}{H_{T,control-scenario}} * 100 \quad [\%]$$

**eq.3. 8**

The calculation of the magnitude of the extreme event with a return period (T) ( $H_{T,C,[\%]}$ ) is displayed in eq.3. 9. The percentage change of the extreme event per return period ( $\Delta H_{T,C,[\%]}$ ) is referred to the extreme event computed with observed data series ( $H_T$ ).

$$H_{T,C,[\%]} = H_T * \left( 1 + \frac{\Delta H_{T,C,[\%]}}{100} \right) \quad [\text{mm/D}] \text{ or } [\text{m}^3/\text{s}]$$

**eq.3. 9**

In the second approach, the magnitude of change ( $\Delta H_{T,C,abs}$ ) is computed with the absolute difference between the extreme event with a return period (T) computed in an IPCC climate change scenario ( $H_{T,IPCC-scenario}$ ) and the corresponding extreme event computed in the control scenario of the past ( $H_{T,control-scenario}$ ).

$$\Delta H_{T,C,abs} = H_{T,IPCC-scenario} - H_{T,control-scenario} \quad [\text{mm/D}] \text{ or } [\text{m}^3/\text{s}]$$

**eq.3. 10**

The absolute value of change of the extreme event ( $\Delta H_{T,C,abs}$ ) is added to the extreme event with a return period (T) computed with observed data series ( $H_T$ ) to calculate the projected magnitude of the extreme event ( $H_{T,C,abs}$ ) under climate change conditions.

$$H_{T,C,abs} = H_T + \Delta H_{T,C,abs} \quad [\text{mm/D}] \text{ or } [\text{m}^3/\text{s}]$$

**eq.3. 11**

### **3.5.2 Computation of Climate Change Factors (CCFs)**

With the computation of climate change factors (CCFs) and statistical evaluations of observed data series ( $H_T$ ), it is possible to obtain the respective extreme rainfall or flood peak events ( $H_{T,C}$ ) for future climate scenarios (C) for further locations in the study area. In this thesis an approach has been developed to calculate the CCF with the average change of an ensemble of scenario study results. It is indicated here as

**Averaging Ensemble CCF** ( $f_{T,C}$ ), which has been derived on the basis of the following equation (eq.3. 12) indicated in [Katzenberger \(2004\)](#).

$$H_{T,C} = f_{T,C} * H_T$$

**eq.3. 12**

CCFs are restricted to be used in the project area where it has been computed. The factor can be calculated with both approaches displayed in 3.5.1. In the percentage change approach, the average over the number of scenario study results ( $n$ ) of the differences of the events per return period ( $\Delta H_{T,C,[\%],n}$ ; eq.3. 8) is calculated.

$$f_{T,C} = \frac{\sum_{n=i}^n \left[ 1 + \frac{(\Delta H_{T,C,[\%],n})}{100} \right]}{n}$$

**eq.3. 13**

In the absolute change approach, the difference between the extreme event under climate change conditions  $H_{T,C,abs}$  (eq.3. 11) and the observed statistical results ( $H_T$ ) is divided by the observed statistical results ( $H_T$ ). And the average is calculated of all scenario study results ( $n$ ).

$$f_{T,C} = \frac{\sum_{n=i}^n \left( 1 + \frac{|H_{T,C,abs,n} - H_{T,n}|}{H_{T,n}} \right)}{n}$$

**eq.3. 14**

### **3.5.3 Design Events for Post-Impact Studies**

For the planning of measures, design conditions have to be determined. Such design conditions are for example the ‘design wave’ for dike constructions or the maximal number of persons with an overall weight, who are allowed to step into an elevator. Different approaches can be used to determine design conditions, e.g. regulations by law, maximal acceptable risk of damages and specific hazards.

It is recommended that at least for the climate scenario with the largest increase in frequency and magnitude of climate change impacts, design rainfall and flood events are created for further post-impact studies of adaptation measures. The changed design conditions are calculated with the magnitudes of change (3.5.1) and with the climate change factors (3.5.2).

#### ***Criteria for deriving design events***

A design flood or rainfall event for further studies could be a calculated (“synthetic”) event or a representative event observed in the past. In this context, a seasonal differentiation of representative design events is recommended. For example, it could be distinguished that summer events are characterised by short term intense rainfall causing high flood peaks, but a lower overall discharge volume, and that winter

rainfall events are defined by a lower intensity, but longer durations, which derives lower discharge peaks, but come along with a larger overall discharge volume.

In this methodology an approach to select a representative observed event is outlined. It is suggested to prefer the largest rainfall or flood event in the data series, if it is defined as representative. Additional criteria are derived, when the scenario study flood event shall be used as well for the adjustment of the representative design rainfall event. In this case the duration of the observed rainfall event shall correspond to the duration of the design conditions. For the adjustment of the magnitude or intensity of the derived design event, matching coefficients have to be calculated.

### ***Calculation of matching coefficients***

Two main strategies can be pursued. In the first approach the matching coefficient is defined with respect to calculate a ***design rainfall event*** with a specific probability of occurrence. In the second approach, the matching coefficient is defined with regard to simulate ***design flood events*** with a specific probability of occurrence. In both approaches the matching coefficients are applied on the rainfall data series for the hydrological simulations of post-impact studies.

In the first approach, the matching coefficient is iteratively calculated for adjusting observed rainfall heights ( $HP_D$ ) with a specific duration ( $D$ ) to the respective design rainfall intensity derived under climate change conditions ( $HP_{D,T,C}$ ).

In the second approach, the matching coefficients have to be obtained by iterative flow simulations with the hydrological model and adjusted rainfall intensities. For this purpose the overall catchment is divided into areas, which drain to specific nodes of interest, and for which the specific matching coefficient can be assigned to simulate design flood events.

## **3.6 Post-Impact Studies to Mitigate Climate Change Impacts on Flood Probability**

It has been defined as an open and required task to develop software tools for modelling sustainable drainage systems (SUDS) as flood probability reduction measures. A variety of state of the art SUDS elements are listed in 2.2.2. It has been detected that modelling green roofs is supplied by only two of the six studied hydrological software tools (Hellmers, 2009), although the effectiveness could be assumed to be significant. Therefore, a focus has been set on modelling the hydrological effectiveness of green as well as brown roofs which can be combined by draining into swales and swale-filter-drain systems.

The developed theoretical approach for modelling SUDS elements is outlined in 3.6.1. For the first verification of the SUDS simulations, testing criteria have been

defined (3.6.2) and in the context of climate change impact studies, a methodology has been derived to set up a variety of future adaptation scenarios with SUDS (3.6.3). For the planning and simulation of SUDS, the main design criteria and the restrictions of their spatial distribution are summarized in 3.6.4.

### 3.6.1 Theoretical Approach to Model SUDS

From a hydrological perspective, SUDSs function like hydrological retention and translation elements in sub-catchments. In this context, the main focus of the developed theoretical approach is set on representing the hydrological retention and horizontal as well vertical water flow processes in SUDS elements.

For this purpose, SUDS elements are divided in layers to simulate the specific infiltration, percolation, evaporation and storage effects. First the developed theoretical approach for green roofs will be explained which is used as well for modelling brown roofs with different soil material or aggregate and without vegetation. Thereafter, the theoretical approach for swales and swale-filter-drain systems will be outlined shortly, which are used for simulating SUDS combinations.

#### 3.6.1.1 Green Roofs

Green roof elements can be subdivided into three main layers: the storage layer, the substrate layer and the filter layer (Fig. 3. 6).

The storage layer is indicated as the first layer in the theoretical approach, where vegetation can be planted. To prevent the overloading of the green roof, an overflow pipe is installed with the height ( $h_{ov}$ ) and above the edge of the overflow pipe a freeboard is provided. The second layer is defined as a substrate layer with top soil. On the plane roof, a filter layer is constructed to drain the water to the down pipe. Below this layer, a root protection and insulation fabric is placed to prevent leakage through the roof.

The change of the soil water content ( $\Delta sw$ ) per time step ( $\Delta t$ ) in the layers is balanced with the continuity equation (eq.3. 15), which is applied for each layer with respective parameters.

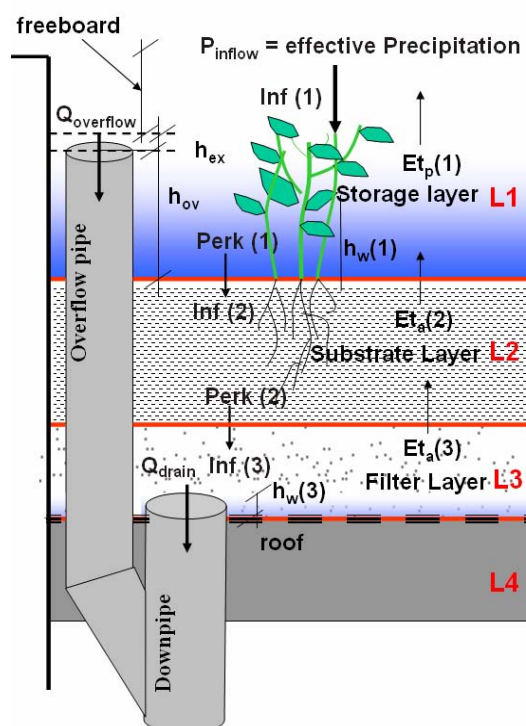


Fig. 3. 6 Concept of the layer theory for green roofs. (published earlier in Brüning & Hellmers, 2009)

$$\frac{\Delta sw(t)[l/m^2]}{\Delta t} = \frac{Inf(t)[l/m^2] - perk(t)[lm^2] - ET_{a/p}(t)[l/m^2]}{\Delta t} - \frac{Q_{outflow}(t)}{A_{greenroof}} \left[ \frac{1}{m^2 * \Delta t} \right]$$

eq.3. 15

The potential inflow (Inf) into the layers is defined as the effective precipitation in the storage layer (L1) and as potential infiltration in the substrate (L2) and the filter layer (L3). The water content which can percolate into the layers below (perk) is the percolation (perk(1)) from the storage layer (L1) into the substrate layer (L2) and the percolation (perk(2)) from the substrate layer (L2) into the filter layer (L3). The percolation (perk(3)) from the filter layer has to be set to zero with respect to the insulation layer on the roof. In the storage layer (L1) the potential evaporation (Et<sub>p</sub>(1)) from the stored water and in the soil layers, the actual evapotranspiration (Et<sub>a</sub>(2)) and (Et<sub>a</sub>(3)) with respect to the vegetation are calculated respectively. Additionally, an outflow through the overflow pipe (Q<sub>outflow</sub> = Q<sub>overflow</sub>) in the storage layer (L1) and the outflow through the rainfall down pipe in the filter layers (Q<sub>outflow</sub> = Q<sub>Down pipe</sub>) reduces the retained water on the green roof.

The overflow from the storage layer (Q<sub>overflow</sub>[mm<sup>3</sup>/s]) depends on the water level (h<sub>ex</sub>[mm]) exceeding the height of the overflow pipe (h<sub>ov</sub>[mm]). The effective minimal (MIN) overflow, is computed with two approaches. On the one hand the inflow into the pipe is calculated with the Poleni equation with the water level above the pipe (h<sub>ex</sub>[mm]), the perimeter of the pipe (d<sub>pipe</sub>[mm]) and the coefficient (μ). According to the technical bulletin [BWK \(1999\)](#) the coefficient μ displays the resistance of the flow from the retained water in the storage layer into the overflow pipe. For the overflow heights (h<sub>ov</sub>[mm]), which are larger than the bottom of the storage layer, the coefficient μ is set to 0.480 ([BWK, 1999](#)). On the other hand the flow is limited by the maximum capacity of the pipe which is calculated according to the Colebrook-White approach with the flow resistance (λ).

$$Q_{overflow}(t) = \text{MIN} \begin{cases} \frac{2}{3} * \pi * d_{pipe} * \mu * \sqrt{2 * g * (h_{ex})^3} & \text{Poleni Approach} \\ \frac{\pi * (d_{pipe})^2}{4} \sqrt{\frac{2 * g * d_{pipe}}{\lambda}} & \text{Colebrook-White Approach} \end{cases}$$

eq.3. 16

The drainage through the down pipe begins when free movable water is accumulated in the filter layer, which exceeds the field capacity of the soil layer. Due to backwater effects at the down pipe a water level (h<sub>w</sub>(3)) is formed. The effective flow through the down pipe is the minimal discharge calculated according to the Poleni equation by taking into account the soil porosity and the maximum capacity of the rainfall down pipe (eq.3. 16). For the Poleni equation in the drainage layer a coefficient of

$\mu=0.577$  is defined for overflow heights of zero according to [BWK \(1999\)](#). The derivation of the equations is given in the Attachment 5.11.

### 3.6.1.2 Swales and Swale-Filter-Drain Systems

The theoretical approach for modelling swales and swale-filter-drain systems have been developed in the Institute of River and Coastal Engineering at the TUHH in the scope of the project “Development of the Decision Support Tool Kalypso-Planer-Client” supported by the Agency for Roads, Bridges and Waters (LSBG) in Hamburg ([Brüning & Hellmers, 2009](#)). These concepts are based as well on the deviation of the SUDS element into respective layers. A swale is computed with a storage layer (L1) and a base layer (L2). A swale-filter-drain system is divided into four layers: the storage layer (L1), the colmation layer (L2), the filter layer (L3) and the base layer (L4). The concepts of the layer theory for swales and swale-filter-drain systems are illustrated in Fig. 3. 7 and Fig. 3. 8.

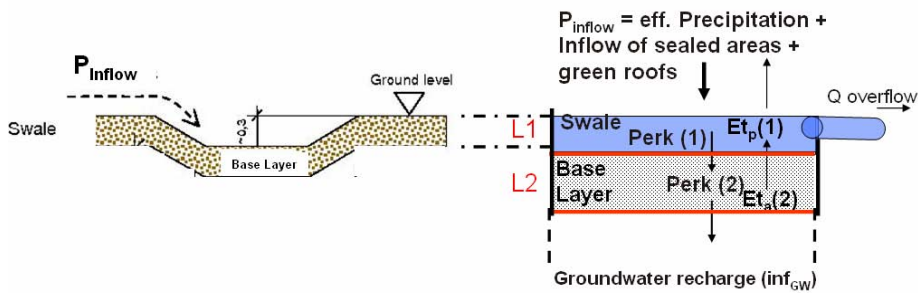


Fig. 3. 7 Concept of the layer theory for swales. (adopted from [Brüning & Hellmers, 2009](#))

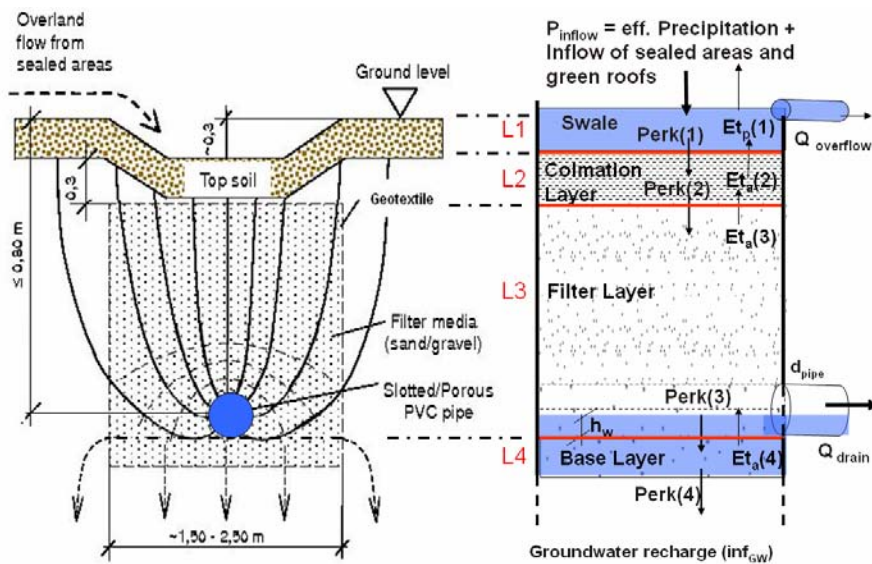


Fig. 3. 8 Concept of the layer theory for swale-filter-drain systems. (adopted from [Brüning & Hellmers, 2009](#))

The water level in the swale is dependent on the inflow and outflow components. The balance of the soil water content (sw) in the layers is based on a continuity equation like displayed for the green roof element, but the inflow ( $P_{inflow}$ ) includes

additionally the discharge from drained sealed areas and it is possible to drain the outflow from green roofs into swale elements additionally.

The accumulation of water in the swale systems depends on the actual and potential percolation as well as on the infiltration between the layers. If the percolation rate into the substratum exceeds the infiltration capacity ( $inf_{GW}$ ), water is retained in the base layer. With respect to the swale element the base layer is defined as the second layer (L2) and for the swale-filter-drain system it is the fourth layer (L4).

The flow through the drain pipe of a swale-filter-drain system begins, when the base layer is saturated and when water is accumulated in the filter layer above the field capacity. The flow into the perforated drain pipe is calculated according to the Poleni approach, like for the green roof modelling theory, by taking into account the soil porosity and the Colebrook-White approach (eq.3. 16 and Attachment 5.11). When the storage capacity in the swale systems is reached the exceeding water volume is drained through an overflow pipe.

### 3.6.2 Criteria for Testing the Approach

The testing of the approach is based on two methods. First method focuses on the overall water balance in the SUDSs. The water balance calculation comprises the inflow and the outflow components as well as the change of retained water in the SUDS elements.

In green roofs, the inflow water volume is the effective rainfall on the roof area and the outflow volume consists of the potential evaporation from the storage layer, the evapotranspiration from soil layers and the drainage through outlet pipes.

The inflow into swales and swale-filter-drain systems comprises additionally the drainage from sealed areas and eventually from green roofs. The outflow processes are defined by the evaporation from the storage layer, the evapotranspiration from soil layers, the percolation into the ground and the overflow from swales in case, the storage capacity is reached. In the swale-filter-drain system an additional outflow process is included, namely the flow through the drain pipe in the filter layer.

In the second approach, the temporal dependency of the soil moisture formation and the flow processes is analysed, with regard on reached field capacities in soil layers, which enables free moveable water and the temporal occurrence of maximums of the flow processes as well as water contents.

Field tests with constructed scale models could not be dealt with in the scope of this thesis.

### 3.6.3 Combination of Adaptation Measure Scenarios

For the assessment of the hydrological effectiveness of SUDS to mitigate the projected future impacts on flood probability in SUCAs, a variety of scenarios are recommended to be considered. For this purpose a methodology has been developed to handle the complexity of scenario set ups in Fig. 3. 9.

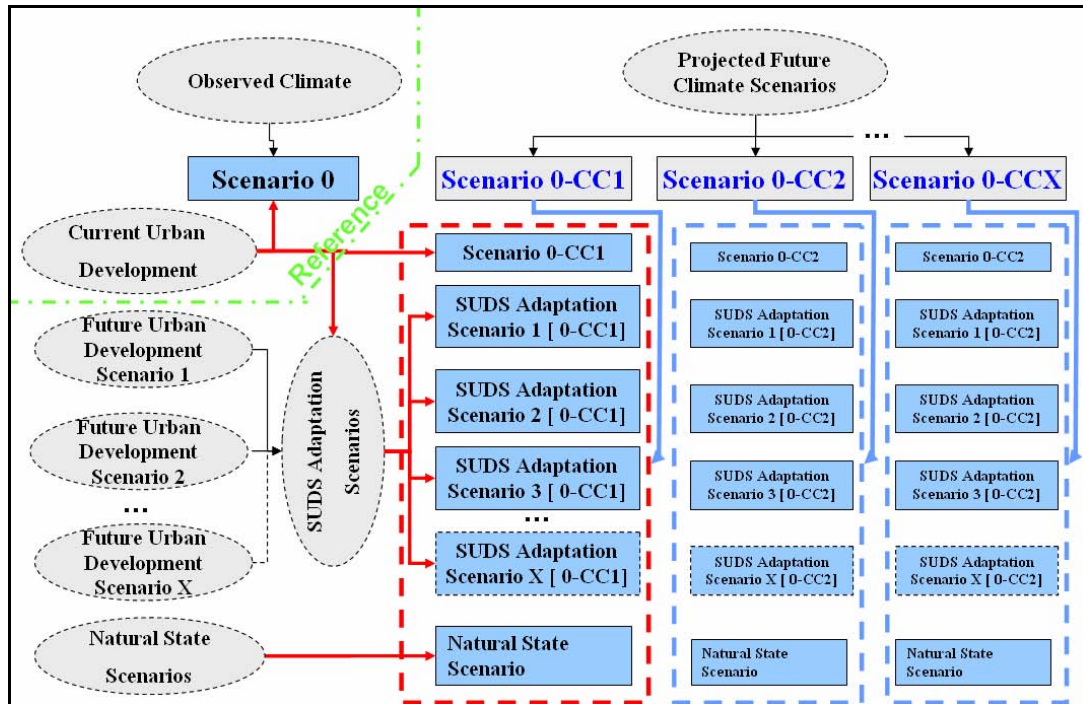


**Fig. 3. 9 Complexity of Climate Scenarios (0-CCX), SUDS Adaptation Scenarios and Future Urban Development Scenarios.**

The scenario set up is derived from the top down with climate scenarios and from the left, with urban development scenarios. From both sides a ‘reference scenario’: observed climate (Scenario 0) and current urban development, provides the basis of comparison for any scenario study.

In the next step, impacts derived by future climate scenarios (0-CCX) can be investigated, which could be derived with IPCC scenarios (e.g. A1B, B1 or A2 = ‘CCX’). On the other hand, future urban developments could be projected with changes in sealing rates in SUCAs and including the implementation of SUDS. But SUDS measures are not necessarily only possible to be implemented in ‘future’ urban developments, but are possible to be planned as well in the current state urban development as indicated in Fig. 3. 9. Additionally, it is possible to simulate natural state scenarios by changing the land use of the catchment into e.g. green fields and forests.

With the variety of climate, urban development and SUDS adaptation scenarios, a complex structure of scenario studies is derived. The scenario set ups considered as significant to be analysed in more detail for the assessment of the effectiveness of SUDSs are indicated in Fig. 3. 9 with red arrows (‘→’).

For the simulation of the reference situation with and without the impacts by climate change, the following two scenarios have to be created without SUDS:

1. Scenario 0 (Current urban development without SUDS)
2. Projected Future Climate Scenario 0-CC1 (Current urban development without SUDS)

For the simulation of SUDS the following adaptation scenarios with (a) single SUDS measures and (b) combined SUDS measures are suggested:

a) Scenarios with single SUDS measures:

3. SUDS Adaptation Scenario 1: Green Roofs
4. SUDS Adaptation Scenario 2: Swales
5. SUDS Adaptation Scenario 3: Swale-filter-drain systems
6. SUDS Adaptation Scenario 4: Unsealing

b) Scenarios with combined SUDS measures:

7. SUDS Adaptation Scenario 5: Combined SUDS Scenario: (e.g. green roofs draining into swales)

A focus has been set on the effectiveness of SUDS to reduce the peak runoff from sealed areas. Therefore it is necessary to define as well the maximum potential reduction under climate change conditions in a scenario of a complete natural state.

8. Climate Change Natural State Scenario

The complexity of the defined scenarios with a variety of ‘SUDS Adaptation Scenarios X’ can be broadened by a selection of ‘Future Urban Development Scenarios X’. This complex combination of scenarios is planned to be studied in further KLIMZUG-Nord projects, but the set up of future urban development scenarios are not worked out in detail in the scope of this thesis.

### **3.6.4 Planning Criteria for Sustainable Drainage Systems**

#### *3.6.4.1 Restrictions of Spatial Distribution*

Planning of SUDS is constrained by local characteristics, which limit the potential spatial distribution. The drainage of rainfall water into receiving rivers as well as the infiltration of water into the ground is defined as utilisation of water bodies in the Act on Managing Water Resources (WHG, 2002). Any negative impacts on the flow velocity as well as quality of receiving waters have to be prevented. The same is stated for impacts on the quality of the soil and the groundwater, especially in water protection zones (WHG, 2002; BBODSCHG, 1998).

#### ***Water protection zones:***

Before planning infiltration facilities, the location of water protection zones has to be detected. Water protection zones are mostly defined in the reach of wells for drinking water supply.

### ***Restriction of rainfall water quality for infiltration:***

For the acceptability of infiltrating rainfall water into the ground, a classification of the water quality from different surface covers has been defined in the technical bulletin [DWA-A 138 \(2005\)](#). The qualitative evaluation is done according to (1) harmless, (2) tolerable and (3) not tolerable water quality. On the basis of this generally accepted definition, federal states and communities in Germany define local regulations for the required quality of rainfall water for infiltration.

### ***Hydrogeological and soil characteristics:***

In-situ soil types with permeability coefficients (kf) larger as  $10^{-6}$ m/s and smaller than  $10^{-3}$ m/s are recommended for infiltration devices ([Röttgers, 2006](#)). Soil types made up of stones and gravel (kf > $10^{-3}$ m/s) are not adequate for the infiltration of rainfall water into the ground due to the too short retention time to assure an appropriate rate of purification ([Röttgers, 2006](#); [DWA-A 138, 2005](#)). Silty or clayey soil types with a permeability coefficient smaller than  $10^{-6}$ m/s are not adequate as well, due to a too low infiltration potential ([Röttgers, 2006](#); [DWA-A 138, 2005](#)). According to the in-situ soil types, specific SUDS measures are recommended by the Ingenieuresellschaft Prof. Dr. Sieker mbH (see [Sieker, 2005](#)).

A minimum depth to the groundwater is required to assure a sufficient leakage path for the purification ([Röttgers, 2006](#)). As stated in the [DWA-A 138 \(2005\)](#), a depth of at least 1m should be available. Exceptionally, the required leakage path can be less than 1m but should be at least 0.5m ([DWA-A 138, 2005](#)). It has to be considered that the flow direction of the infiltrated rainfall water into the ground does not cause water logging or backwater effects in the soil horizons ([Röttgers, 2006](#)). This is especially important close to buildings with cellars.

### ***Site topographical characteristics:***

Restrictions for the planning of SUDS have to be taken into account for areas with higher slopes. Therefore information about the topographical characteristics has to be provided for the planning ([DWA-A 138, 2005](#)).

### ***Landuse types:***

The distribution of flat and slightly pitched roofs has to be determined for the planning of green or brown roofs. Further on, the spatial distribution of green spaces and sealed areas have to be determined for the planning of infiltration devices. It has to be clarified if the available free spaces are adequate for the planning of SUDS locally or if it is necessary to implement larger conveyance systems.

#### *3.6.4.2 Design Criteria of SUDS Measures*

The main design criteria for green roofs, swales and swale-filter-drain systems will be summarized here and for further SUDS techniques references in literature will be provided.

**Green roofs**

There are two major types of green roofs. The differentiation has been made between extensive and intensive green roofs. On extensive green roofs, low growing vegetation are planted with high regeneration potential like moss, herbs and grass. The maintenance of this type of green roof is reduced to about once or twice a year (Optigruen, 2009). On intensive green roofs, larger types of vegetation are planted dependent on the set up of the layers and it is possible to install recreation facilities (e.g. benches, tables). The maintenance requirements are higher than for extensive green roofs.

For the construction of these types of green roofs different materials and layer depths are required. According to Röttgers (2006) layers with a thickness of 4cm to 19cm are recommended for extensive green roofs which are applicable to be installed on existing buildings. The weight is between 55kg/m<sup>2</sup> and 150kg/m<sup>2</sup>. Intensive green roofs are provided with layers of about 15cm up to 200cm, which results in loads of up to 350kg/m<sup>2</sup> (Röttgers, 2006). Green roofs can be installed on roof pitches between 0° and 40° (Röttgers, 2006).

The thickness of the substrate layer depends on the type of use and planting on the green roof. It should be light weight and serve as nutrient supply (DIY Leaflet, 2007). For preventing particles from clogging up the pores in the filter layer, a fabric shall be installed. The filter layer can be made up from a plastic or coarse mineral material like gravel, pumice or expanded shales. About 300m<sup>2</sup> of vegetated roofs can be sufficiently drained per down pipe of a diameter of 100mm (DN<sub>100</sub>) (Optigruen, 2009). In contrast to non vegetated roofs the required drainage capacity is significantly reduced. In Germany down pipes of non-vegetated roofs shall be designed to discharge a rainfall volume of 60 to 100 l/(h\*m<sup>2</sup>) (Vollmer, 2008). The following standard values are defined in Germany:

**Table 3. 2 Standard drained roof area per outlet pipe in Germany.**

| Drained area of non – vegetated roofs per pipe (Lorz, n.d.; Vollmer, 2008) | Diameter of down pipe |
|--|-----------------------|
| 40 m <sup>2</sup>  | 60 mm                 |
| 80m <sup>2</sup>   | 80mm                  |
| 150m <sup>2</sup>  | 100mm                 |
| 270m <sup>2</sup>  | 125mm                 |
| Drained area of vegetated roofs per pipe (Optigruen, 2009)                 | Diameter of down pipe |
| 300m <sup>2</sup>  | 100mm                 |

**Swales and Swale-Filter-Drain Systems**

It is recommended to limit the storage height in swales and swale-filter-drains to a maximum of 30cm to prevent the silting up of the top soil layer and to preserve the habitat for vegetation (DWA-A 138, 2005). Underneath a swale, a top soil cover is constructed with a depth of about 10cm to 30cm (Röttgers, 2006). In case of swale-

filter-drain systems the top soil cover has the function of a colmation layer. It shall be designed with a lower permeability as the filter layer. In this way, the infiltration into the filter layer is controlled and particles as well as pollutants are retained in the colmation layer. In soils of less purification capability, the top soil or colmation layer should be at least 20cm. It is recommended that the drained sealed area ( $A_u$ ) should not exceed 20 times the swale area ( $A_s$ ) in silty soils (DWA-A 138, 2005). According to the DWA-A 138 (2005) distances to the buildings have to be assured to prevent water logging. The distance to cellars should be about 1.5 times the depth of the cellar, but at least 0.5m. Conveyance systems to drain the runoff from sealed areas into swales should be provided with shallow open paved trenches (Röttgers, 2006).

### ***Unsealing***

Unsealing techniques allow rainfall water to pass through the structure of the surface cover and have a positive effect on the microclimate and evaporation as well as the groundwater recharge rate. In residential areas, pavements with larger joints or composite pavement with infiltration openings are recommended. In commercial areas, unsealing of surface covers could be done with water permeable surfaces like porous concrete which are designed for heavier loads (Röttgers, 2006). Unsealing surface covers used for specific purposes and loads are recommended by the Ministry of Environment and Transport in Baden-Württemberg (UMBW, n. d.). In this way, parking places, pedestrian areas, roads and blind arrays can be provided with unsealed surface covers. According to the DWA-A 138 (2005) unsealing measures are not regarded as infiltration devices, which fall under the relevant infiltration techniques described by the WHG (Röttgers, 2006). The reduction of the runoff coefficients from unsealed covers are listed in ATV-DVWK-A117 (2001) and ATV-DVWK-M 153 (2000).

Further SUDS devices comprise rainwater harvesting measures, infiltration filters, drains, soakaways, retention ponds and wet lands. Details about the construction, maintenance and examples of the design are given in Röttgers (2006), DWA-A 138 (2005), Sieker et al. (2006), Kellagher & Laughlan (2005) and UMBW (n. d.).

#### *3.6.4.3 Design Storm Conditions*

For the planning of SUDS, design storm conditions have to be defined. According to the DWA-A 138 (2005) and Sieker (2006), the design of SUDS has to be based on (at least) a rainfall event with a probability of occurrence of once in 5 years ( $HP_5$ ) and a specific duration. The design of the SUDS technique is considered as adequate when the overflow of the SUDS systems does not begin with the design rainfall event. On the other hand it has to be taken into account that the size of the SUDS measures is not over-designed to assure an economical design. The calculation of design rainfall events for climate change impact studies is outlined in 3.5.3.

### **3.7 Comparative and Uncertainty Studies**

The range of varying results is especially large for projections of extreme events like urban flooding, which induce the demand for comparative and uncertainty studies (Handmer et al., 1999; Feyen & Dankers, 2009; Fowler et al., 2007).

In comparative studies the reasonability and appropriateness of scenario study results are discussed, with outcomes of related climate research projects. For this purpose it is advisable, that the studies are based on corresponding future climate periods, an equal range of IPCC scenarios, the data of the same climate models and comparable study areas.

In the context of uncertainty studies, the word ‘uncertainty’ can have different meanings. First it can be defined as ‘spread’, or secondly as ‘distance’ between the actual value to be predicted and its prediction. But uncertainty is not a measure of forecast quality as it is not possible to claim that the future climate will lie between projected scenario boundaries. Therefore ‘uncertainty’ is defined here as ‘spread’ of options which generate a range of uncertainty like done by Déqué et al. (2007).

In EU funded projects like CLAVIER, PRUDENCE, STARDEX, and BALTEX<sup>1</sup> uncertainties of future climate change impacts are discussed. The derived sources of uncertainties can be regarded as elements of a chain, where one element affects as well the other elements. Not all sources of uncertainties have been discussed in research projects and some are considered to cause a higher degree of uncertainty than others (Fowler et al., 2007; Déqué et al., 2007).

Uncertainties spread out while passing through the model chain, which increases the range of possible results. The outcomes of a specific model run have to be discussed in the context of the numerous assumptions at every stage of the model chain (BMVBS, 2007). The complexity of the uncertainties in the model chain and their linkages is depicted in Fig. 3. 10 and Fig. 3. 11. For each element in the uncertainty chain a comprehensive analysis has to be done to assume the overall range of uncertainty. Two elements of Fig. 3. 10 are illustrated in Fig. 3. 11 with the progress of the increasing uncertainty.

---

<sup>1</sup> Descriptions of the research projects are given in chapter 2 and the list of Abbreviations

---

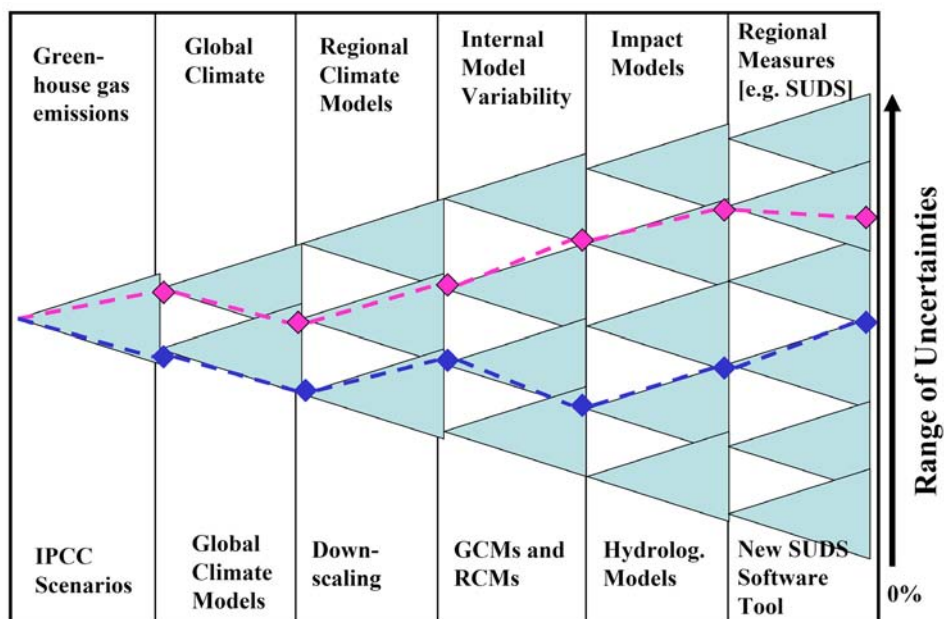


Fig. 3. 10 Simplified illustration of the increasing range of uncertainties in the model chain. (adopted from Viner, 2002)

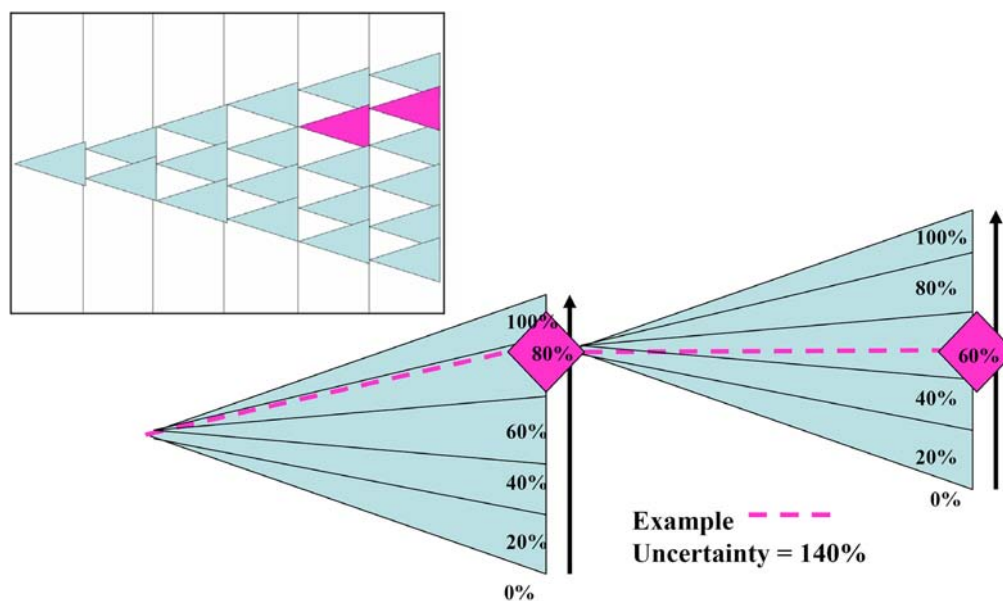


Fig. 3. 11 Simplified illustration of the uncertainties assumed for two elements of the uncertainty chain.

### 1. Uncertainty of Emission Scenarios:

The choice of the IPCC emission scenario reflects the assumption of the trend of greenhouse gas emissions in the future. These estimations are based on worldwide development of population and energy consumption, which is not possible to be predicted with certainty ( 3.3.3). The choice of the emissions scenario can be regarded as initial source of uncertainty in

the chain and has been discussed by Déqué et al. (2007), Frei et al. (2006) and in the projects CLAVIER, ENSEMBLES and PRUDENCE.

### **2. Boundary Uncertainties (Global Circulation Models):**

Global Circulation Models (GCM) provide boundary conditions for regional downscaling models (3.3.2.1.). Their utilized formulations differ and cause another source of uncertainty. This has been discussed for example in the projects CLAVIER, PRUDENCE, ENSEMBLES and the DEFRA project UKCIP09<sup>1</sup>

### **3. Systematic Biases of Regional Climate Models (RCM):**

For impact studies, detailed projections of local climate changes are required which are provided by high resolution RCMs (3.3.2.2). Different numerical methods and physical parameterization are utilized in RCMs to simulate data series of future climate scenarios (CLAVIER [3], 2009). The different applied methods bring along another tier of complexity and uncertainties. This is discussed e.g. in CLAVIER, PRUDENCE, ENSEMBLES and UKCIP09.

### **4. Internal Model Variability:**

The measure for the model's degree of freedom to develop its own dynamics within the given boundary conditions is defined as the internal model variability (CLAVIER[3], 2009). This is discussed in e.g. the projects CLAVIER and UKCIP09.

### **5. Uncertainties derived by Impact Models (e.g. Hydrological Models)**

Hydrological models are based as well on a certain set of parameterizations and modelling features. These models are mostly applied and calibrated for current state situations. Although they provide appropriate results in validations with observed data from the past, it can not be assured that these models show respective applicability in future climate change impact studies. This has been discussed by Ludwig et al. (2009), Goetzinger (2007), Schwandt (2004), Viner (2002) and in the projects HEPEX<sup>2</sup> and CLAVIER.

The analysis of the whole uncertainty chain is very complex and a detailed methodology can not be worked out in the scope of this thesis. However, the results of two research studies about the uncertainties in climate change and hydrological modelling are outlined after the discussion of the scenario results in chapter 6.

---

<sup>1</sup> UKCIP09 = UK climate projections ; <http://ukclimateprojections.defra.gov.uk>

<sup>2</sup> HEPEX = Hydrologic Ensemble Prediction Experiment; <http://hydis8.eng.uci.edu/hepex/>

## 4 Implementation of a SUDS Software Tool

The implementation of the theoretical approach for modelling SUDS has been done in the software Kalypso Hydrology which is a deterministic semi-distributed as well as lumped rainfall-runoff-model, and belongs to the modelling platform Kalypso Enterprise<sup>1</sup>. The approach is based on a catchment level to simulate the effectiveness of SUDSs in SUCAs. The main programmed routines and the procedure of the implementation is illustrated with Nassi-Shneiderman-Diagrams attached to the thesis. These diagrams facilitate the ability to reconstruct the procedure for further software implementation works. An add-on strategy had to be developed for the application of the new software tool with a preliminary assistance tool, till the application of the new developed module is available with the Graphical User Interface (GUI) of the software Kalypso Hydrology.

### 4.1 Catchment Level Approach

Local SUDS can be defined on properties  in sub-catchments, like indicated in the schematic illustration of Fig. 4. 1. Studying the hydrological effects of such single local SUDS on separated properties does not point out the effectiveness in the whole catchment. Therefore SUDS elements of each type are aggregated and assigned to defined land use type areas in the sub-catchment in the data model (Brüning et al., 2009; Pasche et al., 2009).

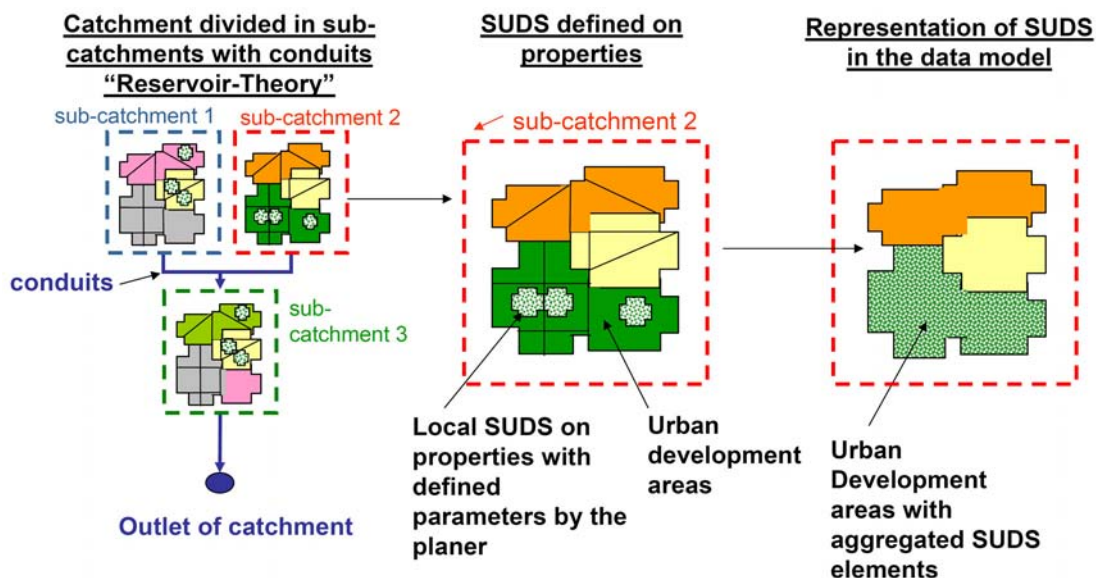


Fig. 4. 1 Representation of SUDS in the data model. (published earlier in Pasche et al., 2009; Brüning et al., 2009; Brüning & Hellmers, 2009)

An additional feature of the model approach is, to compute the overall water balance on the basis of physical processes in the sub-catchments, which are further sub-

<sup>1</sup> <http://sourceforge.net/projects/kalypso/>

divided into hydrological homogeneous response units; defined as ‘hydrotopes’ (Pasche, 2003). Such units are created by intersecting land use areas of sub-catchments with hydrogeological data, and results in areas with specified uniform pedology, hydrology and runoff characteristics. In each hydrotope, hydrological vertical and retention processes, including the evaporation, snow retention, interception as well as the infiltration and percolation, are simulated. This provides the required data to calculate the horizontal flow processes including surface runoff as well as inter-, base- and groundwater flow (Pasche, 2003).

Based on this approach, SUDS areas in the sub-catchments are further processed by intersection with hydrogeological units to create hydrotope areas with the attributes of SUDS. This is illustrated in Fig. 4. 2 with the indicated example of the sub-catchment 2 with SUDS on urban development areas (see Fig. 4. 1).

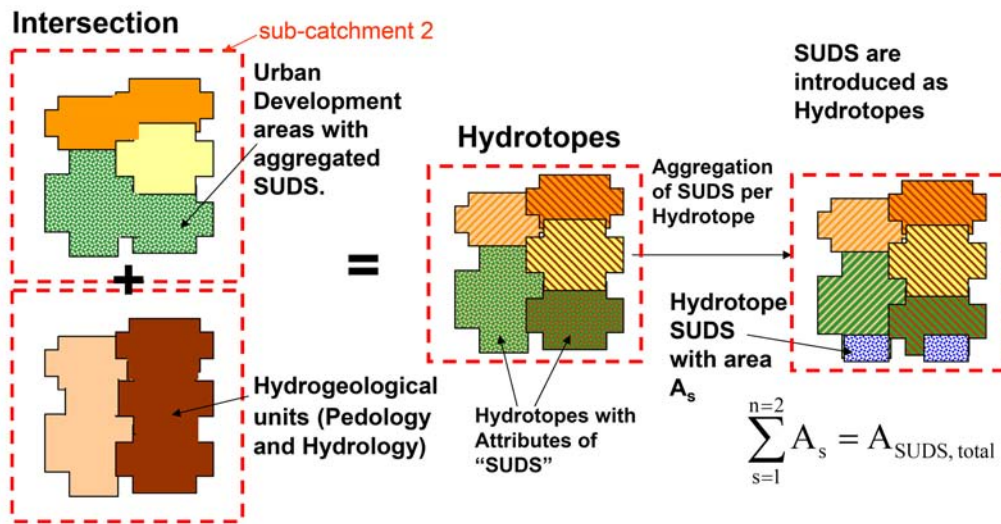


Fig. 4. 2 Creation of hydrotopes with the attributes of SUDS in the data model. (published earlier in Pasche et al., 2009; Brüning et al., 2009; Brüning & Hellmers, 2009)

In the scheme illustrated in Fig. 4. 2, the land use area with the attributes of SUDS is intersected with two hydrogeological units. After the intersection, two hydrotope areas with the attributes of SUDS are created. The area  $A_s$  of the SUDS hydrotope results from the total area of the SUDS ( $A_{SUDS, total}$ ) multiplied with the ratio of the hydrotope area ( $A_{Hydrotope}$ ) to the land use area ( $A_{land\ use\ area}$ ) (Brüning et al., 2009).

$$A_s = A_{SUDS, total} * \frac{A_{Hydrotope}}{A_{land\ use\ area}}$$

eq.4. 1

## 4.2 Implementation Procedure

The core of the Open Source Software application Kalypso Hydrology is based on routines written with the FORTRAN programming language. To prevent redundancies the routines are split into separate sub-routines and functions. Significant sub-routines for modelling the hydrological processes in the sub-

catchment and the embedding of the SUDS sub-routine are illustrated in Fig. 4. 3 and Fig. 4. 4.

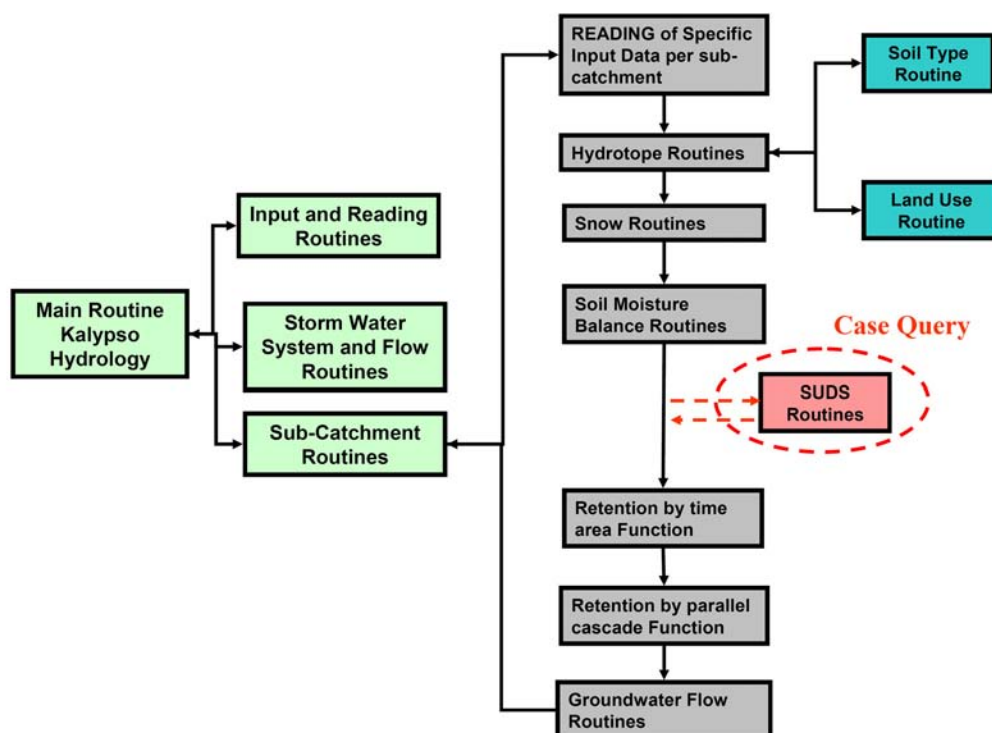


Fig. 4. 3 Outline of the main sub-routines in the Model Kalypso Hydrology and the embedded new sub-routines for simulating SUDS elements.

The main routine 'Kalypso Hydrology' calls the routines to read the input data of the model, the routine to define the flow network with nodes as well as strands, and the routine in which the hydrological processes in sub-catchments are computed. The Sub-Catchment Routine is split in further sub-routines in which specific input data for the sub-catchment is read, the hydrotopes (soil type and land use type) within the sub-catchment are defined, snow retention processes are modelled and the soil moisture is balanced. Additionally, SUDS routines are called with a case query and the outflow from one SUDS type could be defined here as an inflow into another SUDS element. The overland flow (surface runoff) and the drainage from SUDSs, is calculated with time area functions of the respective sub-catchment and parallel cascade functions. In the last called sub-routine the groundwater flow is computed, before the hydrological processes in the following sub-catchment of the model chain are computed.

In the Sub-Catchment Routines the SUDS Type is interrogated in a case query. First the defined green or brown roofs [1] are calculated (if defined), then swales [2] (if defined) and then swale-filter-drain systems [3] (if defined). In this way a SUDS chain can be simulated and the outflow from green or brown roofs can drain into swales as well as swale-filter-drain systems. Likewise the overflow of swales could drain into a swale-filter-drain system (blue lines in Fig. 4. 4.). Otherwise the outflow

from the SUDS element drains into the storm water system, which is further processed in the Sub-Catchment Routine (Fig. 4. 3).

The statements and processes which are equal in each SUDS-Subroutine are defined in further sub-routines, which include the reading of the SUDS input parameters and routines for the calculation of the soil moisture, the evaporation and the interception (green lines in Fig. 4. 4).

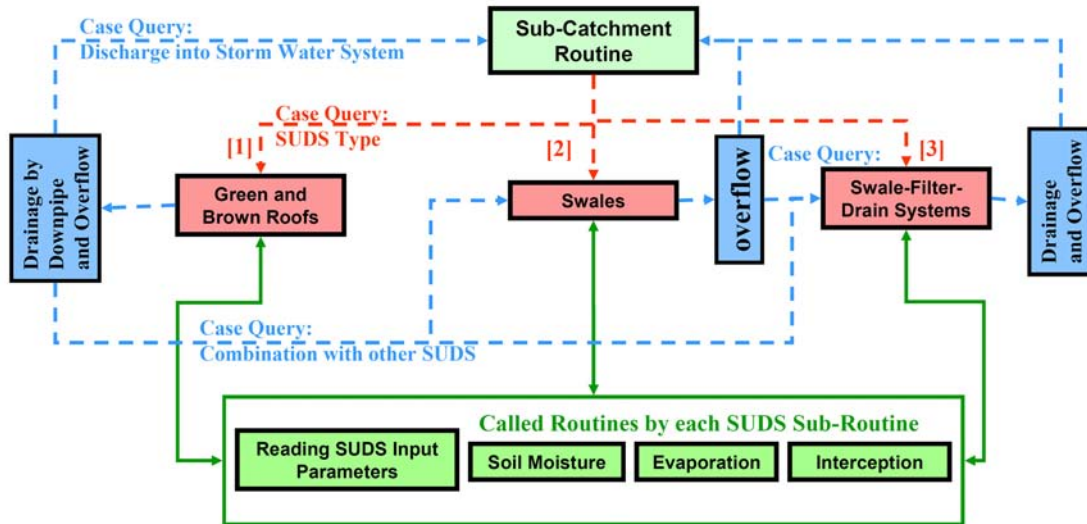


Fig. 4. 4 Outline of the SUDS Sub-Routines.

In the scope of this thesis the routine for modelling green as well as brown roofs has been developed, including the calculation of the flow through the drainage and overflow pipe. Other routines have been only adjusted or upgraded if necessary. The main statements and calculations are illustrated in the Nassi-Shneiderman diagrams in attachment 5. Explanations of the used variables and FORTRAN language definitions are summarized in the introduction of the attachment 5.1. A focus was set on the documentation of the water balance and the flow processes in the layers of the SUDS element. The differentiation between simulating green or brown roofs with the sub-routine is done according to the definition of different materials and with or without vegetation. The sub-routine is as well implemented to simulate brown roofs, but for the documentation the example of green roofs is explained.

The sub-routine for modelling green roofs begins with the definition and initialisation of used variables (Attachment 5.2). Thereafter, a sub-routine is called to import user specific SUDS parameters (e.g. the diameters of the outlet pipes as well as the height of the overflow pipe). Per outlet pipe a specific area can be drained. These sub-areas are initially defined as a standard area. It has been determined that approximately 300m<sup>2</sup> of vegetated roofs can be sufficiently drained per down pipe of a DN<sub>100</sub> (Optigruen, 2009). Nevertheless, the overall roof area per sub-catchment won't be exactly a plural of the defined drained sub-area per outlet pipe. Therefore the area has to be adjusted to define the exact number of outlet pipes and the precise

average drained sub-area per outlet pipe, which is illustrated in the Nassi-Shneiderman diagram in Attachment 5.3 with two examples.

As the next step in the sub-routine (Attach 5.2), the soil parameters of the green roofs are imported and specific parameters are defined like the land use type, the soil type as well as the number of soil layers and the parameters of the vegetation of an extensive or intensive green roof. For the interception and the soil water content, initial values have to be set before hydrological processes are calculated for each time step in loop functions. For long term simulations the time cycle is defined with a length of 365 days and short term simulations are restricted to a maximum of 2880 timesteps, to restrict the required expenditure of calculation time and computer power. In this loop, the water balance and flow processes are computed for each timestep. First the time-dependent parameters of the vegetation are imported, which include the transpiration, root depth and leaf area index. The interception and evapotranspiration from the vegetation on the extensive or intensive green roof are calculated in further sub-routines.

For another internal time loop, timesteps larger than 8 hours are divided by a factor:

$$\text{Internal time loop factor} = \text{INTEGER} \left( \frac{(\Delta \text{timestep}[\text{h}] - 0.01)}{8} + 1 \right)$$

**eq.4. 2**

An example is given in the attachment 5.2 for daily timesteps, where the factor is 3. For simulations with smaller timesteps than 8 hours, the internal timestep loop is passed through once. In this internal time loop, three loops are defined over the number of layers.

The first layer loop (Attach 5.4) runs from the storage layer (L1) to the filter layer (L3). The potential inflow (prinp) into the storage layer (L1) is defined as the effective precipitation (pri). Into the substrate (L2) as well as the filter layer (L3), the inflow is defined as the potential percolation (perkl) into the layer (Attach: if-query 5.4.1). Thereafter, the actual water content (sw), the actual infiltration into the layers and the actual percolation is calculated in a sub-routine. If the potential inflow into the layer is larger than the actual possible infiltration, the water is retained in the layer above (Attach: if-query 5.4.2). The maximal percolation from the filter layer (L3) is set to zero because of the insulation layer on the roof. Therefore, all the water which could potentially percolate (perkl(L3)) is transferred to stored water (pstau). Because the stored water (pstau) is defined for the layer above the regarded one, it is necessary to set the stored water to a fictive layer on the roof (pstau(L4)).

In the second internal layer loop (attach 5.5) the actual water content (sw) is adjusted with the stored water of the layer, pstau (layer) (Attach if-query 5.5.1). The loop

begins with the fictive layer (L4) to add the retained water volume above the layer (p<sub>tau</sub>(4)) to the soil water content in the filter layer (L3). But if the filter layer (L3) is saturated, the exceeding water volume (p<sub>rest</sub>), which can not be retained in the filter layer, has to be added to the soil water content in the layer above, the substrate layer (L2). Respectively the soil water content of the second layer is corrected with the retained water p<sub>tau</sub>(3). When the second layer is saturated the additional water volume (p<sub>rest</sub>) is added to the retained water in the storage layer (sw(1)).

In the third internal layer loop the water levels and the discharge through the outlet pipes on the green roof is calculated (Attach 5.6). This loop begins with the calculations of the processes in the storage layer (L1) and ends with the filter layer (L3). Here the free movable water content (sw<sub>free</sub>) is calculated with the actual water content (sw) and the water volume up to the field capacity (sw<sub>fk</sub>). The field capacity (FK) is the maximum amount of water that a soil type can retain against the force of gravity (Brooks et al., 2003). It is the sum of the water quantity of the permanent wilting point (wp) and the usable field capacity (n<sub>fk</sub>). The water up to the wilting point (wp) is referred to the point where most plants become wilted (Brooks et al., 2003). In the model, this water content is considered as fixed and therefore, it is not included in the water balance calculations. That means, the total water content (sw<sub>total</sub>) is reduced by the water quantity up to the wilting point (wp) already in the input sub-routine. This is important to take into account for any water balance equations in the following SUDS sub-routines.

When the free water content (sw<sub>free</sub>) in the layer is above zero (here: 0.01l/m<sup>2</sup>), the water level is calculated for each internal time step (Δt). The water level is computed with the actual soil water content in the saturated zone (sw<sub>sat</sub>) of the layer, which is the sum of the free water (sw<sub>free</sub>) and the water content up to the field capacity (sw<sub>fk</sub>) which is in the saturated zone but can not be drained. This specific ratio of the water content is calculated by multiplying the water content up to the field capacity (sw<sub>fk</sub>) with the ratio of the actual free water content (sw<sub>free</sub>) to the maximal free water content (sw<sub>maxfree</sub>) (eq.4. 3).

$$sw_{sat} = sw_{free} + \frac{sw_{free}}{sw_{maxfree}} * sw_{fk} \quad [ \frac{l}{m^2} ]$$

**eq.4. 3**

For the calculation of the maximal soil water content (sw<sub>maxtotal</sub>), the volume up to the wilting point (sw<sub>wp</sub>) has to be added to the maximal soil water content (sw<sub>max</sub>).

$$sw_{maxtotal} = sw_{max} + sw_{wp} \quad [ \frac{l}{m^2} ]$$

**eq.4. 4**

The water level (hw) is the hydraulic head in the soil layer. In the scope of this thesis a linear relation has been defined between the depth of the layer and the water content (sw\_sat) in the saturated zone of the layer. This is illustrated in Fig. 4. 5 with the ratio of the layer depth to the maximum soil water content (sw\_max\_total) as the gradient.

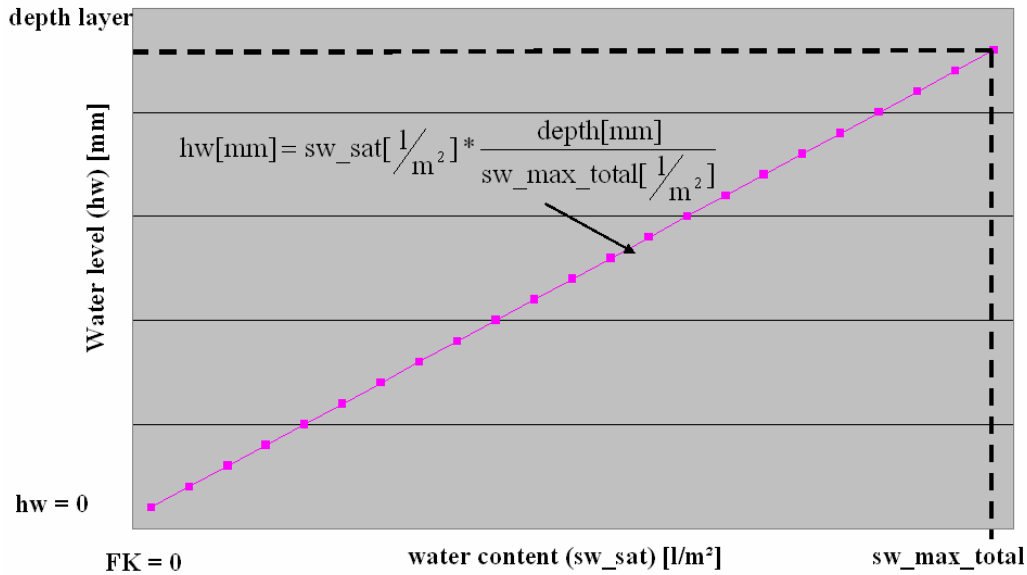


Fig. 4. 5 Relation between water level (hw) and soil water content (sw\_sat) in the software tool

The linear relation is expressed in the equation eq.4. 5:

$$hw[mm] = sw\_sat\left[\frac{l}{m^2}\right] * \frac{depth[mm]}{sw\_max\_total\left[\frac{l}{m^2}\right]}$$

eq.4. 5

The ratio of the maximum soil water content (sw\_max\_total) to the layer depth can be as well defined as the maximal soil porosity.

When the filter layer (L3) is saturated, the water level (hw) is equal to the layer depth (L3) and there is a direct connection between the water in the filter and substrate layer. In this case the hydraulic head is enlarged by the water level in the substrate layer (L2) and results in the effective water level (sum\_hw). If the substrate layer is saturated as well, the effective water level (sum\_hw) is enlarged respectively by the water level in the storage layer (L1). The statements for the water level calculation are illustrated in the attached if-queries 5.6.2 to 5.6.4.

The sub-routine for the calculation of the flow through the outlet pipes is only called when the effective water level (hw\_sum) is above zero (if-query 5.6.5). The call for the sub-routine to calculate the flow through the down pipe and the subsequent water balance adjustment is illustrated in Attach 5.7, whereas the calculation of the flow is depicted in Attach 5.8. For the calculation of the flow through the soil material, the effective porosity in the saturated zone has to be calculated. When the water level is higher than the filter layer, the effective porosity

of the substrate layer has to be taken into account as well. The effective flow is the minimal discharge calculated with the following two approaches in [mm<sup>3</sup>/s].

The flow into the down pipe is calculated with the Poleni equation. The used parameters are the resistance coefficient  $\mu = 0.577$  (BWK, 1999), the diameter of the down pipe ( $d_{\text{pipe}}$ ), the acceleration due to gravity ( $g = 9810\text{mm/s}^2$ ), the water level ( $hw\_sum$ ) and the effective porosity ( $pors\_eff$ ):

$$Q_{\text{Poleni}}[\text{mm}^3/\text{s}] = \frac{2}{3} * \pi * d_{\text{pipe}}[\text{mm}] * \mu * \sqrt{2 * g[\text{mm}/\text{s}^2] * (\text{sum\_hw}[\text{mm}])^{3/2}} * pors\_eff[\%]$$

**eq.4. 6**

Additionally, the maximum capacity of the rainfall down pipe with the diameter ( $d_{\text{pipe}}$ ) limits the maximal discharge from the roof. The maximum flow capacity is calculated with the flow resistance ( $\lambda$ ) according to the Colebrook-White equation with the equivalent sand roughness ( $ks$ ) and the diameter of the down pipe ( $d_{\text{pipe}}$ ):

$$\frac{1}{\sqrt{\lambda}} = -2 * \lg \left( \frac{ks[\text{mm}] / d_{\text{pipe}}[\text{mm}]}{3.71} \right)$$

**eq.4. 7**

$$Q_{\text{max}}[\text{mm}^3/\text{s}] = \frac{\pi * d_{\text{pipe}}[\text{mm}]^2}{4} \sqrt{\frac{2 * g[\text{mm}/\text{s}^2] * d_{\text{pipe}}[\text{mm}]}{\lambda}}$$

**eq.4. 8**

The equivalent sand roughness of the pipe ( $ks$ ) is set as standard value for pipes with the used material. Information about the roughness of pipes is given in: [Schneider “Bautabellen für Ingenieure” \(ed. 16, 2004\)](#) on page 13.13.

The derivations of the equations are outlined in Attachment 5.11. The calculated flow in mm<sup>3</sup>/s ( $q\_gr\_teil\_drain$ ) is the discharge through one rainfall down pipe, but it is required to compute the flow from all roof areas in the sub-catchment. This is calculated by the multiplication of the flow ( $q\_gr\_teil\_drain$ ) with the number of down pipes ( $gr\_teil\_faktor2$ ); eq.4. 9 (step 1). This resulting overall flow in mm<sup>3</sup>/s has to be transferred to a flow of the internal timestep by the multiplication with  $\Delta t$  [h] and 3600 [s/h]; eq.4. 9 (step 2). For the following soil water (sw) balance calculation, the flow has to be referred to the green roof area ( $flaech\_entw\_gr$ ) [in mm<sup>2</sup>]; eq.4. 9 (step3). With these three steps the outflow of the green roofs within a whole catchment is calculated in [mm<sup>3</sup>/mm<sup>2</sup> = mm] of the roof ( $q\_gr\_drain$ ) and per internal timestep  $\Delta t$ :

$$q\_gr\_drain[\text{mm}] = \underbrace{q\_gr\_teil\_drain[\text{mm}^3/\text{s}] * gr\_teil\_faktor2}_{\text{step1}} * \underbrace{3600[\text{s}/\text{h}] * \Delta t[\text{h}]}_{\text{step2}} * \underbrace{\frac{1}{(flaech\_entw\_gr[\text{mm}^2])}}_{\text{step3}}$$

**eq.4. 9**

The flow through the down pipe ( $q_{gr\_drain}$ ) is transferred to the subroutine in Attachment 5.7 and has to be balanced with the available free water content ( $sw\_free$ ) on the roof (if-queri 5.7.1). The flow through the down pipe can be maximal as large as the volume of the free water ( $sw\_free$ ). If the free water ( $sw\_free$ ) is smaller than the flow through the down pipe ( $q_{gr\_drain}$ ) the flow has to be reduced respectively. The water content in the filter layer is reduced to the field capacity, which can not be drained, and the difference between the potential flow ( $g_{gr\_drain}$ ) and the free water ( $sw\_free$ ) is calculated. When the water level is smaller than the depth of the filter layer, the final flow through the down pipe ( $gr\_qabvs$ ) is reduced to the free water content of the filter layer ( $sw\_free(3)$ ). When the soil layer is saturated there is a direct connection between the water volumes of the layers above. Therefore the free water content in the substrate layer adds up to the potential flow through the down pipe when the filter layer (L3) is saturated. For this purpose, another if-query (5.7.2) is introduced in the statement where a balance is done with the difference of the potential flow volume ( $gr\_drain\_diff$ ), which could be drained from the substrate layer. In this way, a water balance over the soil layers and the flow through the down pipe is defined. The water quantity in the storage layer is drained by the overflow pipe above the soil layers and is not taken into account for the calculation of the outflow of the rainfall down pipe which is on the bottom of the soil layers.

The adjusted soil water content ( $sw$ ) is used as an initial value in the following internal timestep ( $\Delta t + 1$ ) for the calculation of the new soil water content ( $sw(\Delta t + 1)$ ) with the inflow ( $prinp$ ) into the respective layer (Attach 5.4). The final flow [ $mm^3$ ] through the down pipe per internal timestep  $\Delta t$  and per  $mm^2$  of the green roof area in the sub-catchment is transferred to the sub-catchment sub-routine (Fig. 4. 4), where it is defined as an input flow into another SUDS-type (e.g. swale) or as inflow into the storm water system.

The flow through the overflow pipe in the storage layer (L1) is calculated in the third internal loop over the green roof layers (Attach 5.6) in the if-query 5.6.6. To prevent redundancies the calculation of the overflow and the balance of the water content on the storage layer is only calculated when the layer equals to one ( $layer = 1$ ) in the calculation loop. The statements of the calculation are illustrated in the Nassi-Shneiderman diagrams in Attach 5.9 and Attach 5.10. The water volume in the storage layer of the roof is the sum of the actual water content ( $sw(1)$ ) and the additional retained water ( $pstau(1)$ ), which is calculated as volume of water [ $mm^3$ ] per  $mm^2$  and forms the water level [ $mm$ ] ( $sum\_hw\_ov$ ) in the storage layer. If the water level in the storage layer ( $sum\_hw\_ov$ ) exceeds the height of the overflow pipe ( $h\_over\_gr$ ) an overflow is calculated and the water content in the storage layer has to be adjusted respectively (if-query 5.9.2). If the water level above the overflow pipe ( $hw\_ex$ ) exceeds the depth of the storage layer inclusive the freeboard, the

---

storage capacity is overloaded (if-query 5.9.3). In this case the water volume which exceeds the storage capacity ( $p_{\text{stau\_over}}$ ) is calculated. This overload is written in the results of the model, so that the modeller can define the rainfall event at which the roof is overloaded and to which extent. The water level above the overflow pipe is adjusted respectively to its maximum, which equals to the freeboard of the roof.

In the storage layer a maximum water content [ $sw\_max$ ] equal to the height of the overflow pipe ( $h\_over\_gr$ ) is retained after the overflow. The correction of the water content in the storage layer  $sw(1)$  is done with the following statement, which is based on the same linear approach as the water level calculation eq.4. 5.

$$sw(1) = h\_exceedence\_gr * \frac{sw\_max(1)}{depth(1)} \quad [\text{mm}]$$

**eq.4. 10**

The water content in the storage layer  $sw(1)$  is calculated like a soil layer with a pore volume of 99% and a wilting point of 1mm/dm. The water level above the overflow pipe has to be corrected with the actual stored water on the roof ( $sw(1)$ ). Because of the approach to model the storage layer like a soil layer, the stored water level remains slightly under the edge of the overflow pipe ( $h\_over\_gr > sw(1)$ ).

With the corrected water level above the overflow pipe, the flow through the pipe is calculated in the routine illustrated in the Nassi-Shneiderman diagram (Attach 5.10).

The effective flow in [ $\text{mm}^3/\text{s}$ ] is the minimum flow calculated with the Poleni approach and the maximal flow capacity through the overflow pipe calculated with the Colebrook-White equation. Like the flow through the down pipe (eq.4. 8), the overflow ( $q\_gr\_over$ ) has to be calculated for all pipes and converted to the flow per internal timestep ( $\Delta t$ ) and per  $\text{mm}^2$  of the roofs.

This overflow is transferred back to the if-query 5.9.5 (Attach. 5.9), where a balance has to be done with the available water above the overflow pipe ( $hw\_ex$ ) and the calculated overflow ( $q\_gr\_over$ ). If the calculated overflow ( $q\_gr\_over$ ) is larger than the available water content above the overflow pipe, the outflow has to be reduced respectively (if-query 5.9.4). If the water content is larger than the overflow ( $q\_gr\_over$ ), the water which can not be discharged ( $diff\_hw\_ex$ ) is added to the water content  $sw(1)$  which is retained in the storage layer. The water volume which exceeds the capacity of the storage layer of the green roof ( $p_{\text{stau\_over}}$ ) and the flow through the overflow pipe are transferred back to the sub-routine of the sub-catchment (Fig. 4. 4) where it is defined as inflow to another SUDS-type (e.g. swale) or to the storm water system.

### 4.3 Development of an Add-On Tool

During the time period of working on the thesis the SUDS simulation tool has been integrated in the new developed, Graphical User Interface (GUI) based software application Kalypso Planer Client. Its functionality is based on several underlying Kalypso modules and the development has been supported by the LSBG in the project: ‘Development of the Decision Support Tool Kalypso-Planer-Client’. The prerequisite for the application of the decision support tool to assess the effectiveness of SUDS is the provision of several Kalypso software models including Kalypso Hydrology, Kalypso WSPM<sup>1</sup>, Kalypso Flood and Kalypso Risk models. The decision support tool enables the quantification of the impacts of future urban developments on the water regime in SUCAs. Further on, the effectiveness of flood probability reduction measures (namely: SUDS) will be possible to be assessed and economical as well as ecological aspects shall be considered in the studies (Küpferle & Pasche, 2008).

In the scope of this thesis the implementation of the SUDS software tool into the separate Kalypso-Hydrology software application has been restricted to the software core. Therefore, the modules for simulating green roofs as well as swales and swale-filter drain systems are not implemented in the GUI of the software application Kalypso-Hydrology up to now. To run simulations with existing Kalypso Hydrology models it has been necessary to develop an add-on tool in the scope of this thesis to assist the application of the new SUDS simulation tool. With the add-on assistance tool, simulations can be executed in console mode, i.e. with the textual file representation (so-called ‘ASCII files’) of a Kalypso Hydrology model and the new core of the software application. On the one hand, working with ASCII files is complex and for a number of processing works, rather time consuming, but on the other hand a detailed definition of all SUDS parameters has been possible in this way.

The experiences of a very detailed adjustment of all SUDS parameters (e.g. materials used as drain or substrate layer, thickness of layers, overflow heights) are useful for the subsequent implementation of the SUDS simulation tool into the GUI of Kalypso Hydrology, where the complexity of SUDS parameter definitions has to be limited.

The most complex and time consuming processing work for simulating SUDS with the ASCII files of Kalypso Hydrology models, is the calculation of the SUDS adjusted hydrotopes in the sub-catchments. An additional aim of this thesis has been defined to reduce this workload for future projects by working out a tool, which calculates the adjusted hydrotopes (including SUDS) with a reasonable number of input data by the user. This tool has been worked out with the spreadsheet

---

<sup>1</sup> Module for computing one-dimensional water surface profiles

application Excel and therefore, no additional software is needed to make any changes in this file later on for other projects.

The required input data to adjust the hydrotopes comprise the following points:

- The status quo hydrotope ASCII file,
- The soil materials of the SUDS,
- The depth of all layers [dm],
- The mean and maximal runoff from sealed areas derived during the design rainfall events for a pre-design calculation [m<sup>3</sup>/s],
- The duration of the design event [h],
- The duration of the infiltration into the ground from SUDS devices [h].

The ASCII file with the hydrotope data is made up of 22 columns and a respective number of rows for the hydrotopes in each sub-catchment of the model (Table 4. 1). In the first row the number of the catchment, the number of hydrotopes and the sealed, natural as well as the total area of the sub-catchment are defined. Additionally, a SUDS switch and the sum of the sealed, natural and total SUDS areas are calculated.

**Table 4. 1 Scheme of the Hydrotope-ASCII file.**

| <b>column</b><br><b>row</b> | <b>1.</b>                         | <b>2.</b>             | <b>3.</b>                           | <b>4.</b>                            | <b>5.</b>                                  | <b>6.</b>       | <b>7.</b>                                  | <b>8. – 22.</b>                          |
|-----------------------------|-----------------------------------|-----------------------|-------------------------------------|--------------------------------------|--|-----------------|--|--|
| <b>1.</b>                   | Sub-Catchment Indication ('Name') | Number of Hydro-topes | Total sealed area [m <sup>2</sup> ] | Total natural area [m <sup>2</sup> ] | Total sub-catchment area [m <sup>2</sup> ] |                 | SUDS switch<br><br>1 = SUDS<br>0 = no SUDS | SUDS cases and areas                     |
| <b>2.</b>                   | Hydrotope area                    | Landuse type          | Soil type                           | Maximal perco-lation rate            | Ground-water factor                        | Hydro-tope nr 1 | Sealing rate                               | Natural and sealed areas drained by SUDS |
| <b>3.</b>                   | Hydrotope area                    | Landuse type          | Soil type                           | Maximal perco-lation rate            | Ground-water factor                        | Hydro-tope nr 2 | Sealing rate                               | Natural and sealed areas drained by SUDS |
| ...                         | ...                               | ...                   | ...                                 | ...                                  | ...  | ...             | ...  | ...                                      |

From the second row on, the areas of the hydrotopes which are not connected to SUDS and other hydrotope parameters (e.g. land use type, soil type, sealing rate) are written in the columns 1 till 7. According to the areas transferred or drained by SUDS (column 8 till 22) the data in the columns 1 till 7 have to be adjusted.

In an input sheet for each SUDS measure (Green Roofs, Swales, Swale-Filter-Drain systems) the user can define the ratio of the sealed area, which shall be assigned to respective SUDS types (see Attachment 6).

Swales and swale-filter-drain systems are situated on green areas within urban catchments like in gardens or free spaces in front of buildings. The required area for swales and swale-filter-drain systems depends on the depth of the storage layer, the runoff volume, which is drained from sealed areas, and the direct rainfall on the area of the SUDS. The infiltration of water into the ground and the evaporation from the water surfaces begins simultaneously with filling up the swale. For a pre-design of the storage capacity of a swale, these processes have to be included.

The infiltration of water during the design rainfall event is calculated with the permeability coefficient of the colmation layer (swale-filter-drain system) or the base layer (swale) in  $\text{m}^3/\text{m}^2$ . The permeability coefficient has been reduced with a factor of 0.5 according to the bulletin [DWA-A 138 \(2005\)](#).

For the calculation of the infiltration volume of the swale, a first assumption of the area is necessary, which is done with the computed runoff volume and the first assumption of the area of the swale. Therewith, the infiltration volume is obtained and the required area for swales and swale-filter-drain systems is calculated.

In literature, recommendations are given by [DWA-A 138 \(2005\)](#) for the ratio of drained sealed areas. For swales and swale-filter-drain systems the maximal drained sealed area shall not exceed 20 times the swale area in silty sandy soils [DWA-A 138 \(2005\)](#). For this purpose a check function has been implemented in the spreadsheet.

With the rough estimations of the infiltration and drainage volume to the swale, inaccuracies have to be taken into account. Therefore the area of the swales and swale-filter-drain systems can be readjusted with SUDS correction factors till the design conditions are fulfilled sufficiently. For the calculation of the new hydrotope areas, the percentage ratio of sealed areas drained by swales and swale-filter-drain systems are used.

For green roofs, the pre-design of the area depends only on the potential spatial distribution of green roofs in the sub-catchments. The user can define a ratio of the sealed area, which shall be simulated as green roofs and this ratio is used in the spreadsheet for the calculation of adjusted hydrotopes.

Another measure planned in the scope of this thesis to reduce the runoff from urban areas is, to replace sealed surfaces with material, which is porous or has gaps, to increase the infiltration rate into the ground. In this way, the runoff coefficient defined according to the [DWA-A 138 \(2005\)](#) can be reduced. In the spreadsheet, the user can define a ratio of the sealed area in sub-catchments, which shall be replaced

by porous surfaces. With this ratio and the potential reduction rate, a factor is calculated which reduces the sealing rate in the sub-catchments.<sup>1</sup>

The potential SUDS combinations in sub-catchments had to be defined specifically for the developed add on spreadsheet tool:

- Possible is the simulation of each SUDS measure separately:
  - Green Roofs,
  - Swales,
  - Swale-filter-drain systems,
  - Unsealing.
- And the simulation of SUDS combinations in system chains:
  - Unsealing of areas and green roofs as well as sealed areas draining into swales,
  - Unsealing of areas and green roofs as well as sealed areas draining into swale-filter-drain systems.

Not possible is the simulation of swales draining into swale-filter-drain systems and the simulation of swales and swale-filter-drain systems in one sub-catchment simultaneously.

### ***Calculation of Hydrotopes***

For the calculation of hydrotopes the status quo hydrotope file (we.hyd) is transferred into the spreadsheet indicated as “statQuo\_we.hyd”. It has to be taken care of keeping the same order of rows and columns. The data of the status quo hydrotopes are linked to the data in the spreadsheet: “Ascii\_file\_SUDS\_we.hyd”. When a completely new hydrotope file shall be created for another project, it is recommended to define new links before beginning any calculations.

Setting up the links and the calculations in the spreadsheet has to be started with calculating the natural areas used by swales and swale-filter-drain systems in column 13 (“20n”: swales) and column 17 (“30n”: swale-filter-drains). Here, the ratio of the natural area used by the swales is multiplied with the total natural area.

The sealed area drained by swales (column 14: “20v”) and by swale-filter-drain systems (column 18: “30v”) is calculated with the ratio computed in the pre-design with the respective losses and the SUDS correction factor. The sealed area transferred to green roofs is calculated with the user defined ratio in percentage of the sealed area in the sub-catchment (e.g. 20%). In the spreadsheet, it is intended that defined green roof areas drain into swales or swale-filter-drain systems (if defined). Therefore, the ratio of the drained sealed areas to swale systems (e.g. 30% of sealed area) is reduced by the area, which is simulated as green roofs (e.g. 20% of sealed area). For the differentiation of the cases, an if-function has been defined.

---

<sup>1</sup> For example a parking place has a surface cover made up of concrete or asphalt which has a runoff coefficient of 0.9. When this parking place is covered with pavement including voids between the elements there could be a potential reduction of the sealing rate of about 0.556.

The sum of the natural and sealed areas comprised by SUDS measures (green roofs, swales and swale-filter-drain systems) are calculated in the columns 8, 9 and 10 in the head row of the sub-catchment data block.

In the next step, the new sealing rates of the hydrotopes have to be calculated by taking into account the reduced sealed areas, drained or transferred to SUDS. For this purpose, the sealed areas have to be calculated in an additional spreadsheet: “auxiliary calculations”. In the first column, the status quo sealed areas of the hydrotopes are calculated and in the following column, the hydrotope area is computed which has been reduced by the SUDS areas.

With the reduced sealed area of the hydrotope the new sealing rate can be calculated in the spreadsheet “Ascii\_file\_SUDS\_we.hyd” (column 7). Here an additional calculation to reduce the sealing rate according to the user defined replacement with e.g. porous pavement is included.

In the following step, the final adjusted sealed area can be calculated in the spreadsheet “auxiliary calculations” for each hydrotope of the sub-catchment. The natural area of each hydrotope is reduced by the areas which are used by swales as well as swale-filter-drain systems and adjusted by the new sealing rate of the hydrotope in the spreadsheet “Ascii\_file\_SUDS\_we.hyd” (column 1). The sum of the adjusted natural and sealed areas of the overall sub-catchment is calculated in column 3 and 4 of the spreadsheet “Ascii\_file\_SUDS\_we.hyd”. The total area of the sub-catchment (not connected to SUDS) is calculated in column 5.

Finally, for the calculation of SUDS, it is important to change the “SUDS-switch” in column 7 of the head row of each sub-catchment data block from 0 to 1, otherwise the SUDS software tool does not run the sub-routines for the calculation of SUDS.

Additionally, two functions have been defined to test the correct data links and calculations of the adjusted hydrotopes in the spreadsheet. In the first test, the overall area of the sub-catchment, with and without adjusted SUDS-hydrotopes, is calculated and in the second test, the adjusted sealing rates are computed with two approaches and compared. The final spreadsheet with the adjusted hydrotopes has to be saved as a Text (MS-DOS) format which can be read by the Kalypso Hydrology core executable. An instruction with screenshots how to start the SUDS simulation is attached to the thesis (Attachment 6).

## **5 Application Scenario Studies**

The developed methodology and the implemented new software tool for simulating SUDS have been applied for climate change and adaptation scenarios in the Krückau catchment, which is located in the Metropolitan Region of Hamburg and involved in the KLIMZUG-Nord project region.

After the hydrological model and the catchment area have been defined (5.1), the climate model as well as scenario data series were selected (5.2). The climate data series have been pre-processed and imported into the hydrological model to simulate the stream flow at specific nodes in the river Krückau in climate scenarios. The results of the climate and flow data series have been processed in analyses to compute extreme rainfall (5.3) and flood peak probability curves (5.4). To calculate the magnitude of change and climate change factors, the results of the statistical evaluations have been post-processed (5.5). Additionally, design rainfall and flood events have been created, which were used for assessing the effectiveness of SUDS in adaptation scenarios to mitigate the impacts on flood probability by climate change (5.6). The results of the climate change and SUDS adaptation scenarios are discussed in chapter 6 in comparative studies.

### **5.1 Applied Hydrological Model of the Krückau Catchment**

#### **5.1.1 Scenario Study Area**

The catchment of the river Krückau is located in the North-German low land area. After a length of about 37km, the river Krückau flows into the river Elbe on a height of 0.1meter above sea level in the north of Seestermühle (NABU-Elmshorn, n.d.). The river has its source in the south of Kaltenkirchen on a height of 30m above sea level. Together with the tributaries: Offenau and Eckholter Au, the Krückau catchment area has a size of about 274 km<sup>2</sup>. To enhance the drainage of agricultural land in the first half of the 20<sup>th</sup> century, the course of the river Krückau has been regulated significantly and therewith the flow velocity in the river Krückau has been increased (NABU-Elmshorn, n.d.). The downstream section of the river, from the urban area of Elmshorn till the outlet, is strongly influenced by the tide.

In the mainly rural Krückau catchment, three urban areas are located. Kaltenkirchen (19 900 inhabitants) is situated upstream of the Krückau catchment and further downstream, the Krückau flows through the low density urban areas of Barmstedt (9700 inhabitants) as well as the outer conurban area of Elmshorn (11 760 inhabitants). The largest urban area is Elmshorn, which is located at the downstream section of the river Krückau with 48 200 inhabitants (Statistikamt Nord, 2009).

A flood barrier was constructed after the storm surge in 1962 downstream of the river Krückau. The barrier protects the catchment area from storm surges, but

problems occur now especially in the urban area of Elmshorn when heavy rainfall events cause the drainage system to be overloaded and the flood barrier has to be closed because of storm surges at the same time.

In 2009 flood risk maps have been published by the Federal State Schleswig-Holstein in the project: ‘*Überprüfung und Neufestlegung von Überschwemmungsgebieten an der Krückau*’ which illustrate the potential number of people who are in risk of being flooded by events which has a defined probability of occurrence (PÜK, 2009). In Elmshorn it has been indicated that the Else-Brandström-School close to the Krückau Park and the adjacent area of the Steindammwiesen Park are situated in flood risk areas (PÜK, 2009). With a research of local newspapers further local hot spots of flooding have been found out which comprise the streets underpass of the Hamburger Strasse known as ‘Badewanne’ [event in June 2005], the Sandberg Nr. 73 [event in July, 2005; July 2002], the Steindammwiesen park [event in January 2004] and the Krückau Park [event in January 2004] (THW-Elmshorn (n.d.); *Elmshorner Nachrichten* (online)). These events point out the current demand for flood probability mitigation measures in Elmshorn. And with regard to climate change impacts in the North German Lowland, an increase of the flood probability is expected.

### 5.1.2 Hydrological Model Set-Up

The model applied for the scenario studies, has been developed by the ‘*Planungsgemeinschaft Überschwemmungsgebiete an der Krückau*’ in short: PÜK, which is formed by the engineers of Klütz & Collegen Itzehoe GmbH together with the EPK-Engineers. The Federal State Schleswig Holstein and the city Elmshorn assigned the PÜK to examine and determine inundation areas in the Krückau catchment (PÜK, 2008).

The model has been build up with the software Kalypso Hydrology. The considered catchment of the river Krückau for the scenario studies has an extension of 185 km<sup>2</sup> covering the upstream catchment area from Kaltenkirchen and the tributaries: Offenau (10.2 km<sup>2</sup>), Eckholter Au (36km<sup>2</sup>), down to the river station close to the sewage treatment plant of Elmshorn. The downstream river Krückau section between the sewerage treatment plant and the outlet into the river Elbe has been neglected in the hydrological model because of the large tidal influence and the constant drainage from the marshy areas behind the dyke by pumps. The catchment area has been divided into 166 sub-catchments with a sub-division in 17 700 hydrotopes, 95 real strands as well as 214 virtual strands, 265 nodes and 28 storage elements (PÜK, 2008).

The soil and pedology in the catchment area is characterised by the old moraine landscape (known as: *Altmoränenlandschaft*) in the upper river catchment area between Kaltenkirchen and Barmstedt. The downstream catchment area of

Elmshorn is characterised by the coastal moorlands with sandy soils of the North German Lowland (known as: Geest) (PÜK, 2008).

The Krückkau catchment is characterised as SUCA<sup>1</sup> with the largest urban area of Elmshorn downstream of predominantly rural areas. The three main urban areas (Kaltenkirchen, Barmstedt and Elmshorn) are defined in the model with sealing rates between 0.25% and 1.0% (Fig. 5. 1). In the Krückkau model, runoff coefficients are defined which may behave differently if climate conditions vary significantly (Staufer et al., 2008). It is expected that with rising air temperature the evaporation rate most probably increase and the infiltration into the soil could decrease, but an adjustment of runoff coefficients in the calibrated Krückkau model could not be covered in the scope of this thesis.

Observed precipitation data series of five rainfall gauging stations have been available with data series from 1969 to 2004 in timesteps of 15minutes. The stations are depicted in (Fig. 5. 1): Horst, Brande, Henstedt-Ulzburg, Bullenkuhlen, Klein Nordende.

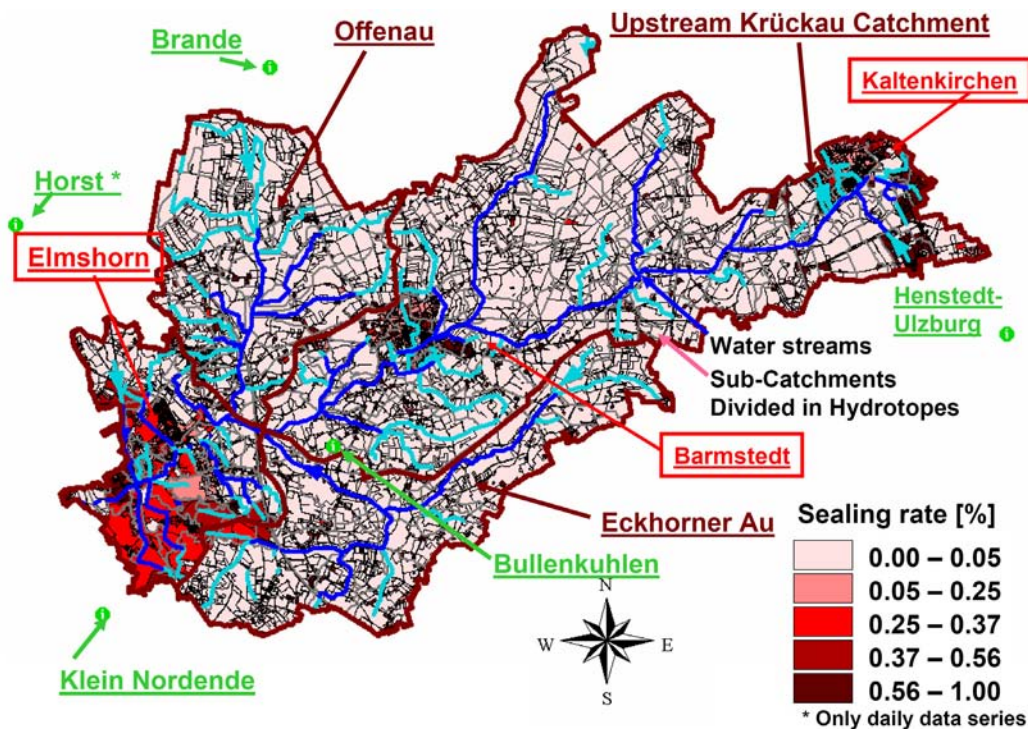


Fig. 5. 1 Map of the Krückkau catchment with the main urban areas, indicated sealing rates and rainfall gauging stations.

The allocation of the rainfall gauging station data series to the corresponding catchment areas has been performed with the Thiessen-Polygon method (PÜK, 2008). In this way rainfall gauging data sets have been gained for about every 30km<sup>2</sup> in the catchment. The distribution is illustrated in Fig. 5. 2 in paragraph 5.2.2. The rainfall data of the station ‘Horst’ has only been available with time steps of 1day.

<sup>1</sup> SUCA = small urban catchment

The calibration of the model has been done with discharge data series of eight gauging stations which have been available with hourly and daily timesteps.

### 5.2 Pre-Processing of Climate Model Data

The climate model data series and the scenario combinations have been selected according to the criteria in (3.3). For the application of the data series, the format as well as the geographical raster of the data series have to be transferred and additional data series (here: potential evaporation) have to be calculated.

#### 5.2.1 Selection of Climate Model Data Series

The selection of the appropriate climate model and scenario data series has been done with the six criteria developed in (3.3). The final selected points are indicated with an arrow: '→'.

1. **Comparability:** In the scope of the KLIMZUG-Nord project ([www.klimzug-nord.de](http://www.klimzug-nord.de)), it has decided that the data of the climate models REMO (dynamical), CLM (dynamical) and optional: WETTREG (statistical) shall be applied as basis for research to render comparability. The temporal coverage has been defined around the year 2050 and the IPCC-scenario A1B shall be preferred before the scenarios B1 and A2.
2. **Climate model type:** The assigned RCMs in the KLIMZUG-Nord project are all driven by the AOGCM ECHAM5 (Attachment 1.1). Due to the physical consistent representation of the water balance processes, the computed results of a dynamical climate model are preferred for hydrological modelling. Information about the different RCMs is provided in the Attachment 1.2.  
→ *Dynamical RCMs are preferred: REMO or CLM.*
3. **Available data values and timesteps:** Only the *datastream D3* of the REMO as well as the CLM dynamical climate models provides all the required data variables for impact studies in this thesis: temperature, precipitation, relative humidity, wind speed and global radiation in the required smallest temporal aggregation in hours and days respectively.  
→ *The datastream D3 is used, which provides data series on a regular geographical grid.*
4. **Required spatial resolution:** For scenario study simulations of flood hydrographs, which depend on the representation of extreme rainfall events, the smallest available spatial resolution is preferred. This is

provided by the REMO model with a resolution of approximately 10 x 10 km (Jacob & Mahrenholz, 2006a-d).<sup>1</sup>

→ *Scenario studies will be based on REMO model data.*

### 5. *Scenario Study Set-Up:*

Two options for scenario combinations have been possible:

- a. Using a variety of climate model results, by applying the A1B scenario data series computed by both dynamical climate models REMO and CLM.
- b. Combination of different IPCC scenarios (A1B, B1 and A2) computed with the REMO model on a higher spatial resolution.

It has been decided to follow the second approach by setting up the scenarios with all three IPCC scenarios (A1B, B1 and A2) provided by the REMO model.

→ *The IPCC scenarios A1B, A2 and B1 of the first realisation of the REMO-UBA experiment, are applied.*

### 6. *Temporal Coverage:*

- a. **Control Scenario:** To define an equal temporal coverage of 30 years of observed (1969 – 2004) and REMO climate model (1961 – 2000) data series, a time period from 1971 to 2000 has been selected.
- b. **Climate Change Scenarios:** The time period considered for the flood probability scenario studies have been set from 2040 to 2070. In this way a comparison with impact studies among the KLIMZUG-Nord project members is provided (around ≈ 2050) and additionally it corresponds to the climate period defined in the Climate Atlas for North Germany (online)<sup>2</sup> for the middle of the 21<sup>st</sup> century.

→ *The covered time period for the control scenario is set from 1971 till 2000, and for the future scenario it is set from 2040 to 2070.*

For the climate scenario studies with the Kalypso Hydrology Model six data sets had to be downloaded from the CERA server for each scenario (C20, A1B, B1 and A2). The data variables and their acronyms as well as descriptions are summarized in attachment 7.

All data series are provided in NetCDF format, whereas finally 24 data series were downloaded and pre-processed. The precipitation data series used in the

---

<sup>1</sup> The CLM model data is displayed on a resolution of approximately 20 x 20km

<sup>2</sup> [www.norddeutscher-klimaatlas.de](http://www.norddeutscher-klimaatlas.de)

application scenarios represent the sum of the convective and the grid scale rainfall. The relative humidity is calculated from the 2m-air temperature (TEMP2) and 2m-dew point temperature (DEW2) on a regular geographical grid. This variable is only provided in the datastream D3, but not in the datastream D2 on a rotated grid. Downward directed data streams (e.g. precipitation) are indicated with a positive algebraic sign. When the vertical processes are directed upwards (e.g. the evaporation; EVAP), it is defined as a loss from the system and is indicated with a negative algebraic sign.

### 5.2.2 Pre-Processing of Climate Model Data Series

The maps of the project area are provided in Gauß-Krüger coordinates. For a first assumption of the required raster of the REMO model data, the borders of the project area have been transferred to geographical coordinates in degrees with the tool: CoordTrans v2.3 developed by Fransen Technology AB (<http://franson.com>).

With this first assumption, the required overall raster covering the project area has been defined with the following expansion:

- Longitude: 9.55° to 10.05°
- Latitude: 53.65° to 53.85°

To display the spatial distribution of the REMO data raster in the map of the project area, the coordinates of the REMO grid cells (in °) have been transferred to Gauß-Krüger-Coordinates indicated with Easting (E) and Northing (N) in the Table 5. 1.

**Table 5. 1 REMO grid cell coordinates (Datastream D3) transferred to Gauß-Krüger-Coordinates (E: Easting [km]; N:Northing [km], left bottom corner of cells).**

|   |  |   |   |   |  |
|---|--|---|---|---|--|
| <b>53.65°/9.55°</b><br>GRID CELL (13)<br>E: 3536.44 km<br>N: 5946.66 km | <b>53.65°/ 9.65°</b><br>GRID CELL (14)<br>E: 3543.05 km<br>N: 5946.72 km | <b>53.65°/9.75°</b><br>GRID CELL (15)<br>E: 3549.66 km<br>N: 5946.78 km | <b>53.65°/9.75°</b><br>GRID CELL (16)<br>E: 3556.26 km<br>N: 5946.84 km | <b>53.65°/9.95°</b><br>GRID CELL (17)<br>E: 3562.89 km<br>N: 5946.94 km | <b>53.65°/10.05°</b><br>GRID CELL (18)<br>E: 3569.50 km<br>N: 5947.03 km |
| <b>53.75°/9.55°</b><br>GRID CELL (7)<br>E: 3536.35 km<br>N: 5957.79 km  | <b>53.75° / 9.65°</b><br>GRID CELL (8)<br>E: 3542.95 km<br>N: 5957.85 km | <b>53.75°/9.75°</b><br>GRID CELL (9)<br>E: 3549.55 km<br>N: 5957.91 km  | <b>53.75°/9.85°</b><br>GRID CELL (10)<br>E: 3556.14 km<br>N: 5957.99 km | <b>53.75°/9.95°</b><br>GRID CELL (11)<br>E: 3562.74 km<br>N: 5958.07 km | <b>53.75°/10.05°</b><br>GRID CELL (12)<br>E: 3569.34 km<br>N: 5958.16 km |
| <b>53.85°/9.55°</b><br>GRID CELL (1)<br>E: 3536.27 km<br>N: 5968.92 km  | <b>53.85°/ 9.65°</b><br>GRID CELL (2)<br>E: 3542.85 km<br>N: 5968.98 km  | <b>53.85°/9.75°</b><br>GRID CELL (3)<br>E: 3549.43 km<br>N: 5969.04 km  | <b>53.85°/9.85°</b><br>GRID CELL (4)<br>E: 3556.01 km<br>N: 5969.12 km  | <b>53.85°/9.95°</b><br>GRID CELL (5)<br>E: 3562.59 km<br>N: 5969.20 km  | <b>53.85°/10.05°</b><br>GRID CELL (6)<br>E: 3569.17 km<br>N: 5969.29 km  |

The size of one grid cell is 0.1 x 0.1 degree. Transferred to Gauß-Krüger coordinates the grid cells display a size of about 11km (Easting) x 6.5km (Northing) with a departure of about 0.65<sup>1</sup>. The REMO model raster, which had been downloaded, comprises 18 grid cell data sets for the listed data values in Attachment 7. For the transformation of the downloaded climate model data, the cdo-tool (provided by the MPI-M) and the additional java-tool (developed by Dejan Antanaskovic from the

<sup>1</sup> The departure is the factor of the distance between meridians and decreases from the equator to the poles for the longitudinal data. In the project area the departure is reduced by a factor of about 0.65 referred to the departure at the Equator (1.0).

Institute of River and Coastal Engineering at the TUHH) have been applied. The required averaging of grid cell data series have been done over four grid cells with the java-tool. The final distribution of the downloaded 18 and the 10 averaged grid cells is depicted in Fig. 5. 2. The data series of the seven indicated grid cells have been allocated to respective sub-catchments to run hydrological simulations and were used for processing analyses.

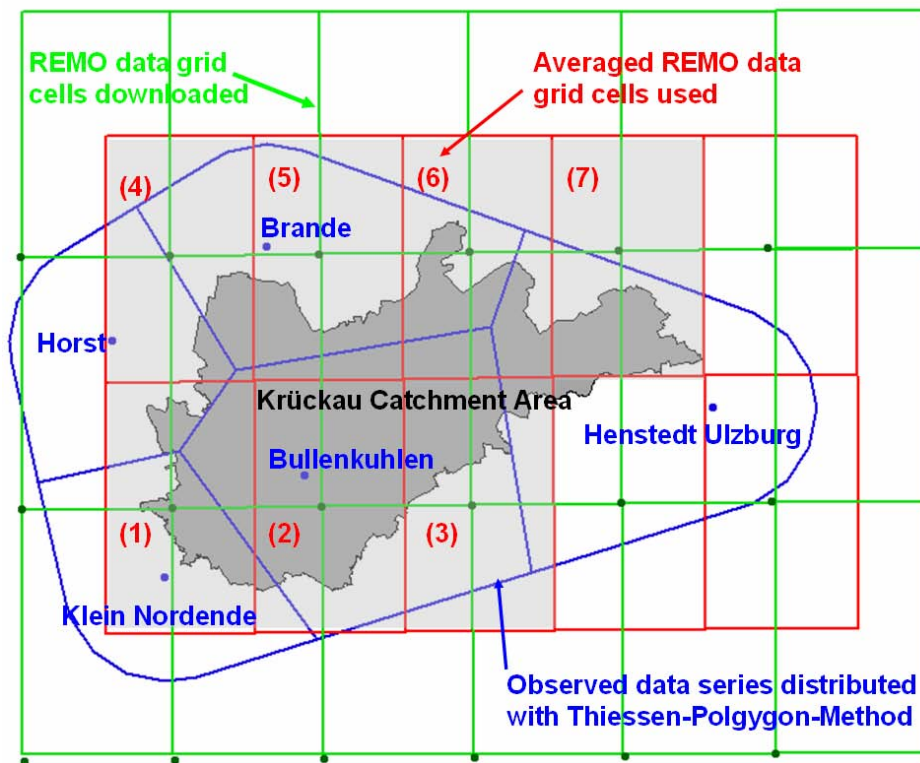


Fig. 5. 2 Rainfall gauging stations (blue) and REMO data raster on a regular grid (red) of the datastream D3 covering the catchment area of the river Krückau. [downloaded REMO data raster: green].

The data series of the potential evaporation have been calculated with the downloaded REMO data series of the wind speed, relative humidity and the global radiation. The procedure as well as the equations are outlined in Attachment 2.

One of the defined open research questions in chapter 2 is: if the smallest spatial resolution of the currently available climate model data is appropriate for flood probability studies. It is illustrated in Fig. 5. 2, that the spatial resolution of the climate model data is adequate for scenario studies in the Krückau catchment, due to the availability of an even finer resolution than provided by observed data series. But the applicability can not be generalised for other study areas. In mountainous or dense urban catchments a finer spatial resolution could be required.

### 5.3 Processing of Results of Climate Variables

The analysis of the scenario data series have been done with periods according to the hydrological year. Summer periods begin May 1<sup>st</sup> and winter periods begin

November 1<sup>st</sup>. The derived changes in the climate data series and the probability of extreme rainfall events is analysed with the data series of the seven REMO grid cells and the five gauging stations which cover the Krückau catchment area (Fig. 5. 2).

### 5.3.1 Climate Control Scenarios[1971 – 2000]

A number of strategies to analyse climate data series have been outlined in the methodology (3.4). For the analysis of the control scenario data series referred to the observed data series of the same time period from 1971 to 2000, two approaches have been applied. First a comparison of average climate data series (temperature, precipitation, potential evaporation) of hydrological year periods has been performed, and secondly a comparison of probability distributions of extreme rainfall events has been worked out.

#### 5.3.1.1 Average Climate Data Results

For the comparison of computed temperature time series with observed data series, the average temperature of the yearly, summer and winter sequences are calculated. For the comparison of the difference in precipitation and potential evaporation, the average sums have been computed. The results of the differences are summarized in Table 5. 2 in [°C] and [%]<sup>1</sup> respectively.

**Table 5. 2 Results of the comparison between observed and REMO control scenario data series.**

| <b>Average over time periods [1971 – 2000]</b> | <b>Average Temperature</b> | <b>Average Precipitation Sum</b> | <b>Average Evaporation Sum</b> |
|--|----------------------------|----------------------------------|--------------------------------|
| <b>summer</b>                                  |                            |                                  |                                |
| observed data series                           | 13.9°C                     | 440.9mm                          | 437.4mm                        |
| control scenario (C20)                         | 13.8°C                     | 565.5mm                          | 464.8mm                        |
| Difference (%)                                 | - 0.4%                     | + 22.0%                          | + 6.3%                         |
| <b>winter</b>                                  |                            |                                  |                                |
| observed data series                           | 5.4°C                      | 372.6mm                          | 178.4mm                        |
| control scenario (C20)                         | 4.5°C                      | 443.3mm                          | 144.8mm                        |
| Difference (%)                                 | - 16.7%                    | + 16.0%                          | -18.8%                         |
| <b>yearly</b>                                  |                            |                                  |                                |
| observed data series                           | 9.7°C                      | 813.5mm                          | 615.7mm                        |
| control scenario (C20)                         | 9.2°C                      | 1008.8mm                         | 609.5mm                        |
| Difference (%)                                 | - 5.0%                     | + 19.4%                          | -1.0%                          |

#### **Temperature:**

The average observed temperature of the summer period is 13.9°C between 1971 and 2000, which is 0.1°C higher than the average computed summer temperature (13.8°C). The average observed temperature of the winter period is 5.4°C and the computed REMO data display an average temperature of 4.5 °C, the difference between the data sets is 0.9°C. The yearly average temperature measured at the

---

<sup>1</sup> The percentage rates are calculated in relation to the results of the observed data series.

gauging stations is 9.7°C. This is 0.5°C higher than the yearly average temperature computed by the climate model REMO (9.2°C).

***Precipitation:***

An average precipitation of 440.9mm has been observed during the summer periods between 1971 and 2000, whereas the average precipitation computed with the climate model is 565.5mm and therewith 22% larger. The difference of the average winter precipitation between the observed (372.6mm) and computed data series (443.3mm) is less significant with 16%. The observed average yearly precipitation is 813.5mm, and the computed average yearly precipitation of the climate model REMO is 1008.8mm, which is 195.3mm (19.4%) higher than the observed data.

***Potential Evaporation:***

A difference of 6.3% has been calculated between the average summer evaporation of the observed data series (437.4mm) and the control scenario data (464.8mm). This difference is reasonable due to the displayed positive difference in precipitation rate (22%) and the low positive difference in temperature (0.4%), whereas the evaporation rate depends to a larger degree on the temperature. It can be assumed that the generation of runoff and drainage simulated with the control scenario data series will be higher than with the observed data series in the summer periods.

Although the computed average precipitation in the hydrological winter sequence is larger (16%) the computed average evaporation is lower by about 18.8%. This is derived by the computed lower temperature (16.7%) in the winter period, which has a high effect on the evaporation. It can be assumed as well that the computed runoff and drainage with the REMO control scenario data will be higher referred to the use of observed data series. The average yearly observed evaporation is 615.7mm which is 1.0% higher than the control scenario C20 evaporation (=609.5mm).

It is expected that the overall runoff and drainage volume simulated with the model Kalypso Hydrology will be higher with the REMO control scenario data than with the observed data series for the time period 1971 to 2000.

### *5.3.1.2 Statistical Evaluations of Rainfall Events*

It is required to calculate probability distribution curves of extreme rainfall events with observed as well as computed climate model data series. The results are post-processed later on to compute the magnitude of climate change impacts, CCFs as well as design rainfall events.

The analysis of probability distributions of extreme rainfall events have been done with hourly and daily data series. The statistical evaluations are worked out according to the approach defined in 3.4. After testing the independency of the rainfall events, a trend adjustment of the data series from 1971 to 2000 ( $M = 30$ ) has

been done for each hydrological year period (yearly, summer, winter) with a partial series of a number of  $N = e \cdot M \approx 82$  rainfall events.

In attachment 8 the results of the trend adjustments are illustrated according to the hydrological year sequences. In the summer periods no significant trend is displayed in the data series of the observed rainfall events, but in the REMO data series a significant decreasing trend towards the year 2000 is illustrated. This decreasing trend is distinguished for the first realisation of the REMO model run and has been detected as well in the UFOPLAN report (Jacob et al., 2008). The winter sequences of the observed and the REMO C20 data series of rainfall events illustrate an increasing trend towards the year 2000. The yearly series mainly comprise larger summer rainfall events. Therefore a similar decreasing trend in the REMO C20 data series and no trend in the observed data series are displayed.

With the trend adjusted data series, the statistical evaluations according to the approach described in the attachment 3 have been worked out. The applied correction factor for the observed data series is 1.03, due to a temporal aggregation of 4 intervals (each 15minutes) for hourly data series. For climate model data series a correction factor of 1.14 has to be defined. After the first statistical evaluations of the observed and computed REMO C20 data series, three outliers have been identified in the hourly and four outliers in the daily data series. The results of the Grubbs Tests are illustrated in Table 5. 3.

**Table 5. 3 Results of the Grubbs Test with the observed and REMO control scenario data series of extreme rainfall events.**

| Data series [1971-2000]          | Seasonal Periods | Extrema   | Date of Rainfall Event | Rainfall Intensity [mm/h] or [mm/d] | $\Delta G$ | Outlier adequately represented? |
|----------------------------------|------------------|-----------|------------------------|-------------------------------------|------------|---------------------------------|
| <b>Hourly Data Series [mm/h]</b> |                  |           |                        |                                     |            |                                 |
| C20 Scenario                     | Summer           | Extrema 1 | 05.09.1973             | 29.55                               | 0.49       | Yes                             |
|                                  | Summer           | Extrema 2 | 11.09.1975             | 33.37                               | 0.99       | No                              |
| Observed Data Series             | Summer           | Extrema 1 | 25.08.1997             | 24.24                               | 1.08       | Yes                             |
| <b>Daily Data Series [mm/d]</b>  |                  |           |                        |                                     |            |                                 |
| C20 Scenario                     | Summer           | Extrema 1 | 28.06.1982             | 125.51                              | 2.27       | No                              |
|                                  | Winter           | Extrema 1 | 04.02.1988             | 66.50                               | 1.92       | No                              |
| Observed Data Series             | Summer           | Extrema 1 | 26.08.1989             | 76.63                               | 2.31       | Yes                             |
|                                  | Winter           | Extrema 1 | 07.01.1998             | 49.34                               | 1.27       | Yes                             |

In the *hourly data series*, computed with the climate model, the rainfall event with an intensity of 33.37mm/h on the 11<sup>th</sup> September 1975 is not adequately displayed in the statistical evaluation; therefore it had to be neglected. The defined outlier on the

5<sup>th</sup> September 1973 (29.55mm/h) with a lower difference between the acceptable value according to DIN 53 804 of  $\Delta G = 0.49$  is adequately displayed in the statistical evaluation with a return period of about once in 50 years ( $T = 50a$ ). In the observed hourly data series an outlier has been defined as well with the Grubbs Test, but it is adequately represented in the statistical evaluation with a return period of about once in 100 years ( $T=100a$ ).

In the *daily data series* an outlier in each of the winter and summer sequences have been defined. Both outliers defined in the computed control scenario data series with REMO are not displayed adequately in the statistical evaluation. In contrast to this, the outliers defined in the observed data series are represented with an adequate higher probability of occurrence. The rainfall events in the summer period (76.63mm/d) and in the winter period (49.34mm/d) are both displayed with a return period of once in 125 years.

After the Grubbs Tests, the trend adjustment has been repeated and the final results are displayed in the attachment 8 according to the period of the hydrological season (summer, winter, yearly) and the duration of the rainfall (daily, hourly). With these data series the final probability distribution curves have been calculated which are transferred to graphs, which illustrate directly the return period  $T$  in years. The rainfall intensities with a specific return period are displayed in tables for each hydrological season and duration (daily, hourly) respectively in the attachment 8. The difference in percentage is referred to the observed data series.

For the short term hourly rainfall intensities the differences are higher than the differences in daily rainfall intensities. The differences cover a range of about 3% ( $T=1a$ ) to about 40% ( $T=100a$ ) in the summer and yearly rainfall intensities (Fig. 5. 3 and Fig. 5. 4). The differences in the winter rainfall intensities increases from about 3% for higher probabilities of occurrence ( $T =1a$ ) to a difference of about 20% for 100year events ( $T=100a$ ).

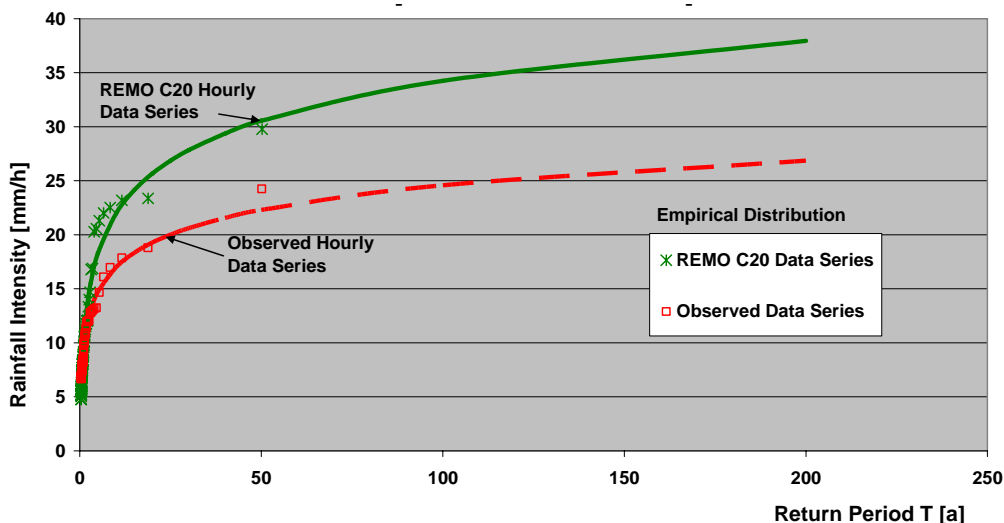
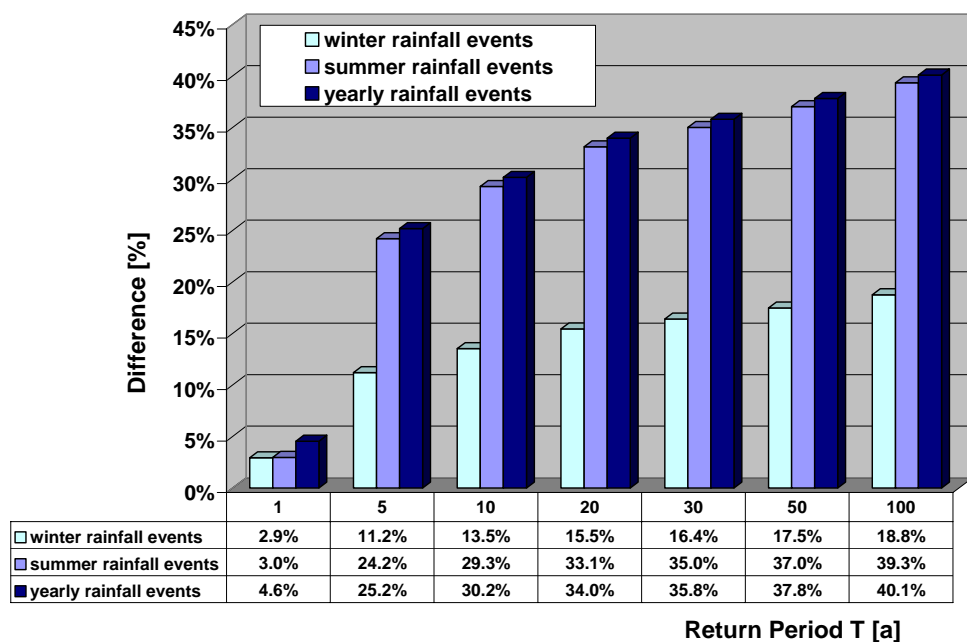


Fig. 5. 3 Probability distribution curves of hourly extreme rainfall events [mm/h] in the summer periods.



**Fig. 5. 4 Differences between the probability distribution curves of REMO climate model and observed hourly data series.**

For daily rainfall intensities, the differences between the REMO and observed data series range from 11% to 33%. The yearly series of rainfall events is mainly composed of summer rainfall events, which results in comparable differences. Between the winter rainfall heights per day, larger differences have been computed for events which have a higher probability of occurrence (e.g. T =1a). The results are displayed in attachment 8.4.

### 5.3.2 Future Climate Scenarios [2040 – 2070]

The changes in climate derived in the IPCC-scenarios for the Krückau catchment area have been analysed with three approaches defined in the methodology. The average change in temperature, precipitation and evaporation are calculated and illustrated with trend analyses. For the studies of extreme rainfall events two approaches are used: first the number of occurrence of daily rainfall heights for hydrological seasons are compared and thereafter short term extreme rainfall intensities (in [mm/h]) are analysed in more detail with statistical evaluations.

#### 5.3.2.1 Trend Line Analysis of Climate Variables

The trend analysis has been done with data series over 100 years from 1970 to 2070 with average temperatures and the summations of precipitation as well as evaporation over the respective summer, winter and yearly sequences. As reference for the trend analysis, the average values of the REMO C20 control scenario data series from 1970 till 2000 have been used. The results of the trend line analysis are displayed in diagrams and tables in attachment 9. In particular, the average projected trend (1), the calculated change for the climate period (2040 to 2070) in percentage

(2) as well as the value of change (3) and the resulting average projected value (4) are outlined. The slope of the trend is calculated per change of [°C] or [%] per decade. A correction of the REMO C20 data series have not been covered in the scope of this thesis. Therefore, the changes in temperature, precipitation and evaporation had to be referred to the observed data series to assume the absolute change in [°C] or [mm] respectively. A summary of the changes per defined hydrological season (summer, winter, year) are given in the Table 5. 4.

**Table 5. 4 Changes per hydrological season of Temperature [°C], Precipitation [%] as well as Evaporation [%].**

| Seasonal Sequences        | IPCC scenario | Temperature                              | Precipitation                            | Evaporation                              |
|---------------------------|---------------|--|--|--|
|                           |               | Average Percentage change [2040 to 2070] | Average Percentage change [2040 to 2070] | Average Percentage change [2040 to 2070] |
| Changes in Summer Periods | B1            | +~ 0.9 to 1.0 °C                         | +~ 2.4 to 3.3 %                          | +~ 2.8 to 4.4 %                          |
|                           | A1B           | +~ 1.3 to 1.6 °C                         | +~ 3.3 to 3.9 %                          | +~ 3.0 to 5.1 %                          |
|                           | A2            | +~ 1.1 to 1.3 °C                         | +~ 1.6 to 2.7 %                          | +~ 4.2 to 7.1 %                          |
| Changes in Winter Periods | B1            | +~ 1.1 to 1.3 °C                         | +~ 10.5 to 14.9 %                        | +~ 4.0 to 5.5 %                          |
|                           | A1B           | +~ 1.4 to 1.7 °C                         | +~ 14.4 to 22.6 %                        | +~ 7.6 to 11.8 %                         |
|                           | A2            | +~ 1.7 to 2.0 °C                         | +~ 11.5 to 18.1 %                        | +~ 7.5 to 11.6 %                         |
| Changes in Yearly Periods | B1            | +~ 0.9 to 1.3 °C                         | +~ 2.7 to 4.2 %                          | +~ 2.2 to 2.6 %                          |
|                           | A1B           | +~ 1.3 to 1.6 °C                         | +~ 5.2 to 9.3 %                          | +~ 3.2 to 4.8 %                          |
|                           | A2            | +~ 1.2 to 1.5 °C                         | +~ 0.0 to 1.6 %                          | +~ 4.1 to 6.3 %                          |

The temperature in the summer period increases by about 0.9°C to 1°C in the B1 scenario, by about 1.3°C to 1.6°C in the A1B scenario and by about 1.1°C to 1.3°C in the A2 scenario. The changes in the average yearly series are slightly higher than in the summer periods. The largest changes are projected for the winter periods, where the temperature increases by about 1.1°C to 1.3°C in the B1 scenario, by about 1.4°C to 1.7°C in the A1B scenario and by about 1.7°C to 2°C in the A2 scenario.

The largest changes in the average precipitation are projected for the winter periods in the A1B scenario with an increase of about 14.4% to 26.6% which corresponds to about 40mm to 80mm more rainfall. The scenarios B1 and A2 display changes between 10% and 18% (39mm to 67mm). In the summer periods the changes of the precipitation are lower and range from 1.6% to 3.9 % (6.9mm to 17mm). Overall the A1B scenario displays higher changes than the other scenarios in seasonal precipitation.

The changes in evaporation are largest in winter periods, which is reasonable due to the larger increases in the temperature and precipitation. The largest changes are displayed by the A1B and the A2 scenarios with 7.5% to 11.8%, which corresponds to an increase of about 13.4mm to 21.1mm. The evaporation in the summer periods changes by about 2.8% to 7.1% in the scenarios A1B and A2.

With the trend line calculations, the average and long term changes in the water budget derived in the climate change scenarios are analysed. But the changes in flood peak formations in catchments are mostly derived by changes in rainfall intensities. For the study of changes in daily precipitation and short term rainfall events, two different approaches are applied; namely the computation of the number of occurrence of threshold events and statistical evaluations.

5.3.2.2 *Number of Occurrence of Daily Rainfall Thresholds*

The changes derived in daily precipitation in the climate scenarios from 2040 to 2070 have been analysed by calculating the days with rainfall heights above defined threshold values. This approach is widely used in climate change studies (e.g. Jacob et al., 2008, Bischoff, 2007, North-German Climate Atlas). The aim is to set up a basis for the comparison of the results with related climate change studies of extreme events. The following threshold values have been defined as described in the methodology:

- Number of days with  $15\text{mm/day} \leq \Sigma P^1 \leq 20 \text{ mm/day}$
- Number of days with  $20\text{mm/day} \leq \Sigma P \leq 25 \text{ mm/day}$
- Number of days ('wet days') with  $25\text{mm/day} \leq \Sigma P$

The results of the number of days which meet the threshold definitions are illustrated in figures attached to the thesis (Attachment 10) and are summarised in Table 5. 5. A differentiation has been done according to the seasons (summer, winter, yearly).

Table 5. 5 Summary of the number of days meeting the defined threshold categories.

|   | Number of Days meeting the Threshold Categories |             |              |             |
|---|---|-------------|--------------|-------------|
|   | Control scenario                                | B1 scenario | A1B scenario | A2 scenario |
|   | 1971 - 2000                                     | 2040 - 2070 |              |             |
| <b>15mm/day <math>\leq \Sigma P \leq 20 \text{ mm/day}</math></b> |   |             |              |             |
| yearly  | ~ 166   | ~ 208       | ~ 243        | ~ 196       |
| summer  | ~ 103   | ~ 133       | ~ 140        | ~ 115       |
| winter  | ~ 63  | ~ 75        | ~ 103        | ~ 81        |
| <b>20mm/day <math>\leq \Sigma P \leq 25 \text{ mm/day}</math></b> |   |             |              |             |
| yearly  | ~ 74  | ~ 85        | ~ 97         | ~ 76        |
| summer  | ~ 47  | ~ 57        | ~ 65         | ~ 45        |
| winter  | ~ 27  | ~ 28        | ~ 32         | ~ 31        |
| <b>25mm/day <math>\leq \Sigma P</math> (wet days)</b>             |   |             |              |             |
| yearly  | ~ 65  | ~ 69        | ~ 96         | ~ 66        |
| summer  | ~ 41  | ~ 43        | ~ 66         | ~ 46        |
| winter  | ~ 24  | ~ 26        | ~ 30         | ~ 20        |

It can be stated, that for all threshold value analyses, more days with higher precipitation occur in the summer than in the winter periods. And the numbers of

<sup>1</sup>  $\Sigma P$  = sum of precipitation per day [mm/day]

days which meet the threshold settings decreases from daily precipitations of the lower threshold values ( $15\text{mm/day} \leq \Sigma P \leq 20 \text{ mm/day}$ ) to the maximum threshold value of wet days.

For the lower threshold value with a precipitation between 15mm/day and 20mm/day the largest increase is projected with the A1B scenario for all seasons. For the summer period an increase of 37 days and for the winter period an increase of 40 days is projected referred to the REMO C20 control scenario [1971 – 2000]. In the scenarios B1 and A2 the increase of the number of days ranges between 30 to 12 days in the summer periods and between 12 to 18 days in the winter periods respectively.

For the second threshold category ( $20\text{mm/day} \leq \Sigma P \leq 25 \text{ mm/day}$ ) the largest increase of days is projected again with the A1B scenario. 65 days are simulated with the defined daily precipitation in the summer periods, which correspond to an increase of 18 days referred to the REMO C20 control scenario. The scenario B1 displays an increase of 10 days in the summer period, whereas the A2 scenario projects a decrease of 2 days. In the winter period only small changes of the number of days (1 to 5days) in all scenarios are projected.

The number of days which are defined as wet days ( $>25\text{mm/day}$ ) are illustrated additionally in Fig. 5. 5. The largest increase of the number of wet days is projected in the scenario A1B with 25 days in the summer period. Overall the number of wet days increases to 66 days in this scenario. The other scenarios B1 and A2 display only small increases of 2 to 5 days in the summer periods.

In the winter periods a slightly increase of wet days is projected in the scenarios B1 (+2days) and A1B (+6days), but in the A2 scenario the number of projected wet days even decrease by about 4 days.

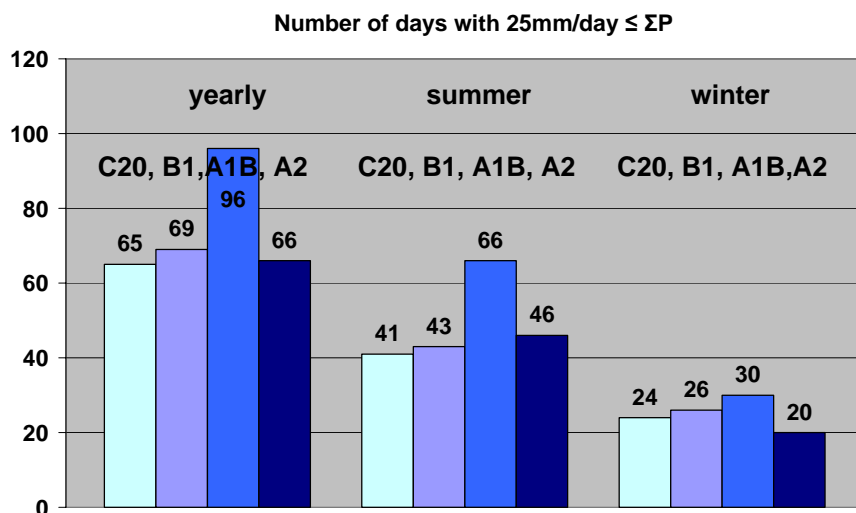


**Fig. 5. 5** Number of days which are defined as wet days ( $>25\text{mm/day}$ ) in the IPCC scenarios (B1, A1B, A2) compared to the computed control scenario (C20).

*5.3.2.3 Statistical Evaluations of Rainfall Events*

The statistical evaluations are calculated with the methodology outlined in Attachment 3, with correction factors of 1.14 and adjustments of trends. Any outliers are identified and discussed with Grubbs Tests.

The final results of the trend adjusted data series of rainfall events for the IPCC scenarios A1B, A2 and B1 are displayed in Attachment 11. In contrast to the trend adjustment of the control scenario (C20) and observed data series, the trend adjustment of projected future IPCC-scenarios have been done to the mean date of the considered time period from 2040 to 2070 (2055), which corresponds to the approach described in the methodology (3.4). As pointed out in the analysis of the previous studies, the climate change effects in the summer and the winter period differs significantly.

In the final scenario data series of the summer periods no significant trend has been detected. In the data series of the winter rainfall events a slightly increasing trend in the B1 scenario and a minor decreasing trend in the A2 scenario has been adjusted. In the yearly data series of rainfall events, an increasing trend in the A1B scenario and a decreasing trend in the A2 scenario had to be adjusted.

For the identification of outliers the Grubbs Test has been applied which is based on the assumption that the data series can be reasonable approximated by a normal distribution (NIST, 2006). This has been tested first with the Kolmogorov-Smirnov Test in the statistic tool provided by the Institute of River and Coastal Engineering at the TUHH. The results of the Grubbs Tests of the scenario studies are displayed in Table 5. 6.

**Table 5. 6 Results of the Grubbs Tests of the future scenario studies of extreme rainfall events.**

| <b>Scenario data series [2040 – 2070]</b> | <b>Seasonal Period</b> | <b>Extrema</b> | <b>Date of Rainfall Event</b> | <b>Rainfall Intensity [mm/h]</b> | <b>ΔG</b> | <b>Outlier adequately represented?</b> |
|---|------------------------|----------------|-------------------------------|----------------------------------|-----------|--|
| <b>A2</b>                                 | Summer                 | Extrema 1      | 06.07.2059                    | 45.10                            | 3.56      | <b>No</b>                              |
|   | Summer                 | Extrema 2      | 25.08.2045                    | 36.06                            | 2.29      | <b>No</b>                              |
|   | Summer                 | Extrema 3      | 22.07.2064                    | 31.63                            | 1.51      | <b>No</b>                              |
| <b>B1</b>                                 | Summer                 | Extrema 1      | 08.08.2065                    | 57.06                            | 2.84      | <b>No</b>                              |
|   | Summer                 | Extrema 2      | 27.08.2047                    | 51.27                            | 2.57      | <b>No</b>                              |
|   | Summer                 | Extrema 3      | 30.08.2048                    | 49.58                            | 2.41      | <b>No</b>                              |
|   | Summer                 | Extrema 4      | 09.10.2056                    | 41.03                            | 1.50      | <b>No</b>                              |
| <b>A1B</b>                                | Winter                 | Extrema 1      | 07.04.2056                    | 14.99                            | 1.26      | <b>No</b>                              |
|   | Winter                 | Extrema 2      | 19.11.2047                    | 14.26                            | 0.99      | <b>No</b>                              |
|   | Winter                 | Extrema 3      | 19.11.2067                    | 12.87                            | 0.51      | <b>Yes</b>                             |

In the data series of the scenario A2 three outliers, in the scenario B1 four outliers and in the scenario A1B two outliers have been defined which are not displayed with an adequate probability of occurrence in the statistical evaluations and distort the results. In the A1B scenario one more outlier has been defined with a rainfall

intensity of 11.29mm/h which differs from the test value according to DIN 53 804 by about  $\Delta G = 0.51$ . This outlier is defined with an adequate probability of occurrence of once in about 52 years in the statistical evaluation and is therefore considered in the analysis. The projected changes of rainfall in the future scenarios are summarized in Table 5. 7 and illustrated in graphs in the attachment 11.

**Table 5. 7 Average change in extreme rainfall [mm/h] derived by future climate scenarios referred to the REMO C20 control scenario.**

| Climate Period<br>[2040 – 2070]                | Return Period T [a] |      |      |      |      |      |      |       |       |   |
|--|---------------------|------|------|------|------|------|------|-------|-------|---|
|  | 1                   | 2    | 3    | 5    | 10   | 20   | 30   | 50    | 100   | a |
| <b>Average Summer Rainfall Differences [%]</b> |                     |      |      |      |      |      |      |       |       |   |
| A1B-Scenario                                   | 63.5                | 44.1 | 37.3 | 31.2 | 25.3 | 21.2 | 19.4 | 17.4  | 15.2  | % |
| B1-Scenario                                    | 27.6                | 18.2 | 14.9 | 11.9 | 9.1  | 7.1  | 6.2  | 5.2   | 4.2   | % |
| A2-Scenario                                    | 29.3                | 15.0 | 10.0 | 5.5  | 1.2  | -1.8 | -3.2 | -4.6  | -6.2  | % |
| <b>Average Winter Rainfall Differences [%]</b> |                     |      |      |      |      |      |      |       |       |   |
| A1B-Scenario                                   | 7.8                 | 7.2  | 7.0  | 6.7  | 6.4  | 6.2  | 6.1  | 6.0   | 5.9   | % |
| B1-Scenario                                    | 7.6                 | 5.1  | 4.0  | 2.8  | 1.6  | 0.6  | 0.2  | -0.4  | -1.0  | % |
| A2-Scenario                                    | 5.0                 | 0.3  | -1.8 | -4.0 | -6.3 | -8.1 | -9.0 | -9.9  | -11.1 | % |
| <b>Average Yearly Rainfall Differences [%]</b> |                     |      |      |      |      |      |      |       |       |   |
| A1B-Scenario                                   | 49.9                | 34.4 | 28.7 | 23.4 | 18.2 | 14.6 | 12.9 | 11.1  | 9.1   | % |
| B1-Scenario                                    | 10.8                | 6.1  | 4.3  | 2.7  | 1.1  | 0.0  | -0.5 | -1.1  | -1.7  | % |
| A2-Scenario                                    | 7.5                 | 0.5  | -2.1 | -4.5 | -6.8 | -8.4 | -9.2 | -10.0 | -10.9 | % |

For all scenarios the largest changes are computed for the summer rainfall events which are illustrated additionally per return period (T) in Fig. 5. 6.

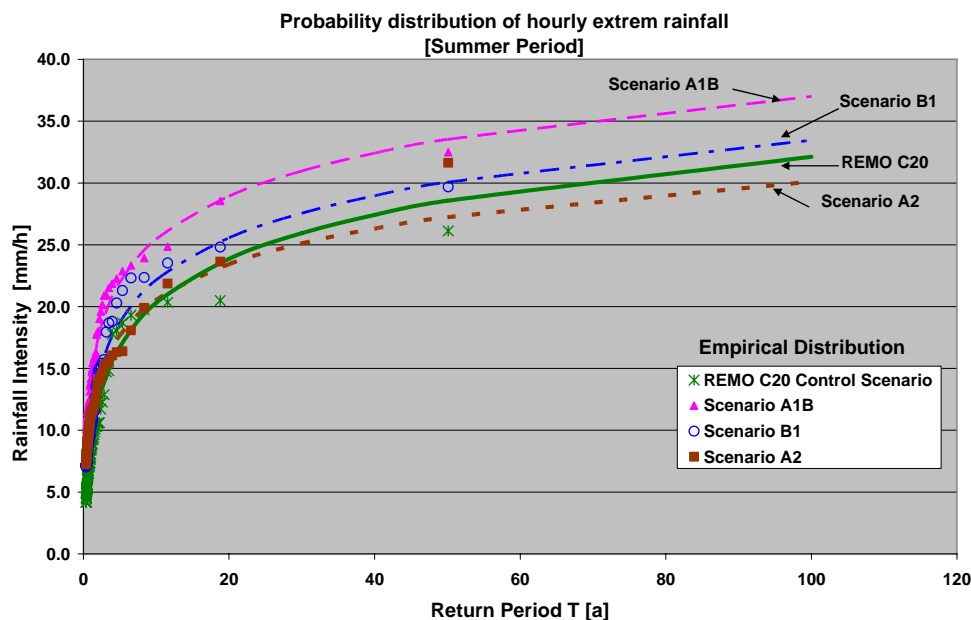


**Fig. 5. 6 Probability distribution curves of summer rainfall intensities in [mm/h] of future climate scenarios A1B, B1 and A2 compared to the control scenario C20.**

The scenario A1B displays the largest increases in the probability distribution curves of the rainfall intensities for all seasons. Especially for the summer rainfall events with a high probability of occurrence of once in a year large changes up to 63.5% are

computed in the A1B. For rainfall events with a low probability of occurrence ( $T > 50a$ ), the changes are below 17%.

The scenario B1 displays lower increases of summer rainfall intensities for larger probabilities of occurrence of about 27.6% and only slight increases for 100year summer events of about 4.2%. In the winter and yearly series decreasing rates are projected for 100year events. In the scenario A2 even lower values are projected than in the B1 scenario and decreasing rates are illustrated for 100year summer, winter and yearly rainfall events.

### ***Referring the projected results of the extreme rainfall events to the trend analyses results:***

By comparing the change of the number of wet days as well as the statistical evaluations of hourly data series, with the trend of the average precipitation per season, it can be stated that the change of extreme rainfall events is reasonable for all seasons. In the A1B scenario the highest increase of average seasonal precipitation, the highest increase of wet days and the largest increase of hourly rainfall heights are projected.

In contradiction to the higher changing rates of wet days and extreme rainfall intensity in the summer periods, there is only a minor increase projected for the average summer precipitation. It can be stated that the increase of extreme rainfall events in the summer period is not caused by the overall increase of average precipitation, but by the increase of the frequency of extreme rainfall events in dryer summers.

In contrast to the simulation results for the summer periods, the average winter precipitation increases by about 14% to 22% in the scenario A1B and by about 10% to 18% in the scenarios B1 and A2. But the number of wet days increases of just 6 days for the scenario A1B and even decreases for the scenario A2. It can be stated that the winter is projected to become wetter, with a decreasing tendency of extreme precipitation events in all scenarios.

With these results of the climate data analysis, it can be already assumed that the projected climate change impacts on the flood probability in the Krückau catchment, will be higher in the summer periods and that the scenario A1B displays the larger changes in extreme events.

## **5.4 Processing of Flood Probability Scenario Results**

For the analysis of flood peak probability changes derived in climate change scenarios specific locations of interest have been defined. These locations are selected with respect to the flood situation in the urban area of Elmshorn and the determined hot spots (see 5.1.1). Before the flood peak simulations have been performed with the climate model data series, a comparison has been done of the

currently used timesteps for the hydrological simulations and the timestep, which is used for the climate scenarios. Overall 750 short term simulations have been run on computers to calculate the required number of flood hydrographs for the statistical evaluations in climate scenarios. The results are processed for the comparison of the control scenario data series and future climate scenarios.

#### 5.4.1 Locations of Interest

For analysing the projected future flood probability situation in the Krückau catchment in climate scenarios, specific nodes and sub-catchments of interest have been defined. Three nodes have been determined, which define the inflow into the river section in Elmshorn. These nodes are situated downstream of the tributaries: Eckhorner Au, Offenau and the upstream section of the Krückau. In Elmshorn a node in the district: Langelohe, and the end node of the whole catchment has been analysed in more detail. The node ‘Langelohe’ is situated close to the Else-Brandström school at the Krückau Park, which is located in a flood risk area and is therefore of special interest. The end node of the whole catchment is located downstream of the densely urbanised city centre of Elmshorn. The flow at the nodes in Elmshorn is influenced by the tidal movement, but these conditions could not be taken into account for the flood probability analysis in this thesis.

Additionally to the nodes in the river sections, the discharge from two sub-catchments have been analysed in more detail, which are pointed out in Fig. 5. 7. In the sub-catchment ELMSH\_06\_02 two hot spots have been defined according to flood events in the past: the street underpass of the ‘Hamburger Strasse’ (known as ‘Badewanne’) and the Steindammwiesen Park. The catchment ELMSH\_E13\_04 drains to the node Langelohe and is of interest for adaptation scenario studies with SUDS later on. These sub-catchments represent the largest urban sub-catchments in Elmshorn, which are characterised by dense residential as well as commercial areas. The identification of the nodes as well as sub-catchments in the Kalypso Hydrology model and the respective drained catchment areas are listed in the Table 5. 8.

**Table 5. 8 Nodes and sub-catchments of interest for the flood probability scenario studies.**

| Location of Interest                          | Term in the Kalypso Hydrology Model | Drained Area [km <sup>2</sup> ] |
|---|-------------------------------------|---------------------------------|
| <b>Tributary Inflow Nodes to Elmshorn</b>     |                                     |                                 |
| Tributary Eckholter Au - Node: ‘Kölln’        | [Eckh_08_1]                         | 35.6                            |
| Upstream Krückau river section - Node: ‘A23’  | [Kruek_23_1 ]                       | 129.9                           |
| Tributary Offenau- Node: ‘Offenau’            | [OFF_10_0]                          | 10.2                            |
| <b>Nodes of interest in Elmshorn</b>          |                                     |                                 |
| Node: ‘Langelohe’                             | [Kruek_29_1 ]                       | 173.4                           |
| End Node of the catchment Krückau             | [ENDKNOTEN]                         | 185.0                           |
| <b>Sub-catchments of interest in Elmshorn</b> |                                     |                                 |
| Sub-catchment ‘ELMS_E06_02’                   | ELMS_E06_02                         | 1.4                             |
| Sub-catchment ‘ELMSH_E13_04’                  | ELMSH_E13_04                        | 2.1                             |

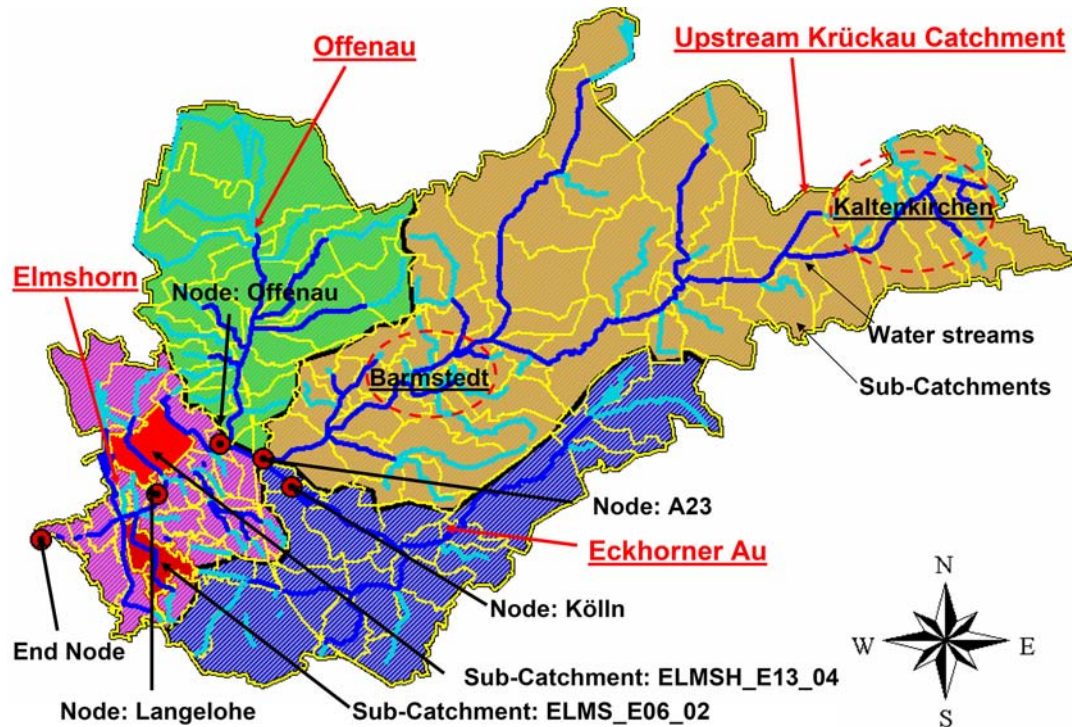


Fig. 5. 7 Nodes and sub-catchments of interest for the flood probability analysis.

#### 5.4.2 Differentiation of Simulation Timesteps

One of the open questions outlined in chapter 2, is the applicability of current climate model data series with the smallest temporal resolution of hourly data series for the simulation of extreme events in hydrological models. For this purpose a short term simulation of the hydrological model has been done with hourly data series and the originally used 15minute data series. The study has been done with the results of an observed flood event in May 1992. The effects of using varying simulation time steps on the flood hydrographs are different for urban and rural sub-catchments. To discuss the differences, a hydrograph of a rural sub-catchment at the ‘Vielmoor Graben’ in the catchment area of the tributary Eckhorner Au and a hydrograph of the urban area ‘ELMS\_E06\_02’ in Elmshorn (Fig. 5. 7) have been analysed in more detail. Additionally, the hydrograph at the node ‘Langelohe’ has been computed to display the differences at a node, which is influenced by a larger catchment including urban as well as rural sub-catchments. The hydrographs are displayed in attachment 12.

For the hourly simulations, the rainfall data series with 15-minute steps have been temporally aggregated to hourly data series. The maximum rainfall last for just 30minutes with a maximum of 2.45mm in 15minutes. By the aggregation of the 15minute data series to hourly data series a maximum rainfall intensity of 5.6mm in 1h is computed for the simulations, but this maximum is computed for an earlier time in the rainfall event. The intensity of rainfall with respect to the timestep is decreasing by the aggregation of the 15minute data series to the hourly data series

which can have significant impacts on the simulation results and (like in this example) the maximal rainfall intensity could be as well shifted in time.

In the rural sub-catchment (3.6km<sup>2</sup>) a peak discharge of 0.126m<sup>3</sup>/s has been calculated with simulation timesteps of 15minutes, and with hourly simulation timesteps, a peak discharge of 0.104m<sup>3</sup>/s has been computed. In the urban sub-catchment (1.4km<sup>2</sup>) the influence of the simulation timesteps is larger because of the faster flow processes on sealed areas. The shift of the maximal rainfall intensity causes as well a shift in the flood peaks. With time steps of 15minutes, a maximal flow peak of 1.01m<sup>3</sup>/s and with hourly time steps a flow peak of 0.59m<sup>3</sup>/s is simulated. In both cases, the flood volume remains almost the same with the different simulation timesteps for both sub-catchments, which is reasonable as the overall precipitation sum does not change with the different simulation time steps.

At the node Langelohé the shift in the maximal rainfall intensity has an influence on the flood peak (Fig. 5. 8). With simulation time steps of 15minutes, a flood peak of 4.26m<sup>3</sup>/s, and with hourly simulation time steps, a flood peak of 4.23m<sup>3</sup>/s is computed. This is a difference of only 0.7%, but the peak is shifted by about 6 hours.

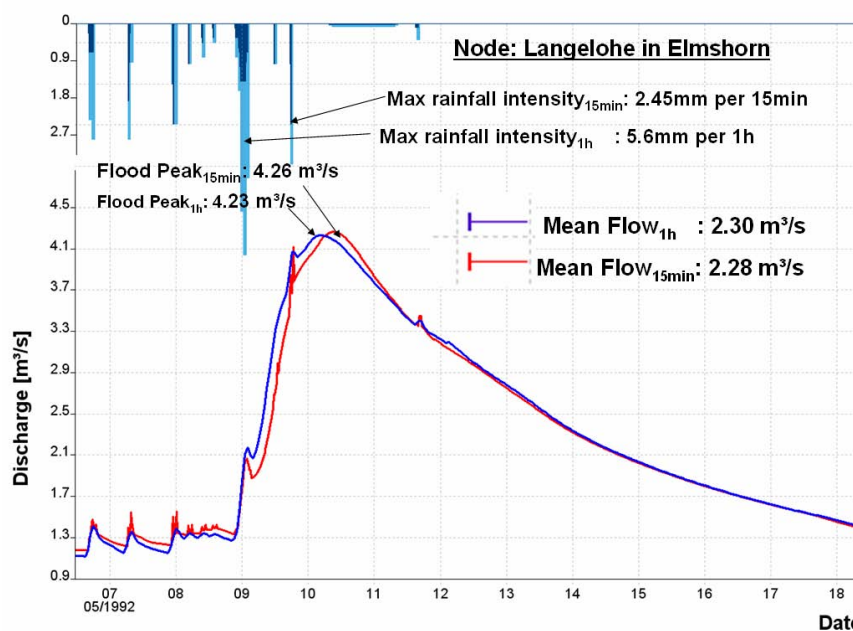


Fig. 5. 8 Results of the flood hydrographs at the node Langelohé with 15minute and hourly simulation timesteps.

### 5.4.3 Statistical Evaluations of Flood Peaks

For the scenario studies, flood hydrographs have been simulated at the nodes and the sub-catchments of interest. According to the methodology described in (3.4.5) a number of two to three simulation results should be used for each winter and summer period. Therefore about 5 flood events have to be computed for every year in the statistical evaluations. Further on, five data series, each covering a time period of 30 years, had to be considered for the scenario studies:

- Scenario i=0: ‘Scenario 0’: status quo flood peak series computed with observed rainfall data series [1971 – 2000]
- Scenario i=1: REMO C20 control scenario run [1971 – 2000]
- Scenario i=2: IPCC scenario A1B [2040 – 2070]
- Scenario i=3 IPCC scenario B1 [2040 – 2070]
- Scenario i=4 IPCC scenario A2 [2040 – 2070]

This results in a number of about 750 short term simulations which have been required for the analysis of the changes in flood probability.

$$\sum_{i=0}^{Z=4} \text{Scenario}_i * 5 \frac{\text{flood events}}{\text{year}} * 30\text{years} = 750 \text{ Short Term Simulation}$$

According to the methodology defined in (3.4) the trend adjustment and the computation of the flood probability curves have to be repeated when outliers are identified in the data series which are not represented with an adequate return period and distort the statistical results. The results of the final outlier Grubbs Tests are listed in Table 5. 9. Thereafter the final results of the trend adjustment and the statistical evaluations are described.

**Identification and discussion of outliers**

Like for the extreme rainfall statistics, the applicability of the Grubbs method for normal distributed data series has been approved with the Kolmogorov Smirnov test. The identified outliers are listed in Table 5. 9 with the flood peaks simulated for the node Langelohé, but these outliers have been defined for all locations.

**Table 5. 9 Identification of outliers in the flood peak data series with the Grubbs Test.**

| Data series                   | Seasonal Period | Extrema   | Date of Flood Event | Flood peak at the node Langelohé [m³/s] | ΔG   | Outlier defined with an adequate probability of occurrence |
|-------------------------------|-----------------|-----------|---------------------|---|------|--|
| <b>[1971 to 2000]</b>         |                 |           |                     |   |      |  |
| <b>Scenario 0 (reference)</b> | Winter          | Extrema 1 | 01/11/1998          | 17.75                                   | 1.10 | <b>Yes</b>   |
| <b>C20 Control Scenario</b>   | Summer          | Extrema 1 | 30/06/1982          | 25.51                                   | 1.58 | <b>No</b>  |
|                               |                 | Extrema 2 | 24/09/1991          | 24.69                                   | 1.45 | <b>Yes</b>   |
|                               | Winter          | Extrema 1 | 19/03/1975          | 25.57                                   | 0.09 | <b>No</b>  |
|                               |                 | Extrema 2 | 06/02/1988          | 28.19                                   | 0.56 | <b>No</b>  |
| <b>[2040 to 2070]</b>         |                 |           |                     |   |      |  |
| <b>A1B Scenario</b>           | Summer          | Extrema 1 | 28/09/2068          | 25.37                                   | 0.04 | <b>Yes</b>   |

When the outlier is defined with an adequate probability of occurrence in the statistical evaluation, the outlier is taken into account. Otherwise the outlier is eliminated from the statistical evaluation.

For the decision of considering an outlier in the statistical evaluation, different criteria have been compared. For the scenario 0, the decision about considering the flood peak simulated on the 01/11/1998 in the statistical evaluation, has been made by comparing results of previous studies done by the PÜK in 2008 for the Krückau catchment (PÜK, 2008). The outlier (17.75m<sup>3</sup>/s) is defined in the statistical evaluation with an adequate return period of once in about 100 years.

In the REMO C20 data series two outliers in the summer and two outliers in the winter period have been identified, whereas one of the outliers in the summer period is taken into account for the statistical evaluation. The summer flood peak outlier (24.69m<sup>3</sup>/s) is defined with an adequate return period of about once in 100 years in the statistical evaluations. For the decision about neglecting the other outliers in the statistical evaluation, the results of a comparable local study in the Metropolitan Region of Hamburg have been referred. The study has been done in 2009 for the catchment of the river Wandse and REMO control scenario data series have been used as well. In the data series only one outlier in the summer periods of the C20 data series has been identified and taken into account for the statistical evaluations (Golder Associates, 2009).

In the IPCC scenario A1B one outlier in the summer period has been detected with a flood peak of 25.37m<sup>3</sup>/s at the node Langeloh. This outlier is represented in the statistical evaluation with an adequate probability of occurrence of about once in 58 years.

Exceptions have been defined in the flood peak results of the Scenario B1 at the node Kölln (Eckhorner Au) and at the node A23, whereas one more summer flood peak outlier has been defined, which distorted the statistical evaluation and the calculation of a Log-Normal-Type III distribution. An additional outlier in the summer flood peak data series of the scenario A2 has been detected, which is represented in the statistical analysis with an adequate return period of once in 100years and is taken into account for the statistical evaluation. In the two sub-catchments in Elmshorn two outliers in the summer periods have been defined, whereas the smaller outlier is represented with an adequate return period of once in 67years, if the other one is not considered in the statistical evaluation.

After the outliers have been discussed, the trend analysis of the data series has been repeated as well as the statistical evaluations.

### ***Trend adjustments***

The trend adjustments have been done with the data series for all scenarios (0, C20, A1B, B1 and A2) according to the hydrological seasons (summer, winter and yearly series) and the nodes of interest. For the sub-catchments in Elmshorn, only the IPCC scenario A1B, which displays the largest changes, has been displayed. Because the focus is set on assessing the maximum climate change impacts and the effectiveness of SUDS.

Overall 93 trend adjustments had to be done:

$$\left. \begin{array}{l} \sum_{i=0}^{Z=4} \text{Scenario}_i * 3_{\text{seasons}} * 5_{\text{Nodes of interest}} = 75 \\ \sum_{i=0}^{Z=2} \text{Scenario}_i * 3_{\text{seasons}} * 2_{\text{Catchments of Interest}} = 18 \end{array} \right\} = 93 \text{ Trend Adjustments}$$

It has been decided to attach only the diagrams of the trend adjustments of the A1B scenario of the summer period to the thesis (Attach. 13). For all locations of interest slightly increasing trends of the summer flood peaks are projected.

**Probability Distribution Curves**

The statistical evaluation of flood peaks have been worked out with the Log-Pearson-Type-III and Log-Normal-Type-III distributions, which have been defined as appropriate for flood peak analysis according to the U.S. Water Resources Council (Fang et al., 1994), the DVWK 101 (1979) and Rao & Srinivas (2008).

For this purpose the statistic tool developed at the Institute of River and Coastal Engineering at the TUHH has been applied. For the seven locations of interest and the hydrological seasons (summer, winter, yearly) 21 probability distribution curves have been worked out.

$$\sum_{i=1}^{L=7} \text{Location}_i * 3_{\text{seasons}} = 21 \text{ Probability Distribution Curves}$$

A comparison of the fitting of all probability distribution curves with the Log-Pearson-Type-III and the Log-Normal-Type-III Distribution has been done. For the goodness-of-fit test, the Kolmogoroff-Smirnov-Test has been applied and the empirical distributions have been computed. The Kolmogoroff-Smirnov-Test has been positive for all Log-Normal-Type-III Distributions after the outlier tests have been done. It displays better fitting with the empirical distribution than the Log-Pearson-Type-III Distribution curves. An example of the comparison is given in Attachment 14.1 for the End Node and the summer, winter as well as yearly flood peak probability curves. In all curves, the Log-Pearson-Type-III Distributions display larger gradients than the Log-Normal-Type-III Distribution, which don't display a good fitting to the empirical distributions. The comparison of the probability distribution curves of the summer flood peaks are illustrated additionally in Fig. 5. 9.

The final results of the Log-Normal-Type III Distribution curves are attached to the thesis in the order of the hydrological seasons: (summer (1), winter (2), yearly (3)) and the locations of interest ([1] node Kölln, [2] node A23, [3] node Offenau, [4] node Langelohé, [5] End Node; the sub-catchments: [6] ELMS\_E06\_02, [7] ELMSH\_E13\_02) and the scenarios: A1B, B1, A2 as well as the REMO control scenario and the scenario 0 results (Attach 14.2).

With regard to the restricted extrapolation of statistical evaluation results, the flood peaks with a return period of once in 100years (HQ<sub>100</sub>) and once in 200years (HQ<sub>200</sub>) are displayed additionally in the graphs, but have to be considered with a higher rate of uncertainty.

**End Node: Probability Distribution of Flood Events - Summer Periods**

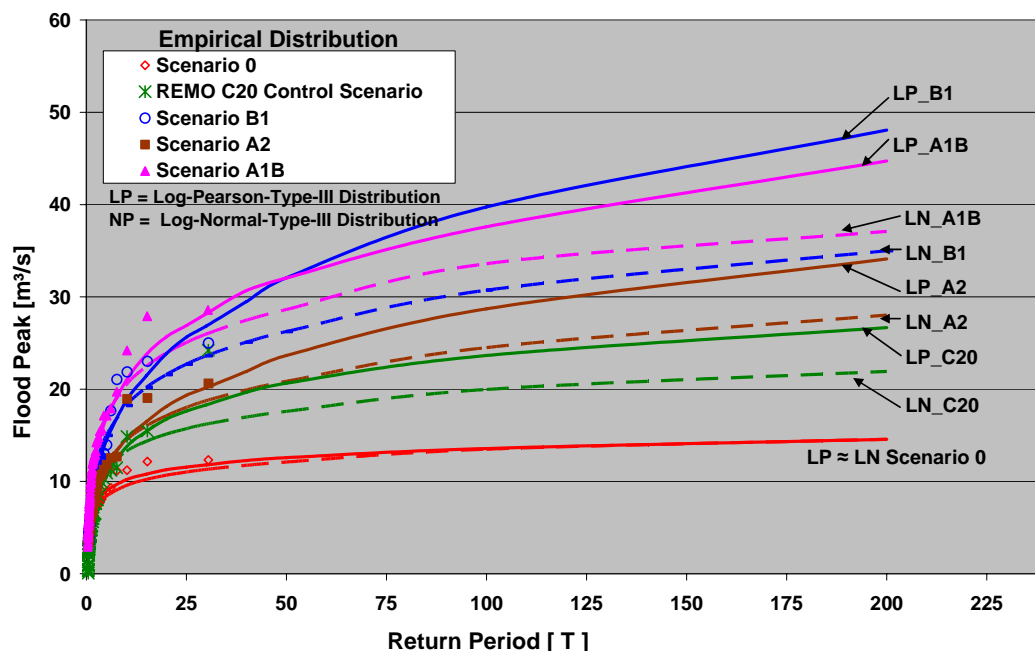


**Fig. 5. 9 Comparison of the Log-Normal Type III and the Log-Pearson Type III Distribution curves of summer flood peaks.**

*5.4.3.1 Climate Control Scenario Results [1971 – 2000]*

A comparison of the computed REMO Control Scenario C20 and the Scenario 0 statistical evaluations has been done like for the results of the rainfall events. The differences between the Scenario 0 and the REMO C20 data series for the time period 1971 to 2000 and locations are listed in tables in the Attachment 14.3. The average changes of the locations for the hydrological year periods are summarized in Table 5. 10.

**Table 5. 10 Average Difference between the REMO C20 and the Scenario 0 flood peak data series for the hydrological year periods.**

| [1971 - 2000]                                    | Return Period T [a] |      |      |      |      |      |      |      |      |   |
|--|---------------------|------|------|------|------|------|------|------|------|---|
|  | 1                   | 2    | 3    | 5    | 10   | 20   | 30   | 50   | 100  | a |
| <b>Average Summer Flood Peak Differences [%]</b> |                     |      |      |      |      |      |      |      |      |   |
| Δ [%]  | -10.1               | 10.8 | 20.1 | 30.3 | 42.5 | 53.6 | 60.1 | 67.7 | 79.7 | % |
| <b>Average Winter Flood Peak Differences [%]</b> |                     |      |      |      |      |      |      |      |      |   |
| Δ [%]  | 19.6                | 22.2 | 22.4 | 22.6 | 22.6 | 21.1 | 19.3 | 18.2 | 16.9 | % |
| <b>Average Yearly Flood Peak Differences [%]</b> |                     |      |      |      |      |      |      |      |      |   |
| Δ [%]  | 16.5                | 20.4 | 22.2 | 23.9 | 25.8 | 27.3 | 28.1 | 29.1 | 30.4 | % |

Especially for summer flood events with low probabilities of occurrence ( T > 50a ) the flood peaks computed with the REMO C20 data series are about 68% to 80% higher than the Scenario 0 probability curve computed with observed rainfall data

series. But for return periods of once in a year ( $T = 1a$ ) the flood peaks computed with the REMO C20 data series are smaller than the Scenario 0 probability curve computed with observed rainfall data series.

The differences of flood events simulated for the winter periods are lower than for the summer flood events. But larger differences are illustrated for flood events with higher probabilities of occurrence ( $T < 5a$ ) than with lower probabilities of occurrence ( $T > 30a$ ). The differences range between 22.6% and 16.9%.

The differences of the REMO C20 Scenario and the Scenario 0 flood peak probability curves over yearly periods, range between 16.5% and 30.4%, which is lower than the differences of the summer flood peaks. The differences are higher for lower probabilities of occurrence ( $T > 50a$ ) than for higher probabilities of occurrence ( $T < 5a$ ).

#### 5.4.3.2 Future Climate Scenario Results [2040 – 2070]

The results of the projected increase derived by the IPCC climate change scenarios referred to the REMO C20 control scenario are computed in percentage for each location of interest. A differentiation according to the seasons: summer, winter and yearly periods has been done for illustrating the results in tables in the Attachment 14.4. The average results of all locations in the Krückau catchment are summarized in Table 5. 11.

**Table 5. 11 Average changes in future climate scenarios referred to the REMO C20 control scenario.**

| [2040 – 2070]                                    | Return Period T [a] |      |      |      |      |      |      |      |      |   |
|--|---------------------|------|------|------|------|------|------|------|------|---|
|  | 1                   | 2    | 3    | 5    | 10   | 20   | 30   | 50   | 100  | a |
| <b>Average Summer Flood Peak Differences [%]</b> |                     |      |      |      |      |      |      |      |      |   |
| A1B-Scenario                                     | 103.3               | 70.0 | 59.8 | 50.5 | 41.3 | 34.4 | 30.8 | 27.0 | 22.5 | % |
| B1-Scenario                                      | 68.8                | 49.5 | 42.9 | 36.6 | 30.1 | 25.0 | 22.5 | 19.7 | 15.2 | % |
| A2-Scenario                                      | 51.9                | 30.0 | 23.3 | 17.3 | 11.5 | 7.3  | 5.2  | 3.0  | -0.4 | % |
| <b>Average Winter Flood Peak Differences [%]</b> |                     |      |      |      |      |      |      |      |      |   |
| A1B-Scenario                                     | 1.3                 | 3.5  | 4.8  | 6.0  | 8.3  | 10.5 | 11.6 | 13.2 | 16.0 | % |
| B1-Scenario                                      | 0.9                 | -0.9 | -1.9 | -3.4 | -4.7 | -6.1 | -7.0 | -8.0 | -9.7 | % |
| A2-Scenario                                      | -2.5                | -3.0 | -3.3 | -3.7 | -3.9 | -4.3 | -4.5 | -4.7 | -5.2 | % |
| <b>Average Yearly Flood Peak Differences [%]</b> |                     |      |      |      |      |      |      |      |      |   |
| A1B-Scenario                                     | 27.4                | 23.8 | 22.2 | 20.3 | 18.1 | 16.3 | 15.1 | 13.7 | 11.8 | % |
| B1-Scenario                                      | 11.3                | 8.8  | 7.5  | 6.0  | 4.1  | 2.7  | 1.9  | 0.1  | -0.2 | % |
| A2-Scenario                                      | 5.9                 | 3.7  | 2.7  | 1.5  | 0.1  | -1.0 | -1.6 | -2.8 | -3.1 | % |

The percentage rate is computed referred to the REMO control scenario results. It has to be taken into account that, the percentage change approach outlines the relative changes. For example an increase of 150% of a summer flood peak with a return period of once in a year ( $T = 1a$ ) is computed for the node Langelohé, which corresponds to a magnitude of change from  $3.0m^3/s$  to  $7.8m^3/s$  with a difference of  $4.7m^3/s$ . But an increase of  $4.1m^3/s$  has been computed as well at the node Langelohé for a summer flood event with a return period of once in 100years, whereas a peak

flow of 27.3m<sup>3</sup>/s is increased to a peak flow of 31.4m<sup>3</sup>/s, which corresponds to an increase of just 23.3%.

It is significant that the increase of the summer and yearly flood peaks are larger for higher probabilities of occurrence (T<5a) than for lower probabilities of occurrence (T>50a). But for the average changes in the winter flood peaks it is the other way around, with larger decreasing rates of flood peaks in the A2 and B1 scenario.

Like for the derived changes in extreme rainfall intensities (5.3.2) higher increasing rates are computed for the flood peak probability curves with the *summer flood events* and the A1B Scenario. For 100year summer flood events, an average increase of 22.5% has been computed with the scenario A1B and for lower probabilities of occurrence (T=1a) an average increase of about 103% is projected. These increasing rates are significantly higher than for the scenarios B1 and A2 which illustrate a range of 15% to 69% and 0% to 52%.

For the locations of interest, higher changes of the *winter flood peaks* are computed for lower probabilities of occurrence (T>50a) than for higher probabilities of occurrence (T<5a). With the A1B scenario increases between 16% (T=100a) and 1.3% (T=1a) are projected. The scenarios B1 and A2 illustrate larger decreasing rates for lower probabilities of occurrence (T=100a) with about 9.7% and 5.2% than for higher probabilities of occurrence (T=5a) with about 1% and 3%. These results are reasonable with the results of the statistical evaluation of extreme rainfall events in the winter periods, where decreasing rates have been computed as well for the scenarios B1 and A2.

In the statistical evaluations of *yearly flood peak* series, larger changes are computed for higher probabilities of occurrence (T<5a) than for lower probabilities of occurrence (T>50a). This corresponds to the changes derived for the flood events in the summer periods but the changes are lower. It ranges between 11.8% (T=100a) and 27.4% (T=1a) for the scenario A1B. The largest change is computed in this case for the node Langeloh in Elmshorn with about 39% (T=1a). In the scenarios B1 and A2, decreases of flood peaks are projected between 0.2% and 3.1% for lower probabilities of occurrence (T=100a).

The yearly flood peaks with higher probabilities of occurrence (T=5a) increase less than the corresponding rainfall events (5.3.2), whereas for lower probabilities of occurrence it is the other way around in the A1B scenario.

## **5.5 Post-Processing of Climate Change Scenario Results**

Two approaches for the post-processing of climate change impact results have been developed to calculate the magnitude of change. These approaches have been indicated as ‘percentage change approach’ and ‘absolute change approach’. The percentage change approach is based on the calculation of relative changes, whereas the absolute change approach is dependent on the correct calculation of the absolute

difference between extreme events in future climate scenarios and in control scenarios. But large differences have been calculated between the reference Scenario 0 and the REMO control scenario C20 results. Therewith, it is questionable, to what extent the calculated changes between REMO control scenario C20 and future scenario data series are affected by systematic biases and how these biases affect the scenario study results. It is not possible to assume the same absolute magnitude of biases for time series of the past as for future simulations, but it is reasonable to take account of relative biases for the climate model data results of the different climate periods. It is stated as well by Fowler et al. (2007) that climate models (here: GCMs) can be assumed to produce more accurately relative changes than absolute values.

Therefore, it is recommended to apply the percentage change approach (3.5.1) to post-process the scenario study results of the Krückau catchment to calculate the magnitude of change in climate scenarios. The A1B scenario projected the largest increases in extreme rainfall as well as flood peak probabilities. Therefore, a focus has been set on this IPCC scenario for further studies. The projected scenario results are indicated as Scenario 0-A1B for rainfall and flood peak events under future climate conditions.

### 5.5.1 Post-Processing of Rainfall Probability Results [Scenario 0-A1B]

The adjusted rainfall intensities derived with the Scenario 0-A1B are displayed in diagrams and tables in Attachment 15.1. With the computed changes in the scenario 0-A1B, a shift in the frequency of rainfall events is projected.

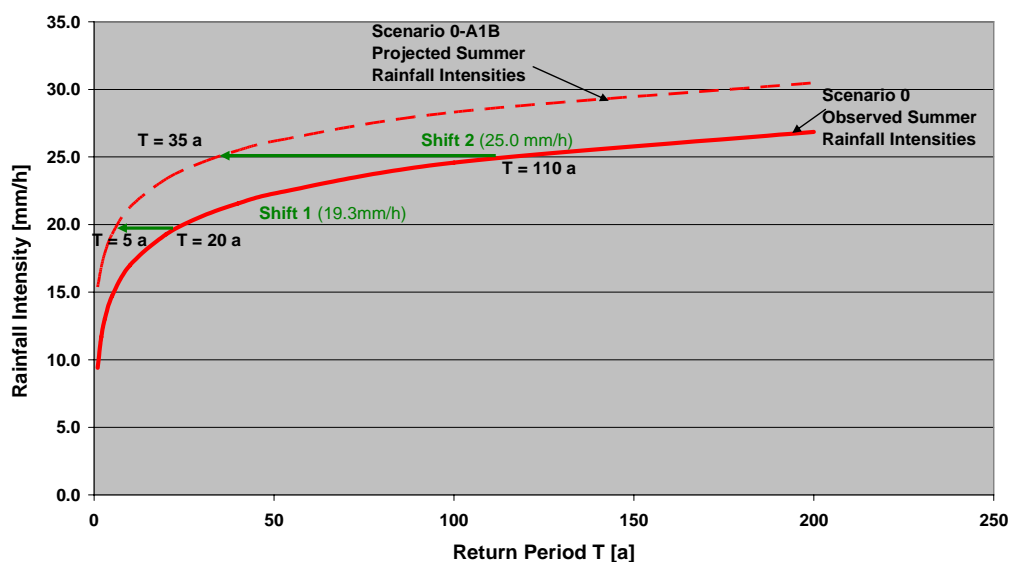


Fig. 5. 10 Illustration of post-processed future summer rainfall intensities and the shift in return periods T [a].

For example in Fig. 5. 10 (shift 1) a summer rainfall event with an intensity of 19.3mm/h has a current probability of occurrence of once in 20 years (T=20a), but in the projected Scenario 0-A1B the return period of such a summer rainfall event is increased to once every 5 years (T=5a). A second shift is illustrated in Fig. 5. 10,

where a current rainfall intensity of 25mm/h is shifted from a return period of once in 110years to a return period of once in about 35 years.

The computation of climate change factors (CCFs) for rainfall is defined in (3.5) with the *Averaging Ensemble CCF* method. It is possible to obtain the respective extreme rainfall events with a specific frequency of occurrence for each location in the Krückau catchment with these CCFs (Table 5. 12).

**Table 5. 12 CCFs for calculating rainfall events with a duration of one hour and specific return periods T (a) with respect to the Scenario 0-A1B results in the Krückau catchment.**

| CCFs – Rainfall Events [Scenario 0-A1B] |      |      |      |      |      |      |      |      |      |      |      |
|---|------|------|------|------|------|------|------|------|------|------|------|
| Return Periods<br>T [a]                 | 1    | 2    | 3    | 5    | 10   | 20   | 30   | 40   | 50   | 100  | 200  |
| Summer Periods                          | 1.63 | 1.44 | 1.37 | 1.31 | 1.25 | 1.21 | 1.19 | 1.18 | 1.17 | 1.15 | 1.13 |
| Winter Periods                          | 1.08 | 1.07 | 1.07 | 1.07 | 1.06 | 1.06 | 1.06 | 1.06 | 1.06 | 1.06 | 1.06 |
| Yearly Periods                          | 1.50 | 1.34 | 1.29 | 1.23 | 1.18 | 1.15 | 1.13 | 1.12 | 1.11 | 1.09 | 1.07 |

Larger changes have been calculated for higher probabilities of occurrence (T =1a) and especially for summer rainfall events.

### 5.5.2 Post-Processing of Flood Peak Probability Results [Scenario 0-A1B]

The changes derived in the scenario A1B for each seasonal differentiation (summer, winter, yearly) and each location of interest are projected on the reference Scenario 0 (computed with observed data series) with the percentage change approach.

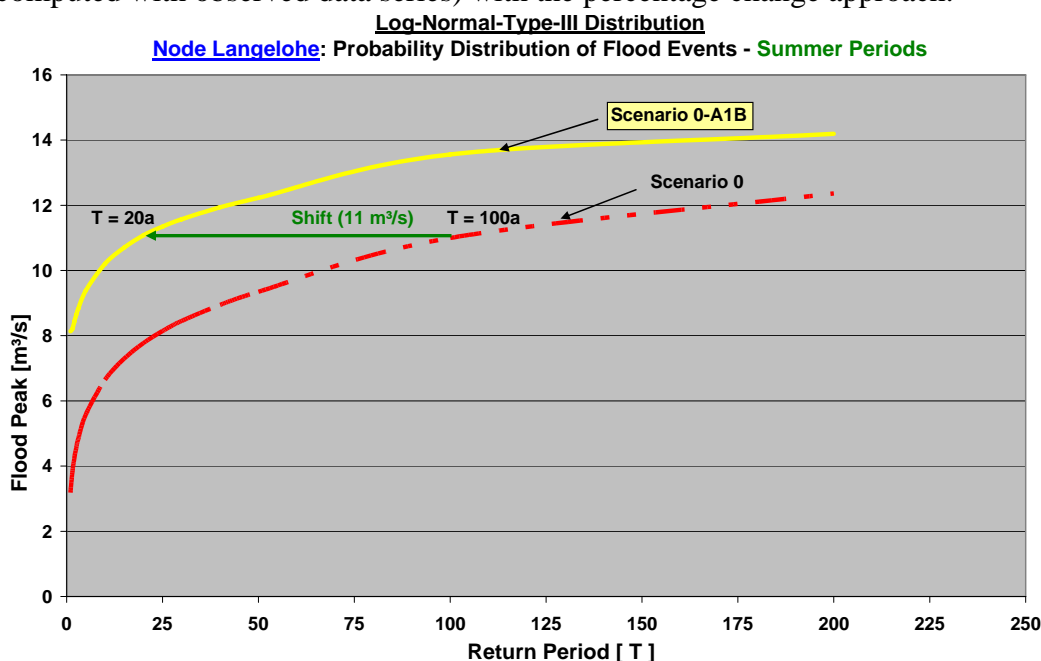


**Fig. 5. 11 Illustration of a shift in return periods of post-processed flood peak probabilities by climate change impacts.**

The resulting curve is indicated as *Scenario 0-A1B* in the diagrams of attachment 14.2 and in the tables in the attachment 15.2 for the seasons: summer (1), winter (2), yearly (3) and according to the seven locations of interest. Especially the projected frequency and magnitude of the summer flood peaks increases significantly (Fig. 5.

11). For example an actual flood peak of 11m<sup>3</sup>/s with a return period of once in 100years (HQ<sub>100</sub>) at the node Langelohé in Elmshorn is possible to occur every 20 years (HQ<sub>20,c</sub>) in the future climate Scenario 0-A1B.

With these results, CCFs have been calculated with the developed *Average Ensemble CCF* method and are listed in Table 5. 13.

**Table 5. 13 CCFs of design flood events for the Krückau catchment for specific return periods (T) to compute the flood peaks with the Scenario 0-A1B results.**

| CCFs – Design Flood Events [Scenario 0-A1B] |      |      |      |      |      |      |      |      |      |
|---|------|------|------|------|------|------|------|------|------|
| Return Period T [ a ]                       | 1    | 2    | 3    | 5    | 10   | 20   | 30   | 50   | 100  |
| Summer Periods                              | 2.03 | 1.70 | 1.60 | 1.51 | 1.41 | 1.34 | 1.31 | 1.27 | 1.22 |
| Winter Periods                              | 1.01 | 1.04 | 1.05 | 1.06 | 1.08 | 1.10 | 1.12 | 1.13 | 1.16 |
| Yearly Periods                              | 1.27 | 1.24 | 1.22 | 1.20 | 1.18 | 1.16 | 1.15 | 1.14 | 1.12 |

The CCFs have been tested, by calculating in turn the results of the simulated Scenario 0-A1B flood peaks per return period. The testing results of the calculations are displayed in Fig. 5. 12 for the node Kölln (Eckhorner Au). A differentiation has been done according to the summer and winter flood occurrences as well as the results for both seasons (yearly periods).

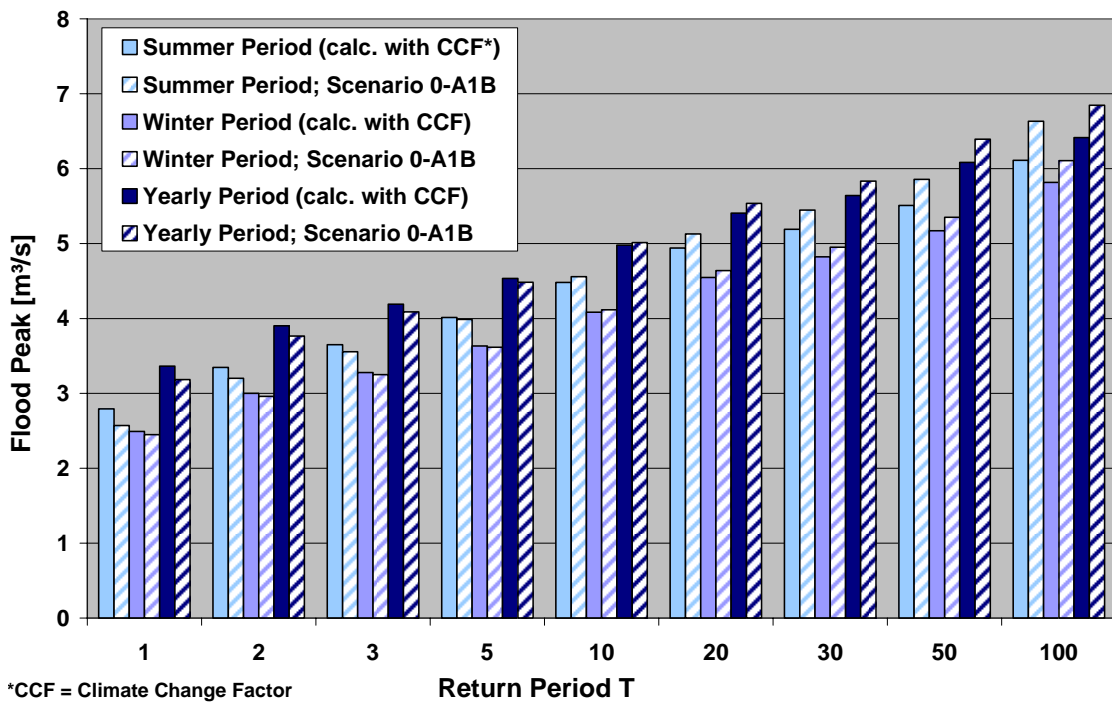


**Fig. 5. 12 Testing results of the climate change factor (CCF) calculations for the node Kölln (Eckhorner Au).**

Differences are displayed especially for flood events with a lower probability of occurrence. For 50year summer flood events differences of 6% (0.4m<sup>3</sup>/s) have been derived. Therefore inaccuracies have to be taken into account by working with CCFs.

### 5.5.3 Design Event for Post-Impact Studies

For further climate change scenario studies, a focus has been set on the larger changes derived for the events in the summer periods. It has been decided to compute a design event on the basis of a reference event observed in the past. In the North German Lowlands, larger rainfall events appear more frequently in the period from July to September in the summer periods. Therefore, the following events in the time period from 1970 to 2000 have been short listed with simulation results: September 1993, August 1989, September 1980, July 1975, July 1974 and July 1971.

It has been decided to apply an event which approximates the statistical results of a rainfall and flood event with return periods of once in five years ( $T=5a$ ). In this context, the observed event in 1971 is considered as most applicable for this purpose. The event is characterised by two intensive showers in 6 hours. In this way the soil moisture in the catchment area is significantly enhanced before the flood event occurs. It is regarded as realistic, that a high rainfall intensity event goes along with other short term rainfall events (showers). At the node Langelohe a peak discharge of  $4.9\text{m}^3/\text{s}$  and a flood volume of  $414\text{m}^3$  has been simulated for the observed event in the past (Fig. 5. 13).

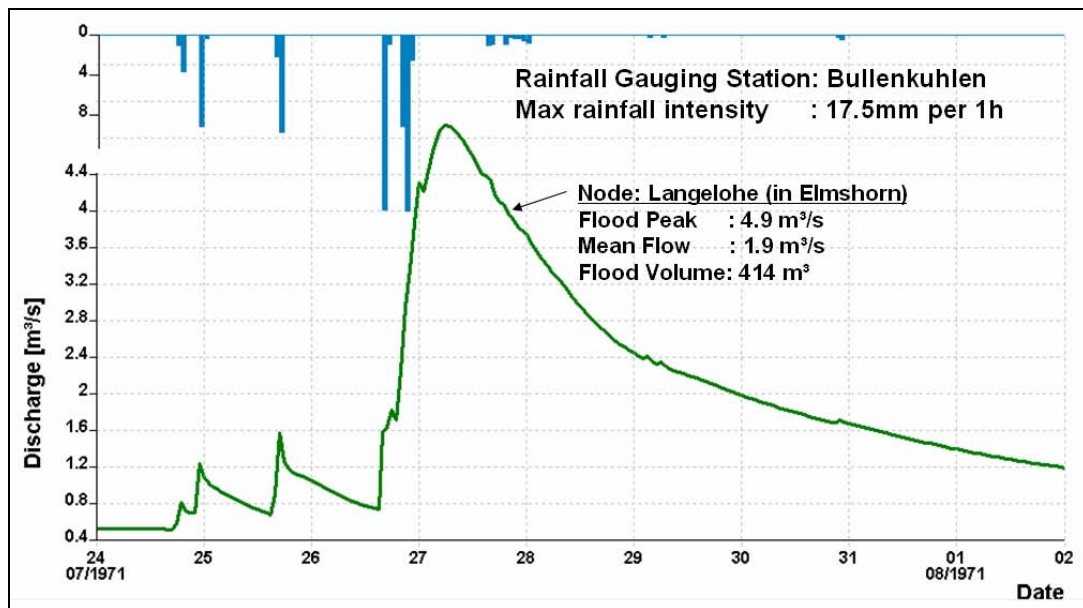


Fig. 5. 13 Design Flood Event selected for Post-Impact Studies.

The maximal measured rainfall intensity at the gauging stations had to be adjusted to an intensity with a return period of once in five years. According to the statistical evaluations, the projected 5year rainfall under climate change conditions (here: Scenario 0-A1B) has an intensity of  $19.3\text{mm}/\text{h}$  (Fig. 5. 10). The matching coefficients for the five rainfall gauging stations in the Krückau catchment have been calculated according to the method in (3.5.3) and are given in Table 5. 14.

**Table 5. 14 Applied matching coefficients for adjusting the observed rainfall intensity to the projected climate change rainfall intensity with a return period of once in five years.**

| Name of Rainfall Gauging Station <sup>1</sup> | Max. observed rainfall intensity | Projected climate change rainfall intensity (T=5a) | Matching Coefficients |
|---|----------------------------------|--|-----------------------|
|   | [mm/h]                           | [mm/h]   |                       |
| <b>Henstedt</b>                               | 15.9                             | 19.3   | <b>1.21</b>           |
| <b>Klein Nordende</b>                         | 14.6                             | 19.3   | <b>1.32</b>           |
| <b>Bullenkühlen</b>                           | 17.5                             | 19.3   | <b>1.10</b>           |
| <b>Brande</b>                                 | 17.3                             | 19.3   | <b>1.12</b>           |

The matching coefficients for adjusting the rainfall intensities for the simulation of design flood events have been derived iteratively. For this purpose matching coefficients have been computed for the sub-catchments, which drain to the nodes of interest. In the scenario studies five nodes of interest and two additional sub-catchment areas in Elmshorn have been regarded (see Fig. 5. 7). The increase of the evaporation and the temperature has been taken into account as well with factors in the hydrological model. The evaporation has been increased by 4% and the temperature by 1.45 °C which has been computed with the A1B scenario in (5.3.2.1) ‘Trend Line Analysis’.

For each of the seven locations of interest and for five climate change flood events (HQ<sub>T,C</sub>) with specific return periods (T =1a, 5a, 20a, 50a and 100a) matching coefficients have been iteratively computed. Overall 35 matching coefficients have been derived with the user interface of Kalypso Hydrology. The average matching coefficients of the Krückau catchment for the simulation of design flood events with the defined return periods are displayed in Table 5. 15.

**Table 5. 15 Average matching coefficients for the simulation of design flood events.**

| HQ <sub>T,C</sub>            | HQ <sub>1,C</sub> | HQ <sub>5,C</sub> | HQ <sub>20,C</sub> | HQ <sub>50,C</sub> | HQ <sub>100,C</sub> |
|------------------------------|-------------------|-------------------|--------------------|--------------------|---------------------|
| <b>Matching coefficients</b> | 1.27              | 1.36              | 1.65               | 1.77               | 1.91                |

The coefficients for the single nodes and sub-catchments differ according to the rainfall gauging station distribution, which had to be adjusted to simulate the design flood events. The lower rainfall data series of the rainfall gauging station Klein Nordende, located in the North-West of Elmshorn had to be increased more than the other rainfall data series.

The selected design rainfall event is indicated with a high short term intensity of rainfall, which approximates an event with a return period of once in 5 years under climate change conditions. It causes a peak flow which had to be adjusted with higher matching coefficients for respective flood events. For example, the average coefficient to adjust the observed rainfall event to an event with a return period of once in five years is about 1.19. But the average matching coefficient to simulate a flood peak with a return period of once in 5 years is 1.36, which results in a rainfall

<sup>1</sup> The locations of the rainfall gauging stations are illustrated in Fig. 5. 2.

intensity of 22.2mm/h and is displayed in the statistical evaluations of rainfall events with a return period of once in about 13 years under climate change conditions.

For the simulation of design flood events with lower probabilities of occurrence, the observed rainfall intensity [here in: mm/h] had to be increased to an even higher ratio.

For the post-impact studies only the design rainfall event with a return period of once in 5 years (HP<sub>5,C</sub>) and the design flood events: HQ<sub>1,C</sub>; HQ<sub>5,C</sub>; HQ<sub>20,C</sub>; HQ<sub>50,C</sub> and HQ<sub>100,C</sub> are used.

### 5.6 Simulation of Adaptation Measures

For the assessment of the effectiveness of SUDS to mitigate increased flood probabilities in the scenario 0-A1B, an assumption of the potential spatial distribution of SUDS in the Krückau catchment and design parameters of the SUDS elements have to be defined. The ASCII files for the application of the new developed SUDS module have been prepared with the additional add-on 'tool' outlined in (4.3). The tool for the simulation of green roofs is applied in this thesis for the first time and therefore, it has been tested in the adaptation scenario studies. Afterwards, the effectiveness of SUDS as flood probability reduction measures has been assessed.

Information about already existing SUDS devices has been obtained from a protocol of an environmental committee meeting in Elmshorn on February the 13<sup>th</sup>, 2008 (Hartwig, 2008). In the area of the Max-Planck-Strasse, the municipal water treatment undertaker of Elmshorn implemented an infiltration device. In this way, the expensive construction of additional rainwater drainage pipes in the ground could be prevented. Further plans of SUDS devices are planned for the areas in the borough of Köhnholz (where problems of the drainage of rainwater have been recorded) and the Rohnstrasse. It has been stated that residents have been interested in the construction of retention and infiltration devices already some years before. And there are residents in Elmshorn who collect the rainwater to water the gardens, for washing and sanitary devices already (Hartwig, 2008).

A special situation is given in the borough of the Danzigerstrasse, Langenmoor and Koppeldamm. According to a regulation by the city of Elmshorn, a number of residents in this area are not allowed to drain the rainwater into the storm water sewer system, but are requested to provide alternative solutions for infiltration in their gardens. Information about the current situation and a former project with the Hafen-City-University of Hamburg about planning rainwater harvesting measures have been provided by a resident of that area (Steinke, 2009). The rainwater from these areas is already retained or infiltrated into the ground locally, therefore no further SUDS measures are planned for the flood probability reduction analysis in this adaptation scenario studies.

### 5.6.1 Design of SUDS Techniques

#### 5.6.1.1 Potential Spatial Distribution of SUDSs

According to the criteria in (3.6.4), the potential spatial distribution of SUDSs has been defined. In the Krückau catchment, water protection zones were enacted by regulations of the federal state Schleswig-Holstein. Background information about this, is published by the Ministry of Environment, Nature and Forests of Schleswig-Holstein (MLUR) (Rittmeier & Viße, 2002). The drinking water in Schleswig-Holstein is mainly taken from groundwater reservoirs (Rittmeier & Viße, 2002), whereas especially in the sandy soils of the old moraine landscape ‘Altmoränenlandschaft’ in the Krückau catchment, the purification capability of water infiltrating into the ground is low. Water protection zones have been defined for the areas:

- Elmshorn-Sibirien (1 110 ha; enacted in 2000)
- Elmshorn Köhnholz/ Krückaupark (4 237ha; enacted in 2002)
- Barmstedt (1 282ha; enacted in 1998)

Further water protection zones are planned in Kaltenkirchen, but it is not taken up by the regulation yet (LLUR<sup>1</sup>, 2009). The sensibility of water protection zones is defined in maps of the agricultural and environmental atlas of Schleswig-Holstein (LLUR, 2009). The infiltration of acceptable and tolerable rainfall water have to be clarified with the governmental agency. In the “Landesverordnung über die Anforderungen an die erlaubnisfreie Versickerung von Niederschlagswasser in das Grundwasser“ published in May 2002, the following requirements are specified for the infiltration of rainfall water (GVOBI<sup>2</sup>, 2002). Permission for the infiltration of rainfall water into the ground is not required outside of water protection zones and contaminated sites, and when the rainfall water is not changed in a negative way by pollutions from households or industry. However, there is a duty to give notice to the responsible water authority one month before using an infiltration measure.

The soil types in the Krückau catchment area are described by LANU<sup>3</sup> (2006) and can be generally defined as sandy soils. Predominantly good infiltration capacity into the ground is provided with relative high permeability coefficients (ca.  $5 \times 10^{-5}$  m/s). Only close to river sections are some areas with peaty soils. These areas have been neglected for the implementation of swales and swale-filter drain systems.

The depth to the groundwater table is indicated on maps published by Tetzlaff et al. (2004). The maps illustrate the groundwater table depth between < 0.4m, 0.4-0.8m, 0.8-1.3m and >1.3m. A more detailed indication of the local groundwater

---

<sup>1</sup> LLUR = The State Agency for Nature and Environment of the Federal State Schleswig-Holstein

<sup>2</sup> GVOBI = Law and Ordinance Gazette of Schleswig-Holstein

<sup>3</sup> LANU= Ministry of agriculture, environment and rural areas of the Federal State Schleswig-Holstein

---

tables has been defined by analysing the measurements of 21 groundwater gauging stations in the Krückau catchment (LLUR, 2009).

In the upper Krückau catchment area (Kaltenkirchen) the depth to the groundwater table is between 5 to 13m deep (source: 3 wells; data series: 1997 – 2009). In the urban area of Barmstedt the measured depth of the groundwater table is about 2.5 to 4m deep (source: 4 wells; data series: 1990 – 2009), in the urban areas of Elmshorn the depth to the groundwater table is only about 1m to 2 m deep (source: 2 wells; data series: 1989 – 2009) (LLUR, 2009).

A restriction of planning swale-filter-drain systems has been defined for the urban areas of Elmshorn. For swales it is considered as potential area with the requirement for further analysis of the exact minimal depth to the groundwater table, because a distance of less than 1m could only be sufficient, if the purification capacity of the planned swales is assured (DWA-A 138, 2005).

The topographical slopes of the catchments are larger in the upper catchment area of the Krückau, but restrictions for the implementation of SUDS are not defined.

To determine the spatial distribution of potential areas for implementing green roofs and the distribution of green spaces in the urban areas for implementing swales and swale-filter-drain systems only a very rough estimation could be done in the scope of this thesis. A detailed analysis by e.g. digitising the urban areas in a detailed way combined with extensive site investigations could not be covered.

The assumption of the spatial distribution has been determined on the example of two urban sub-catchments for the implementation of green roofs combined with swales in Elmshorn (ELMS\_E06\_02 and ELMSH\_E13\_04) and of two urban sub-catchments in Kaltenkirchen (KAKI\_2 and KAKI\_3) for the planning of green roofs combined with swale-filter-drain systems. These four urban sub-catchments have been selected for the purpose to display a range of residential, commercial and industrial uses and to include as well hot spots of flooding.

The selected sub-catchments in Elmshorn have been defined as well as locations of interest for the flood probability analysis in scenario studies in (5.5). In the sub-catchment ELMS\_E06\_02 two hot spots are situated: the ‘Badewanne’ (Hamburger Strasse) and the Steindammwiesen Park area. The sub-catchment area has a size of about 1.4km<sup>2</sup>. The sealing rates in this sub-catchment range from 0.37% (high-density areas) to 0.3% (middle-density areas).

The commercial areas in this sub-catchment include a large estate of a comprehensive school with sports facilities, a primary school, a secondary school, a special school (Paul-Dohrmann-School), a commercial school and a kindergarten. Photos of these commercial facilities have been taken on a site visit in Elmshorn to learn about the potential for planning SUDS (Attach 16). For all these estates and

especially at the large comprehensive school, a quite high potential has been assumed for implementing green roofs, planning shallow swales and for unsealing.

The main area of this sub-catchment is used as residential areas. These comprise single housing, but mostly large apartment buildings with flat roofs. Next to these buildings, larger parking places as well as larger green spaces are often situated. These estates provide as well potential areas for green roofs combined with swales and unsealing of the large parking places. Photos of residential estates in this sub-catchment have been taken as well during the site visit in Elmshorn (Attach 16).

A water protection zone has been enacted in the south-eastern part of the sub-catchment (LLUR, 2009) therefore it has to be agreed upon infiltrating rainfall water with the water authority.

The sub-catchment ELMSH\_E13\_04 drains to the hot spot of the Else-Brandström-school close to the Krückau park (Photo: Attach 16) which is located in a flood risk area. No restriction for infiltrating water is stated by any water protection zone, but the depth to the groundwater table is lower than 1.3m, therefore the planning of infiltration devices has been restricted to shallow swales. The sub-catchment has an area of 2.1km<sup>2</sup>. Commercial estates in this area include a school at the Koppeldamm, a primary school with larger sport facilities and the train station Langenmoor. Like in the sub-catchment ELMS\_E06\_02 these facilities provide larger flat or slightly pitched roofs and adjacent green spaces. The same is given for the residential areas, which comprise larger apartment houses with flat roofs and adjacent green spaces, but mostly single housing with larger gardens.

In the north of the sub-catchment ELMSH\_E13\_04 industrial areas are situated which include the estate of the Claus-Döhling GmbH with large parking places and halls. Smaller industrial areas are used by a welding shop, a coating as well as sand blasting company and a vehicle manufactory.

The borough of the Danzigerstrasse, Langenmoor and Koppeldamm is situated here, where the drainage into the storm water sewer system is restricted since 1950 and infiltration devices are implemented already.

For both sub-catchments in Elmshorn a rough maximal suggestion has been done of a potential spatial distribution of green roofs on 20% of the sealed areas. In a second approach it is assumed that about 30% of the sealed area could be drained to swales and in a third approach, a potential unsealing of 30% of the sealed areas is suggested.

As the simulation of swale-filter-drain systems is not possible in the urban borough of Elmshorn, two sub-catchment areas in Kaltenkirchen have been selected for the assumption of the potential spatial distribution and design of swale-filter-drain systems. In the area of Kaltenkirchen the depth to the ground water table is about 5 to 13 meters, which is sufficient for the planning of any infiltration devices (swales, swale-filter-drain systems as well as soakaways). Up to now there is no water

protection zone defined by law, but it is indicated by LLUR (2009) that a water protection zone is planned. The considered sub-catchments are indicated in the model as KAKI\_2 and KAKI\_3. Both sub-catchments include larger commercial, residential as well as industrial areas. The size of the sub-catchment KAKI\_2 is about 1km<sup>2</sup> and of KAKI\_3 it is about 1.3km<sup>2</sup>. The sealing rates of the sub-catchments are between 0.25% for residential areas, 0.5% for commercial areas and 0.8% for sealed streets as well as places. In the scope of this thesis only a rough suggestion of a potential distribution of SUDS could be done. It has been assumed to simulate 20% of the sealed areas as green roofs and to drain 30% of the sealed areas into swale-filter-drain systems or swales respectively. An unsealing has been assumed to be planned for 30% of the sealed areas (parking places, blind arrays, streets in residential areas). For further urban sub-catchments including the urban area of Barmstedt, the same assumptions have been taken. A summary of the suggested potential spatial distribution of SUDSs in the Krückau catchment is given in Table 5. 16.

**Table 5. 16 Summary of the suggested potential spatial distribution of SUDSs in the urban sub-catchments of Elmshorn, Barmstedt and Kaltenkirchen.**

| SUDS technique             | Percent of sealed area | Specific restrictions in urban areas  |
|----------------------------|------------------------|---|
| Green Roofs                | 20%                    | No  |
| Swales                     | 30%                    | Infiltration in the water protection zones in Elmshorn has to be clarified. |
| Swale-Filter-Drain Systems | 30%                    | Only in urban areas of Kaltenkirchen and Barmstedt                          |
| Unsealing                  | 30%                    | No  |

An example for a combination of the considered SUDS-elements in this thesis is illustrated on a residential estate in Fig. 5. 14.

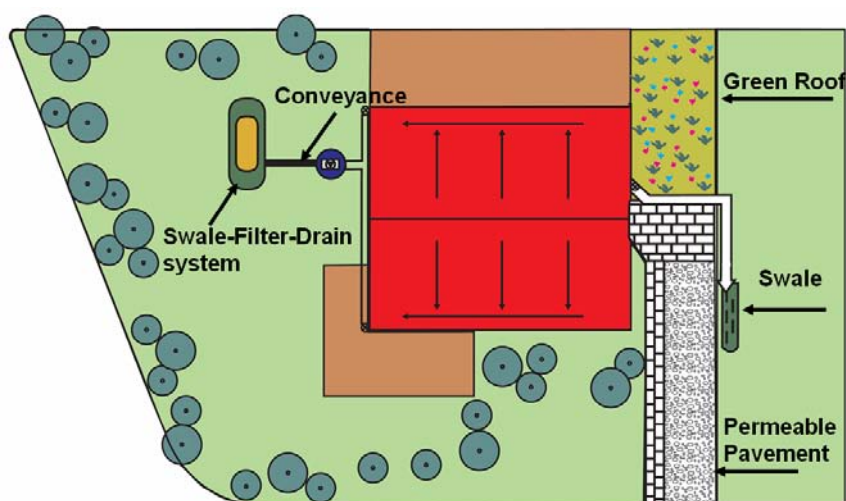


**Fig. 5. 14 Combination of SUDSs on a residential estate. (adopted from UMBW, n.d.).**

### 5.6.1.2 Design of SUDS Elements

For the design of SUDS measures the sizes and materials of the layers as well as the required green spaces have to be defined. The materials and layer set up of the SUDS measures have to be defined in the ASCII files: we\_nat.mr, boden.dat, bod\_art.dat and entered into the add-on spreadsheet. With the spreadsheet, the calculation of the adjusted hydrotopes with SUDS in all urban areas of Elmshorn, Barmstedt and Kaltenkirchen has been prepared for these scenario studies. The parameters defined in this thesis could be as well changed later on for further studies.

The SUDS elements are designed for the projected rainfall event of the Scenario 0-A1B, which has a probability of occurrence of once in 5 years ( $T = 5a$ ). The calculation of this design rainfall event has been outlined in (5.5.3). With the matching coefficients, the observed design rainfall event ( $HP_5$ ) is adjusted to the projected design rainfall ( $HP_{5,C}$ ) representing the computed climate change impacts. It has an intensity of 19.3mm/h. The design of the SUDS elements is considered as adequate, when no overflow of the SUDS systems is generated with the design rainfall event under climate change conditions. On the other hand it has been assured that the size of the SUDS measures is not over-designed, to support an economical design. For this purpose the SUDS application correction factors in the spreadsheet are adjusted.

### ***Design of Green Roofs***

Extensive green roofs with a filter layer of 5cm, a substrate layer of 8cm, an overflow height of 3.5cm and a free board of 10cm have been designed. For the filter layer an inorganic material with a pore volume of 30%, a coefficient of permeability of  $2 \times 10^{-5}$  m/s (1720 mm/d)<sup>1</sup> and a field capacity of 25.5 %<sup>2</sup> has been used. The material used for the substrate layer is made up of inorganic and organic material to provide the nutrient for the plants but provide as well an appropriate storage capacity. Therefore a material with a maximal pore volume of 37.5%, a field capacity of 20% and a lower permeability coefficient of  $4 \times 10^{-6}$  m/s (350mm/d) have been used to retain the water in the storage layer. The material could be compared to a silty sand ([Manual of soil mapping, 2005](#)). The design rainfall event ( $HP_{5,C}$ ) derives a water level in the storage layer of about 2cm, which is just 1.5cm below the overflow pipe. This has been considered in this case as an adequate design.

---

<sup>1</sup> In the ASCII files the permeability coefficient is given in mm/d

<sup>2</sup> In the ASCII files the field capacity is given in mm/dm = %

### *Design of Swales*

Swales are designed with a maximal storage depth of 30cm before the outlet of the overflow pipe is reached. The base layer of the swale is designed with a depth of 30cm made up of a material, which has a pore volume of 41%, a field capacity of 24% and a coefficient of permeability of  $1.8 \times 10^{-5}$  m/s (1570mm/d). This material is comparable with a sandy soil mixed with a lower portion of inorganic material ([Manual of soil mapping, 2005](#)) to serve the planting of the surface cover of the swale with grass or sedum. The pre-designed space required for swales to drain 30% of the sealed areas has been calculated with the add-on spreadsheet. It has been found out that the maximal storage height in this preliminary design has been exceeded in most cases and in some cases the swale areas have been over-designed. Therefore the swale areas have been adjusted with SUDS application correction factors of 1.1 and in some cases of a factor of 0.67 or 2.6. The adjustment had to be done iteratively till a size of the swales has been reached where no overflow is generated, but is at the same time as small as possible. In this way, the water level in the swales derived by a climate change adjusted design rainfall event ( $HP_{5,C}$ ) reaches a height of about 24 to 27cm, which is 3 cm below the overflow pipe. The time period, of water stored in the swale, is about 20 hours for the design rainfall event.

### *Design of Swale-Filter-Drain Systems*

The swale-filter-drain systems are defined with a storage height of 30cm in the swale, a colmation layer thickness of 30cm, a filter layer of 60cm and a base layer of 10cm. The colmation layer has been designed with a lower permeability coefficient of about  $2 \times 10^{-5}$  m/s (1720 mm/d) as the filter layer:  $3 \times 10^{-5}$  m/s (2720mm/d). In this way, the infiltration of water into the filter is controlled by the colmation layer and particles as well as pollutants are retained. The colmation layer is made up of a material with a maximal pore volume of 41% and a field capacity of 15.5%. The filter layer is made up of a soil with a maximal pore volume of about 42% and a field capacity of about 15.5%. The base layer has been defined with a higher field capacity than the filter layer, which facilitates a higher retention of water. Enhanced purification potential has been considered as important with regard to the spatial distribution of water protection zones. Like for swales, the preliminary design with the add-on spreadsheet calculation of the required swale-filter-drain system areas had to be adjusted in some cases with correction factors. It has been detected that the areas of the swale-filter-drain systems had been over-designed in some sub-catchments. Therefore, a factor of 0.8 had been applied to reduce the required areas for this SUDS technique, but in most cases the pre-design with the spreadsheet resulted in a good approximation of the required areas. With the design rainfall event, a maximal water level in the swale is reached of about 23cm to 26cm. The time period of water retained in the storage layer is about 14hours, which is smaller than for swale systems described before.

The unsealing has been designed with a porous pavement with a runoff coefficient of 0.5 according to the [DWA-A 138 \(2005\)](#). A specific pre-design for a rainfall event with a return period of once in 5 years is not required.

A summary of the main important design criteria regarding the size and storage height as well as the duration of water stored in the vegetated layer are summarized in Table 5. 17.

**Table 5. 17 Summary of the results of the SUDS design and simulation with the design rainfall event  $HP_{5,C}$**

| <b>SUDS measure</b>        | <b>Average ratio of reduced sealed areas in the sub-catchments</b> | <b>Average ratio of required natural area</b> | <b>Reached maximal water level</b> | <b>Maximal duration of water stored in the vegetated layer</b> |
|----------------------------|--|---|------------------------------------|--|
| Green roofs                | 20%  | ---   | 2cm                                | About 7 hours  |
| Swales                     | 30%  | 0.85%   | 24 – 27 cm                         | About 20 hours   |
| Swale-filter-drain systems | 30%  | 0.36%   | 23 – 25 cm                         | About 14 hours   |
| Unsealing                  | 30%  | ---   | --                                 | ---  |

### **5.6.2 Testing Results of the SUDS Software Tool**

The testing of the new developed software tool has been done with the results of the projected climate change design rainfall ( $HP_{5,C}$ ). For each implemented SUDS type the results of two sub-catchments have been used for the testing. First the overall water balance has been calculated of the inflow and outflow components of the SUDS elements. By definition the design rainfall event does not cause an overflow of the SUDS element. For testing the corresponding water balance, including the generation of overflow, the results of a rainfall event causing a flood event with a return period of once in 100 years ( $HQ_{100,C}$ ) have been illustrated in tables.

The temporal dependency between the actual soil water content, the percolation into lower layers and into drainage pipes is pointed out in graphs attached to the thesis for the projected climate change design rainfall ( $HP_{5,C}$ ) (Attachment 17). The design event which derives the maximal water level in the SUDS element and the maximal overflow generated of a 100 year flood event are outlined shortly.

#### *5.6.2.1 Simulations of Green Roofs*

The testing of the simulation with green roofs has been done with the results of the two sub-catchments in Elmshorn: ELMS\_E06\_02 and ELMSH\_E13\_04. In both sub-catchments 20% of the sealed areas have been transferred to green roof areas.

The water balances of the green roofs are illustrated in Table 5. 18 and Table 5. 19 for the design rainfall event (HP<sub>5,C</sub>) and the event (HQ<sub>100,C</sub>)<sup>1</sup>. An equal green roof design has been applied for both sub-catchments, but due to the different rainfall gauging stations allocated to the sub-catchments, the projected design rainfall event differs. For the sub-catchment ELMS\_E06\_03 the station Klein Nordende and for the sub-catchment ELMSH\_E13\_04 the station Bullenkuhlen is assigned. The water balance calculation has been done for a unit area of 1m<sup>2</sup> of the green roof.

**Table 5. 18 Water balance calculation results of green roofs [HP<sub>5,C</sub>].**

| Processes in the green roof elements (HP <sub>5,C</sub> )    | Sub-catchment ELMS_E06_02 | Sub-catchment ELMSH_E13_04 | Inflow ↓ or outflow ↑ process |
|--|---------------------------|----------------------------|-------------------------------|
| Total effective rainfall volume [l/m <sup>2</sup> ]          | + 88.1                    | + 92.8                     | ↓                             |
| Potential evaporation from storage layer [l/m <sup>2</sup> ] | - 18.7                    | - 20.1                     | ↑                             |
| Evapotranspiration from the soil layers [l/m <sup>2</sup> ]  | - 18.7                    | - 20.1                     | ↑                             |
| Drainage trough down pipe [l/m <sup>2</sup> ]                | - 40.7                    | - 50.3                     | ↑                             |
| Drainage through overflow pipe [l/m <sup>2</sup> ]           | 0.0                       | 0.0                        | ↑                             |
| Change in soil moisture [l/m <sup>2</sup> ]                  | - 9.9                     | - 5.1                      | ↑                             |
| Difference   | 0.0                       | 0.0                        | --                            |

**Table 5. 19 Water balance calculation results of green roofs [HQ<sub>100,C</sub>].**

| Processes in the green roof elements (HQ <sub>100,C</sub> )  | Sub-catchment ELMS_E06_02 | Sub-catchment ELMSH_E13_04 | Inflow ↓ or outflow ↑ process |
|--|---------------------------|----------------------------|-------------------------------|
| Total effective rainfall volume [l/m <sup>2</sup> ]          | + 181.3                   | + 160.9                    | ↓                             |
| Potential evaporation from storage layer [l/m <sup>2</sup> ] | - 19.8                    | - 18.9                     | ↑                             |
| Evapotranspiration from the soil layers [l/m <sup>2</sup> ]  | - 20.1                    | - 19.5                     | ↑                             |
| Drainage trough down pipe [l/m <sup>2</sup> ]                | - 104.2                   | - 99.9                     | ↑                             |
| Drainage through overflow pipe [l/m <sup>2</sup> ]           | - 17.8                    | - 14.5                     | ↑                             |
| Change in soil moisture [l/m <sup>2</sup> ]                  | - 19.4                    | - 8.0                      | ↑                             |
| Difference [l/m <sup>2</sup> ; %]                            | 0.1<br>(ca. 0.06%)        | 0.1<br>(ca. 0.06%)         | --                            |

<sup>1</sup> The interrelation between a design rainfall event and a design flood event is described in 5.5.3

The input water volume corresponds to the effective rainfall on the area of the green roof. The evaporation from the retained water in the storage layer and the evapotranspiration from the soil layers as well as the drainage through the down pipe and the negative change in the soil moisture are considered as outflow processes from the green roof element. The temporal dependency of the soil moisture, water level and drainage formation has been illustrated in graphs, whereas the results for the green roofs in the sub-catchment ELMSH\_E13\_04 are illustrated in Fig. 5. 15.

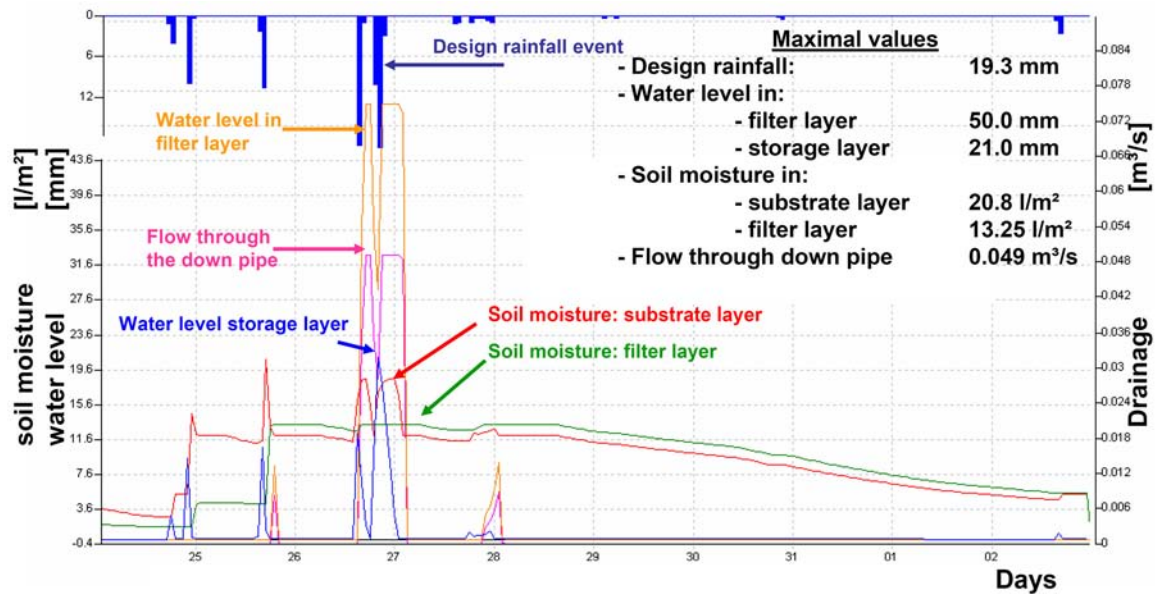


**Fig. 5. 15 Water storage and flow processes in the green roof elements with the design rainfall event (HP<sub>5,C</sub>) [sub-catchment: ELMSH\_E13\_04].**

The water level in the storage layer on the green roof reaches a maximum of 2.1cm in the sub-catchment ELMSH\_E13\_04 with the design rainfall event of 19.3mm/h. The maximum storage height on the green roof before the overflow begins is 3cm. The water stored on the green roof percolates into the substrate layer. When the soil moisture in the substrate layer reaches the field capacity (12 l/m<sup>2</sup>), water percolates into the filter layer, but only as long as the soil moisture in the substrate layer is above the field capacity. The maximum soil moisture in the substrate layer reaches 20.8 l/m<sup>2</sup>. When the soil moisture in the filter layer reaches the field capacity, free movable water is generated, which fills up the layer from the bottom and forms a water level. The maximum water level in the filter layer is 50mm which states that the filter layer is completely saturated. The free movable water volume is drained into the down pipe of the green roof, where a maximum flow of 0.0491m<sup>3</sup>/s is simulated.

The results for the green roofs in the sub-catchment ELMS\_E06\_02, are illustrated in the attachment 17.1.2. The water level in the storage layer on the green roof reaches a maximum of 1.6cm. The maximal soil moisture in the substrate layer is 0.1 l/m<sup>2</sup> lower than in the other sub-catchment and the maximum flow through the down pipe

is larger: 0.0571 m<sup>3</sup>/s. The differences are derived by the design rainfall event which occurs on day 25 and is followed by two smaller showers in the sub-catchment ELMS\_06\_02. This differs to the design rainfall event in the sub-catchment ELMSH\_E13\_04 illustrated in Fig. 5. 15.

The height of the overflow pipe is reached with the adjusted rainfall event, which causes a flood event with a return period of once in 50 years in the sub-catchments. In this case an overflow of the green roof is simulated of 0.09m<sup>3</sup>/s (ELMS\_E06\_02) and 0.12m<sup>3</sup>/s (ELMSH\_E13\_04). With a rainfall event causing a 100year flood event in the sub-catchments, the overflow is about 0.3m<sup>3</sup>/s and 0.35m<sup>3</sup>/s in the sub-catchments ELMS\_E06\_02 and ELMSH\_E13\_04. The height of the freeboard is not reached with the maximal considered design events. Overall, it can be stated that the temporal water storage and drainage processes in green roof elements are appropriately simulated with the criteria defined in (3.6.3).

#### 5.6.2.2 Simulations of Swales

The testing of the simulations with swales has been done with the results of the two sub-catchments in Elmshorn. In both sub-catchments 30% of the sealed areas are suggested to be drained by swales. The results of the water balances are illustrated in Table 5. 20 and Table 5. 21 for the design rainfall event (HP<sub>5,C</sub>) and the 100 year flood event (HQ<sub>100,C</sub>)<sup>1</sup>. The same swale design has been applied for the sub-catchments but the design rainfall data series are different like for the green roof testing. The water balance calculation has been done for a unit area of 1m<sup>2</sup> of the swale.

**Table 5. 20 Water balance calculation results of swales [HP<sub>5,C</sub>].**

| Processes in swale elements (HP <sub>5,C</sub> )            | Sub-catchment ELMS_E06_02 | Sub-catchment ELMSH_E13_04 | Inflow ↓ or outflow ↑ process |
|---|---------------------------|----------------------------|-------------------------------|
| Effective rainfall on swale [l/m <sup>2</sup> ]             | + 88.1                    | + 92.8                     | ↓                             |
| Inflow from sealed areas [l/m <sup>2</sup> ]                | + 793.3                   | + 696.9                    | ↓                             |
| Evaporation from storage layer [l/m <sup>2</sup> ]          | - 18.7                    | - 17.3                     | ↑                             |
| Evapotranspiration from the soil layers [l/m <sup>2</sup> ] | - 28.5                    | - 30.8                     | ↑                             |
| Overflow of the swale [l/m <sup>2</sup> ]                   | 0.0                       | 0.0                        | ↑                             |
| Percolation in the groundwater [l/m <sup>2</sup> ]          | - 836.1                   | - 743.5                    | ↑                             |
| Difference [l/m <sup>2</sup> ; %]                           | -1.9 (ca. 0.2 %)          | -1.9 (ca. 0.2%)            | --                            |

<sup>1</sup> The interrelation between a design rainfall event and a design flood event is described in 5.5.3

**Table 5. 21 Water balance calculation results of swales [HQ<sub>100,C</sub>].**

| Processes in swale elements (HQ <sub>100,C</sub> )          | Sub-catchment ELMS_E06_02 | Sub-catchment ELMSH_E13_04 | Inflow ↓ or outflow ↑ process |
|---|---------------------------|----------------------------|-------------------------------|
| Effective rainfall on swale [l/m <sup>2</sup> ]             | +181.3                    | +160.9                     | ↓                             |
| Inflow from sealed areas [l/m <sup>2</sup> ]                | +1633.5                   | +1207.9                    | ↓                             |
| Evaporation from storage layer [l/m <sup>2</sup> ]          | -19.8                     | -18.9                      | ↑                             |
| Evapotranspiration from the soil layers [l/m <sup>2</sup> ] | -27.5                     | -29.5                      | ↑                             |
| Overflow of the swale [l/m <sup>2</sup> ]                   | -574.4                    | -296.4                     | ↑                             |
| Percolation in the groundwater [l/m <sup>2</sup> ]          | -1195                     | -1025.9                    | ↑                             |
| <b>Difference [l/m<sup>2</sup> ; %]</b>                     | -1.9 (ca. 0.10%)          | -1.9 (ca. 0.14%)           | --                            |

The input water volume is composed of the effective rainfall on the area of the swale and the inflow water volume from sealed areas. The evaporation from the storage layer, the evapotranspiration from the soil, the overflow from the swale as well as the percolation into the groundwater are defined as outflow processes. A difference of 1.9l/m<sup>2</sup> between the inflow and outflow water volume components has been calculated. This difference corresponds to about 0.2% of the whole balanced water volume of the design rainfall event (HP<sub>5,C</sub>) and to about 0.1% to 0.14% for a 100year flood event (HQ<sub>100,C</sub>). This is regarded to be caused by numerical differences due to the explicit continuity equations applied within the model and is considered as an acceptable inaccuracy.

The results of the water storage and infiltration processes in the swale element of the sub-catchment ELMSH\_E13\_04 are displayed in Fig. 5. 16 and the results of the sub-catchment ELMS\_E06\_02 are attached to the thesis (Attach 17.2.2).

The water level in the swale reaches a maximum of 27.3cm in the sub-catchment ELMSH\_E13\_04 with the design rainfall event of 19.3mm/h. The maximum storage height in the swale before the overflow begins is 30cm. The water stored in the swale percolates into the base layer dependent on the infiltration rate. When the soil moisture in the base layer reaches the field capacity, water percolates into the under ground. The field capacity of the base layer is 52 l/m<sup>2</sup> and the maximal reached soil moisture is 79.7 l/m<sup>2</sup>.

In the sub-catchment ELMS\_E06\_02 (Attachment 17.2.2) the water level in the swale reaches a maximum of 27.2cm and the maximum soil moisture in the base layer is 82 l/m<sup>2</sup>.

The maximal storage capacity of the swale is reached with a rainfall, which causes a flood event with a return period of once in 5 years in the sub-catchment. In this case, an overflow of  $0.09\text{m}^3/\text{s}$  in the sub-catchment ELMSH\_E13\_04 and an overflow of maximal  $0.17\text{m}^3/\text{s}$  in the sub-catchment ELMS\_E06\_02 are simulated. With a rainfall causing a flood event with a return period of once in 100years the overflow is about  $0.86\text{m}^3/\text{s}$  in the sub-catchment ELMSH\_E13\_04 and  $0.99\text{m}^3/\text{s}$  in the sub-catchment ELMS\_E06\_02. Overall, it can be stated that the temporal water storage and drainage processes in the swale are sufficiently simulated.

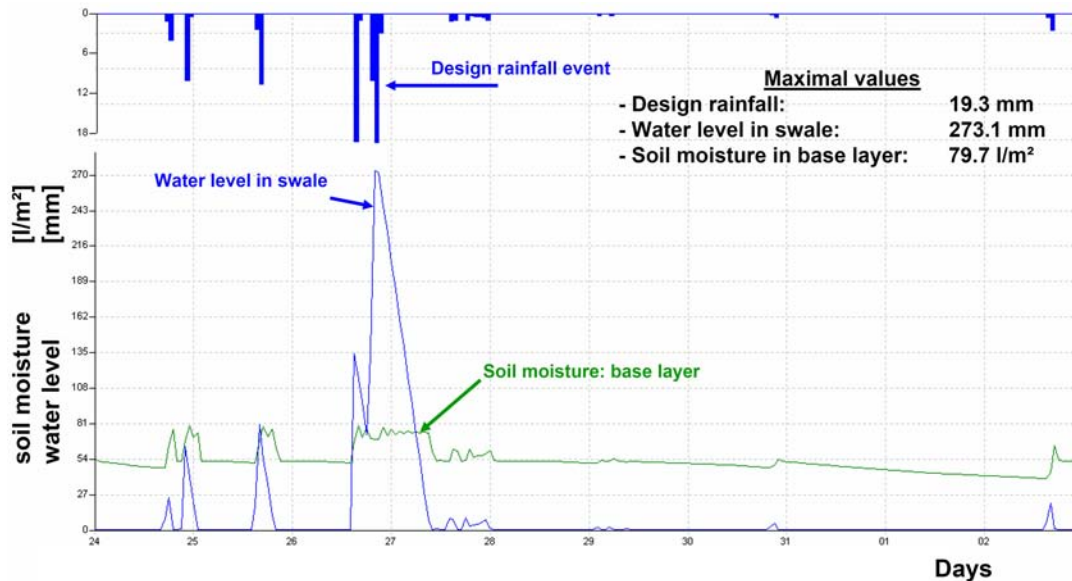


Fig. 5. 16 Water storage and infiltration processes in the swale element of the sub-catchment ELMSH\_E13\_04 with the design rainfall event (HP<sub>5,C</sub>).

### 5.6.2.3 Simulations of Swale-Filter-Drain Systems

With swale-filter-drain systems in the two sub-catchments in Kaltenkirchen (KAKI\_2 and KAKI\_3) the testing results have been calculated. In both sub-catchments 30% of the sealed areas are drained by swale-filter-drain systems.

The water balances of the SUDS elements are illustrated in Table 5. 22 (HP<sub>5,C</sub>) and Table 5. 23 (HQ<sub>100,C</sub>)<sup>1</sup>. The same design of the swale-filter-drain systems has been applied and the rainfall gauging station allocated to both sub-catchments is Henstedt Ulzburg<sup>2</sup>.

The input water volume corresponds to the effective rainfall on the area of the swale-filter-drain system and the water volume from drained sealed areas. The evaporation from the storage layer, the evapotranspiration from the soil layers, the drainage of the filter layer, the overflow from the swale, the percolation into the groundwater as well as the negative change in the soil moisture are defined as outflow processes from the swale system.

<sup>1</sup> The interrelation between a design rainfall event and a design flood event is described in 5.5.3

<sup>2</sup> Location of the rainfall gauging station in Fig. 5.2.

Table 5. 22 Water balance calculation results of swale-filter-drain systems [HP<sub>5,C</sub>].

| Processes in swale-filter-drain systems (HP <sub>5,C</sub> )        | Sub-catchment KAKI_2 | Sub-catchment KAKI_3 | Inflow ↓ or outflow ↑ process |
|---|----------------------|----------------------|-------------------------------|
| Effective rainfall on swale-filter-drain system [l/m <sup>2</sup> ] | + 96.1               | + 96.1               | ↓                             |
| Inflow from sealed areas [l/m <sup>2</sup> ]                        | + 761.7              | + 761.0              | ↓                             |
| Potential evaporation from the storage layer [l/m <sup>2</sup> ]    | - 17.0               | - 17.0               | ↑                             |
| Evapotranspiration from the soil layers [l/m <sup>2</sup> ]         | - 26.2               | - 26.2               | ↑                             |
| Drainage of the filter layer [l/m <sup>2</sup> ]                    | - 8.6                | - 7.6                | ↑                             |
| Overflow of the swale [l/m <sup>2</sup> ]                           | 0.0                  | 0.0                  |                               |
| Percolation in the groundwater [l/m <sup>2</sup> ]                  | - 767.0              | - 767.3              | ↑                             |
| Difference in soil moisture [l/m <sup>2</sup> ]                     | - 39.1               | - 39.1               | ↑                             |
| Difference [l/m <sup>2</sup> ; %]                                   | -0.1<br>(ca. 0.01%)  | -0.1<br>(ca. 0.01%)  | --                            |

Table 5. 23 Water balance calculation results of swale-filter-drain systems [HQ<sub>100,C</sub>].

| Processes in swale-filter-drain systems (HQ <sub>100,C</sub> )      | Sub-catchment KAKI_2 | Sub-catchment KAKI_3 [l/m <sup>2</sup> ] | Inflow ↓ or outflow ↑ process |
|---|----------------------|--|-------------------------------|
| Effective rainfall on swale-filter-drain system [l/m <sup>2</sup> ] | + 104.4              | + 104.4                                  | ↓                             |
| Inflow from sealed areas [l/m <sup>2</sup> ]                        | + 934.5              | + 933.7                                  | ↓                             |
| Potential evaporation from storage layer [l/m <sup>2</sup> ]        | - 17.1               | - 17.1                                   | ↑                             |
| Evapotranspiration from the soil layers [l/m <sup>2</sup> ]         | - 26.1               | - 26.1                                   | ↑                             |
| Drainage of the filter layer [l/m <sup>2</sup> ]                    | - 6.3                | - 5.6                                    | ↑                             |
| Overflow of the swale [l/m <sup>2</sup> ]                           | - 25.4               | - 25.0                                   | ↑                             |
| Percolation in the groundwater [l/m <sup>2</sup> ]                  | - 924.9              | - 925.2                                  | ↑                             |
| Difference in soil moisture [l/m <sup>2</sup> ]                     | - 39.2               | - 39.2                                   | ↑                             |
| Difference [l/m <sup>2</sup> / %]                                   | -0.1 (0.01%)         | -0.1 l/m <sup>2</sup> (0.01%)            | --                            |

The soil moisture and flow processes in the swale-filter-drain systems of both sub-catchments are corresponding, due to the computed equal inflow water volumes and SUDS design. Therefore, only one of the diagrams illustrating the hydrological processes is displayed in Fig. 5. 17 (KAKI\_3).

The complex water storage and flow processes in the layers of the swale-filter-drain system are analysed in more detail. The earlier smaller rainfall event and the resulting soil moisture in the element, is considered as well, to discuss the final water balance processes during the design rainfall event.

The first rainfall event with a height of about 13.2mm/h induces a water level of 94mm in the swale. Which means that about 1/3 of the total volume of the swale is filled up (as the design depth is 300mm). The water infiltrates into the colmation layer within a time of 4.5hours. When the soil moisture in the colmation layer reaches the field capacity (31.5l/m<sup>2</sup>), water infiltrates into the filter layer. The soil moisture in the colmation layer reaches a maximum of about 63.0l/m<sup>2</sup>. By the percolation of the water into the filter layer and no further infiltraton from the stored water of the swale, the soil moisture decreases to the field capacity (31.5l/m<sup>2</sup>) after the first smaller rainfall event.

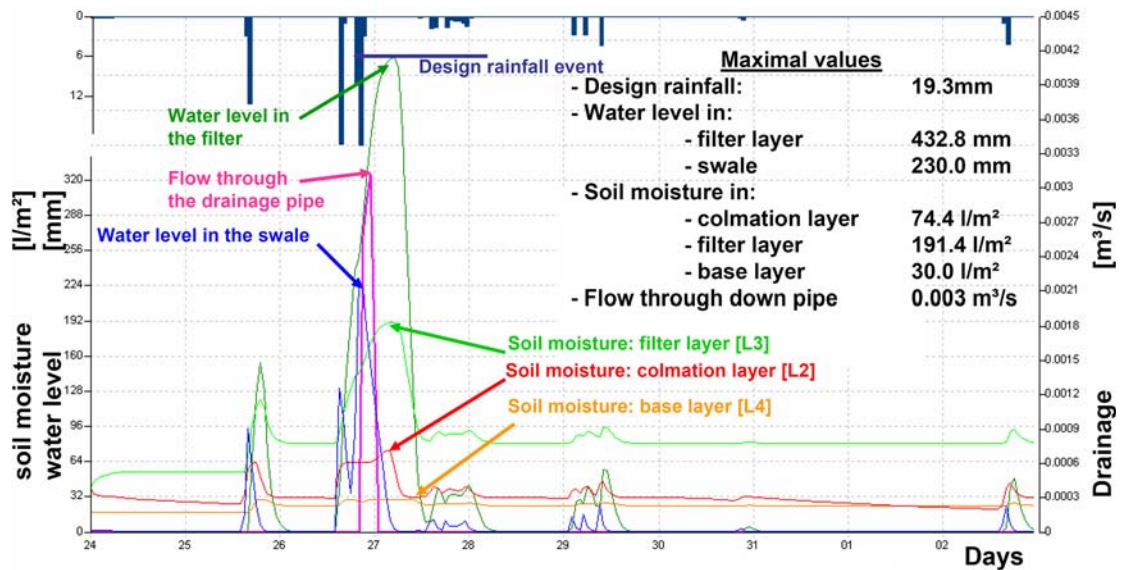


Fig. 5. 17 Water storage and infiltration processes in the swale-filter-drain system of the sub-catchment KAKI\_3 with the design rainfall event (HP<sub>5,C</sub>).

The soil moisture in the filter increases up to 120.3l/m<sup>2</sup> dependent on the percolation of water from the colmation layer. A water level of 154mm is reached in the filter layer after the smaller rainfall event.

Only when the maximum soil moisture in the base layer and the field capacity in the filter layer is reached, water can percolate into the drain pipe and a drainage flow is generated. After the first rainfall event the maximal soil moisture of the base layer is not reached, therefore all the water infiltrates into the ground.

The water level in the swale and the filter layer decreases to zero before the design rainfall event begins with an intensity of 19.3mm/h. The soil moisture in the colmation layer, the filter layer and the base layer are decreased to the respective field capacity.

After the first hour of 19.3mm rainfall on the catchment area, the water level in the swale increases up to 131mm, which decreases within the following 3hours down to 91mm, before the water level in the swale increases again because of another rainfall event with a rainfall height of 19.3mm. This time the water level reaches a maximum of 230mm.

The water percolates into the colmation layer where a maximum of soil moisture of about 74 l/m<sup>2</sup> is reached with simultaneous percolation of water into the filter layer. Only when the whole water from the swale has been infiltrated, the soil moisture in the colmation layer decreases again.

With the infiltration of water from the colmation layer and the simultaneous percolation of water into the base layer and the drain pipe, a maximal soil moisture of 191 l/m<sup>2</sup> is reached in the filter layer. With this soil moisture a water level of maximal 433mm is generated in the filter layer. The flow into the drainpipe reaches a maximum of 0.0031m<sup>3</sup>/s after 2hours of the second larger rainfall.

The base layer is made up of coarse sand with a higher field capacity than the filter layer. Therefore the water is kept back for a longer time in the SUDS element to enhance purification.

The maximum storage capacity in the swale is reached with a rainfall which causes a flood event with a return period of once in 5years. In this case, an overflow of the swale is simulated of 0.009m<sup>3</sup>/s in the sub-catchments of Kaltenkirchen. With a rainfall causing a flood event with a return period of once in 100years, the overflow is maximal about 0.04m<sup>3</sup>/s. This is about 20 times less than with swales.

Overall it can be stated that the temporal water storage and drainage processes in the swale-filter-drain systems are appropriately simulated according to the defined testing criteria.

### **5.6.3 Assessment of the Effectiveness of SUDS in Adaptation Scenarios**

For the simulation of the effectiveness of SUDS to mitigate the increased flood probability computed in climate scenarios, a number of SUDS adaptation scenarios have been developed according to the methodology in (3.6.3). Finally, eight adaptation scenarios have been created, which are given in Table 5. 24.

Like for the post-processing of the statistical evaluations of climate change scenarios, the flood peaks of all SUDS adaptation scenarios with specific return periods have been illustrated in probability curves to assess the effectiveness of the SUDSs. Studies have been done for four nodes of interest: Kölln, A23, Langeloh and the

End Node. Additionally, the effectiveness of the SUDS measures has been quantified in the two urban sub-catchments: ELMSH\_E13\_04 and ELMS\_E06\_02.

Table 5. 24 Eight SUDS adaptation scenarios.

| SUDS Adaptation Scenario                           | Spatial distribution of SUDS | Short description  |
|--|------------------------------|--|
| <b>Green roofs</b><br>[2040 – 2070]                | 20 %                         | 20% of the sealed areas are simulated as green roofs   |
| <b>Swales</b><br>[2040 – 2070]                     | 30 %                         | 30% of the sealed areas are drained by swales  |
| <b>Swale-Filter-Drain systems</b><br>[2040 – 2070] | 30 %                         | 30% of the sealed areas are drained by swale-filter-drain systems (restricted to Kaltenkirchen and Barmstedt)  |
| <b>Unsealing</b><br>[2040 – 2070]                  | 30 %                         | 30% of the sealed areas are covered with unsealing measures  |
| <b>SUDS Combination</b><br>[2040 – 2070]           | Σ of SUDS distributions      | SUDS combination of green roofs (20%) which drain into swales (30%) in Elmshorn or swale-filter-drain systems (30%) in Kaltenkirchen and Barmstedt; additionally 30% of the sealed areas are unsealed. |
| <b>Scenario 0</b><br>[1971 – 2000]                 | No SUDS                      | Reference scenario without climate change impacts or implemented SUDS  |
| <b>Scenario 0-A1B</b><br>[2040 – 2070]             | No SUDS                      | Adjusted climate change scenario without SUDS  |
| <b>Natural State Scenario</b><br>[2040 – 2070]     | No SUDS                      | Climate change scenario with a land use of the whole catchment of 30% forests and 70% meadows  |

### 5.6.3.1 Catchment of the Eckhorner Au

The node of the Eckhorner Au drains a rural, mostly agricultural used catchment of 35.6km<sup>2</sup>. SUDS are simulated only in the industrial area of the south-western part of Elmshorn. In this catchment, swale-filter-drain systems could not be realized as the groundwater table in this area is too high (between 0.9 and max. 1.3m below the surface) and it is situated in a water protection zone. For the infiltration, only flat swales with a depth of maximal 30cm are simulated. The potential mitigation of the peak runoff can maximal reach the natural state scenario results, which are illustrated in attachment 18.1.

The increase of the flood probability in the climate scenario 0-A1B is mostly derived by the discharge from natural areas. As SUDS don't affect the runoff from natural areas, the effectiveness of SUDS to mitigate an increased flood probability by climate change is rather low in this catchment. The combination of SUDS measures

with green roofs, swales and unsealing approximates the natural state scenario, but this is still significantly higher than the reference Scenario 0. The reduction of the peak discharge by SUDS adaptation Scenarios referred to the reference Scenario 0 is about 5% to 13% and with the combination of SUDS measures a reduction of up to 25.7% is achieved. This is illustrated in bar plots in the attachment 18.1 for flood peaks with return periods (T) of once in 1, 5, 20, 50 and 100years.

The discussion of the effectiveness of SUDS is recommended to be done referred to the (climate change) natural state scenario. For this purpose additional bar plots have been worked out with the potential percentage reduction by SUDS measures referred to the projected (climate change) natural state scenario. The combined SUDS measures reduce the flood peak by about 70% to 80% referred to the natural state scenario. The maximal reduction by separate SUDS measures like unsealing is 21%, by green roofs 29.2% and with swales 43% for flood peaks with return periods of once in 5years.

### 5.6.3.2 *Upper Krückau Catchment ( Kaltenkirchen and Barmstedt)*

The node A23 drains the upper catchment of the river Krückau including the urban sub-catchments in Kaltenkirchen as well as Barmstedt. The catchment is mainly made up of green fields and agricultural areas with smaller villages. The situation is similar to the catchment area of the Eckhorner Au. The flood probability with climate change impacts from the catchment in a completely natural state is larger than from the reference situation with sealed areas. Like in the catchment area of the Eckhorner Au, the combined SUDS measures illustrate the highest effectiveness to reduce the flood probability. Related to the reference Scenario 0 and the (climate change) natural state scenario, a reduction of up to 50% is achieved with the SUDS adaptation scenario of combined measures. The largest effectiveness of single SUDS measures is displayed by swales of 22.4% for flood events with a return period of once in 50years, followed by green roofs (19.9%), swale-filter-drain systems (15.7%)<sup>1</sup> and unsealing (14.7%). The results are provided in Attachment 18.2.

### 5.6.3.3 *Elmshorn - Node Langelohe*

The node Langelohe is situated in Elmshorn downstream of the nodes A23, Eckhorner Au and Offenau. The node is located close to the Else-Brandström school in a flood risk area at the Krückau Park. Like in the catchments further upstream, the increased flood probability derived from the projected (climate change) natural state scenario is larger than the reference scenario 0 of the year 2000. The peak discharge at this node is mainly affected by the drainage from natural areas of the Krückau catchment upstream.

---

<sup>1</sup> The spatial distribution of swale-filter-drain systems is restricted to the urban areas of Kaltenkirchen and Barmstedt

The simulated swale-filter-drain systems in Kalttenkirchen and Barmstedt show only a minor effectiveness at the node Langeløhe. With the SUDS combination scenario, a potential reduction of about 22% to 50% referred to the Scenario 0, and a reduction of about 55% to 70% of the flood probability referred to the (climate change) natural state scenario could be reached. The separate SUDS measures reach a reduction between 10% to maximal 40% with green roofs or swales referred to the (climate change) natural state scenario. With these results it is expected that the flood risk at the school close to the Krückau park will increase under this projected climate change scenario conditions (A1B Scenario), because even the projected (climate change) natural state scenario illustrate an increase referred to the status quo scenario 0 (see Fig. 5. 18).

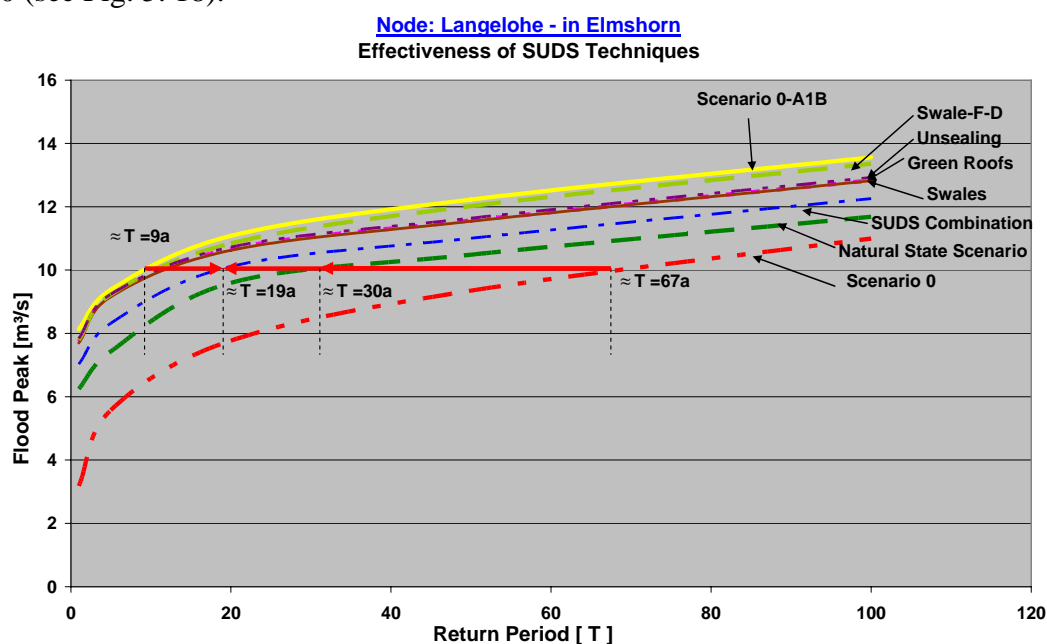


**Fig. 5. 18 Flood peak probability curves of the climate change and SUDS adaptation scenarios at the node: Langeløhe in Elmshorn.**

The mitigation effectiveness of the projected flood peaks is illustrated in Fig. 5. 18 with a shift in the flood probability curves. For example a projected future flood peak of about 10.0m³/s with a return period of once in about 9years ( $T = 9a$ ), is projected to occur once in 19years in the SUDS combination scenario. But in the current state scenario 0 this flood peak is projected to have a return period of once in about 67years. The maximal reduction of the probability of occurrence of this flood peak by SUDS is to a return period of once in about 30 years, represented by the natural state scenario.

The comparison of flood hydrographs computed with the SUDS scenarios is illustrated additionally in Fig. 5. 19 for an  $HQ_{100}$ .

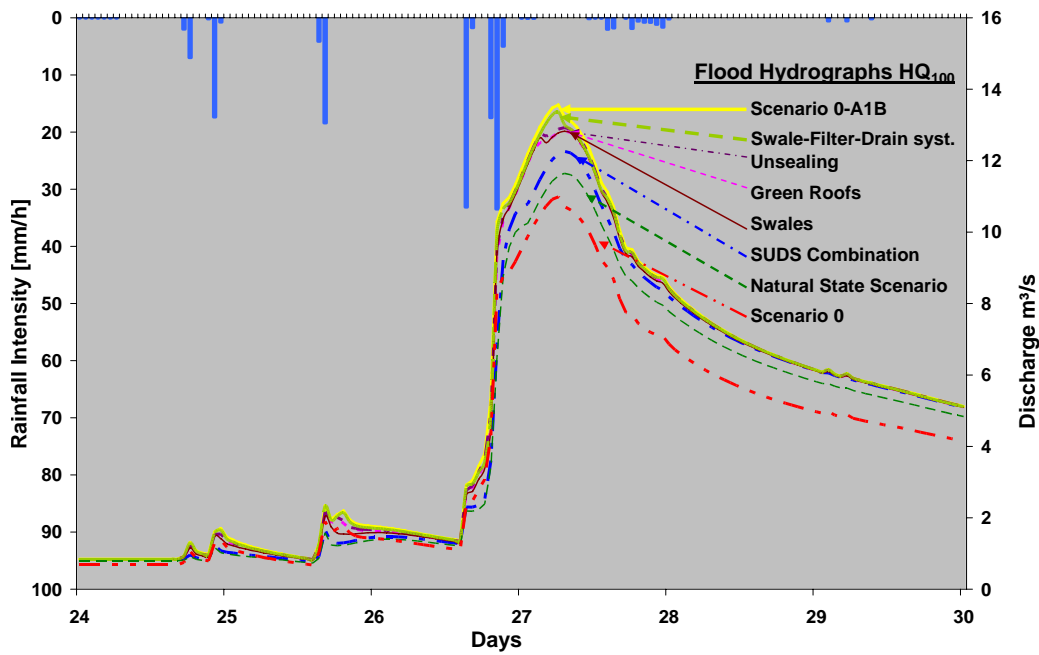


Fig. 5. 19 Flood peaks (HQ<sub>100</sub>) in hydrographs of SUDS adaptation and climate scenarios [node Langeloh in Elmshorn].

5.6.3.4 Elmshorn - End Node of Krückkau Catchment

The End Node of the Krückkau catchment is situated downstream of Elmshorn and drains additional sealed areas which include the industrial area of Elmshorn in the north, the city centre of Elmshorn with high sealing rates and further dense urban sub-catchments. The peak discharge is mainly generated from the sealed urban areas in contrast to the other nodes considered before.

Krückkau Catchment End Node: Elmshorn  
Effectiveness of SUDS Techniques

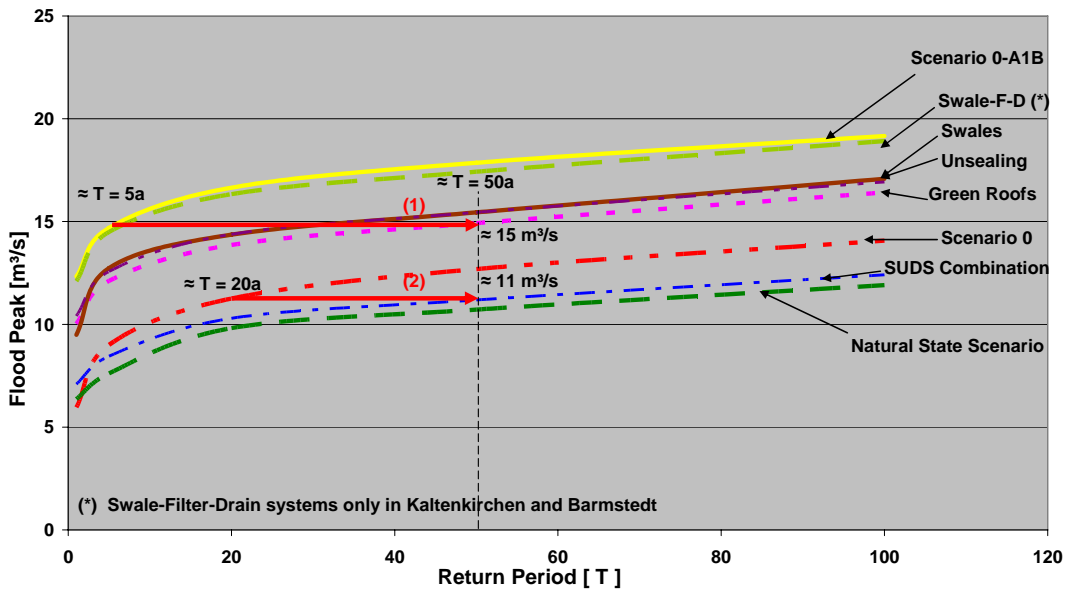


Fig. 5. 20 Flood peak probability curves of the climate change and SUDS adaptation scenarios at the End Node of the Krückkau Catchment.

The flood peaks in the (climate change) natural state scenario are lower than the flood peaks in the reference Scenario 0 with the sealed areas. A larger potential is displayed in this case, that the increase of the peak discharge derived with the climate change scenario 0-A1B can be compensated with SUDS measures.

Draining about 30% of the sealed areas in the urban sub-catchments of Kaltenkirchen und Barmstedt by swale-filter-drain systems reduces the flood peak probability in Elmshorn by about 6% only, because of a restricted spatial distribution. Therefore it has not been taken into account for the comparison.

For floods with a return period of once in 50years, the largest reduction of the peak discharge by separated SUDS measures is achieved by green roofs with a reduction of 57% followed by swales and unsealing with a reduction of 46.7% referred to the scenario 0. The flood peak mitigation effectiveness by green roofs is illustrated in Fig. 5. 20 with the shift (1). A flood peak of 15m<sup>3</sup>/s under climate change conditions is projected with a return period of once in 5years. In the SUDS adaptation scenario with implemented green roofs, this flood peak is computed to occur only once in 50years.

With the combination of SUDS, the flood peak probability is even reduced below the reference scenario 0 by about 30% (reduction of 130%: see Fig. 5. 21). This is illustrated in Fig. 5. 20 with the shift (2) of a flood peak with 11m<sup>3</sup>/s. In the reference scenario 0, the flood peak is computed to occur once in about 20 years, but it is projected to occur only once in 50years in the SUDS combination scenario under climate change conditions.

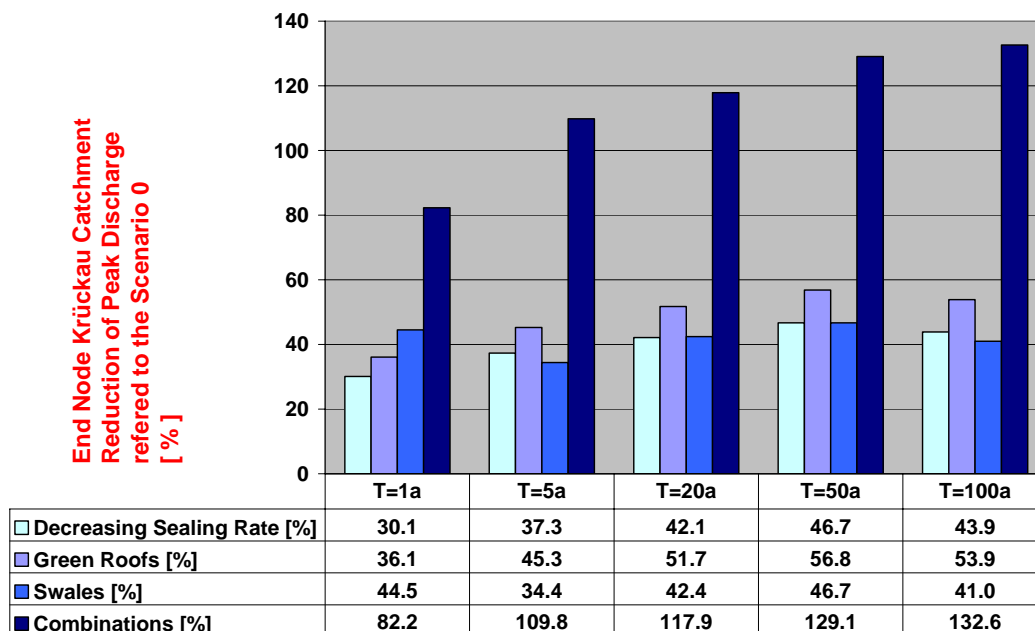


Fig. 5. 21 Reduction of the flood peaks by projected (climate change) SUDS adaptation scenarios related to the reference Scenario 0 at the End Node of the Krückkau catchment.

The SUDS combination scenario approximates the projected (climate change) natural state scenario by about 90%, as illustrated in the bar plot (Fig. 5. 22). With the

scenario of green roofs in all urban sub-catchments, a decrease of the peak discharge of about 40% and by swales a reduction of maximal 30% is achieved referred to the maximal reduction in the natural state scenario. It is significant that the effectiveness of swales decreases with larger rainfall intensities. This points out, that the SUDS measures loose there effectiveness, when the storage capacity is reached and an overflow of the systems is generated. This is less significant with the combined SUDS chain, where for example the overflow from green roofs drains into swales first. Another SUDS scenario has been defined with 30% unsealing of urban areas in Kaltenkirchen, Barmstedt and Elmshorn. Therewith the peak discharge can be reduced maximal by about 34% referred to the natural state scenario.

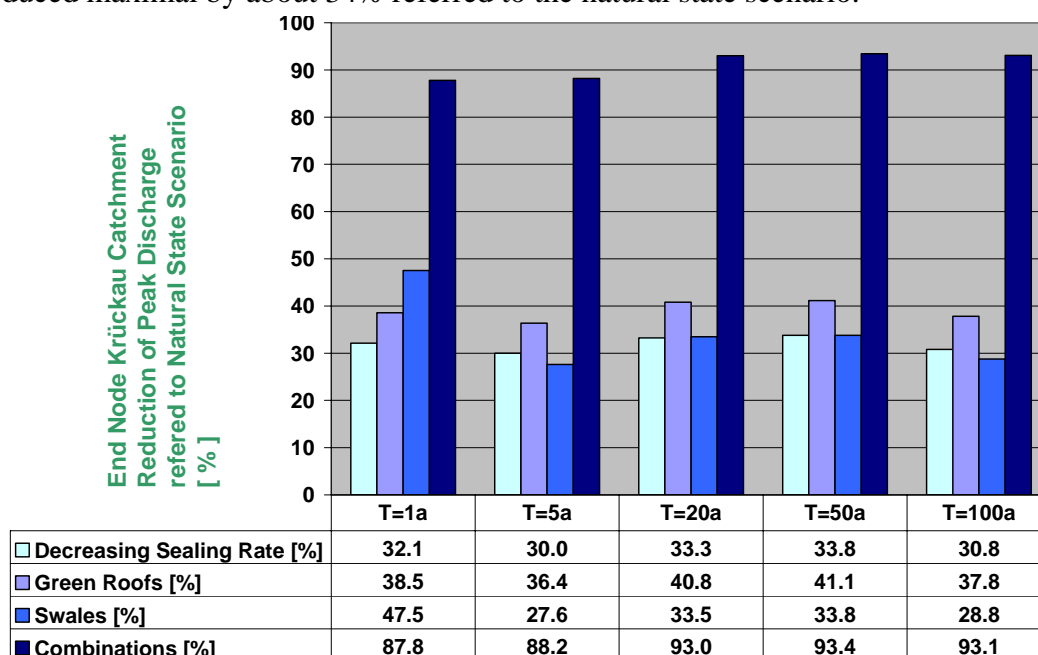


Fig. 5. 22 Reduction of the flood peaks referred to the projected (climate change) Natural State Scenario at the End Node of the Krückau catchment.

### 5.6.3.5 Sub-Catchments in Elmshorn

The results of the SUDS adaptation scenarios in the sub-catchments of Elmshorn are provided in the Attachment 18.5. The flood probability curve of the sub-catchment ELMS\_E06\_02 with the hot spots of the ‘Badewanne’ (Hamburger Strasse) and the Steindammwiesen Park is given in Fig. 5. 23.

All SUDS measures reduce the projected increase of the flood peak probability derived in the climate change scenario 0-A1B below the reference scenario 0. For events with higher probabilities of occurrence ( $T < 5a$ ), swales display the best reduction potential. But when this measure is overloaded ( $T > 5a$ ) and the overflow is drained to the storm water system, the effectiveness is reduced. For larger storm events, green roof elements display better mitigation results than swales or unsealing of surfaces. In Fig. 5. 23 the shift of the probability of occurrence of a peak discharge with  $2.5m^3/s$  is illustrated. In the reference scenario 0, the peak discharge is

computed to have a return period of once in 20 years. This probability of occurrence is increased in the climate change scenario 0-A1B to once in about 10years. In the SUDS adaptation scenario with green roofs, the probability of occurrence is reduced to once in 30years and with the SUDS combinations it is even reduced to once in about 91 years.

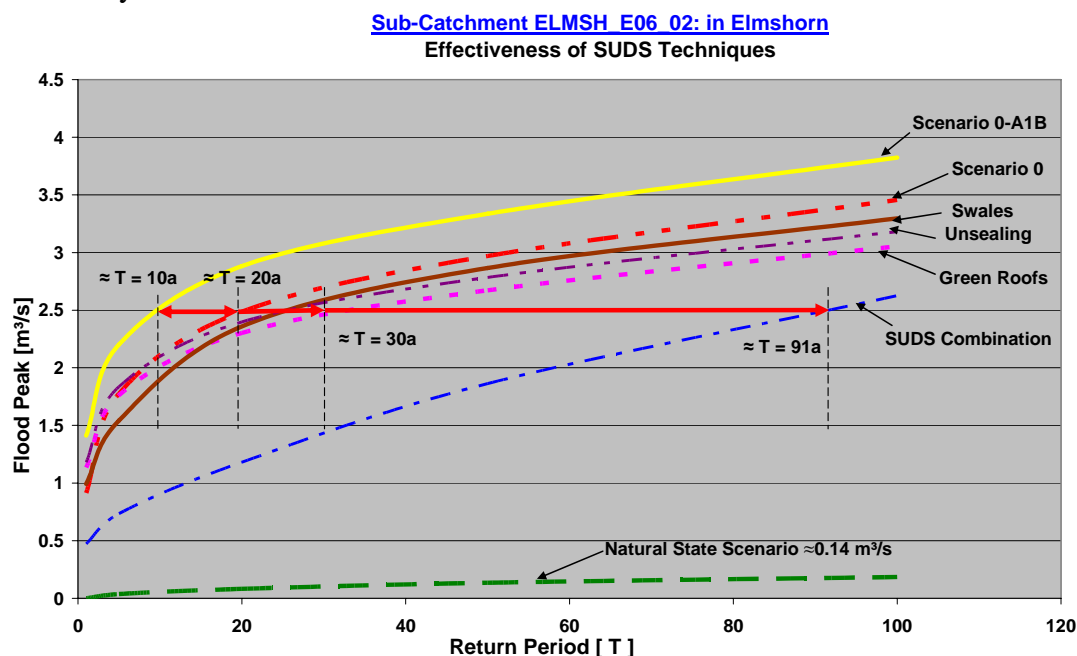


**Fig. 5. 23 Flood peak probability curves of the climate change and SUDS adaptation scenarios of the Sub-catchment ELMS\_E06\_02.**

The magnitude of mitigation is given in bar plots related to the reference Scenario 0 (Fig. 5. 24) and related to the (climate change) natural state scenario (Fig. 5. 25).

By unsealing measures, a reduction of the peak discharge of about 46% to 175% is achieved, whereas the largest reduction is illustrated for the event with a probability of occurrence of once in 100years. With green roofs, a flood event with a return period of once in 20years is reduced by about 47% below the reference scenario 0 and for a 100year flood event the flood peak is even reduced by two times the impacts derived by climate change (210%). The overflow of green roofs is generated above an event with a return period of 50years and it could be stated, that the storage height of 3cm on the green roof could be reduced to 2.5cm.

The simulation of swales display the highest effectiveness for events with a return period of once in 5years and thereafter the effectiveness is reduced. This is caused by the generation of overflow from the swales, which drains into the storm water sewage systems. However, with swales the impacts derived by climate change on the flood probability could be compensated completely in the sub-catchment ELMS\_E06\_02. A mitigation of the flood peak of 50% below the reference Scenario 0 is achieved.

With a combination of SUDS, the largest effectiveness is displayed for a 20year event with a reduction of about 4times the impacts by climate change (430%). This is due to the high effectiveness of SUDS combinations, which approximate the (climate change) natural state scenario by about 61% to 68% (Fig. 5. 25), which displays much lower discharge peaks than the reference Scenario 0 with dense urbanised areas (Fig. 5. 23).

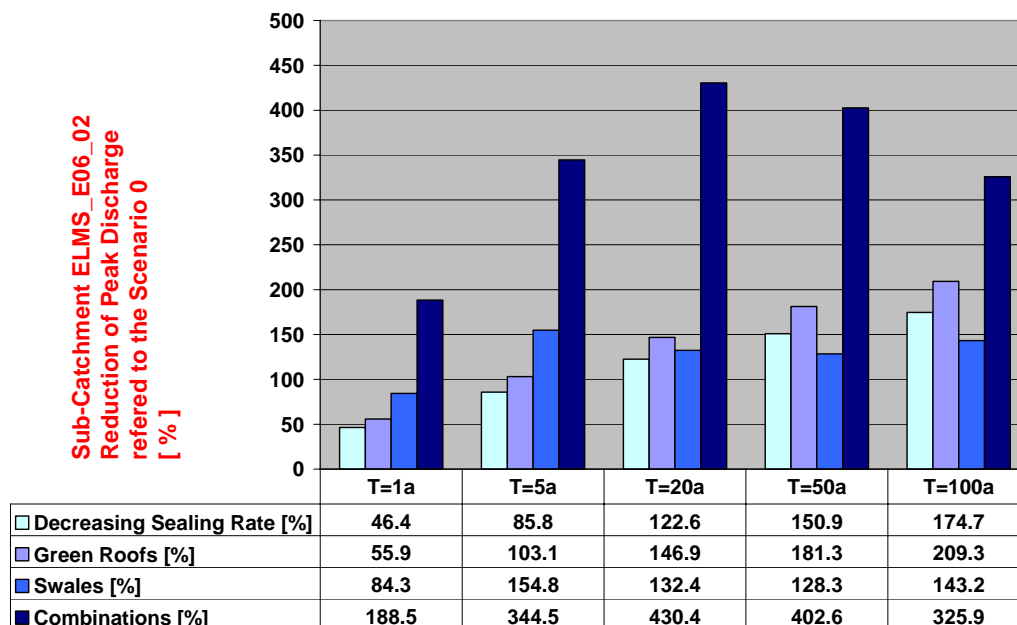


Fig. 5. 24 Reduction of the flood peaks by projected (climate change) SUDS adaptation scenarios related to the reference Scenario 0 of the Sub-catchment ELMS\_E06\_02.

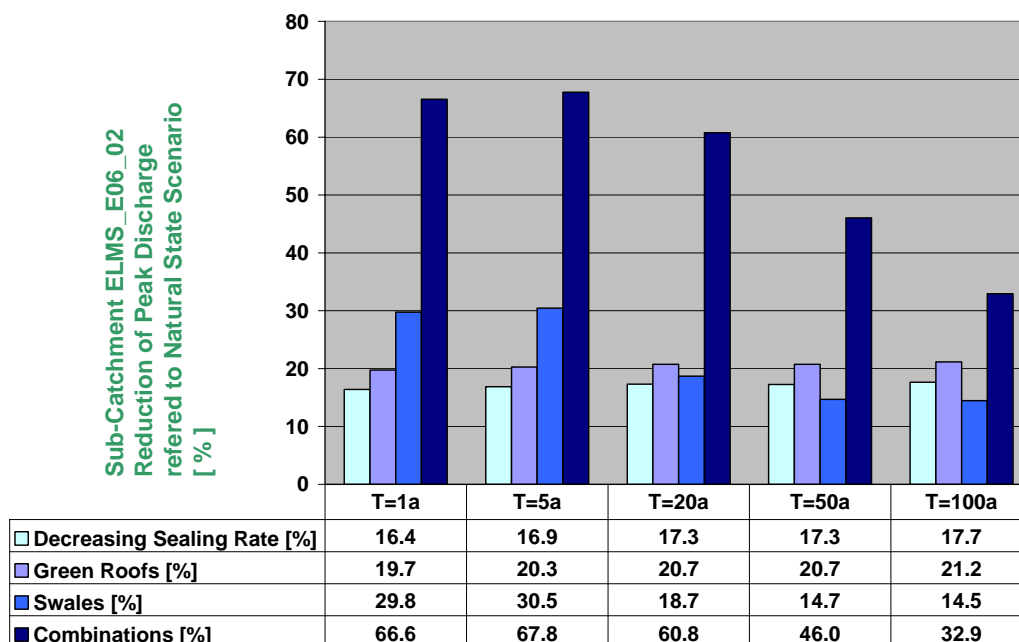


Fig. 5. 25 Reduction of the flood peaks referred to the projected (climate change) natural state scenario of the Sub-catchment ELMS\_E06\_02.

The simulation results of the sub-catchment ELMSH\_E13\_04 are comparable, considering the SUDS adaptation scenarios of unsealing, green roofs and the SUDS-combination scenario. But the simulation of swales does not project a compensation of the climate change impacts on the flood probability in this sub-catchment (Attachment 18.5). The turning point of the effectiveness of swales is again for an event with a return period of once in 5 years, but almost no effectiveness is displayed anymore for 100year peak discharges in this sub-catchment.

## **6 Discussion**

The results of the application scenario studies are summarized to discuss their appropriateness in comparison with outcomes of related projects (6.1), and the range of uncertainties in climate change studies using add-on hydrological models is pointed out (6.2).

### **6.1 Comparative Studies**

For the discussion of changes in flood probabilities, it is important to analyse as well the impacts on climate variables (precipitation, temperature and evaporation) with a focus on extreme rainfall, which are the external drivers for the water balance and flood regime simulations in catchments. The projected changes of the climate variables as well as the results of the flood probability calculations are discussed in comparative studies with the following related projects (UFOPLAN: [Jacob et al., 2008](#); [Bischoff, 2007](#); [PÜK, 2008](#); INKLIM 2012 II Plus: [Brahmer, 2008](#); Wandse project: [Golder Associates, 2009](#)).

For the discussion of SUDS adaptation scenario results, comparative studies are rare up to now, especially considering the effectiveness to compensate climate change impacts. Therefore, the discussion is based on the testing criteria of the implemented software tool.

#### **6.1.1 Discussion of Changes in Climate Variables**

##### *6.1.1.1 Climate Control Scenario Results [1971 – 2000]*

##### ***Differences in Temperature***

The differences between the computed control scenario data (REMO C20, 1971 – 2000) and the observed data series (1971 – 2000) are outlined in (5.3.1). The average summer temperature of the REMO data series compared to the observed data series is about 0.1°C lower and the winter temperature is about 0.9°C lower for the Krückau catchment. In the UFOPLAN project report is stated that the REMO data overestimates the average summer temperature by about 1°C to 2°C and that the winter temperatures are underestimated by about 1°C ([Jacob et al., 2008](#)). The scenario study results in this thesis for the winter temperature correspond to the published underestimation, but for the summer period a slightly lower temperature difference has been computed. This could be derived from the different definition of the seasonal periods. In the UFOPLAN report, the summer period is defined for June, July and August (JJA) ([Jacob et al., 2008](#)), but in the scenario studies of this thesis the differentiation of the seasons have been done according to a hydrological year from May to October.

### ***Differences in Precipitation***

The seasonal precipitation display larger differences between the REMO and observed data series. In summer periods a difference of +22%, in yearly periods a difference of +19% and in the winter periods a difference of +16% has been calculated of the REMO data series compared to the observed data series. The REMO control scenario data series are affected by climate variability and systematic inaccuracies of the climate models. On the other hand, it has been stated by [Rudolf & Rubel \(2005\)](#) that underestimations of 10% to 50% have to be taken into account when observed rainfall data series are used, due to systematic errors. These biases or inaccuracies in precipitation data series depend on wind velocity, temperature and the season ([Rudolf & Rubel, 2005](#)). Because the largest computed differences between the REMO control scenario data and the observed rain gauge data is 22% for the Krückau catchment in this thesis, the differences of the precipitation data series are regarded as reasonable.

### ***Differences in Evaporation***

Comparative studies about evaporation data series of the control scenario (1971 – 2000) are not available. Therefore, the REMO data series have been discussed with the differences in temperature and precipitation. It has been concluded that 6.3% more evaporation in the summer periods is reasonable due to the higher computed precipitation with the REMO climate model. The projected evaporation data series in the winter periods is 18.8% lower than the observed data series, which is explainable with the computed lower temperature data series.

### ***Differences in Extreme Rainfall Events***

In the computed extreme rainfall events of the REMO C20 control scenario run a negative trend from 1970 to 2000 has been detected which does not correspond to the observations in that time period. This is due to the climate variability projected in the REMO-UBA model realisation and has been stated as well in the UFOPLAN report ([Jacob et al., 2008](#)).

In the statistical evaluations of rainfall intensities, daily and hourly data series have been compared with specific return periods. The differences in the computed REMO C20 control scenario data series and the observed data series are larger for the statistical evaluations of the short term hourly rainfall durations. This has been detected as well by [Bischoff \(2007\)](#), who compared rainfall intensities with durations of 1hour, 6hours and 24hours for the region of Hamburg. One result of his analyses is given in chapter 2 (Fig. 2.2). In the study results for hourly extreme rainfall intensities for Hamburg by [Bischoff \(2007\)](#) differences of 40% to 60% are displayed and in this thesis, differences of up to 40% have been calculated.

These validation results of the REMO control scenario data series and observed data series confirm the need to discuss uncertainties in climate scenario studies.

*6.1.1.2 Future Climate Scenario Results [2040 – 2070]*

The changes in climate variables derived in the IPCC scenarios A1B, A2 and B1 have been analysed with regard on temperature, precipitation and evaporation with trend analyses in (5.3.2). The results of the final UFOPLAN report for Hamburg and Schleswig Holstein are referred in this context, to discuss the results for the Krückau catchment area. But a comparison has to be done of data series for different future climate periods. In the UFOPLAN, periods from 2021 to 2050 and from 2071 to 2100 are related to the control scenario time period from 1961 to 1990. In this thesis a future climate period from 2040 to 2070 related to the control scenario period from 1971 to 2000 has been analysed. Additionally, it has to be taken into account that the summer and winter periods are differently defined. Therefore only a rough comparison and discussion of the results can be obtained.

***Average changes in Temperature***

In the UFOPLAN, the minimal and maximal projected yearly temperature increases from 2021 to 2050 by about 0.6°C to 1.5 °C (Table 6. 1) and for the climate period from 2071 to 2100 by about 1.9°C to 2.9°C (Table 6. 2) for the scenarios A1B, A2 and B1.

**Table 6. 1 Relative change of temperature published in the UFOPLAN for the period: 2021-2050 and the scenarios A1B, A2 and B1 related to (1961 – 1990). (adopted from [Jacob et al., 2008](#))**

| Changes in Temperature (2021 – 2050) | Winter (DJF) <sup>1</sup> |       | Spring (MAM) |       | Summer (JJA) |       | Autumn (SON) |       | Yearly |       |
|--------------------------------------|---------------------------|-------|--------------|-------|--------------|-------|--------------|-------|--------|-------|
|                                      | Hamburg                   | 0.9°C | 1.8°C        | 0.0°C | 1.0°C        | 0.7°C | 1.4°C        | 0.6°C | 1.7°C  | 0.6°C |
| Schleswig-Holstein                   | 0.8°C                     | 1.8°C | 0.1°C        | 1.1°C | 0.7°C        | 1.4°C | 0.7°C        | 1.7°C | 0.6°C  | 1.5°C |

**Table 6. 2 Relative change of temperature published in the UFOPLAN for the period: 2071-2100 and the scenarios A1B, A2 and B1 related to (1961 – 1990). (adopted from [Jacob et al., 2008](#))**

| Changes in Temperature (2071 – 2100) | Winter (DJF) |       | Spring (MAM) |       | Summer (JJA) |       | Autumn (SON) |       | Yearly |       |
|--------------------------------------|--------------|-------|--------------|-------|--------------|-------|--------------|-------|--------|-------|
|                                      | Hamburg      | 2.5°C | 3.6°C        | 1.2°C | 2.1°C        | 1.8°C | 2.9°C        | 2.1°C | 3.1°C  | 1.9°C |
| Schleswig-Holstein                   | 2.5°C        | 3.5°C | 1.4°C        | 2.2°C | 1.8°C        | 2.7°C | 2.1°C        | 3.0°C | 1.9°C  | 2.9°C |

<sup>1</sup> DJF = December, January, February; MAM = March, April, May; JJA = June, July, August; SON = September, October, November

**Table 6. 3 Changes per hydrological season in Temperature [°C] (2040 – 2070) calculated for the Krückkau catchment related to the period 1971 – 2000.**

| Changes in Temperature (2040 – 2070) | Changes in Summer Periods (May – Oct.) | Changes in Winter Periods (Nov. – April) | Changes in Yearly Periods |
|--------------------------------------|--|--|---------------------------|
| <b>B1 Scenario</b>                   | +~ 0.9 to 1.0 °C                       | +~ 1.1 to 1.3 °C                         | +~ 0.9 to 1.3 °C          |
| <b>A1B Scenario</b>                  | +~ 1.3 to 1.6 °C                       | +~ 1.4 to 1.7 °C                         | +~ 1.3 to 1.5 °C          |
| <b>A2 Scenario</b>                   | +~ 1.1 to 1.3 °C                       | +~ 1.7 to 2.0 °C                         | +~ 1.2 to 1.5 °C          |

In this thesis a minimal average yearly temperature increase of 0.9°C and a maximal increase of 1.5°C have been computed for the future time period 2040 to 2070 related to the control scenario (1970 to 2000) (Table 6. 3). The results of this thesis are only slightly higher than the projected results in the UFOPLAN report for the earlier climate period (2021 – 2050) (Jacob et al., 2008). This could be derived by the considered later control scenario period from 1971 to 2000 in this thesis, which results in lower changing rates respectively.

The calculated increase of the average summer temperatures, published in the UFOPLAN report range between 0.7°C and 1.4°C (2021 – 2050) and between 1.8°C and 2.9°C (2071 to 2100) (Jacob et al., 2008). In this thesis, summer temperature increases between 0.9°C and 1.6°C have been calculated, which approximates again the displayed changes of the earlier climate period results in the UFOPLAN report.

The maximum and minimum temperature increase in the winter periods computed in the study results of this thesis are between 1.1°C and 2.0°C. These changes approximate as well the results for the earlier climate period of the UFOPLAN report, which range between 0.8°C and 1.8°C (Jacob et al., 2008).

***Average changes in Precipitation***

The computed average precipitation changes in this thesis are as well in the range of the results published in the UFOPLAN report for Hamburg and Schleswig-Holstein. In the UFOPLAN, the maximal and minimal yearly precipitation increase of the scenarios (A1B, B1 and A2) range from 2% to 8% for the climate period from 2021 to 2050 and from 4% to 9% for the climate period from 2071 to 2100 (Table 6. 4 and Table 6. 5). In this thesis, no change of the yearly precipitation in the A2 scenario, and a maximal increase of 9.3% in the A1B scenario have been calculated for the climate period from 2040 to 2070 (Table 6. 6).

For the average summer precipitation an increase between 1.6% and 3.9% for the climate period 2040 to 2070 has been calculated for the Krückkau catchment in this thesis. The projected results in the UFOPLAN report display a larger range between a decrease of 11% and an increase of up to 8% (2021 - 2050), whereas for the climate period from 2071 to 2100 a decrease of precipitation in all scenarios is projected.

The calculated increase in winter precipitation is in the range of 10.5% to 22.6% for the Krückau catchment area for the climate period from 2040 to 2070. The published increases in the UFOPLAN report are smaller for the climate period from 2021 to 2050 (4% to 15%) and larger for the time period from 2071 to 2100 (19% to 27%). The computed climate changes for the Krückau catchment are considered as reasonable and comparable with the results of the UFOPLAN report. The differences of the data results can be ascribed to the restricted rough comparison with different climate periods as well as different spatial distributions.

**Table 6. 4 Change of precipitation published in the UFOPLAN for the period: 2021-2050 and the scenarios A1B, A2 and B1 related to (1961 – 1990). (adopted from Jacob et al., 2008)**

| Changes in Precipitation (2021 – 2050) | Winter (DJF) |       | Spring (MAM) |      | Summer (JJA) |       | Autumn (SON) |       | Yearly |      |
|--|--------------|-------|--------------|------|--------------|-------|--------------|-------|--------|------|
|  | Hamburg      | 4,0%  | 12,0%        | 1,0% | 5,0%         | -7,0% | 8,0%         | 7,0%  | 20,0%  | 4,0% |
| Schleswig Holstein                     | 7,0%         | 15,0% | -3,0%        | 6,0% | -11,0%       | 6,0%  | 7,0%         | 12,0% | 2,0%   | 8,0% |

**Table 6. 5 Change of precipitation published in the UFOPLAN for the period: 2071-2100 and the scenarios A1B, A2 and B1 related to (1961 – 1990). (adopted from Jacob et al., 2008)**

| Changes in Precipitation (2071 – 2100) | Winter (DJF) |     | Spring (MAM) |     | Summer (JJA) |      | Autumn (SON) |     | Yearly |    |
|--|--------------|-----|--------------|-----|--------------|------|--------------|-----|--------|----|
|  | Hamburg      | 19% | 23%          | 5%  | 14%          | -13% | -11%         | 14% | 20%    | 6% |
| Schleswig Holstein                     | 22%          | 27% | 7%           | 15% | -18%         | -13% | 9%           | 14% | 4%     | 7% |

**Table 6. 6 Relative changes per hydrological season in precipitation [%] (2040 – 2070) calculated for the Krückau catchment related to the period from 1971 to 2000.**

| Changes in Precipitation (2040 – 2070) | Changes in Summer Periods | Changes in Winter Periods | Changes in Yearly Periods |
|--|---------------------------|---------------------------|---------------------------|
| B1 Scenario                            | + 2.4 to 3.3 %            | + 10.5 to 14.9 %          | + 2.7 to 4.2 %            |
| A1B Scenario                           | + 3.3 to 3.9 %            | + 14.4 to 22.6 %          | + 5.2 to 9.3 %            |
| A2 Scenario                            | + 1.6 to 2.7 %            | + 11.5 to 18.1 %          | + 0.0 to 1.6 %            |

**Average changes in Evaporation**

The changes derived in the evaporation are neither calculated in the UFOPLAN (Jacob et al., 2008) nor in the North-German Climate Atlas<sup>1</sup>, but the plausibility of the changes derived in evaporation has been discussed with the changes in temperature as well as precipitation. In the summer periods an increase of evaporation between 2.5% and 7.1% has been calculated (Table 6. 7). This increase is due to the increase in temperature as well as the increase of precipitation. The change of evaporation in the winter period is significantly higher with an increase of

<sup>1</sup> [www.norddeutscher-klimaatlas.de](http://www.norddeutscher-klimaatlas.de)

up to 11.8%. This is reasonable due to the larger increase of precipitation in the winter period of up to 22.6% (A1B Scenario).

**Table 6. 7 Relative changes per hydrological season in evaporation [%] (2040 – 2070) calculated for the Krückau catchment related to the period from 1971 to 2000.**

| <b>Changes in Evaporation (2040 – 2070)</b> | <b>Changes in Summer Periods</b> | <b>Changes in Winter Periods</b> | <b>Changes in Yearly Periods</b> |
|---|----------------------------------|----------------------------------|----------------------------------|
| <b>B1 Scenario</b>                          | + 2.8 to 4.4 %                   | + 4.0 to 5.5 %                   | + 2.2 to 2.6 %                   |
| <b>A1B Scenario</b>                         | + 3.0 to 5.1 %                   | + 7.6 to 11.8 %                  | + 3.2 to 4.8 %                   |
| <b>A2 Scenario</b>                          | + 4.2 to 7.1 %                   | + 7.5 to 11.6 %                  | + 4.1 to 6.3 %                   |

### *Changes in Extreme Daily Rainfall Events*

With the number of daily rainfall heights above defined threshold values, the changes derived in climate scenarios have been analysed. This approach is widely used in climate change studies (e.g. [Jacob et al., 2008](#); [Bischoff, 2007](#); North-German Climate Atlas). In this thesis the number of days with a precipitation height above 25mm (= 'wet days') have been analysed (5.3.2) like done in the UFOPLAN ([Jacob et al., 2008](#)). The comparability is restricted again due to the considered different climate periods. Additionally, the results in the UFOPLAN cover all federal states of Germany, whereas in this thesis only the small spatial distribution of the Krückau catchment has been considered. A large increase of 25 wet days has been computed for the A1B scenario in summer periods for the Krückau catchment. This is not displayed in the UFOPLAN report, where a slightly larger increase of wet days has been illustrated for the B1 scenario for the time period 2021 to 2050 (see Fig. 2.1). For the time period 2071 to 2100 the difference between the IPCC scenarios is not significant as well, but a slightly larger increase is computed for the A2-scenario ([Jacob et al., 2008](#)).

However, the scenario study results in this thesis are comparable with the outcomes of a dissertation worked out at the MPI-M, which has been finished in December 2009. In the dissertation, an investigation of regional climate change signals of means and extremes with precipitation distribution functions have been analysed by [Bülow \(2009\)](#). The results display as well larger changes in heavy precipitation in the scenario A1B than for the scenarios A2 and B1 ([Bülow, 2009](#)).

In the statistical evaluations of short term extreme rainfall events, larger increases have been calculated as well for the IPCC-Scenario A1B. Only some related studies can be referred here, which worked out comparable statistical evaluations for future climate scenarios. This is due to the larger uncertainties which are derived within extreme event investigations with current state of the art climate models ([Fowler & Ekström, 2009](#)). In this thesis, statistical evaluations have been worked out with partial series of hourly rainfall heights in [mm/h] with about 82 values for each

climate period: 1971 to 2000 and 2040 to 2070 and each scenario. Especially for summer rainfall events with high probabilities of occurrence, which means with return periods of once in a year ( $T=1a$ ), a significant increase has been calculated in the scenario A1B by about 63.5% in rainfall height [mm/h]. For summer rainfall events with a lower probability of occurrence ( $T = 100a$ ) an increase of the rainfall intensity of about 15.2% for the A1B scenario has been computed. The increase of hourly rainfall heights with specific return periods for winter periods in the A1B scenario ranges between 7.8% for events with  $T=1a$  and 5.6% for events with  $T=100a$ . The computed statistical evaluation results of both seasons together (yearly periods) display an increase of 49.9% for events with higher probabilities of occurrence ( $T=1a$ ) and an increase of 9.1% for events with lower return periods ( $T=100a$ ) in the A1B scenario. The statistical evaluation results of the scenario B1 display lower increases and in the A2 scenario even decreases of extreme rainfall intensities have been calculated for the future climate scenarios.

In a comparable climate change study of the Wandse catchment area in Hamburg, statistical evaluations have been worked out with yearly series of rainfall intensities with durations of 2 hours from 2001 till 2100 (Golder Associates, 2009). For this purpose, REMO model data series of the A1B scenario have been used. The data series for the statistical evaluations differ to the data series used in this thesis with regard on the considered rainfall duration (1hour; 2hours), the climate period (2040-2070; 2001-2100), the differentiation of seasons and the application of yearly instead of partial series. Due to the deviating data sources, only a rough comparative study is possible. The statistical results of the Wandse project illustrate larger increases of the extreme rainfall intensities of about 30% for events with a lower probability of occurrence ( $T=100a$ ) and lower increases of about 14% for extreme rainfall events with higher probability of occurrences ( $T<5a$ ).

Because of these differing results, the plausibility of the statistical evaluations of the changes in extreme rainfall, have been additionally discussed with the statistical evaluation results of the changes in flood probability in this thesis. Larger increases of the flood peaks have been computed for events with higher probabilities of occurrence ( $T < 5a$ ) than for flood peaks with lower probabilities of occurrence (e.g.  $T = 100a$ ). This tendency corresponds to the statistical evaluations of the extreme rainfall events and is therefore regarded as reasonable.

### **6.1.2 Discussion of Changes in Flood Probability**

Discussions of the flood probability results are done for the comparison of the simulation results using observed data series of the past (1971 to 2000), applying REMO control scenario data series of the past (1971 to 2000) and using future climate scenario data series (2040 – 2070).

### 6.1.2.1 Reference Scenario 0 Results [1971 – 2000]

The results of the statistical evaluations of the flood peak probability curves computed with observed data series (Scenario 0) in this thesis are discussed with the results of a previously worked out project by the cooperation of the EPK<sub>2</sub> Engineers GbR and the Engineers of Klütz & Collegen Itzehoe GmbH. The team of engineers has been named: *Planungsgemeinschaft Überschwemmungsgebiete an der Krückau*; in short: PÜK. The PÜK developed the hydrological model used in this thesis and worked out statistics for specific nodes (river stations) upstream of Elmshorn till the node A23 with yearly flood peak data series from 1969 to 2004. For the climate change scenario studies in this thesis, it was necessary to apply a different statistical evaluation approach with partial series for the climate period from 1971 to 2000 and with a differentiation of summer as well as winter periods of a hydrological year.

For the comparability, the flood peaks in the years 2000 till 2004 computed by the PÜK had to be transferred to the scenario 0 flood peak series worked out in this thesis. The comparison of the statistical evaluations has been done for the node A23<sup>1</sup>. The results of the Gumbel and Gamma distribution curves computed by the PÜK are illustrated in Fig. 6. 1 together with the Log-Normal Type III and Log-Pearson Type III Distribution curves calculated in this thesis.

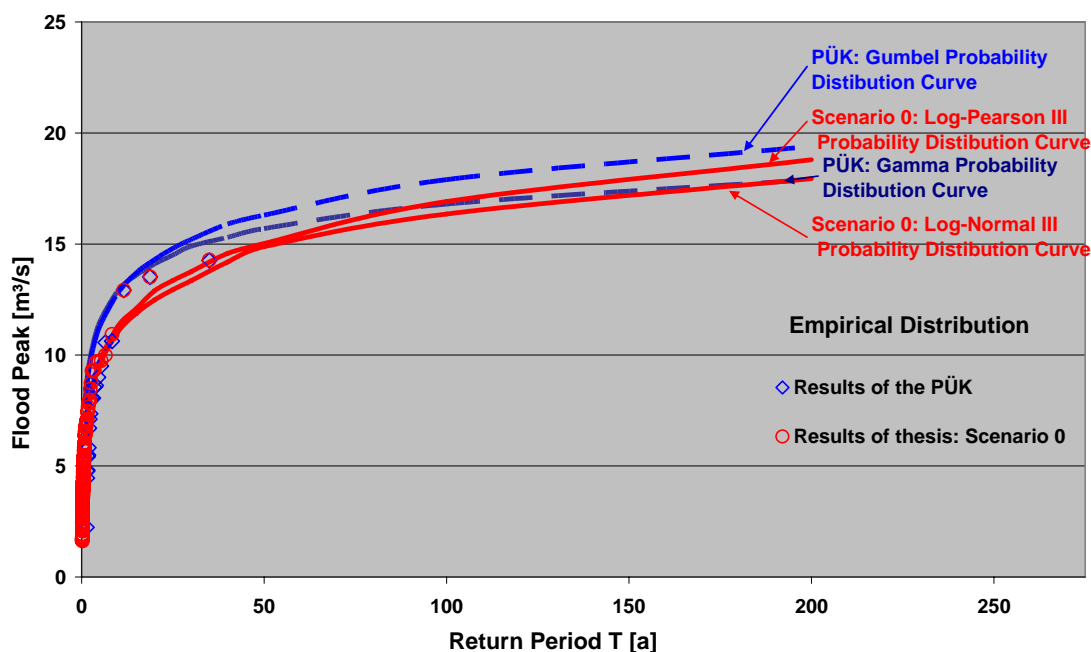


Fig. 6. 1 Comparison of the statistical evaluations of the PÜK and the computed Scenario 0 in this thesis

The differences between the statistical evaluations are about 7.5% for flood peaks with small return periods of once every 1 to 5 years and a higher difference of up to 17% has been calculated for events with return periods of once in 100 years. Because

<sup>1</sup> The location of this node is displayed in Figure 5.7

different probability distribution functions and partial instead of yearly series have been applied, the outcomes compared with the results of the PÜK are regarded as comparable and reasonable.

### *6.1.2.2 Climate Control Scenario Results [1971 – 2000]*

The differences in the flood probability simulations with observed data series (Scenario 0) and the REMO control scenario data series (Scenario C20) are discussed with the results of the study done for the catchment area of the Wandse in 2009. In this project the software Kalypso Hydrology has been applied for simulating a yearly series of flood peaks for three nodes in the catchment (Golder Associates, 2009). The computed average differences of the results range between 8% for events with small return periods of once in a year and increases up to 100% for events with return periods of once in 100years. This is comparable with the results in the scenario studies in this thesis for summer periods, where rather low differences for events with small return periods ( $T < 5a$ ) have been calculated of about 11% and the difference increases up to an average difference of 80% for a return period of the flood peaks of once in 100years (Attachment 14.3). For the yearly period differences are computed between 16% ( $T=1a$ ) and 30% ( $T=100a$ ) in this thesis. In both project studies, the differences between the flood peaks are significant for extreme flood events with lower probabilities of occurrence. The reason for these differences needs to be further discussed as stated in the outlook of this thesis.

### *6.1.2.3 Future Climate Scenario Results [2040 - 2070]*

For the discussion of the computed changing rate of flood probability curves derived in future climate scenarios, the results of the project INKLIM 2012 II plus (Brahmer, 2008) and the results of the local study of the Wandse catchment are referred.

In the INKLIM 2012 II plus project the increase of flood peaks in the Lahn catchment area derived with the IPCC scenarios A1B, B1 and A2 has been analysed. The applied climate data series have been computed with the statistical RCM WETTREG<sup>1</sup>. For the simulation of stream flow for the past (1961 to 1990) and the future (2051 to 2080) climate periods, the hydrological model LARSIM<sup>2</sup> has been applied (Brahmer, 2008). Like in the scenario studies of this thesis, the largest changes have been computed for the Scenario A1B with an increase of about 20% for extreme flood peaks with return periods of once in 100years (Brahmer, 2008). In this thesis, an increase of 27% has been computed for summer flood peaks in the scenario A1B in the Krückau catchment. However, it has been pointed out that there is a low confidence in computing changes in flood probability, which can vary significantly between scenarios and study locations (Brahmer, 2008).

---

<sup>1</sup> Features of the RCM WETTREG are listed in Attachment 1.2.

<sup>2</sup> LARSIM = <http://larsim.sourceforge.net/>.

In the Wandse project, REMO data series for the IPCC scenario A1B have been applied for different climate periods from 2001 to 2100, from 2051 to 2100, from 2076 to 2100 and yearly series of flood peaks have been computed with the software Kalypso Hydrology. The results in this thesis approximate the statistical evaluation results of the Wandse project for the climate period from 2076 to 2100. For three nodes in the Wandse catchment, average increases of about 28% are illustrated for events with higher probabilities of occurrence of once in a year (T=1a) and for events with lower probabilities of occurrence (T=100a) an average change of about 11.9% has been displayed (Golder Associates, 2009). In this thesis, for events with higher probabilities of occurrence (T=1a) an increase of maximal 27.4% and for events with lower probabilities of occurrence (T=100a) an increase of about 11.8% has been calculated. The results in the Wandse report for the other climate periods from 2001 to 2100 and from 2051 to 2100, display lower changes in flood peak probabilities.

In comparison with the increase of the rainfall intensities, it can be stated that in the A1B scenario the summer flood peaks increase with a higher percentage rate than the summer rainfall intensities. The yearly flood peaks with a larger probability of occurrence (T = 5a) increases less than the corresponding rainfall events, whereas for events with lower probabilities of occurrence it is the other way around. The rainfall intensities in the winter period increase only by about 5.7% to 7.8%, but the flood peaks in the winter period increases between 11.8% and 27.4%. It can be stated that the overall tendency of increase corresponds between the extreme rainfall and flood events, but the rate and magnitude of increase differs in the A1B scenario, which displayed the largest changes and is regarded as most important for the following discussion of the post-processing results.

### 6.1.3 Discussion of Post-Processing Results

For calculating the magnitude of the projected climate change impacts of extreme rainfall and flood peaks, two approaches have been developed, namely the percentage change and the absolute change approach (3.5.1). In this thesis, the percentage change approach has been identified to be the appropriate one to be used, to take account of relative magnitudes of biases for the climate model data results of the different climate periods.

For the application of the computed impacts on design rainfall and flood events with specific return periods, it is recommended to calculate climate change factors (CCFs). In this thesis, the CCFs are computed with the developed *Averaging Ensemble CCF* method (3.5.2). This approach is discussed with the results by applying another calculation method, where the projected change in runoff per km<sup>2</sup> of the catchment is calculated with the flood peak probability changes in future climate scenarios. This has been applied in the Wandse project (Golder Associates, 2009) and is indicated here as *Delta Runoff Rate CCF*. With the computed flood

probability results of the projected climate change Scenario 0-A1B, the Averaging Ensemble CCF and the Delta Runoff Rate CCF for the Krückkau catchment have been computed with the equations summarized in Attachment 19. The equations for calculating the Delta Runoff Rate CCF have been developed by recalculating the published results in the Wandse project report (Golder Associates, 2009). With the resulting CCFs, control calculations have been done by computing the projected climate change design floods with specific return periods ( $HQ_{C,T}$ ) on the basis of the current design floods ( $HQ_T$ ) for the specific locations of interest in the catchment. The results for flood events with a return period of once in 5 years are illustrated in attachment 19 and the results for 100year flood events are displayed in Fig. 6. 2.

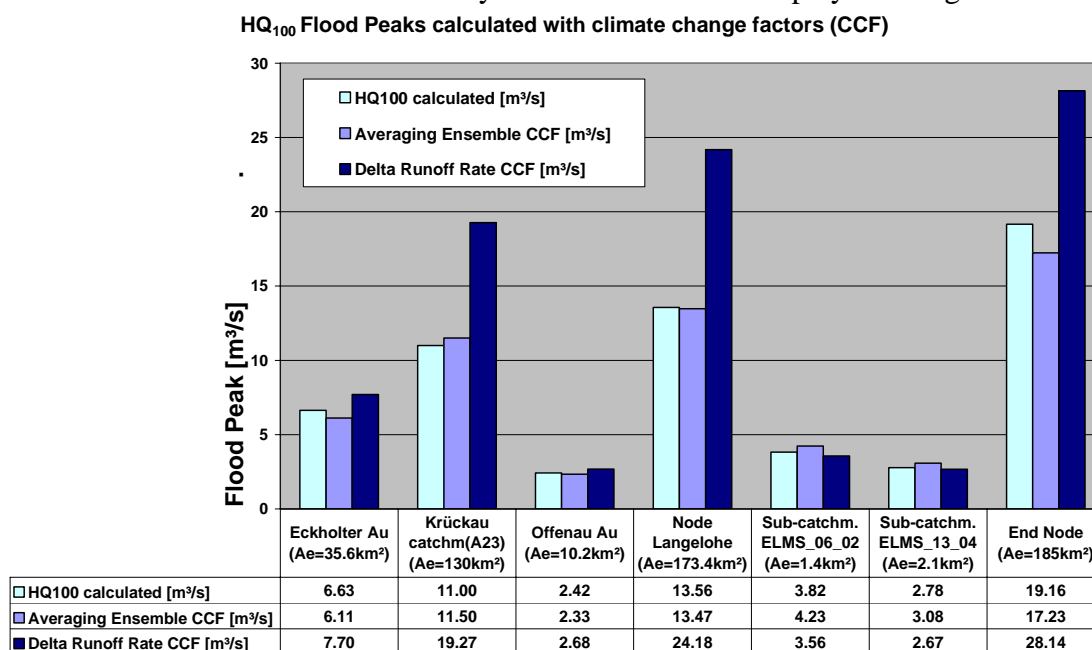


**Fig. 6. 2 Comparison of the approaches to calculate climate change factors (CCFs)**

With the Averaging Ensemble CCF, minor differences are calculated for all nodes referred to the simulated results of the Scenario 0-A1B. Therefore, the method is considered as appropriate.

With the Delta Runoff Rate CCF, minor differences of flood peaks are as well calculated for the nodes draining smaller catchments, but significant differences are computed for nodes draining larger catchments. In this method, the changes of runoff rates are derived with the flood peak changes and in the dependency on the catchment area in km<sup>2</sup>. In the scenario studies, the flood probability calculations have been done for catchments with rather different sizes, ranging from 1.4km<sup>2</sup> to the whole catchment size of 185km<sup>2</sup> (see Fig. 6. 2) and with different land use types. In this case, it is not reasonable to relate the average change in runoff directly to the change in the peak flow at specific nodes draining specific areas of the catchment. This leads to an overestimation of the flood peaks at nodes draining larger

catchments. Therefore, the Delta Runoff Rate CCF method is considered to be less appropriate for computing overall CCFs of catchments.

#### **6.1.4 Discussion of SUDS Adaptation Scenario Results**

The developed SUDS simulation software tool for green roofs in this thesis has been tested together with the software tools for simulating swales and swale-filter-drain systems. The testing results of the SUDS display a difference in the water balance calculations of 0.1% to 0.01%. This is considered as acceptable in the scope of this thesis, but could be further optimised. The hydrological processes in the SUDS elements have been discussed with graphical illustrations and demonstrated a good correspondence of all outflow and inflow processes in each SUDS element.

The effectiveness of SUDS as flood probability reduction measures has been successfully simulated with the new developed software tool. Especially the combination of SUDS with green roofs draining into swales or swale-filter-drain systems plus unsealing displayed a large effectiveness. In this adaptation scenario, the sealed urban areas drained by storm water sewer systems have been reduced by about 80%. For discussing these results, a scenario has been created under climate change conditions of the post-processed scenario 0-A1B, whereas the whole Krückau catchment has been changed to green fields and forests. In this way, the maximal achievable reduction of the flood probability by SUDS under climate change conditions could be displayed and compared with the results of SUDS adaptation scenarios. In this context, it could be demonstrated that the large effectiveness of the combination of SUDS, reach the natural state scenario results by about 90% at the End Node, by about 70% at the node Langelohe and by about 68% at the urban sub-catchments in Elmshorn for events with shorter return periods of once in a year. The effectiveness of the SUDS measures decreases in extremer events, which is reasonable due to the restricted storage capacity and the generation of overflow.

With these results, it can be stated that the new software tool for modelling SUDSs provide appropriate and detailed simulations of hydrological processes in each element, but as well the overall simulation of SUDS on a catchment level is enabled.

## **6.2 Uncertainty Analysis in Climate Change Impact Studies**

In the comparative studies, a range of differences have been defined which are considered as appropriate and reasonable in current state of the art climate change scenario analyses. These differences are derived due to different sources of uncertainties, which are outlined in 3.6 and have to be taken into account for any climate change studies.

For hydrological impact studies it is not only important to analyse which sources of uncertainties have to be taken into account, but to assess the magnitude of the uncertainty. Only in a few research studies, an assessment of the magnitude of uncertainties in climate model projections have been done up to now (e.g. Déqué et al., 2007; Goetzinger, 2007; BALTEX). The computation of specific uncertainty ranges for the scenario study results of the Krückau catchment could not be done due to the restricted variety of scenarios and work load in this thesis. But the results of two studies about climate as well as hydrological modelling are outlined to give an assumption of the uncertainty range in the model chain.

In the study, published by Déqué et al. (2007), the sources of uncertainties derived with Emission Scenarios [1], Boundary Uncertainties (GCM) [2], RCM model inaccuracies [3] and internal model variability [4] are evaluated with the data results of the PRUDENCE project. The aim of the study by Déqué et al. (2007) has been, to assess the uncertainties in model projections of temperature and precipitation by using as many model runs as possible of all European sub-regions which are defined according to Christensen et al. (2007): British Islands, Iberian Peninsula, France, Middle Europe, Scandinavia, Alps, Mediterranean and Eastern Europe. The eight sub-regions are defined according to the assumption, that the climate in each zone is relatively homogeneous (Déqué et al., 2007). The studied climate model combinations comprise:

- Two IPCC scenarios (A2 and B2),
- The output of three GCMs for the creation of boundary conditions,
- The data series of ten RCMs,
- Three runs of each model combination over 30 year climate periods,
- One control scenario run for each combination (1961 – 1990).

From all model combinations a set of 25 future scenario combination runs for the climate period from 2071 to 2100 and 18 control scenario runs from 1961 to 1990 were taken for the uncertainty analysis by Déqué et al. (2007). For precipitation data series, the results of the variance in percentage derived by the four uncertainty sources are given for middle Europe (Germany and the Netherlands) in Table 6. 8. A differentiation is done for the winter period: December, January, February (DJF) and the summer period: June, July and August (JJA).

**Table 6. 8 Total variance of precipitation in [%] derived by four sources of uncertainty (adopted from Déqué et al., 2007).**

| Sub-region: middle Europe<br>(Germany and the Netherlands) | Emissions<br>Scenario [%] | GCM<br>[%] | RCM<br>[%] | Model Variability [%] |
|--|---------------------------|------------|------------|-----------------------|
| Winter seasons (DJF)                                       | 12%                       | 65%        | 31%        | 8%                    |
| Summer seasons (JJA)                                       | 36%                       | 50%        | 27%        | 5%                    |

The uncertainty derived by the choice of the GCM (Boundary Uncertainty) is largest out of the four sources. The most climate variables depend on the general lateral circulations, which are strongly influenced by the boundary conditions (Déqué et al., 2007). Especially the German and Dutch coastal line is under oceanic influence, where changes in the general circulation introduced by the GCMs produce regional climate changes. The uncertainty due to the selected emissions scenario is lower than the uncertainties derived by the GCMs or RCMs. The uncertainty due to the internal model variability is projected to be lowest (<10%). Déqué et al. (2007) concluded that the number of used GCMs should be at least as high as the number of applied RCMs for uncertainty analysis. Using several models reveals on the one hand the magnitude of uncertainty and on the other hand the uncertainty could be reduced as well, by taking into account the range of results.

Little quantitative knowledge is available up to now about the source of uncertainty derived by hydrological models in climate change impact studies (Ludwig et al., 2009). An approach to study this source of uncertainty has been done by Ludwig et al. (2009) with the application of three hydrological models: PROMET<sup>1</sup>, Hydrotel<sup>2</sup> and HSAMI<sup>3</sup>. The applied hydrological models are based on different complexity and structures. The Ammer catchment (709 km<sup>2</sup>) in the Bavarian alpine forelands has been used as study area. The computed climate data series of the climate models CGCM<sup>4</sup> and the CRCM<sup>5</sup> have been taken to simulate climate change projections for the IPCC scenario A2. Therewith, control scenario model runs (1971 – 2000) and future scenario model runs (2071 – 2100) have been done with all three hydrological models.

It was demonstrated in a validation of the mean annual discharge [m<sup>3</sup>/s] over a 30 year period by Ludwig et al. (2009) that all three hydrological models perform well when driven by the same observed data series supplied by the German Weather

<sup>1</sup> PROMET = Processes of Radiation, Mass and Energy Transfer; a spatial raster-based distributed hydrological model; developed and tested by Ludwig Maximillians University Munich (Ludwig et al., 2009).

<sup>2</sup> HYDROTEL: Semi-distributed model on small sub-catchments; developed by the Institute National de la Recherche Scientifique in Quebec City. (Ludwig et al., 2009).

<sup>3</sup> HSAMI: Lumped bucket-type conceptual model with low physical complexity; developed by the Institute Hydro Quebec (Ludwig et al., 2009).

<sup>4</sup> CGCM = Canadian Global Climate Model.

<sup>5</sup> CRCM = Canadian Regional Climate Model.

Service (DWD). But differences are pointed out by analyzing the magnitude of discharge for specific flood probabilities and especially for the future climate scenario A2. In Fig. 6. 3 are the discharges with a return period of once in 2, 5 and 10 years illustrated, which have been derived by using the regional climate model data of the past: 1971 – 2000 (solid bars) and the future climate scenario A2: 2071 – 2100 (striped bars). A differentiation between the summer and winter events has not been done.

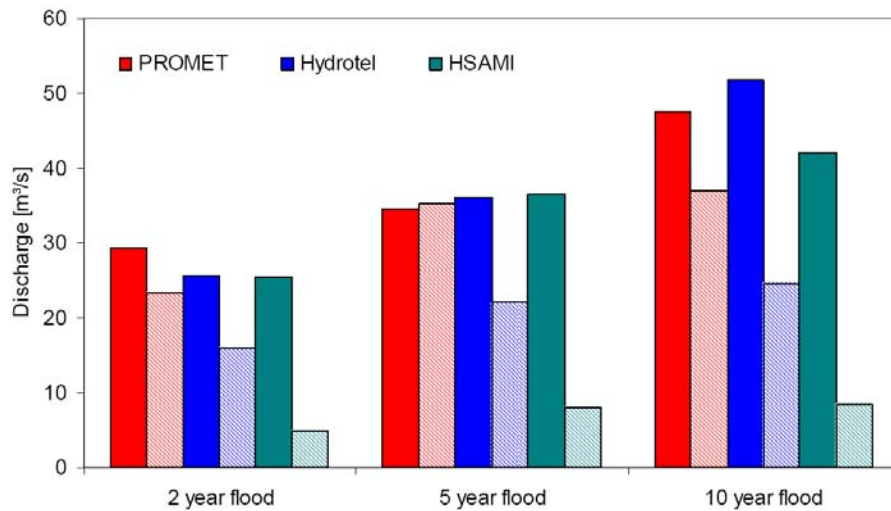


**Fig. 6. 3 Comparison of flood peak probabilities simulated with three hydrological models using the climate data series of the CGCM2 (past [1971-2000] = solid bars; future A2 [2071-2100] = striped bars) (adopted from Ludwig et al., 2009)**

It has been stated that the hydrological models with lower physical complexity (HSAMI) and the models which are calibrated for current climate conditions (HSAMI and Hydrotel) are less adequate for climate change studies, but this considered as arguable in this thesis. This points out the requirement for further studies about the quantification of uncertainties derived by hydrological models in climate change studies.

## **7. Conclusion and Outlook**

In this thesis, a methodology has been developed to study climate change impacts on the flood probability in Small Urban Catchments (SUCAs). For this purpose, a systematic procedure has been worked out with state of the art as well as a number of new developed approaches and data series with a high spatial as well as temporal resolution have been required. The calculated future climate scenario results of flood probabilities in SUCAs have to be considered in a range of uncertainty. Therefore, flexible and ‘no-regret’ solutions are required to compensate impacts on flood probability in the future. In this context, Sustainable Drainage Systems (SUDS) have been identified as appropriate measures.

The effective and successful application of the methodology has been demonstrated for climate change scenario studies in a river catchment, which is situated in the KLIMZUG-Nord project region.

### **7.1 Conclusion**

The main steps of the work flow in the developed methodology are illustrated in Fig. 7. 1 to quantify the hydrological impacts by climate change on the flood probability in SUCAs and the subsequent simulation of adaptation measure scenarios with SUDS. Features to optimize the work flow and the application of the implemented new SUDS simulation tool are indicated additionally.

In the *pre-processing*, criteria for selecting climate model and scenario data series have been defined, which could assist further projects to create a basis for comparability. The file formats provided by a variety of climate models differ significantly. Therefore, tools are provided to transfer climate model data files (e.g. NetCDF, ASCII, IEG files) into usable formats for impact studies, but the handling of the tools as well as the required further data processing is left to the climate model data user. For the transformation of the often used NetCDF format, the procedure is described in the developed methodology and a Java tool has been created at the Institute of River and Coastal Engineering in Hamburg for further applications. The computation of additional variables of climate model data series has been depicted in this thesis with the calculation of potential evaporation data series on the basis of available data series of the climate models REMO and CLM. Calculating such additional data series depends on the required input data series for the applied hydrological model.

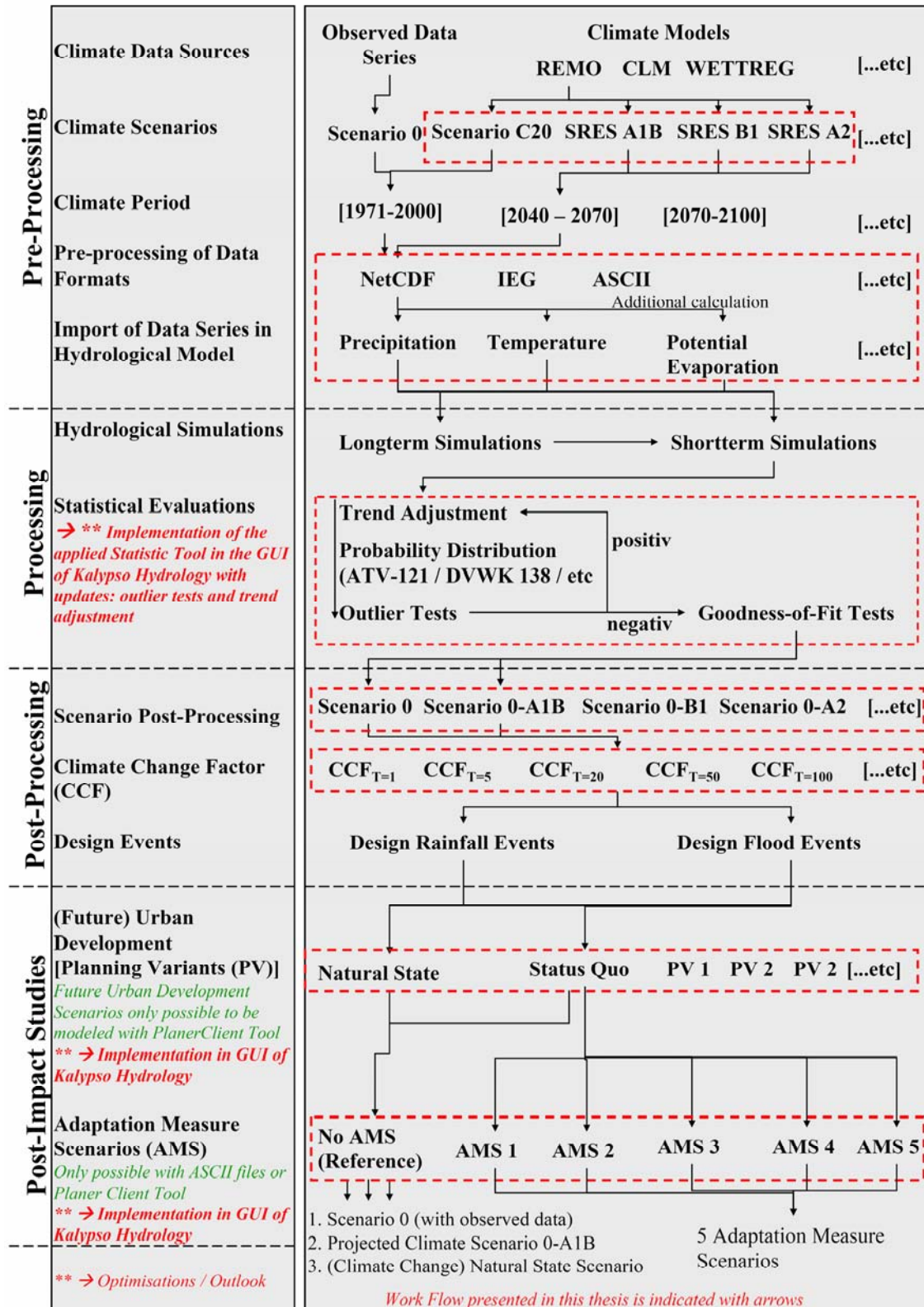


Fig. 7. 1 Illustration of the work flow to quantify climate change impacts on the flood probability in SUCAs and simulating adaptation measure scenarios (SUDS-Scenarios); with notes for optimisation and outlook.

It has been defined as an open question, if the spatial resolution of the currently available climate model data is adequate for the complex flood probability studies in SUCAs. It has been illustrated in the application scenario studies, that the spatial resolution of about 11km x 6.5km provided by the climate model REMO in the datastream D3 interpolated on a regular grid, is appropriate for the scenario studies in the Krückau catchment, which is characterised by rural areas. The displayed spatial resolution is finer as provided by the observed climate data series of gauging stations ( $\approx 30\text{km} \times 30\text{km}$ ), used for the calibration of the hydrological model. But the applicability can not be generalised for other study areas. In mountainous or dense urban catchments a finer spatial resolution could be required and has to be analysed further on.

The restricted temporal resolution of data series provided by climate models has been analysed in comparative studies. The results of flood hydrographs with hourly and 15-minute simulation time steps have been compared for a rural, an urban and a discharge node in the urban area of Elmshorn. The differences between these two simulations are significant for the urban sub-catchments and therefore smaller timesteps than hourly data series are required for flood probability simulations in SUCAs.

Climate data series describe the statistical sums and averages of weather phenomena. Therefore, climate data series neither of the past nor of the future can be analysed according to a specific event or short term trend. Therefore, strategies have been outlined for the *processing* of the data series, to analyse the overall changes of the climate variables and derived impacts in a whole climate period. The most important results for flood probability analyses are gained by statistical evaluations, which are less often applied in climate change studies up to now and only some related studies can be referred here. In this thesis, for each of the five scenarios (0, C20, A1B, B1 and A2) and seasonal differentiation (summer, winter and yearly) statistical evaluations have been computed. In this way, fifteen statistical evaluations have been worked out with the results of overall 750 short term flood peak simulations after respective long term simulations. In the developed methodology, a calculation loop for statistical evaluations has been introduced. This loop starts with the trend adjustment of data series over the climate period for a reference year and the results are used for the calculation of probability distribution curves. If outliers are detected in the distribution curves, which are not appropriately represented and distort the statistical evaluation results, these outliers have to be handled separately and the loop has to be repeated with the trend adjustment till the outlier test is negative. Additionally, the representativeness of the probability distribution curve is controlled with goodness-of-fit tests as the last step.

With the results of the statistical evaluations, another open question has been discussed, namely if the IPCC scenario representing the largest increase in CO<sub>2</sub> emissions and which projects the highest temperature changes, also leads to a larger increase of the probability of extreme rainfall events as well as flood events. In the studies of this thesis, the largest changes in flood probability compared to the reference year 2000, are displayed by the A1B scenario, which is by definition a medium emissions scenario (see 3.2). Therewith, shifts in the probability of design events in the Krückau catchment area has been computed; e.g. an actual summer flood peak of 11m<sup>3</sup>/s with a return period of once in 100years (HQ<sub>100</sub>) at the node Langeloh in Elmshorn changes due to the projected effects in the A1B scenario to a flood event with a return period of once in 20years (HQ<sub>20,C</sub>). Extreme summer rainfall events with a current probability of occurrence of once in 100years (T=100a) and an intensity of 24.6mm/h, are calculated to be shifted to an event with a return period of once in 30years (T = 30a). The highest emissions scenario analysed in the application studies, is the A2 scenario which displayed lower changes in flood probability and extreme rainfall for the climate period from 2040 to 2070. These outcomes of the statistical evaluations have been discussed in chapter 6 with results of the INKLIM 2012 II Plus project, where the largest changes in flood probability have been defined as well for the A1B scenario with comparable results.

Furthermore, it has been stated as questionable, if interdependencies between the average changes in climate scenarios and the changes in extreme events can be detected. It has been found out that the correlation between average climate changes published in research studies can not be taken as a basis to provide a statement about the changes of extreme rainfall or flood probabilities in a local study area. Statistical evaluations or the number of occurrence of events above a defined threshold value have to be quantified for this purpose. Additionally, it can not be stated that extreme flood events change in a corresponding way like extreme rainfall events in climate change scenarios with specific return periods as discussed in this thesis, where only a corresponding tendency of increase could be identified. Overall, larger increases of flood and extreme rainfall events in the summer periods are calculated than in the winter periods. In the scenarios A2 and B1 even a decrease of extreme events is computed for the winter periods, although the average winter precipitation is calculated to be increased significantly.

The differences in the results of using computed control scenario data series in comparison to the results using observed data series are significant. Therefore in the outlined *post-processing* methodology, two approaches are derived, namely the ‘percentage change approach’ and the ‘absolute change approach’, to handle the differences and to calculate the magnitude of climate change impacts. For the applicability of the climate change scenario study results in practice, climate change

factors (CCFs) are calculated. These factors are applied to obtain the respective design rainfall or flood peak event with a specific return period under climate change conditions for further locations in the study areas. The developed *Averaging Ensemble CCF* method has been proved to be more applicable, compared to another approach (namely the '*Delta Runoff Rate CCF*') discussed in (6.1.3).

The results of the post-processing are further used in *post-impact studies*, like done in this thesis for the assessment of the effectiveness of flood risk mitigation measures in SUCAs. In this context, Sustainable Drainage Systems (SUDSs) have been identified as appropriate flexible and no-regret strategies, which can be adapted to uncertain future impacts derived by climate change and urban developments. The focus has been set on green roofs combined with swales, swale-filter-drain systems and unsealing. For this purpose, a new software tool has been implemented to simulate the effectiveness of green roofs (chapter 4). It is based on a catchment level approach and enables the simulation of the complex hydrological vertical (e.g. infiltration, percolation, evaporation) as well as horizontal (e.g. flow trough drainage layer) and the storage processes of water in each layer of the SUDS element. In this way, a detailed and comprehensive simulation of SUDSs is facilitated. The functions and calculations in the developed sub-routines, written in the FORTRAN programming language, have been described with Nassi-Shneiderman diagrams to provide a detailed documentation for further studies and software updates. The software tool has been implemented in the development of the Decision Support Tool Kalypso Planer Client, which was supported by the Agency for Roads, Bridges and Waters in Hamburg (LSBG). Additionally, an add-on tool had to be worked out, to assist the simulation of SUDS with a separate Kalypso Hydrology model. The simulations are restricted to be done with ASCII files and the executable of the core up to now. Testings of the developed SUDS simulation software tool for green roofs have been performed in combination with testing the software tools of swales and swale-filter-drain systems and if required, these tools have been revised in the scope of this thesis. The results of the SUDS simulations display acceptable differences in the water balance calculations of 0.1% to 0.01%. Additionally, a discussion of the effectiveness of SUDS compared to the results of a natural state scenario has been done. Therewith, it can be stated that not just the simulation of the hydrological processes of each SUDS element is adequately enabled, but that the assessment of the effectiveness of SUDS on a catchment level is appropriately and successful facilitated.

In the SUDS application scenarios (5.6) it has been found out that SUDS display larger effectiveness for flood probability mitigation as closer as the measures are located to the urban areas of interest. In the sub-catchments with the hot spots of the "Badewanne" and the Steindammwiesen Park in Elmshorn, the projected flood peak probabilities are even reduced below the current reference situation (Scenario

0). But this high effectiveness of SUDS can only be reached in dense urban areas and for events with higher probabilities of occurrence. By rainfall and flood events with lower return periods of e.g. once in 30years or 50years, the effectiveness of the SUDS technique is reduced due to the generation of overflow from the limited storage capacity of SUDS.

Finally, the implemented combination of SUDS comprising green roofs, swales, swale-filter-drain systems and unsealing of surfaces, illustrated high potential to mitigate and even compensate climate change impacts on the flood probability in the Krückau catchment.

## **7.2 Outlook**

For optimising the work flow of the developed methodology to quantify the impacts of climate change on flood probabilities, it is required to upgrade and implement the indicated issues in Fig. 7. 1. The expertise gained in this thesis could be used to improve and enhance the applied external Java statistic tool, to implement it in the user interface of Kalypso Hydrology. In the work flow, the required expenditure of time could be reduced considerably in this way for future projects.

Secondly, the simulation of future urban developments or planning variants is not possible currently with the Kalypso Hydrology software application, but with the Planer Client tool. Implementing the features as well in the Kalypso Hydrology tool could improve significantly the modelling applicability. Likewise, the availability to simulate SUDS not only with the complex ASCII files of an existing hydrological model, but with the user interface of Kalypso Hydrology, is an important step to be realised (Fig. 7. 1).

It has been concluded in this thesis that the spatial resolution of climate model data series has been appropriate for studies in the mostly rural Krückau catchment, but this can not be generalized for more urbanised catchments like in the city of Hamburg. A study about using further downscaled data series provided by the mesoscale climate model METRAS, is planned in the scope of the KLIMZUG-Nord project for a dense urban area.

The computed differences in the control scenario data series of the climate model and the observed data series are significant. This has been calculated in this thesis, but as well in other climate change research studies (CLAVIER; Bischoff, 2007; Jacob et al., 2008; Golder Associates, 2009). There is a need for applying correction measures on the computed climate data series, which has to be studied in more detail. It is appreciated to enhance the variety of scenario studies, which had to be restricted in this thesis, where only the projections of three IPCC scenarios could be compared. This has to be continued by e.g. applying scenario A1B data series computed by

different climate models and with respective different realisations. Additionally, the studies of uncertainties could be broadened by using as well a variety of hydrological models as discussed in chapter 6.

It is essential that the uncertainties are communicated to the public in an appropriate, reasonable and comprehensible way. The results of future climate scenarios had to be regarded as plausible ways in which the future *could* unfold without causing panic on the one hand, but in turn, being prepared as well for even more extreme impacts.

In this context, planners can not wait for more advanced models and till all uncertainties have been discussed in detail. Many decisions about implementing adaptation measures have to be taken now. For example, flood prevention measures, which involve developments in major infrastructure, require long term planning. Additionally, this planning is influenced by other factors like future urban developments. Decisions of such adaptation measures have to be tackled shortly and the simulation of future urban developments is important here as well.

With regard to the ranges of uncertainty, it is worthwhile to look on the main model consensus, qualitative agreement and general tendencies. A foundation of knowledge for taking action, capacity to learn from experiences and effective response as well as adaptation to change in a timely manner is needed (EEA, 2008). Therefore it is urgent that more studies about climate change impacts and adaptation measures are done.

A focus has been set in this thesis on the study of changes in flood probabilities derived by climate change impacts in SUCAs, but it could not be analysed, how the flood volume, the inundated area and the flood consequences are influenced in the scenario studies to compute the change in flood risk. Therefore, further studies about the change in flood risk and flood hazard for the residents, due to the change in flood probability are an important task for further studies. Concerning this matter, it is also important to correlate the changes in flood risk to monetary and economical aspects, which provides another basis to discuss the realisation of adaptation measures like SUDS techniques.

In this thesis, the simulation of SUDS with the new developed software tool has been tested on the basis of physical and mathematical calculations. Testing the simulation results further on with practical models in the field is important to validate and calibrate the simulations with the software tool.

When implemented in larger urban areas, SUDS could have as well an effect on the microclimate, which in turn could have an impact on the generation of more evaporation, the reduction of the formation of heat islands but as well on the initiation of intensive rainfall. Studies about these issues are planned in the scope of the KLIMZUG-Nord project in cooperation between the Institute of River and

Coastal Engineering at the TUHH and the Centre for Marine and Atmospheric Sciences (ZMAW) in Hamburg. The results of the Model Kalypso Hydrology with the simulation of adaptation measures and the results of the mesoscale climate model METRAS are intended to be used to study the effects of climate change and adaptation measures (e.g. SUDS) in combination. It has been stated by [Hoffmann \(2009\)](#) that especially highly dense urban areas like Hamburg could have an effect on the initiation of heavy rainfall. Thus, it appears that the Wandse catchment in Hamburg is selected as an appropriate area for further studies in the scope of the KLIMZUG-Nord project.

An additional important contribution of SUDSs is the enhanced infiltration of rainfall water into the ground which increases the ground water recharge rate and low flow conditions. This could be an important issue for future agricultural land use.

Further on, SUDS measures provide potential for purification of rainfall water combined with a reduction of the runoff velocity in urban areas. In this way, the pollution load of surface runoff could be reduced before entering storm water drainage systems. The reduction of the pollution load has not been studied in this thesis, but is another important issue. Additionally, climate change has an impact on insects, small animals and vegetation, whereas SUDS could display potential new habitats in urban areas.

As shown in the climate change scenario studies in this thesis, SUDSs are appropriate measures for flood risk mitigation under climate change conditions in SUCAs and are applicable for a variety of further forward-looking climate change impact studies.

## **8 Bibliography**

- ASCE (1996): American Society of Civil Engineers (ASCE); *Hydrology Handbook – second edition*; ASCE Manual and Reports on Engineering Practice 28, New York, 1996.
- ATV-A 121, 1985; Abwassertechnische Vereinigung e.V. (ATV); *Merkblatt ATV-A 121 - Starkregenauswertung nach Wiederkehrzeit und Dauer*; Regelwerk; Köllendruck & Verlag GmbH, Bonn, 1985.
- ATV-DVWK-A 117 (2001): Deutsche Vereinigung für Wasserwirtschaft, Abwasser und Abfall e.V. (DVWK); *Merkblatt-DVWK-A 117 - Bemessung von Regenrückhalte-räumen*; ATV-DVWK-Regelwerk, Hennef, 2001.
- ATV-DVWK-M 153 (2000): Deutsche Vereinigung für Wasserwirtschaft, Abwasser und Abfall e.V.; *Merkblatt ATV-DVWK-M 153 - Handlungsempfehlungen zum Umgang mit Regenwasser*; ATV-DVWK-Regelwerk, Hennef, 2000.
- BACC (2008): BALTEX Assessment of Climate Change for the Baltic Sea Basin (BACC) Author Team; *Assessment of Climate Change for the Baltic Sea Basin*; Series Editors: H.-J. Bolle, M. Menenti, I. Rasool, [e-book] Springer Verlag, Berlin Heidelberg, 2008.
- Bader et al. (2008): Bader, D.C., Covey, C., Gutowski, W.J., Held, I.M., Kunkel, K.E., Miller, R.L, Tokmakian, R.T., Zhang, M.H.; *Climate Models: An Assessment of Strengths and Limitations - A Report by the U.S. Climate Change Science Program.3.1*; [e-book] chapter 7, U.S. Department of Energy, Washington, DC, USA (2008). [accessed online, January 2010]  
<http://www.climatescience.gov/Library/sap/sap3-1/final-report/sap3-1-final-ch7.pdf>
- BBODSCHG (1998); Bundes-Bodenschutzgesetz (BBODSCHG); *Gesetz zum Schutz vor schädlichen Bodenveränderungen und zur Sanierung von Altlasten*; Homepage von Beratung Forschung Management Umwelt (bfm umwelt). [accessed online, 4 June 2009] <http://www.bundes-bodenschutzgesetz.de/>
- Bischoff (2007): Bischoff, G.; *Characterisierung und Validierung von simulierten Niederschlagsdaten des Klimamodells REMO unter Hinzuziehung von Niederschlagsaufzeichnungen der Hamburger Stadtentwässerung*; Diploma Thesis; Hafen City University Hamburg, Department of Civil Engineering, July 2007.
- Blyth (2009): Blyth, E.; *Process that impact runoff generation in Northern Latitudes*; WATCH Technical Report No. 16, WATCH, 2009. [accessed online 25 May 2009]  
<http://nora.nerc.ac.uk/6318/1/BlythN006318CR.pdf>
- BMVBS (2007): Federal Ministry of Transport, Building and Urban Affairs (BMVBS); *Navigation and Waterways in Germany – Meeting the Challenges of Climate Change (A Review)*; Federal Ministry of Transport, Building and Urban Affairs, Directorate-General Waterways and Shipping, printed by BMVBS, Bonn, 2007.
- Brahmer (2008): Brahmer, G.; *Untersuchung der Auswirkungen des Klimawandels auf Hochwasserscheitelabflüsse und Abflussverhalten im Lahnggebiet und im hessischen Mainingebiet*; project report: INKLIM 2012 II plus; Hessian Agency for Environment and Geology, Wiesbaden, 2008. [accessed online, December 2009]  
[http://www.hlug.de/klimawandel/inklim\\_plus/dokumente/berichte/abfluss.pdf](http://www.hlug.de/klimawandel/inklim_plus/dokumente/berichte/abfluss.pdf)
-

---

## Bibliography

---

- Brooks et al. (2003): Brooks, K.N., Ffolliott P.F., Gregersen H.M. DeBano L.F.; *Hydrology and the Management of Watersheds*; third edition; Blackwill Publishing Professional, Iowa State Press, Iowa, 2003.
- Brüning et al. (2009): Brüning, C., Pasche, E., Hellmers, S., Manojlovic, N., Behzadnia, N.; *Modelling the Flood Attenuation of combined SUDS in Urban Areas*; conference Paper, COST22, Paris, November 2009.
- Brüning & Hellmers (2009): Brüning, C., Hellmers, S.; *Entwicklung des Entscheidungshilfesystems KALYPSO-Planer-Client auf Basis des Feinkonzeptes. Teil 1: Theoretischer Hintergrund der Simulation von SUDS im Fortran-Rechenkern*; [unpublished draft] Hamburg, Dezember 2009.
- Bruntland (1987): Bruntland, G.; *Our common future: The World Commission on Environment and Development*; chapter 2; Oxford University Press, Oxford, 1987. [accessed online, September 2009] <http://www.un-documents.net/ocf-02.htm#I>
- Bülow (2009): Bülow, K. (in press); *Zeitreihenanalyse von regionalen Temperatur- und Niederschlagssimulation in Deutschland*; Ph.D. Max-Planck-Institute for Meteorology, Hamburg.
- BWK (1999): Bund der Ingenieure für Wasserwirtschaft, Abfallwirtschaft und Kulturbau (BWK) e.V.; *Hydraulische Berechnung naturnaher Fließgewässer - Teil 1: Stationäre Berechnung der Wasserspiegellinie unter besonderer Berücksichtigung von Bewuchs und Bauwerkseinflüssen*; Merkblatt 1; Bund der Ingenieure für Wasserwirtschaft, Abfallwirtschaft und Kulturbau (BWK) e.V., Düsseldorf, 1999.
- Christensen et al. (2007): Christensen, J.H., Christensen, O.B.; *A summary of the PRUDENCE model projections of changes in European climate by the end of this century*; Journal Climate Change, Volume 81; pages. 7 – 30, Springer Netherlands, 2007. [accessed online, June 2009] <http://www.springerlink.com/content/ex762443118rgvp3/>
- CLAVIER Final Report published online: <http://www.clavier-eu.org/>; *Climate Change and Variability: Impact on Central and Eastern Europe (CLAVIER)* [accessed online, November 2009]  
CLAVIER[1], 2009 : <http://www.clavier-eu.org/?q=node/862>  
CLAVIER[2], 2009 : <http://www.clavier-eu.org/?q=node/876>  
CLAVIER[3], 2009 : <http://www.clavier-eu.org/?q=node/877>
- DIY Leaflet (2007); University of Sheffield, Groundwork Sheffield, Sheffield city council; *DIY Green Roofs*; The Green Roof Forum; Part-financed by the European Union European Regional Development Fund. [accessed online, January 2010] <http://www.thegreenroofcentre.co.uk/pages/DIY%20Leaflet.pdf>
- Déqué et al. (2007): Déqué, M., Rowell, D. P. , Lüthi, D. ,Giorgi, F., Christensen, J. H., Rockel, B., Jacob, D., Kjellström, E., de Castro, M., van den Hurk, B.; *An intercomparison of regional climate simulations for Europe: assessing uncertainties in model projections*; Journal of Climatic Change; Volume 81; pages 53 -70; Springer Netherlands, 2007. [accessed online, June 2009]. <http://www.springerlink.com/content/m35mu141g142112q/?p=98597816e57741aab32d17e753b3a7a&pi=3>
-

---

## Bibliography

---

- Durner (1999): Durner W.; *Einführung in die Statistik*; Script of lecture at the University of Bayreuth – SS, 1999.
- DVWK -101 (1979): Deutscher Verband für Wasserwirtschaft und Kulturbau e.V. (DVWK); *Empfehlung zur Berechnung der Hochwasserwahrscheinlichkeit*, DVWK-Merkblatt 101; Verlag Paul Parey, 1979.
- DVWK-238 (1996): Deutscher verband für Wasserwirtschaft und Kulturbau e.V. (DVWK); *Ermittlung der Verdunstung von Land- und Wasserflächen*; Moser Durich + Verlag GmbH; Rheinbach, 1996.
- DWA-A 138 (2005): Deutsche Vereinigung für Wasserwirtschaft, Abwasser und Abfall e.V. (DWA-A); *Planung, Bau und Betrieb von Anlagen zur Versickerung von Niederschlagswasser*; DWA-Regelwerk, Hennef, 2005.
- EEA (2004): European Environment Agency; *EEA Signals 2004 - A European Environment Agency update on selected issues*; EEA, Copenhagen, 2004. [accessed online, April 2009] <http://www.eea.europa.eu/publications/signals-2004/ENSIGNALS2004WEB.PDF>
- EEA (2008): European Environment Agency; *Impacts of Europe's changing climate - 2008 indicator-based assessment*; Joint EEA-JRC-WHO report No 4/2008; EEA, Luxembourg, 2008. [accessed online, January 2009] [http://www.eea.europa.eu/publications/eea\\_report\\_2008\\_4](http://www.eea.europa.eu/publications/eea_report_2008_4)
- Elmshorner Nachrichten (online); [accessed online, June 2009] <http://www.en-online.de/>
- Enke & Kreienkamp (2006): Enke, W.; Kreienkamp, F., *WETTREG A1B Scenario run, UBA Project, World Data Center for Climate: CERA-DB*, 2006. [accessed online, January 2010] [http://cera-www.dkrz.de/WDCC/ui/Compact.jsp?acronym=WR\\_A1B\\_2021\\_2030](http://cera-www.dkrz.de/WDCC/ui/Compact.jsp?acronym=WR_A1B_2021_2030)
- European Commission (2009): *White paper - Adapting to climate change: towards a European framework for action*; Brussels, 2009. [accessed online, May 2009] <http://eur-lex.europa.eu/LexUriServ/LexUriServ.do?uri=CELEX:52009DC0147:EN:NOT>
- European Parliament (2000): *Directive 2000/60/EC of the European Parliament and of the Council establishing a framework for Community action in the field of water policy*; Official Journal of the European Union – Directives; OJ L 327, 22.12.2000, p. 1–73. [accessed online, June 2009] <http://eur-lex.europa.eu/LexUriServ/LexUriServ.do?uri=CELEX:32000L0060:EN:NOT>
- European Parliament (2007): *Directive 2007/60/EC of the European Parliament and of the Council of 23. October 2007 on the assessment and management of flood risk*; Official Journal of the European Union – Directives; OJ L 288, 6.11.2007, p. 27–34; European Parliament; Straßburg, 2007. [accessed online, June 2009] <http://eur-lex.europa.eu/LexUriServ/LexUriServ.do?uri=CELEX:32007L0060:EN:NOT>
-

## Bibliography

---

- Fang et al. (1994): Fang, X. Y., Naghavi, B., Singh, V. P. and Wang, G.T.; *MMO: An improved estimator for log-Pearson type-3 distribution*; in Journal: Stochastic Hydrology and Hydraulics; Volume 8, Number 3, Springer Berlin / Heidelberg; pages 219-231, September 1994. [accessed online, November 2009]  
<http://www.springerlink.com/content/114461x45275p3w0/>
- The Federal Government (2008): *German Strategy for Adaptation to Climate Change*; adopted by the German federal cabinet on 17th December 2008. [accessed online, November 2009]  
[http://ccsl.iccip.net/das\\_gesamt\\_en\\_bf.pdf](http://ccsl.iccip.net/das_gesamt_en_bf.pdf)
- Feyen & Dankers (2009): Feyen, L., Dankers, R.; *Impact of climate change on flood hazard*; Homepage of the JRC - FLOODS Portal; 22 June 2009. Adopted from: Feyen, L., Dankers, R. (2009): *The impact of global warming on streamflow drought in Europe*; J. Geophys. Res., 114, D17116, doi:10.1029/2008JD011438. [accessed online, July 2009]  
[http://floods.jrc.ec.europa.eu/index.php?option=com\\_content&view=article&id=146&Itemid=225](http://floods.jrc.ec.europa.eu/index.php?option=com_content&view=article&id=146&Itemid=225)
- Fowler et al. (2007): Fowler, H. J., Blenkinsop, S., Tebaldi, C.; *Review: Linking climate change modelling to impacts studies: recent advances in downscaling techniques for hydrological modelling*; International Journal of Climatology No. 27; Wiley InterScience, 2007. [accessed online, June 2009]  
[http://www.staff.ncl.ac.uk/h.j.fowler/Fowleretal2007\\_reviewpaper.pdf](http://www.staff.ncl.ac.uk/h.j.fowler/Fowleretal2007_reviewpaper.pdf)
- Fowler & Ekström (2009): Fowler, H. J., Ekström, M.; *Multi-model ensemble estimates of climate change impacts on UK seasonal precipitation extremes*; International Journal of Climatology; Volume 29(3), pages 385-416. [accessed online, October 2009]  
[http://www.staff.ncl.ac.uk/h.j.fowler/fowler&ekstrom\\_ijc09.pdf](http://www.staff.ncl.ac.uk/h.j.fowler/fowler&ekstrom_ijc09.pdf)
- Frei et al. (2006): Frei, C., R. Schöll, S. Fukutome, J. Schmidli, and P. L. Vidale; *Future change of precipitation extremes in Europe: Intercomparison of scenarios from regional climate models*, Journal of Geophysical Research – Atmospheres, 111. [accessed online, July 2009]  
<http://www.agu.org/pubs/crossref/2006/2005JD005965.shtml>
- Golder Associates (2009): Golder Associates GmbH; *Fachliche Analyse des Klimazuschlages für Bemessungsabflüsse im Einzugsgebiet der Wandse*; Agency for Roads, Bridges and Waters (LSBG); Hamburg, 2009.
- Götzinger (2007): Götzinger, J.; *Distributed Conceptual Hydrological Modelling - Simulation of Climate, Land Use Change Impact and Uncertainty Analysis*; Mitteilungen, Heft 164; Institute for River and Coastal Engineering, University Stuttgart, Stuttgart, 2007. [accessed online, May 2009]  
[http://elib.uni-stuttgart.de/opus/volltexte/2007/3349/pdf/Diss\\_Goetzinger\\_ub.pdf](http://elib.uni-stuttgart.de/opus/volltexte/2007/3349/pdf/Diss_Goetzinger_ub.pdf)
- GVOBI (2002): Law and Ordinance Gazette of Schleswig Holstein; *Landesverordnung über die Anforderungen an die erlaubnisfreie Versickerung von Niederschlagswasser in das Grundwasser*, enacted on 25 May 2002; Ministry of Environment, Nature and Forests of the Federal State Schleswig-Holstein, 2002. [accessed online, December 2009] [www.sh.juris.de/sh/gesamt/VersickV\\_SH.htm](http://www.sh.juris.de/sh/gesamt/VersickV_SH.htm)

---

## Bibliography

---

- Hagemann et al. (2005): Hagemann, S., Arpe, K.; *Bengtsson, L.; Validation of the hydrological cycle of ERA40*; Reports on Earth System Science; Hamburg, 2005. [accessed online, September 2009]  
<http://edoc.mpg.de/get.epl?fid=17555&did=249272&ver=0>
- Handmer et al. (1999); Handmer, J.W., Penning-Rowsell, E.C, and Tapsell, S.; *Flooding in a warmer world: the view from Europe*. In: Downing, T. E., Olsthoorn, A. A., Tol, R. S. J. (1999): *Climate, Change and Risk*; pages 125-161, Routledge, London, 1999
- Hänggi & Weingartner (2009): Hänggi, P., Weingartner, R.; *Analyse von quantitativen Veränderungen hydrologischer Systeme mit Hilfe von Verteilungsparametern*; in: Fohrer, N., Schmalz, B., Hörmann, G., Bieger, K.; *Forum für Hydrologie und Wasserbewirtschaftung - Hydrologische Systeme im Wandel*; Contribution to the day of Hydrology on 26./27. March 2009 at the Christian-Albrechts-University of Kiel; booklet 26.09, ISBN: 978-3-941089-54-9. [accessed online, November 2009]  
[http://fghw.lfi.rwth-aachen.de/chapvero/docs/inhalt\\_forum2609.pdf](http://fghw.lfi.rwth-aachen.de/chapvero/docs/inhalt_forum2609.pdf)
- Hanson et al. (2007): Hanson, C. E., Palutikof, J. P., Livermore, M. T. J., Barring, L., Bindi, M., Corte-Real, J., Durao, R., Giannakopoulos, C., Good, P., Holt, T., Kundzewicz, Z., Leckebusch, G. C., Moriondo, M., Radziejewski, M., Santos, J., Schlyter, P., Schwarb, M., Stjernquist, I., Ulbrich, U.; *Modelling the impact of climate extremes: an overview of the MICE project*; in Journal: *Climatic Change* 81; pages 163–177; Springer Science + Business Media B.V., 2007. [accessed online, June 2009]  
<http://www.springerlink.com/content/31gu620751607x60/>
- Hartwig (2008): *Über die Sitzung des Umweltausschusses am Mittwoch dem 13.02.2008. um 18:00 im Mehrzweckraum des Rathauses*; Environmental Committee Elmshorn; Protocol (01/2008). [accessed online, December 2009]  
[http://www.stadt-elmshorn.de/files/ua\\_protokoll\\_2008-02-13.pdf](http://www.stadt-elmshorn.de/files/ua_protokoll_2008-02-13.pdf)
- Hellmers, 2009: Hellmers, S.; *Sustainable Concepts of Urban Drainage in the UK and Assessment Methods of their Effectiveness – Case Study West Garforth*; Project Work; Institute of River and Coastal Engineering, Hamburg, March 2009.
- HLUG (2005): Hessian Agency for the Environment and Geology (HLUG); *Integriertes Klimaschutzprogramm Hessen – INKLIM 2012; Projektbaustein II: Klimawandel und Klimafolgen in Hessen*; Final Report, 2005. [accessed online, January 2010]  
[http://www.hlug.de/klimawandel/inklimate/dokumente/abschlussbericht\\_II.pdf](http://www.hlug.de/klimawandel/inklimate/dokumente/abschlussbericht_II.pdf)
- Hoffmann (2009): Hoffmann, P.; *Modifikation von Starkniederschlägen durch urbane Gebiete*; Diploma Thesis; Institute of Meteorology; University of Hamburg, 2009.
- Iorio et al. (2004): Iorio, J. P., Duffy, P. B., Govindasamy, B., Thompson, S. L., Khairoutdinov, M., Randall, D.; *Effects of model resolution and subgrid-scale physics on the simulation of precipitation in the continental United States*; Journal: *Climate Dynamics* Volume 23; pages 243 – 258; Springer-Verlag Berlin / Heidelberg, 2004. [accessed online, June 2009]  
<http://www.springerlink.com/content/6xj0aw1llj3exnc0/>
-

---

## Bibliography

---

- IPCC (2000): Intergovernmental Panel on Climate Change (IPCC); *Emissions Scenarios – IPCC Special Report. Summary for Policymakers*; Contribution of Working Group III to the Third Assessment Report of the Intergovernmental Panel on Climate Change; Cambridge University Press, Cambridge, UK, 2000.  
[accessed online, June 2009]  
[http://www.grida.no/publications/other/ipcc\\_sr/?src=/climate/ipcc/emission/031.htm](http://www.grida.no/publications/other/ipcc_sr/?src=/climate/ipcc/emission/031.htm)
- IPCC TAR (2001): Intergovernmental Panel on Climate Change; [eds. Houghton, J. T., Ding, Y., Griggs, D.J. , Noguer, M. , van der Linden P. J. and Xiaosu D.]; *Climate Change 2001: The Scientific Basis. Contribution of Working Group I to the Third Assessment Report of the Intergovernmental Panel on Climate Change*, Cambridge University Press, Cambridge, UK. [accessed online, June 2009]  
<http://www.ipcc.ch/ipccreports/tar/wg1/088.htm>
- IPCC AR4 (2007a/b): Intergovernmental Panel on Climate Change (IPCC); [eds. Solomon, S., Qin, D., Manning, M., Chen, Z., Marquis, M., Averyt, K.B., Tignor, M., Miller, H.L.]; *Climate Change 2007: The Physical Science Basis. Contribution of Working Group I to the Fourth Assessment Report of the Intergovernmental Panel on Climate Change*; Cambridge University Press, Cambridge, UK and NY, USA. [accessed online 11 January 2010]  
IPCC AR4 (2007a):  
<http://www.ipcc.ch/pdf/assessment-report/ar4/wg1/ar4-wg1-chapter8.pdf>  
IPCC AR4 (2007b):  
[http://www.ipcc.ch/publications\\_and\\_data/ar4/wg1/en/ch3s3-1.html](http://www.ipcc.ch/publications_and_data/ar4/wg1/en/ch3s3-1.html)
- IPCC AR4 (2007c/d/e): Intergovernmental Panel on Climate Change (IPCC); [eds. Parry, M. L.; Canziani, O. F.; Palutikof, J. P.; van der Linden, P. J. and Hanson, C.E.]; *Climate Change 2007: Impacts, Adaptation and Vulnerability. Contribution of Working Group II to the Fourth Assessment Report of the Intergovernmental Panel on climate Change*; Cambridge University Press, Cambridge, UK.  
IPCC AR4 (2007c)  
[http://www.ipcc.ch/publications\\_and\\_data/ar4/wg2/en/ch1s1-3.html](http://www.ipcc.ch/publications_and_data/ar4/wg2/en/ch1s1-3.html)  
IPCC AR4 (2007d)  
[http://www.ipcc.ch/publications\\_and\\_data/ar4/wg2/en/ch3s3-5-2.html](http://www.ipcc.ch/publications_and_data/ar4/wg2/en/ch3s3-5-2.html)  
IPCC AR4 (2007e)  
[http://www.ipcc.ch/publications\\_and\\_data/ar4/wg2/en/contents.html](http://www.ipcc.ch/publications_and_data/ar4/wg2/en/contents.html)
- Jacob & Lorenzo (2009): Jacob, D., Tomassini, L.; *REMO A1B SCENARIO RUN, BFG PROJECT, 0.088 DEGREE RESOLUTION, monthly data*; World Data Center for Climate, CERA-DB, 2009. [accessed online, December 2009]  
[http://cera-www.dkrz.de/WDCC/ui/Compact.jsp?acronym=REMO\\_BFG\\_A1B\\_MM](http://cera-www.dkrz.de/WDCC/ui/Compact.jsp?acronym=REMO_BFG_A1B_MM)
- Jacob & Mahrenholz (2006a): Jacob, D., Mahrenholz, P.; *REMO C20 SCENARIO RUN, UBA PROJECT, DATASTREAM 3*; World Data Center for Climate; CERA-DB.  
[accessed online July 2009]  
[http://cera-www.dkrz.de/WDCC/ui/Compact.jsp?acronym=REMO\\_UBA\\_C20\\_D3](http://cera-www.dkrz.de/WDCC/ui/Compact.jsp?acronym=REMO_UBA_C20_D3)
- Jacob & Mahrenholz (2006b): Jacob, D., Mahrenholz, P.; *REMO A1B SCENARIO RUN, UBA PROJECT, DATASTREAM 3*; World Data Center for Climate; CERA-DB.  
[accessed online July 2009]  
[http://cera-www.dkrz.de/WDCC/ui/Compact.jsp?acronym=REMO\\_UBA\\_A1B\\_D3](http://cera-www.dkrz.de/WDCC/ui/Compact.jsp?acronym=REMO_UBA_A1B_D3)
- Jacob & Mahrenholz (2006c): Jacob, D., Mahrenholz, P.; *REMO A2 SCENARIO RUN, UBA PROJECT, DATASTREAM 3*; World Data Center for Climate; CERA-DB.  
[accessed online July 2009]  
[http://cera-www.dkrz.de/WDCC/ui/Compact.jsp?acronym=REMO\\_UBA\\_A2\\_D3](http://cera-www.dkrz.de/WDCC/ui/Compact.jsp?acronym=REMO_UBA_A2_D3)
-

---

## Bibliography

---

- Jacob & Mahrenholz (2006d): Jacob, D., Mahrenholz, P.; *REMO B1 SCENARIO RUN, UBA PROJECT, DATASTREAM 3*; World Data Center for Climate; CERA-DB.  
[accessed online July 2009]  
[http://cera-www.dkrz.de/WDCC/ui/Compact.jsp?acronym=REMO\\_UBA\\_B1\\_D3](http://cera-www.dkrz.de/WDCC/ui/Compact.jsp?acronym=REMO_UBA_B1_D3)
- Jacob et al. (2008): Jacob, D., Göttel, H., Kotlarski, S., Lorenz, P., Sieck, K.; *Klimaauswirkungen und Anpassung in Deutschland – Phase 1: Erstellung regionaler Klimaszenarien für Deutschland*; Abschlussbericht zum UFOPLAN-Vorhaben 204 41 138, UBA-FB 000969, Umweltbundesamt, Dessau-Roßlau, August 2008 [accessed online, May 2009]  
[www.umweltdaten.de/publikationen/fpdf-l/3513.pdf](http://www.umweltdaten.de/publikationen/fpdf-l/3513.pdf)
- Katzenberger (2004): Katzenberger, B.; *Bisherige Erkenntnisse aus KLIWA – Handlungsempfehlungen*; page 197 - 204.-; in: Fachvorträge: *Klimaveränderung und Konsequenzen für die Wasserwirtschaft*. 2. KLIWA Symposium 2004; 3. – 4. 05.2004 Würzburg ISBN: 3-937911-16-2; Druckhaus Fritz König GmbH, München.  
[accessed online, June 2009]  
<http://www.kliwa.de/download/KLIWAHeft4.pdf>
- Kellagher & Laughlan (2005): Kellagher, R.B.B., Laughlan, C.S.; *Use of SUDS in High Density Developments – Guidance Manual*; Report SR 666; Release 4; HR Wallingford, Wallingford, October 2005.
- KLIWA (2006): German Weather Service (DWD), State Environment, Measurement and Nature Conservation Agency (LUBW), Bavarian State Environment Agency (LfU); *Our climate is changing - Consequences-Extend-Strategies, Impact on Water Resources Management in Southern Germany*; ÖkoMedia PR, Stuttgart, 2006.  
[accessed online, January 2010] [http://www.kliwa.de/download/KLIWA\\_en.pdf](http://www.kliwa.de/download/KLIWA_en.pdf)
- KOSTRA-Atlas (1997): Bartels, H., Malitz, G., Asmus, S., Albrecht, F.M., Dietzer, B., Günther, T., Ertel, H.; *Niederschlagshöhen für Deutschland – KOSTRA: Koordinierte Starkniederschlags-Regionalisierungs-Auswertungen*; Selbstverlag des Deutschen Wetterdienstes, Offenbach am Main, 1997.
- Küpferle & Pasche (2008): Küpferle, C., Pasche, E.; *Feinkonzept: Implementierung des Kalypso-Planer-Clients auf Basis von Kalypso für die Freie und Hansestadt Hamburg*; supplied by the Agency for Roads, Bridges and Waters (LSBG); Version 2.0; 20.05.2008.
- Kyoto Protocol (1997): Conference Secretariat; *Official Web Site of the Third Conference of the Parties*; Kyoto, December 1 – 10, 1997. [accessed online, May 2009]  
<http://unfccc.int/cop3/>
- LANU (2006): Ministry of agriculture, environment and rural areas Federal State Schleswig-Holstein (LANU); *Die Böden Schleswig-Holsteins, Entstehung, Verbreitung, Nutzung, Eigenschaften und Gefährdung, Schriftenreihe LANU-SH – Geologie und Boden (1)*; Pirwitz druck & design, Kiel, 2006. [accessed online, December 2009]  
[http://www.umweltdaten.landsh.de/nuis/upool/gesamt/geologie/boden\\_sh.pdf](http://www.umweltdaten.landsh.de/nuis/upool/gesamt/geologie/boden_sh.pdf)
-

---

## Bibliography

---

- Lautenschlager et al. (2009); Lautenschlager, M., Keuler, K., Wunram, C., Keup-Thiel, E., Schubert, M., Will, A., Rockel, B., Boehm, U.; *Climate Simulation with CLM, Scenario A1B run no.1, Data Stream 3: European region MPI-M/MaD*; World Data Center for Climate; CERA-DB. [accessed online July 2009]  
[http://cera-www.dkrz.de/WDCC/ui/Entry.jsp?acronym=CLM\\_A1B\\_1\\_D3](http://cera-www.dkrz.de/WDCC/ui/Entry.jsp?acronym=CLM_A1B_1_D3)
- LLUR (2009): The State Agency for Nature and Environment of the Federal State Schleswig-Holstein; *Agrar- und Umweltatlas des Landes Schleswig Holstein*. [accessed online, December 2009]  
<http://www.umweltdaten.landsh.de/atlas/script/index.php>
- Lorz (n.d.); Lorz, B., Lorz, D; *Homepage: Haus-Umbau, Lexikon: Fallrohre*. [accessed online, September 2009] <http://www.haus-umbauen.de/lexikon/fallrohr>
- Ludwig et al. (2009): Ludwig, R., May, I., Turcotte, R., Vescovi, L., Braun, M., Cyr, J.-F., Fortin, L.-G., Chaumont, D., Biner, S., Chartier, I., Caya, D., Mauser, W.; *The role of hydrological model complexity and uncertainty in climate change impact assessment*; Journal Adv. Geosci., 21, pages 63–71, 2009. [accessed online, September 2009] <http://www.adv-geosci.net/21/63/2009/adgeo-21-63-2009.pdf>
- Manual of soil mapping (2005); Ad-Hoc-Arbeitsgruppe Boden: Eckelmann, W., Sponagel, H., Grotenthaler, W., a.o.; *Bodenkundliche Kartieranleitung. 5. verbesserte und erweiterte Auflage*; Bundesanstalt für Geowissenschaften und Rohstoffe in Zusammenarbeit mit den Staatlichen Geologischen Diensten der Bundesrepublik Deutschland, Hannover, 2005.
- NIST (2006): NIST/SEMATECH; *e-Handbook of Statistical Methods*. [e-book accessed online, December 2009] <http://www.itl.nist.gov/div898/handbook/> (Last updated: 7/18/2006).
- North German Climate Atlas (online): [accessed online, September 2009].  
[www.norddeutscher-klima-atlas.de](http://www.norddeutscher-klima-atlas.de)
- Pfister et al. (2005); Pfister, C., Schellnhuber, H. J., Rahmstorf, S., Graßl, H.; *Weather catastrophes and climate change*; Münchener Rückversicherungs-Gesellschaft; Druckerei Fritz Kriechbaumer, Munich, 2005: ISBN 3-937624-81-3.
- NABU-Elmshorn (n.d.): Nature and Biodiversity Conservation Union Elmshorn; *Projektraum mittlere Krückau*; Homepage of the NABU Elmshorn. (accessed online, September 2009) [http://www.nabu-elmshorn.de/nabue\\_06.htm](http://www.nabu-elmshorn.de/nabue_06.htm)
- Pasche (2003): Pasche, E.; *Wasserbau – fünf Jahre: Alles fließt*; River and Coastal Engineering at the Technical University Hamburg Harburg; Schüthedruck GmbH, Hamburg, 2003. (accessed online, January 2010)  
<http://doku.b.tu-harburg.de/volltexte/2003/50/pdf/wasserbau.pdf>
- Pasche et al. (2008): Pasche E., Lawson N., Ashley, R., Schertzer, D.; *Risk Assessment and Risk in Small Urban Catchments*, ed: Crue Funding Initiative on Flood Risk Management Research.

---

## Bibliography

---

- Pasche et al. (2009): Pasche, E., Behzadnia, N., Brüning, C., Hellmers, S., Manojlovic, N.; *Hydrologic Sensitivity Analysis - contribution to assessment of efficiency of SUDS in small urban catchments*, Paper, 33rd IAHR Conference, August 9-14, Vancouver BC, Canada.
- Optigrüen (2009): Optigrün international AG: *Systemlösungen zur Dachbegrünung mit Optigrün Produkten*; Homepage. [accessed online, September 2009]  
[www.optigruen.de](http://www.optigruen.de)
- PÜK (2008): Planungsgemeinschaft Überschwemmungsgebiete an der Krückau (PÜK); EPK<sub>2</sub> Engineers GbR, Engineers of Klütz & Collegen Itzehoe GmbH; *Überprüfung und Neufestlegung von Überschwemmungsgebieten an der Krückau – Hochwasserrisikokarten; Erläuterungsbericht – Modellaufbau und Modellkalibrierung Niederschlagsabflussmodell*; LANU Schleswig Holstein, Itzehoe, Hamburg, 29.02.2008.
- PÜK (2009): Planungsgemeinschaft Überschwemmungsgebiete an der Krückau (PÜK); EPK<sub>2</sub> Engineers GbR, Engineers of Klütz & Collegen Itzehoe GmbH; *Überprüfung und Neufestlegung von Überschwemmungsgebieten an der Krückau – Hochwasserrisikokarten*; Hochwasserrisikokarten Nr. 1 – Nr. 14, LANU Schleswig Holstein, 27.08.2009 – 01.09.2009.
- Rao & Srinivas (2008): Rao, A.R., Srinivas, V.V.; *Regionalization of Watersheds: An approach based on Cluster Analysis*; Water Science and Technology, Vol. 58; Springer Science + Business Media B.V., 2008.
- Rudolf & Rubel (2005): Rudolf, B., Rubel, F.; *Global Precipitation*. In: Hantel (2005): *Observed Global Climate*; Landolt-Börnstein: *Numerical Data and Functional Relationships*; New Series; chapter 11; pages 11-22; Group V: Geophysics, Volume 6, Springer-Verlag Berlin Heidelberg New York. [accessed online, July 2009]  
[http://www.dwd.de/bvbw/generator/Sites/DWDWWW/Content/Oeffentlichkeit/KU/KU4/KU42/en/Reports\\_Publications/Global\\_Precipitation\\_LB.templateId=raw.property=publicationFile.pdf/Global\\_Precipitation\\_LB.pdf](http://www.dwd.de/bvbw/generator/Sites/DWDWWW/Content/Oeffentlichkeit/KU/KU4/KU42/en/Reports_Publications/Global_Precipitation_LB.templateId=raw.property=publicationFile.pdf/Global_Precipitation_LB.pdf)
- REMO User Leaflet (n. d.): Max-Planck Institute of Meteorology, *Hinweise für REMO-Datennutzer*, no date. [accessed online, May 2009]  
[http://www.mpimet.mpg.de/fileadmin/staff/pfeifersusanne/REMO\\_UBA/REMO-UBA-Hinweise.pdf](http://www.mpimet.mpg.de/fileadmin/staff/pfeifersusanne/REMO_UBA/REMO-UBA-Hinweise.pdf)
- Rittmeier & Viße (2002): Rittmeier, M., Viße, C.; *Wasserschutzgebiete in Schleswig-Holstein*; Hintergrund Nr. 1/2002; Ministry of Environment, Nature and Forests of the Federal State Schleswig-Holstein, 2002. [accessed online, November 2009]  
[http://www.hampel-knappert.de/download/wasserschutzgebiete\\_sh.pdf](http://www.hampel-knappert.de/download/wasserschutzgebiete_sh.pdf)
- Röttgers (2006): Röttgers, M.: *Broschüre - Dezentrale naturnahe Regenwasserbewirtschaftung. Ein Leitfaden für Planer, Architekten, Ingenieure und Bauunternehmer*; Behörde für Stadtentwicklung und Umwelt der Freien und Hansestadt Hamburg (BSU), Hamburg, 2006.
- Tourbier et al. (2007): Tourbier, J.T., White, I.; *Sustainable Measures for Flood Attenuation: Sustainable Drainage and Conveyance Systems SUDACs*. In: Ashley, R., Garvin, S., Pasche, E., Vassilopoulos, A., Zevenbergen, C.; *Advances in Urban Flood Management*; Taylor & Francis Group, London, 2007.
-

---

## Bibliography

---

- Schättler (2009): Schättler, U.; *A Description of the Nonhydrostatic Regional COSMO-Model- Part V: Preprocessing: Initial and Boundary Data for the COSMO-Model*; German Weather Service (DWD), Offenbach, Germany; 2009. [accessed online, January 2010]  
<http://www.cosmo-model.org/content/model/documentation/core/cosmoInt2lm.pdf>
- Schendera (2007): Schendera, C.F.G.; *Datenqualität mit SPSS*; Oldenbourg Wissenschaftsverlag, München, 2007. [accessed online, January 2010]  
[http://www.oldenbourg-wissenschaftsverlag.de/fm/694/3-486-58214\\_v.pdf](http://www.oldenbourg-wissenschaftsverlag.de/fm/694/3-486-58214_v.pdf)
- Schneider (2004): Schneider, K.-J.: *Bautabellen für Ingenieure*. 16. Auflage. Werner, Düsseldorf, 2004.
- Schwandt (2004): Schwandt, D.; *Abflussentwicklung in Teileinzugsgebieten des Rheins - Simulationen für den Ist-Zustand und für Klimaszenarien*; Dissertation; PIK Report No. 88; Potsdam Institute Climate Change Impacts Research (PIK), Potsdam. [accessed online, June 2009]  
<http://www.pik-potsdam.de/research/publications/pikreports/.files/pr88.pdf>
- Sieker (2005): Ingenieurgesellschaft Prof. Dr. Sieker mbH; *Maßnahmen zur Regenwasserbewirtschaftung – Versickerung*, Homepage. [accessed online, September 2009]  
[http://www.sieker.de/MKat/rw\\_bewirt\\_versickerung.htm](http://www.sieker.de/MKat/rw_bewirt_versickerung.htm)
- Sieker et al. (2006): Sieker, F., Kaiser, M., Sieker, H.: *Dezentrale Regenwasserbewirtschaftung im privaten, gewerblichen und kommunalen Bereich (Grundlagen und Ausführungsbeispiele)*; Fraunhofer IRB-Verlag, Stuttgart, 2006.
- Spekat et al. (2007); Spekat, A., Enke, W., Kreienkamp, F.; *Neuentwicklung von regional hoch aufgelösten Wetterlagen für Deutschland und Bereitstellung regionaler Klimaszenarios auf der Basis von globalen Klimasimulationen mit dem Regionalisierungsmodell WETTREG auf der Basis von globalen Klimasimulationen mit ECHAM5/MPI-OM T63L31, 2010 bis 2100 für die SRES Szenarios B1, A1B und A2*; Forschungsprojekt im Auftrag des Umweltbundesamtes, FuE-Vorhaben Förderkennzeichen 204 41 138; Umweltbundesamt Fachbibliothek Umwelt, 2007. [accessed online, May 2009] <http://www.umweltdaten.de/publikationen/fpdf-l/3133.pdf>
- STARDEX Final Report (n. d.): *STARDEX – downscaling climate extremes*; Final Report; Climatic Research Unit, Norwich, no date. [accessed online, May 2009]  
[http://www.cru.uea.ac.uk/projects/stardex/reports/STARDEX\\_FINAL\\_REPORT.pdf](http://www.cru.uea.ac.uk/projects/stardex/reports/STARDEX_FINAL_REPORT.pdf)
- Statistikamt Nord (2009): Statistisches Amt für Hamburg und Schleswig-Holstein; *Bevölkerung der Gemeinden in Schleswig-Holstein am 31.12.2008*; Statistische Berichte; A I 2 - vj 4/08 S; 8 October 2009. [accessed online, January 2010]  
[http://www.statistik-nord.de/uploads/tx\\_standocuments/A\\_I\\_2\\_vj084\\_S.pdf](http://www.statistik-nord.de/uploads/tx_standocuments/A_I_2_vj084_S.pdf)
- Staufer et al. (2008): Staufer, P., Siekmann, M., Roder, S., Pinnekamp, J.; *Sustainable development of regional water resources management confronting climate trends and extreme weather*; Proceedings, 11th International Conference on Urban Drainage, Edinburgh, Scotland, UK.
-

---

## Bibliography

---

- Steinke (2009): Steinke W.; With reference to the Klimzug-Nord Project and the presentation on the 8th December 2009 in Elmshorn; Email to Prof. Dr.-Ing. E. Pasche about the local rainwater drainage situation in the Danzigerstrasse, Langenmoor, Koppeldamm [Email] (Personal communication, 9 December 2009)
- Tetzlaff et al. (2004): Tetzlaff, B., Kunkel, R., Taug, R., Wendland, F.; *Grundlagen für eine nachhaltige Bewirtschaftung von Grundwasserressourcen in der Metropolregion*; Hamburg Schriften des Forschungszentrums Jülich, Reihe Umwelt/Environment; Band/Volume 46; Grafische Betriebe, Forschungszentrum Jülich GmbH, Jülich, 2004. [accessed online, November 2009]  
[http://juwel.fz-juelich.de:8080/dspace/bitstream/2128/349/1/Umwelt\\_46.pdf](http://juwel.fz-juelich.de:8080/dspace/bitstream/2128/349/1/Umwelt_46.pdf)
- THW-Elmshorn (n.d.): Homepage of the German Federal Agency for Technical Relief (THW) of Elmshorn. [accessed online, June 2009] [www.thw-elmshorn.de](http://www.thw-elmshorn.de)
- TU Dresden (2009): Technical University Dresden, Institute of Food Chemistry; *Verfahrensanweisung - statistische Tests*; [online], adopted from: *DIN 53 804 Teil 1 Statistische Auswertungen - Meßbare (kontinuierliche) Merkmale, Abs. 8.2, Ausreißertest nach Grubbs*, September 1981. [accessed online, December 2009]  
[http://www.chm.tu-dresden.de/lc/praktikum/karlfischer/verfahrensanweisungen\\_KF.doc](http://www.chm.tu-dresden.de/lc/praktikum/karlfischer/verfahrensanweisungen_KF.doc)
- UCAR (2007): University Corporation for Atmospheric Research (UCAR); *NetCDF-format definitions*; Homepage of the UCAR. [accessed online, June 2009]  
<http://www.image.ucar.edu/GSP/Software/Netcdf/> (last modified 2007)
- UMBW (n d.): Agency for Environment and Transport Baden-Württemberg (UMBW); *Naturverträgliche Regenwasserbewirtschaftung – Leitfaden für Planer, Ingenieure, Architekten, Kommunen und Behörden*; UMBW; Rösler Druck GmbH, Schorndorf. [accessed online, May 2009]  
<http://www.um.baden-wuerttemberg.de/servlet/is/37009/>
- Van Pelt et al. (2009): van Pelt, S. C., Kabat, P., Maat, H. W., van den Hurk, B. J. J. M., Weerts, A. H.; *Discharge simulations performed with a hydrological model using bias corrected regional climate model input*; Journal: *Hydrological Earth System Science* No.13, 2009. [accessed online, January 2010]  
<http://www.hydrol-earth-syst-sci.net/13/2387/2009/hess-13-2387-2009.pdf>
- VICAIRE, 2006; Virtual campus in hydrology and water resources management; [accessed online, January 2010] <http://echo.epfl.ch/VICAIRE/> (last modified 2006)
- Viner (2000); Viner, D.; *Information sheets - 8: Modelling Climate Change*; Homepage of the Climatic Research Unit (CRU). [accessed online, May 2009]  
<http://www.cru.uea.ac.uk/cru/info/modelcc/>
- Viner (2002): Viner D.; *A qualitative assessment of the sources of uncertainty in climate impacts assessment studies*; Climatic Research Unit (CRU), pages 139-149, in: Beniston, M.: *Climatic Change: Implications for the Hydrological Cycle and for Water Management*; book series: *Advances in Global Change Research*, Volume 10; Springer Netherlands, Norwich, UK.
-

## Bibliography

---

- Vollmer (2008); Homepage des Bedachungszentrums: Verbund deutscher Dachdeckervereine und Händler. [accessed online, September 2009]  
<http://lexikon.bedachungszentrum.de/fallrohr.html>
- Yao Hu, 2008: *Development of post-processing capabilities in the rainfall runoff model Kalypso NA to derivate design flood by implementation of the flood frequency analysis*; Project Work; Institute of River and Coastal Engineering, Technical University Hamburg Harburg, 2008.
- WHG (2002): Federal Environmental Agency; *Act on Managing Water Resources*; (Wasserhaushaltsgesetz, WHG); Bundesgesetzblatt Jahrgang 2002, Teil I Nr. 59. [accessed online, May 2009] <http://bundesrecht.juris.de/whg/index.html>
- WMO/GWP (2008): World Meteorological Organisation (WMO), Global Water Partnership (GWP); *Urban Flood Risk Management - A Tool for Integrated Flood Management*; Technical Document No. 11; Flood Management Tools Series, 2008. [accessed online, May 2009]  
[http://www.apfm.info/pdf/ifm\\_tools/Tools\\_Urban\\_Flood\\_Risk\\_Management.pdf](http://www.apfm.info/pdf/ifm_tools/Tools_Urban_Flood_Risk_Management.pdf)
- Zebisch et al. (2005): Zebisch, M., Grothmann, T., Schröter, D., Hasse, C. Fritsch, U., Cramer, W.; *Klimawandel in Deutschland - Vulnerabilität und Anpassungsstrategien klimasensitiver Systeme*; Forschungsbericht UFOPLAN: 201 41 253 Umweltbundesamt, Dessau, 2005. [accessed online, May 2009]  
<http://www.umweltdaten.de/publikationen/fpdf-l/2947.pdf>

## Attachment 1

## Climate Models

## Attachment 1.1: Global Circulation Model List

| <b>Atmospheric Ocean Global Circulation Model (AOGCM)</b> | <b>CGCM<sub>3.1</sub> (T47) and CGCM<sub>3.1</sub> (T63)</b>   | <b>ECHAM5</b>  | <b>HadCM3</b>  |
|---|--|--|--|
| <b>Developed by</b>                                       | Canadian Centre for Climate Modelling and Analysis, Canada.  | Max Planck Institute for Meteorology, Germany.   | Hadley Centre for Climate Prediction and Research, Met Office, United Kingdom.   |
| <b>Atmospheric Spatial Resolution [in °]</b>              | T47 = 2.8° x 2.8°<br>T63 = 1.9° x 1.9°   | T63 = 1.9° x 1.9°  | latitude:2.75°<br>longitude:3.75°  |
| <b>Provided Specific Selected Land Features</b>           | Representation of soil moisture in a multi-layered scheme, presence of canopy, river routine scheme is implemented.<br>(IPCC AR4, 2007a) | Representation of soil moisture in a single layer bucket scheme, presence of canopy, river routine scheme is implemented.<br>(IPCC AR4, 2007a) | Representation of soil moisture in a multi-layered scheme, presence of canopy, river routine scheme is implemented.<br>(IPCC AR4, 2007a) |
| <b>IPCC - Scenarios</b>                                   | A1B, A2 and B1   | A1B, A2 and B1   | A1B, A2 and B1   |
| <b>Formats</b>  | NetCDF   | NetCDF   | NetCDF   |
| <b>Availability</b>                                       | <a href="http://cera-www.dkrz.de/">http://cera-www.dkrz.de/</a>  | <a href="http://cera-www.dkrz.de/">http://cera-www.dkrz.de/</a>  | <a href="http://cera-www.dkrz.de/">http://cera-www.dkrz.de/</a>  |
| <b>Literature / References</b>                            | <a href="http://www.cccma.bc.ec.gc.ca">http://www.cccma.bc.ec.gc.ca</a>  | <a href="http://www.mpimet.mpg.de">www.mpimet.mpg.de</a>   | <a href="http://www.metoffice.gov.uk/">http://www.metoffice.gov.uk/</a>  |

**Attachment 1.2: Regional Climate Model List**

| <b>Regional Climate Models (RCM)</b>   | <b>REMO</b><br>(Regional Climate Model)  | <b>CLM</b><br>(Climate Local Model)  | <b>WETTREG</b><br>(WETterlagen-basierte REGionalisierungsmethode)  |
|--|--|--|--|
| <b>Type</b>  | Dynamical Regional Climate Model   | Dynamical Regional Climate Model   | Statistical Regional Climate Model   |
| <b>Developed by:</b>   | Max-Planck-Institute of Meteorology in Hamburg (MPI-M) - <a href="http://www.mpimet.mpg.de">www.mpimet.mpg.de</a>                    | Consortium for small-scale modelling (COSMO) in collaboration with various universities, the GKSS <sup>1</sup> and DWD <a href="http://clm.gkss.de">http://clm.gkss.de</a> | Climate and Environment Consulting Potsdam GmbH (CEC) <a href="http://www.cec-potsdam.de">www.cec-potsdam.de</a> |
| <b>Scenarios and Model Realisations</b><br><br>*_1 : first model run<br>*_2 : second model run | Control scenarios:<br>C20_1 (1960 - 2000)<br>C20_2 (1950 - 1990)<br><br>IPCC-Scenarios:<br>A1B_1, A1B_2,<br>B1_1, A2_1 (2001 - 2100) | Control scenarios:<br>C20_1, C20_2, C20_3 (1960 - 2000)<br><br>IPCC-Scenarios:<br>A1B_1, A1B_2;<br>B1_1, B1_2 (2001 - 2100)  | Control Data Series:<br>1961 - 2000<br><br>IPCC-Scenarios: A1B, B1, A2 (2001 - 2100=)                            |
| <b>Spatial Resolution</b>  | Germany:<br>(ca. 10km x 10km)<br>ca. 0.1° x 0.1°<br><br>( <i>doubled nested RCM results</i> )  | Europe:<br>(ca. 20km x 20km)<br>ca. 0.2° x 0.2°  | Data series for 282 climate stations and 1695 rainfall gauging stations in Germany                               |
| <b>Spatial Distribution</b>  | Datastream 2: rotated geographical raster<br><br>Datastream 3: regular geographical grid   | Datastream 2: rotated geographical raster<br><br>Datastream 3: regular geographical grid   |  |
| <b>Smallest Time Step Sequences</b>  | 1h, 6h, 24h  | 1h, 3h, 24h  | Daily (24h)  |
| <b>Data Formats</b>  | NetCDF and IEG formats   | NetCDF and ASCII format  | csv-files  |
| <b>Availability</b>  | <a href="http://cera-www.dkrz.de/">http://cera-www.dkrz.de/</a>  | <a href="http://cera-www.dkrz.de/">http://cera-www.dkrz.de/</a>  | <a href="http://cera-www.dkrz.de/">http://cera-www.dkrz.de/</a>  |
| <b>Literature</b>  | Jacob & Mahrenholz, 2006   | Lautenschlager et al., 2009  | Enke & Kreienkamp, 2006  |

<sup>1</sup>GKSS = Gesellschaft für Kernenergieverwertung in Schiffbau und Schifffahrt

## Attachment 2

### Calculation of Additional Climate Change Data Series

*Calculation of the potential evaporation with data series of the regional climate models REMO or CLM.*

A differentiation is done between the maximal possible evaporation ( $ET_p$ ) and the actual evapotranspiration ( $ET_a$ ) (DVWK-238, 1996). In times of high soil moisture and frequent rainfall events the actual Evapotranspiration ( $ET_a$ ) approximates the potential evaporation ( $ET_p$ ), otherwise the actual evapotranspiration is limited by the actual water balance.

On the basis of the Penman-Monteith equation, physically based methods have been developed to calculate the potential evaporation ( $ET_p$ ) by taking into account the energy balance of the atmosphere (DVWK-238, 1996). E.g. the FAO-Standard has been developed on the basis of the Penman-Monteith method which is based on the assumption of a land cover of low grass fields. It is also known as “grass-reference-evaporation” ( $ET_0$ ) and is recommended to be used as potential evaporation, according to the technical bulletin DVWK-238 (1996).

For daily data series, the calculation of the “grass-reference-evaporation” ( $ET_0$ ) is defined by Wendling (1995) in the technical bulletin DVWK-238 (1996):

$$ET_0 = g(T, v) * \left( \frac{R_n}{L} + f(T) * t * v_2 * \left(1 - \frac{U}{100}\right) \right) \quad [\text{mm}] \quad \text{eq. 1}$$

With the dimensionless functions:

$$g(T, v) = \frac{s}{s + \gamma * (1 + 0.34 * v_2)} \quad \text{eq. 2}$$

$$f(T) = \frac{e_s(T)}{s} * \frac{\gamma * 3.75}{T + 273} \quad \text{eq. 3}$$

$$e_s(T) = 6.11 * 10^{\frac{7.48 * T}{237 + T}} \quad \text{eq. 4}$$

with:

- $R_n$  = Net solar radiation [ $\text{J}/\text{cm}^2$ ]
- $L$  = Specific evaporation heat [ $\text{J}/(\text{cm}^2 * \text{mm})$ ]
- $t$  = Timestep [1 day]
- $T$  = Daily average air temperature in  $^{\circ}\text{C}$  (2m above surface)
- $v_2$  = Daily average wind velocity in m/s (2m above surface)

- $U$  = Average daily relative air moisture in % (2m above surface)
- $s$  = Slope of the saturation vapor pressure curve for water
- $\gamma$  = Latitude of catchment area [°]

Based on this approach, a Java application has been created to calculate the “grass-reference-evaporation” per day in the Institute of River and Coastal Engineering at the TUHH. For the application of the tool, the required climate model input data is reduced to:

- The latitude of the project area in [°]
- Precipitation sum [mm/d]
- Average temperature [°C/d]
- Average wind velocity [Beaufort/d]
- Average relative air moisture [%/d]
- Sun shine duration [h/d]

Further processing of climate model data is required to obtain the necessary input data for the tool. In the climate model REMO, the sun shine duration ( $S$ ) in [h/d] is not provided. But with the data series of the global radiation ( $R_G$ ) delivered by the climate models (e.g. REMO or CLM), the following approach is advised with the Ångström – equation to calculate the required sunshine duration data series.

$$R_G = R_0 * \left( a + b * \frac{S}{S_0} \right) \quad [\text{J/cm}^2]$$

**eq. 5**

With:

- $a$  and  $b$  being coefficients of the Ångström – equation ([DVWK 238, 1996](#)); for Germany:

$$a = 0.19$$

$$b = 0.55$$

- $R_G$  = Global radiation [J/cm<sup>2</sup>]
- $R_0$  = Extraterrestrial radiation [J/cm<sup>2</sup>]
- $S$  = Sunshine duration of the day [h]
- $S_0$  = Astronomical possible sunshine duration of the day [h]
- $T$  = Average daily temperature [C°]
- $U$  = Average relative Air Moisture [%/d]

The Ångström – equation can be revised to compute the sun shine duration ( $S$ ):

$$S = \frac{S_0}{b} * \left( \frac{R_G}{R_0} - a \right) \quad [\text{h}]$$

**eq. 6**

For the calculation of the extraterrestrial radiation ( $R_0$ ) and the astronomical sunshine duration ( $S_0$ ) the following equations according to the [DVWK-238 \(1996\)](#) bulletin are supposed:

$$S_0 = 12.3 + \sin \zeta * \left( 4.3 + \frac{\gamma - 51}{6} \right) \quad [\text{h}]$$

**eq. 7**

$$R_0 = 245 * \left[ 9.9 + 7.08 * \sin \xi + 0.18 * (\gamma - 51) * (\sin \zeta - 1) \right] \quad [\text{J/cm}^2]$$

**eq. 8**

$$\zeta = 0.0172 * JT - 1.39$$

**eq. 9**

With:

- $\gamma$  = Latitude of the project area in [ $^\circ$ ] (e.g. Hamburg  $\gamma = \text{ca. } 54^\circ$ )
- $JT$  = Number of the day since the 01.01 of the year

## Attachment 3 Statistical Evaluations

### 3.1 Adjustment of Trends in Data Time Series

The trend magnitude for each value in the data series can be computed e.g. with the function TREND() in the Microsoft-Office-Program EXCEL. The required variables in the function are the data values of the time series (e.g. peak discharge [m<sup>3</sup>/s] or rainfall intensity [mm/h]) as matrix of  $Y_k$  (ordinate) and the dates of the time series as matrix of  $X_k$  (abscissa) (Fig. 1). With the function TREND () the resulting value on the trend line for each point in the data series is computed.

| Partielle Serie [2040 - 2070] A1B Scenario |            |                               |                |  |                   |   |   |   |
|--|------------|-------------------------------|----------------|--|-------------------|---|---|---|
|  | $X_k$      | $Y_k$                         | $Y_{k\_trend}$ | $Y_k'$                                     |                   |   |   |   |
| counter                                    | Date       | Discharge [m <sup>3</sup> /s] | Trend Value    | trend adjusted value                       |                   |   |   |   |
| k  |            |                               |                | 1  | 2                 | 3 | 4 | 5 |
| 1  | 03/01/2040 | 12.985                        | 10.35006835    | =TREND(\$C\$9:\$C\$162,\$B\$9:\$B\$162,B9) |                   |   |   |   |
| 2  | 14/02/2040 | 10.375                        | 10.35190876    | 10.6204                                    | 2.36278           |   |   |   |
| 3  | 10/08/2040 | 7.339                         | 10.35971708    | 7.5766                                     |                   |   |   |   |
| 4  | 19/09/2040 | 23.307                        | 10.36147176    | 23.5429                                    | =-\$D\$83-D11+C11 |   |   |   |
| 5  | 18/12/2040 | 8.635                         | 10.36541979    | 8.8669                                     | 2.18233           |   |   |   |
| 6  | 25/01/2041 | 7.94                          | 10.36708673    | 8.1703                                     | 2.10050           |   |   |   |
| 7  | 18/04/2041 | 7.147                         | 10.37072769    | 7.3736                                     | 1.99791           |   |   |   |
| 8  | 23/07/2041 | 5.696                         | 10.37493892    | 5.9184                                     | 1.77807           |   |   |   |
| 9  | 26/09/2041 | 8.073                         | 10.37779027    | 8.2926                                     | 2.11536           |   |   |   |
| 10   | 03/11/2041 | 18.297                        | 10.37945722    | 18.5149                                    | 2.91858           |   |   |   |
| 11   | 02/03/2042 | 14.291                        | 10.38467739    | 14.4937                                    | 2.67371           |   |   |   |
| 12   | 07/05/2042 | 4.662                         | 10.3875726     | 4.8718                                     | 1.58346           |   |   |   |
| 13   | 07/06/2042 | 6.482                         | 10.38893248    | 6.6904                                     | 1.90068           |   |   |   |
| 14   | 30/06/2042 | 14.014                        | 10.38994142    | 14.2214                                    | 2.65475           |   |   |   |

Fig. 1 Example of a trend adjustment.

The magnitude of the trend adjustment ( $Y_k'$ ) is computed by calculating the difference between the reference value on the trend line ( $Y_{reference}$ ) and the considered value of the data time series ( $Y_{k\_trend}$ ). This difference is added to the respective value in the data series  $Y_k$  (Fig. 1).

$$\begin{aligned}
 Y_1' &= Y_{reference} - Y_{1\_trend} + Y_1 \\
 Y_2' &= Y_{reference} - Y_{2\_trend} + Y_2 \\
 Y_3' &= Y_{reference} - Y_{3\_trend} + Y_3 \\
 &\dots \\
 Y_k' &= Y_{reference} - Y_{k\_trend} + Y_k
 \end{aligned}$$

### 3.2 Statistical Evaluation of Extreme Rainfall Events with Partial Series

The Exponential-Distribution function for partial series of extreme rainfall events is defined according to the KOSTRA-Atlas (1997) and ATV-A 121 (1985):

$$h_{P(T_n, D)} = u_p(D) + w_p(D) * \ln(T) \tag{eq. 1}$$

With:

- $h_p$  = Rainfall height [mm]
- $T$  = Assumption of the return period (“plotting position”)[a]
- $u_p$  and  $w_p$  = Parameters of the distribution function
- $D$  = Duration [h]

The assumption of the return period ( $T_n$ ) with partial series is done with the following equation (KOSTRA-Atlas, 1997; ATV-A 121, 1985):

$$T_k(D) = \frac{N + 0.2}{k - 0.4} * \frac{M}{N} \quad \text{eq. 2}$$

With:

- $M$  = Length of the data series [a]
- $D$  = Duration of rainfall [h]
- $N$  = Number of values in the data series
- $k$  = Index of the data series sorted according to the magnitude
  - $k = 1$  as largest value
  - $k = N$  as smallest value

It is recommended to set up partial series with a number of values ( $N$ ) between 2 to 3 times the lengths of the covered time period ( $M$ ) in years, or it can be calculated with the equation given in the KOSTRA-Atlas (1997):

$$N = e * M \quad \text{eq. 3}$$

- $M$  = length of the data series [a]
- $N$  = number of values in the data series
- $e$  = EULER’s number (2.718)

For the analysis of climate change impacts it is important to differentiate between the summer and winter rainfall events. For this purpose it is “suggested” in this thesis to use a number of at least two to three events ( $N$ ) per winter and summer period for each year in the time period ( $M$ ).

Example:

In a partial series with a time period length of  $M = 30$  years and a number of  $N = e * 30 = 81.55$  (ca. 82) values, the return period of the largest and smallest value in the partial series is assumed to  $T_1 = 50.12$  and  $T_{82} = 0.37$ .

The calculation of the parameters of the distribution function  $w_p$  and  $u_p$  can be done with the equations given in the ATV-A 121 (1985) or graphically according to KOSTRA-Atlas (1997).

Mathematical calculation of  $u_p$  and  $w_p$  (ATV-A 121, 1985):

$$w_p = \frac{\sum_{k=1}^N (h_{p,k} * Ln(T_k) - L * \overline{h_p} * \overline{Ln(T)})}{\sum_{k=1}^N ((Ln(T_k))^2 - N * (\overline{Ln(T)})^2)} \quad \text{eq. 4}$$

$$u_p = \overline{h_p} - w_p * \overline{Ln(T)} \quad \text{eq. 5}$$

With the arithmetical averages of  $h_p$  and  $Ln(T)$ :

$$\overline{h_p} = \frac{1}{N} * \sum_{k=1}^N h_{p,k} \quad \text{eq. 6}$$

$$\overline{Ln(T)} = \frac{1}{L} * \sum_{k=1}^N (Ln(T_k)) \quad \text{eq. 7}$$

Additionally to the mathematical calculation of the parameters  $w_p$  and  $u_p$  the graphical illustration of the probability distribution should be done (ATV-A 121, 1985).

Graphical determination of  $u_p$  and  $w_p$  (KOSTRA-Atlas, 1997):

The precipitation heights ( $h_p$ ) are plotted into a graph with the values of  $h_p$  on the ordinate and the values of  $Ln(T)$  on the abscissa. Through the plotted series of data with assumed return periods, a distribution curve is determined as regression line. The parameter of the distribution function  $u_p$  is the intercept on the ordinate ( $h_p$ ) for  $Ln(T) = 0$ , and  $w_p$  is the slope of the distribution curve.

Example:

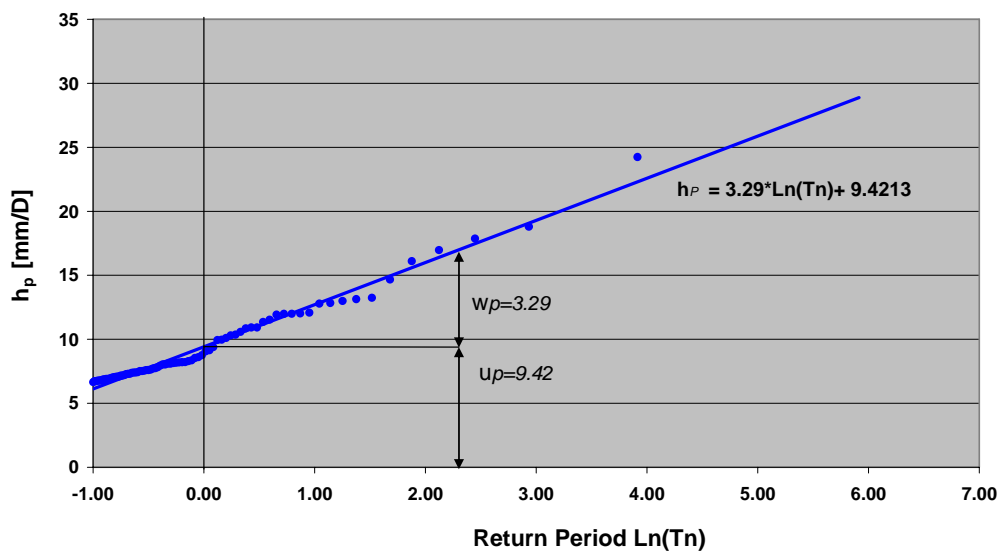


**Fig. 2 Graphical determination of the parameters of the distribution function  $w_p$  and  $u_p$ .**

The determination of the return period (T) of a specific precipitation height ( $h_p$ ) can be optimised by transferring the logarithmical illustration to a non-logarithmical graph. This can be done by calculating a series of significant return periods of  $h_p$  with the determined exponential distribution equations.

For example the logarithmical graph of the example above is transferred with the exponential distribution equation  $h_p(T, D) = 3.29 * \ln(T) + 9.42$  to the probability distribution curve illustrated in Fig. 3.

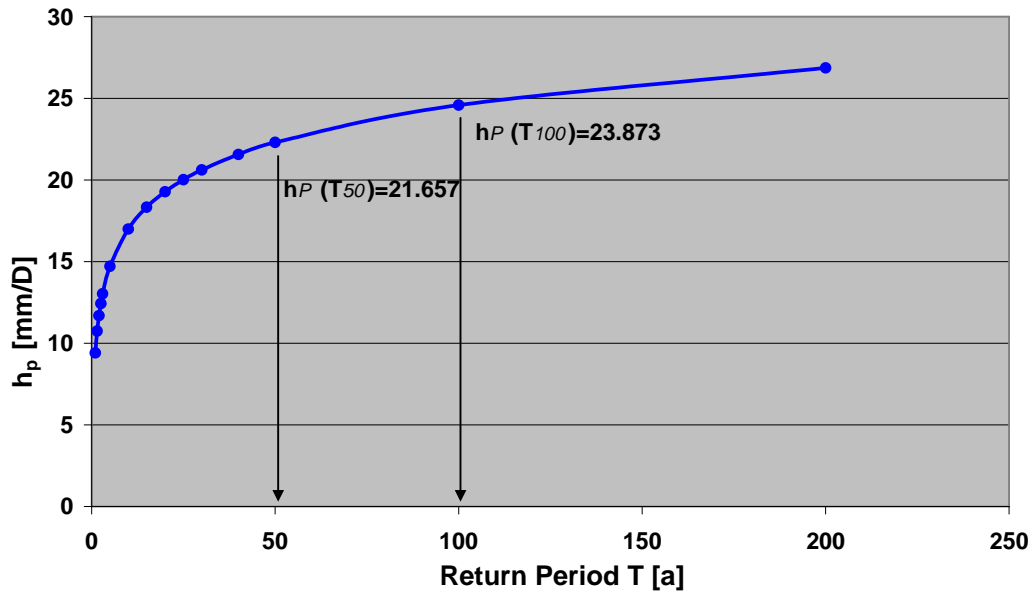


**Fig. 3 Probability distribution curve.**

According to the [ATV-A 121 \(1985\)](#) the rainfall volume ( $r_{D;n}$  in [l/s\*ha]) is defined for the specific duration (D) and return period (T) of the rainfall event  $h_p$  with:

$$r_{D,n} = 166.6 \cdot \frac{h_p}{D}$$

With:

- $r_{D,n}$  = rainfall volume in [l/s\*ha]
- $h_p$  = rainfall height [mm]
- $D$  = duration [min]

## Attachment 4

## Grubbs Test Values (G) (DIN 53 804)

(Table adopted from [TU Dresden, 2009](#))

n = number of values in the statistical evaluation

| n  | G               |                 | n   | G               |                 |
|----|-----------------|-----------------|-----|-----------------|-----------------|
|    | Significance    |                 |     | Significance    |                 |
|    | $\alpha = 0.05$ | $\alpha = 0.01$ |     | $\alpha = 0.05$ | $\alpha = 0.01$ |
| 3  | 1.153           | 1.155           | 29  | 2.73            | 3.085           |
| 4  | 1.463           | 1.492           | 30  | 2.745           | 3.103           |
| 5  | 1.672           | 1.749           | 35  | 2.811           | 3.178           |
| 6  | 1.822           | 1.944           | 40  | 2.866           | 3.24            |
| 7  | 1.938           | 2.097           | 45  | 2.914           | 3.292           |
| 8  | 2.032           | 2.221           | 50  | 2.956           | 3.336           |
| 9  | 2.11            | 2.323           | 55  | 2.992           | 3.376           |
| 10 | 2.176           | 2.41            | 60  | 3.025           | 3.411           |
| 11 | 2.234           | 2.485           | 65  | 3.055           | 3.442           |
| 12 | 2.285           | 2.55            | 70  | 3.082           | 3.471           |
| 13 | 2.331           | 2.607           | 75  | 3.107           | 3.496           |
| 14 | 2.371           | 2.659           | 80  | 3.13            | 3.521           |
| 15 | 2.409           | 2.705           | 85  | 3.151           | 3.543           |
| 16 | 2.443           | 2.747           | 90  | 3.171           | 3.563           |
| 17 | 2.475           | 2.785           | 95  | 3.189           | 3.582           |
| 18 | 2.504           | 2.821           | 100 | 3.207           | 3.6             |
| 19 | 2.532           | 2.854           | 105 | 3.224           | 3.617           |
| 20 | 2.557           | 2.884           | 110 | 3.239           | 3.632           |
| 21 | 2.58            | 2.912           | 115 | 3.254           | 3.647           |
| 22 | 2.603           | 2.939           | 120 | 3.267           | 3.662           |
| 23 | 2.624           | 2.963           | 125 | 3.281           | 3.675           |
| 24 | 2.644           | 2.987           | 130 | 3.294           | 3.688           |
| 25 | 2.663           | 3.009           | 135 | 3.309           | 3.7             |
| 26 | 2.681           | 3.029           | 140 | 3.318           | 3.712           |
| 27 | 2.698           | 3.049           | 145 | 3.328           | 3.723           |
| 28 | 2.714           | 3.068           |     |                 |                 |

## Attachment 5.1

### Definitions and Auxiliary Explanations

Definitions and auxiliary explanations of the variables used in the Nassi-Shneiderman diagrams:

*List of Variables:*

- anzlayy = Number of layers: here 4
- depth = Layer thickness [mm]
- drd = Diameter of rainfall down pipe ( $d_{\text{downpipe}}$ )
- flaech\_entw\_gr = Initial drained area per outlet pipe [m<sup>2</sup>]
- flaechgr = Sum of green roof areas per sub-catchment [m<sup>2</sup>]
- gr\_drain\_diff = Difference of soil water, which can not be drained through the outlet pipe in that time step and is retained in the soil layer [mm]
  
- gr\_qabvs = Actual flow through the outlet pipe [mm]
- gr\_teil = Uncorrected drained roof area [m<sup>2</sup>]
- gr\_teil\_diff = Difference of the drained green roof area [m<sup>2</sup>] between the overall green roof area (flaechgr) and the sum of uncorrected drained roof areas (gr\_teil)
  
- gr\_teil\_entw = Corrected drained roof area [m<sup>2</sup>]
- gr\_teil\_faktor1 = Uncorrected number of outlet pipes per sub-catchment
- gr\_teil\_faktor2 = Corrected number of outlet pipes per sub-catchment
- h\_over\_gr = Height of the overflow pipe [mm]
- hw(layer) = Water level in layer [mm]
- hw\_ex = Water level above the overflow pipe [mm]
- Inf (layer) = Infiltration of water into the layer [l/m<sup>2</sup>]
- ks = Roughness of pipes [mm]
- $\lambda$  = Flow resistance (Colebrook White equation) [-]
- nfk = Usuable field capacity [l/m<sup>2</sup>]
- $\mu$  = Overflow coefficient (Poleni equation) [-]
- perkl(layer) = Percolation from the layer above [l/m<sup>2</sup>]
- prest = Additional water volume in the layer [l/m<sup>2</sup>]
- pri = Effective rainfall on the roof area [l/m<sup>2</sup>]
- prinp = Potential water inflow volume into the layer per timestep [l/m<sup>2</sup>]
  
- pors\_eff = Effective porosity [%]
- pstau(layer) = Retained water in the layer above the regarded one [l/m<sup>2</sup>]
- pstau\_over = Water volume which cause on overload of the green roof [l/m<sup>2</sup>]
  
- q\_gr\_drain/over = Potential flow trough all outlet pipes [mm]
- q\_gr\_teil\_drain/ex = Potential flow per outlet pipe [mm<sup>3</sup>/s]
- Q\_max = Flow calculated with the Colebrook White equation [mm<sup>3</sup>/s]
  
- Q\_poleni = Flow calculated with the Poleni equation [mm<sup>3</sup>/s]
- sw (layer) = Soil moisture of the layer (in core: bf) [l/m<sup>2</sup>]
- sw\_fk(layer) = Soil water in the layer up to the field capacity [l/m<sup>2</sup>]
- sw\_free(layer) = Free moveable water content in the soil layer [l/m<sup>2</sup>]

- `sum_hw` = Total water level in the layers of the green roof [mm]
- `sum_hw_ov` = Actual water level in the storage layer of the roof [mm]
- `sw_max (layer)` = Maximal soil moisture of the layer, without the water volume up to the wilting point (in core: `bfmax`) [l/m<sup>2</sup>]
- `sw_max_free(layer)` = Maximal free moveable water content in the soil layer [l/m<sup>2</sup>]
- `sw_max_total` = Maximal soil water content inclusive the water volume up to the wilting point [l/m<sup>2</sup>]
- `sw_sat (layer)` = Actual soil water content in the saturated zone of the layer [l/m<sup>2</sup>]
- `sw_wp (layer)` = Soil water content up to the wilting point [l/m<sup>2</sup>]
- `Δt` = Internal simulation time step [s]

***Important constants:***

- L1 = Storage layer = Layer 1
- L1 = Substrate layer = Layer 2
- L3 = Filter layer = Layer 3
- L4 = Fictive roof layer = Layer 4

*“variable (layer)” : the variable is defined as an array over the layers. The variable for the first, the storage layer, of the green roof would be defined as “variable (1)” and the variable for the second, the substrate layer, of the green roof is defined as “variable (2)”.*

*Note of units:*

- [mm] = [l/m<sup>2</sup>]

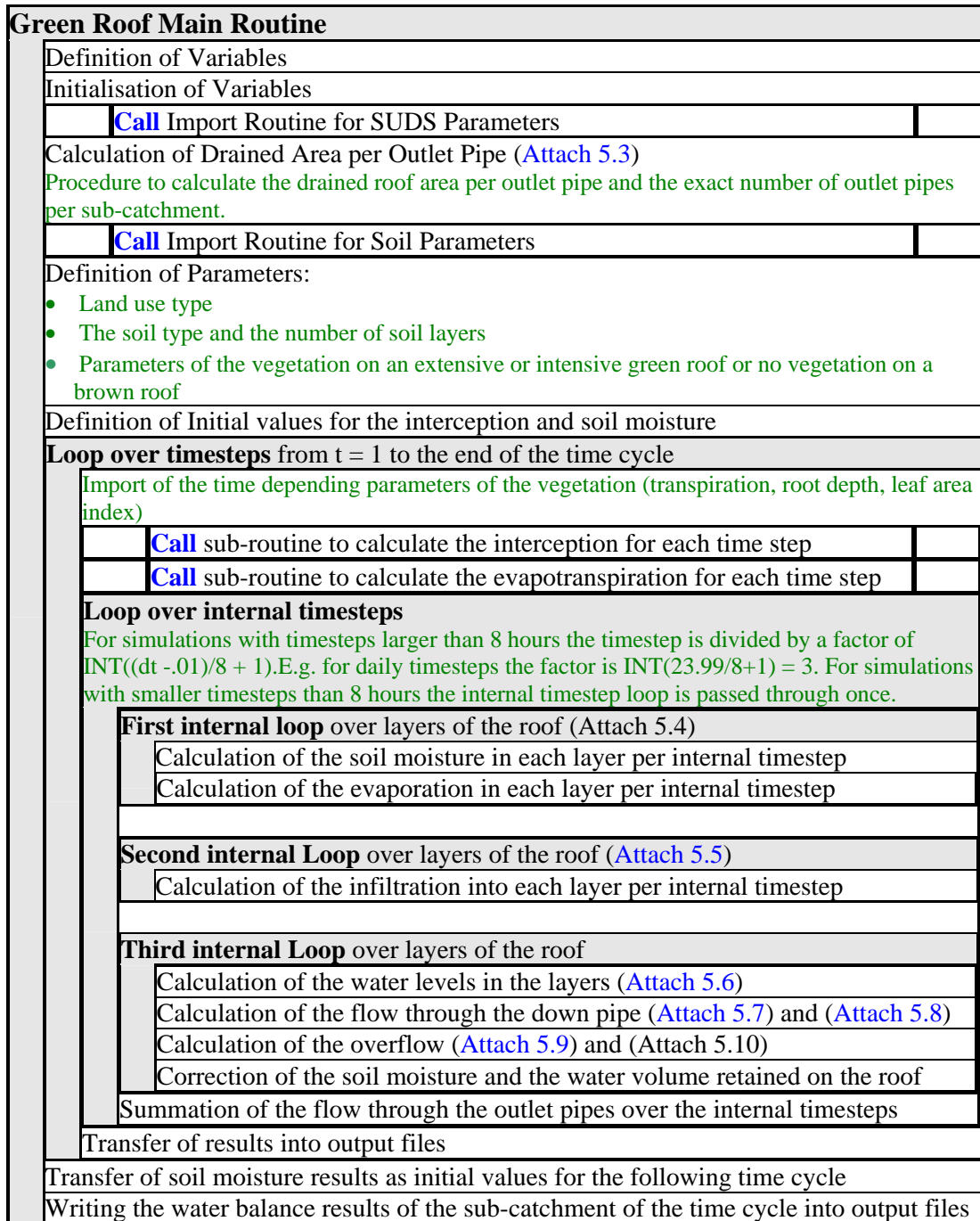
***Important Functions:***

- `INT(value or calculation)` The integer of the value or the result of a calculation is given
- `MIN (variable, variable,...)` Intrinsic function to determine the minimal value of the variables

*The initialisations and summations are not depicted in the Nassi-Shneiderman diagrams. A focus was set on the significant processes for the calculation of the water balance in the layers of the green roof and the flow through the outlet pipes.*

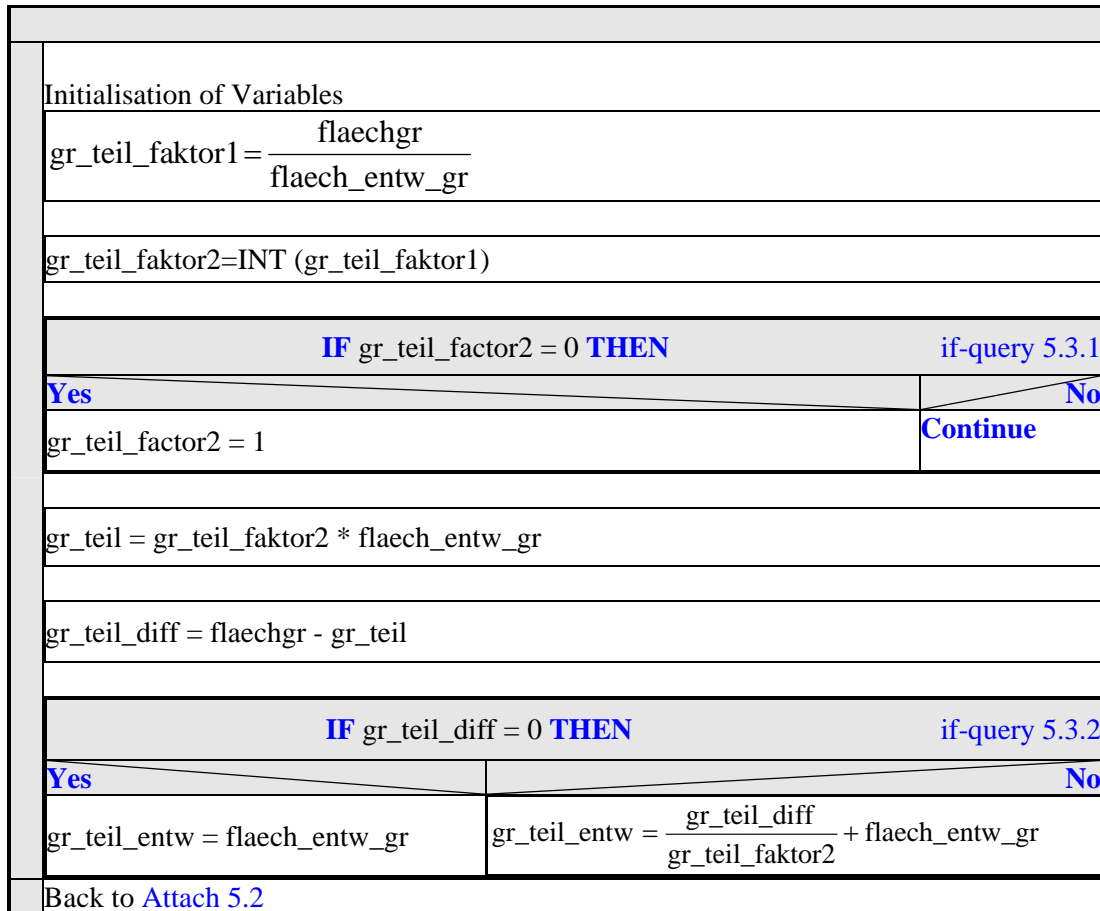
## Attachment 5.2

## Nassi-Shneiderman-Diagram: Green Roof Main Routine



## Attachment 5.3

## Nassi-Shneiderman-Diagramm: Drained Area per Outlet Pipe

**Important Variables:**

flaech\_entw\_gr = Initial drained area [m<sup>2</sup>] per outlet pipe  
 flaechgr = Sum of green roof areas per sub-catchment [m<sup>2</sup>]

gr\_teil = Uncorrected drained roof area [m<sup>2</sup>]  
 gr\_teil\_diff = Difference of the drained green roof area [m<sup>2</sup>] between the overall green roof area (flaechgr) and the sum of uncorrected drained roof areas (gr\_teil)  
 gr\_teil\_entw = Corrected drained roof area [m<sup>2</sup>]

gr\_teil\_faktor1 = Uncorrected number of outlet pipes per sub-catchment  
 gr\_teil\_faktor2 = Corrected number of outlet pipes per sub-catchment

**Example 1:**

In a sub-catchment an overall green roof area of 2000m<sup>2</sup> (=flaechgr) is defined whereas the outlet pipes are designed with a diameter of 100mm (=drd). A roof area

of 300m<sup>2</sup> (=flaech\_entw\_gr) can be drained per outlet pipe. The number of necessary outlet pipes (= gr\_teil\_factor1) is 6.67 (=2000m<sup>2</sup>/300m<sup>2</sup>). This number of outlet pipes is converted to an integer of 6 (=gr\_teil\_factor2) with the function INT (gr\_teil\_factor1) and used to calculate the roof area drained by 6 outlet pipes (gr\_teil) 1800m<sup>2</sup> (= 6 x 300m<sup>2</sup>).

The difference of 200m<sup>2</sup> (gr\_teil\_diff) between the partial area (gr\_teil = 1800m<sup>2</sup>) and the overall green roof area in the sub-catchment (2000m<sup>2</sup>) have to be drained additionally by the 6 outlet pipes. In the ‘if query’ (5.3.2) the average sub area drained per outlet pipe results to 333.3 m<sup>2</sup> (=gr\_teil\_entw) by dividing the additional sub-area of 200m<sup>2</sup> (=gr\_teil\_diff) by 6 outlet pipes (=gr\_teil\_factor2) and adding this to the initial drained area per outlet pipe of 300m<sup>2</sup> (= flaech\_entw\_gr).

**Results:**

The corrected drained green roof sub-area per outlet pipe is 333.3 m<sup>2</sup>.

The exact number of outlet pipes in the sub-catchment area is 6.

**Example 2:**

In a sub-catchment an overall green roof area of 100m<sup>2</sup> (= flaechgr) is defined, but in this example the initial area drained per pipe is 150m<sup>2</sup> (flaech\_entw\_gr). The number of necessary outlet pipes (gr\_teil\_factor1) is 0.67 (=100m<sup>2</sup>/150m<sup>2</sup>). This number of outlet pipes is converted to an integer of 0.00 (=gr\_teil\_factor2) with the function INT (gr\_teil\_factor1). The calculation with a zero number of outlet pipes would result in an error of the model and not correct results. Therefore, the number of outlet pipes is corrected to 1 in the ‘if-query’ (5.3.1).

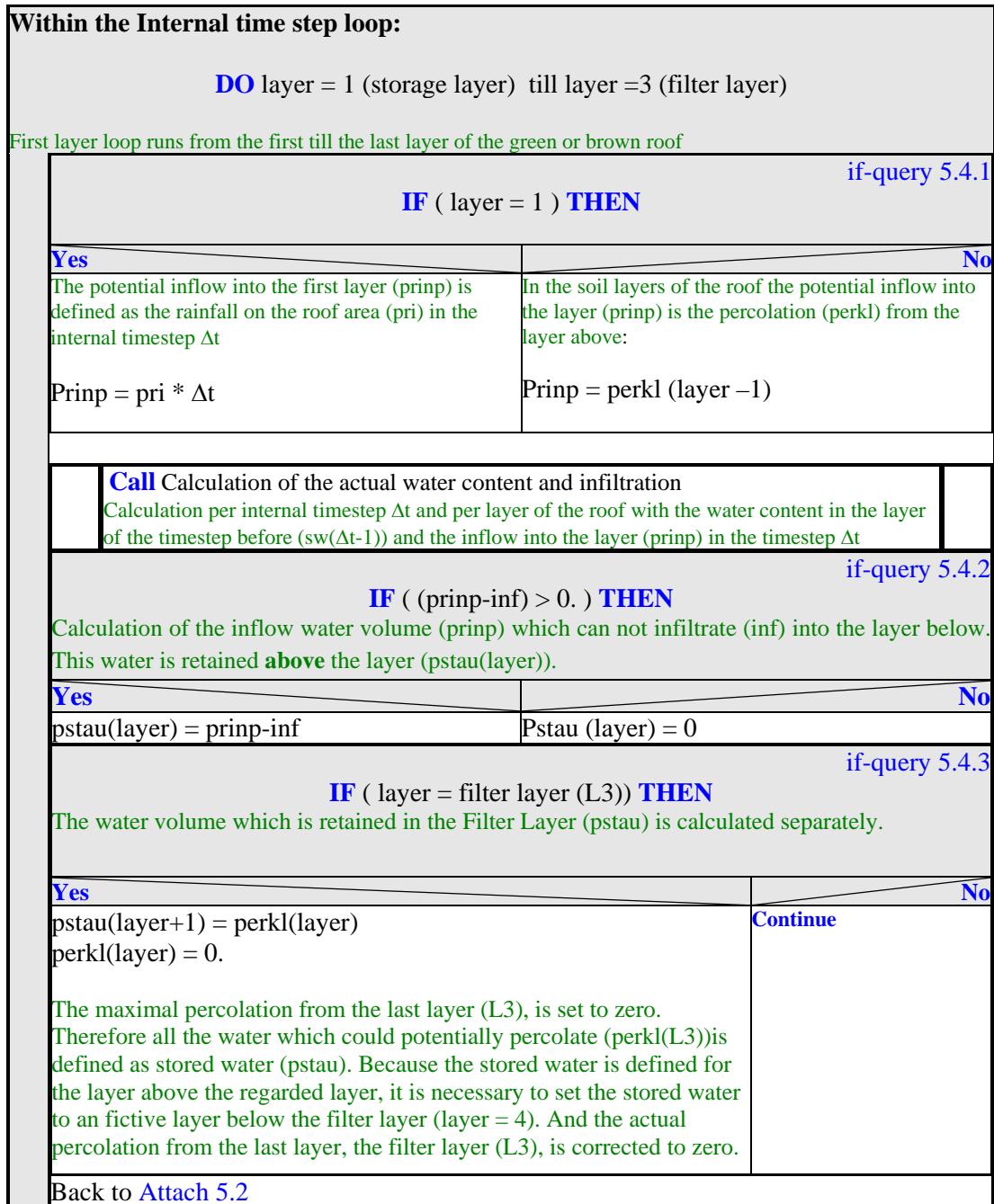
The negative difference of 50m<sup>2</sup> between the initial drained area (gr\_teil = 150m<sup>2</sup>) and the overall green roof area in the sub-catchment (100m<sup>2</sup>) have to be subtracted from the drained green roof area. When the overall green roof area is smaller than the initial drained green roof area, the actual drained area per outlet pipe is equal to the overall green roof area in the sub-catchment.

**Results:**

The drained green roof area per outlet pipe is 100 m<sup>2</sup> by one outlet pipe and one overflow pipe in the sub-catchment.

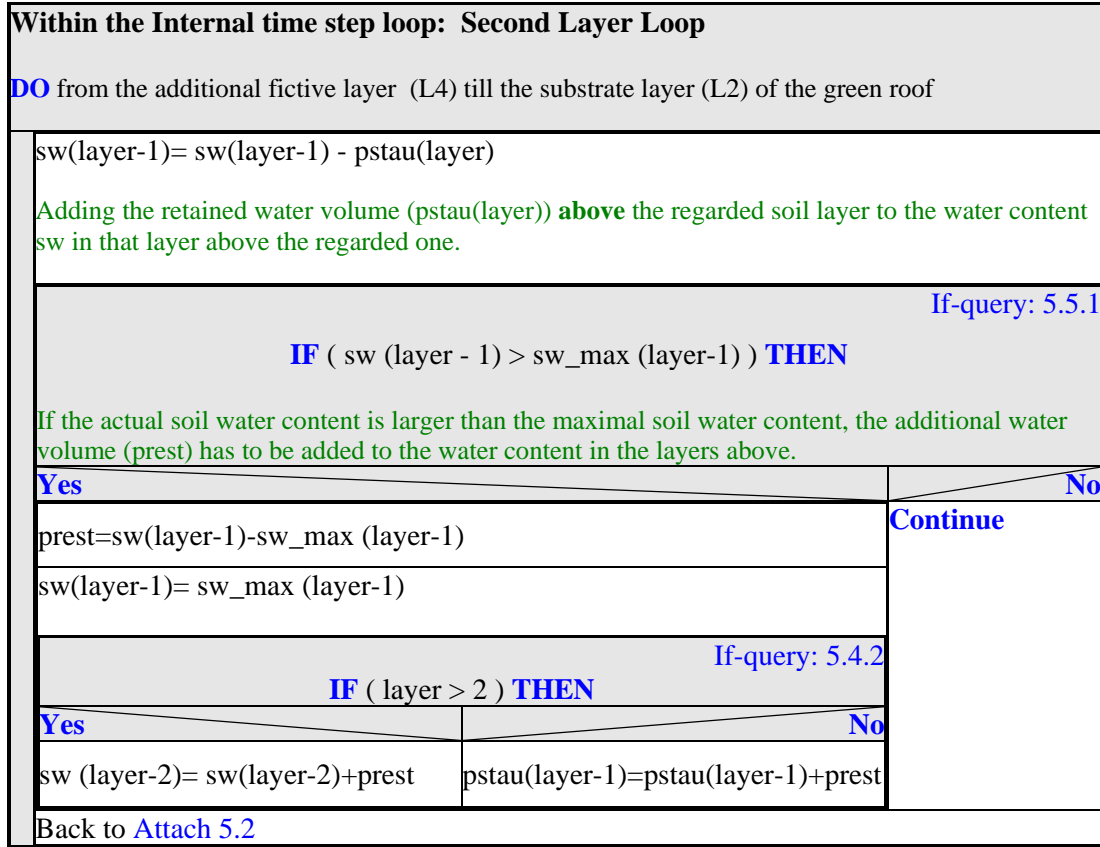
## Attachment 5.4

## Nassi-Shneiderman-Diagram: First Internal Layer Loop



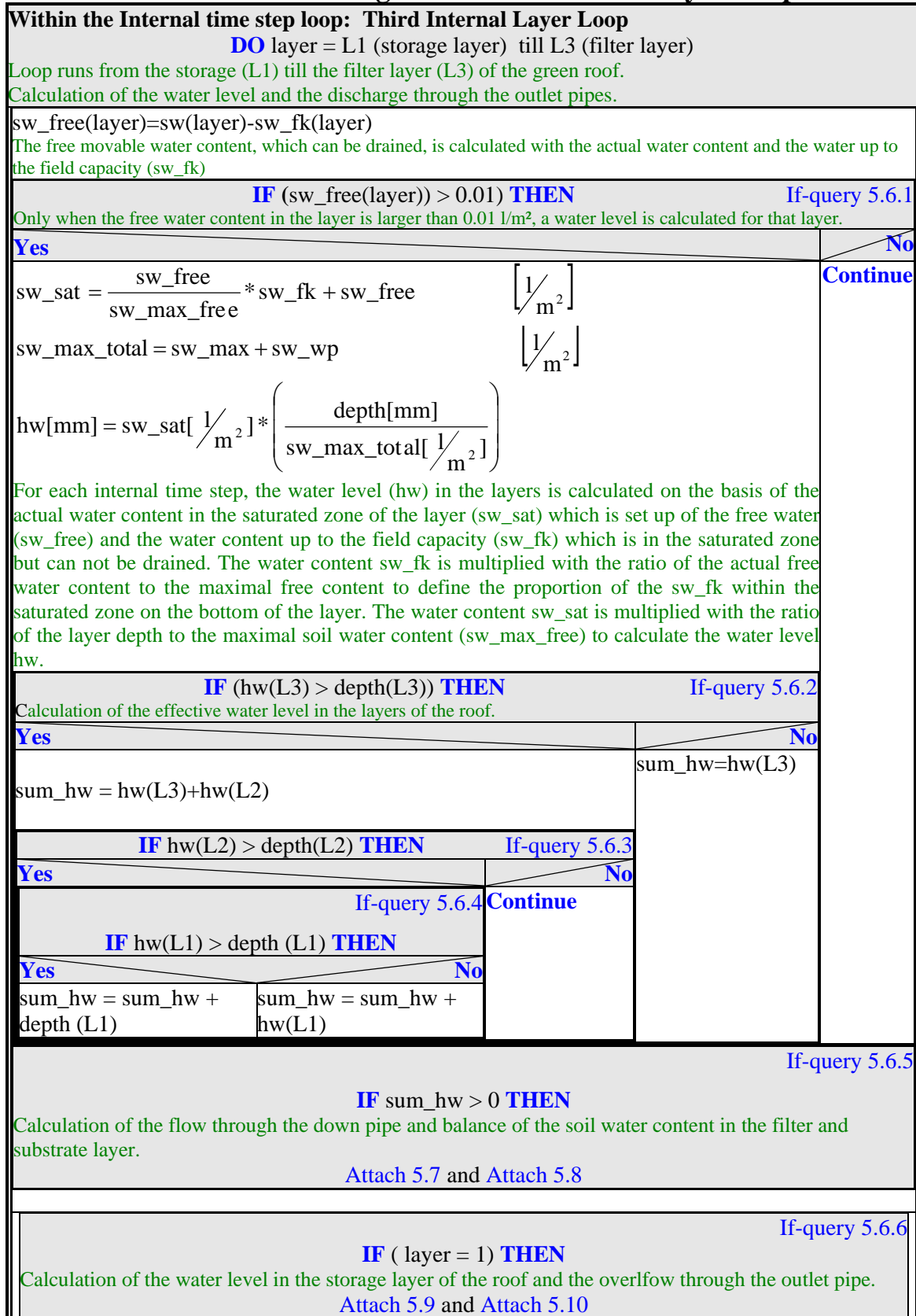
## Attachment 5.5

### Nassi-Shneiderman-Diagram: Second Layer Loop



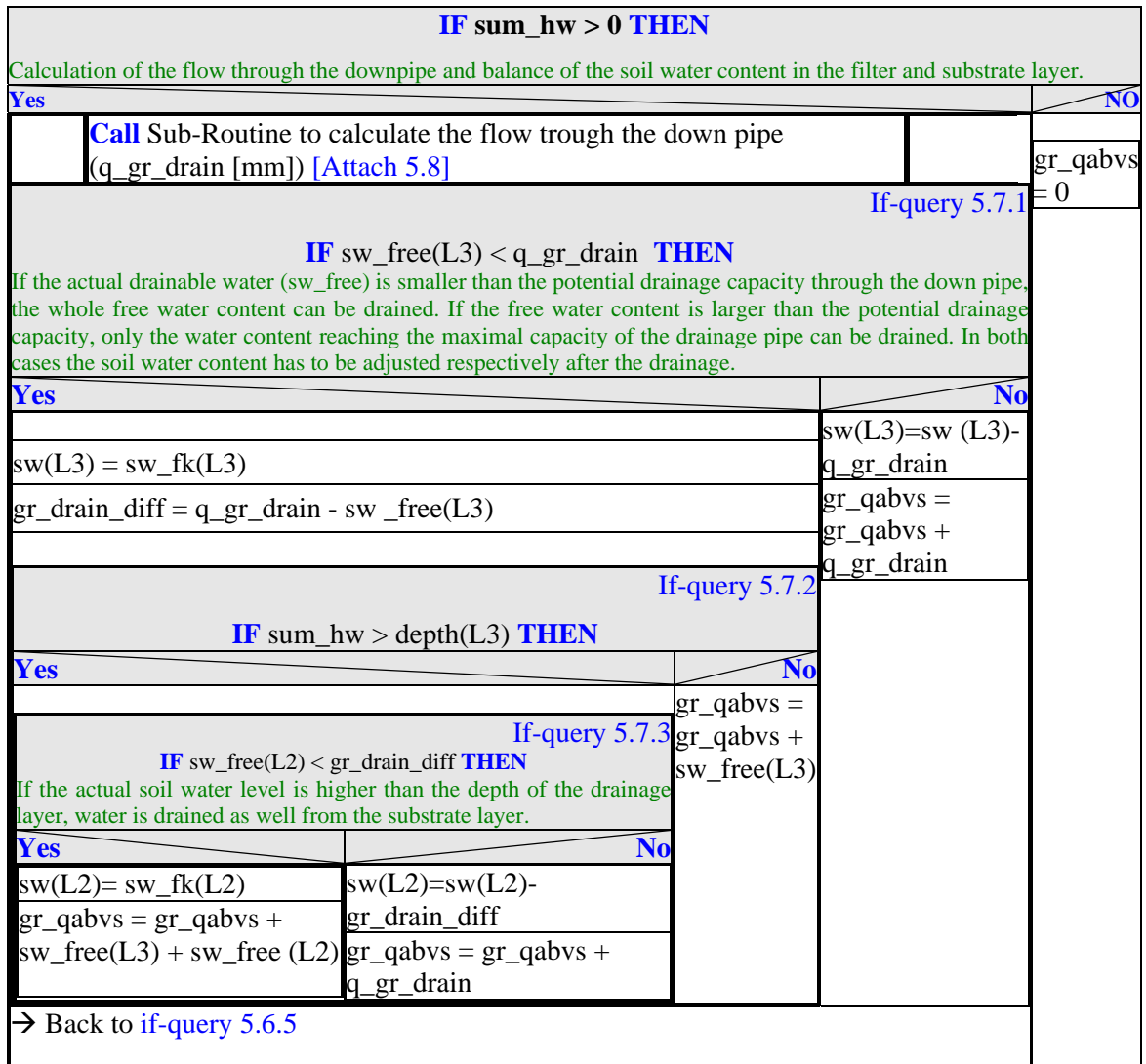
## Attachment 5.6

## Nassi-Shneiderman-Diagram: Third Internal Layer Loop

→ Back to [Attach 5.2](#)

## Attachment 5.7

### Nassi-Shneiderman-Diagram: Water Balance in Drainage and Substrate Layer



## Attachment 5.8

## Nassi-Shneiderman-Diagram: Flow Through Down Pipe

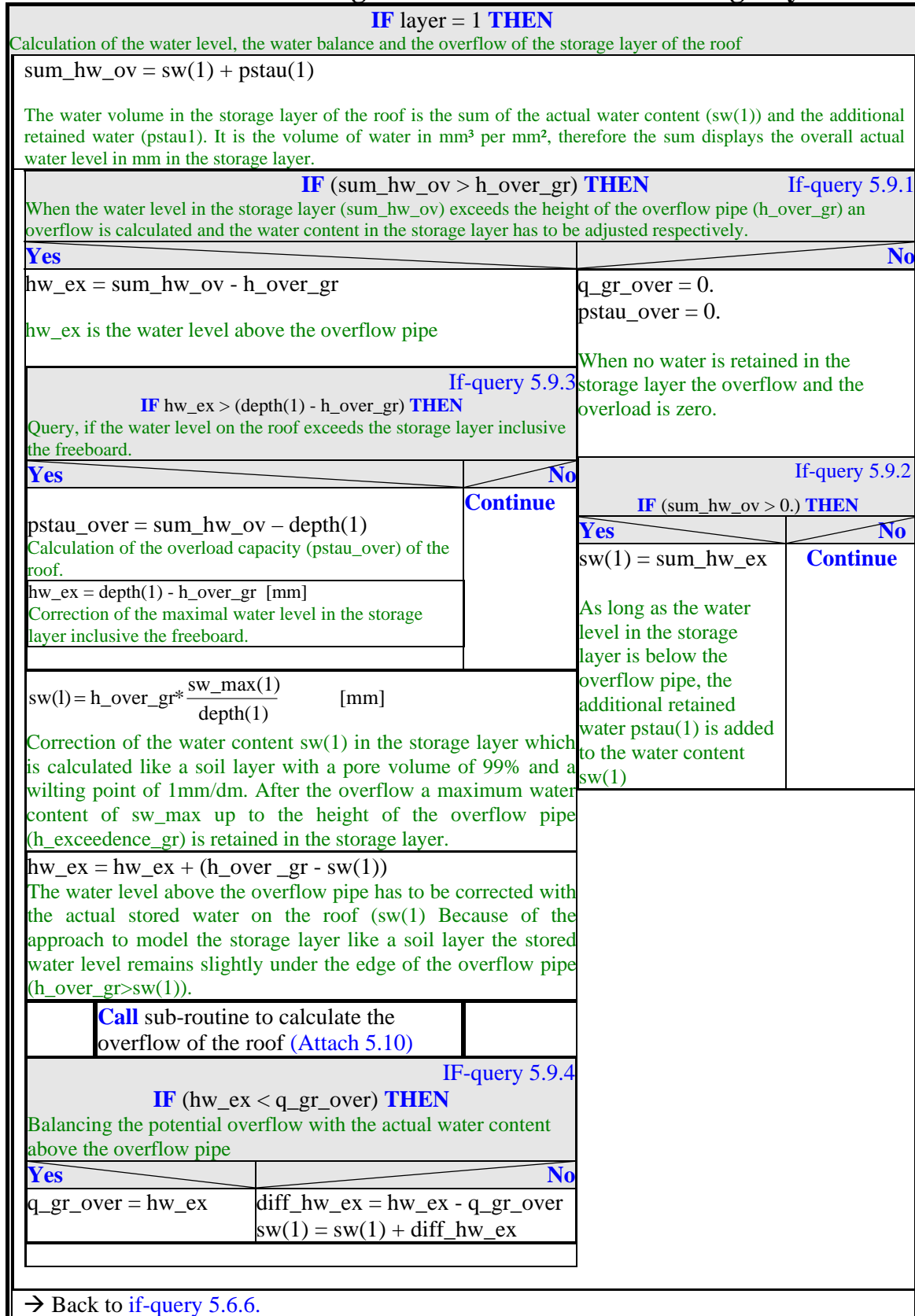
|  |   |
|--|---|
| Calculation of the flow through the down pipe in a separate sub-routine  |   |
| <b>IF</b> sum_hw < depth(L3) <b>THEN</b>   |   |
| Calculation of the effective porosity according to the height of the effective water level in the soil layers of the roof.   |   |
| <b>Yes</b>   | <b>No</b>   |
| $\text{Pors\_eff} = \frac{\text{sw\_max}(3)}{100} \quad [\%]$  | $\text{Pors\_eff} = \frac{\text{sw\_max}(3) + \text{sw\_max}(2)}{2 * 100} \quad [\%]$ |
| Calculation of the flow with the Poleni equation.  |   |
| $Q\_Poleni = \frac{2}{3} * \pi * d_{\text{downpipe}} * \mu * \sqrt{2 * g * (\text{sum\_hw})^{3/2}} * \text{pors\_eff} \quad [\text{mm}^3/\text{s}]$  |   |
| According to BWK, 1999 page 52 for overflow obstructions of a height of zero the coefficient $\mu = 0.577$   |   |
| Calculation of the flow resistance in the pipe according to Colebrook White equation for turbulent flow: $\text{drd} = d_{\text{downpipe}}$  |   |
| $\frac{1}{\sqrt{\lambda}} = -2 * \lg \left( \frac{ks / d_{\text{downpipe}}}{3.71} \right)$   |   |
| Calculation of the maximal flow through the rainfall downpipe:   |   |
| $Q\_max = \frac{\pi * (d_{\text{downpipe}})^2}{4} \sqrt{2 * g * d_{\text{downpipe}} * \frac{1}{\lambda}} \quad [\text{mm}^3/\text{s}]$   |   |
| $q\_gr\_teil\_drain = \text{MIN} ( Q\_poleni, Q\_max )$  |   |
| MIN = Intrinsic function to determine the minimal flow through one rainfall downpipe   |   |
| $q\_gr\_drain [\text{mm}] = \underbrace{q\_gr\_teil\_drain [\text{mm}^3/\text{s}]}_{\text{step1}} * \underbrace{gr\_teil\_faktor2 * 3600 [\text{s}/\text{h}]}_{\text{step2}} * \underbrace{\Delta t [\text{h}]}_{\text{step3}} * \frac{1}{(\text{flaech\_entw\_gr} [\text{mm}^2])}$  |   |
| Calculation of the flow through all downpipes in the catchment per internal timestep $\Delta t$ in [h] and per $\text{mm}^2$ of the average drained roof area per downpipe. This has to be multiplied with the number of downpipes in the sub-catchment to gain the overall discharge through all the downpipes in the sub-catchment.<br>( $\rightarrow$ variables explained in ATTACH 5.1 and in the chapter 4 of thesis) |   |
| $\rightarrow$ Back to <a href="#">Attach 5.7</a>   |   |

Note:

The derivation of the equations is outlined in [Attach 5.11](#).

## Attachment 5.9

### Nassi-Shneiderman-Diagram: Water Balance in Storage layer



## Attachment 5.10

## Nassi-Shneiderman-Diagram: Flow Through Overflow Pipe

| Calculation of the flow through the overflow pipe   |  |
|---|--|
| Calculation of the overflow with the Poleni equation.   |  |
| $Q_{\text{Poleni}} = \frac{2}{3} * \pi * d_{\text{pipe}} * \mu * \sqrt{2 * g * (hw_{\text{ex}})^{3/2}} \quad [\text{mm}^3/\text{s}]$  |  |
| According to <a href="#">BWK (1999) page 52</a> for the flow over obstructions with larger losses, because of a larger height ( $h_{\text{over\_gr}}$ ) compared to the water level ( $hw_{\text{ex}}$ ) above the pipe, the <b>coefficient <math>\mu</math> is about 0.480</b>   |  |
| Calculation of the flow resistance in the overflow pipe:  |  |
| $\frac{1}{\sqrt{\lambda}} = -2 * \lg \left( \frac{ks / d_{\text{pipe}}}{3.71} \right)$  |  |
| Calculation of the maximal flow through the rainfall downpipe.  |  |
| $Q_{\text{max}} = \frac{\pi * (d_{\text{pipe}})^2}{4} \sqrt{2 * g * d_{\text{pipe}} * \frac{1}{\lambda}} \quad [\text{mm}^3/\text{s}]$  |  |
| $q_{\text{gr\_teil\_ex}} = \text{MIN} (Q_{\text{wehr}}, Q_{\text{max}})$  |  |
| Intrinsic function to determine the minimal flow through one rainfall downpipe  |  |
| $q_{\text{gr\_over}} [\text{mm}] = \underbrace{q_{\text{gr\_teil\_ex}} [\text{mm}^3/\text{s}] * gr_{\text{teil\_faktor2}}}_{\text{step1}} * \underbrace{3600 [\text{s/h}] * \Delta t [\text{h}]}_{\text{step2}} * \underbrace{\frac{1}{(flaech_{\text{entw\_gr}} [\text{mm}^2])}}_{\text{step3}}$   |  |
| Calculation of the overflow through all pipes in the catchment per internal timestep $\Delta t$ in [h] and per $\text{mm}^2$ of the average drained roof area per overflow pipe. This has to be multiplied with the number of overflow pipes in the sub-catchment to gain the overall flow through all the overflow pipes in the sub-catchment. |  |

→ Back to [Attach 5.9](#)

Note:

Derivations of the equations are depicted in [Attach 5.11](#)

## Attachment 5.11 Derivation of Equations

### 5.11.1. The Poleni equation is derived according to the [BWK, 1999](#):

$$Q_{\text{Poleni}} = \frac{2}{3} * w * \mu * \sqrt{2 * g * (\text{sum\_hw})^{3/2}}$$

The parameters are explained in [Attach 5.1](#).

(w = width of a weir)

It is assumed that the porosity in the soil material reduces the flow. Therefore, the equation is multiplied with the effective porosity:

$$Q_{\text{Poleni}} = \frac{2}{3} * w * \mu * \sqrt{2 * g * (\text{sum\_hw})^{3/2}} * \text{pors\_eff}$$

Further on, the “weir” on the green roof is considered as the inflow into the pipe with the width of the perimeter of the pipe ( $\pi * d_{\text{pipe}}$ ):

$$Q_{\text{Poleni}} = \frac{2}{3} * \pi * d_{\text{pipe}} * \mu * \sqrt{2 * g * (\text{sum\_hw})^{3/2}} * \text{pors\_eff}$$

### 5.11.2 Maximal flow capacity of a pipe is calculated with the Colebrook White approach:

The Colebrook White equation is defined as:

$$\frac{1}{\sqrt{\lambda}} = -2 * \lg \left( \underbrace{\frac{ks/d_{\text{pipe}}}{3.71}}_{\text{term1}} + \underbrace{\frac{2.51}{\text{Re} * \sqrt{\lambda}}}_{\text{term2}} \right)$$

When turbulent flow is calculated, the Reynolds number ( $Re$ ) is very high and the term 2 can be neglected from the equation.

$$\frac{1}{\sqrt{\lambda}} = -2 * \lg \left( \frac{ks/d_{\text{pipe}}}{3.71} \right)$$

The velocity in the pipe is calculated with the following approach:

$$v = \sqrt{2 * g * d_{\text{pipe}} * \frac{1}{\lambda}}$$

With the equation of the velocity and the friction coefficient, the maximal flow through the pipe can be calculated with:

$$Q = A * v = A * \sqrt{2 * g * d_{\text{pipe}} * \frac{1}{\lambda}} = \frac{\pi * (d_{\text{pipe}})^2}{4} * \sqrt{2 * g * d_{\text{pipe}} * \frac{1}{\lambda}}$$

## Attachment 6

## Application of Spreadsheet and ASCII Files

## 1. Definition of SUDS

To define SUDS in the Krückau catchment, an excel file has been worked out: 'hydrotope\_sheet.xls'. In the first sheet, the ratio of sealed areas drained or transferred to SUDS can be defined for each sub-catchment. The acronyms of the sub-catchments are given in the input sheet, whereas the locations as well as attributes of these sub-catchments are defined in the Kalypso Hydrology model developed by the PÜK (2008).

|    | A                  | B               | C                   | D            | E              | F |
|----|--------------------|-----------------|---------------------|--------------|----------------|---|
| 55 |                    |                 |                     |              |                |   |
| 56 |                    |                 | <b>sub-cachment</b> | <b>ratio</b> |                |   |
| 57 | <b>Green Roofs</b> | <b>Elmshorn</b> | K37_01              | 20 %         | of sealed area |   |
| 58 |                    |                 | K37_02              | 20 %         | of sealed area |   |
| 59 |                    |                 | Elmsh_E13_04        | 20 %         | of sealed area |   |
| 60 |                    |                 | Elmsh_E07           | 20 %         | of sealed area |   |
| 61 |                    |                 | Elmsh_E06_03        | 20 %         | of sealed area |   |
| 62 |                    |                 | Elmsh_E06_04        | 20 %         | of sealed area |   |
| 63 |                    |                 | Elmsh_E06_01        | 20 %         | of sealed area |   |
| 64 |                    |                 | ELMS_E06_02         | 20 %         | of sealed area |   |
| 65 |                    |                 | Elms_E32            | 20 %         | of sealed area |   |
| 66 |                    |                 | K16_04              | 20 %         | of sealed area |   |
| 67 |                    |                 | K17_01              | 20 %         | of sealed area |   |
| 68 |                    |                 | K17_02              | 20 %         | of sealed area |   |
| 69 |                    |                 | K16_07              | 20 %         | of sealed area |   |
| 70 |                    |                 | K18                 | 20 %         | of sealed area |   |
| 71 |                    |                 | K15                 | 20 %         | of sealed area |   |
| 72 |                    |                 | Sandkamp            | 20 %         | of sealed area |   |
| 73 |                    |                 | K16_01              | 20 %         | of sealed area |   |
| 74 |                    |                 | K16_02              | 20 %         | of sealed area |   |
| 75 |                    |                 | Kruek_24            | 20 %         | of sealed area |   |
| 76 |                    |                 | Kruek_25            | 20 %         | of sealed area |   |
| 77 | Kruek_26           | 20 %            | of sealed area      |              |                |   |
| 78 | Kruek_27           | 20 %            | of sealed area      |              |                |   |
| 79 | Kruek_28           | 20 %            | of sealed area      |              |                |   |

Fig. 1 The user can define the spatial distribution of SUDS.

It is possible to define green roofs, swales and unsealing in all urban sub-catchments (Elmshorn, Barmstedt, Kaltenkirchen), but it is recommended to define swale-filter-drain systems only in the urban sub-catchments of Kaltenkirchen and Barmstedt as indicated in the sheet 'Swale-Filter-Drain Systems'. The methodology, calculations and input data are described in more detail in chapter 4.

In the sheet: 'Ascii\_file\_SUDS\_we.hyd' the ASCII file with the adjusted hydrotopes is calculated. In the first row, short descriptions of the data in each column are given. This sheet has to be saved as 'Text (MS-DOS) (\*.txt)' – file in the folder 'hydrotope\_file\_templates' → 'we.hyd\_acronym'. A number of files are provided, which have been developed in the Master's Thesis as examples (Fig.2).

The hydrotope file, which shall be used for the calculation, has to be copied to the folder 'inp.dat', where all input files are provided, which are actually used by the software code. The name of the hydrotope file has to be changed to 'we.hyd'.

| Name                                      | Ext | Size      | ↓Date      |
|---|-----|-----------|------------|
| ↑...[-.]                                  |     | <DIR>     | 03/02/2010 |
| we.hyd_SUDScombination                    | txt | 2,421,353 | 05/01/2010 |
| we.hyd_Unsealing_30percent                | txt | 2,407,096 | 05/01/2010 |
| we.hyd_Swales_upper_Krueckau_30percent    | txt | 2,411,150 | 05/01/2010 |
| we.hyd_Swales_30percent                   | txt | 2,415,487 | 05/01/2010 |
| we.hyd_green_roofs_20percent              | txt | 2,412,263 | 05/01/2010 |
| we.hyd_Swales_Elmshorn_20Percent          | txt | 2,410,783 | 05/01/2010 |
| we.hyd_groof_roofs_10percent              | txt | 2,411,155 | 04/01/2010 |
| we.hyd_swale_filter_drains_upper_Krueckau | txt | 2,410,564 | 04/01/2010 |

Fig. 2 Provided Hydrotape files with defined SUDS.

## 2. Definition of the return period of the flood event

For the simulation of SUDS scenarios, different flood events with defined rainfall intensities can be simulated, which have been calculated with the IPCC Scenario 0-A1B.

| Name                              | Ext | Size   | Date       |
|-----------------------------------|-----|--------|------------|
| ↑...[-.]                          |     | DIR    | 06/01/2010 |
| we_nat.geb_T5_designRainfallEvent |     | 70,633 | 02/01/2010 |
| we_nat.geb_HQ100                  |     | 70,467 | 29/12/2009 |
| we_nat.geb_HQ50                   |     | 70,446 | 29/12/2009 |
| we_nat.geb_HQ20                   |     | 70,467 | 29/12/2009 |
| we_nat.geb_HQ5                    |     | 70,467 | 28/12/2009 |
| we_nat.geb_HQ1                    |     | 70,387 | 29/12/2009 |

Fig. 3 Files with defined matching coefficients for the simulation of specific events

In this thesis, the SUDS measures (green roofs, swales, swale-filter-drain systems) have been designed with the rainfall event, which has a return period of once in 5years ('T5'). Further on, five flood events with a return period of once in 1year, once in 5years, once in 20years, once in 50years and once in 100years have been developed. The file which shall be used has to be copied to the 'inp.dat' folder and renamed to 'we\_nat.geb'. Therewith, the existing file has to be overwritten.

## 3. Running the Calculation

Before running a calculation it has to be controlled if a folder is defined, where the results are saved. This folder has to be named 'out\_we.nat'.

When there are existing results in the folder 'out\_we.nat' and not renamed, the files are overwritten during the following calculation. For the simulation results an additional folder 'Results\_MasterThesis' has been created to save all the simulation results. The results of this thesis are calculated with a spatial distribution of green roofs on 20% of the sealed areas, 30% of the sealed areas drained by swales or swale-filter-drain systems (only Kalttenkirchen and Barmstedt), unsealing of 30% of the sealed areas and the combination of all SUDS.

Fig. 4 Overview of required files for the simulations

| Name                   | Ext | Size       | Date           |
|------------------------|-----|------------|----------------|
| ..                     |     |            | DIR 06/01/2010 |
| zufuss                 |     |            | DIR 22/12/2009 |
| start                  |     |            | DIR 05/01/2010 |
| Results_MasterThesis   |     |            | DIR 06/01/2010 |
| out_we.nat             |     |            | DIR 06/01/2010 |
| lzsims                 |     |            | DIR 22/12/2009 |
| klima.dat              |     |            | DIR 22/12/2009 |
| inp.dat                |     |            | DIR 06/01/2010 |
| hydro.top              |     |            | DIR 05/01/2010 |
| namodellBerechnung.gml |     | 2,202,534  | 07/12/2009     |
| IdMap.txt              |     | 123,579    | 07/12/2009     |
| hydrotape_sheet.xls    |     | 24,908,800 | 06/01/2010     |
| Grafik.Pro             |     | 1,000      | 06/01/2010     |
| grafik.ini             |     | 696        | 05/01/2010     |
| grafik.exe             |     | 654,336    | 16/08/2004     |
| exe.log                |     | 97,352     | 07/12/2009     |
| exe.err                |     | 23         | 07/12/2009     |

A variety of variables can be calculated and defined in the folder 'start' → 'we\_nat\_start.txt'. Here a 'j' stands for calculation and a 'n' stands for no calculation.

Table 1 Variables to be calculated.

| n/j | German description        | English description                          |      |
|-----|---------------------------|--|------|
| n/j | Temperatur                | Temperature                                  | .tmp |
| n/j | Niederschlag              | Precipitation                                | .pre |
| n/j | Schnee                    | Snow   | .sch |
| n/j | Bodenfeuchte              | Soil Moisture                                | .bof |
| n/j | Bodenspeicher             | Soil Storage Volume                          | .bsp |
| n/j | Grundwasserstand          | Ground water level                           | .gws |
| n/j | Gesamtabfluss Knoten      | Discharge at nodes                           | .qgs |
| n/j | Gesamtabfluss TG          | Discharge of sub-catchments                  | .qgg |
| n/j | nat. Oberflaechenabfluss  | Discharge of natural areas in sub-catchments | .qna |
| n/j | Interflow                 | Interflow                                    | .qif |
| n/j | Abfluss vers. Flächen     | Discharge from sealed areas                  | .qvs |
| n/j | Basisabfluss              | Base flow                                    | .qbs |
| n/j | Kluftgrundw1              | Deep groundwater level                       | .qt1 |
| n/j | Kluftgrundw               | Deep ground water flow                       | .qtg |
| n/j | Grundwasserabfluss        | Groundwater flow                             | .qgw |
| n/j | Kapil.Aufstieg            | Capillary apprise                            | .kap |
| n/j | Evapotranspiration        | Evapotranspiration                           | .vet |
| n/j | Ausgabe Hydrotape         | Output of Hydrotapes                         | .hyd |
| n/j | Abflussbilanz             | Water and flow balance                       | .bil |
| n/j | Statistische Abflusswerte | Statistical flow values                      | .nmq |
| n/j | Speicherinhalt            | Storage volume                               | .spi |
| n/j | Speicherüberlauf          | Storage overflow                             | .sup |
| n/j | Gründach Überlauf         | Overflow of green roofs                      | .qgu |
| n/j | Gründach Drainrohr        | Drainage of green roofs                      | .qgr |
| n/j | Überlauf Mulden-Rigolen   | Overflow of swale-filter-drain systems       | .que |
| n/j | Drainrohr Mulden-Rigolen  | Drainage of swale-filter-drain systems       | .qmr |
| n/j | Überlauf Mulden           | Overflow of swales                           | .mul |

#### 4. Illustration of the Results

The results are saved in the folder 'out\_we.nat'. To open the results in a diagram a graphic tool (developed by Björnсен Consulting Engineers GmbH; [www.bjoernsen.de](http://www.bjoernsen.de)) can be used.



The functions of this graphic tool are the same as in the user interface of Kalypso Hydrology.

| Name              | Ext | Size      | Date       | Time     |
|-------------------|-----|-----------|------------|----------|
|                   | DIR |           | 06/01/2010 | 00:17:09 |
| stat.txt          |     | 434       | 05/01/2010 | 23:22:34 |
| LAST.TPL          |     | 1,769     | 05/01/2010 | 23:21:30 |
| grafik.ini        |     | 704       | 06/01/2010 | 00:17:09 |
| 710724_uh_ger.dat |     | 261,568   | 05/01/2010 | 23:14:25 |
| 710724_qvs.dat    |     | 2,864,803 | 05/01/2010 | 23:14:26 |
| 710724_que.dat    |     | 2,864,803 | 05/01/2010 | 23:14:26 |
| 710724_qna.dat    |     | 2,864,793 | 05/01/2010 | 23:14:26 |
| 710724_qmr.dat    |     | 2,864,804 | 05/01/2010 | 23:14:26 |
| 710724_qgu.dat    |     | 2,864,797 | 05/01/2010 | 23:14:26 |
| 710724_qgr.dat    |     | 2,864,802 | 05/01/2010 | 23:14:26 |
| 710724_qbs.dat    |     | 249,520   | 05/01/2010 | 23:14:26 |
| 710724_pre.dat    |     | 147,518   | 05/01/2010 | 23:14:25 |
| 710724_mul.dat    |     | 2,864,795 | 05/01/2010 | 23:14:26 |

Fig. 5 Results Folder

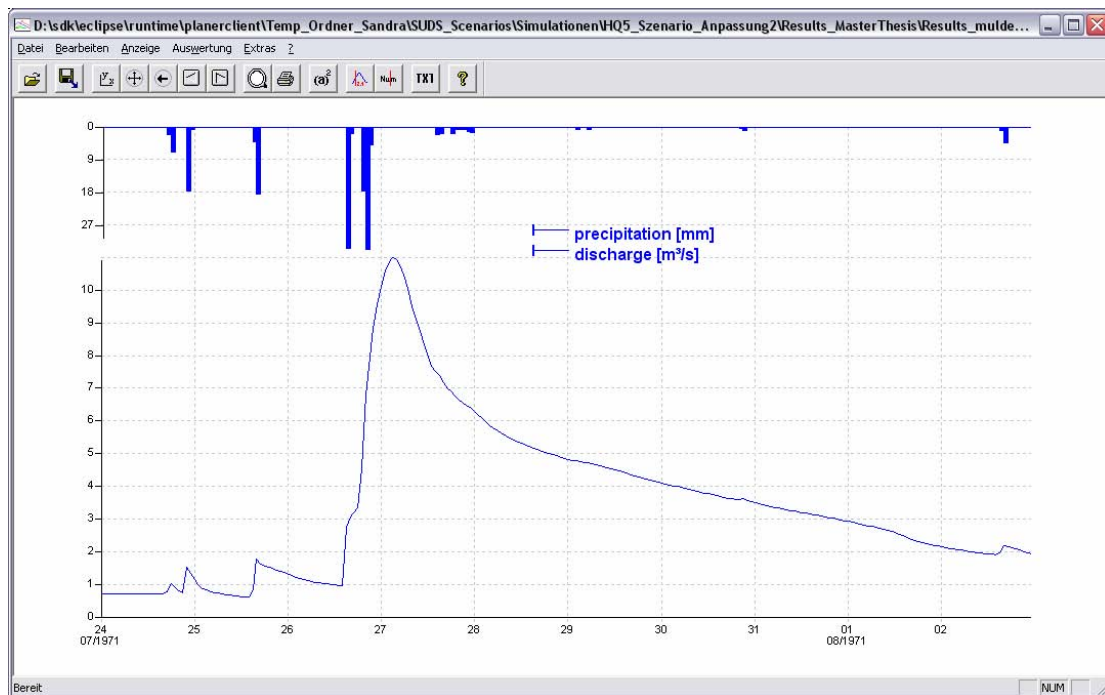


Fig. 6 Example of hydrograph illustrated with the graphic tool

The numbers of the sub-catchments, nodes and strands are explained in the file: IDMap.txt of the model-folder.



## Attachment 7

## Climate Model Data Variables

REMO-UBA data series used for scenario studies in this thesis.

(Source: [Jacob & Mahrenholz, 2006a-d](#))

Temporal Coverage                      Scenario: 'SR': scenario run data series: C20, A1B, B1 or A2  
 1/1/1960 - 31/12/2000                      (C20)  
 1/1/2001 - 31/12/2100                      (A1B, B1, A2)

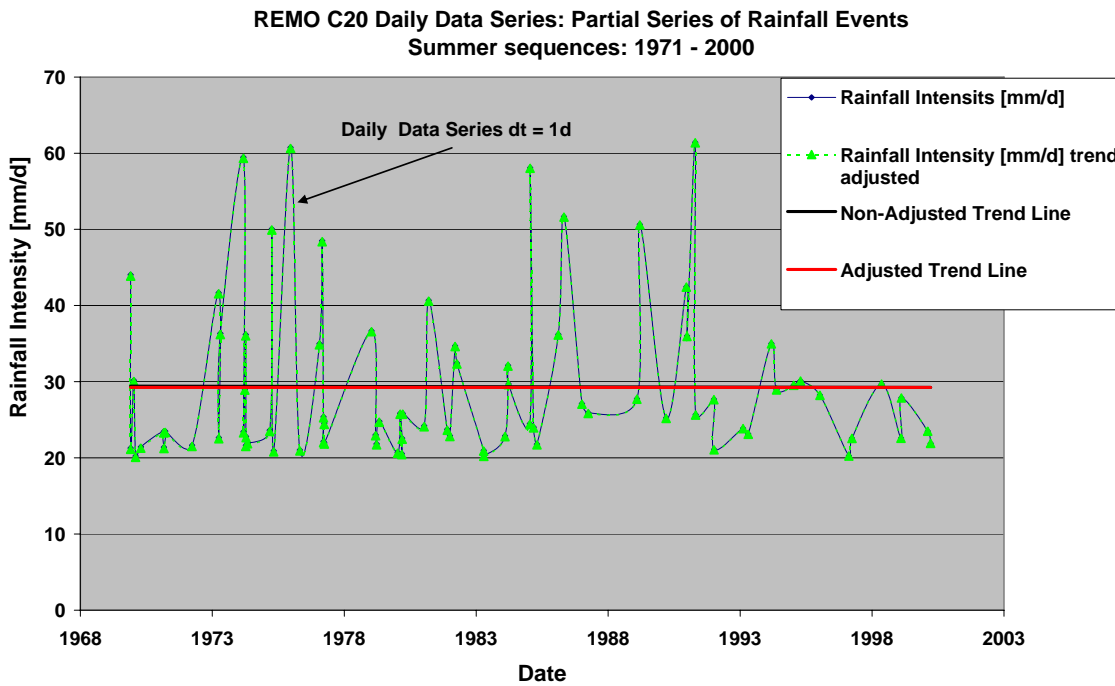
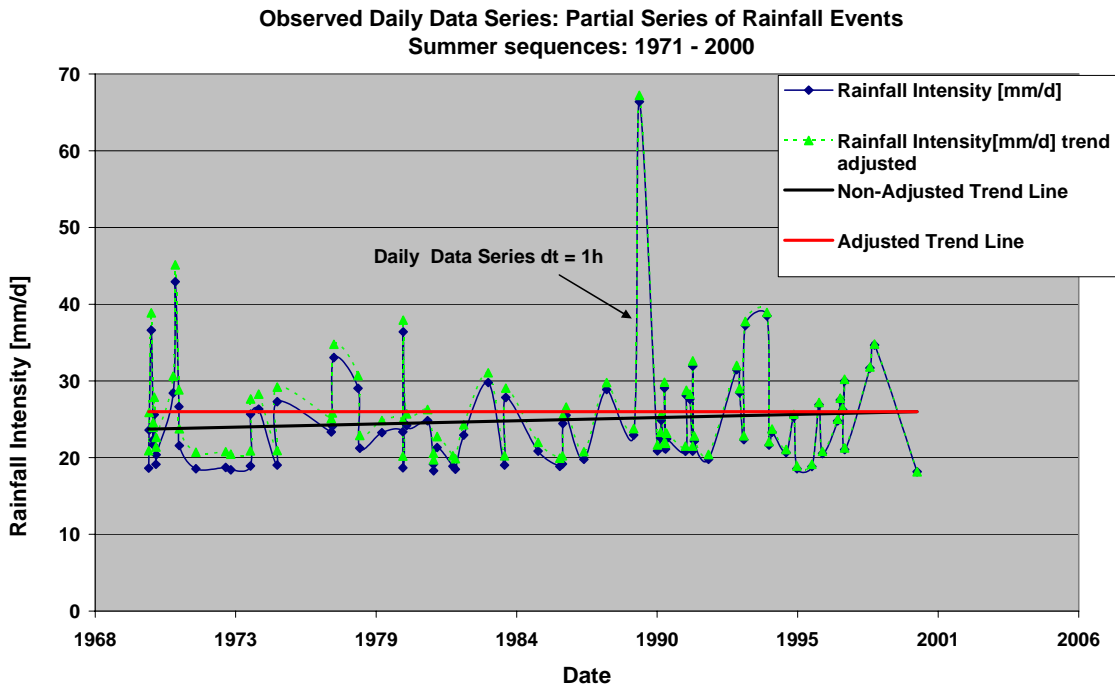
| Data Variable          | Acronym    | Topic [CERA-Server]          | Unit                | Temporal Aggregation | Description [CERA-Server]   | Date of creation |
|------------------------|------------|------------------------------|---------------------|----------------------|---|------------------|
| Temperature            | TEMP2      | RE_UBA_'SR'_D3_DM_TEMP2      | [K]<br>Kelvin       | Daily mean           | Air temperature-at 2m above surface   | 19/10/2006       |
| Wind Speed             | WIND_SPEED | RE_UBA_'SR'_D3_DM_WIND_SPEED | [m/s]               | Daily mean           | Value of the wind speed in 10m altitude   | 19/10/2006       |
| Relative Humidity      | REL_HUM    | RE_UBA_'SR'_D3_DM_REL_HUM    | [%]                 | Daily mean           | Post processed value of the relative humidity with respect to water saturation                        | 19/10/2006       |
| Global Radiation       | SRADO      | RE_UBA_'SR'_D3_DM_SRADO      | [W/m <sup>2</sup> ] | Daily mean           | Net shortwave radiation (at model top)  | 19/10/2006       |
| Precipitation [daily]  | PRECIP_TOT | RE_UBA_'SR'_D3_DS_PRECIP_TOT | [mm/d]              | Daily sum            | Post-processed value of convective [APRC] and grid scale precipitation [APRL], sum over time interval | 04/10/2006       |
| Precipitation [hourly] | PRECIP_TOT | RE_UBA_'SR'_D3_1H_PRECIP_TOT | [mm/h]              | Hourly sum           | Post-processed value of convective and grid scale precipitation, sum over time interval               | 04/10/2006       |

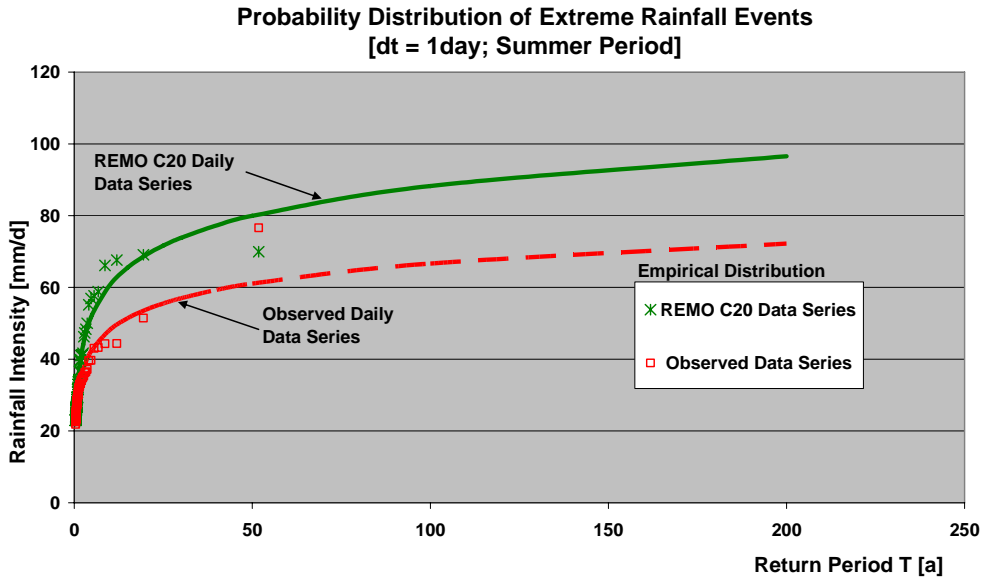
# Attachment 8

## Probability of Extreme Rainfall Events in the Past [1971 - 2000]

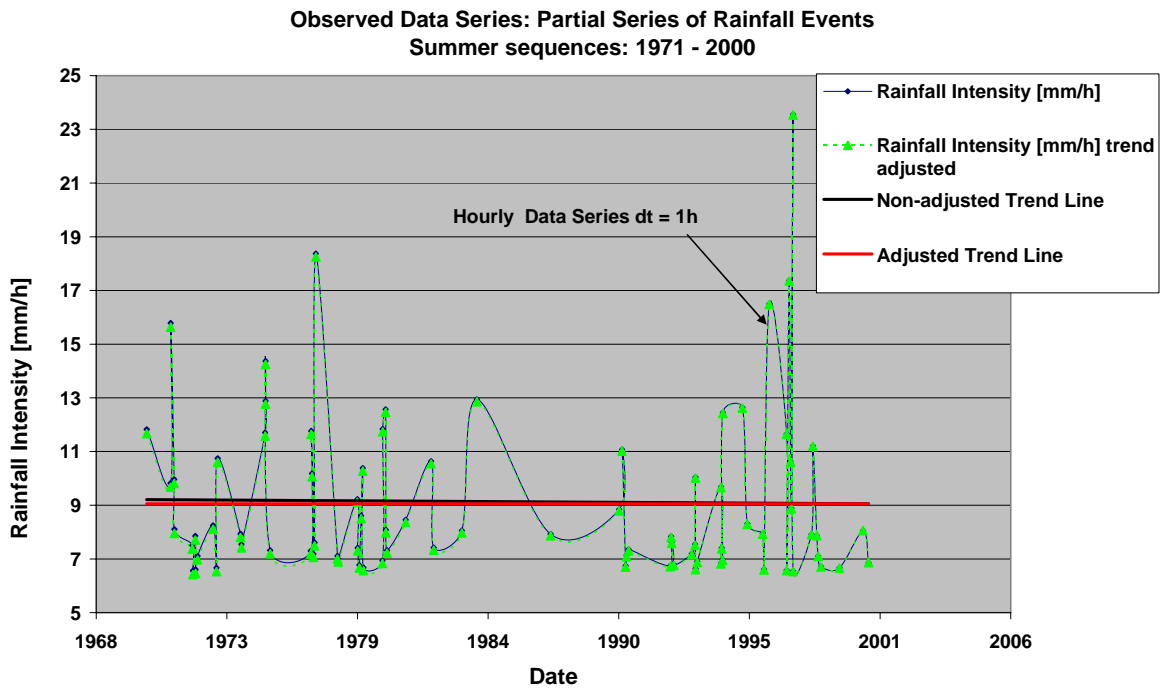
### 8.1 Summer Periods

#### 8.1.1 Daily Data Series:

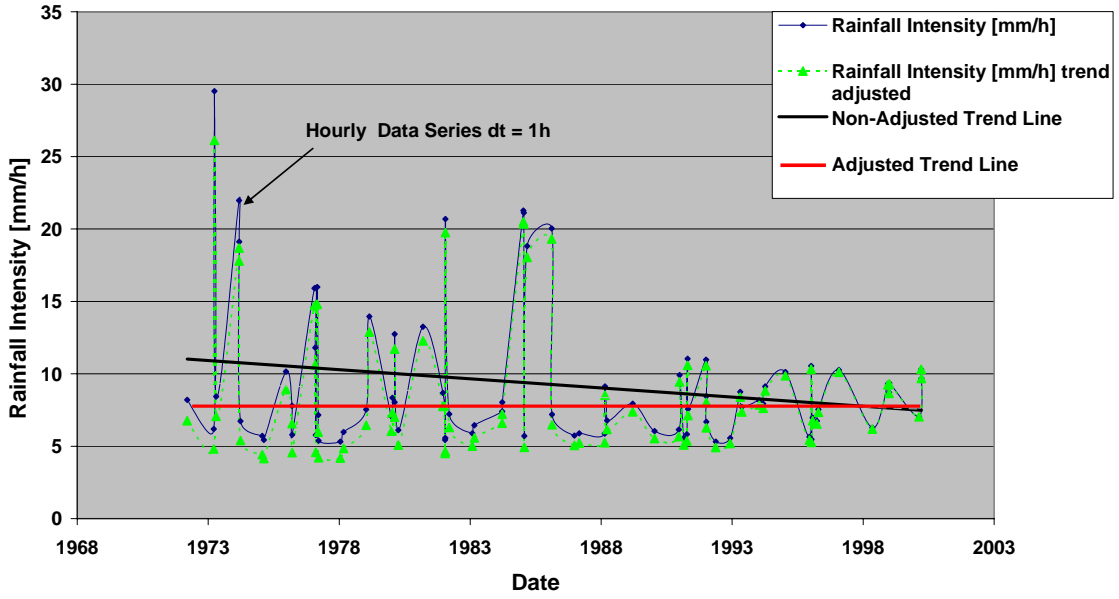




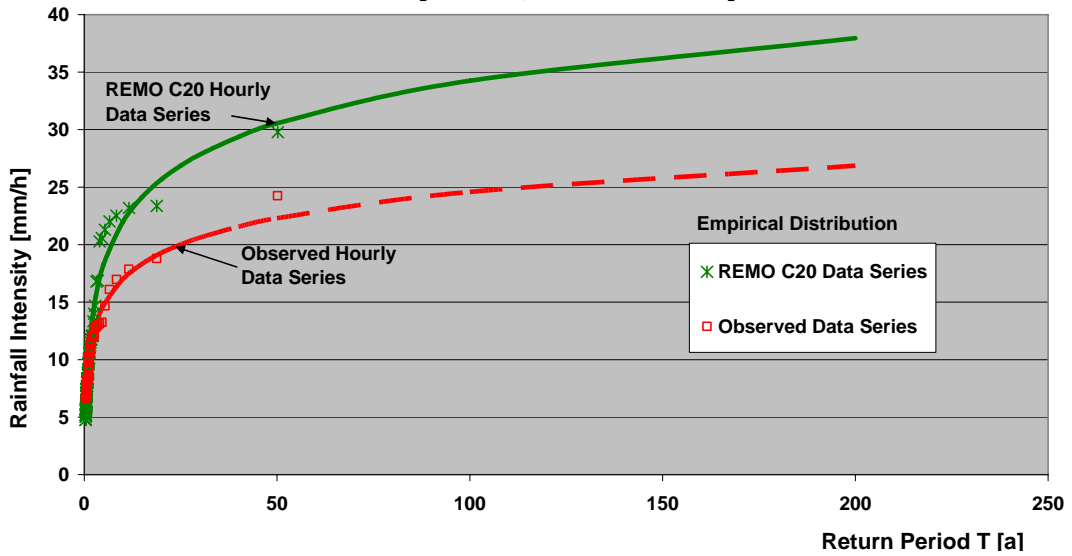
### 8.1.2 Hourly Data Series



REMO C20 Hourly Data Series: Partial Series of Rainfall Events  
Summer sequences: 1971 - 2000



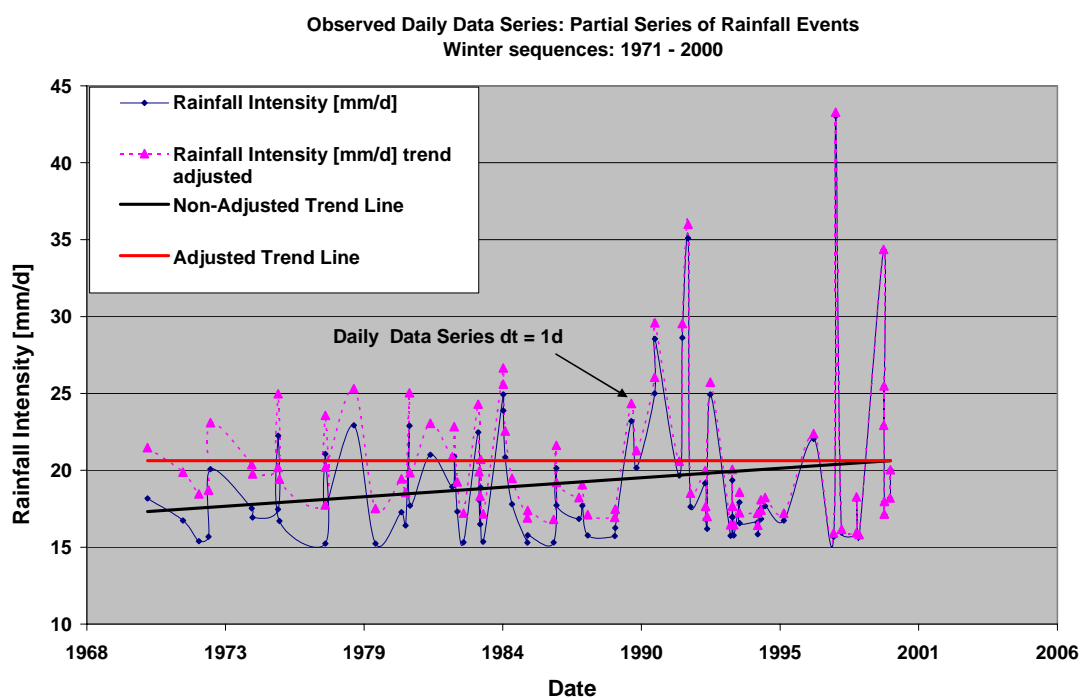
Probability Distribution of Extreme Rainfall Events  
[dt = 1hr; Summer Period]

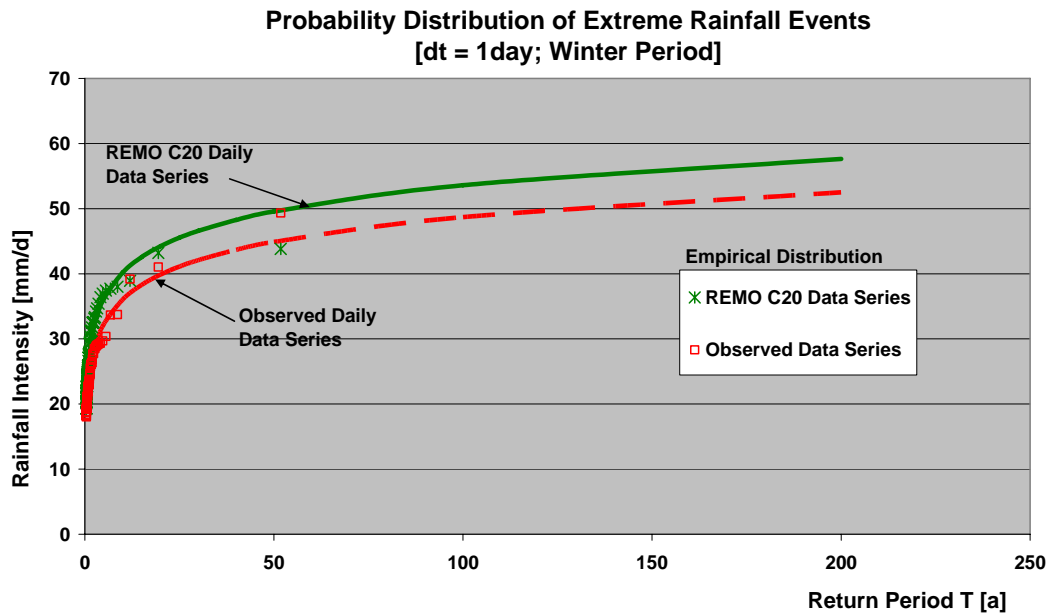
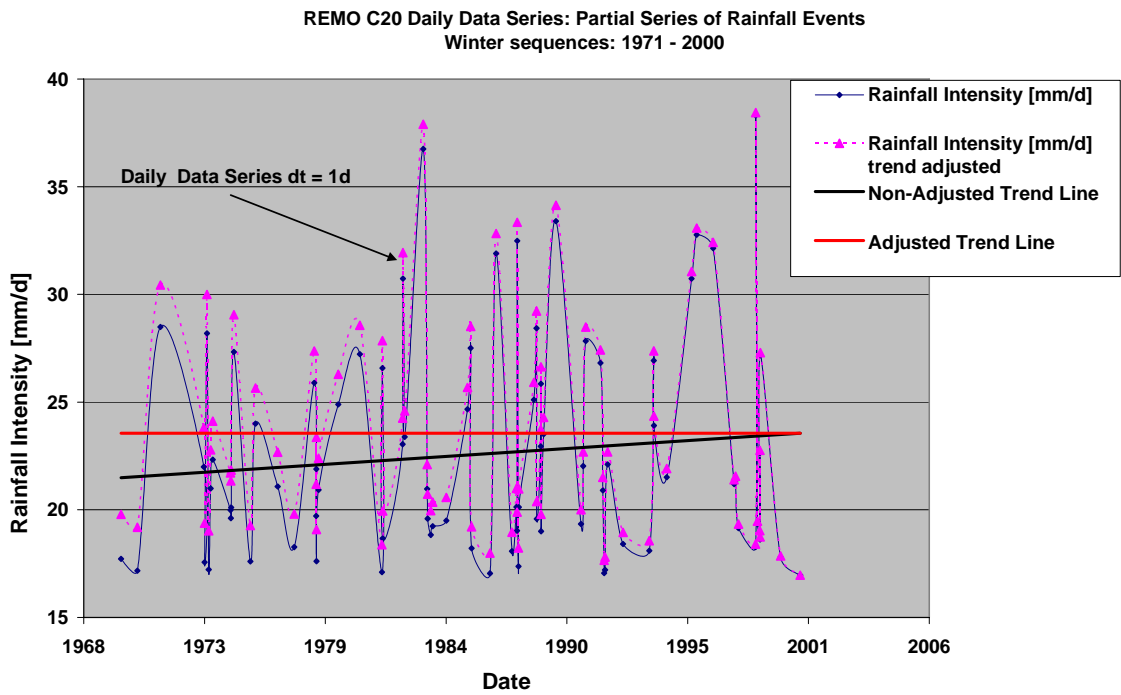


| Summer Periods | Hourly Data series  |                             | Daily Data Series           |                             |
|----------------|---------------------|-----------------------------|-----------------------------|-----------------------------|
|                | Return Period T [a] | Observed Data Series [mm/h] | REMO C20 Data Series [mm/h] | Observed Data Series [mm/d] |
| 1              | 9.4                 | 9.7                         | 29.7                        | 33.1                        |
| 2              | 10.7                | 11.9                        | 32.9                        | 37.9                        |
| 2              | 11.7                | 13.4                        | 35.3                        | 41.4                        |
| 3              | 12.4                | 14.6                        | 37.0                        | 44.0                        |
| 3              | 13.0                | 15.5                        | 38.5                        | 46.2                        |
| 5              | 14.7                | 18.3                        | 42.6                        | 52.4                        |
| 10             | 17.0                | 22.0                        | 48.2                        | 60.7                        |
| 15             | 18.3                | 24.1                        | 51.4                        | 65.5                        |
| 20             | 19.3                | 25.7                        | 53.7                        | 69.0                        |
| 25             | 20.0                | 26.9                        | 55.5                        | 71.6                        |
| 30             | 20.6                | 27.8                        | 57.0                        | 73.8                        |
| 40             | 21.6                | 29.4                        | 59.3                        | 77.3                        |
| 50             | 22.3                | 30.6                        | 61.1                        | 80.0                        |
| 100            | 24.6                | 34.2                        | 66.7                        | 88.3                        |
| 200            | 26.9                | 37.9                        | 72.2                        | 96.6                        |

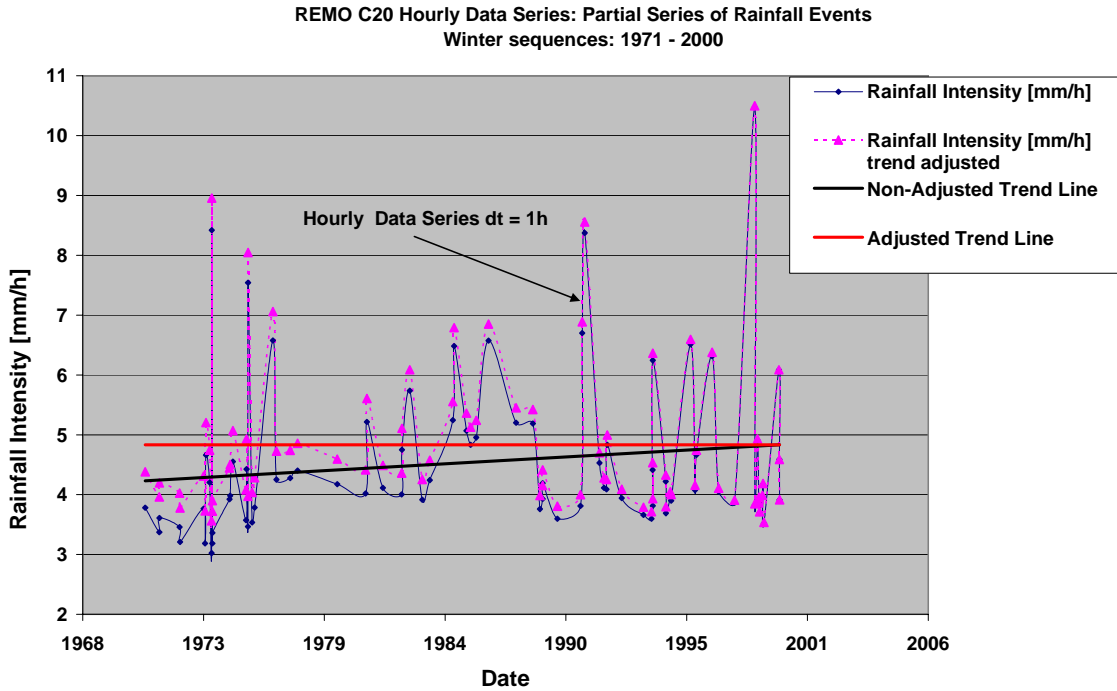
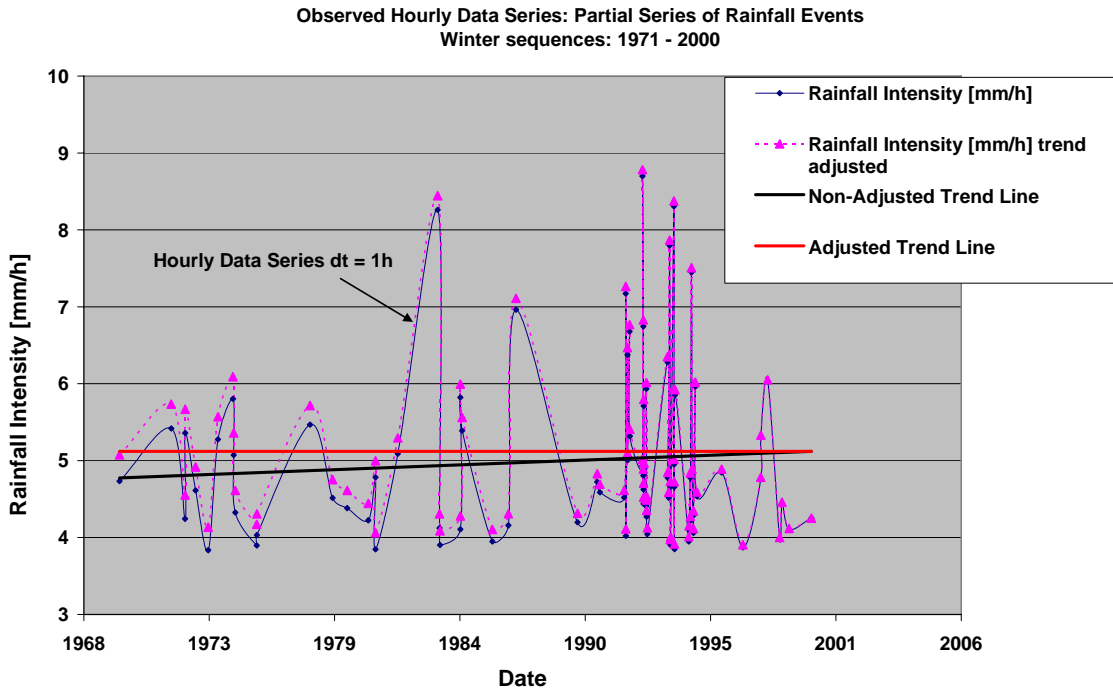
## 8.2 Winter Periods

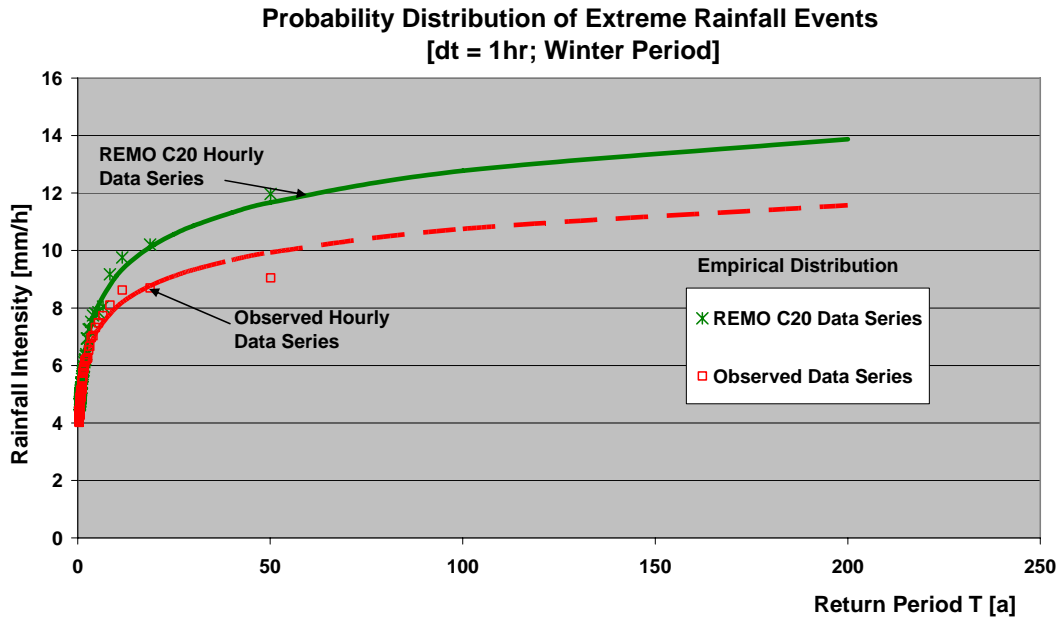
### 8.2.1 Daily Data Series:





8.2.2 Hourly Data Series

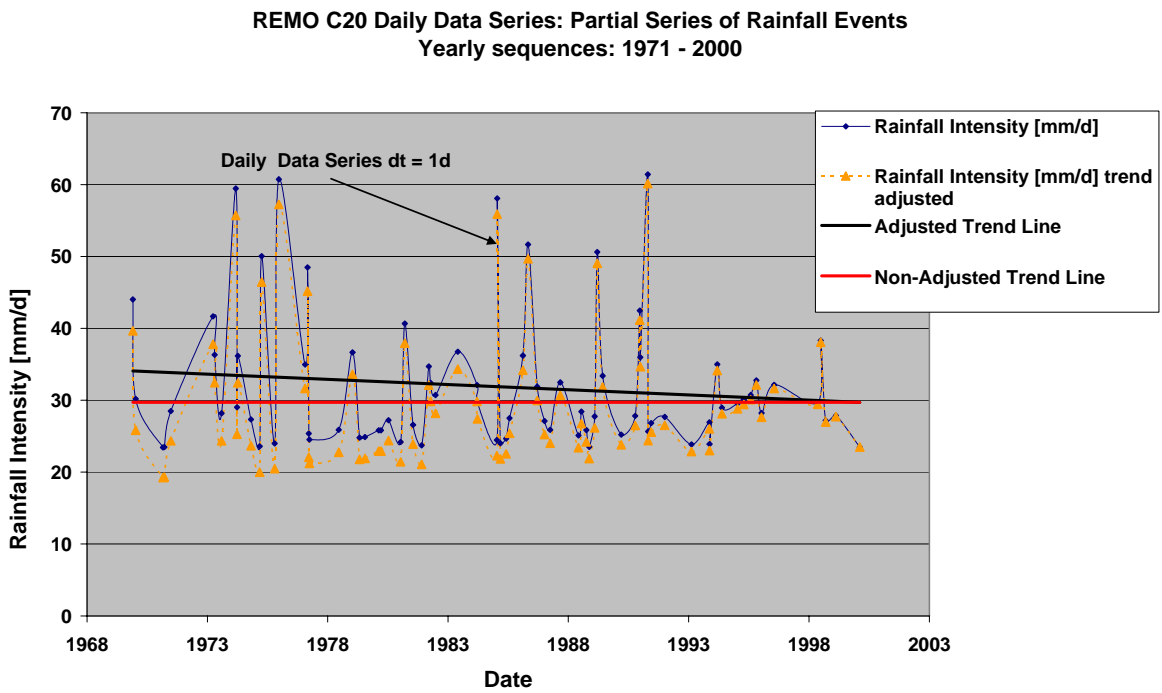
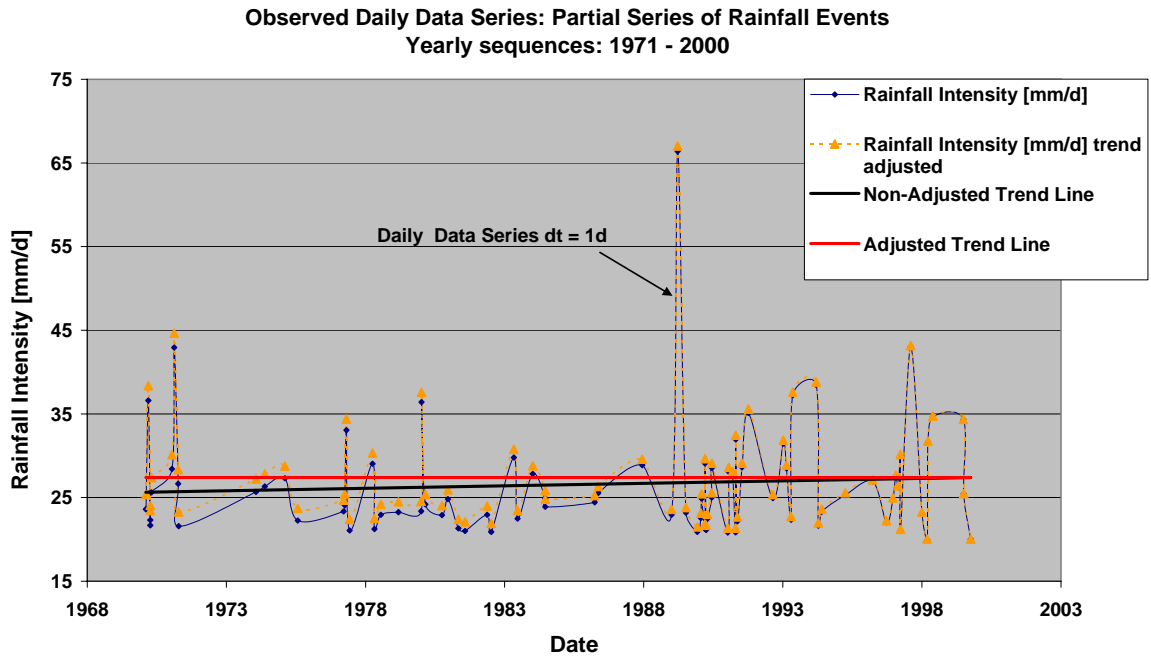


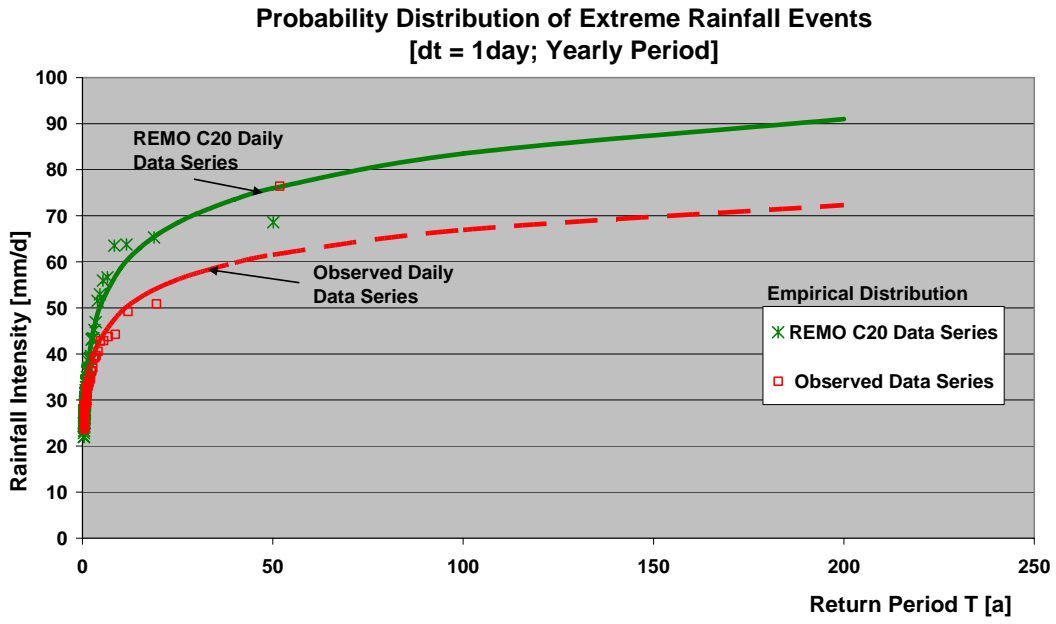


| Winter Periods | Hourly Data series  |                             | Daily Data Series           |                             |
|----------------|---------------------|-----------------------------|-----------------------------|-----------------------------|
|                | Return Period T [a] | Observed Data Series [mm/h] | REMO C20 Data Series [mm/h] | Observed Data Series [mm/d] |
| 1              | 5.3                 | 5.4                         | 23.4                        | 26.8                        |
| 2              | 5.8                 | 6.1                         | 25.6                        | 29.2                        |
| 2              | 6.1                 | 6.5                         | 27.2                        | 30.8                        |
| 3              | 6.4                 | 6.9                         | 28.4                        | 32.1                        |
| 3              | 6.6                 | 7.2                         | 29.4                        | 33.2                        |
| 5              | 7.2                 | 8.0                         | 32.3                        | 36.2                        |
| 10             | 8.0                 | 9.1                         | 36.1                        | 40.2                        |
| 15             | 8.5                 | 9.8                         | 38.3                        | 42.6                        |
| 20             | 8.8                 | 10.2                        | 39.9                        | 44.2                        |
| 25             | 9.1                 | 10.6                        | 41.1                        | 45.5                        |
| 30             | 9.3                 | 10.9                        | 42.1                        | 46.6                        |
| 40             | 9.7                 | 11.3                        | 43.7                        | 48.3                        |
| 50             | 9.9                 | 11.7                        | 44.9                        | 49.6                        |
| 100            | 10.8                | 12.8                        | 48.7                        | 53.6                        |
| 200            | 11.6                | 13.9                        | 52.5                        | 57.6                        |

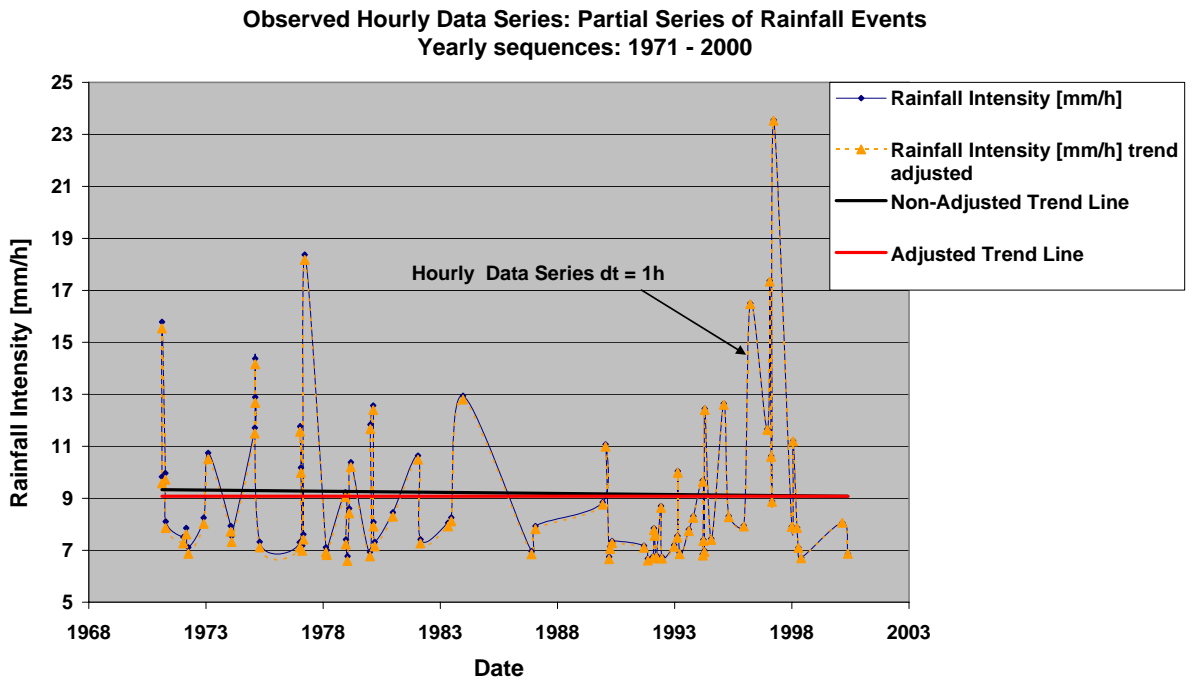
### 8.3 Yearly Periods

#### 8.3.1 Daily Data Series:

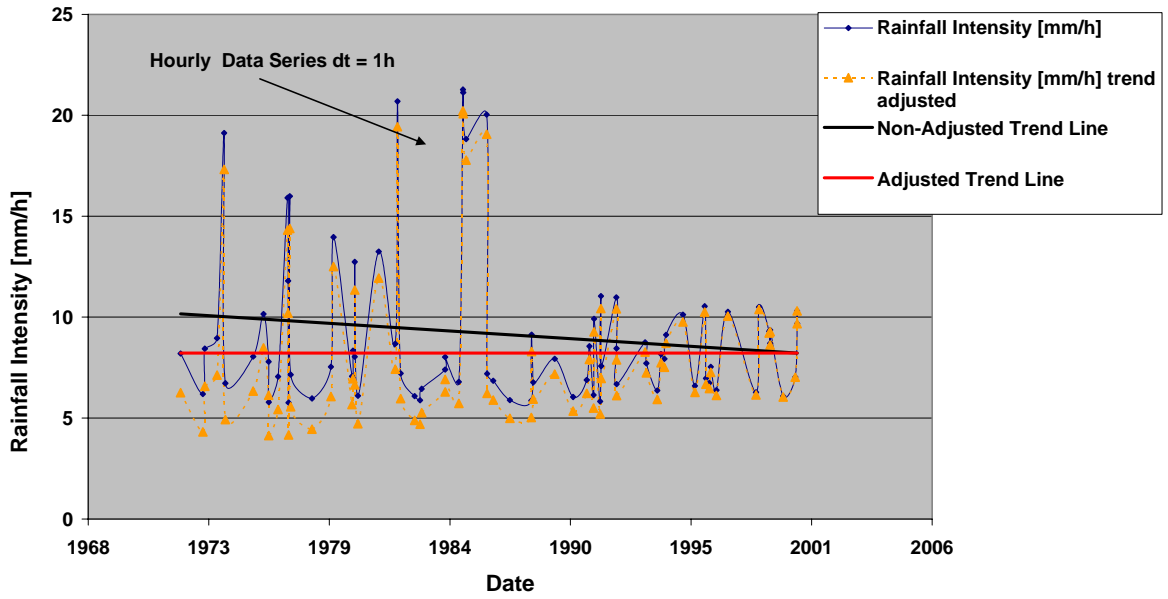




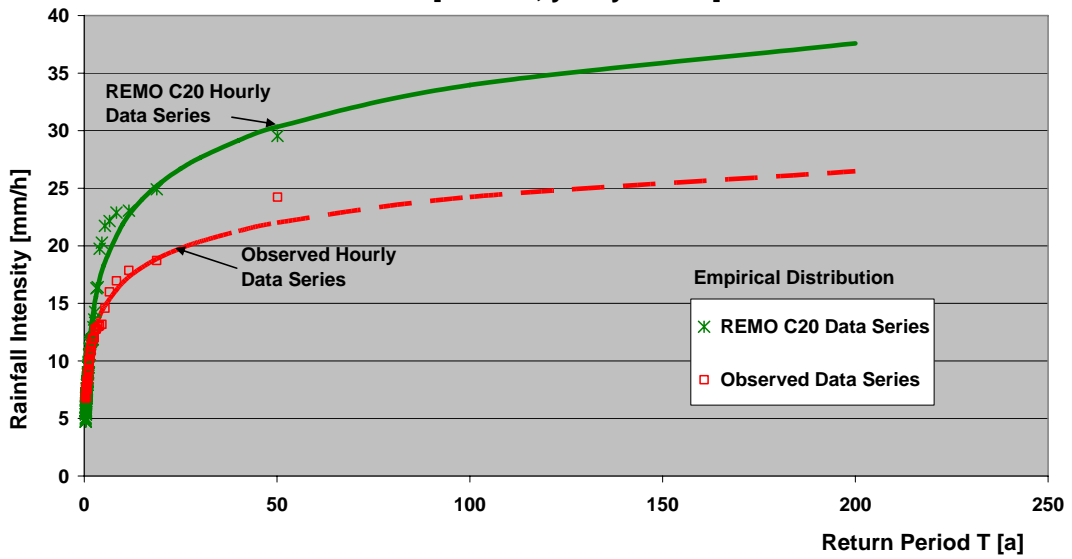
**8.3.2 Hourly Data Series:**



REMO C20 Hourly Data Series: Partial Series of Rainfall Events  
Yearly sequences: 1971 - 2000

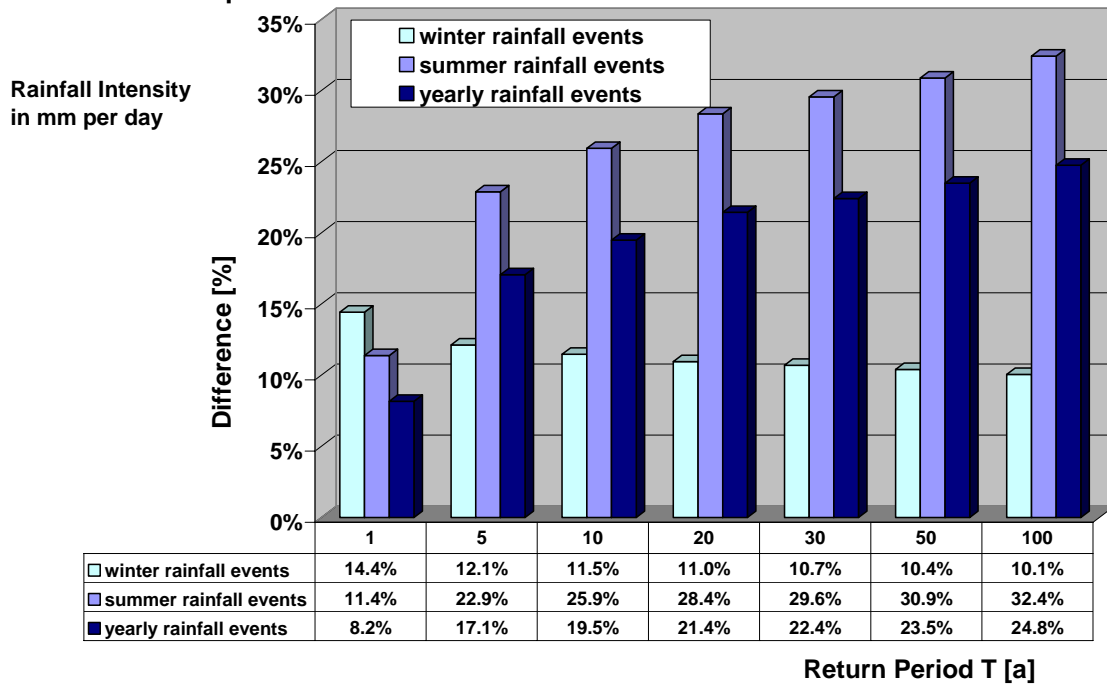


Probability Distribution of Extreme Rainfall Events  
[dt = 1hr; yearly Period]

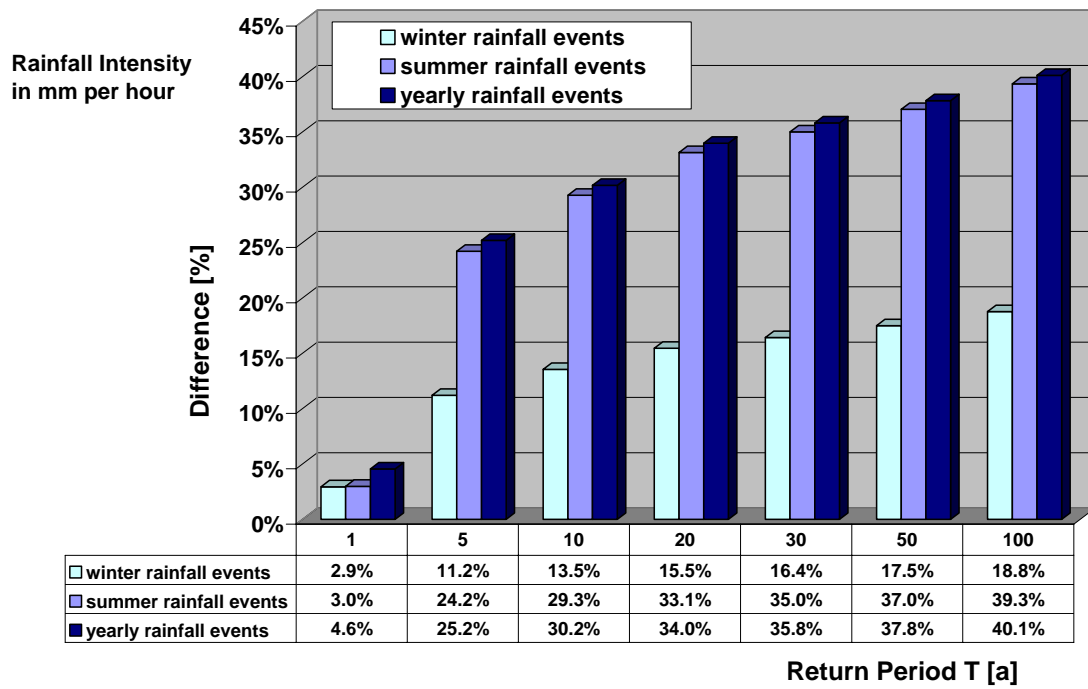


| Yearly Periods      | Hourly Data series          |                             | Daily Data Series           |                             |
|---------------------|-----------------------------|-----------------------------|-----------------------------|-----------------------------|
| Return Period T [a] | Observed Data Series [mm/h] | REMO C20 Data Series [mm/h] | Observed Data Series [mm/d] | REMO C20 Data Series [mm/d] |
| 1                   | 9.4                         | 9.8                         | 31.1                        | 33.6                        |
| 2                   | 10.7                        | 12.0                        | 34.3                        | 38.0                        |
| 2                   | 11.6                        | 13.5                        | 36.5                        | 41.1                        |
| 3                   | 12.4                        | 14.6                        | 38.2                        | 43.6                        |
| 3                   | 12.9                        | 15.6                        | 39.6                        | 45.5                        |
| 5                   | 14.6                        | 18.3                        | 43.6                        | 51.1                        |
| 10                  | 16.8                        | 21.9                        | 49.0                        | 58.6                        |
| 15                  | 18.1                        | 24.0                        | 52.2                        | 62.9                        |
| 20                  | 19.1                        | 25.5                        | 54.4                        | 66.1                        |
| 25                  | 19.8                        | 26.7                        | 56.1                        | 68.5                        |
| 30                  | 20.4                        | 27.6                        | 57.5                        | 70.4                        |
| 40                  | 21.3                        | 29.2                        | 59.8                        | 73.6                        |
| 50                  | 22.0                        | 30.3                        | 61.5                        | 76.0                        |
| 100                 | 24.2                        | 34.0                        | 66.9                        | 83.5                        |
| 200                 | 26.5                        | 37.6                        | 72.3                        | 91.0                        |

**8.4 Differences in Percentage**



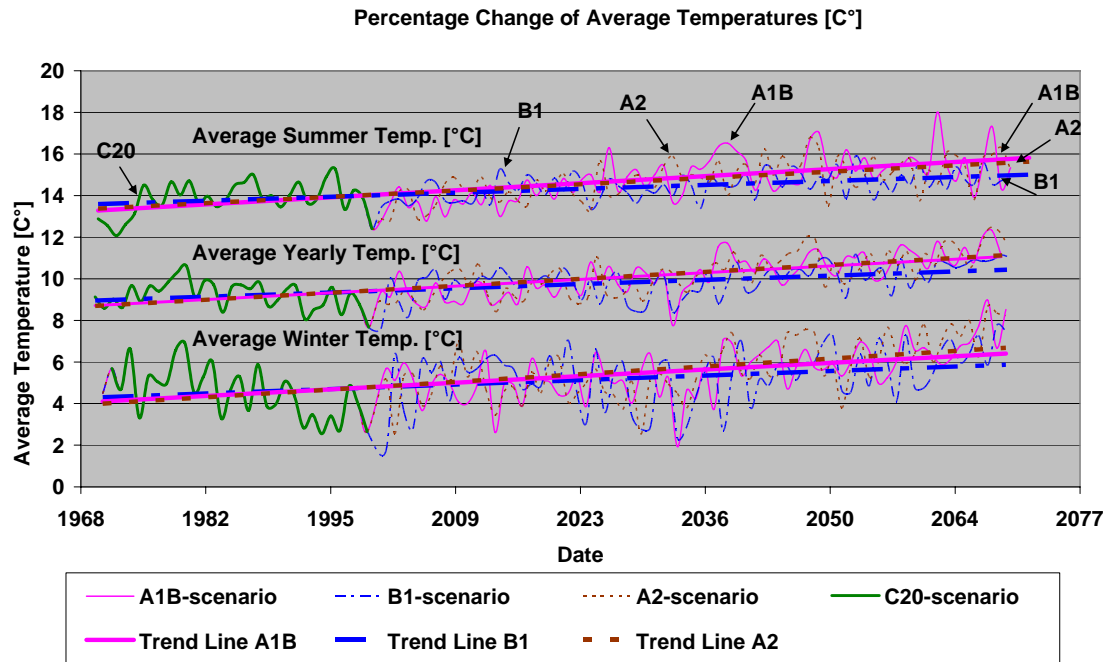
## Attachment 8



## Attachment 9

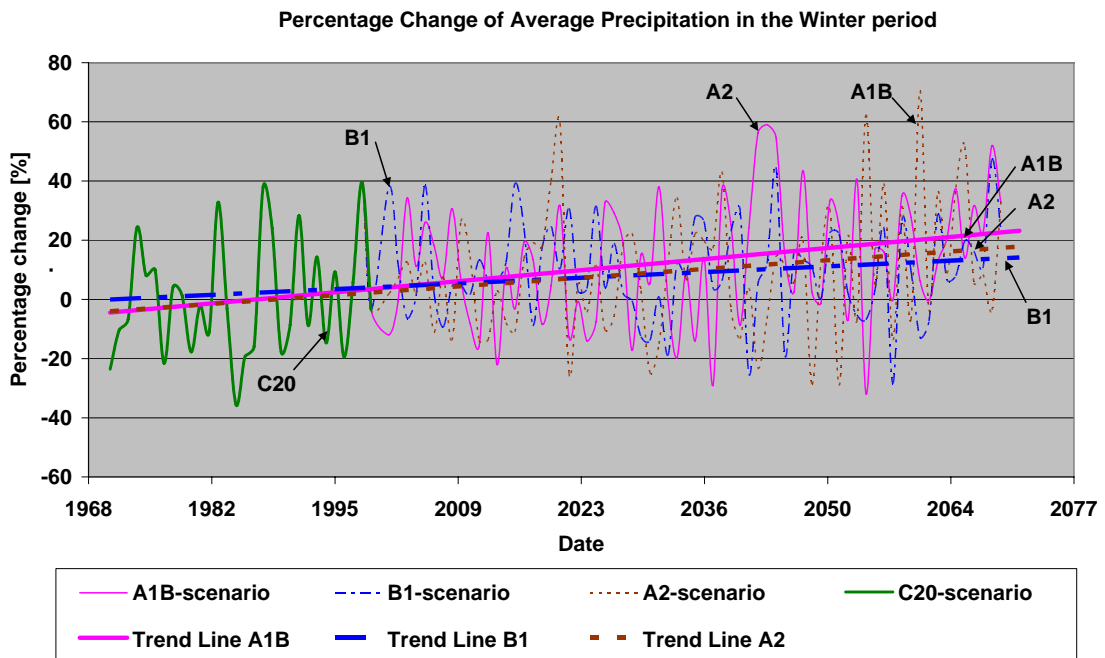
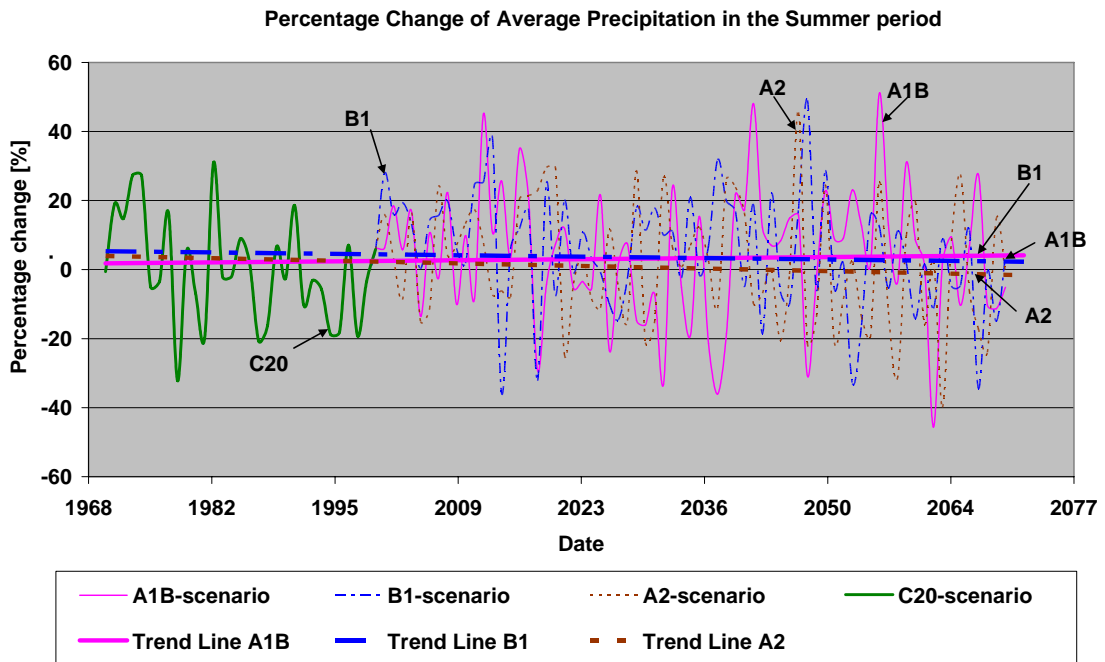
### Average Changes in Climate Variables [2040 - 2070]

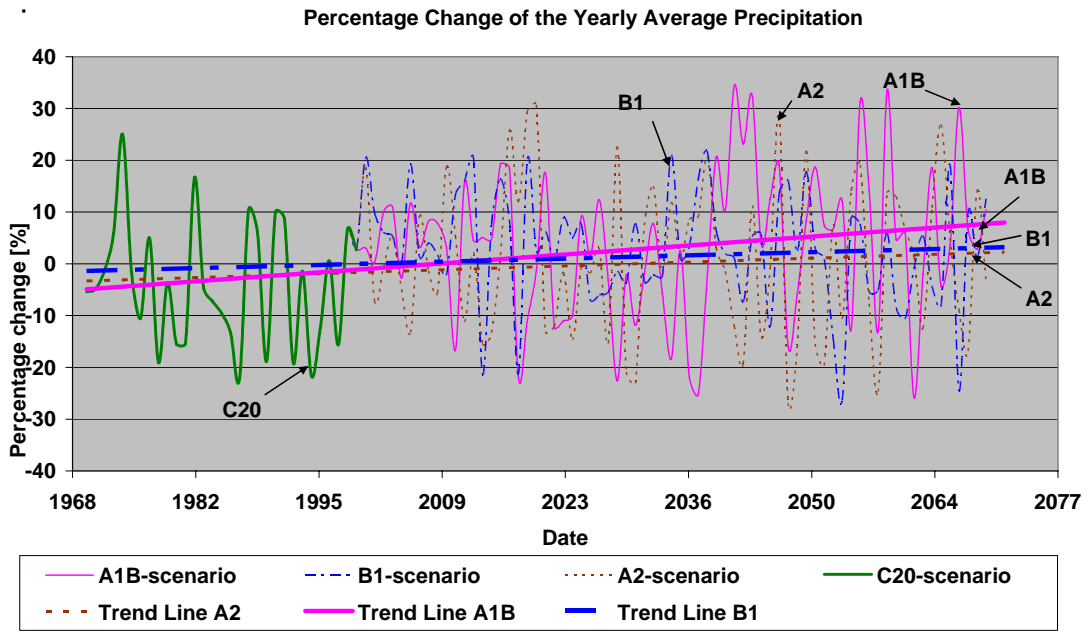
#### 9.1 Temperature Trend Line Analysis:



| Sequences                         | Reference Observed Data Series (1970-2000) | IPCC scenario | Trend [°C/decade] | Average Percentage change [2040 to 2070] | Average change [°C] [2040 to 2070] | Average Temperature [°C] - [2040 - 2070] |
|-----------------------------------|--|---------------|-------------------|--|------------------------------------|--|
| Average Summer Period Temperature | 13.9 °C                                    | B1            | + 4.E-04          | + ~ 6.3 to 7.3 %                         | + ~ 0.9 to 1.0 °C                  | ~ 14.8 to 14.9 °C                        |
|                                   |  | A1B           | + 7.E-04          | + ~ 9.7 to 11.5 %                        | + ~ 1.3 to 1.6 °C                  | ~ 15.2 to 15.5 °C                        |
|                                   |  | A2            | + 6.E-04          | + ~ 8.0 to 9.6 %                         | + ~ 1.1 to 1.3 °C                  | ~ 15.0 to 15.2 °C                        |
| Average Winter Period Temperature | 5.4 °C                                     | B1            | + 4.E-04          | + ~ 19.8 to 23.3 %                       | + ~ 1.1 to 1.3 °C                  | ~ 6.5 to 6.7 °C                          |
|                                   |  | A1B           | + 6.E-04          | + ~ 26.4 to 31.5 %                       | + ~ 1.4 to 1.7 °C                  | ~ 6.8 to 7.1 °C                          |
|                                   |  | A2            | + 7.E-04          | + ~ 30.6 to 36.6 %                       | + ~ 1.7 to 2.0 °C                  | ~ 7.1 to 7.4 °C                          |
| Yearly Average Temperature        | 9.7 °C                                     | B1            | + 4.E-04          | + ~ 9.0 to 13.9 %                        | + ~ 0.9 to 1.3 °C                  | ~ 10.6 to 11.0 °C                        |
|                                   |  | A1B           | + 7.E-04          | + ~ 13.0 to 15.6 %                       | + ~ 1.3 to 1.5 °C                  | ~ 11.0 to 11.2 °C                        |
|                                   |  | A2            | + 7.E-04          | + ~ 12.7 to 15.4 %                       | + ~ 1.2 to 1.5 °C                  | ~ 10.9 to 11.2 °C                        |

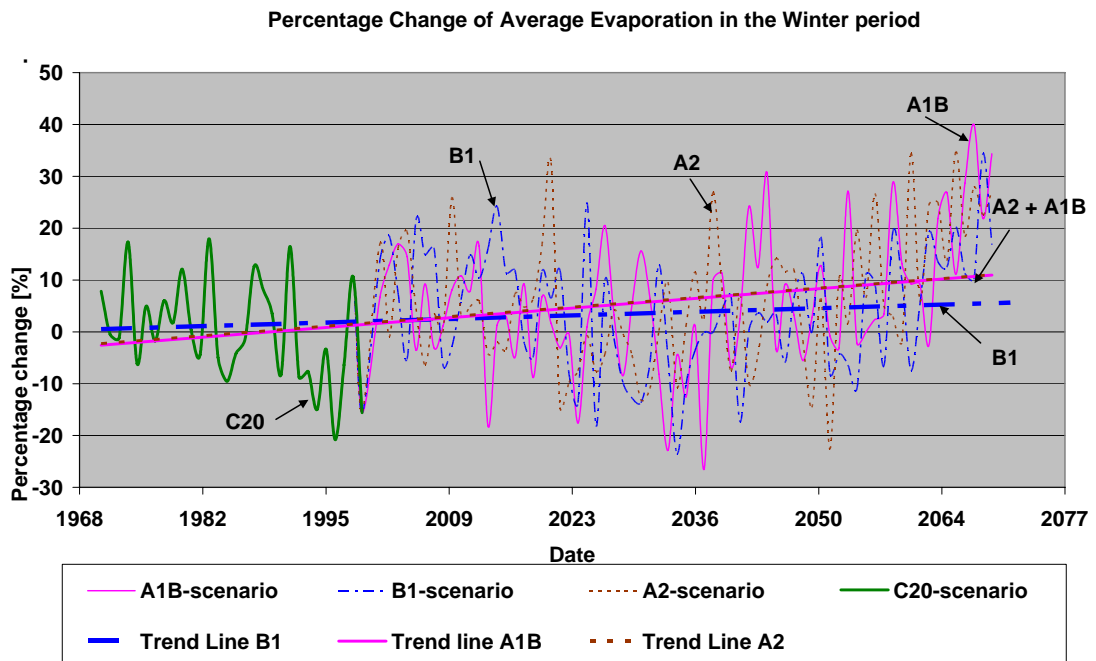
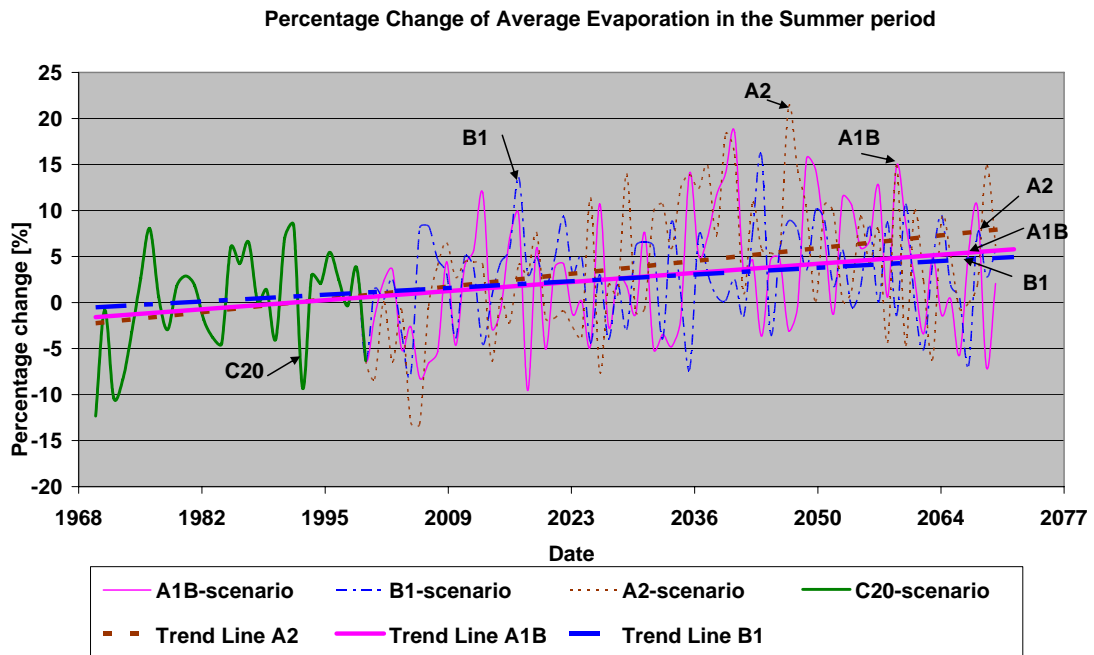
## 9.2 Precipitation Trend Line Analysis



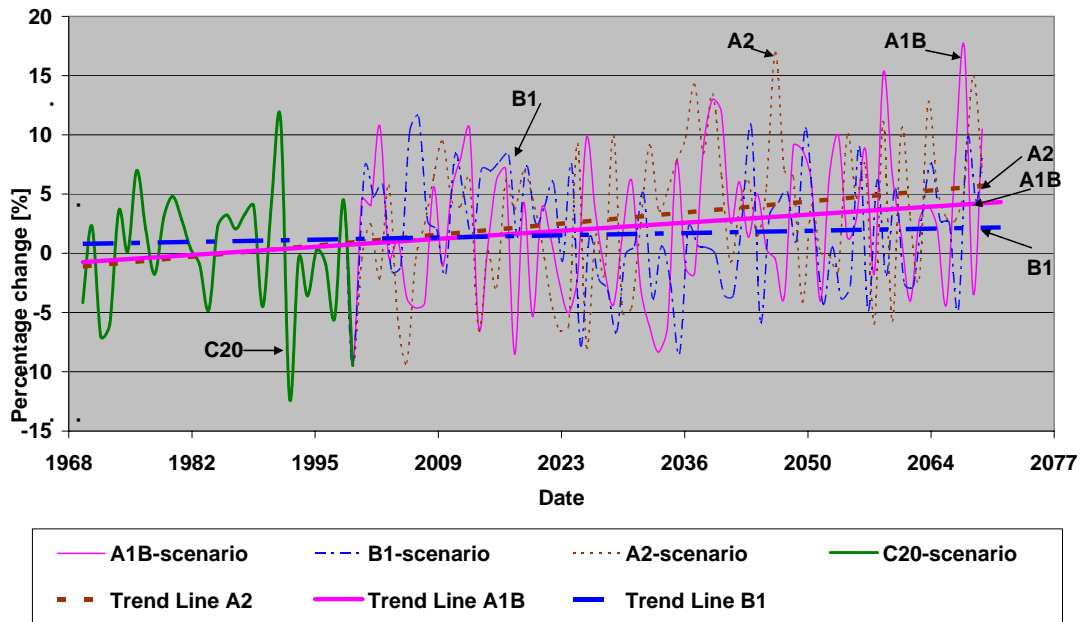


|                                  | Reference Observed Data Series (1970-2000) | scenario study | Trend [%/decade] | Average Percentage change [2040 to 2070] | Average change [mm] - [2040 to 2070] | Average Precipitation Sum [mm] - [2040 - 2070] |
|----------------------------------|--|----------------|------------------|--|--------------------------------------|--|
| Average Summer Precipitation Sum | 440.9 mm                                   | B1             | + -8.E-04        | + ~ 2.4 to 3.3 %                         | + ~ 10.6 to 14.5 mm                  | ~ 451.5 to 455.4 mm                            |
|                                  |  | A1B            | + 6.E-04         | + ~ 3.3 to 3.9 %                         | + ~ 14.5 to 17.4 mm                  | ~ 455.4 to 458.3 mm                            |
|                                  |  | A2             | + -1.E-03        | + ~ 1.6 to 2.7 %                         | + ~ 7.1 to 11.9 mm                   | ~ 448.0 to 452.8 mm                            |
| Average Winter Precipitation Sum | 372.6 mm                                   | B1             | + 4.E-03         | + ~ 10.5 to 14.9 %                       | + ~ 39.2 to 55.5 mm                  | ~ 411.8 to 428.1 mm                            |
|                                  |  | A1B            | + 7.E-03         | + ~ 14.4 to 22.6 %                       | + ~ 53.8 to 84.2 mm                  | ~ 426.4 to 456.8 mm                            |
|                                  |  | A2             | + 6.E-03         | + ~ 11.5 to 18.1 %                       | + ~ 43.0 to 67.5 mm                  | ~ 415.6 to 440.1 mm                            |
| Yearly Average Precipitation Sum | 813.5 mm                                   | B1             | + 1.E-03         | + ~ 2.7 to 4.2 %                         | + ~ 21.6 to 34.0 mm                  | ~ 835.1 to 847.5 mm                            |
|                                  |  | A1B            | + 4.E-03         | + ~ 5.2 to 9.3 %                         | + ~ 42.6 to 75.5 mm                  | ~ 856.1 to 889.0 mm                            |
|                                  |  | A2             | + 1.E-03         | + ~ 0.0 to 1.6 %                         | + ~ 0.4 to 12.9 mm                   | ~ 813.9 to 826.4 mm                            |

9.3 Evaporation Trend Line Analysis



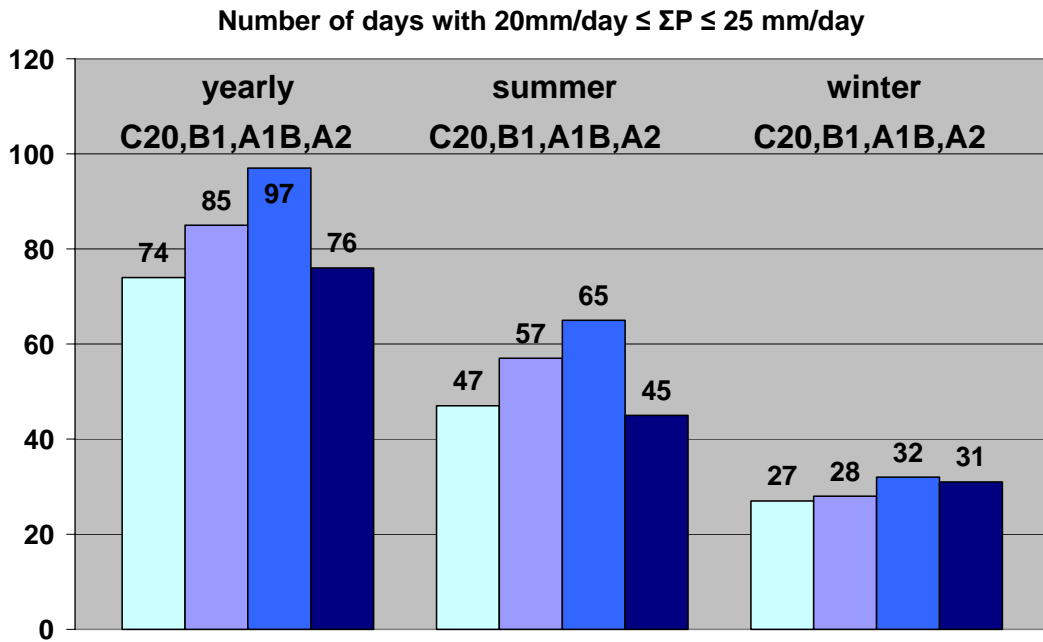
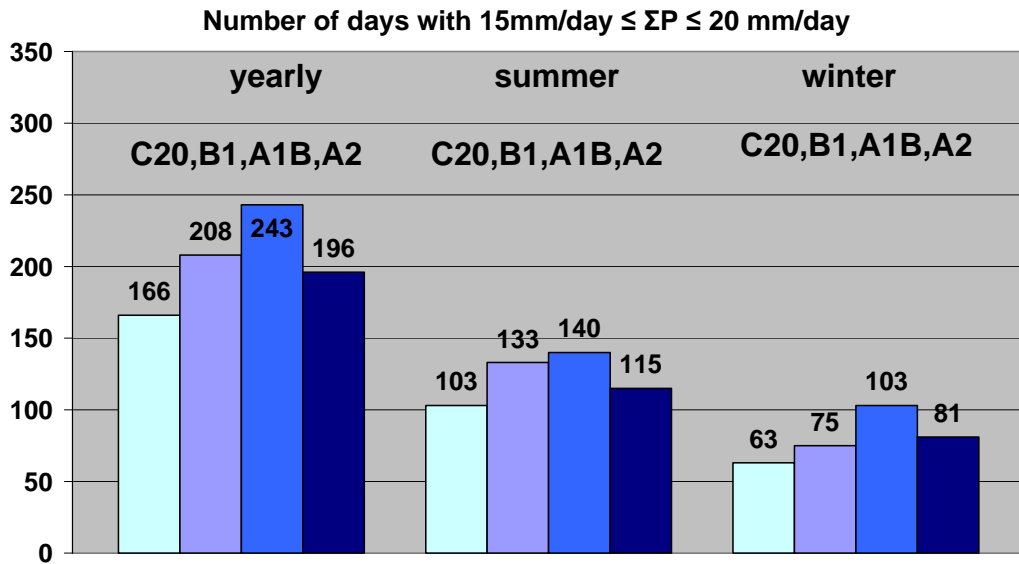
Percentage Change of Average Yearly Evaporation

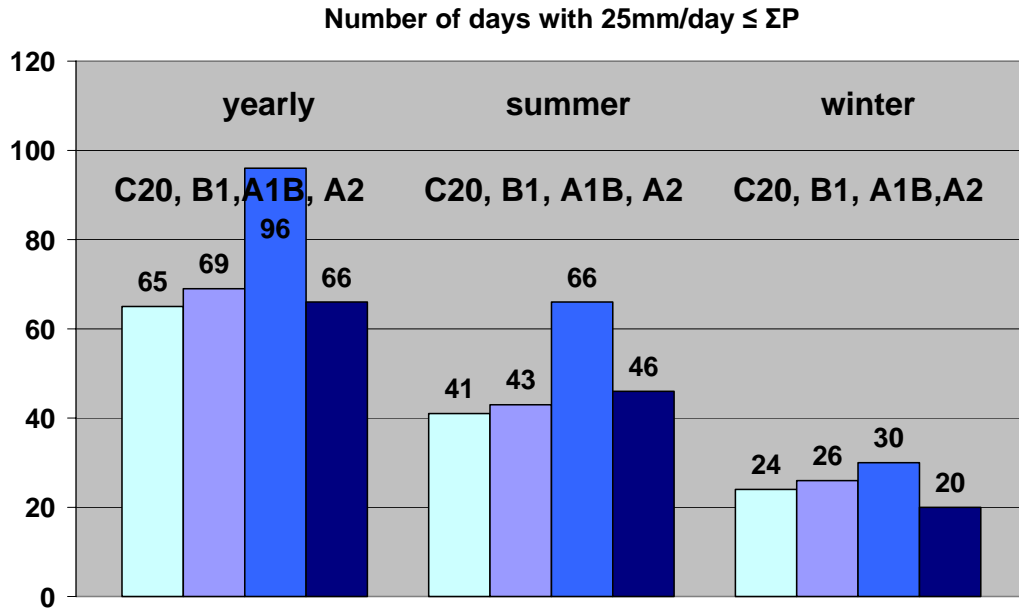


|                                | Reference Observed Data Series (1970-2000) | scenario study | Trend [%/decade] | Average Percentage change [2040 to 2070] | Average change [mm] - [2040 to 2070] | Average Evaporation Sum [mm] - [2040 - 2070] |
|--------------------------------|--|----------------|------------------|--|--------------------------------------|--|
| Average Summer Evaporation Sum | 437.4 mm                                   | B1             | + 1.E-03         | + ~ 2.8 to 4.4 %                         | + ~ 12.4 to 19.0 mm                  | ~ 449.8 to 456.4 mm                          |
|                                |  | A1B            | + 2.E-03         | + ~ 3.0 to 5.1 %                         | + ~ 13.3 to 22.4 mm                  | ~ 450.7 to 459.8 mm                          |
|                                |  | A2             | + 3.E-03         | + ~ 4.2 to 7.1 %                         | + ~ 18.4 to 31.1 mm                  | ~ 455.8 to 468.5 mm                          |
| Average Winter Evaporation Sum | 178.4 mm                                   | B1             | + 1.E-03         | + ~ 4.0 to 5.5 %                         | + ~ 7.2 to 9.9 mm                    | ~ 185.6 to 188.3 mm                          |
|                                |  | A1B            | + 4.E-03         | + ~ 7.6 to 11.8 %                        | + ~ 13.5 to 21.1 mm                  | ~ 191.9 to 199.5 mm                          |
|                                |  | A2             | + 4.E-03         | + ~ 7.5 to 11.6 %                        | + ~ 13.4 to 20.8 mm                  | ~ 191.8 to 199.2 mm                          |
| Yearly Average Evaporation Sum | 615.7 mm                                   | B1             | + 4.E-04         | + ~ 2.2 to 2.6 %                         | + ~ 13.2 to 16.3 mm                  | ~ 628.9 to 632.0 mm                          |
|                                |  | A1B            | + 1.E-03         | + ~ 3.2 to 4.8 %                         | + ~ 19.8 to 29.6 mm                  | ~ 635.5 to 645.3 mm                          |
|                                |  | A2             | + 2.E-03         | + ~ 4.1 to 6.3 %                         | + ~ 25.4 to 38.6 mm                  | ~ 641.1 to 654.3 mm                          |

## Attachment 10

### Number of Occurrence of Daily Precipitation Intensities [2040 - 2070]



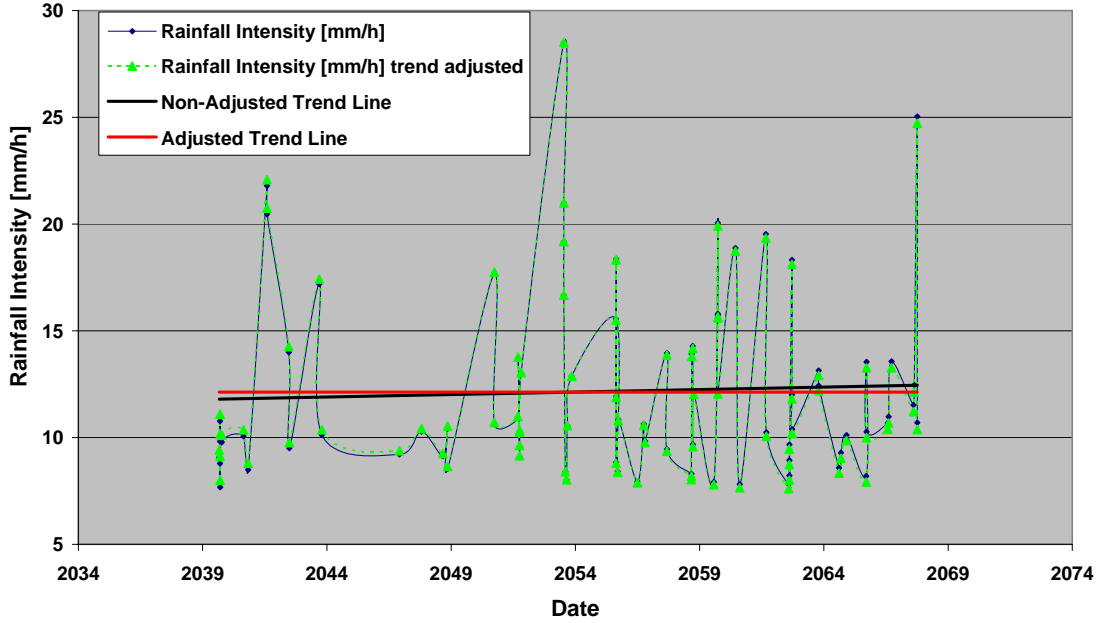


# Attachment 11

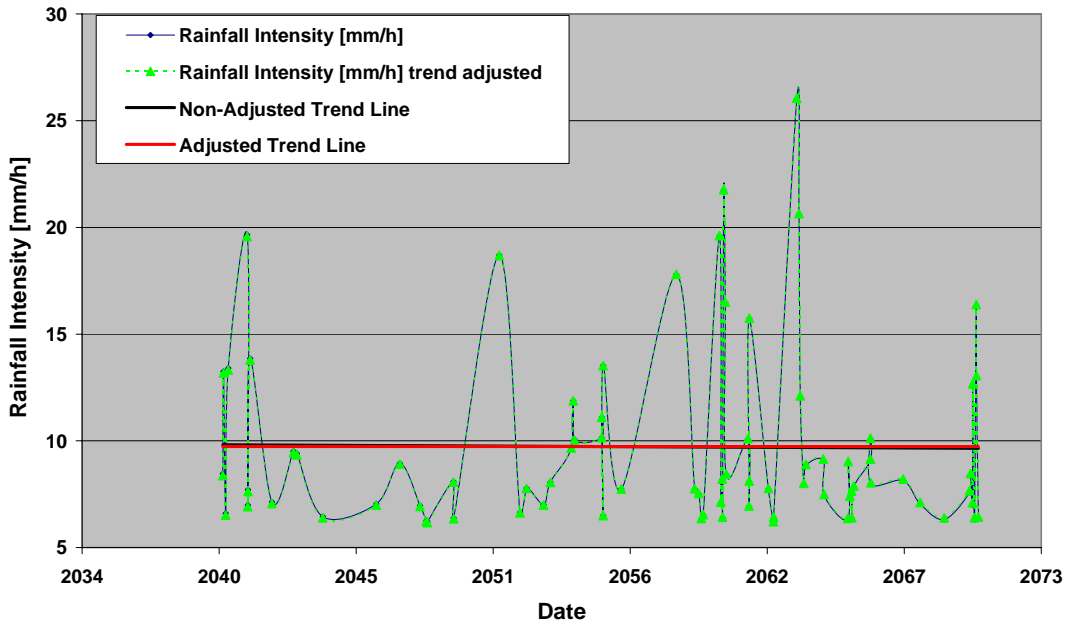
## Probability of Extreme Rainfall Events in the Future [2040 - 2070]

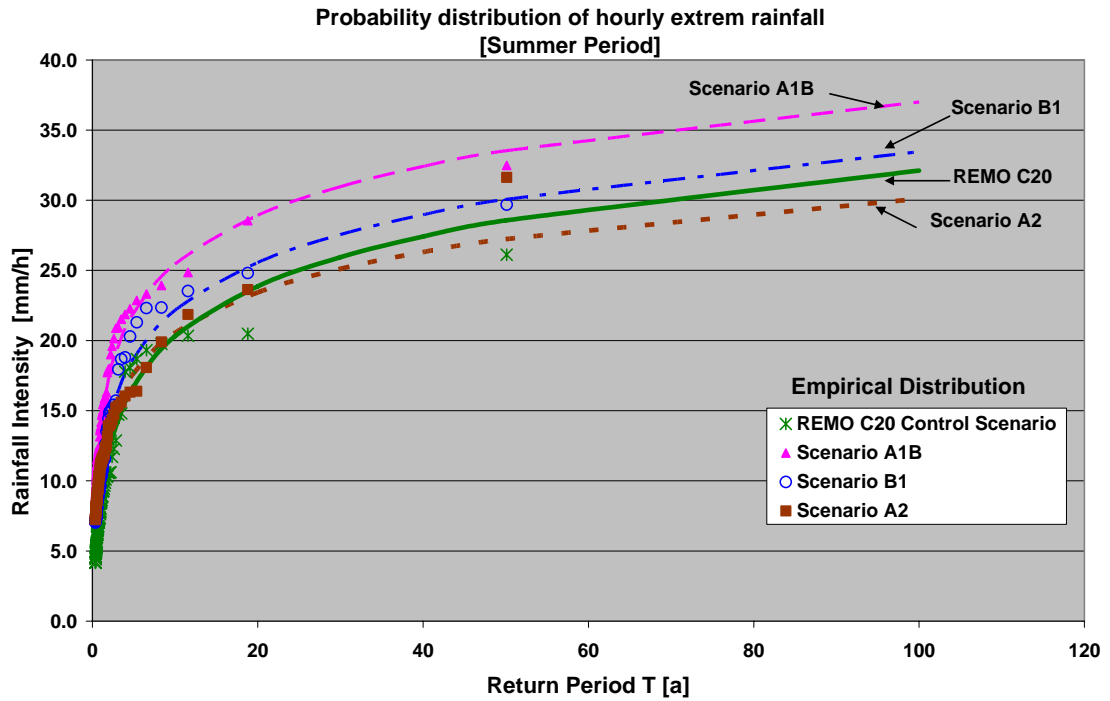
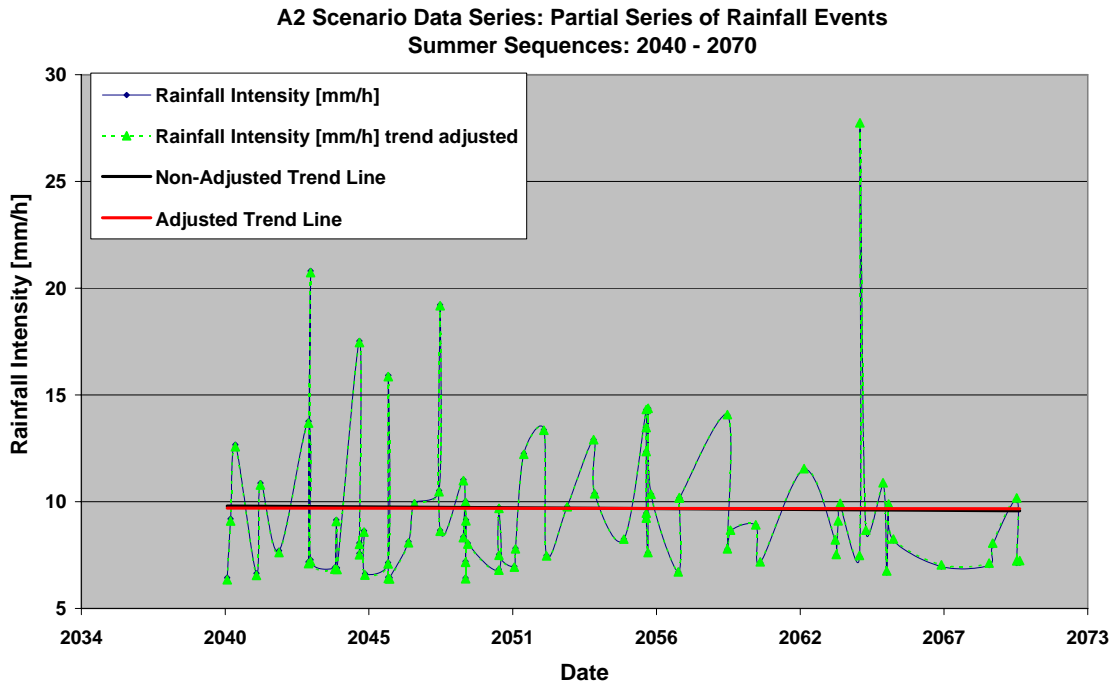
### 11.1 Summer Period

A1B Scenario Data Series: Partial Series of Rainfall Events - Summer Sequences: 2040 - 2070

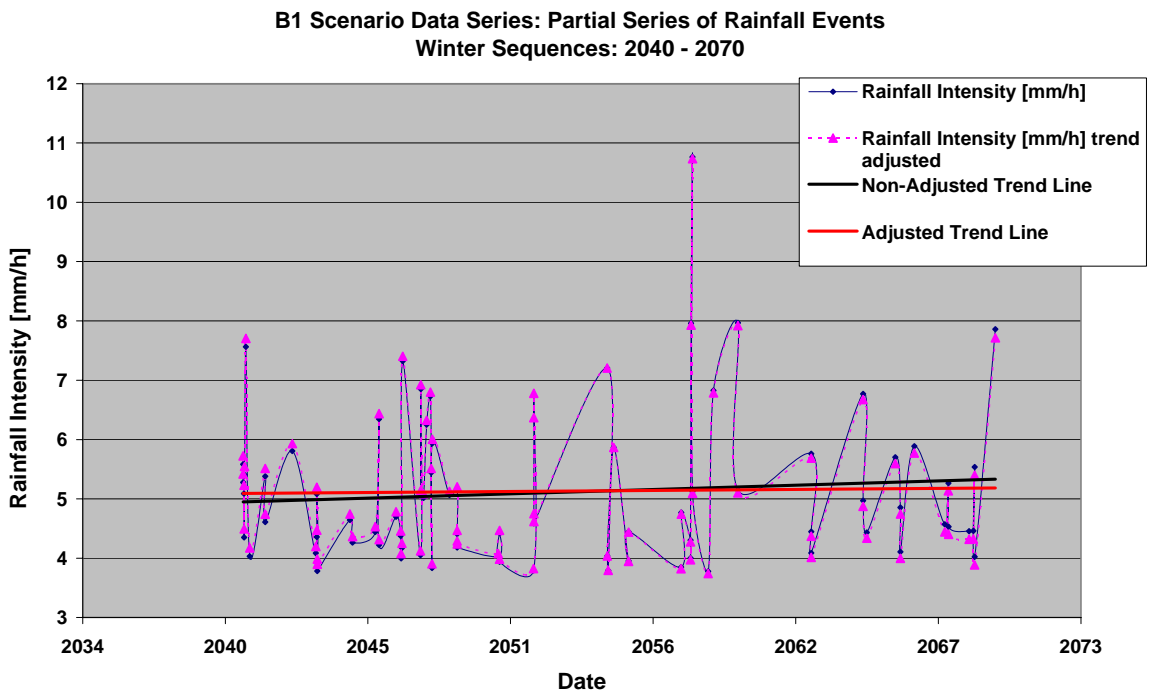
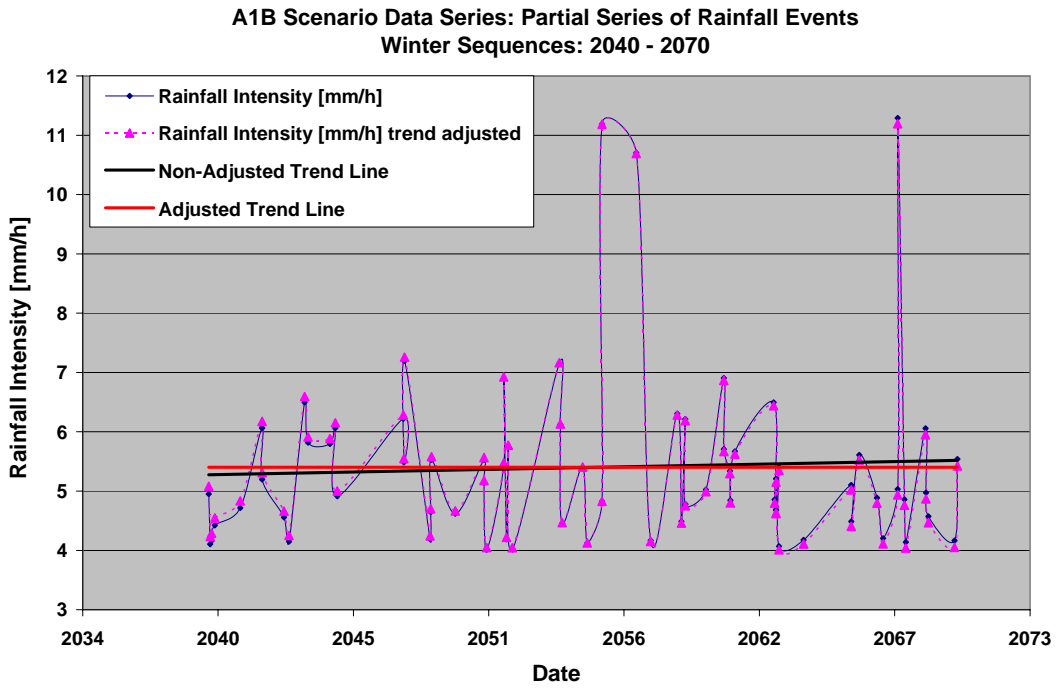


B1 Scenario Data Series: Partial Series of Rainfall Events Summer Sequences: 2040 - 2070

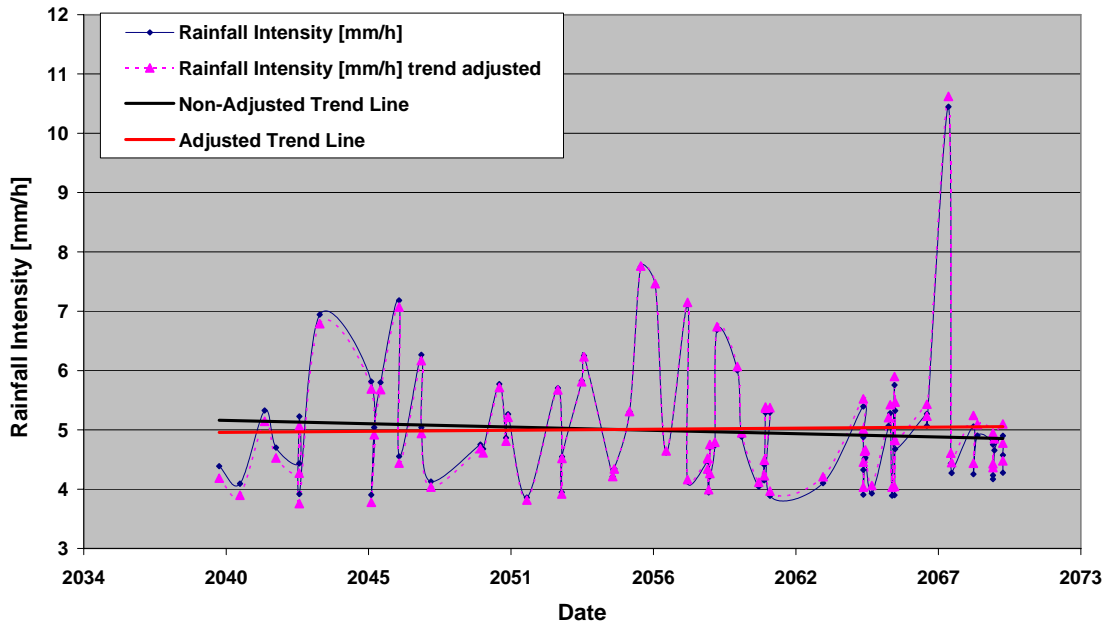




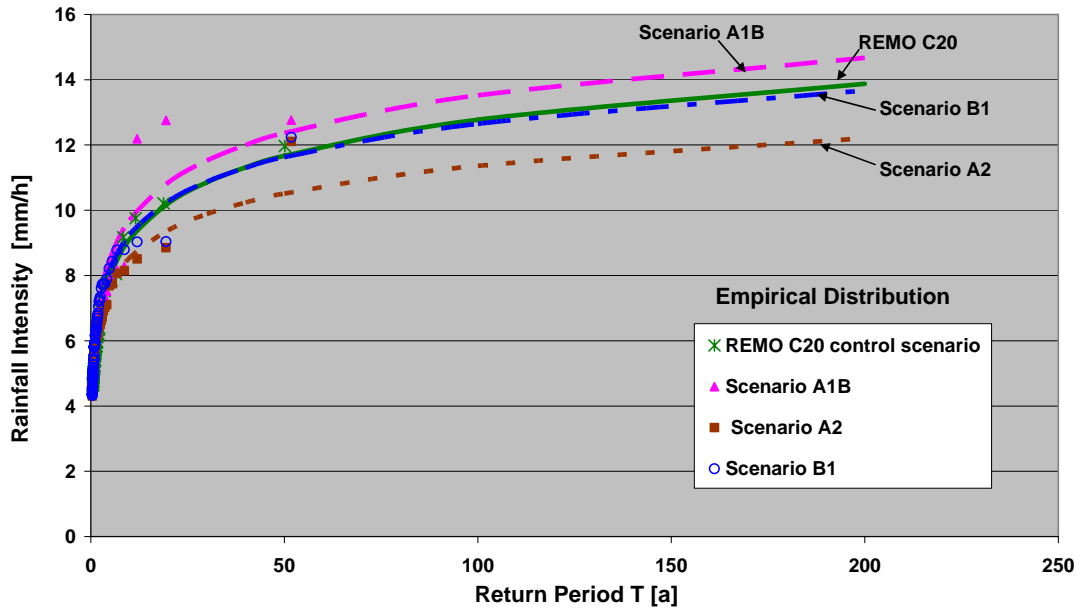
### 11.2 Winter Period



A2 Scenario Data Series: Partial Series of Rainfall Events  
Winter Sequences: 2040 - 2070

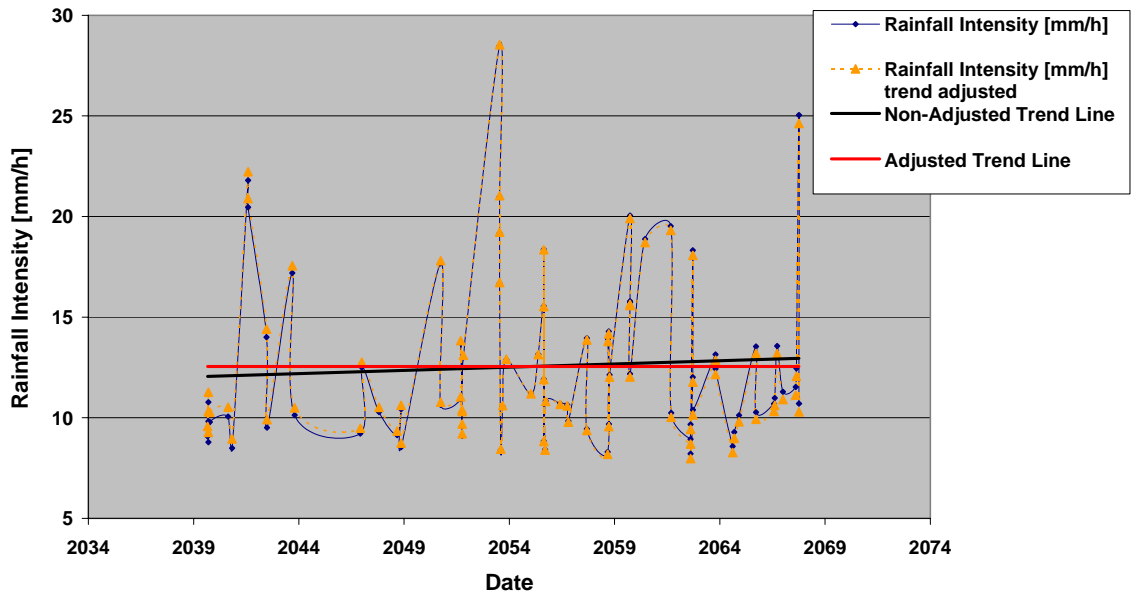


Probability distribution of hourly extrem rainfall events  
[Winter Period]

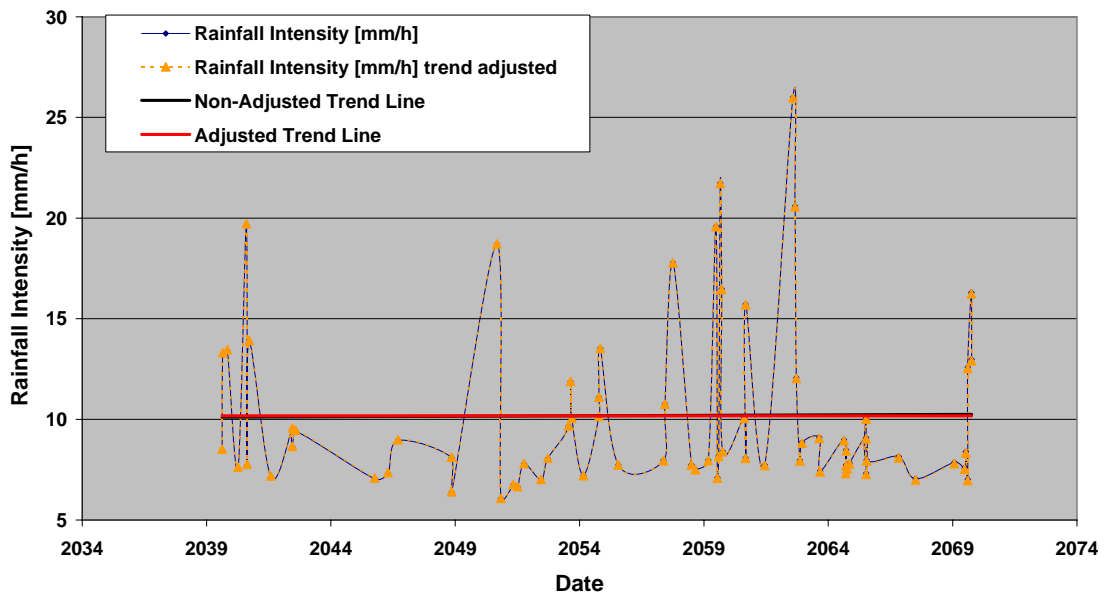


### 11.3 Yearly Periods

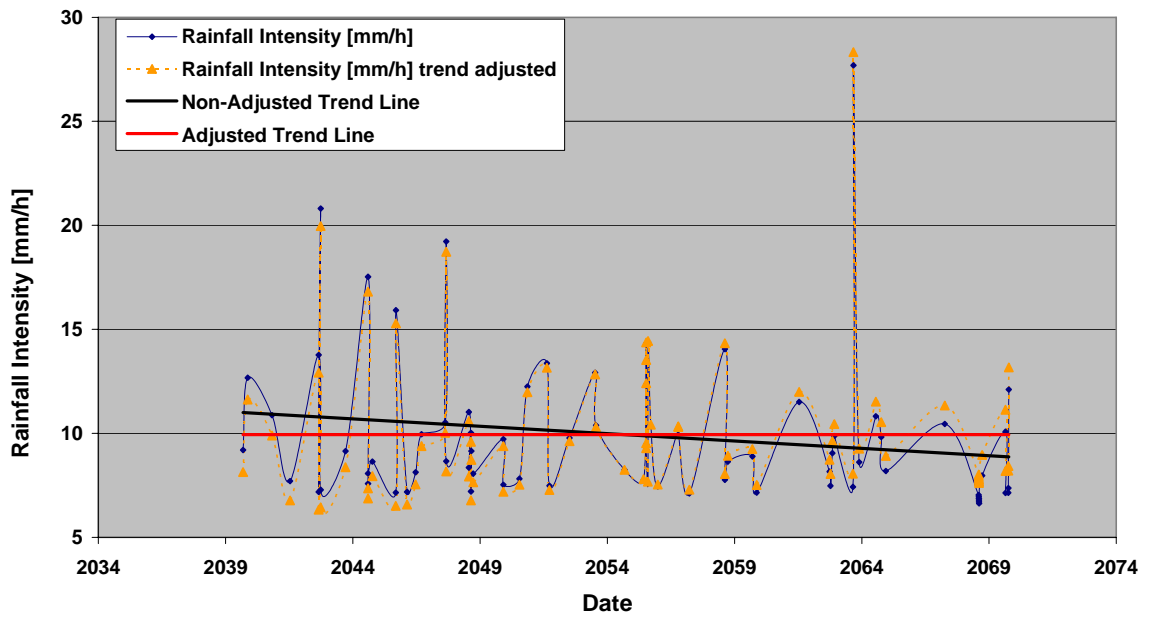
A1B Scenario Data Series: Partial Series of Rainfall Events  
Yearly Sequences: 2040 - 2070



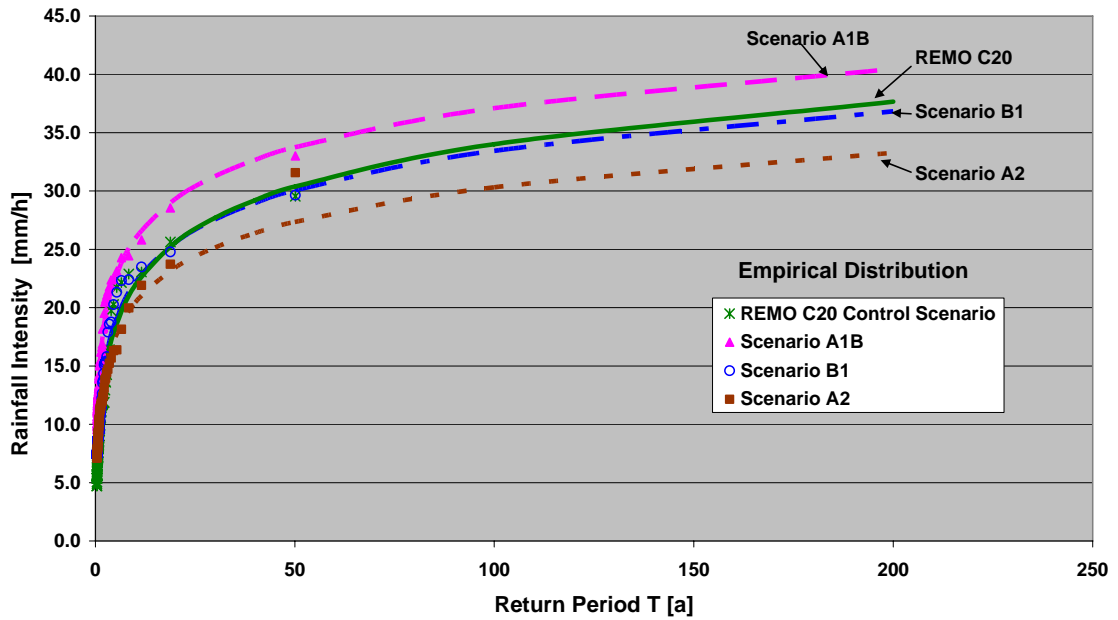
B1 Scenario Data Series: Partial Series of Rainfall Events  
Yearly Sequences: 2040 - 2070



A2 Scenario Data Series: Partial Series of Rainfall Events  
Yearly Sequences: 2040 - 2070

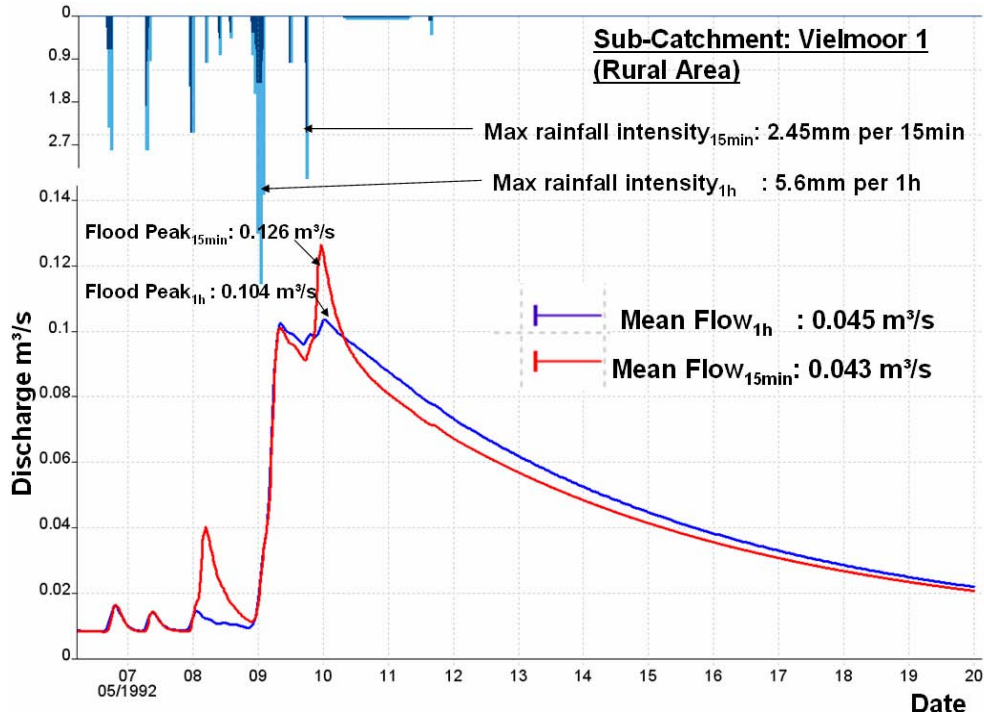


Probability distribution of hourly extrem rainfall events  
[Yearly Periods]

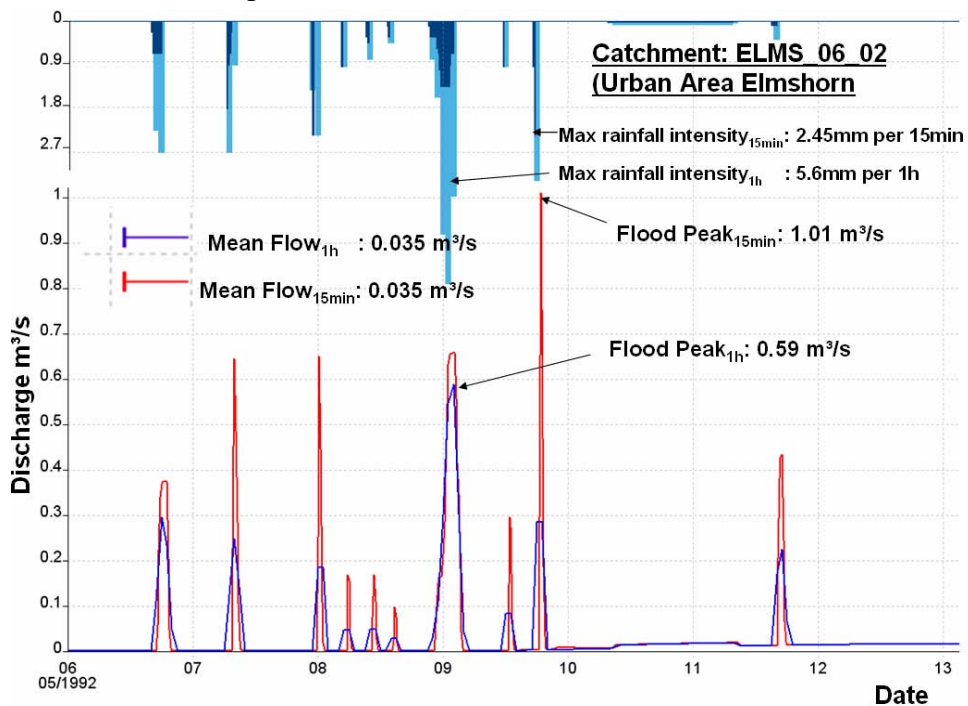


## Attachment 12

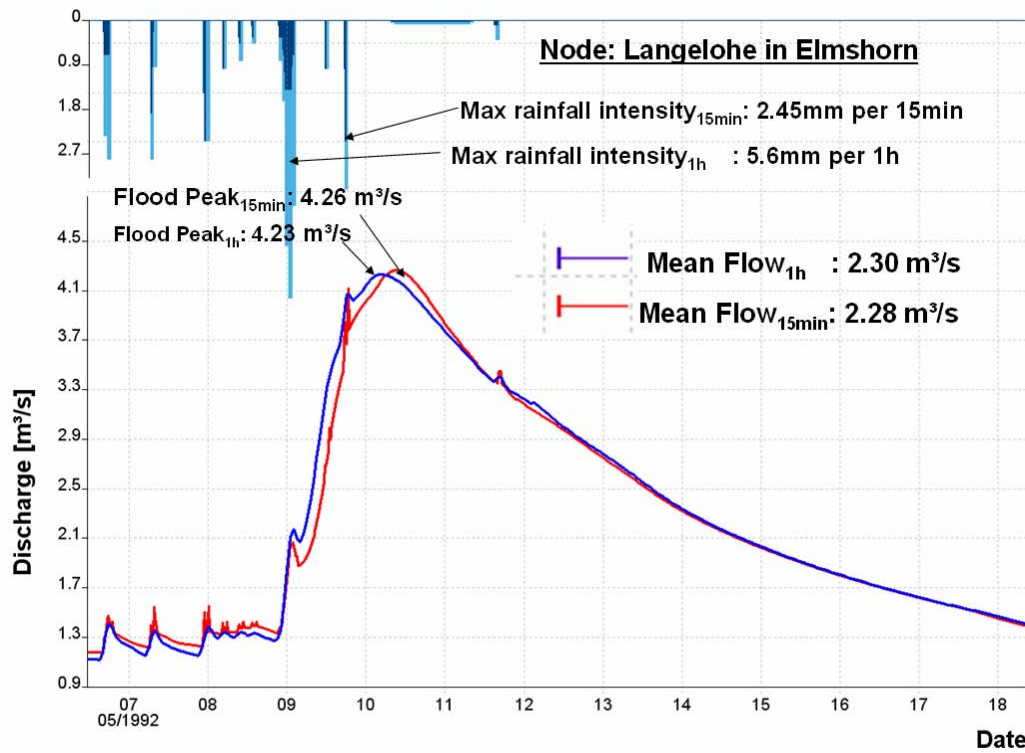
### Differentiation of Simulation Time Steps



Discharge hydrograph results of the rural sub-catchment: 'Vielmoor1', for different simulation timesteps (15minutes and 1h).



Discharge hydrograph results for the urban sub-catchment: ELMS\_06\_02, with different simulation timesteps (15minutes and 1h).

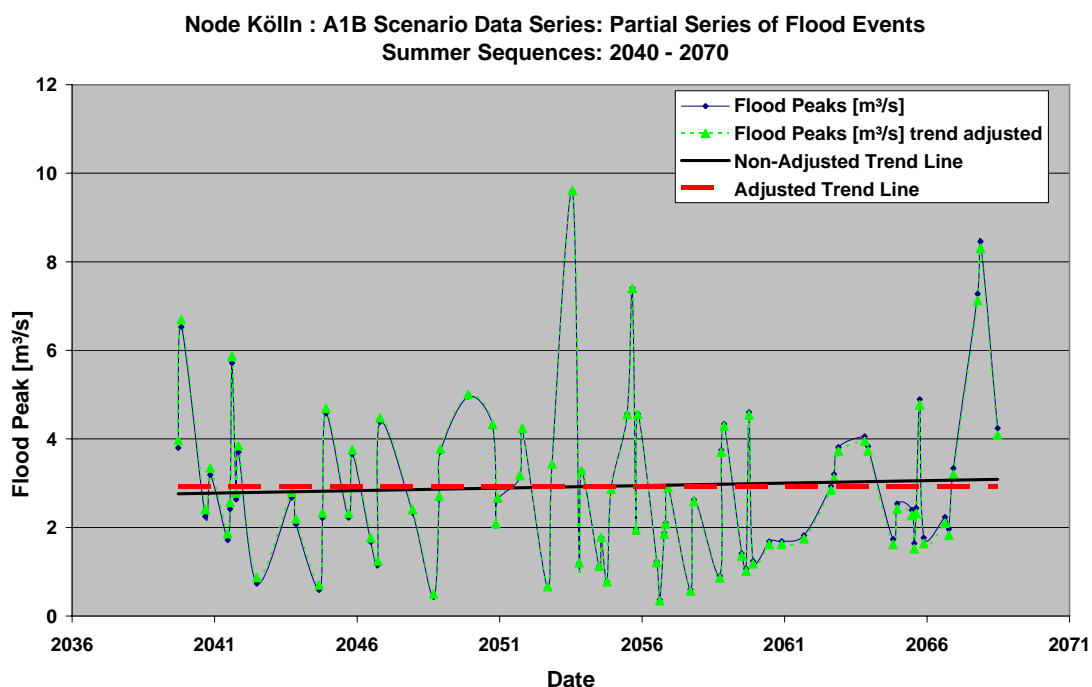


Discharge hydrograph results for the node: Langelohe in Elmshorn, with different simulation timesteps (15minutes and 1h).

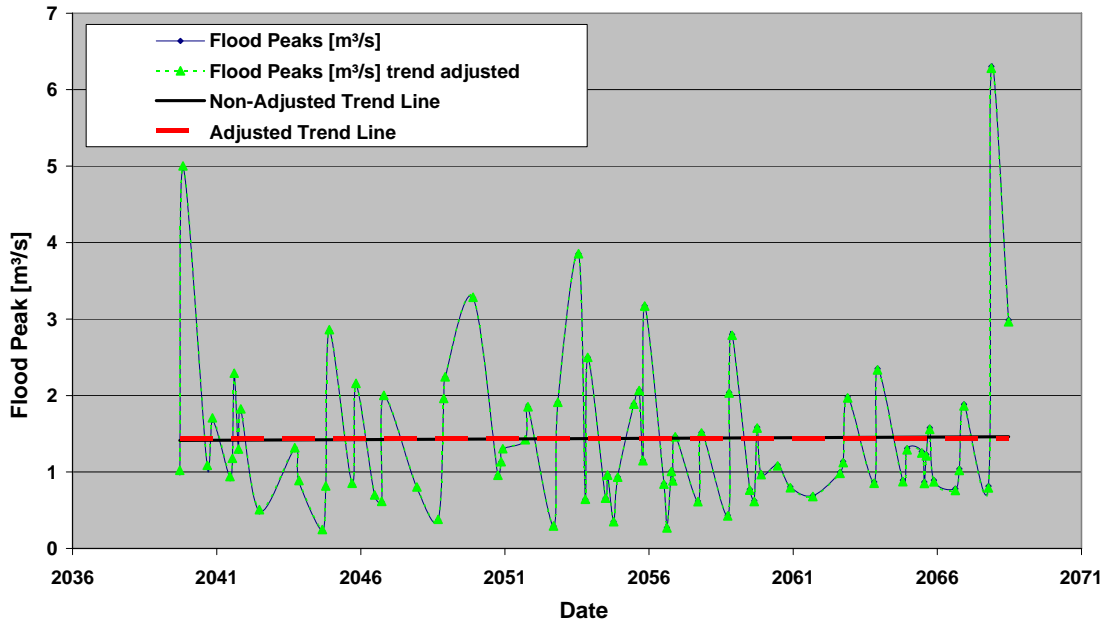
## Attachment 13

### Trend Adjustment of Flood Peak Data Series

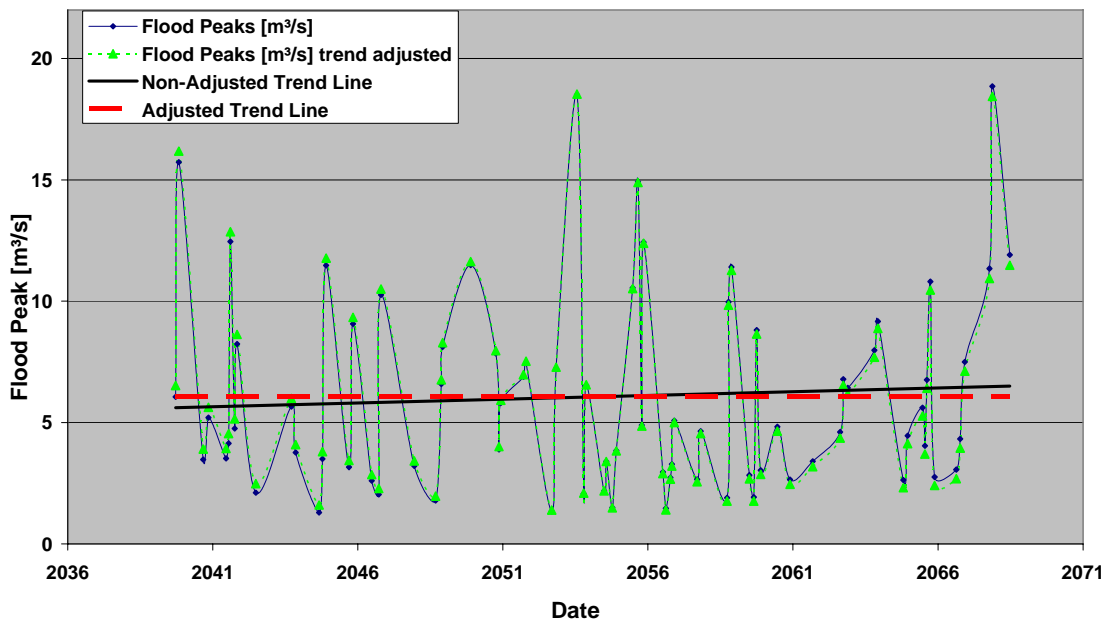
For the analysed five nodes and two sub-catchments, the trend adjustment diagrams for the summer periods, which have been worked out with the IPCC scenario A1B, are illustrated in this attachment. These diagrams are taken from 93 diagrams, which have been created for the seasons (summer, winter, yearly) and for all scenarios (0, C20, A1B, B1, A2) as well as nodes and both sub-catchments in Elmshorn.



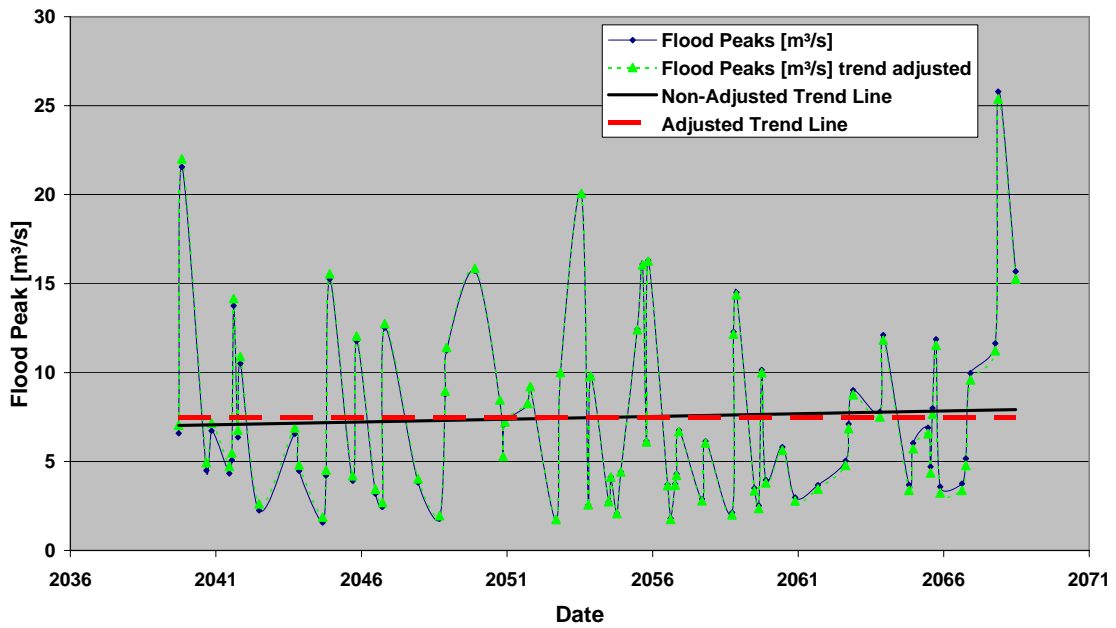
Node Offenau : A1B Scenario Data Series: Partial Series of Flood Events  
Summer Sequences: 2040 - 2070



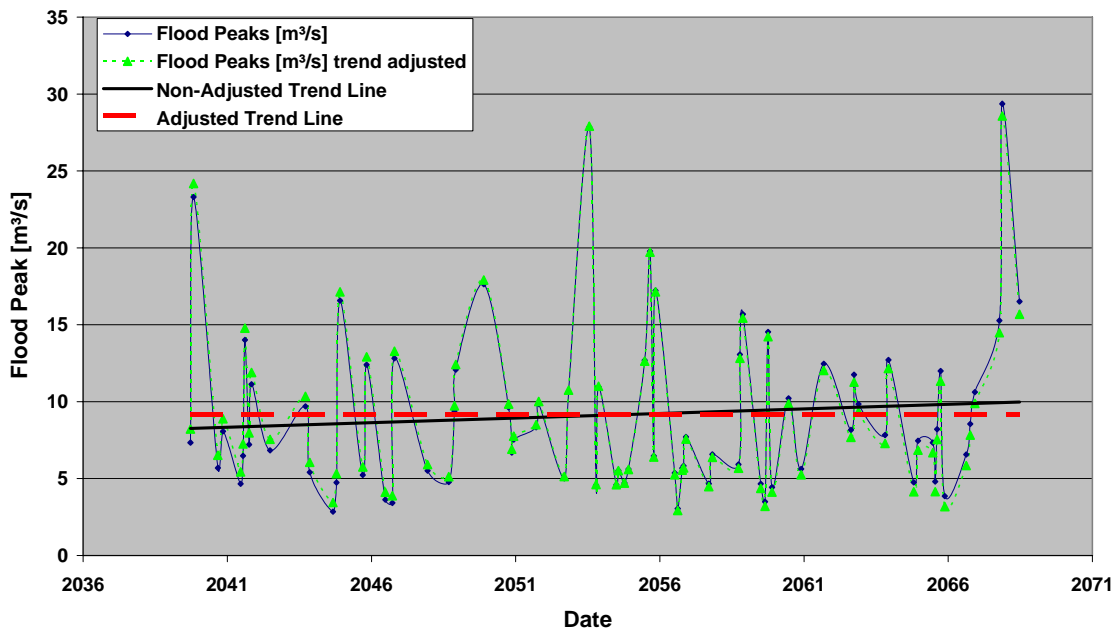
Node A23 : A1B Scenario Data Series: Partial Series of Flood Events  
Summer Sequences: 2040 - 2070



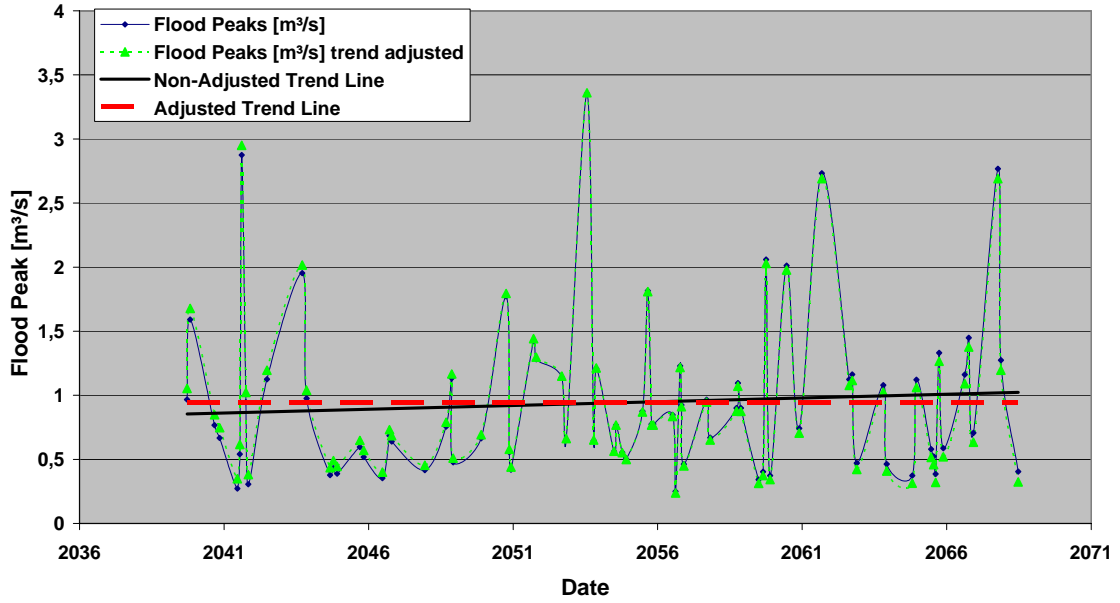
Node Langelohe : A1B Scenario Data Series: Partial Series of Flood Events  
Summer Sequences: 2040 - 2070



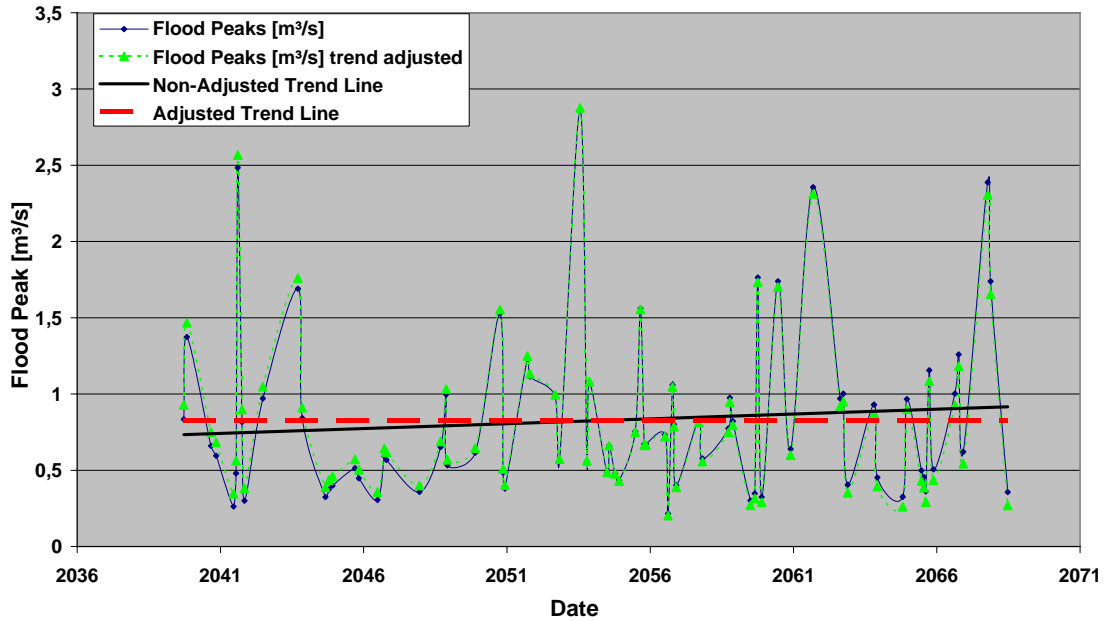
End Node (Elmshorn) : A1B Scenario Data Series: Partial Series of Flood Events  
Summer Sequences: 2040 - 2070



Sub-Catchment ELMS\_E06\_02 : A1B Scenario Data Series:  
Partial Series of Flood Events in Summer Sequences: 2040 - 2070



Sub-Catchment ELMSH\_E13\_04 : A1B Scenario Data Series:  
Partial Series of Flood Events in Summer Sequences: 2040 - 2070

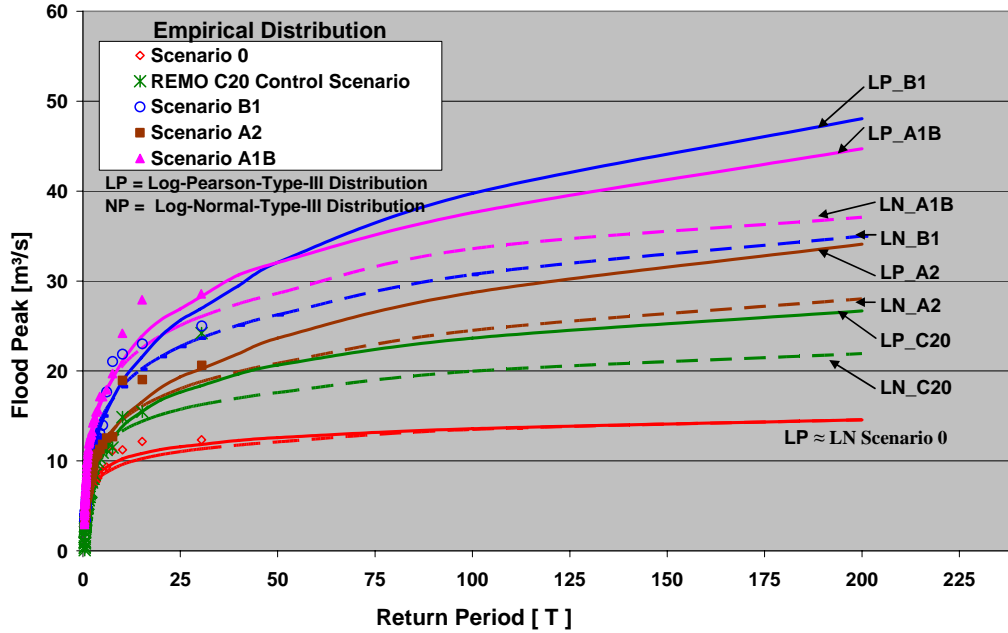


# Attachment 14

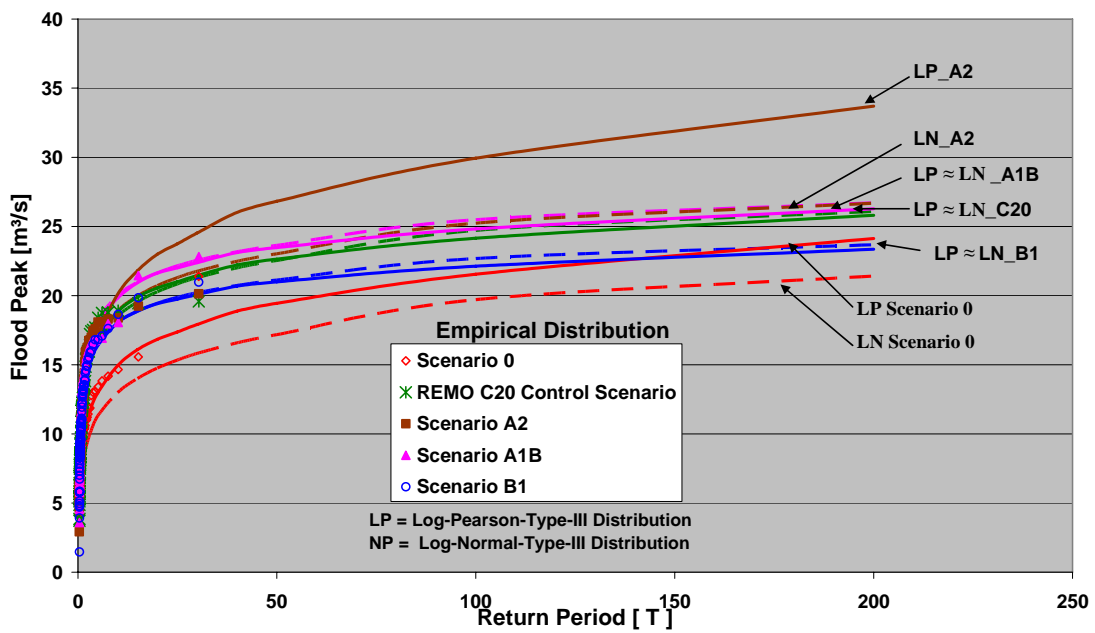
## Probability of Flood Peak Events

### 14.1 Log-Pearson Type III and the Log-Normal Type III Distributions

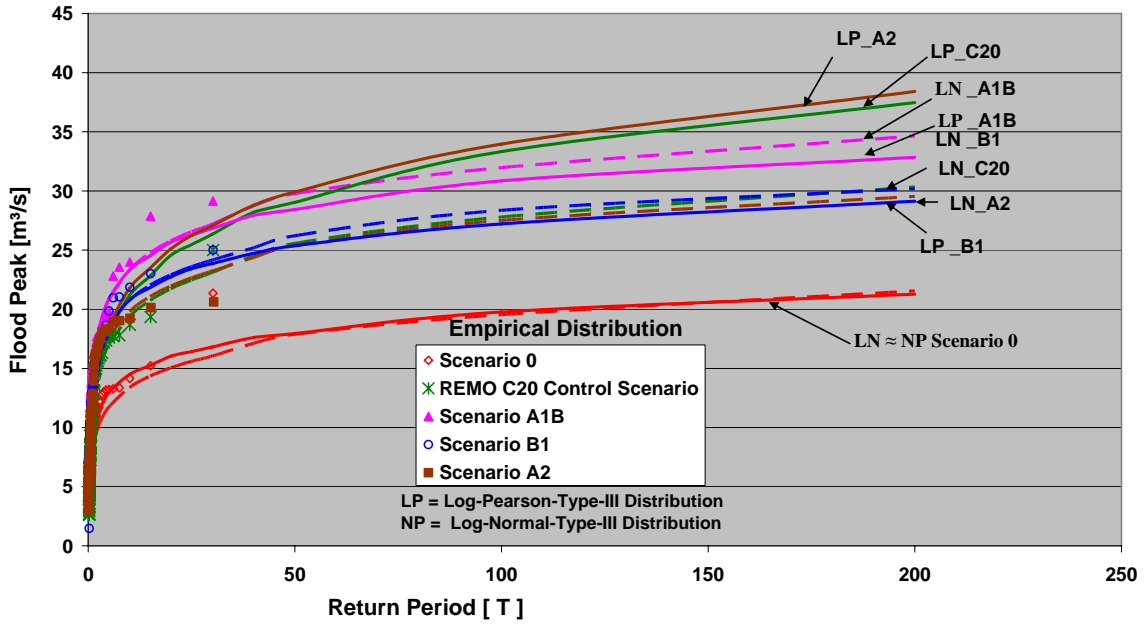
**End Node: Probability Distribution of Flood Events - Summer Periods**



**End Node: Probability Distribution of Flood Events - Winter Periods**



**End Node: Probability Distribution of Flood Events - Yearly Periods**

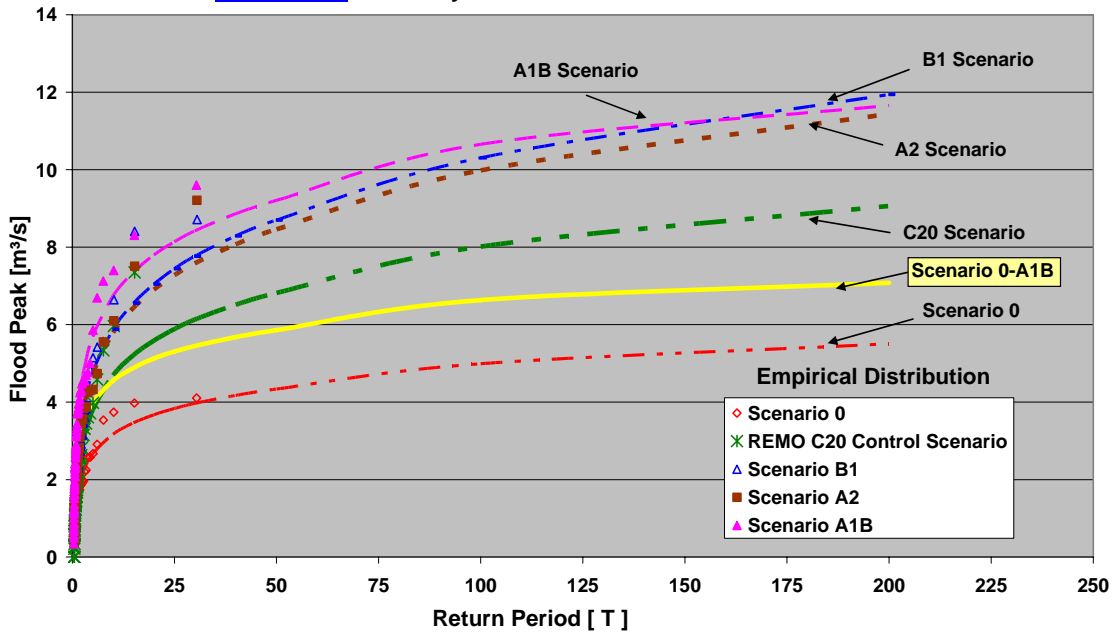


**14.2 Flood Probability Distribution Curves**

**14.2.1 Flood Probability Distribution Curves (Summer Periods)**

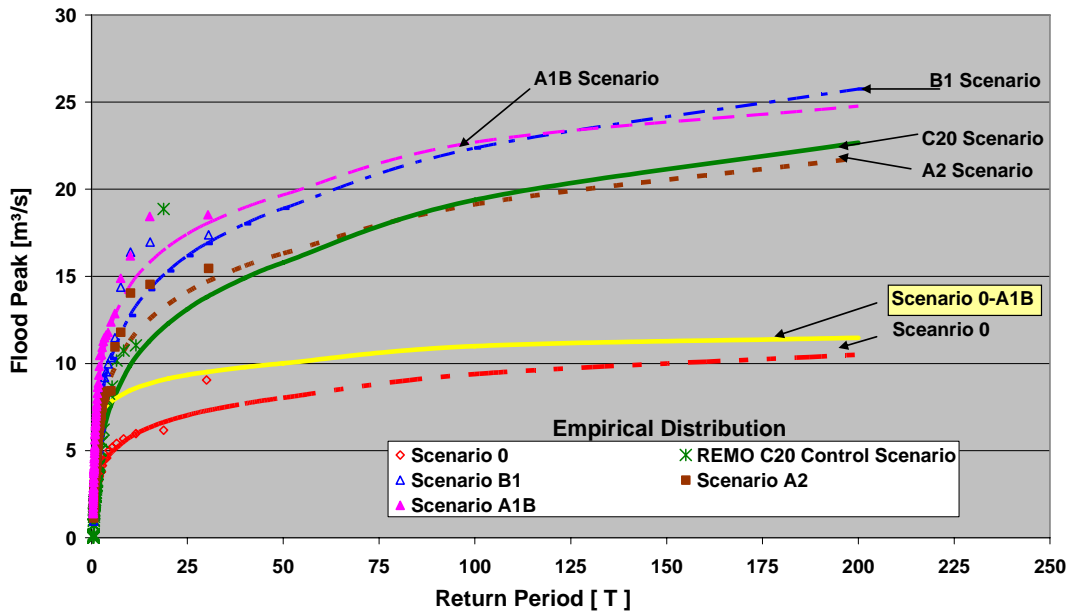
**Log-Normal-Type-III Distribution**

**Node Kölln: Probability Distribution of Flood Events - Summer Periods**

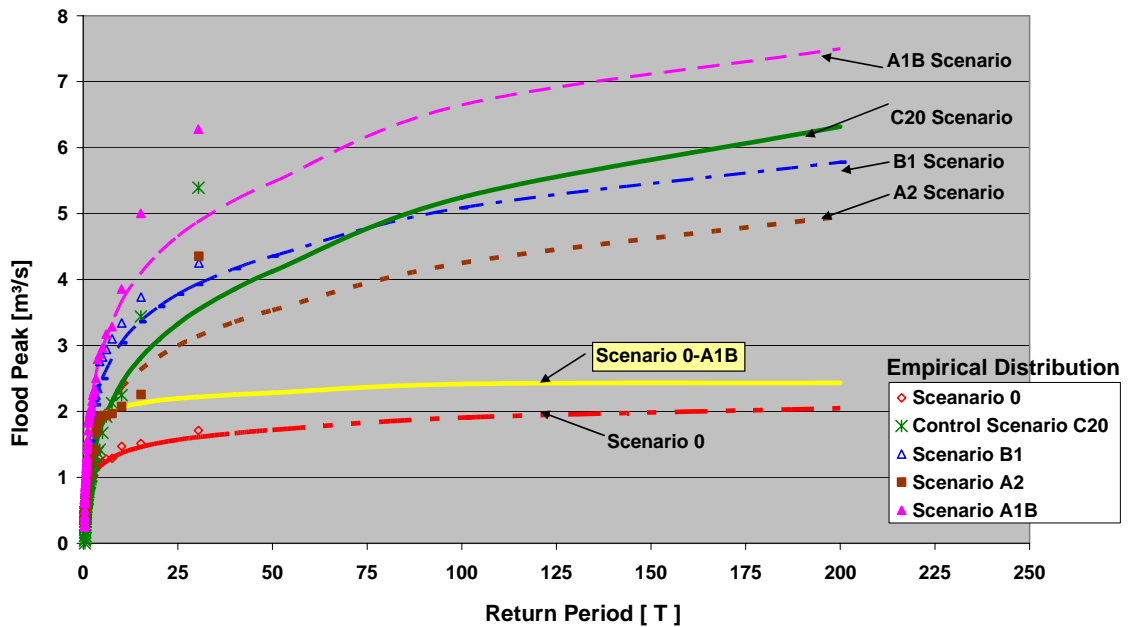


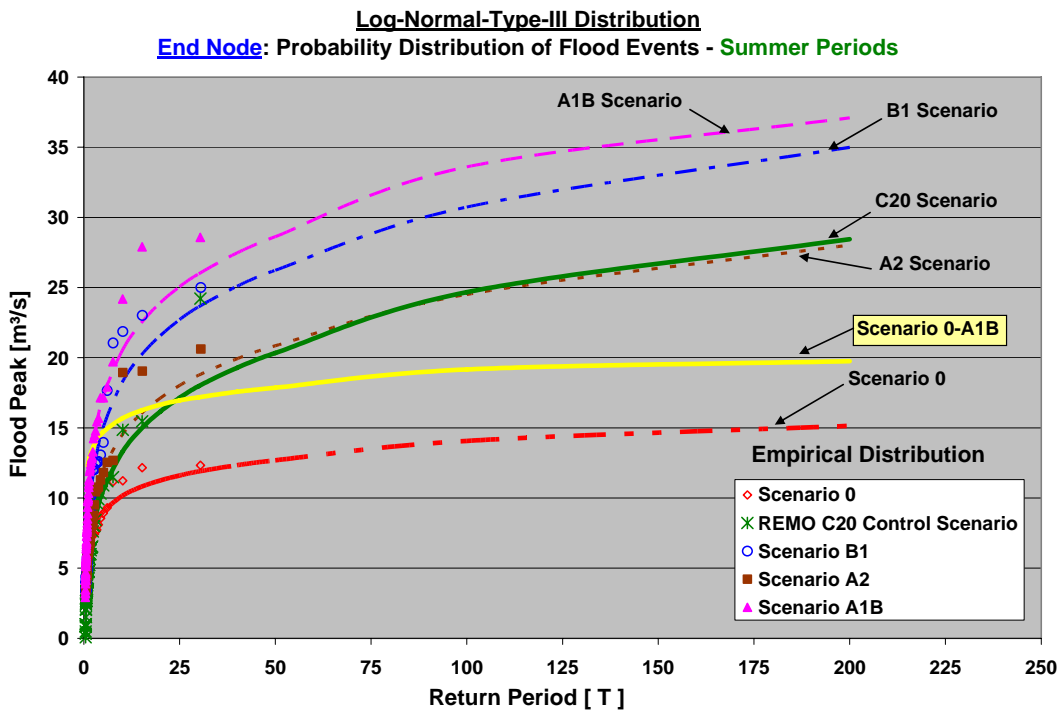
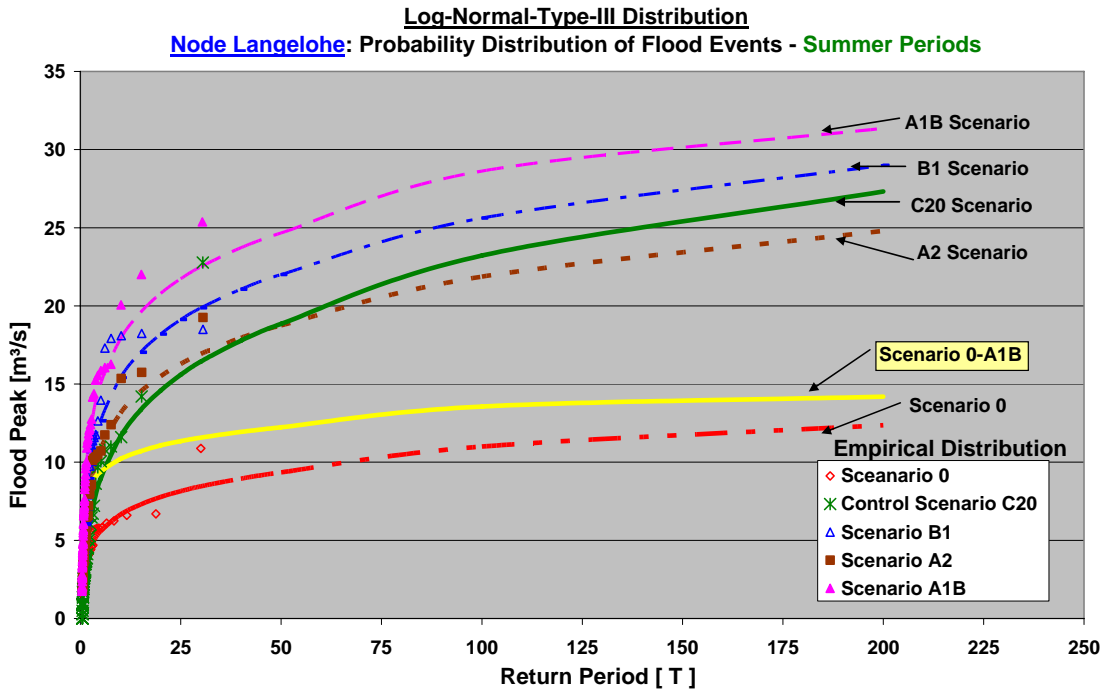
**Note: Scenario 0-A1B:** In the post-processing, the derived largest changes by the IPCC Scenario A1B have been referred to the Scenario 0 probability distribution curves, which results in the Scenario 0-A1B curve. [Explained in 5.5.2]

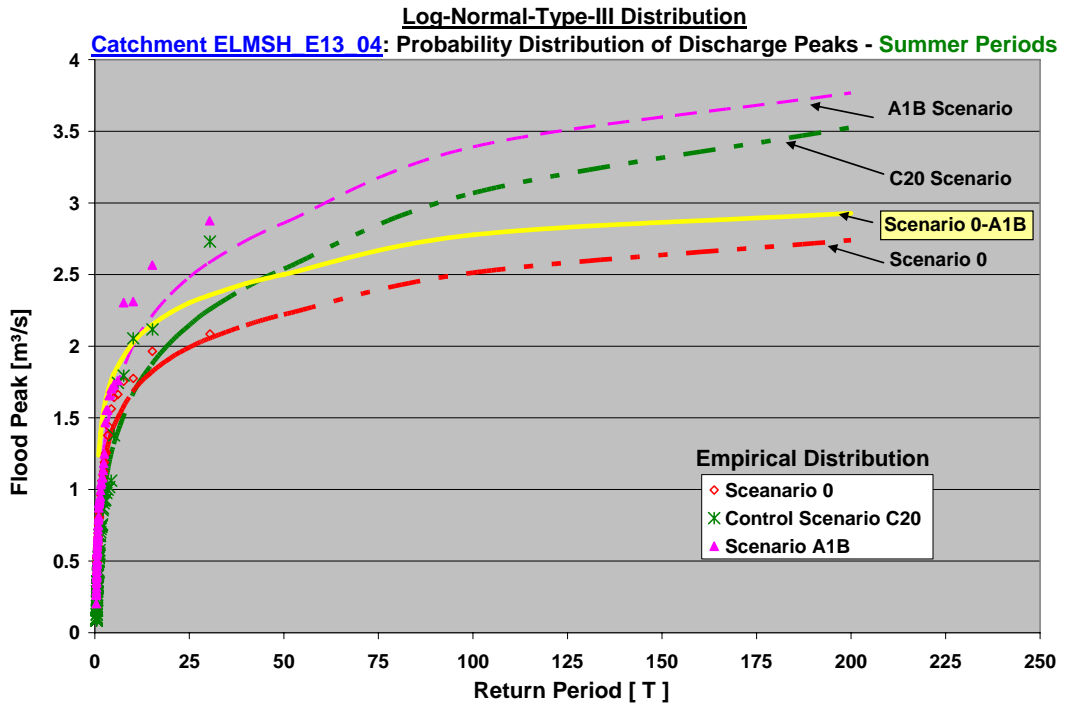
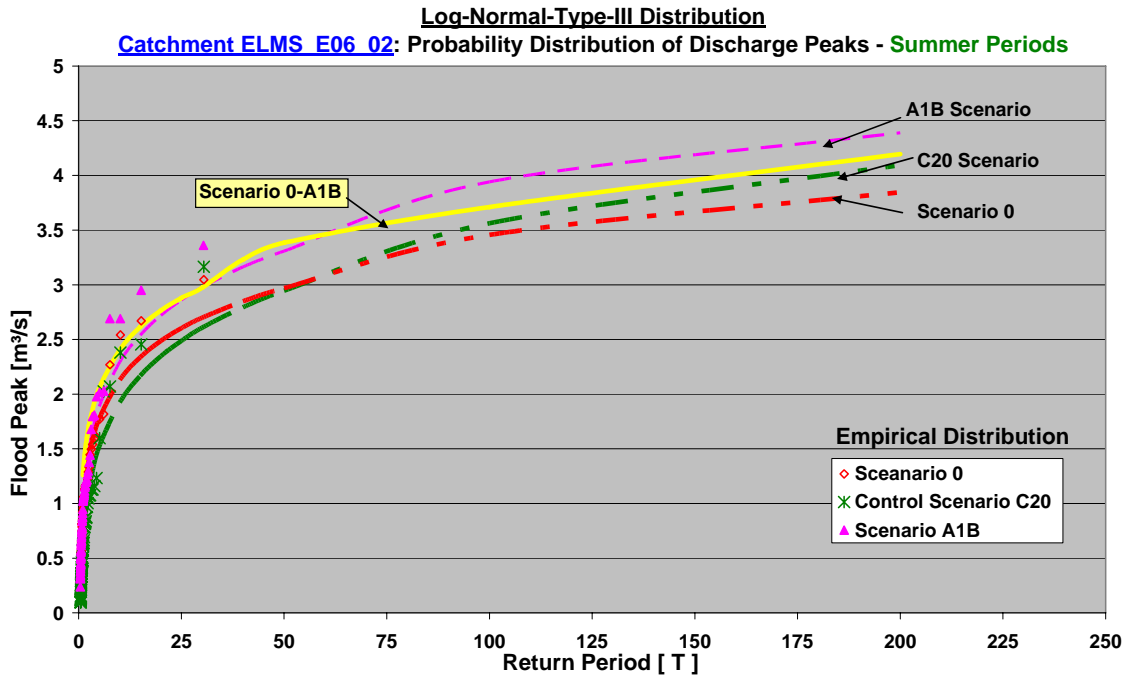
**Log-Normal-Type-III Distribution**  
**Node A23: Probability Distribution of Flood Events - Summer Periods**



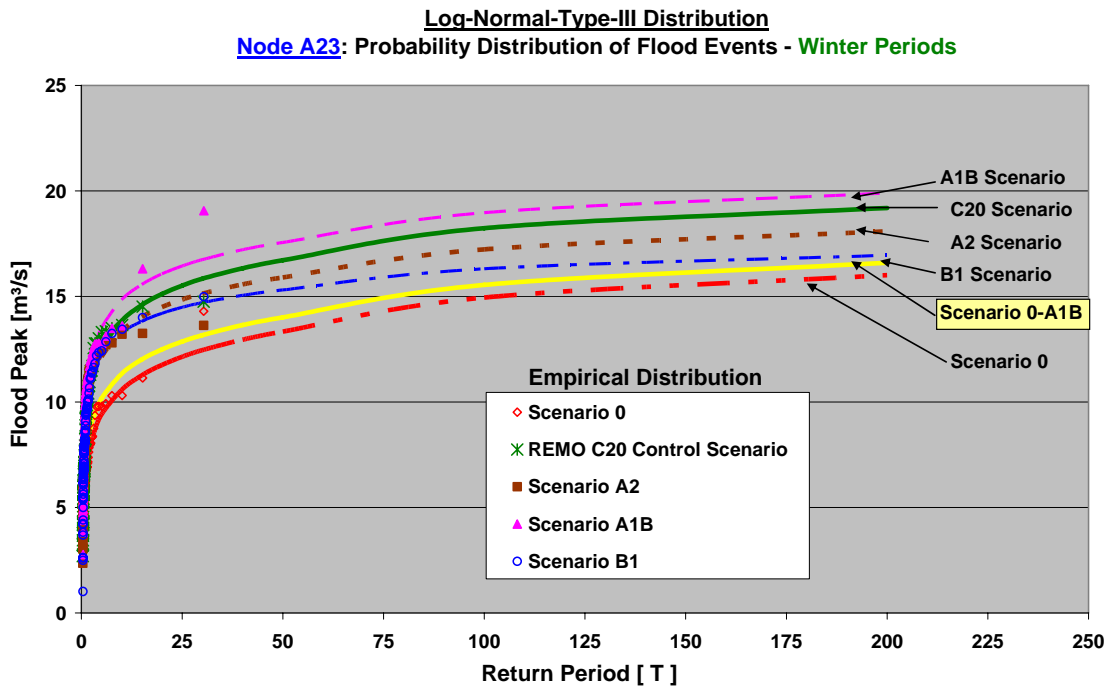
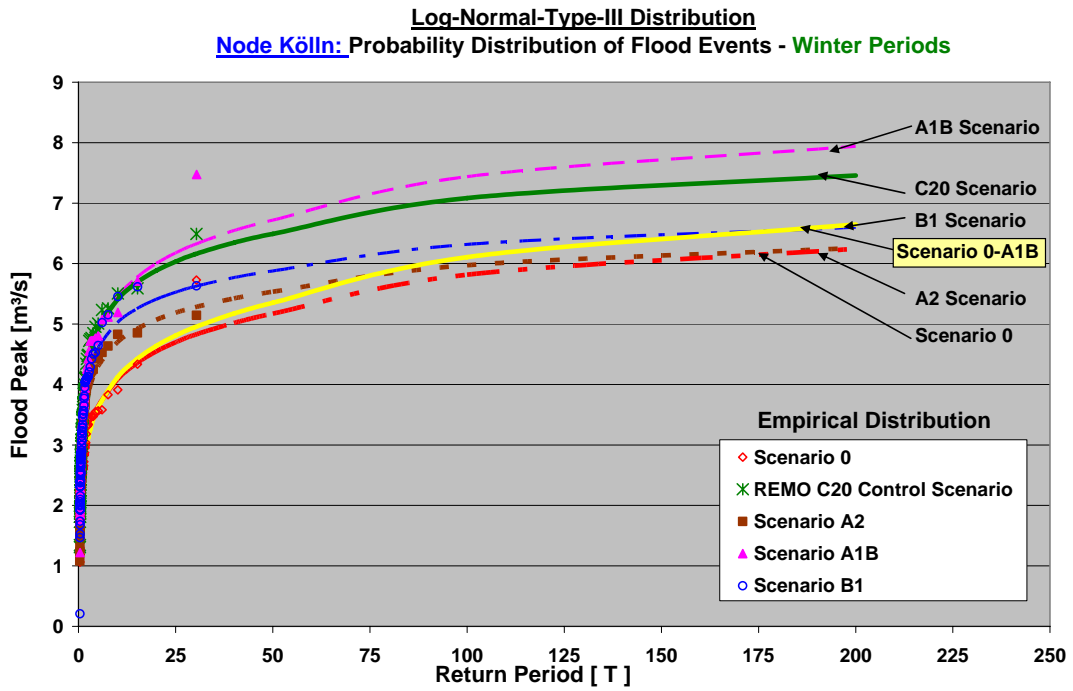
**Log-Normal-Type-III Distribution**  
**Node Offenau: Probability Distribution of Flood Events - Summer Periods**

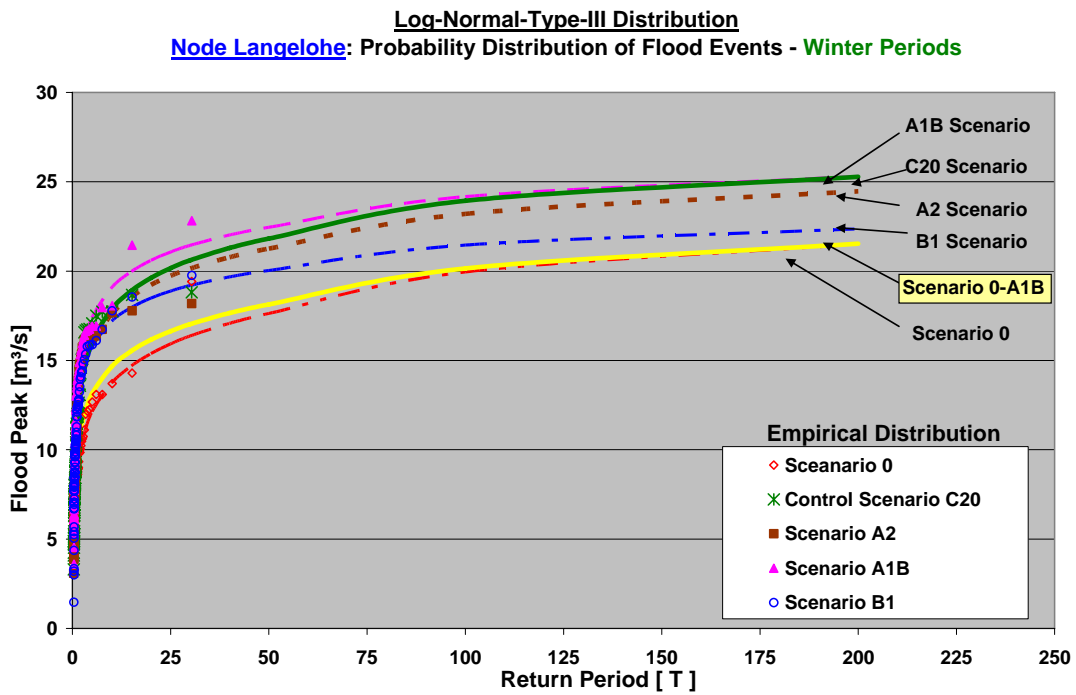
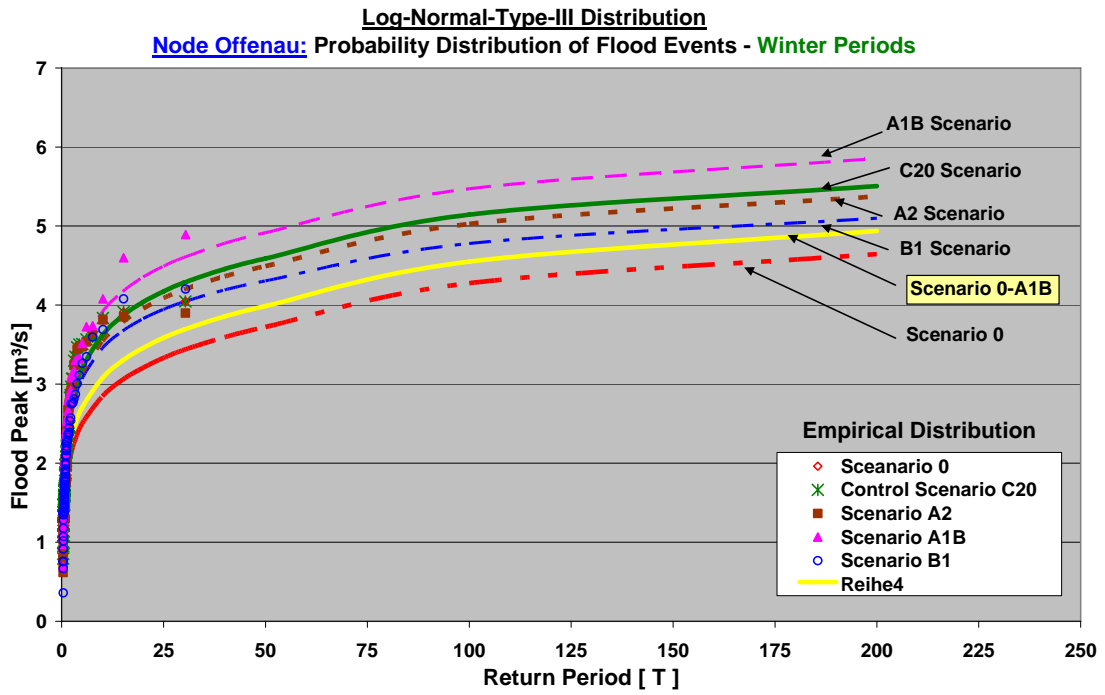


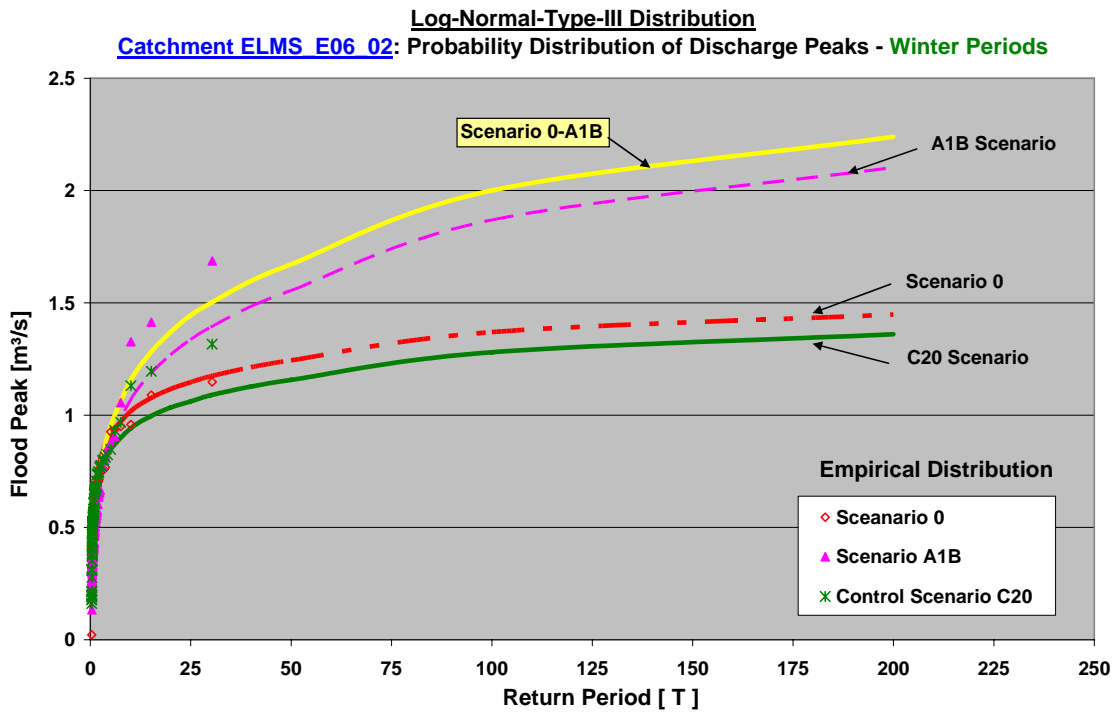
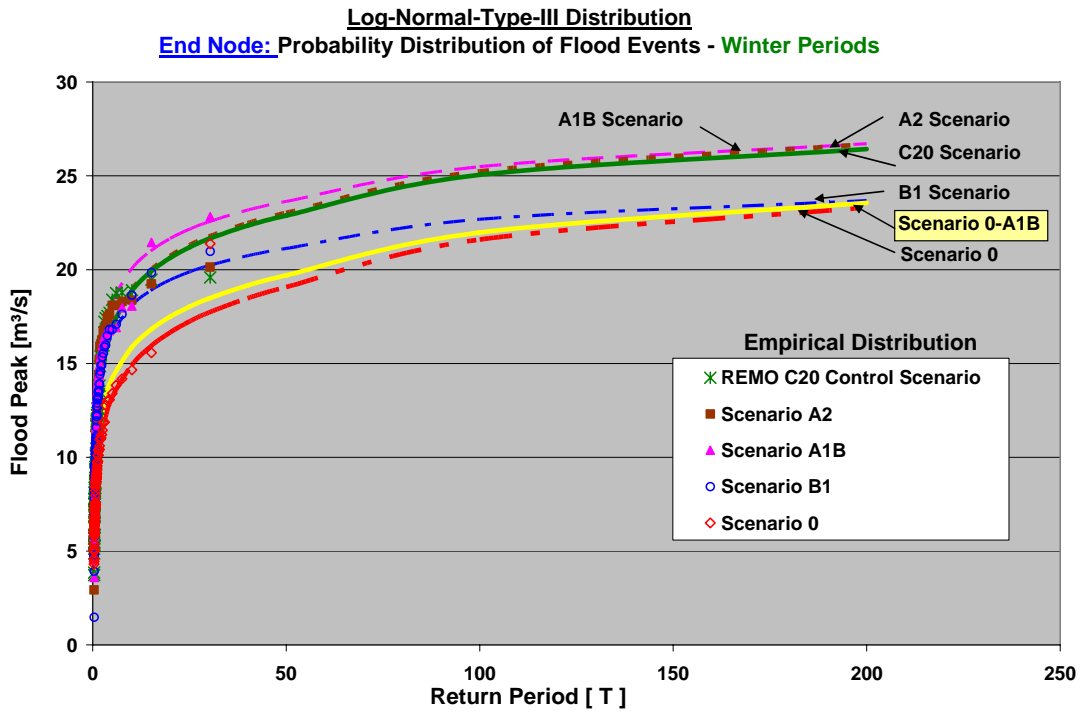


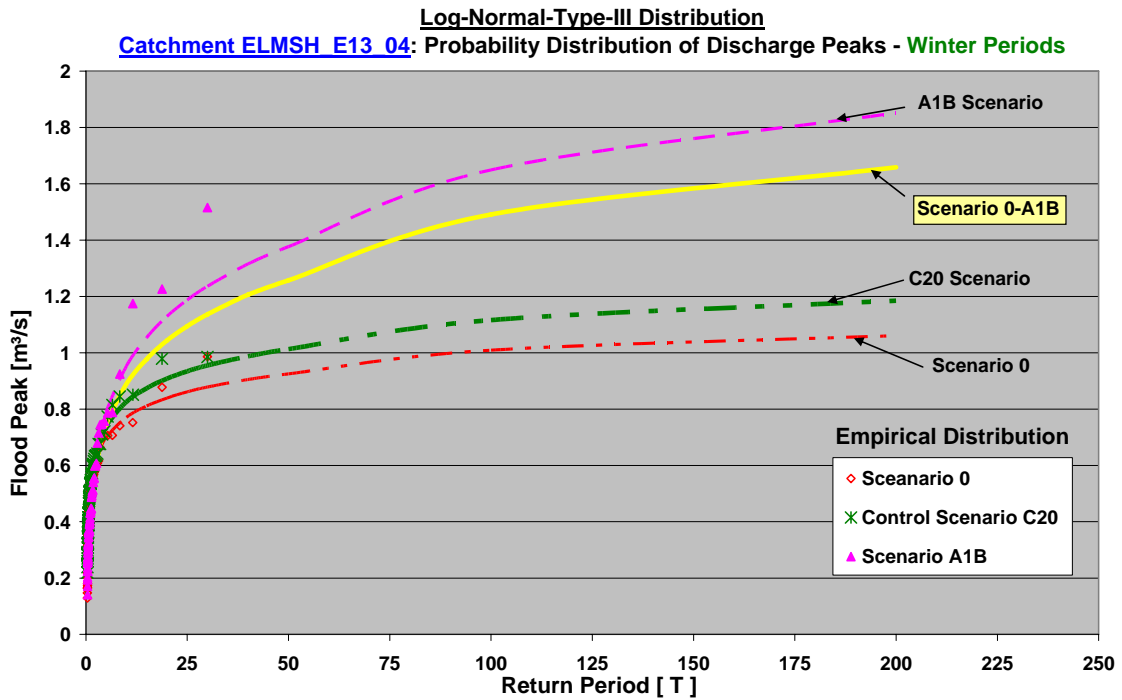


14.2.2 Flood Probability Distribution Curves (Winter Periods)

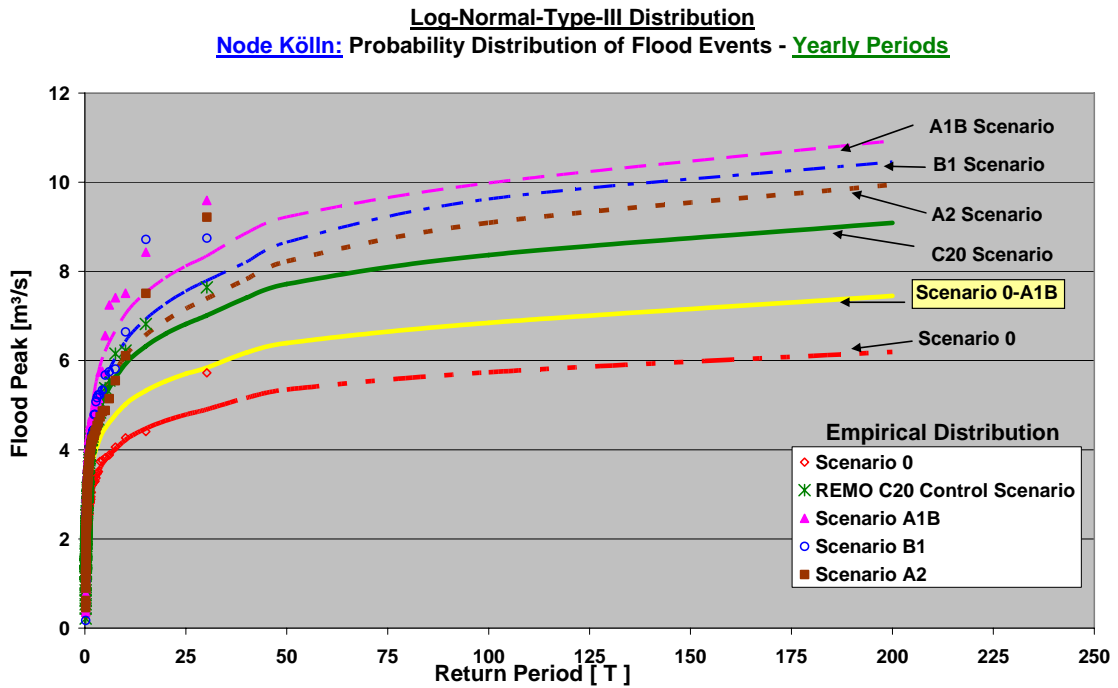


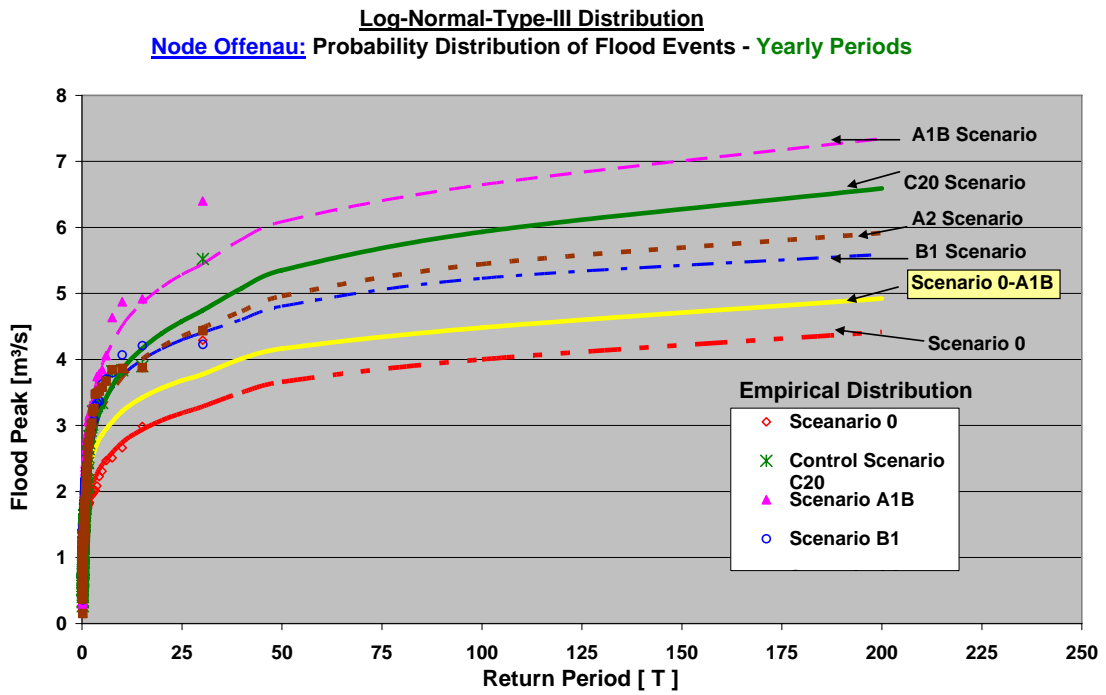
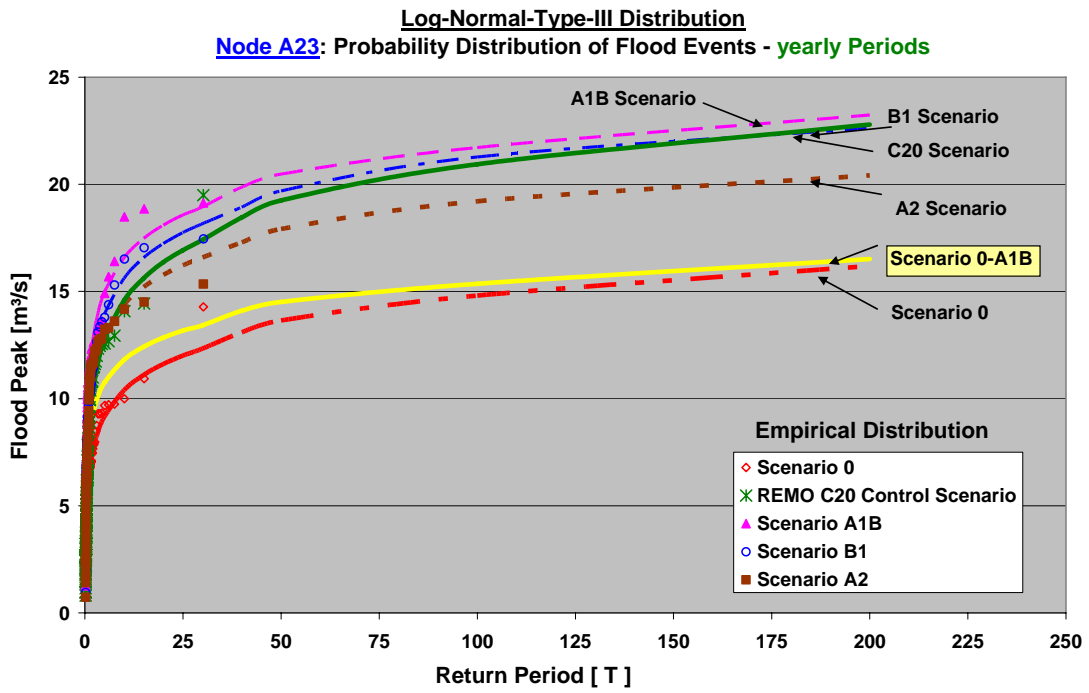


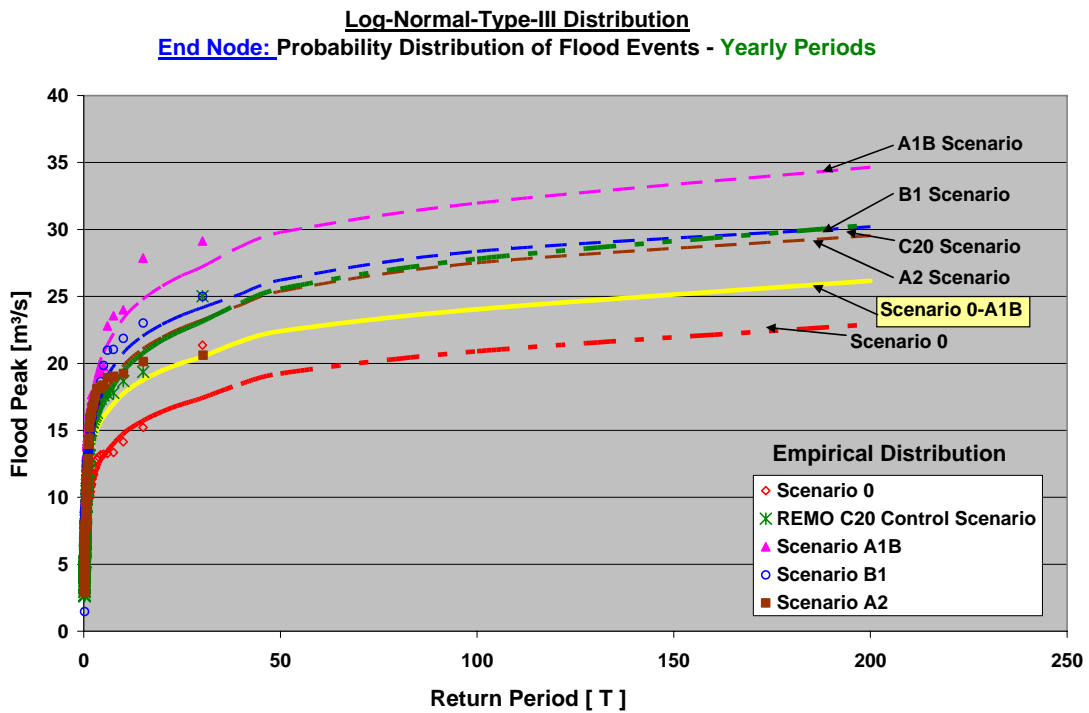
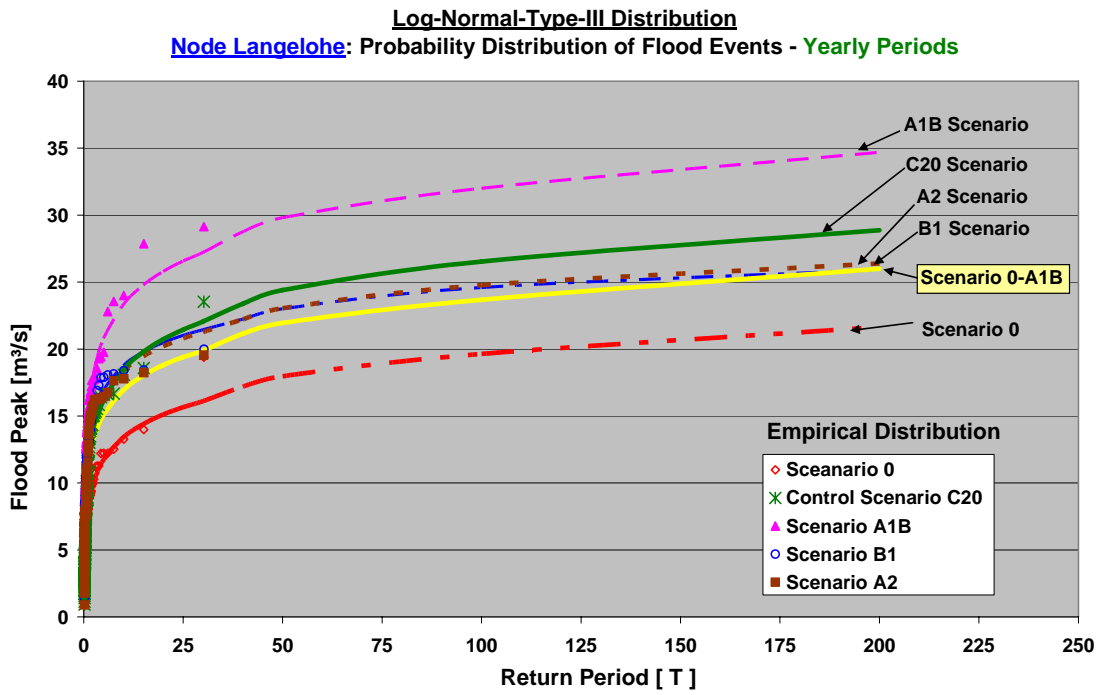


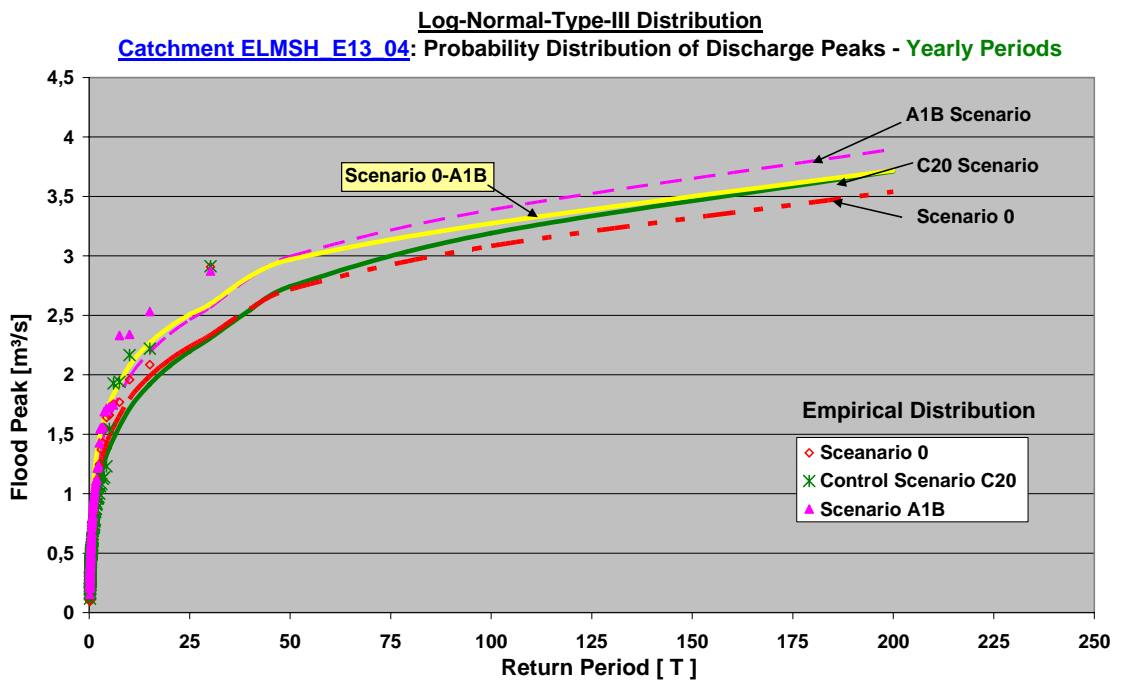
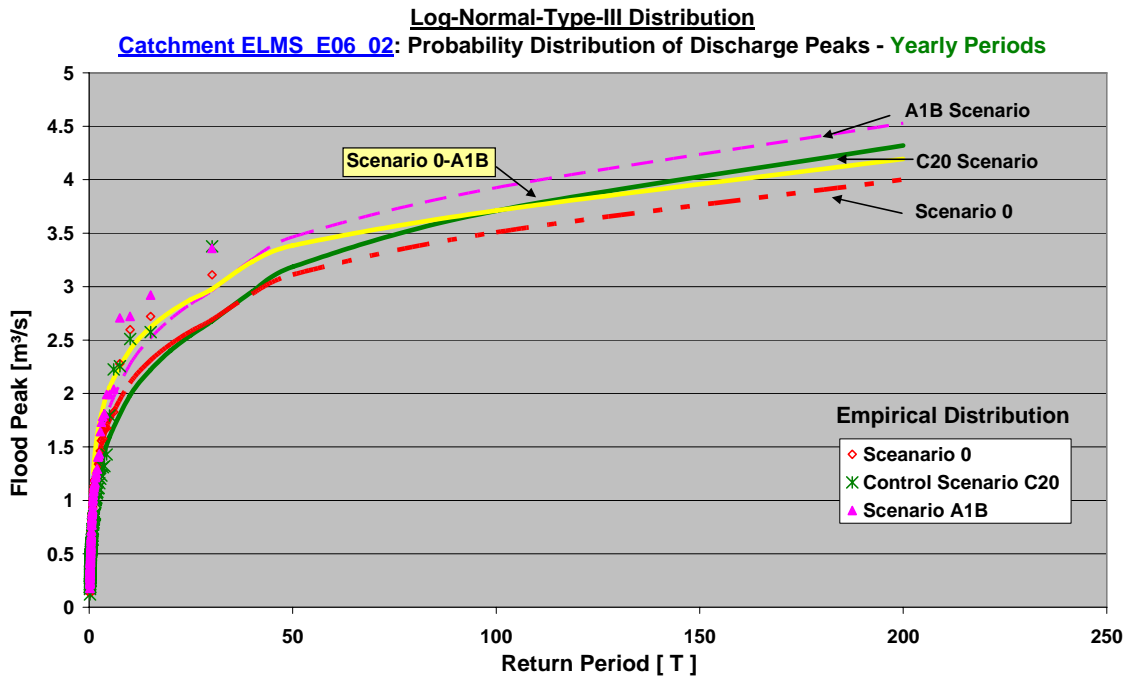


14.2.3 Flood Probability Distribution Curves (Yearly Periods)









## 14.3 Tables: Control Scenario Results [1971 - 2000]

| Summer<br>Periods            | [1971 - 2000] |             |             |             |             |             |             |             |             | Return Period T [a] |
|------------------------------|---------------|-------------|-------------|-------------|-------------|-------------|-------------|-------------|-------------|---------------------|
|                              | 1             | 2           | 3           | 5           | 10          | 20          | 30          | 50          | 100         |                     |
| <b>Eckhorner Au</b>          |               |             |             |             |             |             |             |             |             |                     |
| Δ [%]                        | 20.3          | 33.2        | 37.9        | 42.7        | 47.9        | 52.1        | 54.5        | 57.1        | 60.6        | %                   |
| <b>Offenau</b>               |               |             |             |             |             |             |             |             |             |                     |
| Δ [%]                        | -10.3         | 17.3        | 32.4        | 51.2        | 76.9        | 103.0       | 119.3       | 139.8       | 175.2       | %                   |
| <b>Node A23</b>              |               |             |             |             |             |             |             |             |             |                     |
| Δ [%]                        | -3.6          | 29.7        | 43.0        | 56.4        | 71.1        | 83.0        | 89.5        | 96.6        | 106.4       | %                   |
| <b>Node Langelohe</b>        |               |             |             |             |             |             |             |             |             |                     |
| Δ [%]                        | -4.0          | 31.4        | 45.6        | 59.9        | 75.4        | 87.8        | 94.5        | 101.7       | 111.1       | %                   |
| <b>End Node</b>              |               |             |             |             |             |             |             |             |             |                     |
| Δ [%]                        | -23.7         | -3.8        | 5.9         | 16.9        | 30.7        | 43.7        | 51.2        | 60.3        | 75.3        | %                   |
| <b>Catchment ELMS_E06_02</b> |               |             |             |             |             |             |             |             |             |                     |
| Δ [%]                        | -32.1         | -22.4       | -18.4       | -14.3       | -9.6        | -5.6        | -3.4        | -0.8        | 3.1         | %                   |
| <b>Catchment ELMS_E06_02</b> |               |             |             |             |             |             |             |             |             |                     |
| Δ [%]                        | -17.7         | -9.9        | -5.8        | -1.0        | 5.4         | 11.4        | 15.0        | 19.3        | 26.5        | %                   |
| <b>Average</b>               |               |             |             |             |             |             |             |             |             |                     |
| Δ [%]                        | <b>-10.1</b>  | <b>10.8</b> | <b>20.1</b> | <b>30.3</b> | <b>42.5</b> | <b>53.6</b> | <b>60.1</b> | <b>67.7</b> | <b>79.7</b> | <b>%</b>            |

| Winter<br>Periods            | [1971 - 2000] |             |             |             |             |             |             |             |             | Return Period T [a] |
|------------------------------|---------------|-------------|-------------|-------------|-------------|-------------|-------------|-------------|-------------|---------------------|
|                              | 1             | 2           | 3           | 5           | 10          | 20          | 30          | 50          | 100         |                     |
| <b>Eckhorner Au</b>          |               |             |             |             |             |             |             |             |             |                     |
| Δ [%]                        | 39.5          | 38.3        | 37.0        | 35.0        | 32.3        | 29.4        | 27.7        | 25.5        | 21.8        | %                   |
| <b>Offenau</b>               |               |             |             |             |             |             |             |             |             |                     |
| Δ [%]                        | 21.2          | 26.2        | 27.3        | 28.1        | 27.2        | 25.9        | 24.8        | 23.3        | 20.3        | %                   |
| <b>Node A23</b>              |               |             |             |             |             |             |             |             |             |                     |
| Δ [%]                        | 33.6          | 34.6        | 34.1        | 33.0        | 30.9        | 28.6        | 27.2        | 25.3        | 22.0        | %                   |
| <b>Node Langelohe</b>        |               |             |             |             |             |             |             |             |             |                     |
| Δ [%]                        | 32.2          | 34.0        | 33.6        | 32.4        | 30.2        | 27.5        | 25.9        | 23.8        | 20.0        | %                   |
| <b>End Node</b>              |               |             |             |             |             |             |             |             |             |                     |
| Δ [%]                        | 27.6          | 29.9        | 29.7        | 28.7        | 26.5        | 23.8        | 22.2        | 20.0        | 16.0        | %                   |
| <b>Catchment ELMS_E06_02</b> |               |             |             |             |             |             |             |             |             |                     |
| Δ [%]                        | -6.3          | -0.4        | 0.9         | 5.6         | 13.0        | 13.3        | 7.2         | 7.6         | 14.7        | %                   |
| <b>Catchment ELMS_E06_02</b> |               |             |             |             |             |             |             |             |             |                     |
| Δ [%]                        | -10.5         | -7.3        | -5.8        | -4.4        | -2.2        | -0.5        | 0.5         | 1.6         | 3.5         | %                   |
| <b>Average</b>               |               |             |             |             |             |             |             |             |             |                     |
| Δ [%]                        | <b>19.6</b>   | <b>22.2</b> | <b>22.4</b> | <b>22.6</b> | <b>22.6</b> | <b>21.1</b> | <b>19.3</b> | <b>18.2</b> | <b>16.9</b> | <b>%</b>            |

**Attachment 14**

| Yearly Periods               | [1971 - 2000]       |             |             |             |             |             |             |             |             |          |
|------------------------------|---------------------|-------------|-------------|-------------|-------------|-------------|-------------|-------------|-------------|----------|
|                              | Return Period T [a] |             |             |             |             |             |             |             |             |          |
|                              | 1                   | 2           | 3           | 5           | 10          | 20          | 30          | 50          | 100         | a        |
| <b>Eckhorner Au</b>          |                     |             |             |             |             |             |             |             |             |          |
| Δ [%]                        | 32.9                | 35.7        | 37.0        | 38.5        | 40.4        | 41.9        | 42.9        | 44.2        | 45.8        | %        |
| <b>Offenau</b>               |                     |             |             |             |             |             |             |             |             |          |
| Δ [%]                        | 24.2                | 30.8        | 33.8        | 36.9        | 40.2        | 42.8        | 44.3        | 46.2        | 48.3        | %        |
| <b>Node A23</b>              |                     |             |             |             |             |             |             |             |             |          |
| Δ [%]                        | 32.3                | 36.4        | 37.9        | 39.2        | 40.3        | 40.9        | 41.2        | 41.1        | 41.4        | %        |
| <b>Node Langelohe</b>        |                     |             |             |             |             |             |             |             |             |          |
| Δ [%]                        | 33.0                | 36.3        | 37.2        | 37.7        | 37.8        | 37.2        | 36.9        | 35.8        | 35.1        | %        |
| <b>End Node</b>              |                     |             |             |             |             |             |             |             |             |          |
| Δ [%]                        | 20.5                | 26.0        | 28.0        | 29.9        | 31.5        | 32.4        | 32.8        | 32.9        | 33.0        | %        |
| <b>Catchment ELMS_E06_02</b> |                     |             |             |             |             |             |             |             |             |          |
| Δ [%]                        | -17.4               | -13.6       | -11.5       | -9.0        | -5.6        | -2.5        | -0.5        | 2.3         | 5.8         | %        |
| <b>Catchment ELMS_E06_02</b> |                     |             |             |             |             |             |             |             |             |          |
| Δ [%]                        | -10.1               | -8.6        | -7.4        | -6.0        | -4.0        | -2.0        | -0.7        | 1.2         | 3.6         | %        |
| <b>Average</b>               |                     |             |             |             |             |             |             |             |             |          |
| Δ [%]                        | <b>16.5</b>         | <b>20.4</b> | <b>22.2</b> | <b>23.9</b> | <b>25.8</b> | <b>27.3</b> | <b>28.1</b> | <b>29.1</b> | <b>30.4</b> | <b>%</b> |

**14.4 Tables: Future Scenario Results [2040 - 2070]**

| Summer Periods                | [2040 - 2070]                         |             |             |             |             |             |             |             |             |          |
|-------------------------------|---------------------------------------|-------------|-------------|-------------|-------------|-------------|-------------|-------------|-------------|----------|
|                               | Return Period [T] ; HQ <sub>T,C</sub> |             |             |             |             |             |             |             |             |          |
|                               | 1                                     | 2           | 3           | 5           | 10          | 20          | 30          | 50          | 100         | a        |
| <b>Eckhorner Au</b>           |                                       |             |             |             |             |             |             |             |             |          |
| A1B-Scenario                  | 87.1                                  | 62.6        | 55.6        | 49.5        | 43.7        | 39.5        | 37.3        | 35.0        | 32.9        | %        |
| B1-Scenario                   | 38.1                                  | 28.4        | 26.4        | 25.4        | 25.3        | 26.1        | 26.7        | 27.6        | 28.6        | %        |
| A2-Scenario                   | 38.7                                  | 28.3        | 26.0        | 24.4        | 23.6        | 23.5        | 23.7        | 24.1        | 24.5        | %        |
| <b>Offenau</b>                |                                       |             |             |             |             |             |             |             |             |          |
| A1B-Scenario                  | 116.1                                 | 84.4        | 73.3        | 62.6        | 51.3        | 42.6        | 37.8        | 32.7        | 26.7        | %        |
| B1-Scenario                   | 81.0                                  | 58.2        | 48.2        | 37.7        | 25.9        | 16.3        | 11.2        | 5.6         | -3.0        | %        |
| A2-Scenario                   | 44.5                                  | 20.5        | 12.5        | 4.9         | -2.7        | -8.4        | -11.2       | -14.3       | -19.0       | %        |
| <b>Node A23</b>               |                                       |             |             |             |             |             |             |             |             |          |
| A1B-Scenario                  | 146.7                                 | 91.6        | 75.4        | 60.9        | 46.6        | 36.0        | 30.5        | 24.6        | 17.1        | %        |
| B1-Scenario                   | 71.9                                  | 48.9        | 41.9        | 35.6        | 29.3        | 24.6        | 22.3        | 19.7        | 15.4        | %        |
| A2-Scenario                   | 64.5                                  | 37.4        | 29.2        | 21.8        | 14.5        | 9.0         | 6.3         | 3.3         | -1.3        | %        |
| <b>Node Langelohe</b>         |                                       |             |             |             |             |             |             |             |             |          |
| A1B-Scenario                  | 155.5                                 | 99.5        | 83.0        | 68.2        | 53.6        | 42.6        | 36.9        | 30.8        | 23.3        | %        |
| B1-Scenario                   | 91.9                                  | 61.2        | 51.2        | 41.8        | 32.2        | 24.7        | 20.9        | 16.7        | 10.3        | %        |
| A2-Scenario                   | 73.1                                  | 40.3        | 30.4        | 21.5        | 12.8        | 6.3         | 3.0         | -0.5        | -5.8        | %        |
| <b>End Node</b>               |                                       |             |             |             |             |             |             |             |             |          |
| A1B-Scenario                  | 106.8                                 | 80.4        | 71.4        | 63.1        | 54.5        | 47.9        | 44.5        | 40.7        | 36.2        | %        |
| B1-Scenario                   | 61.1                                  | 51.1        | 46.8        | 42.4        | 37.5        | 33.4        | 31.4        | 29.0        | 24.6        | %        |
| A2-Scenario                   | 38.5                                  | 23.6        | 18.5        | 13.9        | 9.3         | 5.9         | 4.3         | 2.5         | -0.7        | %        |
| <b>Catchment ELMS_E06_02</b>  |                                       |             |             |             |             |             |             |             |             |          |
| A1B-Scenario                  | 54.6                                  | 34.9        | 29.1        | 24.0        | 19.2        | 15.9        | 14.2        | 12.3        | 10.6        | %        |
| <b>Catchment ELMSH_E13_04</b> |                                       |             |             |             |             |             |             |             |             |          |
| A1B-Scenario                  | 56.1                                  | 36.5        | 30.6        | 25.4        | 20.2        | 16.5        | 14.7        | 12.6        | 10.5        | %        |
| <b>Average</b>                |                                       |             |             |             |             |             |             |             |             |          |
| A1B-Scenario                  | <b>103.3</b>                          | <b>70.0</b> | <b>59.8</b> | <b>50.5</b> | <b>41.3</b> | <b>34.4</b> | <b>30.8</b> | <b>27.0</b> | <b>22.5</b> | <b>%</b> |
| B1-Scenario                   | <b>68.8</b>                           | <b>49.5</b> | <b>42.9</b> | <b>36.6</b> | <b>30.1</b> | <b>25.0</b> | <b>22.5</b> | <b>19.7</b> | <b>15.2</b> | <b>%</b> |
| A2-Scenario                   | <b>51.9</b>                           | <b>30.0</b> | <b>23.3</b> | <b>17.3</b> | <b>11.5</b> | <b>7.3</b>  | <b>5.2</b>  | <b>3.0</b>  | <b>-0.4</b> | <b>%</b> |

**Attachment 14**

| <b>Winter<br/>Periods</b>     | <b>[2040 - 2070]</b>                          |             |             |             |             |             |             |             |             |          |
|-------------------------------|---|-------------|-------------|-------------|-------------|-------------|-------------|-------------|-------------|----------|
|                               | <b>Return Period T [a] ; HQ<sub>T,C</sub></b> |             |             |             |             |             |             |             |             |          |
|                               | 1   | 2           | 3           | 5           | 10          | 20          | 30          | 50          | 100         | a        |
| <b>Eckhorner Au</b>           |   |             |             |             |             |             |             |             |             |          |
| A1B-Scenario                  | -1.8  | -1.3        | -0.9        | -0.4        | 0.8         | 2.0         | 2.6         | 3.5         | 5.0         | %        |
| B1-Scenario                   | -4.0  | -4.6        | -5.1        | -6.1        | -7.0        | -8.0        | -8.7        | -9.4        | -10.8       | %        |
| A2-Scenario                   | -9.7  | -10.9       | -11.5       | -12.4       | -13.0       | -13.8       | -14.3       | -14.8       | -15.7       | %        |
| <b>Offenau</b>                |   |             |             |             |             |             |             |             |             |          |
| A1B-Scenario                  | 7.8   | 8.6         | 8.6         | 8.2         | 8.1         | 7.8         | 7.4         | 7.1         | 6.4         | %        |
| B1-Scenario                   | -2.4  | -2.9        | -3.3        | -4.1        | -4.6        | -5.2        | -5.7        | -6.2        | -7.1        | %        |
| A2-Scenario                   | -3.2  | -2.4        | -2.2        | -2.1        | -2.0        | -2.0        | -2.1        | -2.1        | -2.3        | %        |
| <b>Node A23</b>               |   |             |             |             |             |             |             |             |             |          |
| A1B-Scenario                  | 12.1  | 10.2        | 9.3         | 8.1         | 7.2         | 6.3         | 5.7         | 5.1         | 4.0         | %        |
| B1-Scenario                   | 3.8   | 1.1         | -0.3        | -2.3        | -4.1        | -6.1        | -7.1        | -8.4        | -10.6       | %        |
| A2-Scenario                   | -0.2  | -1.5        | -2.1        | -3.0        | -3.5        | -4.1        | -4.5        | -4.9        | -5.5        | %        |
| <b>Node Langelohe</b>         |   |             |             |             |             |             |             |             |             |          |
| A1B-Scenario                  | 14.0  | 11.5        | 10.2        | 8.4         | 6.7         | 5.0         | 4.0         | 2.9         | 1.0         | %        |
| B1-Scenario                   | 4.5   | 1.7         | 0.2         | -1.8        | -3.8        | -5.7        | -6.9        | -8.2        | -10.4       | %        |
| A2-Scenario                   | 1.0   | 0.0         | -0.5        | -1.2        | -1.5        | -2.0        | -2.3        | -2.6        | -3.1        | %        |
| <b>End Node</b>               |   |             |             |             |             |             |             |             |             |          |
| A1B-Scenario                  | 12.1  | 10.2        | 9.1         | 7.6         | 6.4         | 5.0         | 4.2         | 3.3         | 1.7         | %        |
| B1-Scenario                   | 2.6   | 0.3         | -0.9        | -2.6        | -4.1        | -5.7        | -6.6        | -7.6        | -9.5        | %        |
| A2-Scenario                   | -0.6  | -0.1        | 0.0         | -0.1        | 0.3         | 0.5         | 0.5         | 0.6         | 0.7         | %        |
| <b>Catchment ELMS_E06_02</b>  |   |             |             |             |             |             |             |             |             |          |
| A1B-Scenario                  | -20.3   | -8.9        | -3.0        | 3.9         | 13.5        | 22.7        | 27.8        | 34.4        | 46.0        | %        |
| <b>Catchment ELMSH_E13_04</b> |   |             |             |             |             |             |             |             |             |          |
| A1B-Scenario                  | -15.0   | -5.5        | 0.0         | 6.6         | 15.4        | 24.3        | 29.4        | 35.9        | 47.8        | %        |
| <b>Average</b>                |   |             |             |             |             |             |             |             |             |          |
| <b>A1B-Scenario</b>           | <b>1.3</b>                                    | <b>3.5</b>  | <b>4.8</b>  | <b>6.0</b>  | <b>8.3</b>  | <b>10.5</b> | <b>11.6</b> | <b>13.2</b> | <b>16.0</b> | <b>%</b> |
| <b>B1-Scenario</b>            | <b>0.9</b>                                    | <b>-0.9</b> | <b>-1.9</b> | <b>-3.4</b> | <b>-4.7</b> | <b>-6.1</b> | <b>-7.0</b> | <b>-8.0</b> | <b>-9.7</b> | <b>%</b> |
| <b>A2-Scenario</b>            | <b>-2.5</b>                                   | <b>-3.0</b> | <b>-3.3</b> | <b>-3.7</b> | <b>-3.9</b> | <b>-4.3</b> | <b>-4.5</b> | <b>-4.7</b> | <b>-5.2</b> | <b>%</b> |

**Attachment 14**

| Yearly Periods                | [2040 - 2070]                           |             |             |             |             |             |             |             |             |          |
|-------------------------------|---|-------------|-------------|-------------|-------------|-------------|-------------|-------------|-------------|----------|
|                               | Return Period T [a] ; HQ <sub>T,C</sub> |             |             |             |             |             |             |             |             |          |
|                               | 1                                       | 2           | 3           | 5           | 10          | 20          | 30          | 50          | 100         | a        |
| <b>Eckhorner Au</b>           |   |             |             |             |             |             |             |             |             |          |
| A1B-Scenario                  | 20.6                                    | 19.5        | 19.2        | 19.0        | 18.9        | 19.0        | 19.0        | 19.5        | 19.3        | %        |
| B1-Scenario                   | 5.0                                     | 5.7         | 6.3         | 7.2         | 8.6         | 10.2        | 11.1        | 12.2        | 15.0        | %        |
| A2-Scenario                   | 0.4                                     | 0.7         | 1.3         | 1.9         | 3.1         | 4.5         | 5.4         | 6.6         | 8.6         | %        |
| <b>Offenau</b>                |   |             |             |             |             |             |             |             |             |          |
| A1B-Scenario                  | 24.7                                    | 22.0        | 20.6        | 19.2        | 17.4        | 15.9        | 14.9        | 13.7        | 12.0        | %        |
| B1-Scenario                   | 10.4                                    | 6.2         | 3.8         | 1.1         | -2.4        | -5.3        | -7.0        | -10.2       | -11.9       | %        |
| A2-Scenario                   | 4.5                                     | 2.0         | 0.8         | -0.9        | -2.8        | -4.6        | -5.5        | -7.3        | -8.2        | %        |
| <b>Node A23</b>               |   |             |             |             |             |             |             |             |             |          |
| A1B-Scenario                  | 29.3                                    | 23.2        | 20.3        | 17.3        | 13.6        | 10.6        | 8.8         | 6.3         | 3.7         | %        |
| B1-Scenario                   | 15.3                                    | 12.4        | 10.9        | 9.2         | 7.0         | 5.3         | 4.3         | 2.3         | 1.6         | %        |
| A2-Scenario                   | 9.1                                     | 5.3         | 3.4         | 1.2         | -1.4        | -3.6        | -4.8        | -6.9        | -8.3        | %        |
| <b>Node Langelohe</b>         |   |             |             |             |             |             |             |             |             |          |
| A1B-Scenario                  | 39.2                                    | 33.4        | 31.0        | 28.7        | 26.3        | 24.4        | 23.4        | 22.2        | 20.6        | %        |
| B1-Scenario                   | 14.7                                    | 10.0        | 7.7         | 5.0         | 1.6         | -1.2        | -2.8        | -5.7        | -7.3        | %        |
| A2-Scenario                   | 9.2                                     | 5.5         | 3.9         | 1.8         | -0.5        | -2.5        | -3.6        | -5.5        | -6.6        | %        |
| <b>End Node</b>               |   |             |             |             |             |             |             |             |             |          |
| A1B-Scenario                  | 29.2                                    | 25.7        | 24.0        | 22.3        | 20.3        | 18.7        | 17.7        | 16.5        | 15.0        | %        |
| B1-Scenario                   | 11.2                                    | 9.5         | 8.6         | 7.4         | 5.9         | 4.6         | 3.9         | 2.2         | 1.8         | %        |
| A2-Scenario                   | 6.2                                     | 4.8         | 4.1         | 3.2         | 2.0         | 1.0         | 0.5         | -0.7        | -1.0        | %        |
| <b>Catchment ELMS_E06_02</b>  |   |             |             |             |             |             |             |             |             |          |
| A1B-Scenario                  | 23.8                                    | 21.1        | 19.5        | 17.5        | 14.7        | 12.3        | 10.7        | 8.8         | 5.8         | %        |
| <b>Catchment ELMSH_E13_04</b> |   |             |             |             |             |             |             |             |             |          |
| A1B-Scenario                  | 24.9                                    | 22.1        | 20.5        | 18.3        | 15.5        | 12.9        | 11.2        | 9.2         | 6.1         | %        |
| <b>Average</b>                |   |             |             |             |             |             |             |             |             |          |
| A1B-Scenario                  | <b>27.4</b>                             | <b>23.8</b> | <b>22.2</b> | <b>20.3</b> | <b>18.1</b> | <b>16.3</b> | <b>15.1</b> | <b>13.7</b> | <b>11.8</b> | <b>%</b> |
| B1-Scenario                   | <b>11.3</b>                             | <b>8.8</b>  | <b>7.5</b>  | <b>6.0</b>  | <b>4.1</b>  | <b>2.7</b>  | <b>1.9</b>  | <b>0.1</b>  | <b>-0.2</b> | <b>%</b> |
| A2-Scenario                   | <b>5.9</b>                              | <b>3.7</b>  | <b>2.7</b>  | <b>1.5</b>  | <b>0.1</b>  | <b>-1.0</b> | <b>-1.6</b> | <b>-2.8</b> | <b>-3.1</b> | <b>%</b> |

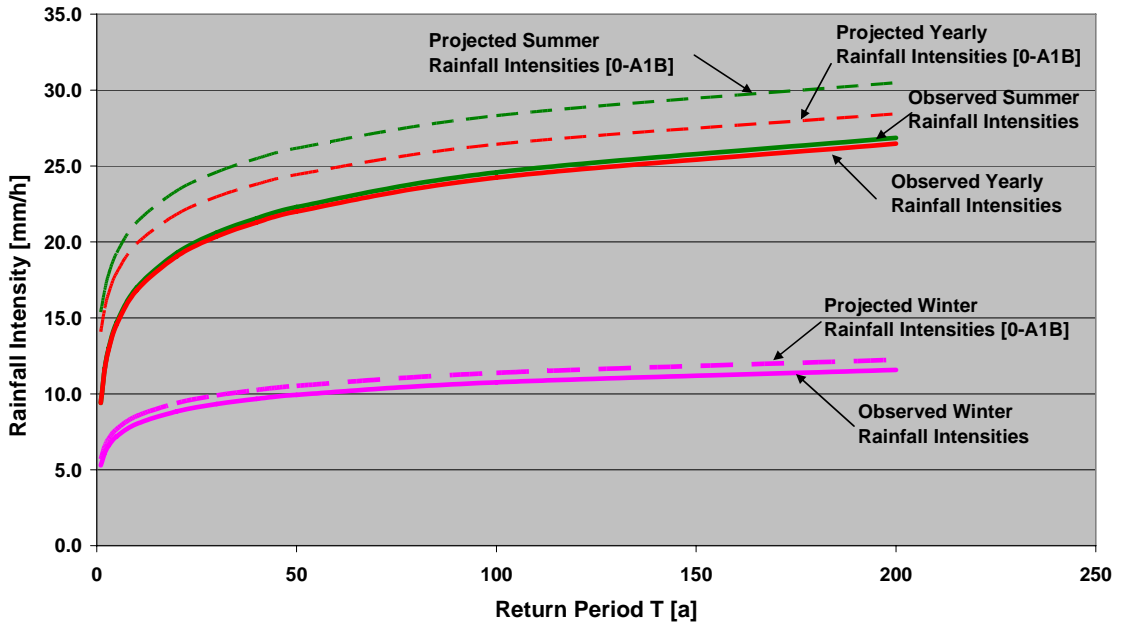
# Attachment 15

## Post-Processing Results

### 15.1 Post-Processing of Design Rainfall Events

|                              | Return Periods T [a] |      |      |      |      |      |      |      |      |      |      |
|------------------------------|----------------------|------|------|------|------|------|------|------|------|------|------|
|                              | 1                    | 2    | 3    | 5    | 10   | 20   | 30   | 40   | 50   | 100  | 200  |
| <b>Summer Periods (mm/h)</b> |                      |      |      |      |      |      |      |      |      |      |      |
| <b>Scenario 0</b>            | 9.4                  | 11.7 | 13.0 | 14.7 | 17.0 | 19.3 | 20.6 | 21.6 | 22.3 | 24.6 | 26.9 |
| <b>Scenario 0-A1B</b>        | 15.4                 | 16.9 | 17.9 | 19.3 | 21.3 | 23.4 | 24.6 | 25.5 | 26.2 | 28.3 | 30.5 |
| <b>Δ %</b>                   | 63.5                 | 44.1 | 37.3 | 31.2 | 25.3 | 21.2 | 19.4 | 18.2 | 17.4 | 15.2 | 13.5 |
| <b>Winter Periods (mm/h)</b> |                      |      |      |      |      |      |      |      |      |      |      |
| <b>Scenario 0</b>            | 5.3                  | 6.1  | 6.6  | 7.2  | 8.0  | 8.8  | 9.3  | 9.7  | 9.9  | 10.8 | 11.6 |
| <b>Scenario 0-A1B</b>        | 5.7                  | 6.6  | 7.1  | 7.7  | 8.5  | 9.4  | 9.9  | 10.3 | 10.5 | 11.4 | 12.2 |
| <b>Δ %</b>                   | 7.8                  | 7.2  | 7.0  | 6.7  | 6.4  | 6.2  | 6.1  | 6.0  | 6.0  | 5.9  | 5.7  |
| <b>Yearly Periods (mm/h)</b> |                      |      |      |      |      |      |      |      |      |      |      |
| <b>Scenario 0</b>            | 9.4                  | 11.6 | 12.9 | 14.6 | 16.8 | 19.1 | 20.4 | 21.3 | 22.0 | 24.2 | 26.5 |
| <b>Scenario 0-A1B</b>        | 14.1                 | 15.6 | 16.7 | 18.0 | 19.9 | 21.8 | 23.0 | 23.8 | 24.4 | 26.4 | 28.4 |
| <b>Δ %</b>                   | 49.9                 | 34.4 | 28.7 | 23.4 | 18.2 | 14.6 | 12.9 | 11.8 | 11.1 | 9.1  | 7.5  |

Projected Scenario 0- A1B results on the Observed Data Series



## 15.2 Post-Processing of Design Flood Events

1. Scenario 0 =  $HQ_T$   
 2. Scenario 0-A1B =  $HQ_{T,C}$

| Summer Periods                | Return Period T [ a ] |      |      |      |      |      |      |      |      |                   |
|-------------------------------|-----------------------|------|------|------|------|------|------|------|------|-------------------|
|                               | 1                     | 2    | 3    | 5    | 10   | 20   | 30   | 50   | 100  | a                 |
| <b>Eckhorner Au</b>           |                       |      |      |      |      |      |      |      |      |                   |
| Scenario 0                    | 1.4                   | 2.0  | 2.3  | 2.7  | 3.2  | 3.7  | 4.0  | 4.3  | 5.0  | m <sup>3</sup> /s |
| Scenario 0-A1B                | 2.6                   | 3.2  | 3.6  | 4.0  | 4.6  | 5.1  | 5.4  | 5.9  | 6.6  | m <sup>3</sup> /s |
| Δ %                           | 87.1                  | 62.6 | 55.6 | 49.5 | 43.7 | 39.5 | 37.3 | 35.0 | 32.9 | %                 |
| <b>Offenau</b>                |                       |      |      |      |      |      |      |      |      |                   |
| Scenario 0                    | 0.7                   | 1.0  | 1.1  | 1.2  | 1.4  | 1.5  | 1.6  | 1.7  | 1.9  | m <sup>3</sup> /s |
| Scenario 0-A1B                | 1.6                   | 1.8  | 1.9  | 2.0  | 2.1  | 2.2  | 2.2  | 2.3  | 2.4  | m <sup>3</sup> /s |
| Δ %                           | 116.1                 | 84.4 | 73.3 | 62.6 | 51.3 | 42.6 | 37.8 | 32.7 | 26.7 | %                 |
| <b>Node A23</b>               |                       |      |      |      |      |      |      |      |      |                   |
| Scenario 0                    | 2.7                   | 3.7  | 4.2  | 4.8  | 5.8  | 6.7  | 7.3  | 8.0  | 9.4  | m <sup>3</sup> /s |
| Scenario 0-A1B                | 6.7                   | 7.0  | 7.3  | 7.8  | 8.4  | 9.1  | 9.5  | 10.0 | 11.0 | m <sup>3</sup> /s |
| Δ %                           | 146.7                 | 91.6 | 75.4 | 60.9 | 46.6 | 36.0 | 30.5 | 24.6 | 17.1 | %                 |
| <b>Node Langelohé</b>         |                       |      |      |      |      |      |      |      |      |                   |
| Scenario 0                    | 3.2                   | 4.2  | 4.8  | 5.6  | 6.6  | 7.8  | 8.5  | 9.3  | 11.0 | m <sup>3</sup> /s |
| Scenario 0-A1B                | 8.1                   | 8.4  | 8.8  | 9.4  | 10.2 | 11.1 | 11.6 | 12.2 | 13.6 | m <sup>3</sup> /s |
| Δ %                           | 155.5                 | 99.5 | 83.0 | 68.2 | 53.6 | 42.6 | 36.9 | 30.8 | 23.3 | %                 |
| <b>End Node</b>               |                       |      |      |      |      |      |      |      |      |                   |
| Scenario 0                    | 6.0                   | 7.4  | 8.1  | 9.0  | 10.1 | 11.3 | 11.9 | 12.7 | 14.1 | m <sup>3</sup> /s |
| Scenario 0-A1B                | 12.3                  | 13.3 | 13.9 | 14.7 | 15.7 | 16.6 | 17.2 | 17.9 | 19.2 | m <sup>3</sup> /s |
| Δ %                           | 106.8                 | 80.4 | 71.4 | 63.1 | 54.5 | 47.9 | 44.5 | 40.7 | 36.2 | %                 |
| <b>Catchment ELMS E06_02</b>  |                       |      |      |      |      |      |      |      |      |                   |
| Scenario 0                    | 0.9                   | 1.3  | 1.5  | 1.8  | 2.1  | 2.5  | 2.7  | 3.0  | 3.5  | m <sup>3</sup> /s |
| Scenario 0-A1B                | 1.4                   | 1.8  | 2.0  | 2.2  | 2.5  | 2.9  | 3.1  | 3.3  | 3.8  | m <sup>3</sup> /s |
| Δ %                           | 54.6                  | 34.9 | 29.1 | 24.0 | 19.2 | 15.9 | 14.2 | 12.3 | 10.6 | %                 |
| <b>Catchment ELMSH E13_04</b> |                       |      |      |      |      |      |      |      |      |                   |
| Scenario 0                    | 0.8                   | 1.1  | 1.3  | 1.4  | 1.7  | 1.9  | 2.1  | 2.2  | 2.5  | m <sup>3</sup> /s |
| Scenario 0-A1B                | 1.2                   | 1.5  | 1.6  | 1.8  | 2.0  | 2.2  | 2.4  | 2.5  | 2.8  | m <sup>3</sup> /s |
| Δ %                           | 56.1                  | 36.5 | 30.6 | 25.4 | 20.2 | 16.5 | 14.7 | 12.6 | 10.5 | %                 |

| Winter Periods                | Return Period [ T ] |      |      |      |      |      |      |      |      |                   |
|-------------------------------|---------------------|------|------|------|------|------|------|------|------|-------------------|
|                               | 1                   | 2    | 3    | 5    | 10   | 20   | 30   | 50   | 100  | a                 |
| <b>Eckhorner Au</b>           |                     |      |      |      |      |      |      |      |      |                   |
| Scenario 0                    | 2.5                 | 3.0  | 3.3  | 3.6  | 4.1  | 4.5  | 4.8  | 5.2  | 5.8  | m <sup>3</sup> /s |
| Scenario 0-A1B                | 2.4                 | 3.0  | 3.3  | 3.6  | 4.1  | 4.6  | 4.9  | 5.4  | 6.1  | m <sup>3</sup> /s |
| Δ %                           | -1.8                | -1.3 | -0.9 | -0.4 | 0.8  | 2.0  | 2.6  | 3.5  | 5.0  | %                 |
| <b>Offenau</b>                |                     |      |      |      |      |      |      |      |      |                   |
| Scenario 0                    | 1.7                 | 2.1  | 2.3  | 2.5  | 2.8  | 3.2  | 3.4  | 3.7  | 4.3  | m <sup>3</sup> /s |
| Scenario 0-A1B                | 1.9                 | 2.2  | 2.4  | 2.7  | 3.1  | 3.5  | 3.7  | 4.0  | 4.5  | m <sup>3</sup> /s |
| Δ %                           | 7.8                 | 8.6  | 8.6  | 8.2  | 8.1  | 7.8  | 7.4  | 7.1  | 6.4  | %                 |
| <b>Node A23</b>               |                     |      |      |      |      |      |      |      |      |                   |
| Scenario 0                    | 6.4                 | 7.8  | 8.5  | 9.4  | 10.6 | 11.8 | 12.5 | 13.3 | 14.9 | m <sup>3</sup> /s |
| Scenario 0-A1B                | 7.2                 | 8.5  | 9.3  | 10.2 | 11.3 | 12.5 | 13.2 | 14.0 | 15.5 | m <sup>3</sup> /s |
| Δ %                           | 12.1                | 10.2 | 9.3  | 8.1  | 7.2  | 6.3  | 5.7  | 5.1  | 4.0  | %                 |
| <b>Node Langelohe</b>         |                     |      |      |      |      |      |      |      |      |                   |
| Scenario 0                    | 8.2                 | 9.9  | 10.9 | 12.1 | 13.7 | 15.4 | 16.4 | 17.6 | 20.0 | m <sup>3</sup> /s |
| Scenario 0-A1B                | 9.3                 | 11.1 | 12.0 | 13.1 | 14.7 | 16.2 | 17.0 | 18.1 | 20.1 | m <sup>3</sup> /s |
| Δ %                           | 14.0                | 11.5 | 10.2 | 8.4  | 6.7  | 5.0  | 4.0  | 2.9  | 1.0  | %                 |
| <b>End Node</b>               |                     |      |      |      |      |      |      |      |      |                   |
| Scenario 0                    | 9.0                 | 10.9 | 11.9 | 13.2 | 14.9 | 16.7 | 17.7 | 19.1 | 21.6 | m <sup>3</sup> /s |
| Scenario 0-A1B                | 10.1                | 12.0 | 13.0 | 14.2 | 15.8 | 17.5 | 18.5 | 19.7 | 22.0 | m <sup>3</sup> /s |
| Δ %                           | 12.1                | 10.2 | 9.1  | 7.6  | 6.4  | 5.0  | 4.2  | 3.3  | 1.7  | %                 |
| <b>Catchment ELMS_E06_02</b>  |                     |      |      |      |      |      |      |      |      |                   |
| Scenario 0                    | 0.6                 | 0.8  | 0.8  | 0.9  | 1.0  | 1.1  | 1.2  | 1.2  | 1.4  | m <sup>3</sup> /s |
| Scenario 0-A1B                | 0.5                 | 0.7  | 0.8  | 0.9  | 1.2  | 1.4  | 1.5  | 1.7  | 2.0  | m <sup>3</sup> /s |
| Δ %                           | -20.3               | -8.9 | -3.0 | 3.9  | 13.5 | 22.7 | 27.8 | 34.4 | 46.0 | %                 |
| <b>Catchment ELMSH_E13_04</b> |                     |      |      |      |      |      |      |      |      |                   |
| Scenario 0                    | 0.5                 | 0.6  | 0.6  | 0.7  | 0.8  | 0.8  | 0.9  | 0.9  | 1.0  | m <sup>3</sup> /s |
| Scenario 0-A1B                | 0.4                 | 0.6  | 0.6  | 0.7  | 0.9  | 1.0  | 1.1  | 1.3  | 1.5  | m <sup>3</sup> /s |
| Δ %                           | -15.0               | -5.5 | 0.0  | 6.6  | 15.4 | 24.3 | 29.4 | 35.9 | 47.8 | %                 |

| Yearly Periods                | Return Period [ T ] |      |      |      |      |      |      |      |      |                   |
|-------------------------------|---------------------|------|------|------|------|------|------|------|------|-------------------|
|                               | 1                   | 2    | 3    | 5    | 10   | 20   | 30   | 50   | 100  | a                 |
| <b>Eckhorner Au</b>           |                     |      |      |      |      |      |      |      |      |                   |
| Scenario 0                    | 2.6                 | 3.2  | 3.4  | 3.8  | 4.2  | 4.7  | 4.9  | 5.4  | 5.7  | m <sup>3</sup> /s |
| Scenario 0-A1B                | 3.2                 | 3.8  | 4.1  | 4.5  | 5.0  | 5.5  | 5.8  | 6.4  | 6.8  | m <sup>3</sup> /s |
| Δ %                           | 20.6                | 19.5 | 19.2 | 19.0 | 18.9 | 19.0 | 19.0 | 19.5 | 19.3 | %                 |
| <b>Offenau</b>                |                     |      |      |      |      |      |      |      |      |                   |
| Scenario 0                    | 1.6                 | 2.0  | 2.2  | 2.4  | 2.7  | 3.1  | 3.3  | 3.7  | 4.0  | m <sup>3</sup> /s |
| Scenario 0-A1B                | 2.0                 | 2.4  | 2.6  | 2.9  | 3.2  | 3.6  | 3.8  | 4.2  | 4.5  | m <sup>3</sup> /s |
| Δ %                           | 24.7                | 22.0 | 20.6 | 19.2 | 17.4 | 15.9 | 14.9 | 13.7 | 12.0 | %                 |
| <b>Node A23</b>               |                     |      |      |      |      |      |      |      |      |                   |
| Scenario 0                    | 6.2                 | 7.5  | 8.3  | 9.2  | 10.4 | 11.6 | 12.3 | 13.6 | 14.8 | m <sup>3</sup> /s |
| Scenario 0-A1B                | 8.1                 | 9.3  | 9.9  | 10.7 | 11.8 | 12.8 | 13.4 | 14.5 | 15.4 | m <sup>3</sup> /s |
| Δ %                           | 29.3                | 23.2 | 20.3 | 17.3 | 13.6 | 10.6 | 8.8  | 6.3  | 3.7  | %                 |
| <b>Node Langelohe</b>         |                     |      |      |      |      |      |      |      |      |                   |
| Scenario 0                    | 7.8                 | 9.5  | 10.5 | 11.7 | 13.4 | 15.1 | 16.1 | 18.0 | 19.6 | m <sup>3</sup> /s |
| Scenario 0-A1B                | 10.9                | 12.7 | 13.8 | 15.1 | 16.9 | 18.8 | 19.9 | 22.0 | 23.7 | m <sup>3</sup> /s |
| Δ %                           | 39.2                | 33.4 | 31.0 | 28.7 | 26.3 | 24.4 | 23.4 | 22.2 | 20.6 | %                 |
| <b>End Node</b>               |                     |      |      |      |      |      |      |      |      |                   |
| Scenario 0                    | 9.3                 | 11.0 | 11.9 | 13.1 | 14.7 | 16.4 | 17.4 | 19.2 | 20.9 | m <sup>3</sup> /s |
| Scenario 0-A1B                | 12.0                | 13.8 | 14.8 | 16.0 | 17.7 | 19.5 | 20.5 | 22.4 | 24.0 | m <sup>3</sup> /s |
| Δ %                           | 29.2                | 25.7 | 24.0 | 22.3 | 20.3 | 18.7 | 17.7 | 16.5 | 15.0 | %                 |
| <b>Catchment ELMS E06_02</b>  |                     |      |      |      |      |      |      |      |      |                   |
| Scenario 0                    | 1.0                 | 1.3  | 1.5  | 1.8  | 2.1  | 2.5  | 2.7  | 3.1  | 3.5  | m <sup>3</sup> /s |
| Scenario 0-A1B                | 1.3                 | 1.6  | 1.8  | 2.1  | 2.4  | 2.8  | 3.0  | 3.4  | 3.7  | m <sup>3</sup> /s |
| Δ %                           | 23.8                | 21.1 | 19.5 | 17.5 | 14.7 | 12.3 | 10.7 | 8.8  | 5.8  | %                 |
| <b>Catchment ELMSH E13_04</b> |                     |      |      |      |      |      |      |      |      |                   |
| Scenario 0                    | 0.8                 | 1.1  | 1.3  | 1.5  | 1.8  | 2.1  | 2.3  | 2.7  | 3.1  | m <sup>3</sup> /s |
| Scenario 0-A1B                | 1.0                 | 1.3  | 1.5  | 1.8  | 2.1  | 2.4  | 2.6  | 3.0  | 3.3  | m <sup>3</sup> /s |
| Δ %                           | 24.9                | 22.1 | 20.5 | 18.3 | 15.5 | 12.9 | 11.2 | 9.2  | 6.1  | %                 |

## Attachment 16

### Photos of Site Visit in Elmshorn [9 October 2009]

#### 16.1 Hot Spots:

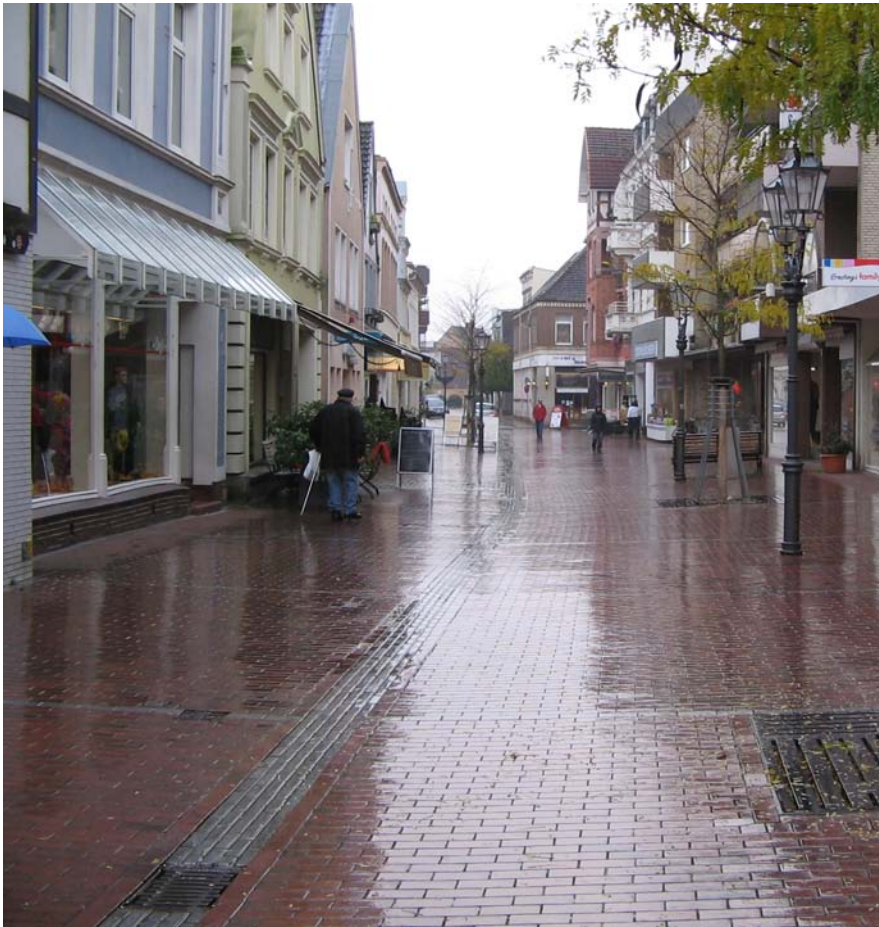
##### Else-Brandström School close to the Krückau Park:



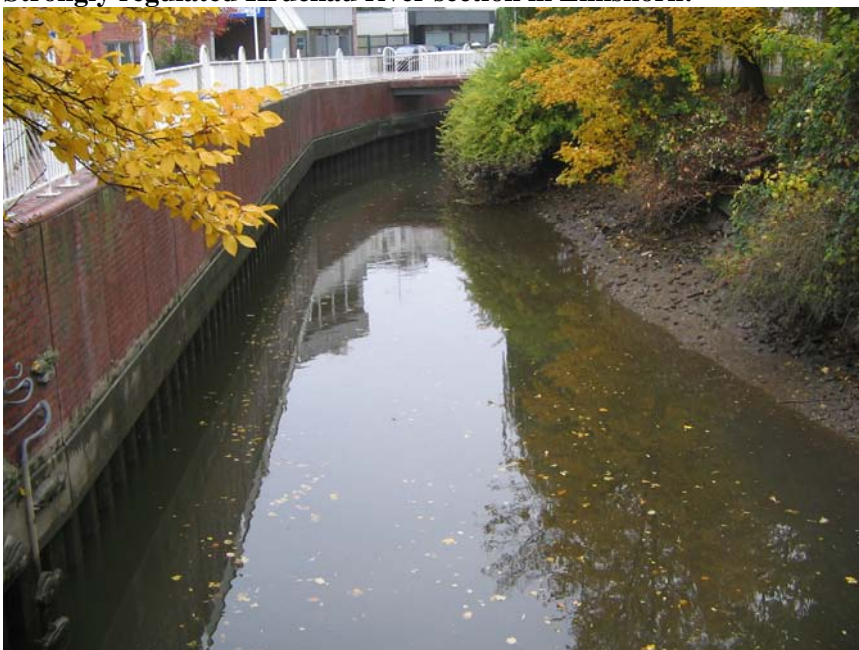
##### The “Badewanne” (Hamburger Strasse):



**City Centre Elmshorn:**



**Strongly regulated Krückau river section in Elmshorn:**



**16.2 Commercial Areas:**

**Kindergarten:**



**Paul-Doormann School:**

**Mostly low buildings with slightly pitched roofs and green spaces in front.**



**Large estate of a comprehensive school with sports facilities:  
Mostly flat roofs and sealed surface covers.**



**Commercial school:  
Flat roofs with green spaces in front.**



**16.3 Photo of a residential area with apartment houses and green spaces for infiltration devices:**



**Parking Place in a residential area:**



**16.4 Example of Existing SUDS.**

**Unsealed parking place in the northern industrial area of Elmshorn:  
Material: concrete blocks filled with grass (“Rasengittersteine”).**

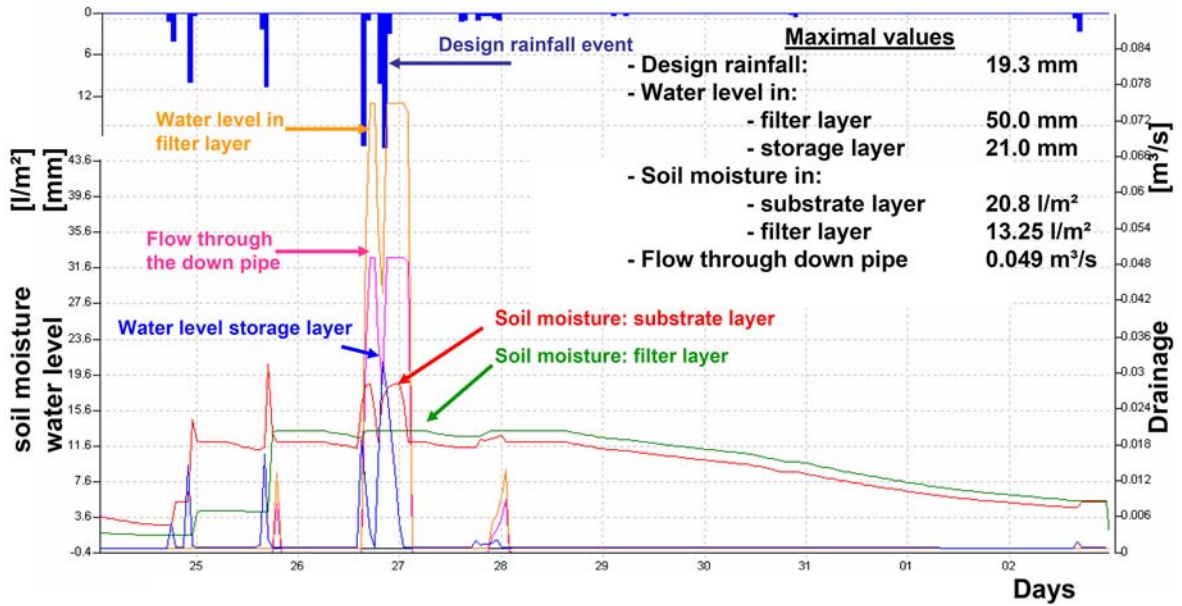


# Attachment 17

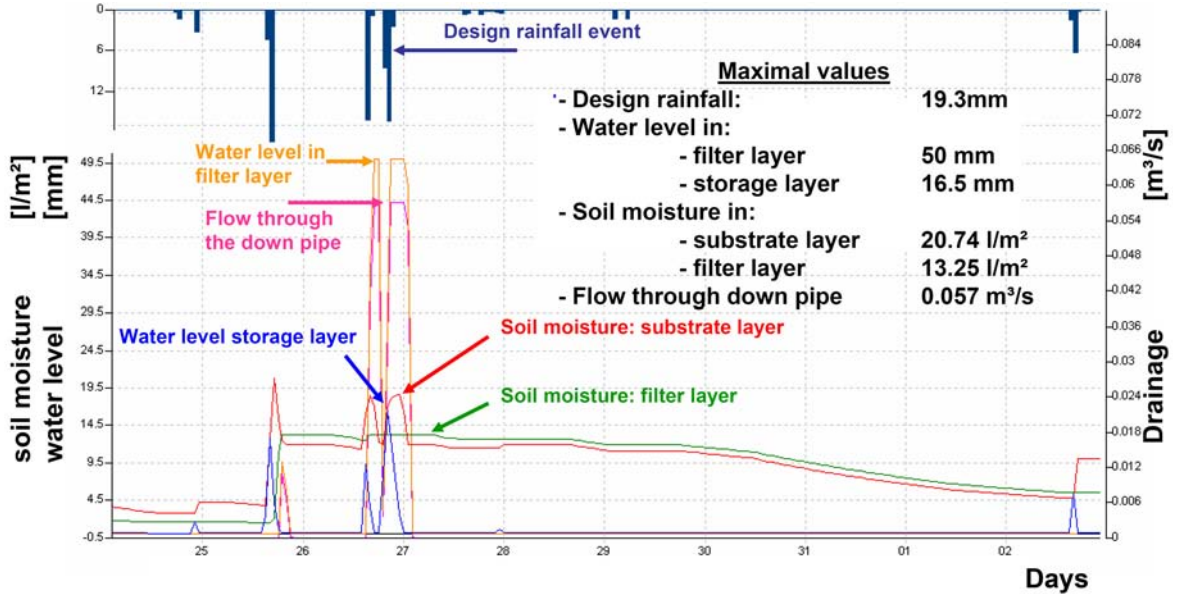
## Testing Results of Software Tool

### 17.1 Testing Results of Green Roofs

#### 17.1.1 Sub-catchment: ELMSH\_E13\_04

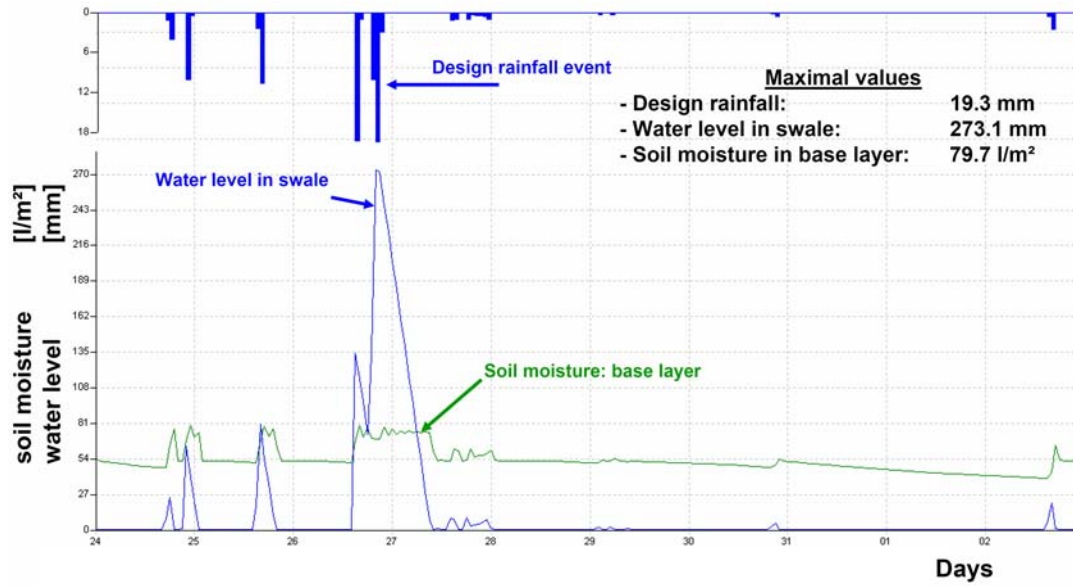


#### 17.1.2 Sub-catchment ELMS\_E06\_02

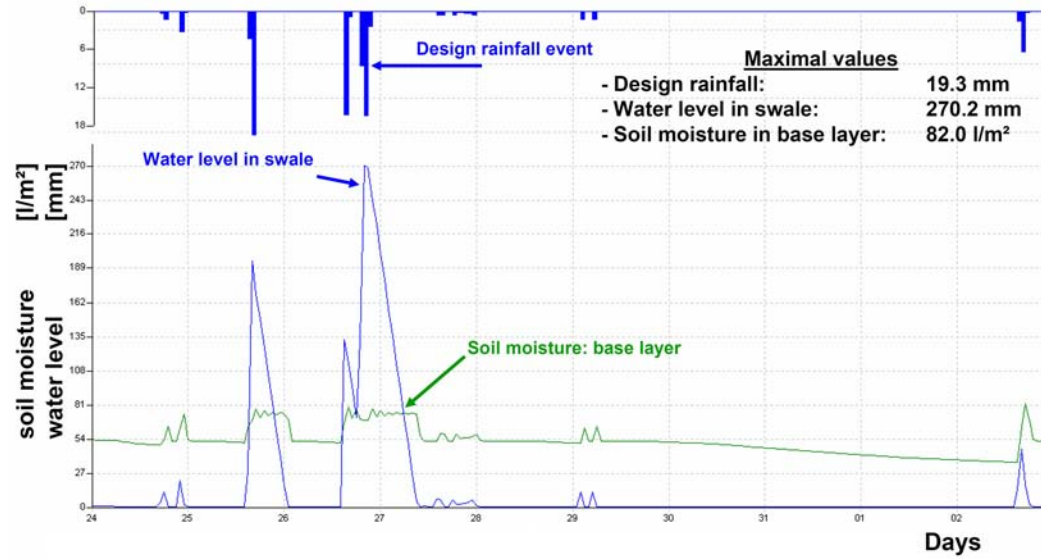


## 17.2 Testing Results of Swales

### 17.2.1 Sub-catchment: ELMSH\_E13\_04

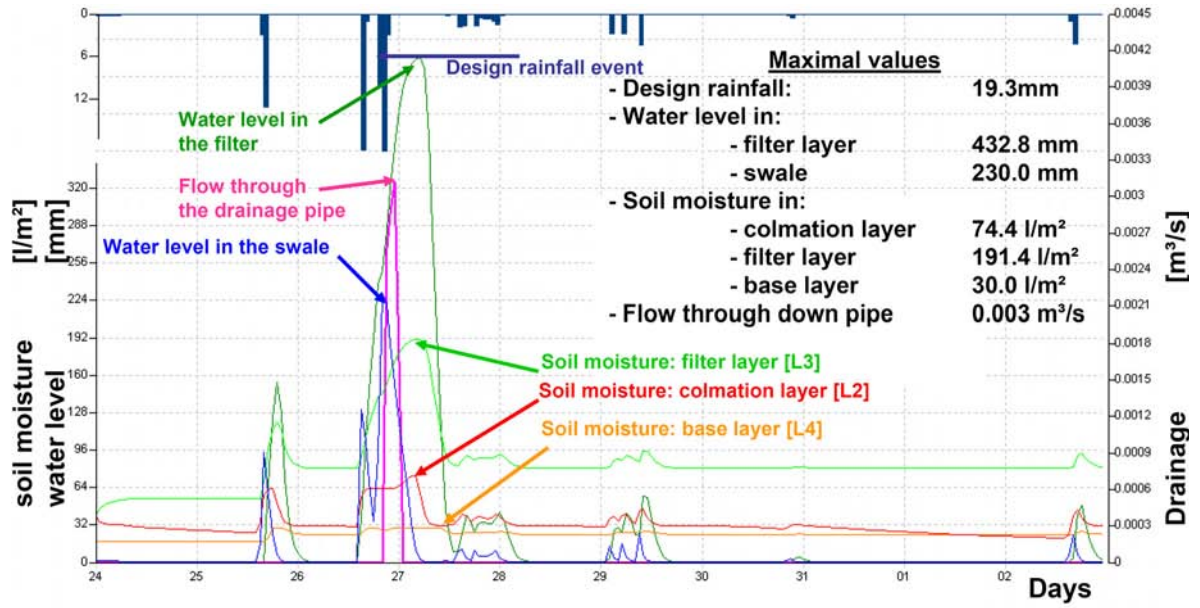


### 17.2.2 Sub-catchment: ELMS\_E06\_02



17.3 Testing Results of Swale-Filter-Drain systems

17.3.1 Sub-catchments: KAKI\_2 and KAKI\_3



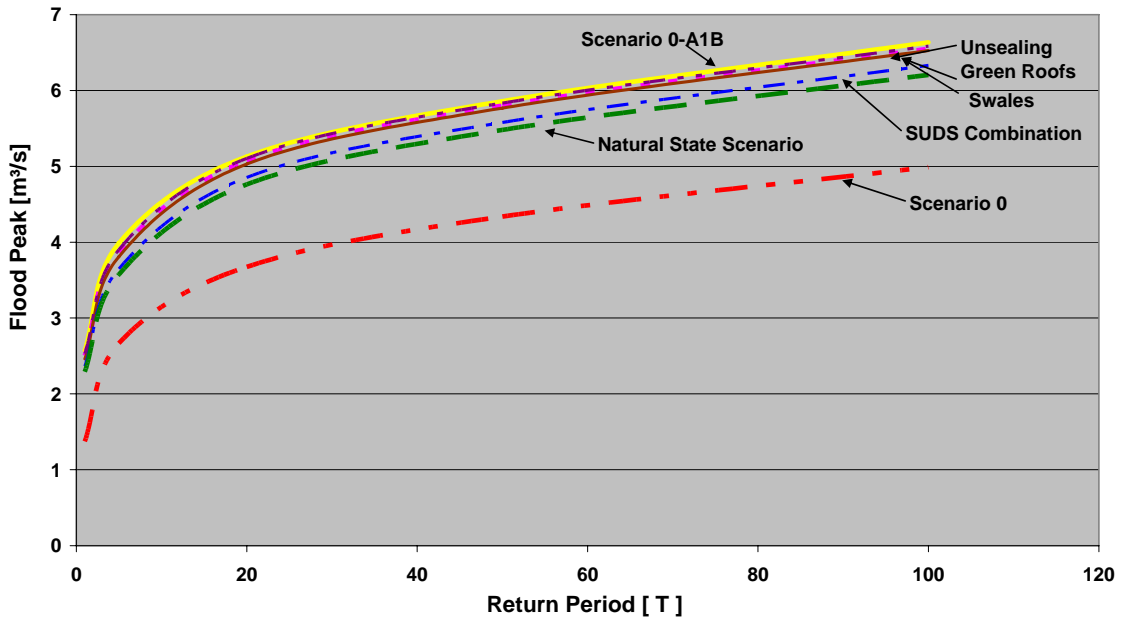
# Attachment 18

## Results of SUDS Adaptation Scenarios

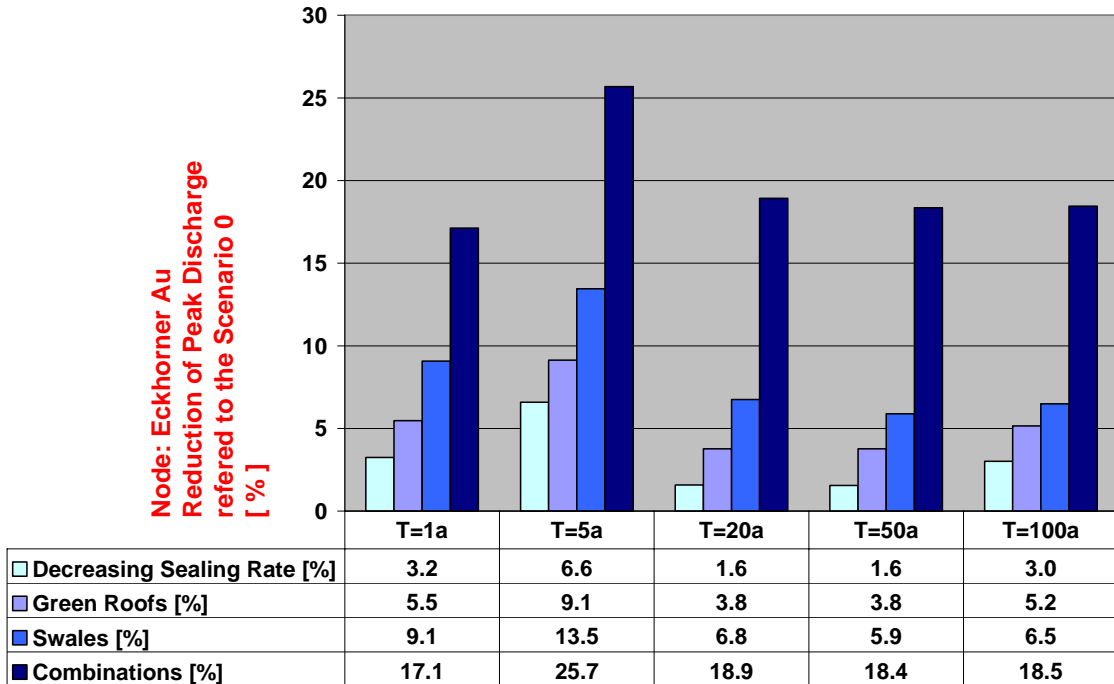
### 18.1 Catchment Eckhorner Au:

[Node: Eckhorner Au](#)

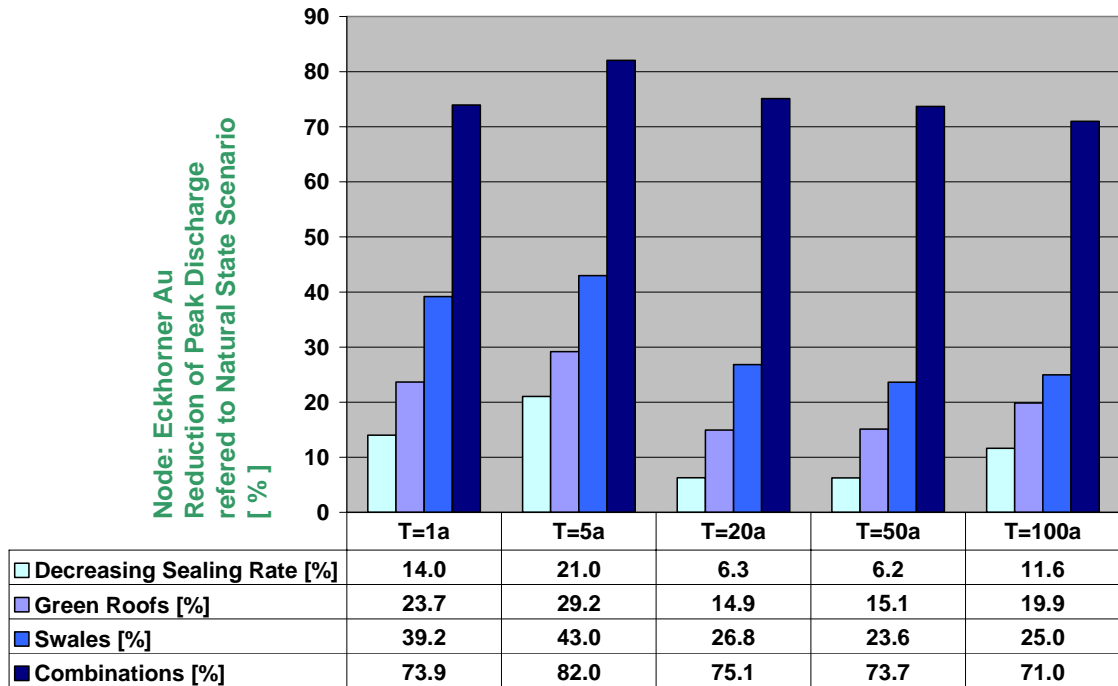
Effectiveness of SUDS Techniques



Reduction of the Peak Discharge related to the reference Scenario 0:

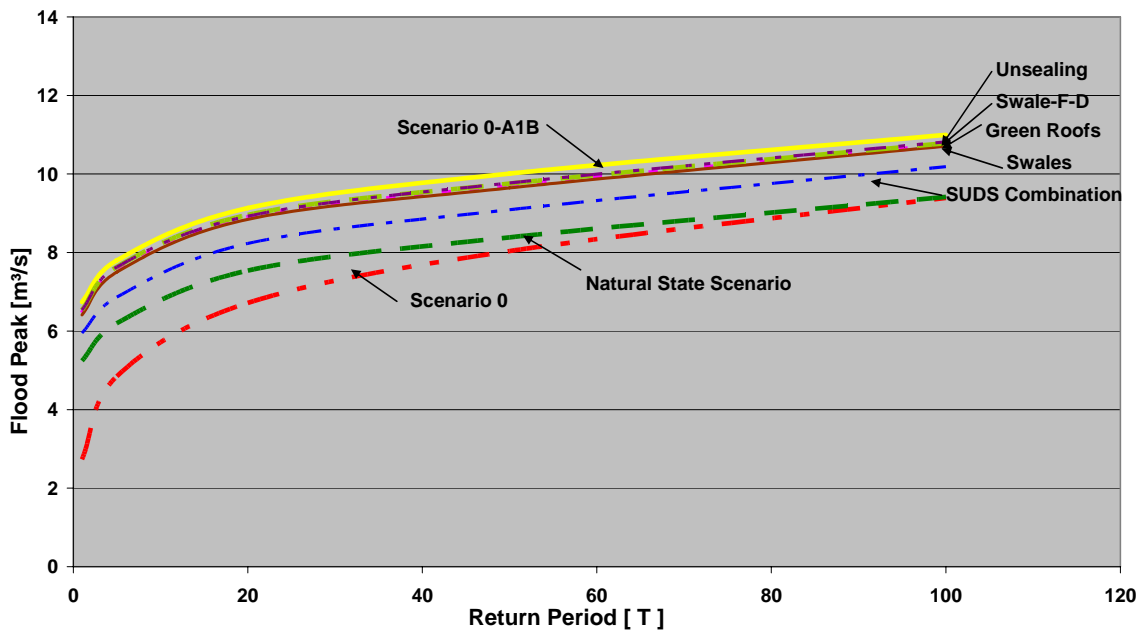


Reduction of the Peak Discharge referred to the projected (climate change) Natural State Scenario:

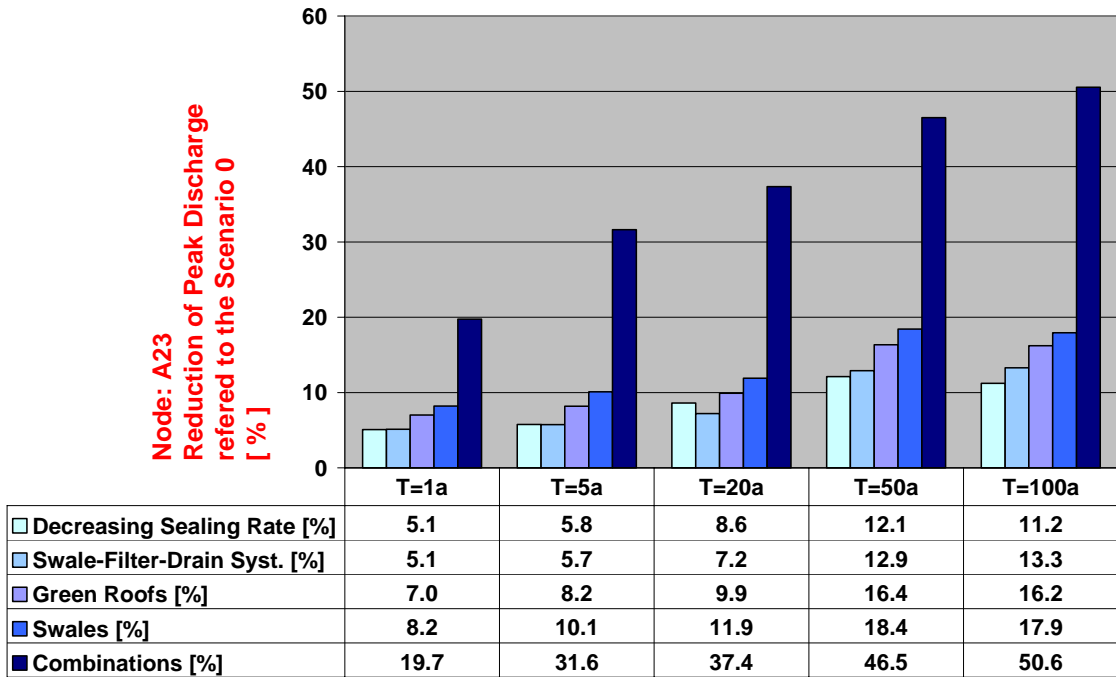


### 18.2 Upper Krückkau catchment with Kaltenkirchen and Barmstedt:

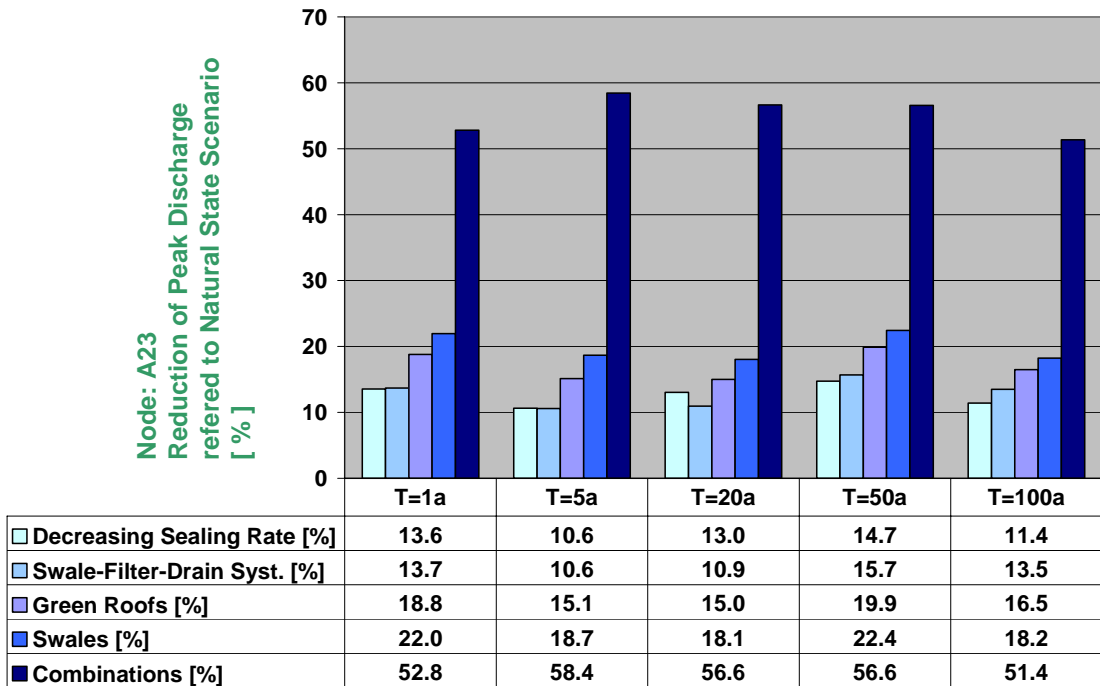
Node: A23 - Upper Krückkau catchment  
Effectiveness of SUDS Techniques



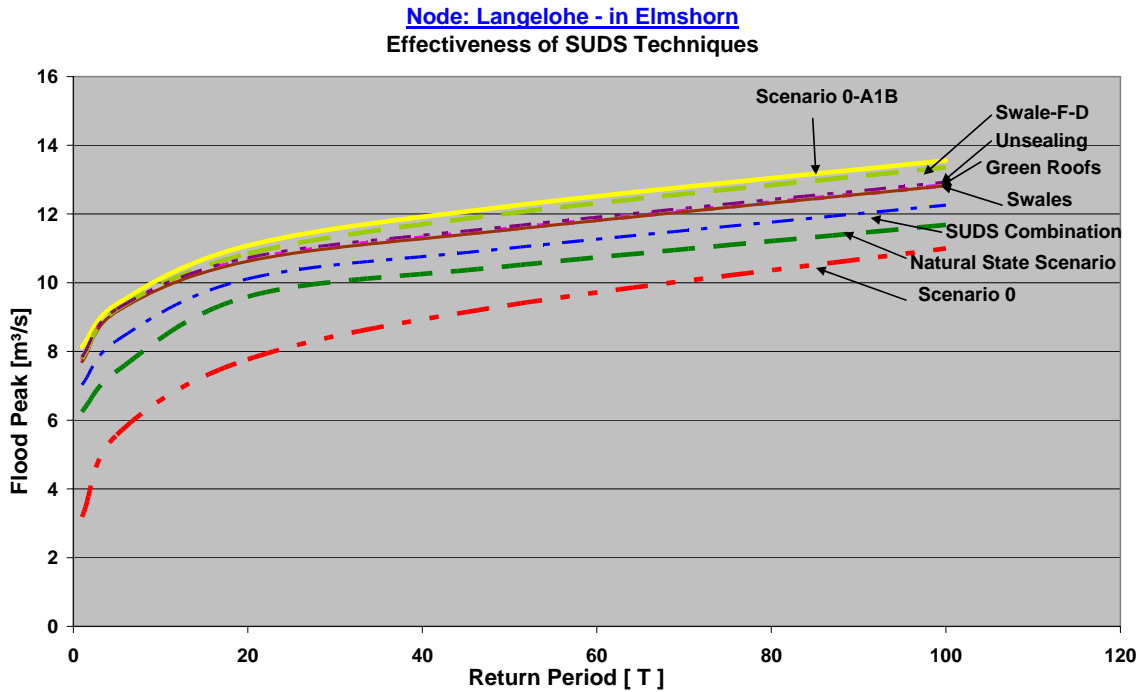
Reduction of the Peak Discharge related to the reference Scenario 0:



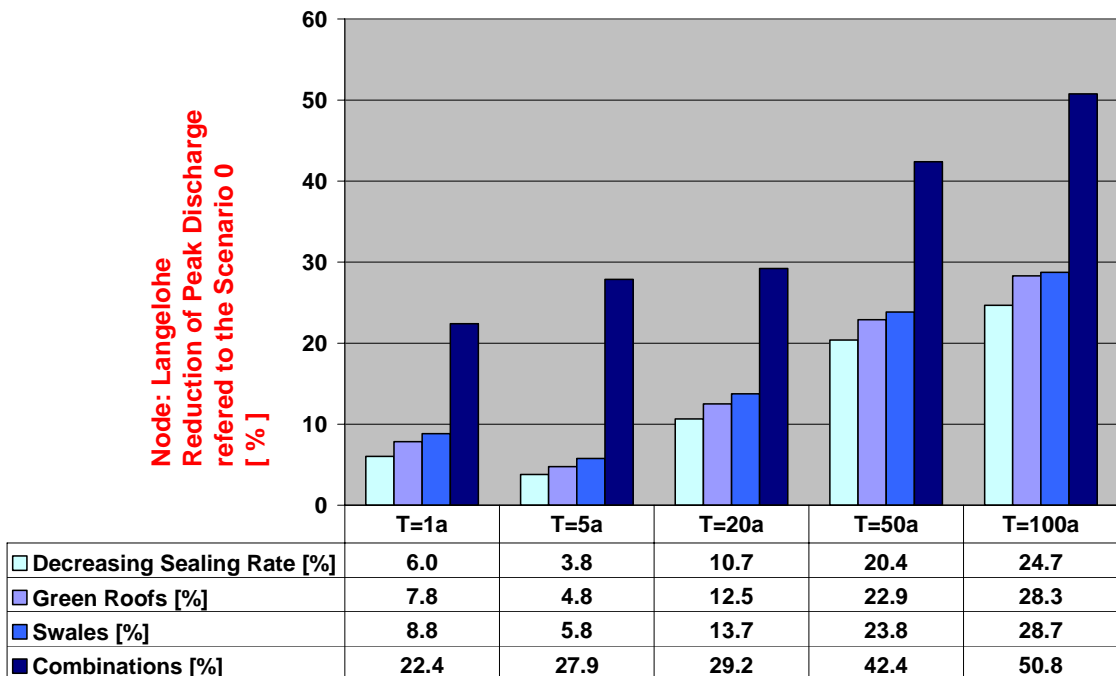
Reduction of the Peak Discharge referred to the projected (climate change) Natural State Scenario:



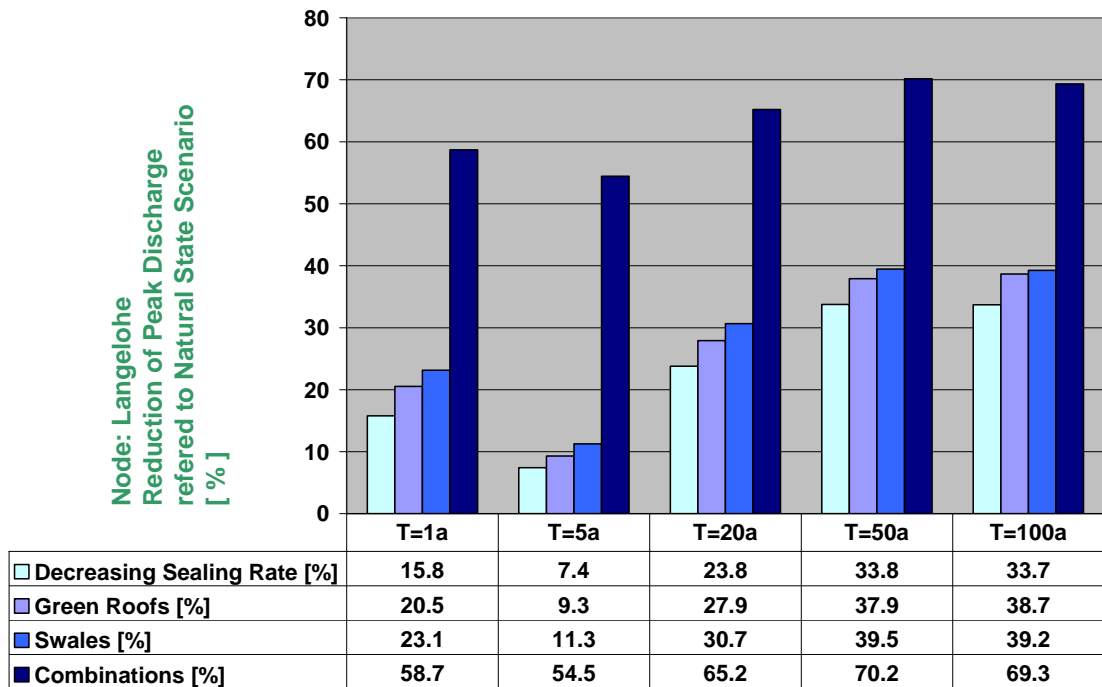
18.3 Node Langelohé in Elmshorn



Reduction of the Peak Discharge related to the status quo Scenario 0:

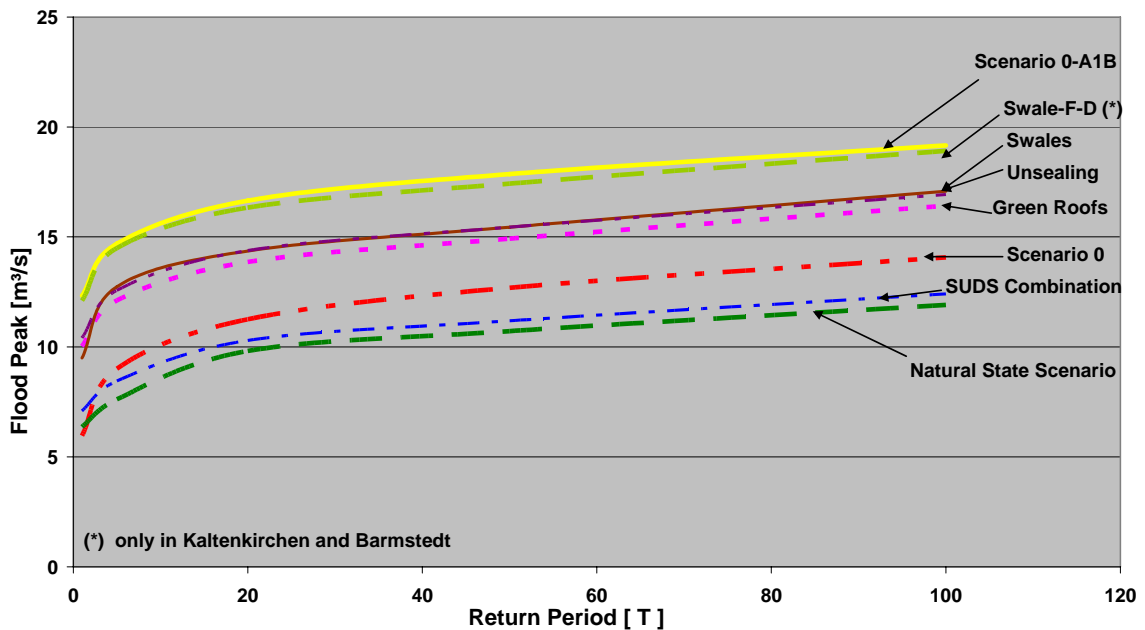


Reduction of the Peak Discharge referred to the projected (climate change) Natural State Scenario:

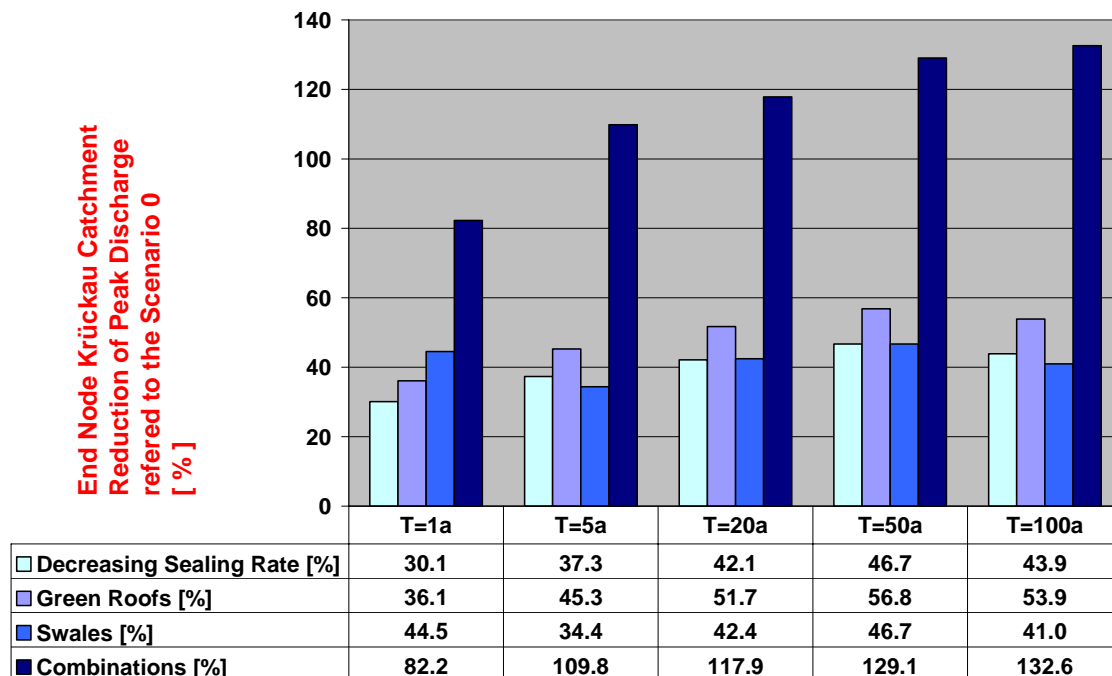


18.4 End Node of the Krückkau catchment area downstream of Elmshorn

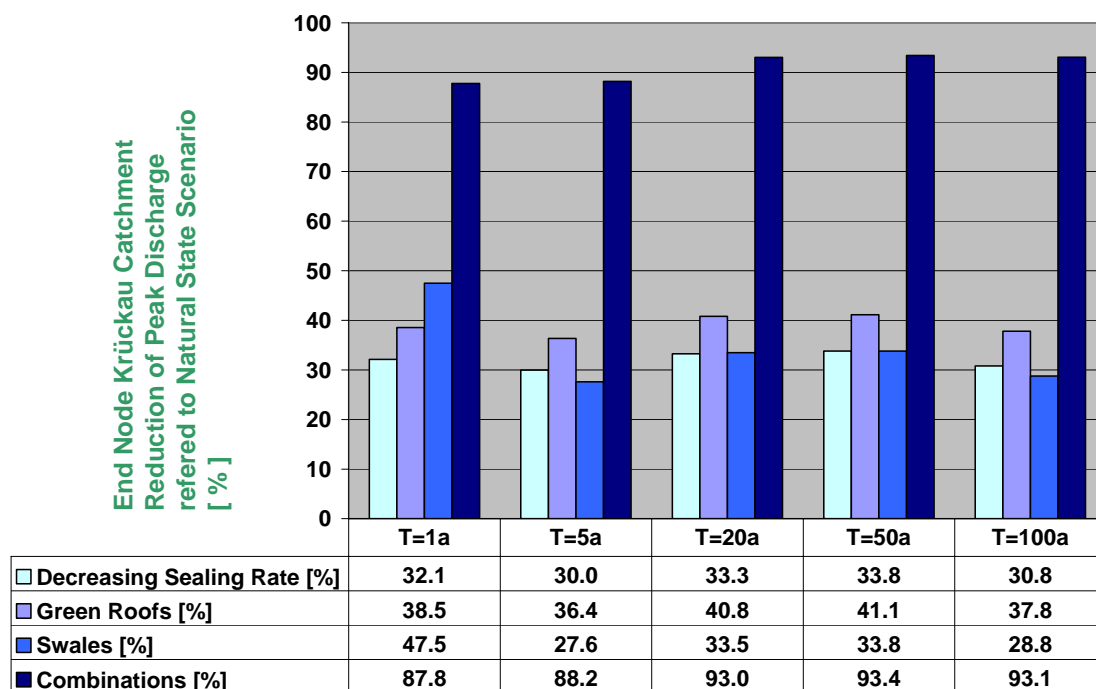
Krückkau Catchment End Node: Elmshorn  
Effectiveness of SUDS Techniques



*Reduction of the Peak Discharge related to the reference Scenario 0:*

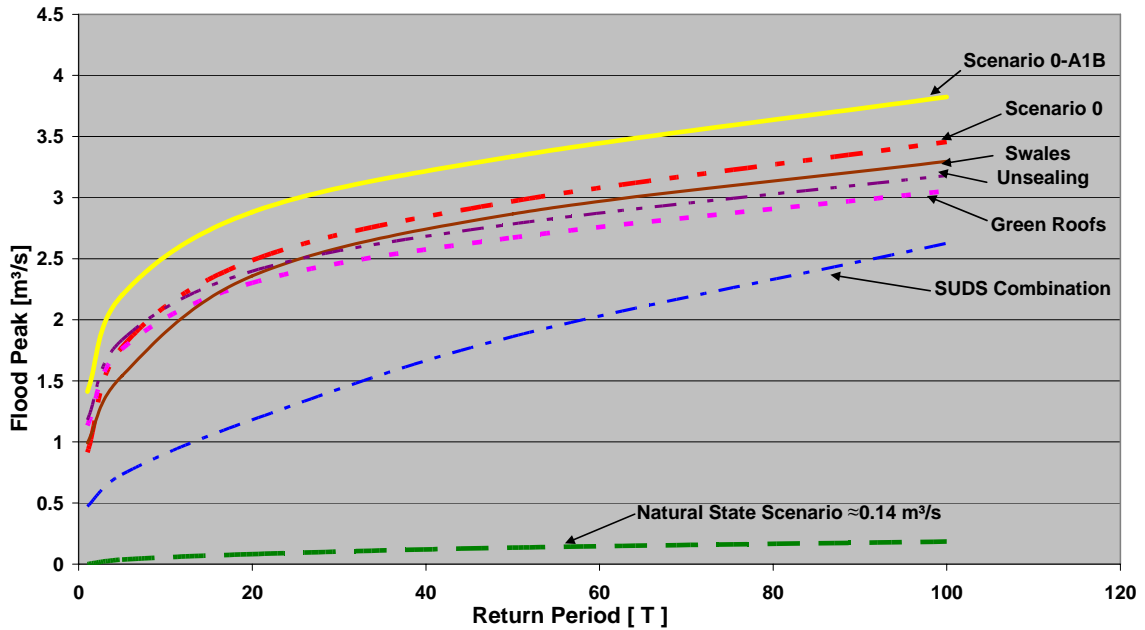


*Reduction of the Peak Discharge referred to the projected (climate change) Natural State Scenario:*

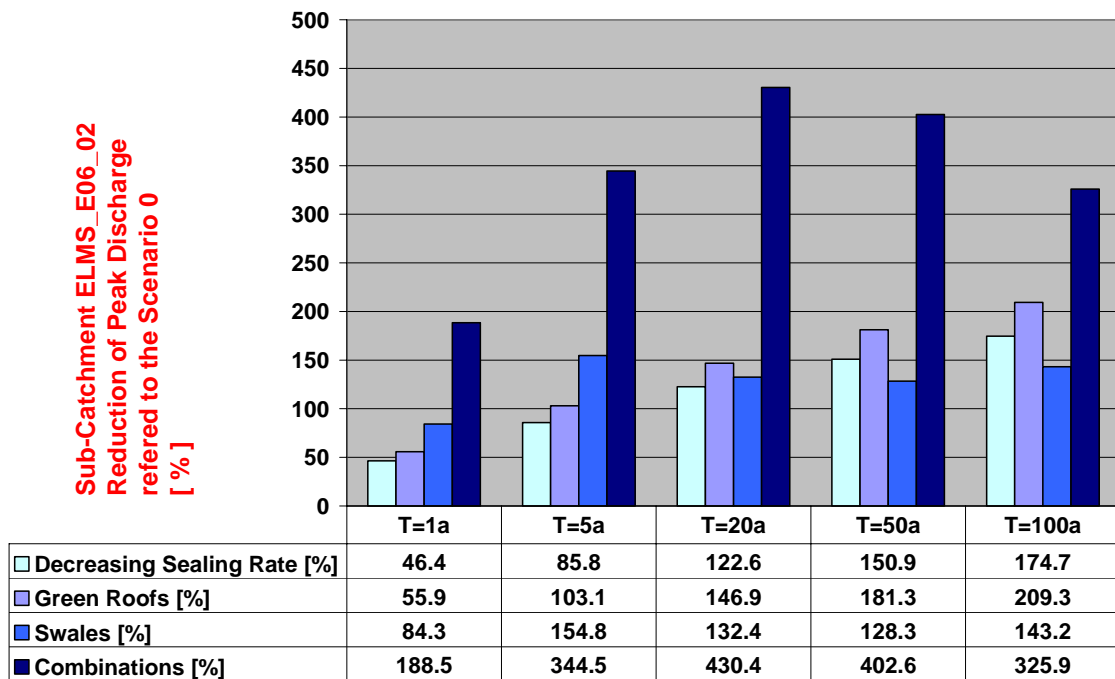


18.5 Results of Sub-Catchments in Elmshorn

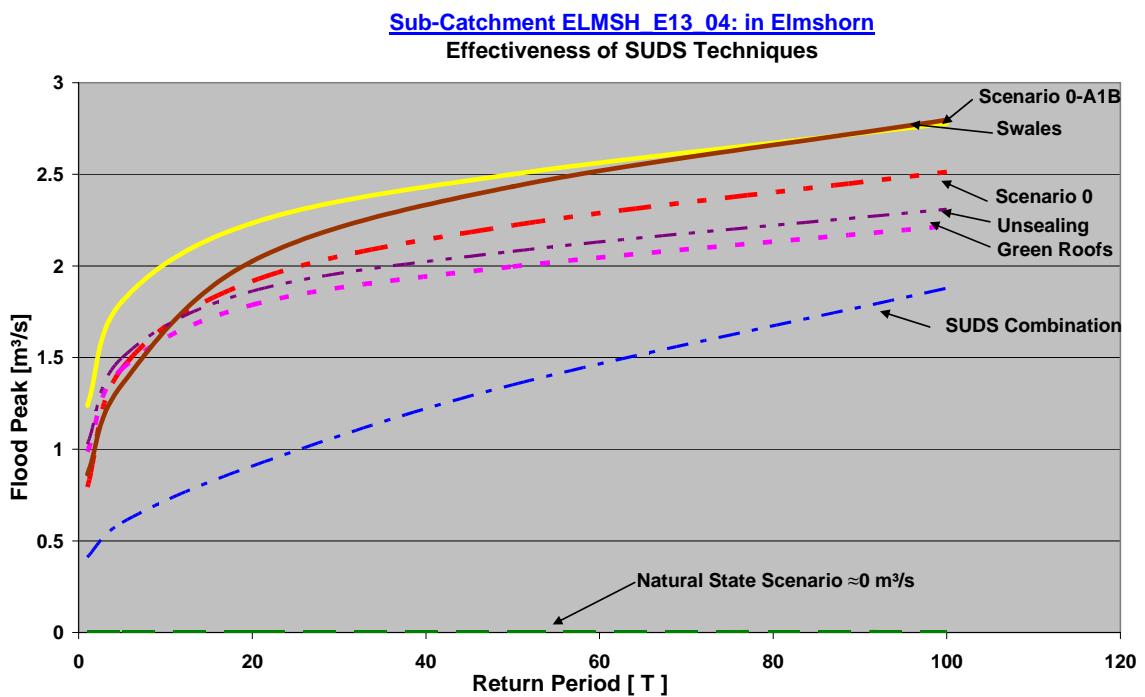
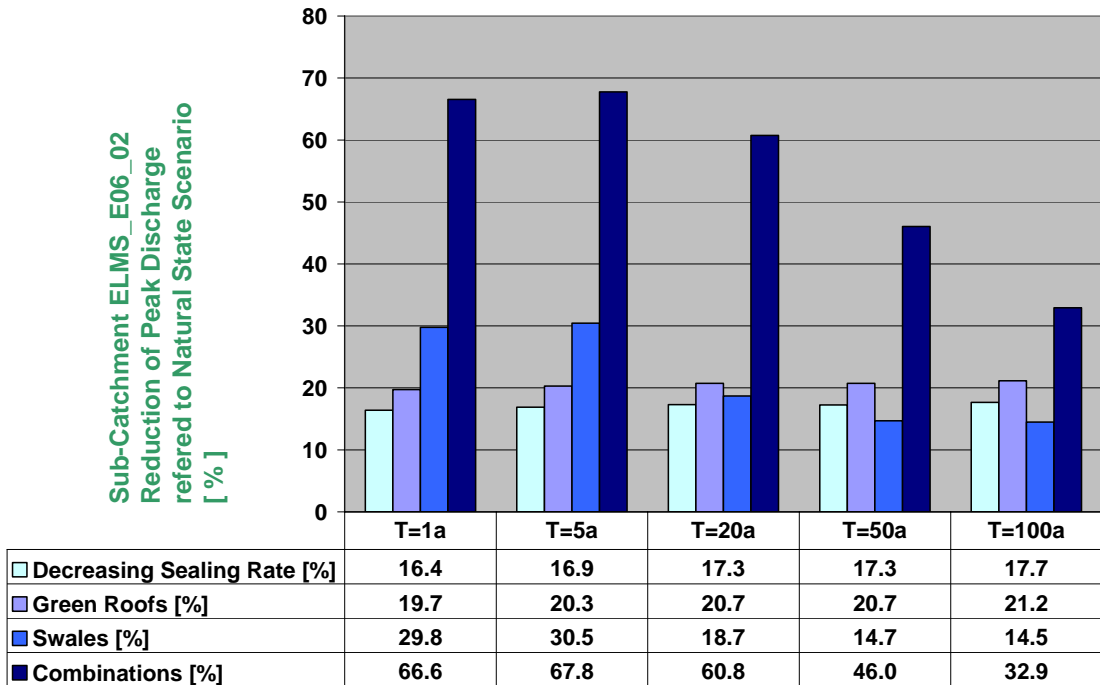
Sub-Catchment ELMSH E06\_02: in Elmshorn  
Effectiveness of SUDS Techniques



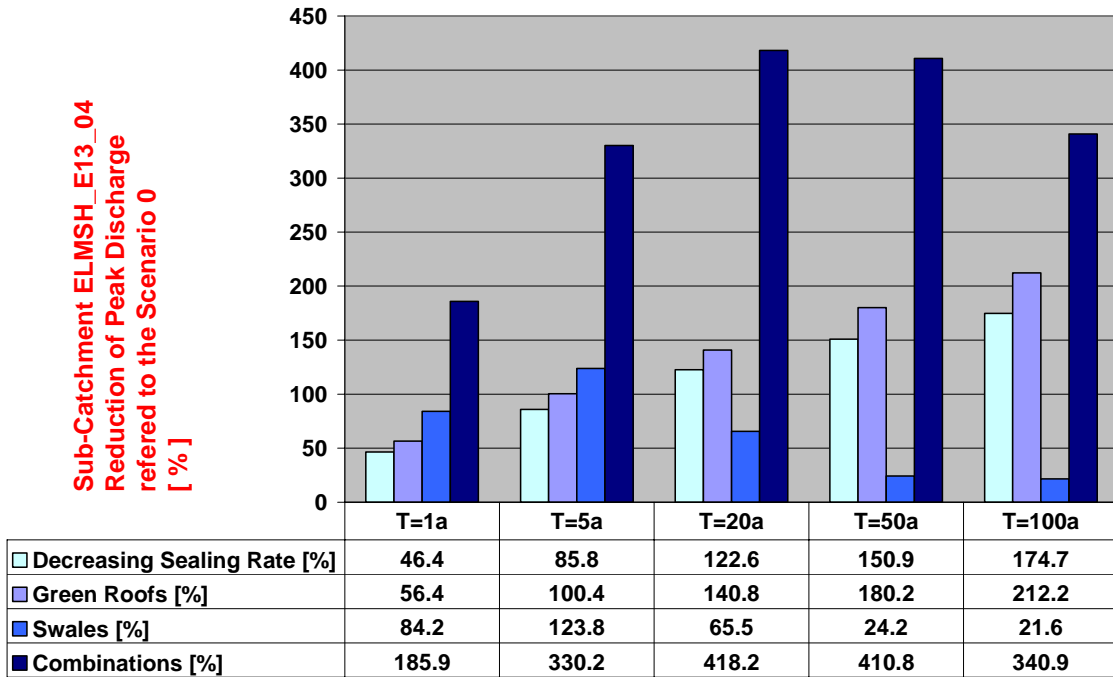
*Reduction of the Peak Discharge related to the reference Scenario 0:*



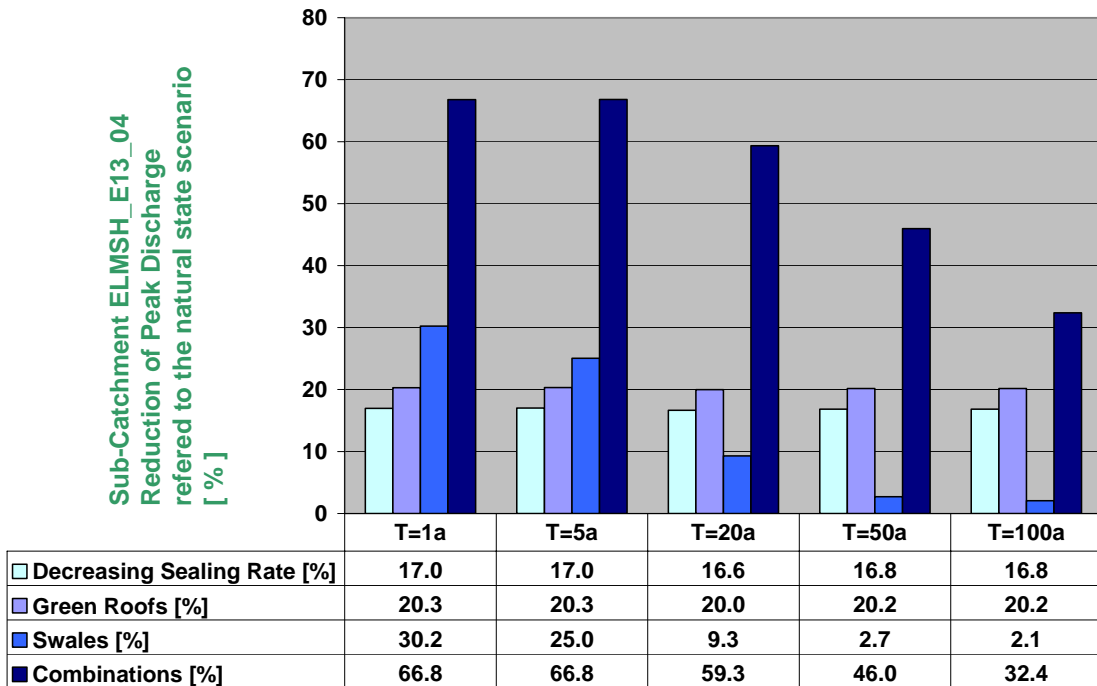
Reduction of the Peak Discharge referred to the projected (climate change) Natural State Scenario:



Reduction of the Peak Discharge related to the reference Scenario 0:



Reduction of the Peak Discharge referred to the projected (climate change) Natural State Scenario:



## Attachment 19

### Discussion About Climate Change Factor (CCF) Calculations

#### Definition of Variables:

- $A_e$  = Catchment area drained by the specific node ( $n$ ) [km<sup>2</sup>].
- $f_{T,C}$  = Climate change factor [ - ].
- $HQ_T$  = Flood peak with a return period ( $T$ ) computed with observed data series [m<sup>3</sup>/s].
- $\Delta HQ_{T,C,[\%]}$  = Percentage change of the flood event under climate change conditions ( $C$ ) with a specific return period ( $T$ ) [%]
- $HQ_{T,C,[\%]}$  = Magnitude of the flood peak with a return period ( $T$ ) for an IPCC scenario ( $C$ ) [m<sup>3</sup>/s].
- $HQ_{T,C}$  = Magnitude of the flood peak with a return period ( $T$ ) for an IPCC scenario ( $C$ ) [m<sup>3</sup>/s].
- $\Delta HQ_{T,C,control-scenario}$  = Flood peak with a return period ( $T$ ) computed in the control scenario of the past [m<sup>3</sup>/s].
- $\Delta HQ_{T,C,IPCC-scenario}$  = Flood peak with a return period ( $T$ ) computed in an IPCC climate scenario ( $C$ ) [m<sup>3</sup>/s].
- $n$  = Number of statistical evaluations [ - ].
- $T$  = Return Period [a]

Calculation of the percentage change of the flood peak per probability of occurrence  $\Delta HQ_{T,C,[\%]}$  (see 3.5.1 for details)

$$\Delta HQ_{T,C,[\%]} = \frac{(HQ_{T,C,IPCC-scenario} - HQ_{T,C,control-scenario})}{HQ_{T,C,control-scenario}} * 100 \quad [\%]$$

#### 1. Averaging Ensemble CCF (Developed in this thesis; chapter 3.5.2)

Calculation of the climate change factor with the percentage change approach:

$$f_{T,C} = \frac{\sum_{n=i}^n \left[ 1 + \frac{(\Delta HQ_{T,C,[\%]})}{100} \right]}{n}$$

Calculation of the adjusted design flood for a specific return period ( $T$ ):

$$HQ_{T,C} = f_{T,C} * HQ_T$$

2. Delta Runoff Rate CCF (adopted from Golder Associates, 2009)

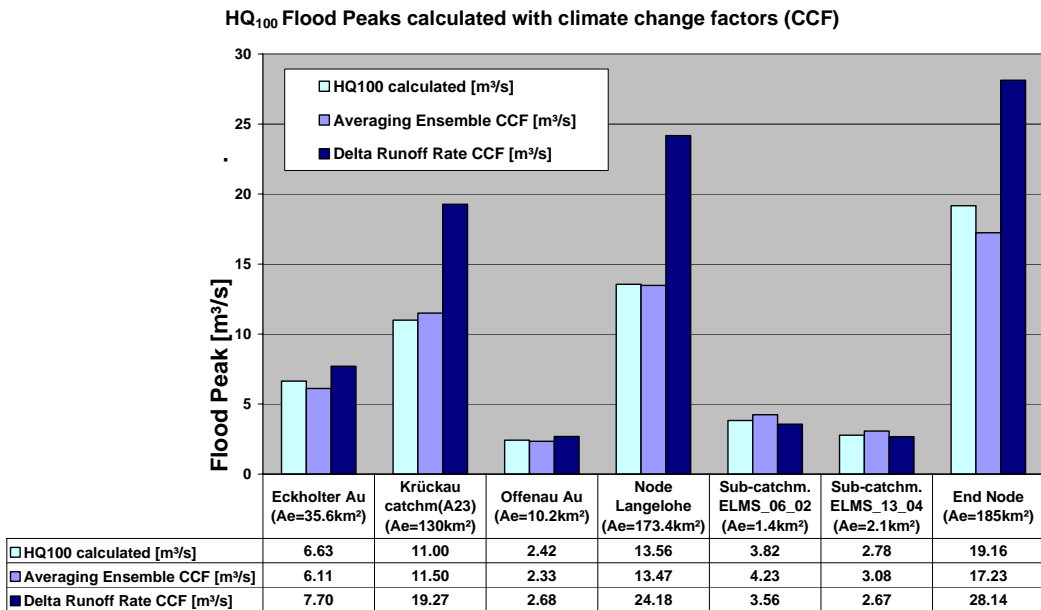
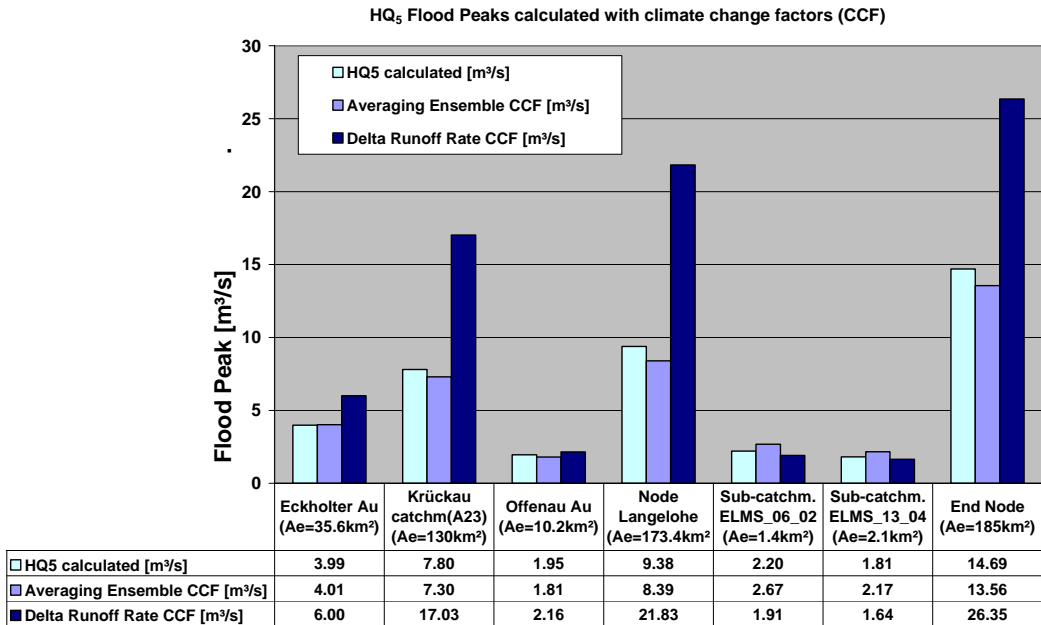
The equations for the calculation of the Delta Runoff Rate CCF have been developed by recalculating the published results in Golder Associates (2009):

$$\Delta q_{T,C} = \frac{\sum_{n=i}^n \left[ \frac{\Delta HQ_{T,C,[\%]} * HQ_T}{A_e(n) * 100} \right]}{n}$$

Calculation of the adjusted design flood for a specific return period:

$$HQ_{T,C}(n) = HQ_T(n) + \Delta q * A_e(n)$$

3. Comparison of Results





ISBN 978-3-937693-13-2



9 783937 693132 >